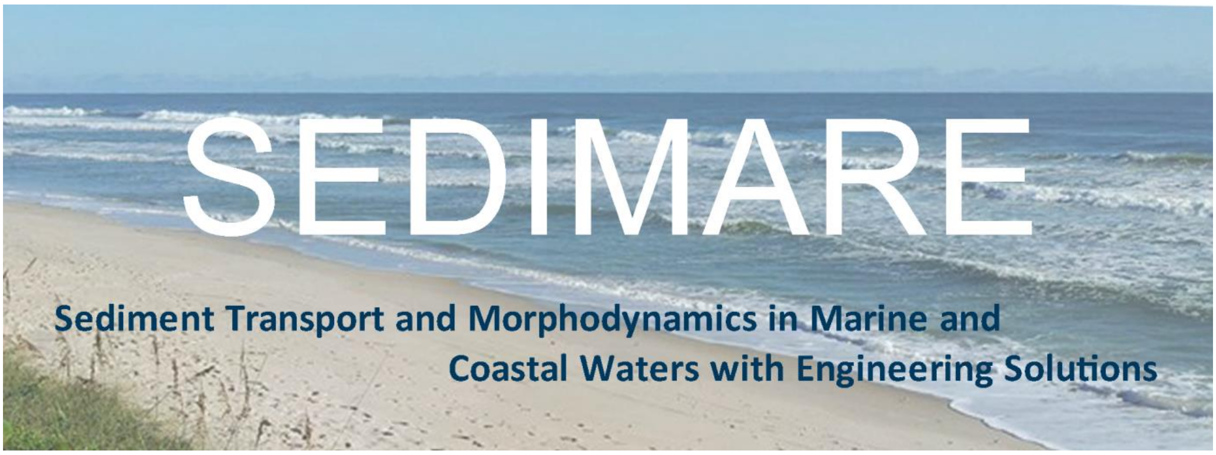

Project Number: 101072443

1st NETWORK TRAINING SCHOOL

Deliverable 4.2

Dissemination level: PU - Public

Prepared by:

Athanassios Dimas, Coordinator, University of Patras

This project has received funding from the European Union's (EU) Horizon Europe Framework Programme (HORIZON) under Grant Agreement No. 101072443 as a MSCA Doctoral Network (HORIZON-MSCA-2021-DN-01).

Document Information

Project Title	Sediment Transport and Morphodynamics in Marine and Coastal Waters with Engineering Solutions
Project Acronym	SEDIMARE
Grant Agreement No.	101072443
Call	MSCA Doctoral Networks 2021 (HORIZON-MSCA-2021-DN-01)
Start Date of Project	01-02-2023
Duration of Project	48 months
Deliverable	D4.2: 1st NETWORK TRAINING SCHOOL
No. of pages including cover	379

Version	Publication Date	Author(s)	Change
1.0	29.05.2024	Athanassios Dimas	Initial version
2.0	28.06.2024	Athanassios Dimas	Addition of EU funding acknowledgment on page 1 and disclaimer text on page 2. Addition of new Section 2.

Date and Signature of Author(s): ATHANASIOS DIMAS 28/06/2024 19:51

Table of Contents

1. Overview

The SEDIMARE "Introductory Training School" was organized at the University of Nottingham (UNOTT), Nottingham, UK, on 22-24 April 2023. Local organizers were Prof. N. Dodd and Prof. R. Briganti. The training event was attended in person by DCs 1, 2, 4, 5, 6, 7, 8, 9, 10 and 11, and remotely (due to travel obligations) by DCs 3 and 12. The program of the event is shown in Table 1.

Table 1. Program of the SEDIMARE "1st Network Training School"

Time	**April 22, Monday (Day 1)**
9:00-10:30	• Introduction: Short introduction by the REA Project Officer (Dr. Vyzikas) and the Project Coordinator on the purpose of the Mid-Term Meeting. • SEDIMARE Research teams: All scientists-in-charge from Beneficiaries and Associated Partners should briefly present their research team and describe their role within the Network. • REA Project officer presentation: Presentation on the monitoring of project implementation, reporting and purpose of the mid-term check, including: o MTM objective o Assessment of recruitment / Reminder of DCs rights & obligations o Project Management o Reporting & finance o Communication, Dissemination, Exploitation, Synergies Useful links & reference documents
10:45-11:00	Coffee / Tea
11:00-12:30	• Project Coordinator's presentation: Presentation of the Network and the progress covering the following aspects: o State of play of the recruitment, deliverables and milestones; o Management activities (Supervisory board activities, etc.); o Financial aspects; o Critical implementation risks and mitigation actions; o Document management and Open Science. • DC introductions: The 12 DCs will present themselves, their background and their individual research project (foreseen research, training, secondments, etc.). Scientific results are not expected at this stage.
12:30-14:00	Lunch
14:00-15:30	DC presentations: The 12 DCs will present work done so far especially in terms of literature review and research planning.
15:30-17:00	Restricted session with the DCs: the session is intended to allow the researchers to discuss with the REA representative about their experiences within the network in terms of training foreseen, supervision

	arrangements, progress and impact on their future careers. *This session was postponed (Dr. Vyzikas was under the weather); it was scheduled and held one week later.* Discussion between the SEDIMARE scientists and DCs on issues and ways to improve the Network impact.
17:00-17:30	Restricted session: Meeting between Project Coordinator and Project Officer to discuss any issue. *This session was also postponed; Dr. Vyzikas sent his remarks to the Coordinator one week later via email.*
	April 23, Tuesday (Day 2)
08:45-09:00	Announcements
09:00-10:30	"Q2Dmorfo: a reduced complexity model for long term coastal dynamics" (Invited Speaker **Albert Falqués**, Universitat Politècnica de Catalunya)
10:30-11:00	Coffee / Tea
11:00-12:15	"Find your course in choosing between coarse grids, fine grids, unstructured grids, quadtree grids and subgrids" (**N. Volp**, UTWENTE)
12:15-14:00	Lunch
14:00-15:15	"Modelling of coupled hydrodynamics, sediment transport and bed morphodynamics" (**A. Dimas**, UPATRAS)
15:15-15:45	Coffee / Tea Break
15:45-17:00	"Application of the projection method for the Navier Stokes equations to two-phase flow solvers" (**M. Papalexandris**, UCL)
	April 24, Wednesday (Day 3)
09:00-10:15	"Blending coastal morphodynamic models and observations through data assimilation" (**M. Alvarez**, FIHAC)
10:15-10:45	Coffee / Tea
10:45-12:00	"Wave resolving numerical modelling of swash zone hydro- and morphodynamics" (**R. Briganti**, UNOTT)
12:00-14:00	Lunch
14:00-15:15	"Modelling eddies and coherent structures in the coastal area." (**M. Postacchini**, UNIVPM)
15:15-15:45	Coffee / Tea
15:45-17:00	"Calibration and verification of sediment transport models in the real world" (**M. Knaapen**, HRW)

2. Extracts from the Presentations

The theme of the 1st Network Training School was "Numerical Methods in Coastal Hydrodynamics and Sediment Transport". Therefore, the scope of the presentations was on the fundamentals and the applications of numerical methods to be used by the DCs in their research.

Characteristic parts of corresponding presentations are shown in the next pages but first the presentations of all DCs in terms of literature review, work done so far and research planning are included.

DC Presentations

Hydraulic Engineering Laboratory
Department of Civil Engineering
University of Patras

Literature Review & Research Planning

Ioannis Gerasimos Tsipas Ph.D Candidate

Objective

- Development of large-eddy simulation (LES) software to model turbulent oscillatory flow and sediment transport induced by waves over a flat or rippled sandy bed.
- Sediment transport module with the capability to model sand composed by grains of single size.✓
- <u>The sediment transport module will have the capability to model sand composed by grains of mixed and not single size.</u>

Literature Review

- Depth-Averaged Two-Dimensional Numerical Modeling of Unsteady Flow and Non-uniform Sediment Transport in Open Channels (Weiming Wu, M.ASCE)
- 2D numerical modeling of grain-sorting processes and grain size distributions (Yi Xiao, Hong Wang, Xuejun Shao, Journal of Hydro-environment Research)
- Non-uniform sediment transport in alluvial rivers (Weiming Wu, Sam S.Y. Wang & Yafei Jia, Journal of Hydraulic Research)

Methodology

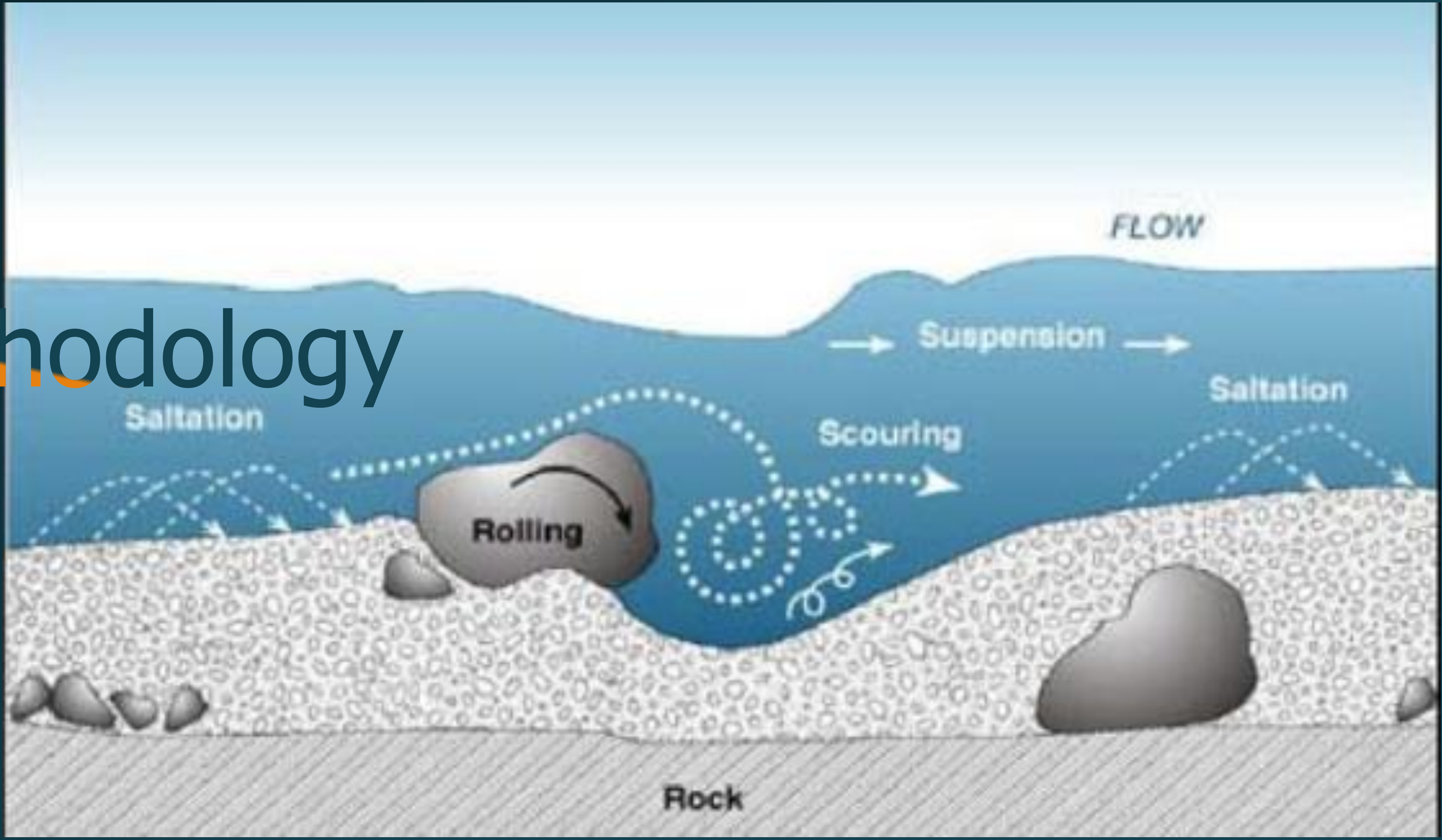

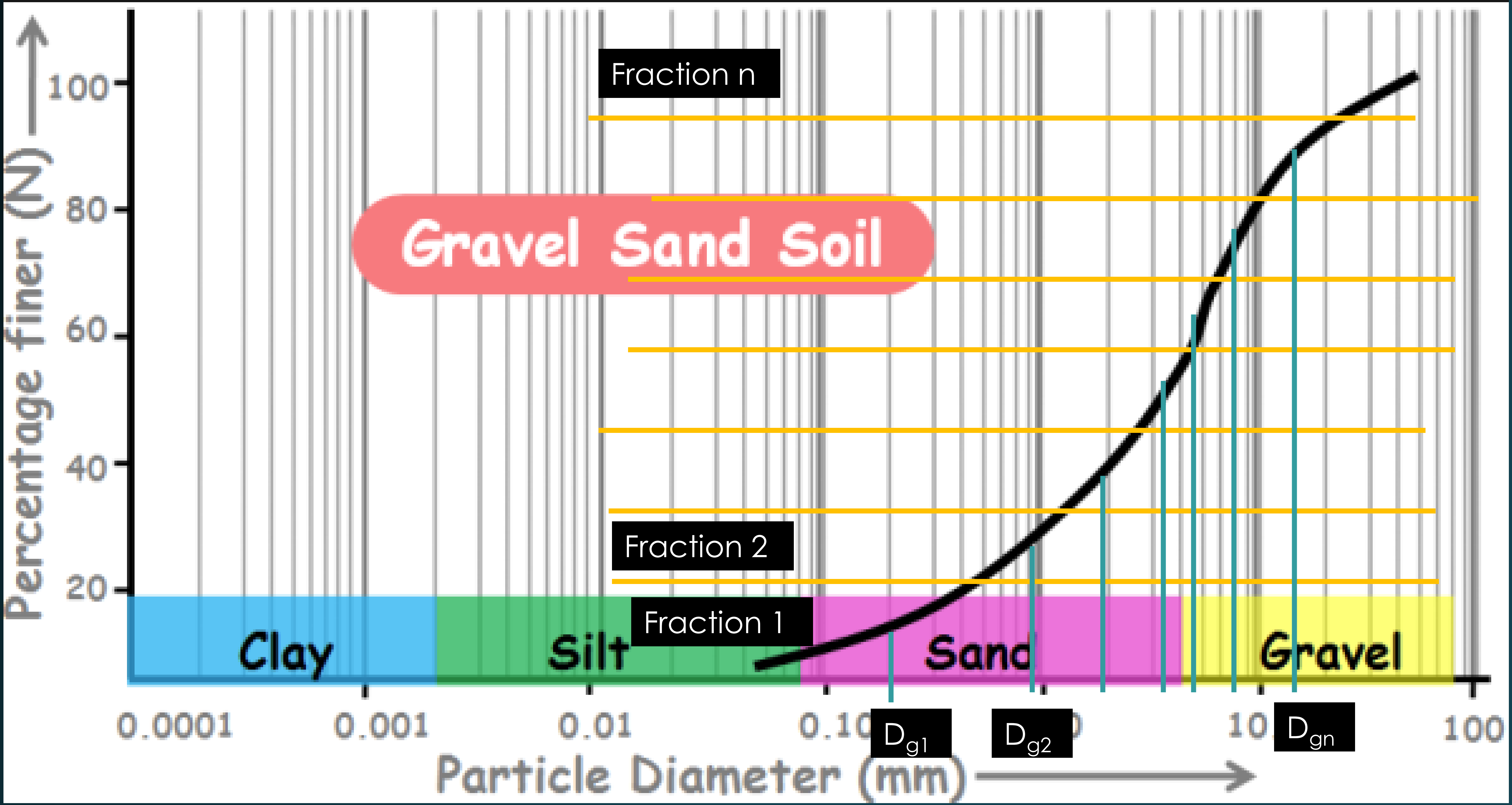

Gravel Sand Soil
Fraction n
Fraction 2
Fraction 1
Percentage finer (N)
100
80
60
40
20
Clay
Silt
Sand
Gravel
0.0001
0.001
0.01
0.10
10
100
D_{g1}
D_{g2}
D_{gn}
Particle Diameter (mm)

Sediment Transport Equations, Bed Load

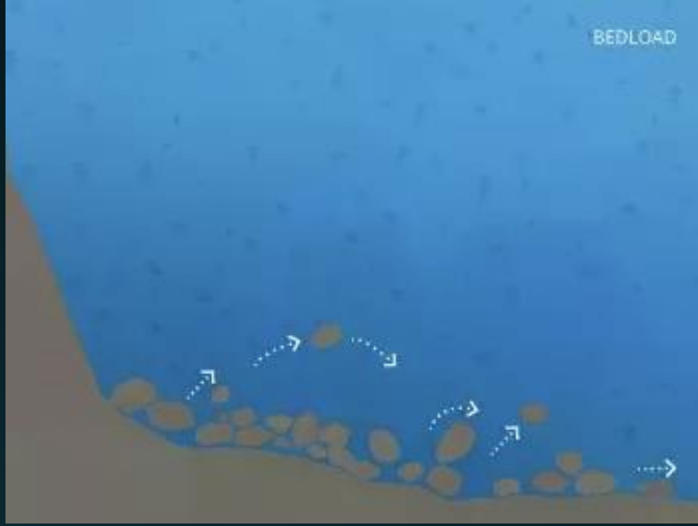

Bed load transport rate

1

$$\frac{Q_b}{\sqrt{(S-1)gD_g^3}} = \Phi_b(\theta, \theta_c, Dg)$$

Shields number

$$\theta = \frac{\tau_b}{\rho(S-1)gD_g^3}$$

2

Critical Shields number

$$\theta_c = \theta_c(\varphi, tan\beta, \theta_{co})$$

Critical Shields number (Horizontal Bed)

$$\theta_{co} = f(D_*)$$

(van Rijn, 1984)

Dimensionless grain size

$$D_* = D_g\left[(S-1)g/v^2\right]^{1/3}$$

1 Non-dimensional fractional bed-load transport rate

$$\Phi_{bi} = \frac{Q_{bi}}{f_{b,i}\sqrt{(S-1)gD_{gi}^3}}$$

- Q_{bi} : transport rate of the ith fraction of bed-load per unit width (m^2 /s)
- f_{bi} : percentage of bed particles in fraction "i" with mean diameter D_{gi}

2 Critical Shields number

$$\theta_{c,i} = \theta_{c,i}(\varphi_i, tan\beta, \theta_{co\,i})$$

- θ_c, can be interpreted as the non-dimensional critical shear stress for the corresponding uniform sediment or the mean size of bed materials for each "i" fraction.

Sediment Transport Equations ,Suspended Sediment

Advection-Diffusion Equation

$$\frac{\partial c_i}{\partial t} + u_j \frac{\partial c_i}{\partial x_j} - w_s \frac{\partial c_i}{\partial z} = \frac{1}{Re{\cdot}Sc} \frac{\partial^2 c_i}{\partial x_j^2} - \frac{\partial \chi_{j,i}}{\partial xj}$$

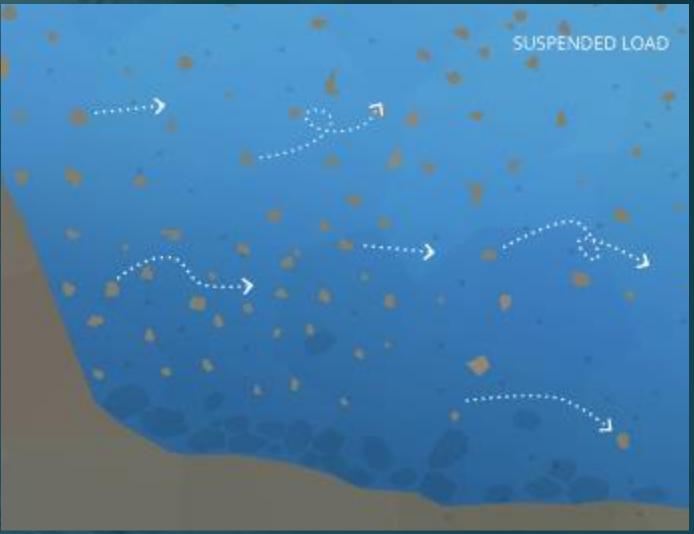

Bed Boundary Condition (Dirichlet)

$$C_{a,i} = c_{a,i}\,(\theta, \theta_c, D_g)$$ (van Rijn 1984)

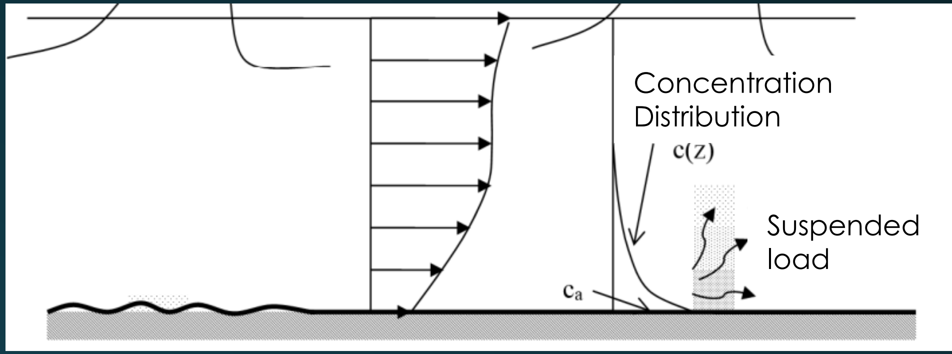

Transport rate of suspended sediment

$$q_{s,x,i}(x,y,t) = \int_{z_a}^{h} (uc)dz \quad , \quad q_{s,y,i}(x,y,t) = \int_{z_a}^{h} (vc)dz$$

The Boundary Condition should change for every fraction “i” of the model, so the advection diffusion equation shall be solved for each sediment fraction ,i.

Morphology Evolution Equations

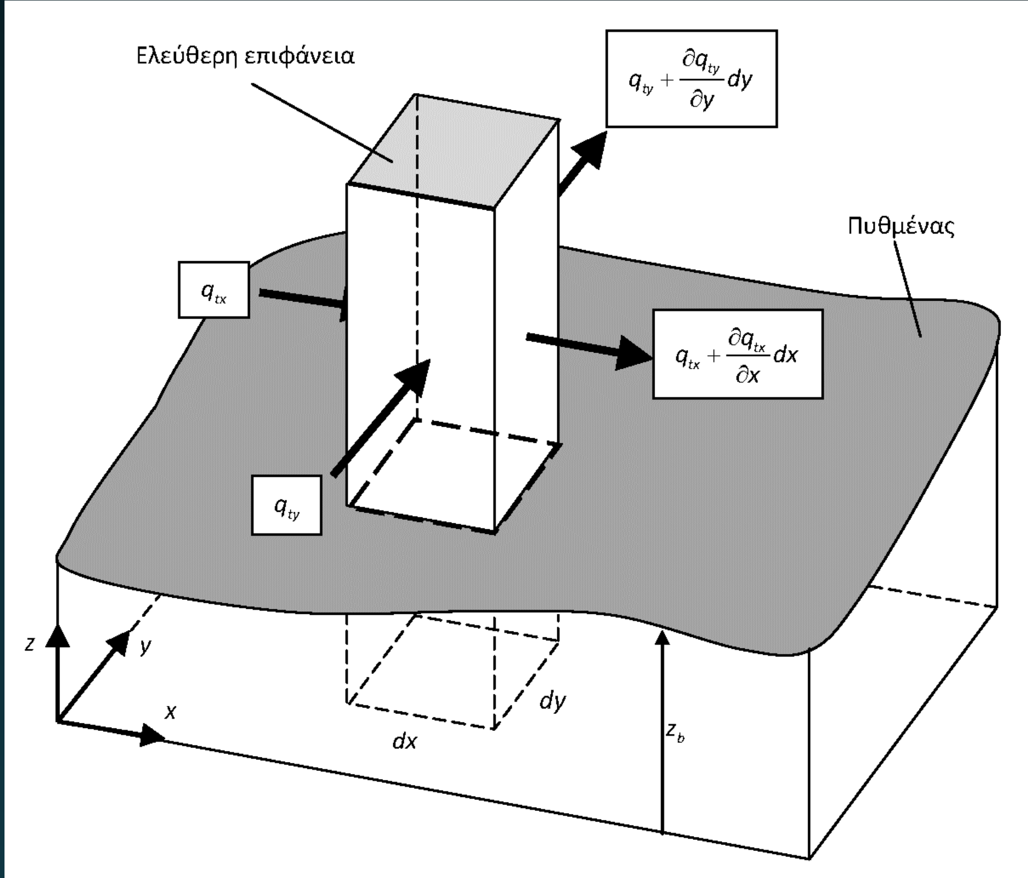

Conservation of sediment mass equation (Exner equation)

3

$$\left(\frac{\partial z_B}{\partial t}\right)_i + \frac{1}{1-n_p}\frac{\partial}{\partial t}\left(\int_{z_a}^{h} c_i dz\right) = -\frac{1}{1-n_p}\left(\frac{\partial q_{t,x}}{\partial x} + \frac{\partial q_{t,y}}{\partial y}\right)_i$$

$$q_{t,i} = q_{b,i} + q_{s,i}$$

$$z_B = z_{B1} + z_{B2} + \cdots + z_{Bn}$$

The total depth results from the sum of each depth of the respective fractions

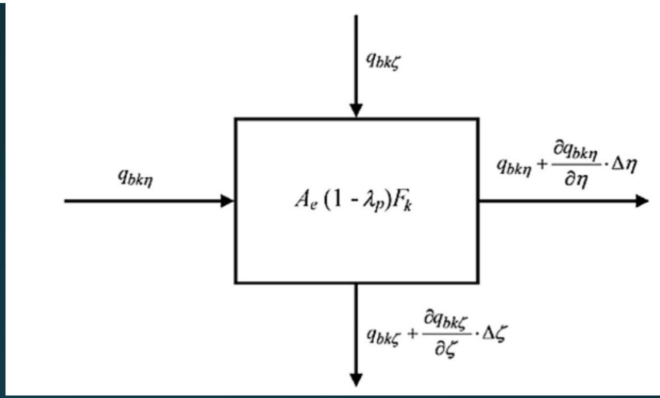

3 $\left(\frac{\partial z_b}{\partial t}\right)_i$ =bed change rate corresponding to the i^{th} fraction of sediment

The morphology equation shall be calculated for each “i” fraction of sediment

Thank you for your attention

UNIVERSITÀ POLITECNICA DELLE MARCHE

Ingegneria

SEDIMARE DC MEETING

22.04.2024-24.04.2024

Nottingham, the UK

Nearshore Wave Processes by Remote Sensing

Name	Muhammed Said Parlak
Project	Coastal Resilience
Supervisors	Maurizio Brocchini Nicholas Dodd Matteo Postacchini

Coastal Dynamics by Remote Sensing

→ Monitoring by videocameras
  - Quantification of sand bars

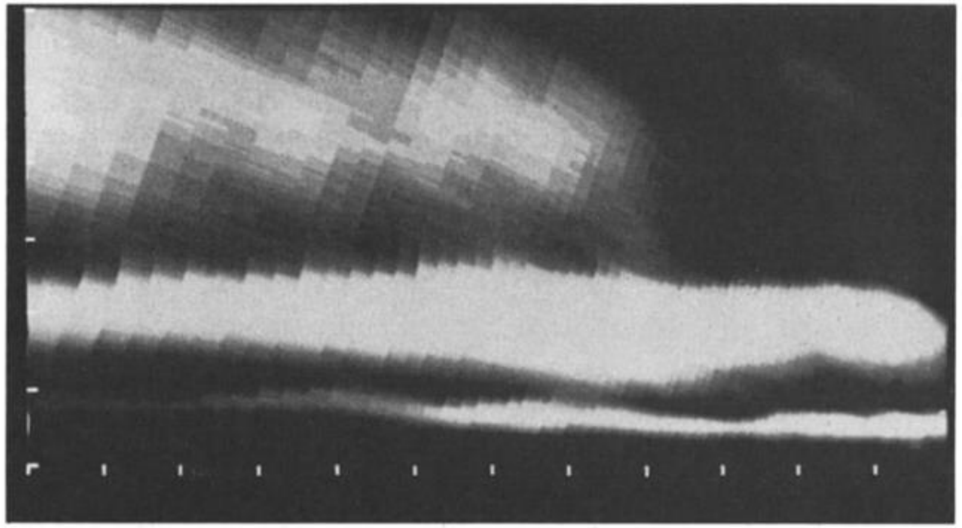

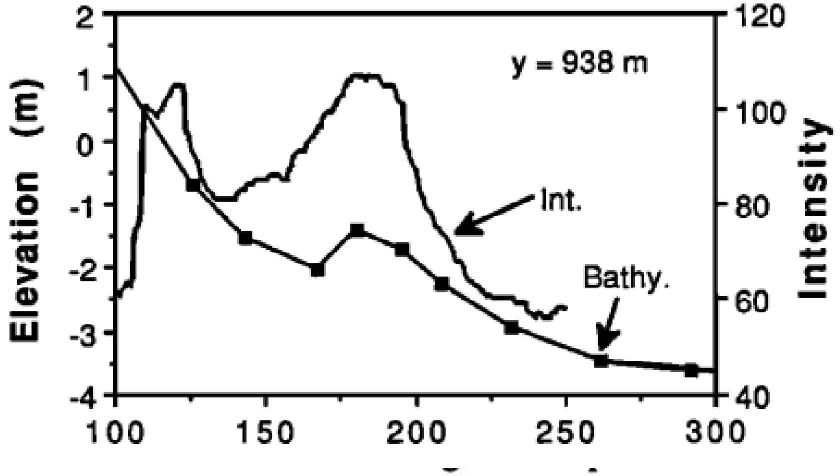

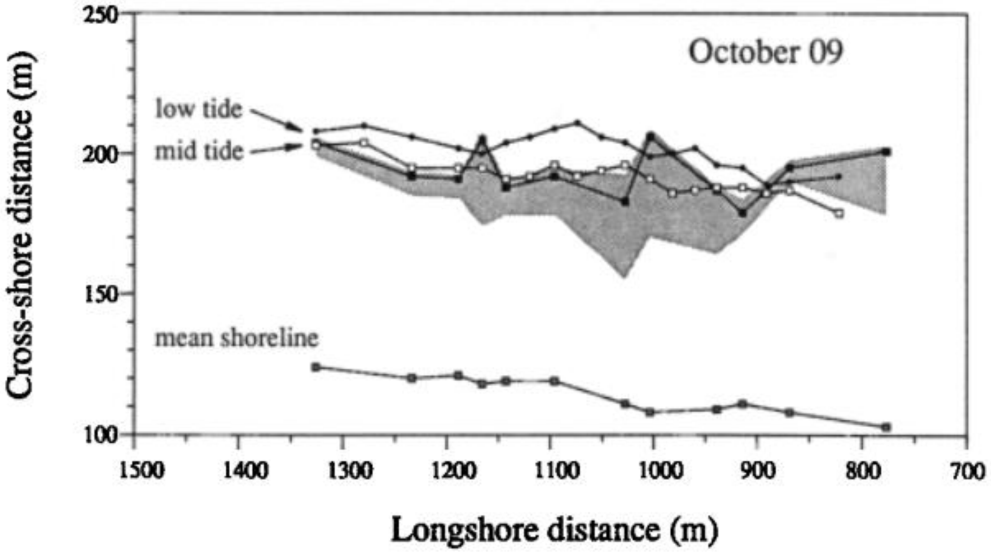

[Lipmann and Holman, 1989]

Coastal Dynamics by Remote Sensing

→ Monitoring by videocameras
  - Wave characteristics

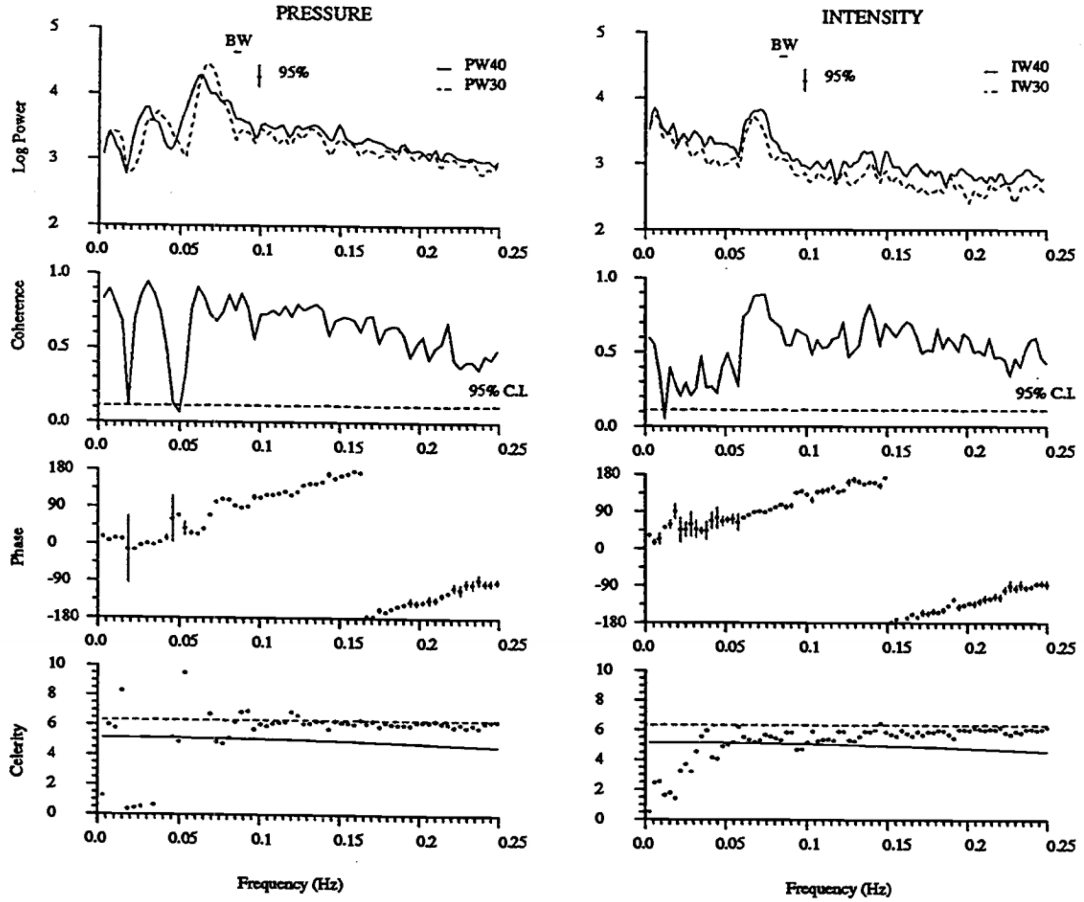

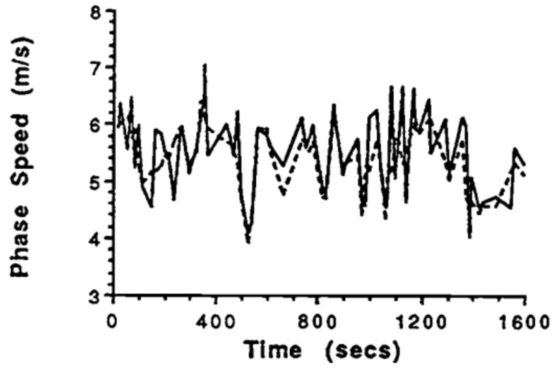

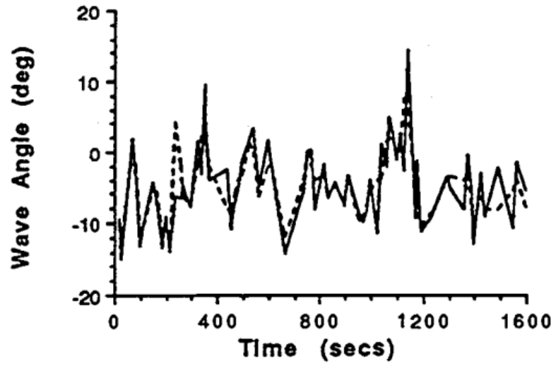

[Lipmann, 1993]

Coastal Dynamics by Remote Sensing

→ Monitoring by videocameras
  - Identification of wave breaking

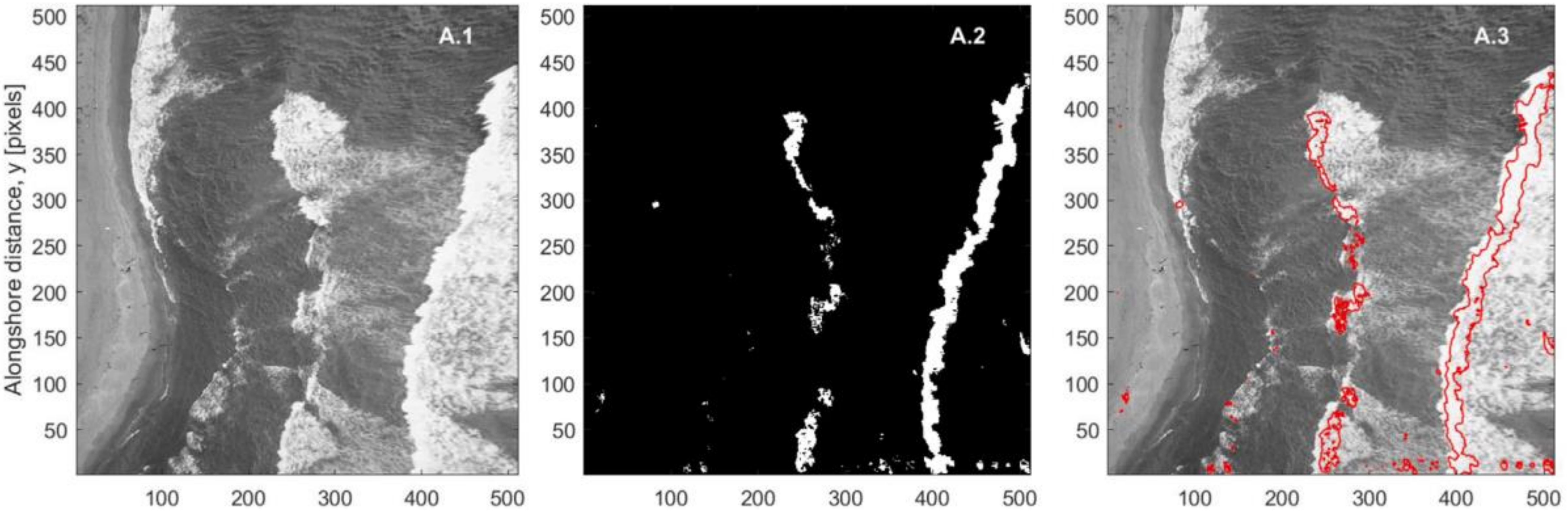

[Sáez et al., 2021]

Coastal Dynamics by Remote Sensing

→ Monitoring by radar system
  - Evaluation of wave characteristics

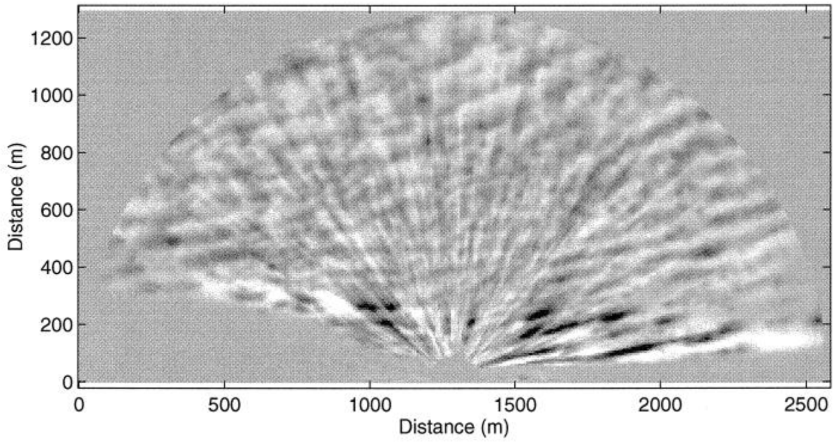

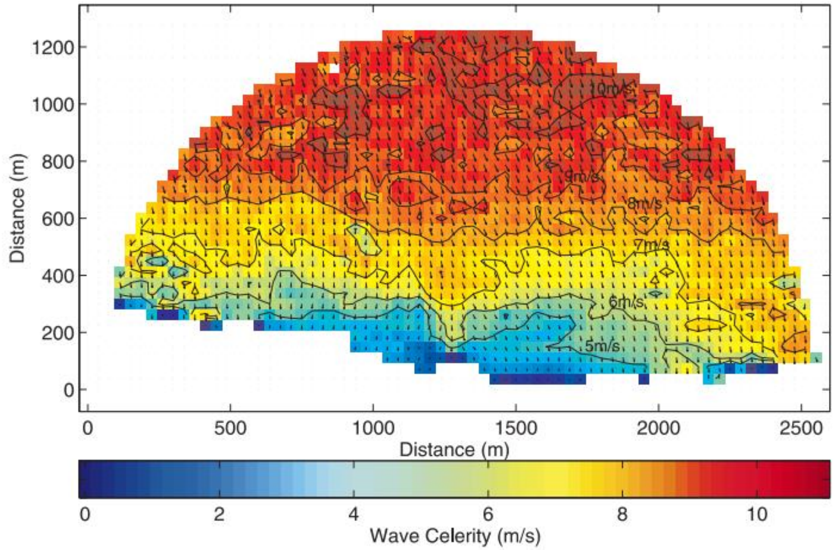

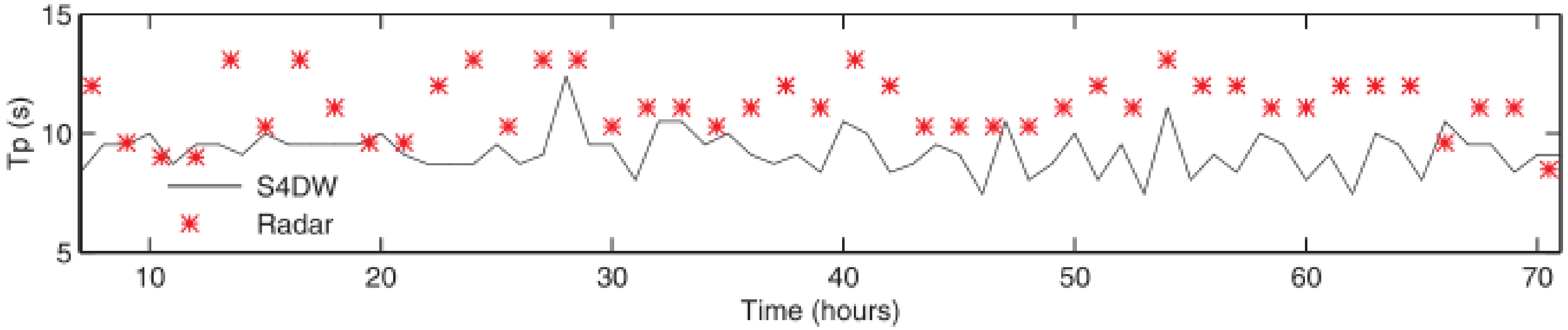

[Bell, 1999]

Coastal Dynamics by Remote Sensing

→ Monitoring by radar system
  - Evaluation of wave characteristics

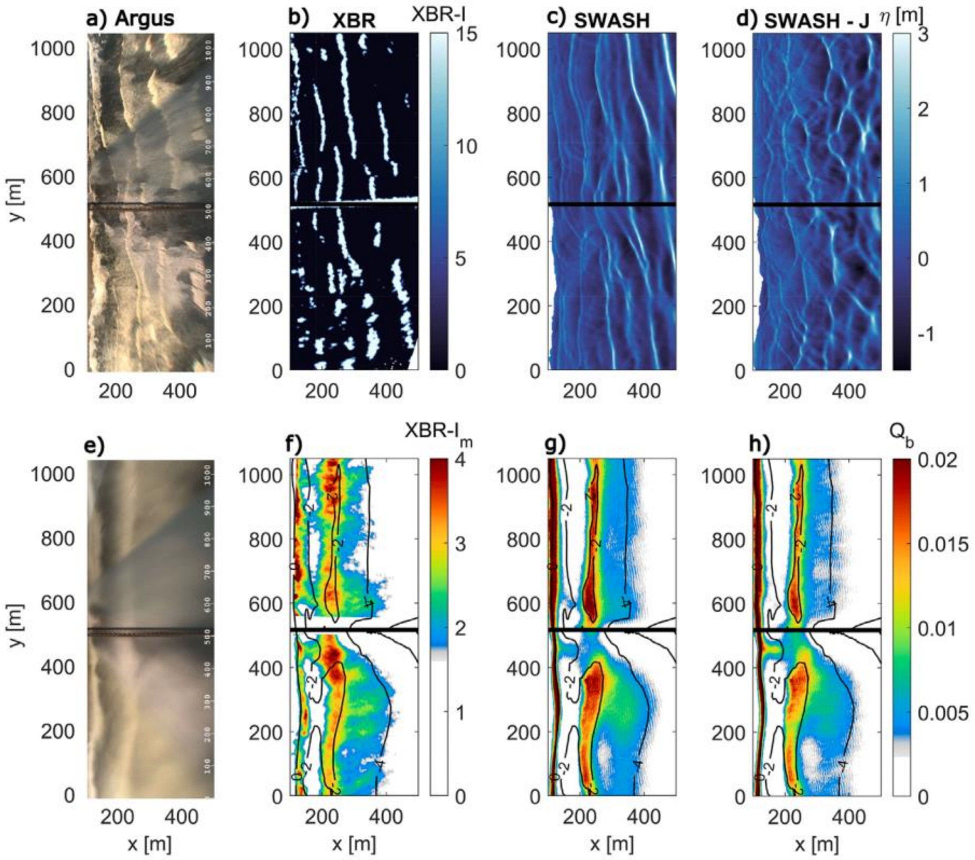

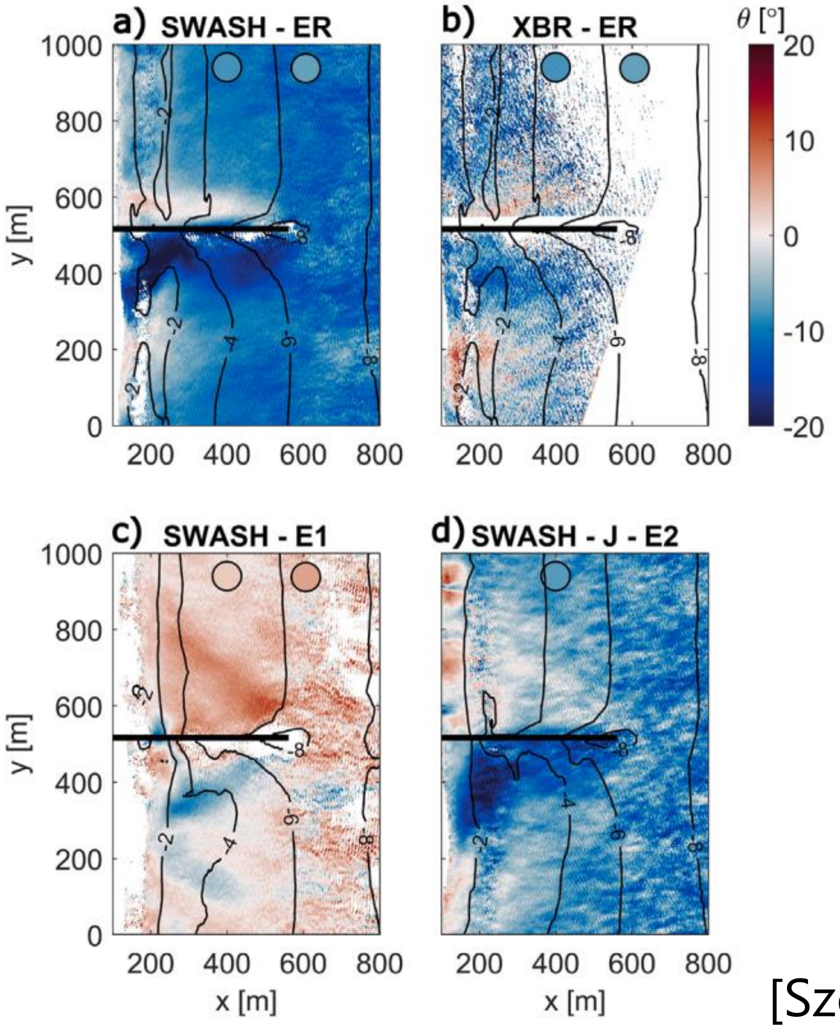

[Szczyrba et al., 2023]

Coastal Dynamics by Remote Sensing

→ Combined use of tools

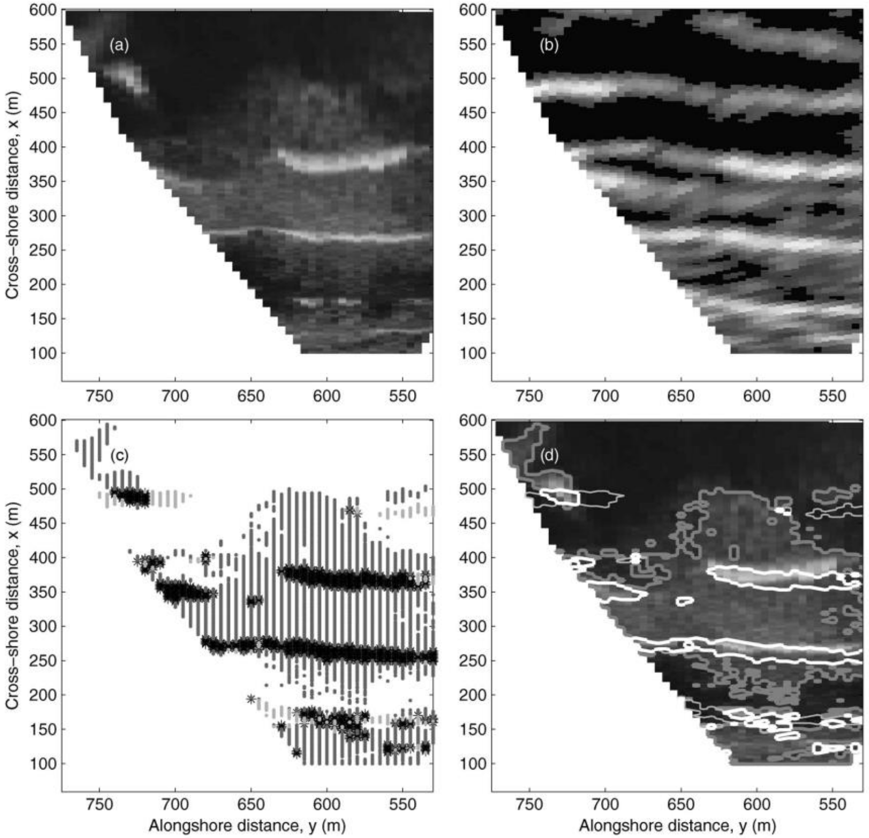

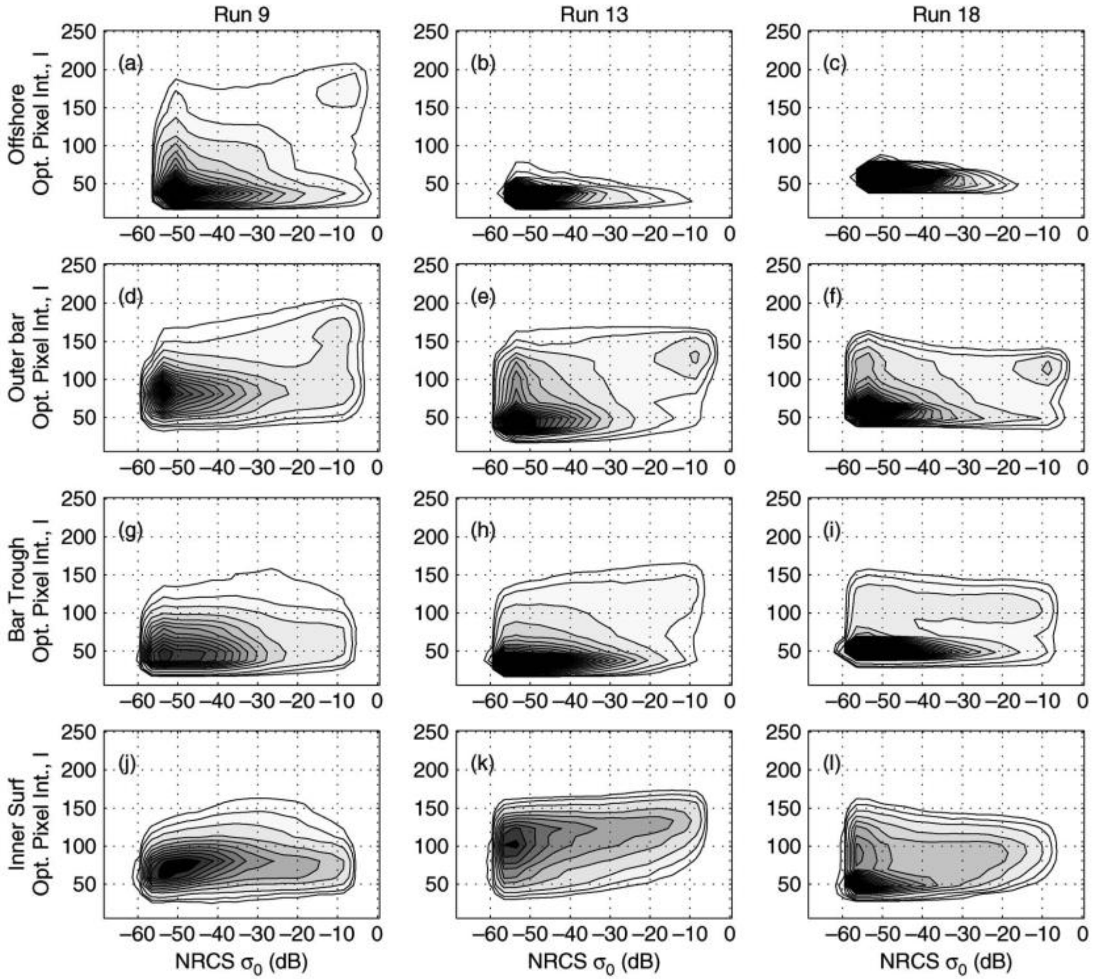

[Catalán et al., 2011]

Coastal Dynamics by Remote Sensing

→ Combined use of tools

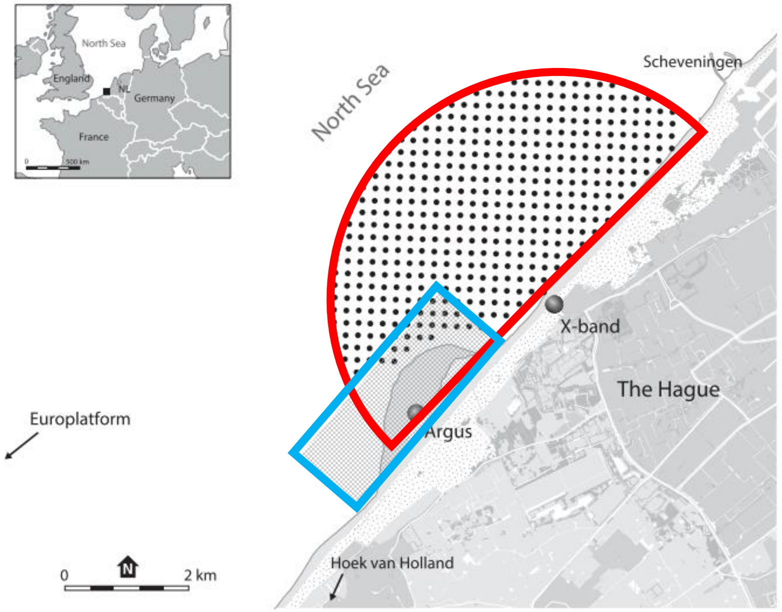

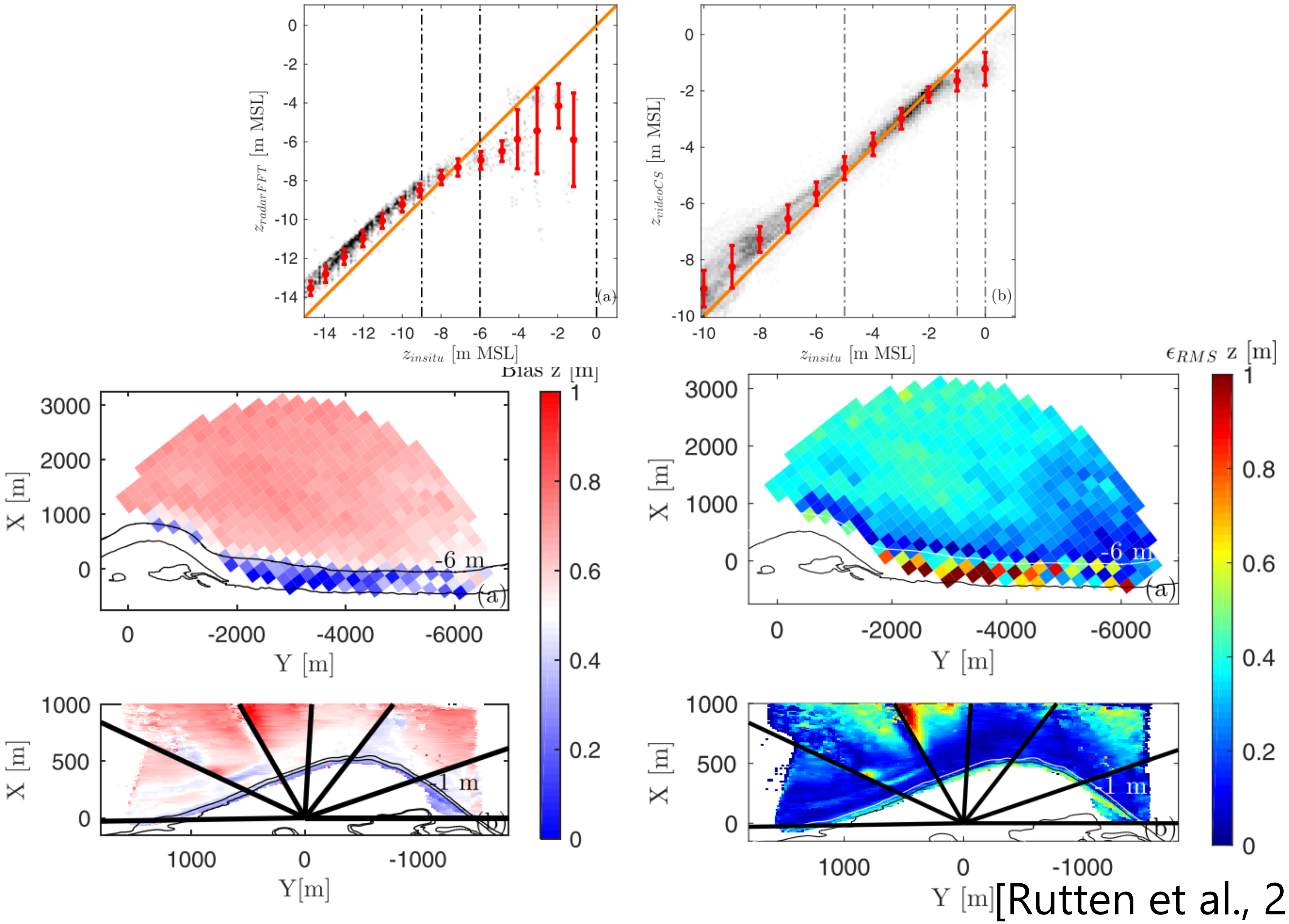

[Rutten et al., 2017]

Aim

→ Investigate nearshore wave processes by combining remote sensing, in-situ data and numerical modelling. [D3.1, D2.6]

→ Efforts on better understanding of wave propogation impacts on the coastal resilience. [D3.1, D2.6]

→ Investigate other indicators for coastal resilience and develop an analytical, quick, approach. [D3.1]

→ Test the approach for selected Eueopean beaches by using numerical models and available data. [D3.6]

→ Forecast the coastal resilience by accounting for SLR. [D3.6]

Methodology and Preliminary Analyses

→ Study site

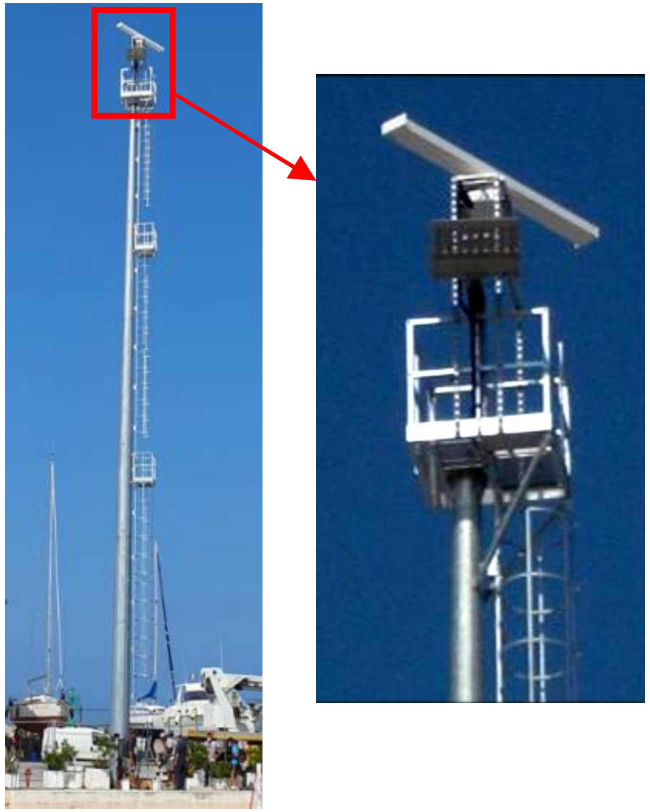

X-Band Radar System
REMOCEAN

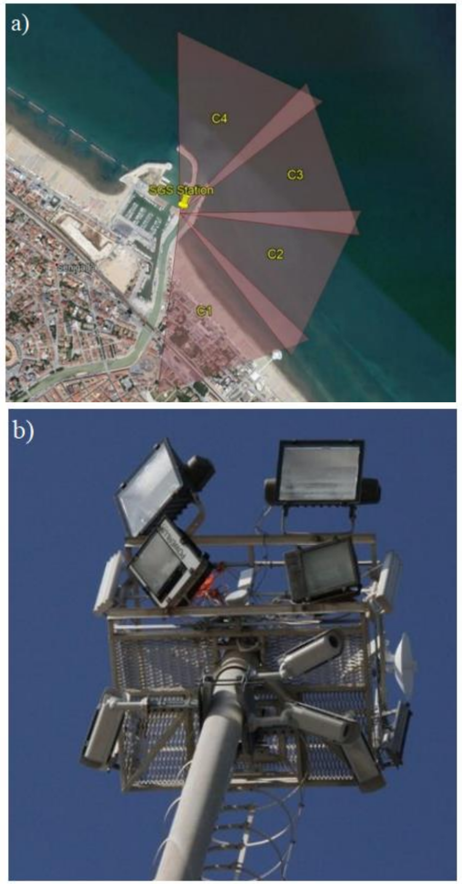

SGS Video
Monitoring System

Methodology and Preliminary Analyses

→ Processing data obtained from remote sensing tools.
- REMOCEAN

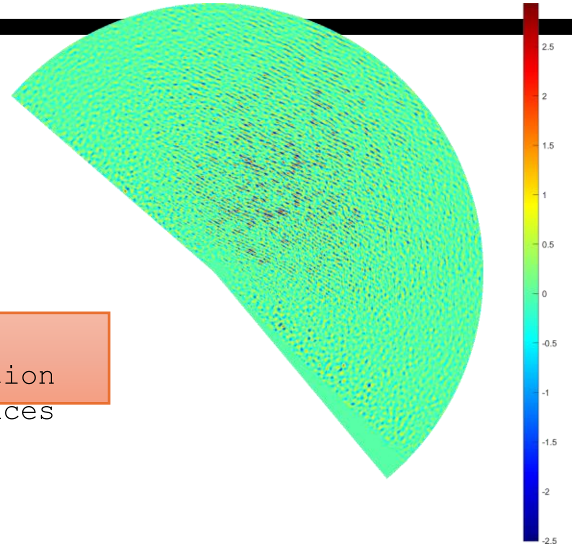

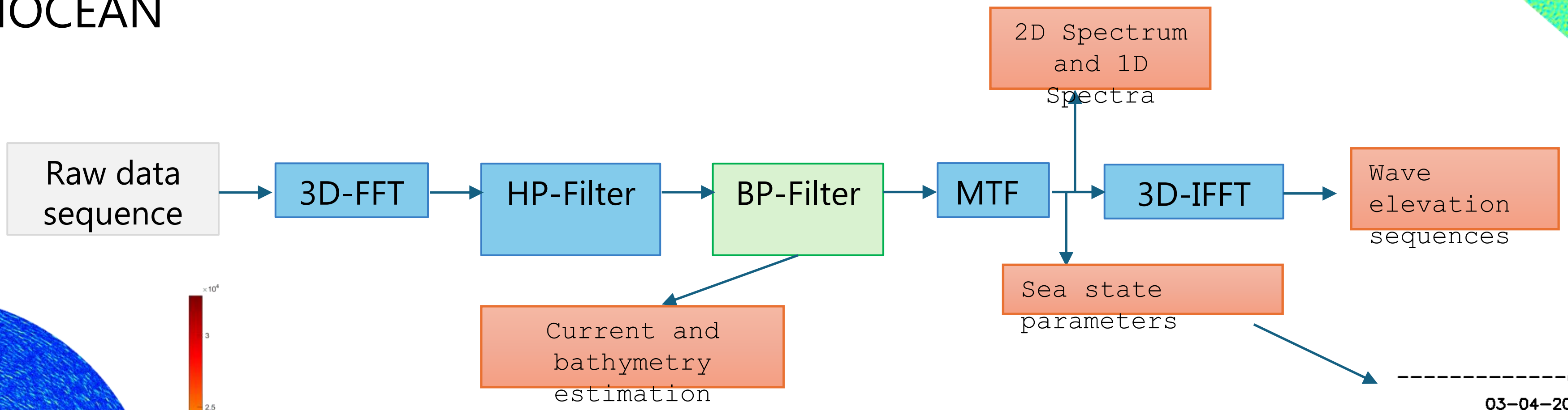

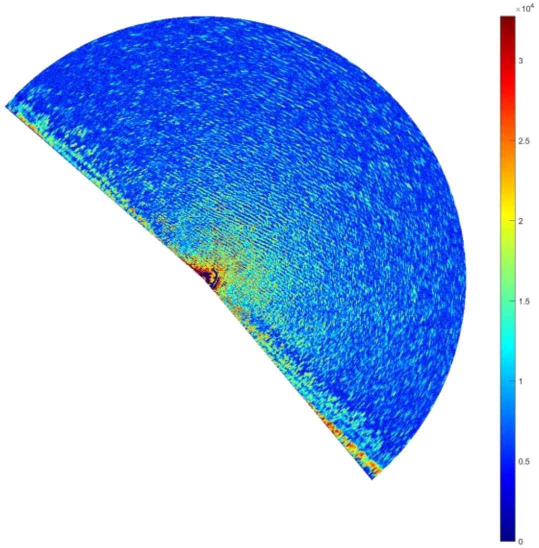

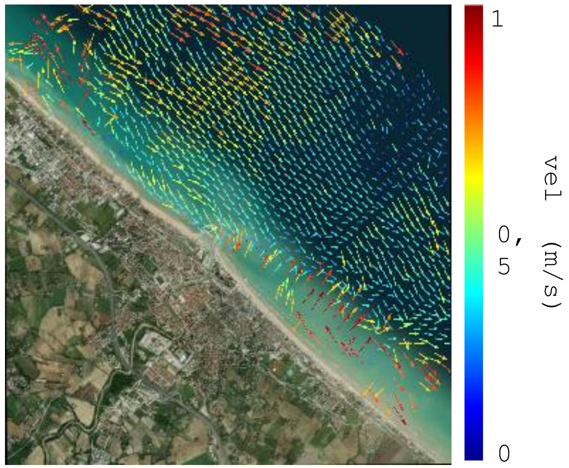

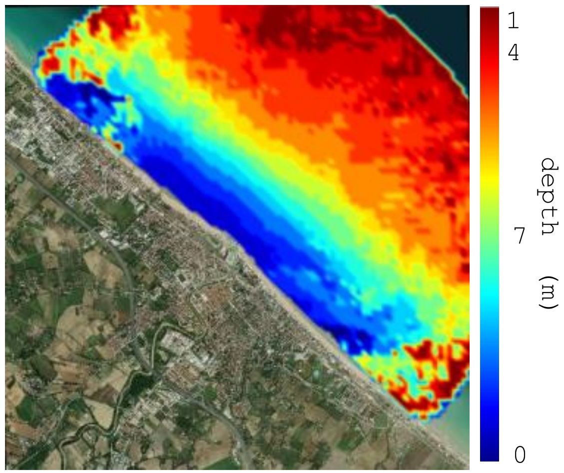

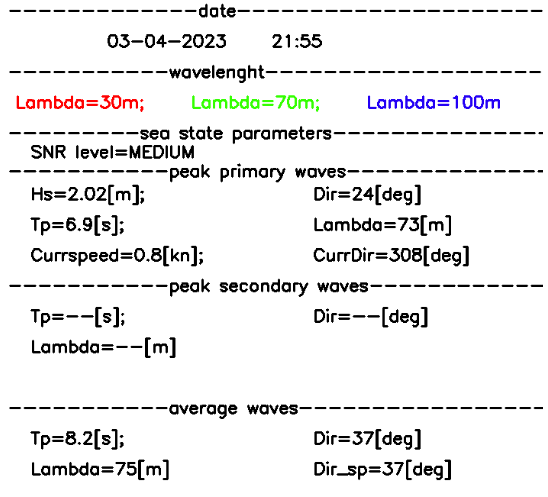

[Serafino et al., 2012]

Methodology and Preliminary Analyses

→ Processing data obtained from remote sensing tools.
- REMOCEAN

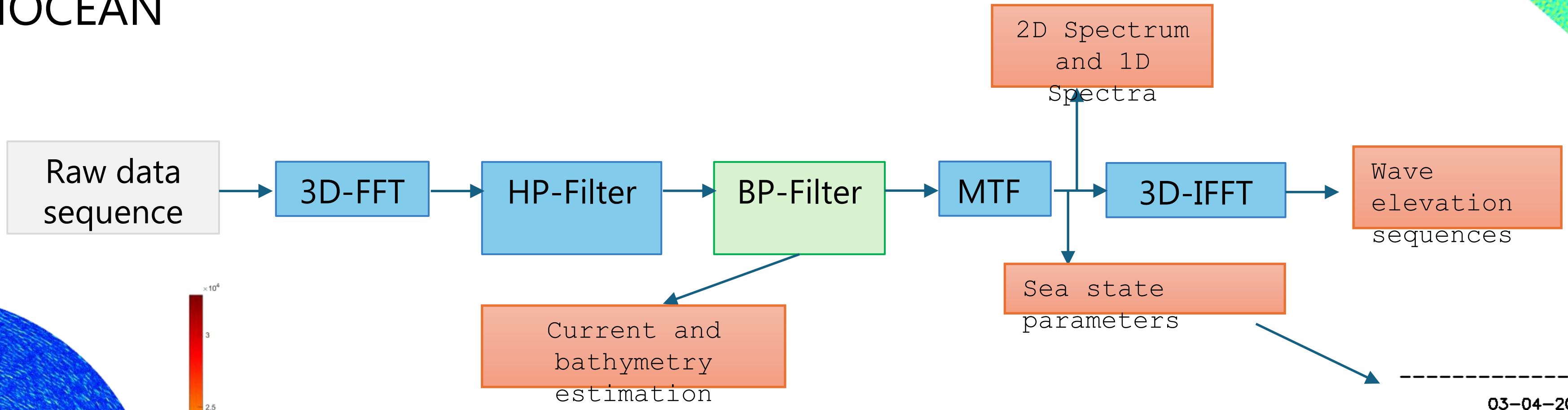

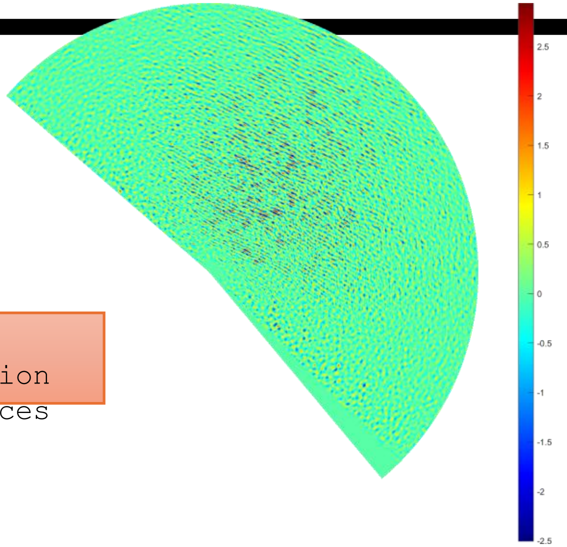

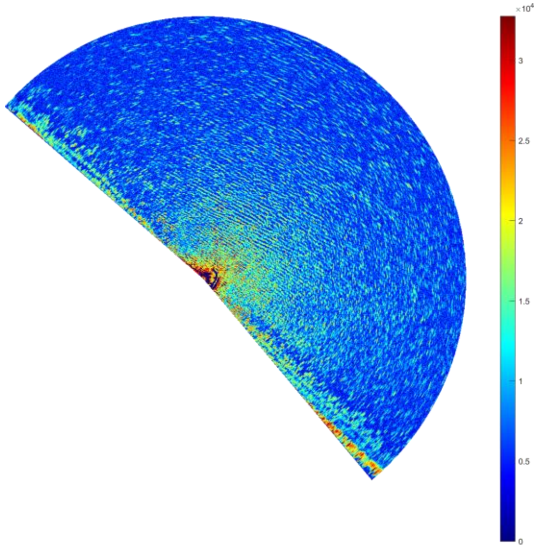

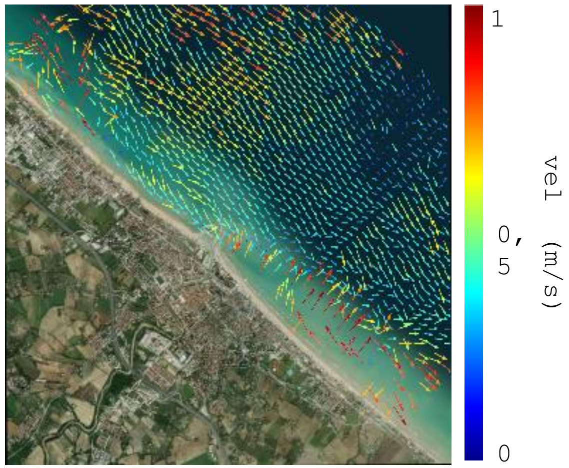

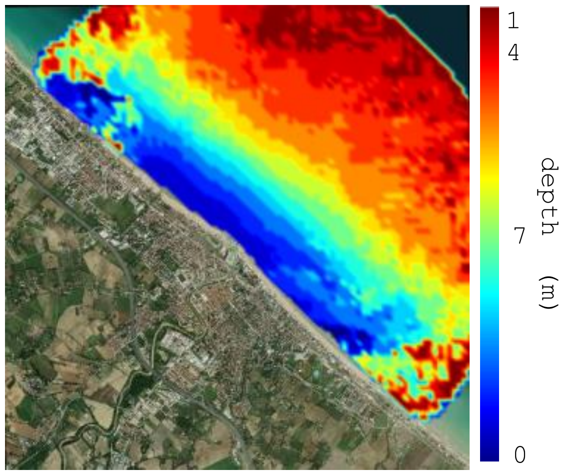

--------------date--------------------
03-04-2023 21:55
------------wavelenght--------------------
Lambda=30m; Lambda=70m; Lambda=100m
----------sea state parameters---------------
SNR level=MEDIUM
------------peak primary waves--------------
Hs=2.02[m]; Dir=24[deg]
Tp=6.9[s]; Lambda=73[m]
Currspeed=0.8[kn]; CurrDir=308[deg]
------------peak secondary waves-------------
Tp=--[s]; Dir=--[deg]
Lambda=--[m]

------------average waves------------------
Tp=8.2[s]; Dir=37[deg]
Lambda=75[m] Dir_sp=37[deg]

single value for whole domain

[Serafino et al., 2012]

Methodology and Preliminary Analyses

→ Processing data obtained from remote sensing tools.
  - Efforts to resolve spatiotemporal wave processes

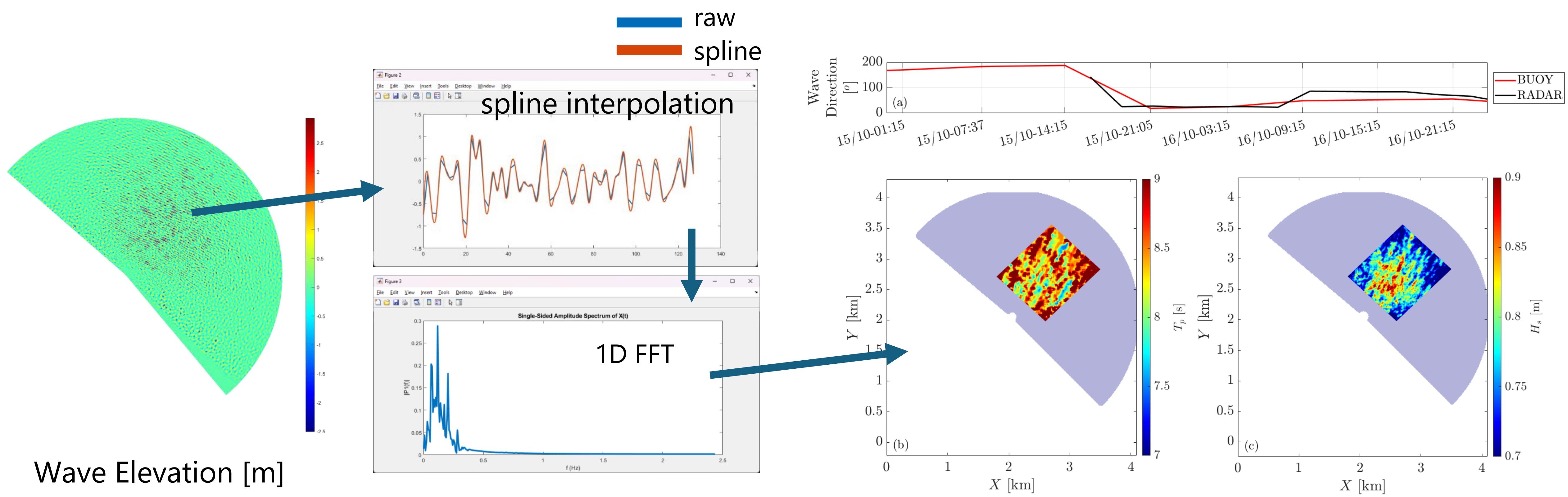

Methodology and Preliminary Analyses

→ Processing data obtained from remote sensing tools.
- Efforts to resolve spatiotemporal wave processes

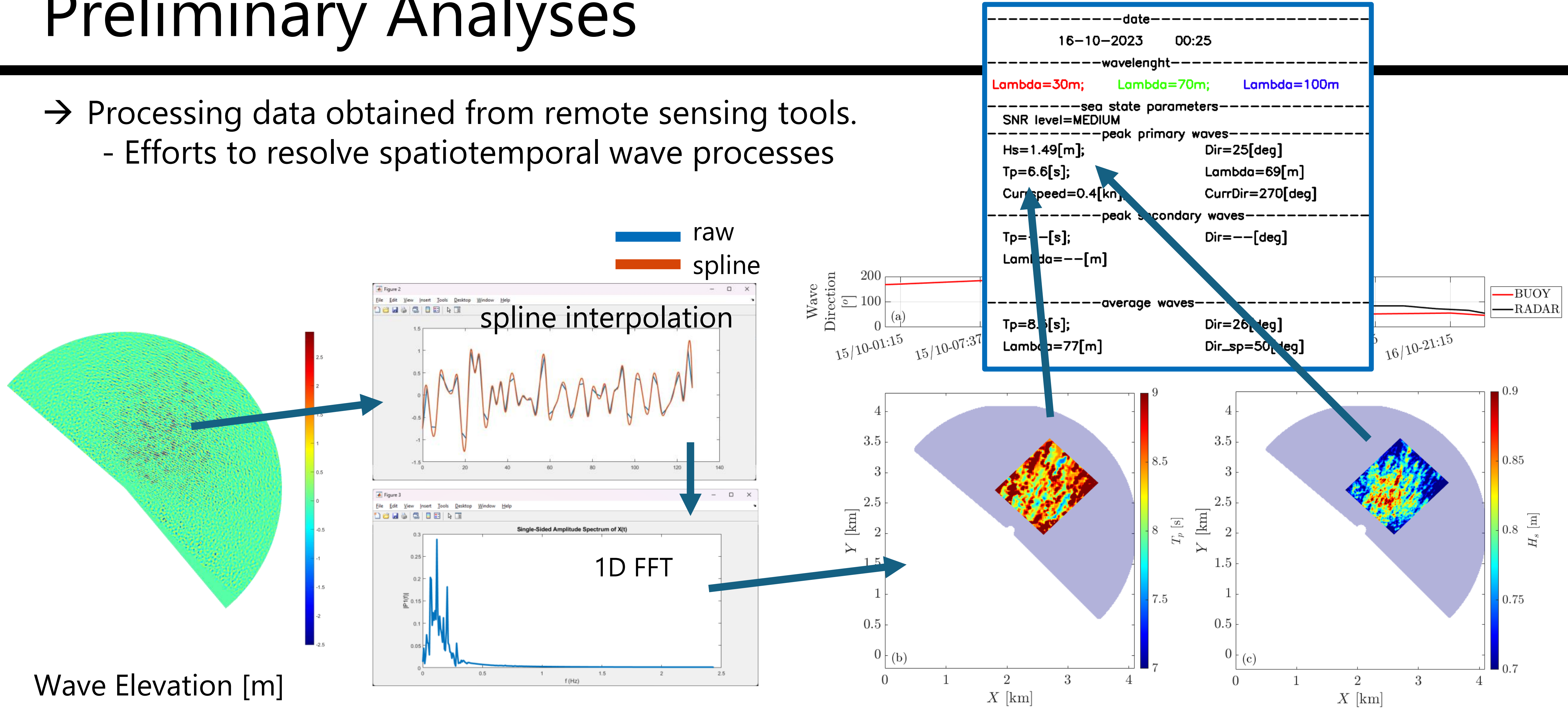

Methodology and Preliminary Analyses

→ Processing data obtained from remote sensing tools.
- cBathy

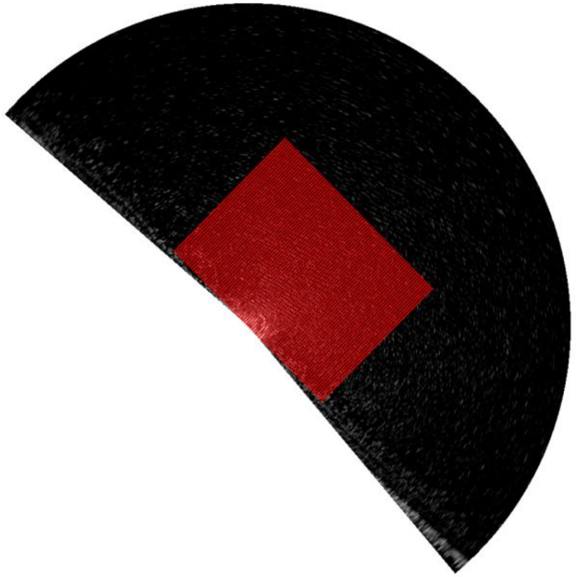

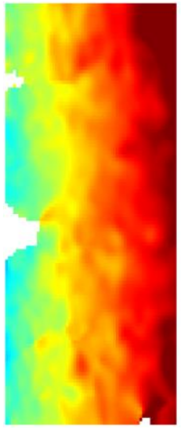

cBathy

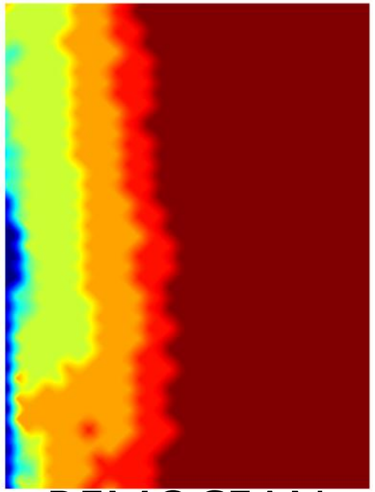

REMOCEAN

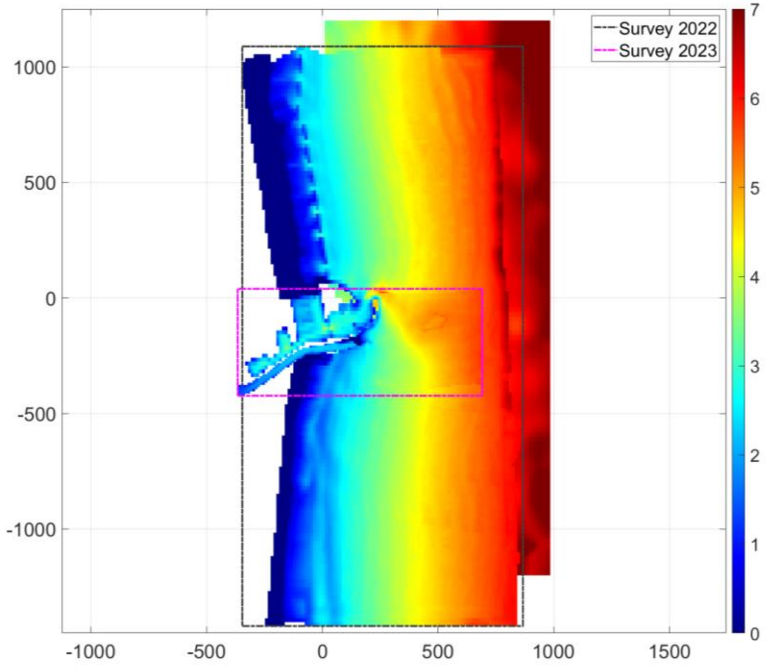

[16.10.2023-00:25]

Methodology and Preliminary Analyses

→ Processing data obtained from remote sensing tools.

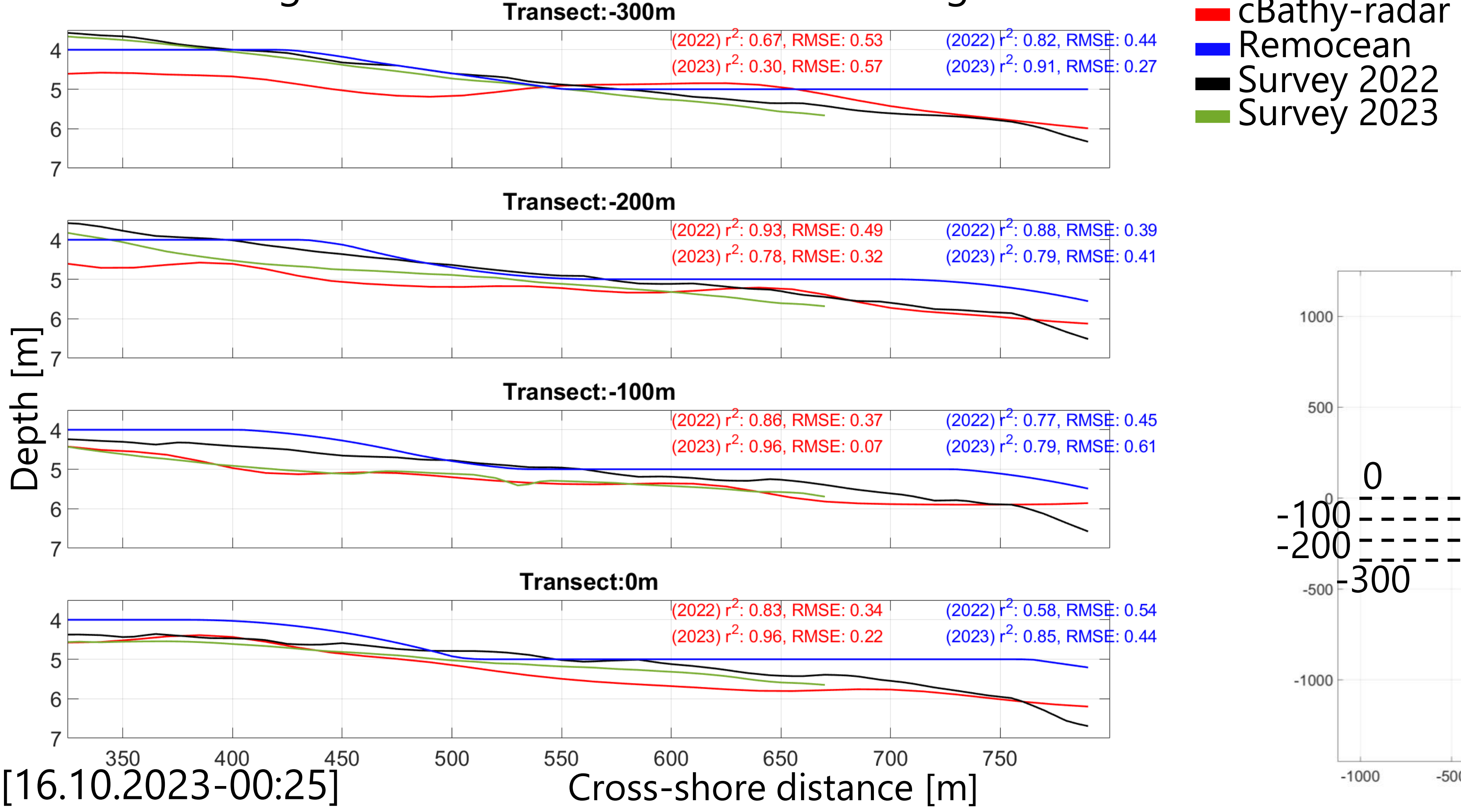

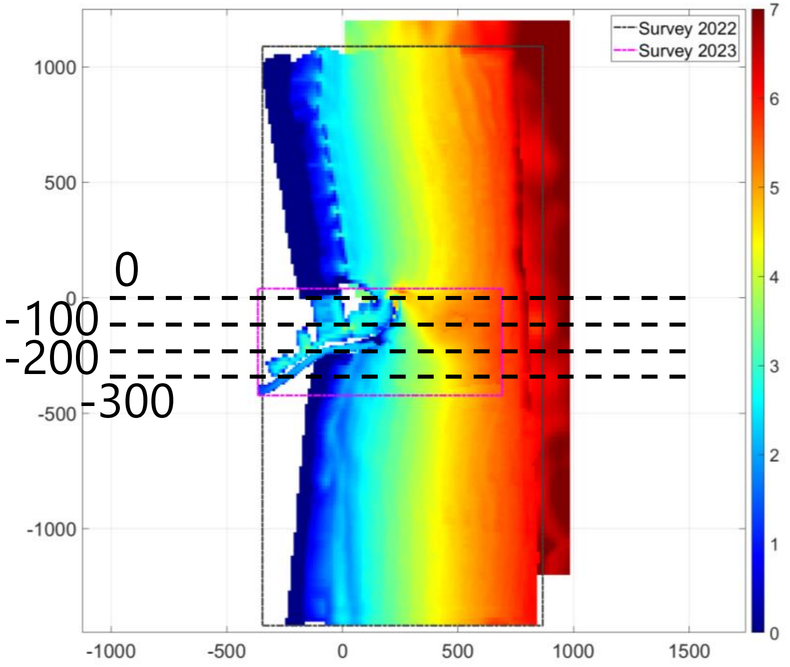

[16.10.2023-00:25]

Methodology and Preliminary Analyses

→ Efforts to resolve spatiotemporal wave processes (cBathy)

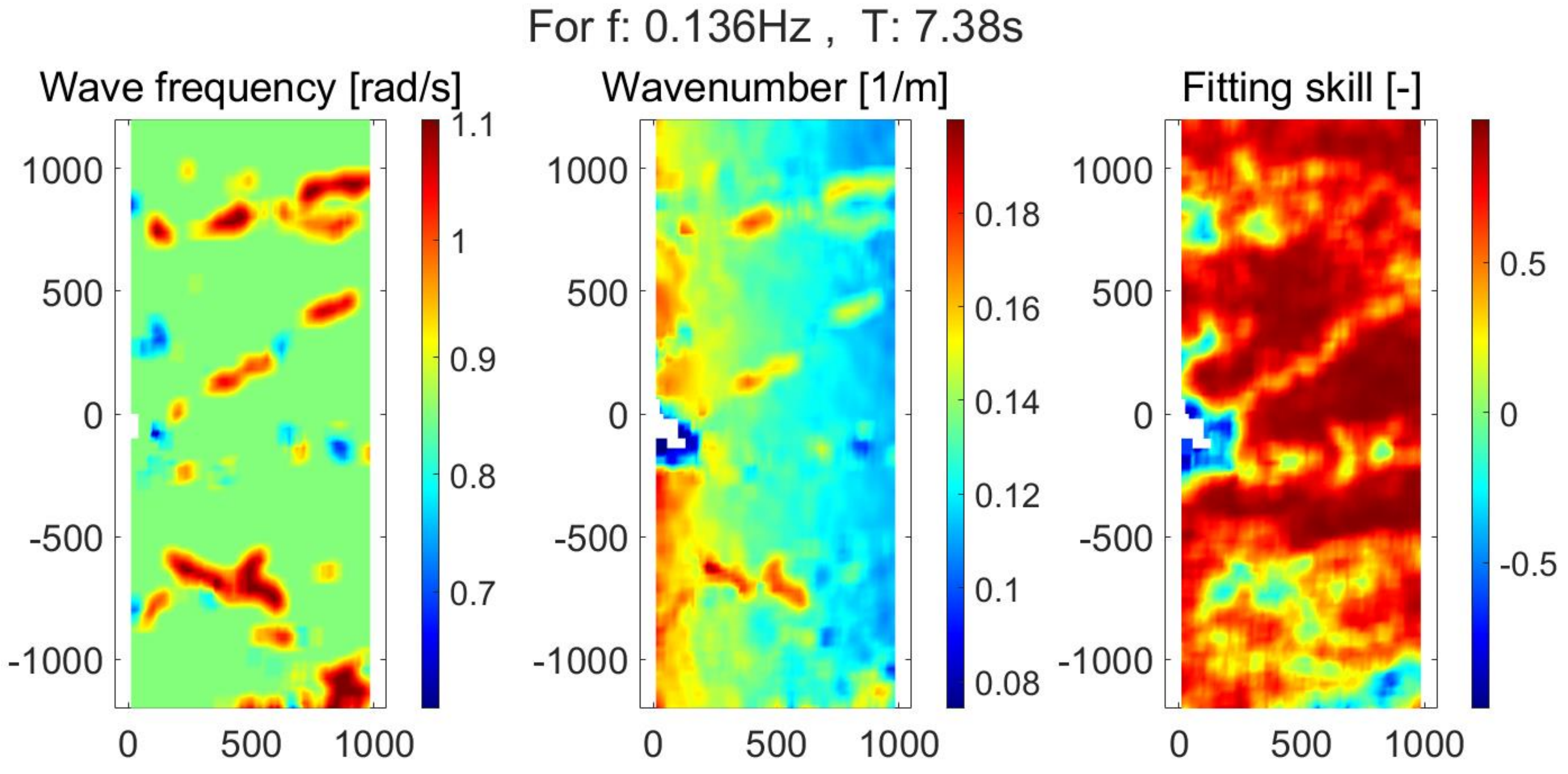

[16.10.2023-00:25]

Methodology and Preliminary Analyses

→ Efforts to resolve spatiotemporal wave processes (cBathy)

→ Approximation of wave height from amplitude dispersion

$$c = \sqrt{g(d + \alpha_{ad} H)}, \qquad d = \frac{H}{\gamma},$$

→ α_{ad}: calibration coefficient to what extent amplitude dispersion is considered (α_{ad}=0 → shallow, α_{ad}=1 → solitary).

→ γ: breaker parameter

$$H = \frac{c^2}{g\left(\frac{1}{\gamma} + \alpha_{ad}\right)}, \qquad c = \frac{\omega}{\kappa}$$

$H_p = \sim 1.6 - 2.0 * H_s$ [Goda, 2000]

[Stresser et al. 2022]

Methodology and Preliminary Analyses

→ Efforts to resolve spatiotemporal wave processes (cBathy)

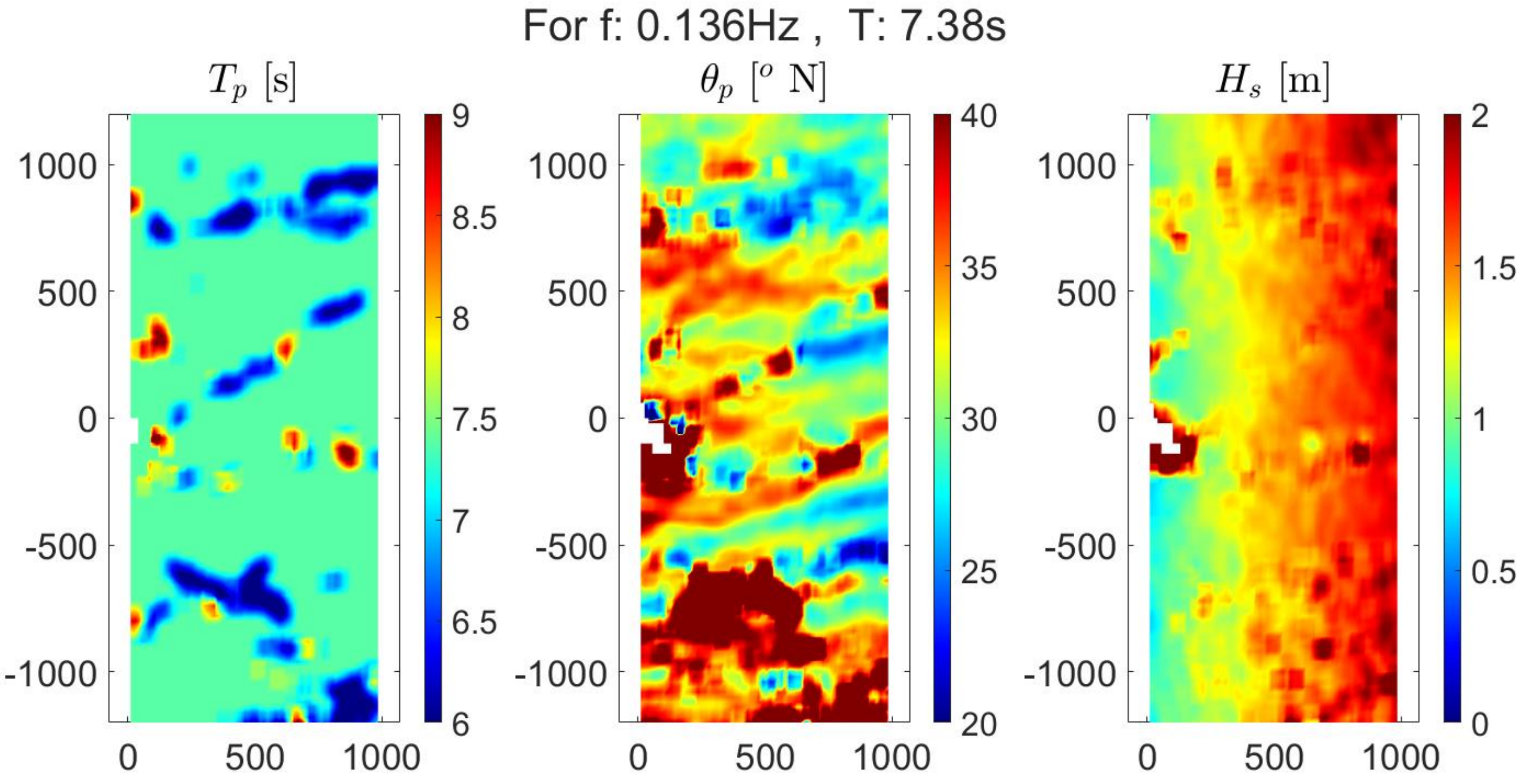

[16.10.2023-00:25]

Methodology and Preliminary Analyses

→ Efforts to resolve spatiotemporal wave processes (cBathy)
- Comparison with available data

Model → 5-6 m

Buoy → 70 m

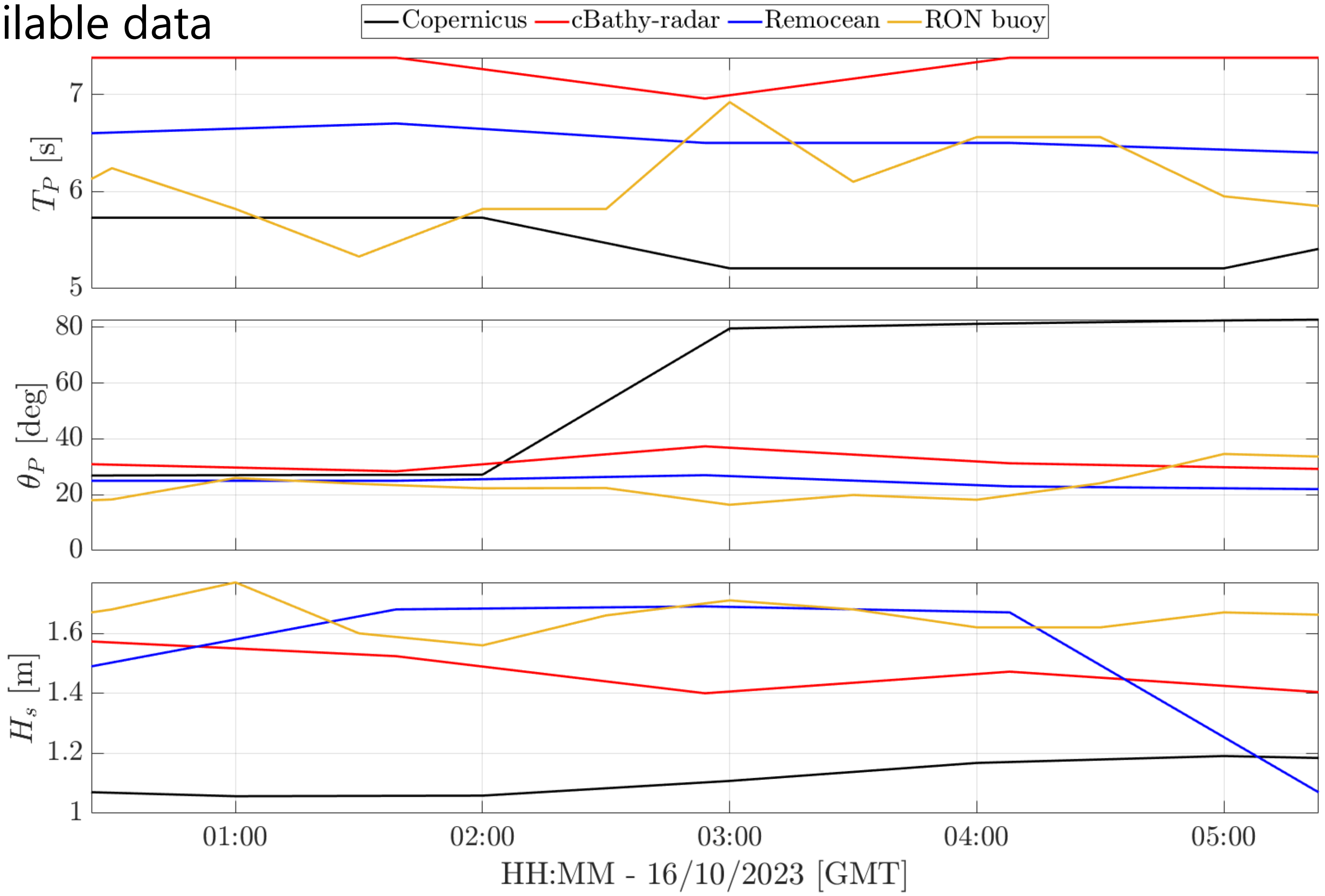

Ongoing Studies

→ Improving skill of the cBathy

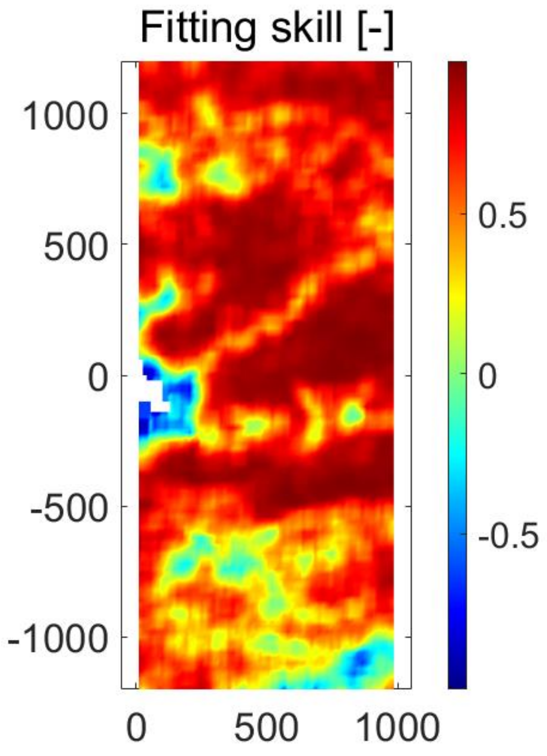

Ongoing Studies

→ Improving skill of the cBathy

- Increasing the recording number

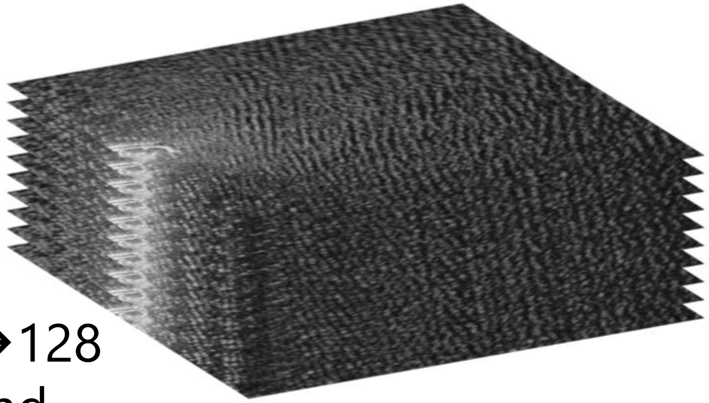

63→128
and
more

Ongoing Studies

→ Improving skill of the cBathy
- Increasing the recording number
- Apply phase correction

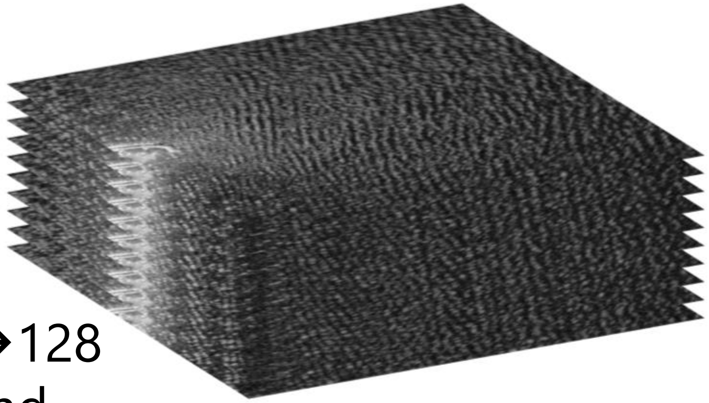

63→128
and
more

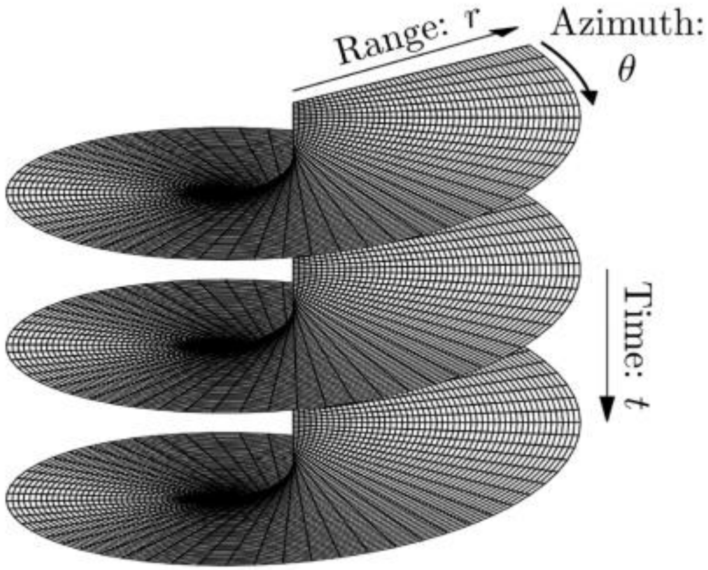

Ongoing Studies

→ Improving skill of the cBathy
- Increasing the recording number
- Apply phase correction
- Combine with camera system (wave characteristics and breaking analyses)

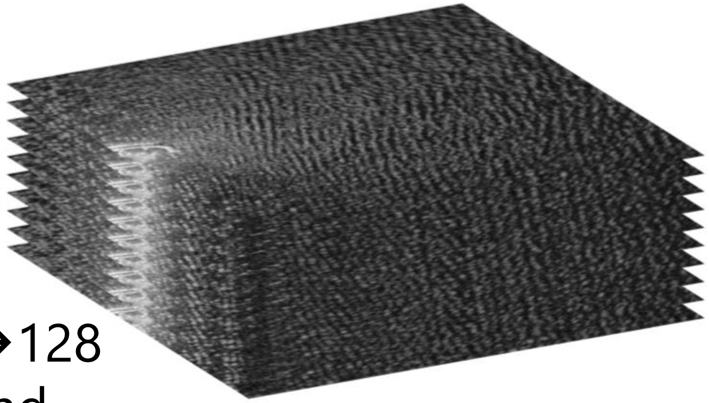

63→128 and more

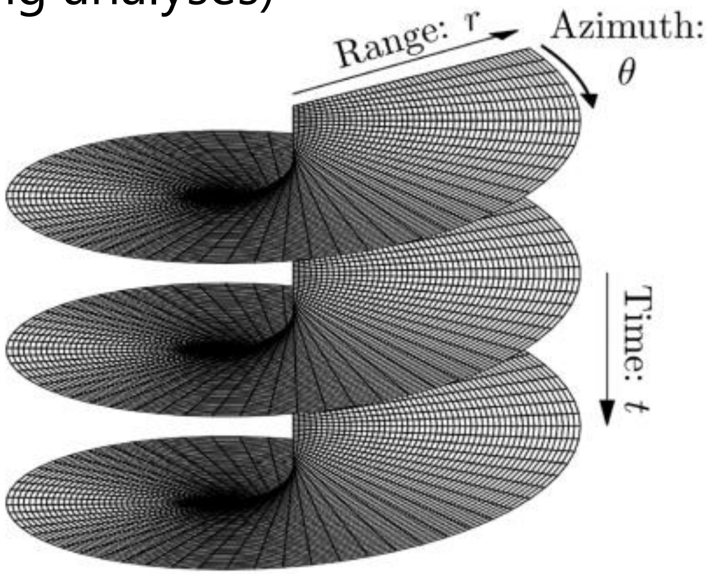

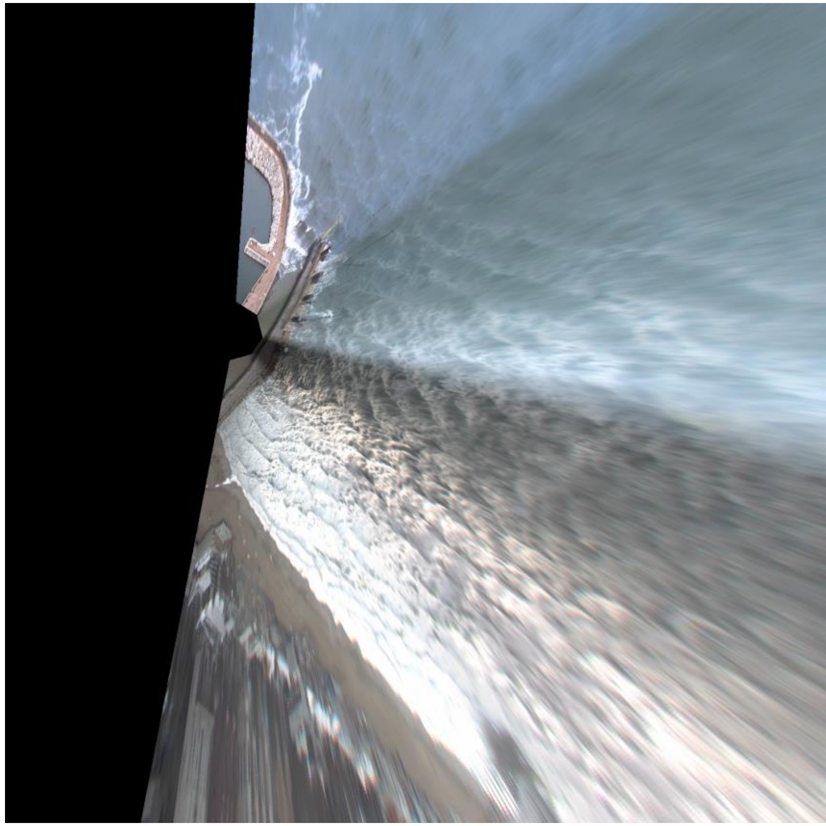

SEDIMARE DC MEETING

22.04.2024-24.04.2024

Nottingham, the UK

THANKS

UNIVERSITY OF TWENTE.

SEDIMARE 2023 - 2027

Sediment Transport and Morphodynamics in Marine and Coastal Waters with Engineering Solutions

EROSION AND TRANSPORT OF SAND-SILT MIXTURES

Nottingham Meeting

INTRODUCTION OF DC #3 IN SEDIMARE PROJECT

PhD Candidate: Nguyen, Thi To Van (Van)
Promotor: P.C. Roos (Pieter)
Co-promotor: J.J. van der Werf (Jebbe)

Date: 2024 Apr 22nd

INTRODUCTION

Research background

2015 – 2019

- **Bachelor program**

2020 – 2022

- **Master program**

2023 – 2027

- **PhD program**

Taking bachelor degree at the ***Oceanology Department***, **University of Science, HCMC, Vietnam**.

Master trainning at **COAST** (***Coastal Ocean And Sediment Transport***) research group, **National Central University, Taiwan**.

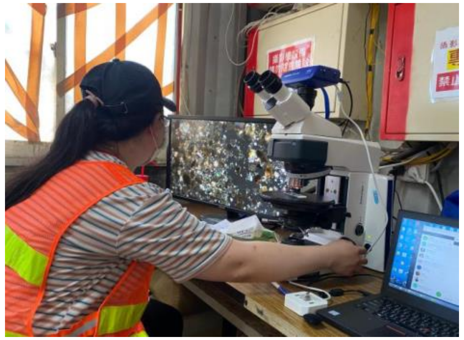

國立中央大學
National Central University

UNIVERSITY OF TWENTE.

Studying the PhD program in the **University of Twente, Netherlands**. I am working on the SEDIMARE project under supervision of ***Dr. ir. Jebbe van der Werf*** and ***Dr. ir. Pieter Roos***.

The interdisciplinary training of 12 Doctoral Candidates (DC) in coastal processes and engineering, aiming towards a sustainable coastal use and protection.

SEDIMARE 2023 - 2027

Sediment Transport and Morphodynamics in Marine and Coastal Waters with Engineering Solutions

SEDIMARE #3:
Erosion and transport of sand-silt mixtures.

SEDIMARE #7 (Jowi Miranda)

Practical morphological modelling of sand-mud mixtures

Collecting dataset of erosion and transport of sand-silt mixtures from laboratory experiments

→ Observe, identify and quantify the influence of silt on the erosion and transport of sand-silt mixtures.

→ Obtained knowledge will be translated into empirical models which can be easily be implemented in modeling (e.g. Delft3D and Xbeach)

SEDIMARE #3 PROJECT

Current progress

Natural sediments primarily exist in mixtures of sand (63 µm ≤ *D* < 2,000 µm) and fine sediments (*D* < 63 µm). These fine sediments are usually collectively called mud, and consist of silt (4 µm ≤ *D* < 63 µm) and clay (*D* < 4 µm). Mixed sediments are prevalent in less dynamic systems (e.g. tidal basins, estuaries, rivers).

Mangrove forest with silty sediments in Mekong Delta (Vietnam)
[Photo by ManqLub project]

Silt in the Tamar River, Tasmania, Australia.
[Photo by ABC Northern Tasmania: Craig Heerey]

Western Scheldt (river), Netherlands
Photo by MUSA 1 project]

SEDIMARE #3 PROJECT

Current progress

Recently, there have been more studies focusing on the transport of mixed sediment. However, most of these studies treated clay and silt collectively as mud (*Mitchener and Torfs, 1996; Van Ledden, 2003; Jacobs, 2011; Winterwerp et al., 2012; Colina Alonso et al., 2023*). This is despite the fact that clay and silt are different in properties and behaviors and there are also many notable silt-dominated systems. **We still lack a thorough understanding of the role of silt in the erosion of sand-silt mixtures.**

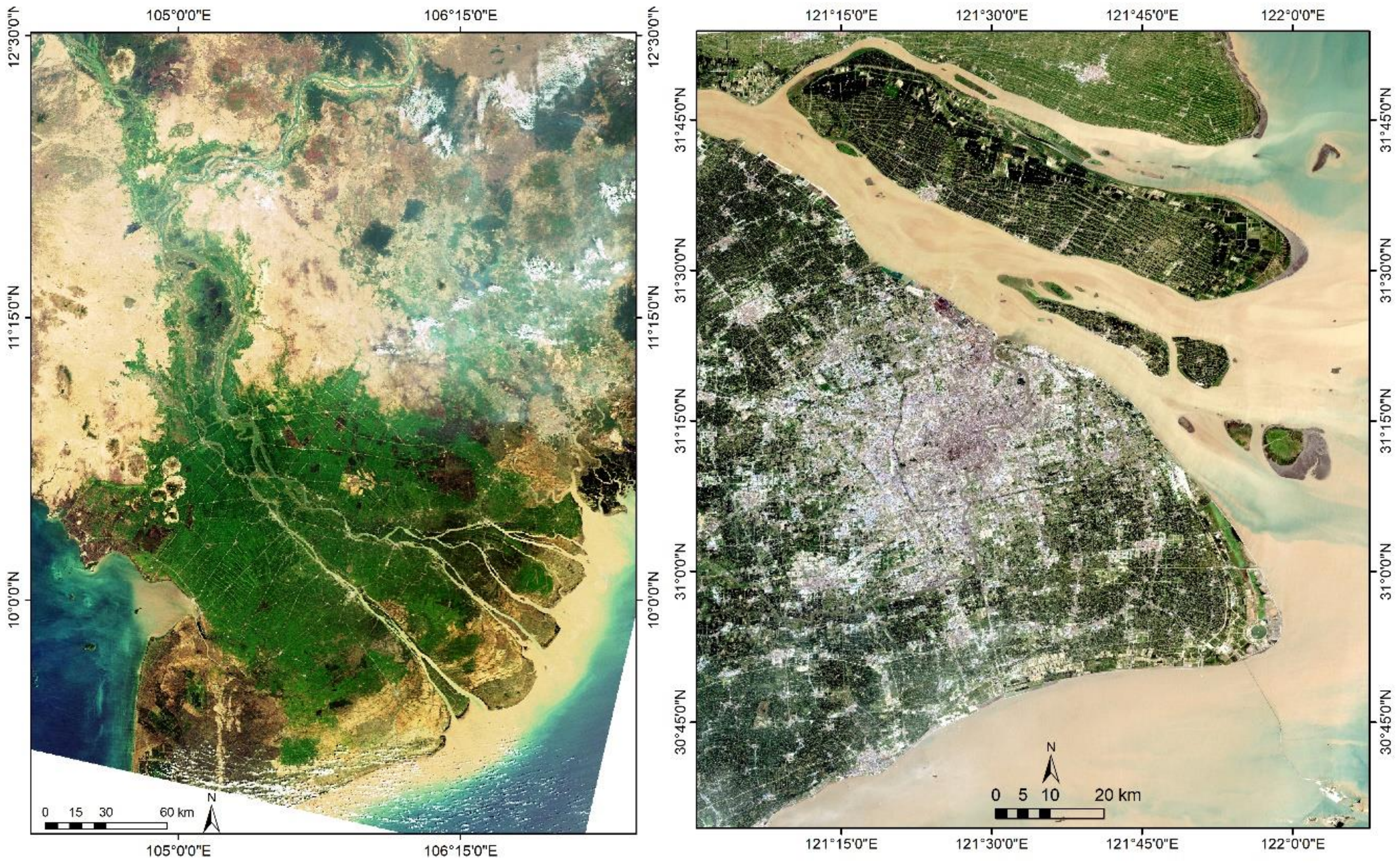

Figure 1. Satellite images of the Mekong Delta (a) taken by Envisat and the Yangtze Delta (b) taken by Shanghai Landsat 7, respectively.

OBJECTIVE OF OUR PROJECT:

Collecting dataset of erosion and transport of sand-silt mixtures from **laboratory experiments.**

→ Observe, identify and quantify the influence of silt on the erosion and transport of sand-silt mixtures.

→ Obtained knowledge will be translated into empirical models which can be easily be implemented in modeling (e.g. Delft3D and Xbeach)

The **laboratory experiments** will be carried out at the **University of Aberdeen (UK)** in collaboration with Dr. ir. Dominic van der A and Prof. Dr. Thomas O'Donoghue.

Main experiment

(10 m long, 0.75 m high and 0.3 m wide)

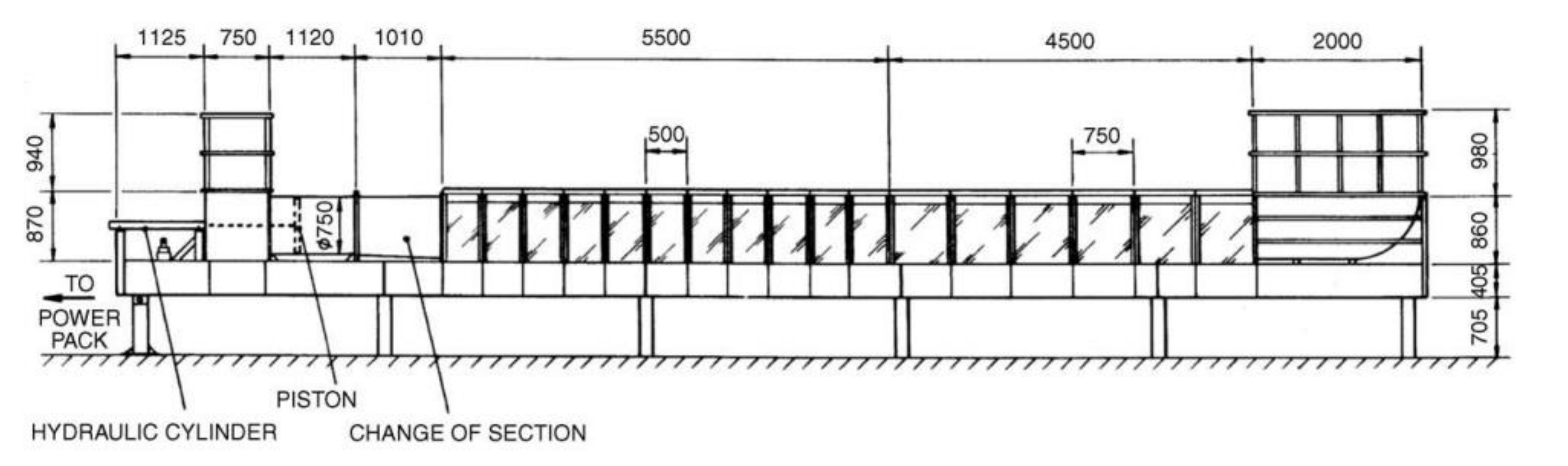

The Aberdeen oscillatory flow tunnel (**AOFT**) at the University of Aberdeen (van der Werf et al., 2006)

Current progress

Before conducting the main experiments in AOFT, we will carry out a preparatory experiment in the small-scale oscillatory tunnel, also known as the **Aberdeen Mini Tunnel** (AMT).

Observations, results, and experiences obtained from the preparatory experiments will inform the conditions, bed configurations and procedures of the main AOFT experiments.

Preparatory experiment

The Aberdeen Mini Tunnel (AMT) at the University of Aberdeen.

SEDIMARE #3 PROJECT

Current progress

September 2023

- Collected literature on dynamics of mixed sediments.
- Explored and found opportunities to collaborate with other institutions on laboratory experiments.
- Took background/skill courses and served as a teaching assistant at UT.

January 2024

- Summarized and wrote literature review.
- Prepared and wrote plans for preparatory experiments in Aberdeen.
- Wrote research proposal.

April

- Working on preparatory experiments in Aberdeen.

May

- Finishing preparatory experiments.
- 17th May: Qualified exam

Research timeline

Task	Year 1				Year 2				Year 3				Year 4			
Literature review																
Research proposal																
Preparatory experiments																
Qualifier			Q													
Main experiments																
Data analysis for erosion of sand-silt mixtures (RQ1)																
Writing paper 1									P1							
Data analysis for transport of sand-silt mixtures (RQ2)																
Writing paper 2											P2					
Data analysis to improve empirical formulas (RQ3)																
Writing paper 3													P3			
Writing dissertation																
Submit & Defense																D


THANK YOU FOR YOUR ATTENTION

UNIVERSITÀ POLITECNICA DELLE MARCHE

Nasim Soori

Supervisors:
Prof. Maurizio Brocchini – UNIVPM
Prof. Athanassios Dimas – UPATRAS
Prof. Matteo Postacchini – UNIVPM

DC 4: Mixing and transport in the coastal area

22 Apr., 2024

- The focus of this research project is the **development of a 2D numerical solver** for the hydro-morphodynamics in the nearshore area to extract the Lagrangian motion/flow field, also with the support of UPATRAS (where a secondment period is planned).
- In my project, **to extract the Lagrangian motion and flow field**, the open solver **FUNWAVE-TVD** will be utilized. It uses a Total Variation Diminishing (**TVD**) scheme, which helps to maintain the accuracy and stability of the numerical solutions. **FUNWAVE-TVD** is an example of the recently improved models implementing a high-order adaptive time-stepping.
- I am working on simple cases on FUNWAVE TVD for my case study to analysis a simulation of nearshore processes and providing insights into wave-sediment interactions and their impact on nearshore morphology

- To gather data and validate numerical models for investigating the mixing and transport of particles due to different characteristics:

Numerical modeling	Real-world nearshore cases will be numerically modeled, where mixing easily occurs and significantly impacts on the transported particles (sediments or pollutants)
Laboratory experiments	Controlled experiments will be conducted to model physical processes occurring around breakwater and the motion of suspended particles for monitoring and analyzing
Field measurements	The video-monitoring system at the Misa River Estuary will be used to track surficial sediment transport and circulation patterns around existing coastal structures

Inrtoduction

- ❑ The **Sea of Marmara** is a permanently stratified water body:
  - *Differences in salinity* in the two large adjacent basins
  - *Stratified based on temperature*

✓ So, due to variations in salinity or temperature, **pycnocline** forms (sharp gradients in density).

- **Gemlik Bay** is an inlet of the Sea of Marmara, in the Marmara region of **Turkey**, which is located in the southwestern part of the sea of Marmara.

✓ Gemlik Bay is **open to the waves** coming from the band between northwest and southwest.

❑ Based on measurements in the Sea of Marmara, three **"warm and saline"** and **upwelling events** were observed **during autumn and winter** scientific expeditions.

➢ Using **Delft-3D**: circulation flow was simulated in Gemlik bay.

➢ Using **Delft-3D**: investigating how varying salinity and temperature over time and at different depths by consideration of Bosphorus trait entering the sea Marmara salinity flow from Agean Sea (Next step)

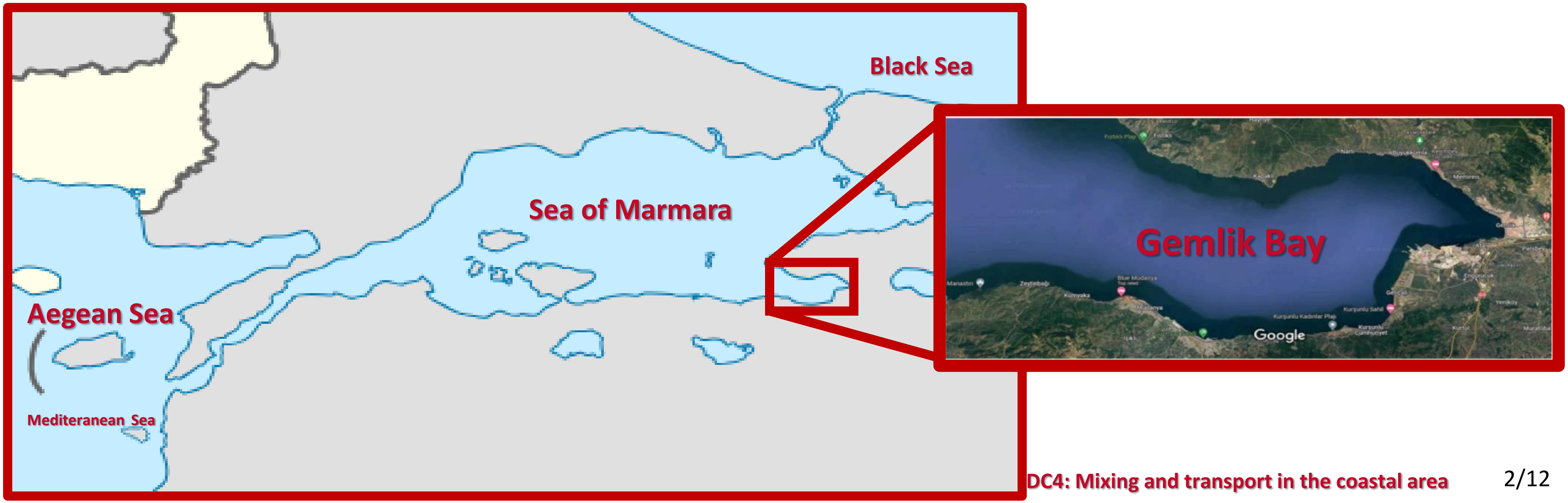

Numerical part: Delft-3D

- To investigate the flow circulation in Gemlik Bay, the hydrodynamic module, **Delft-3D- Flow**, was used.

➢ **Depth averaged velocity after 1, 3, 7 days:**

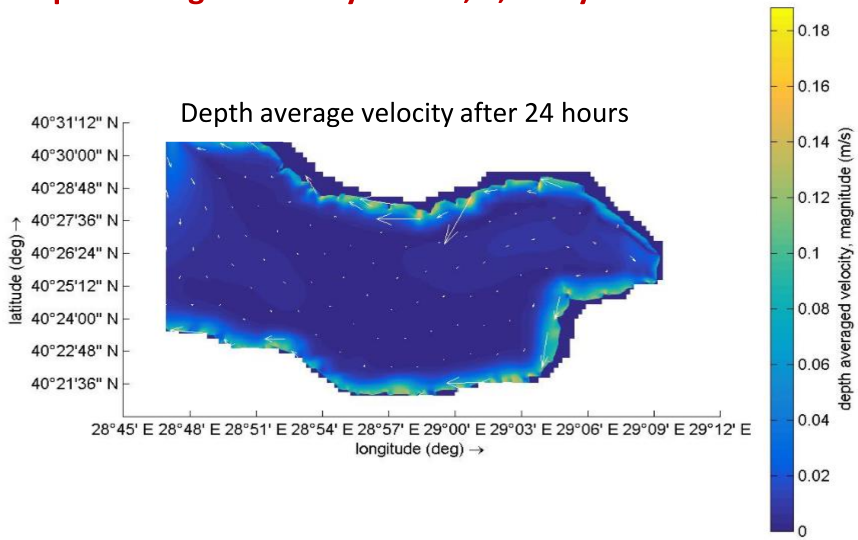

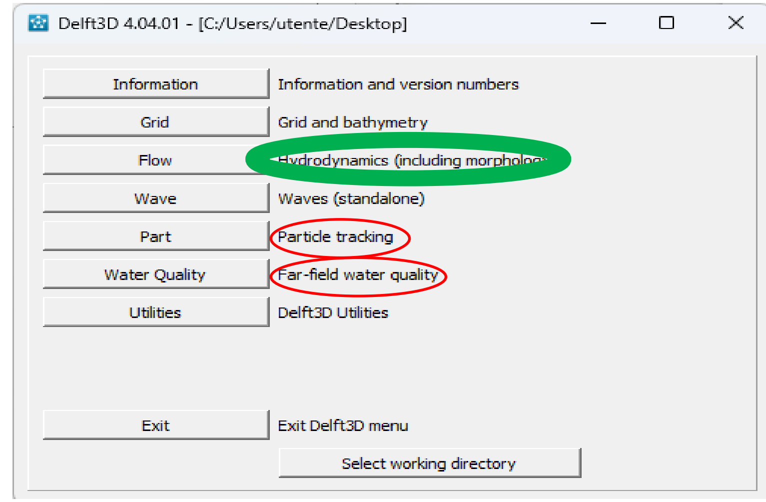

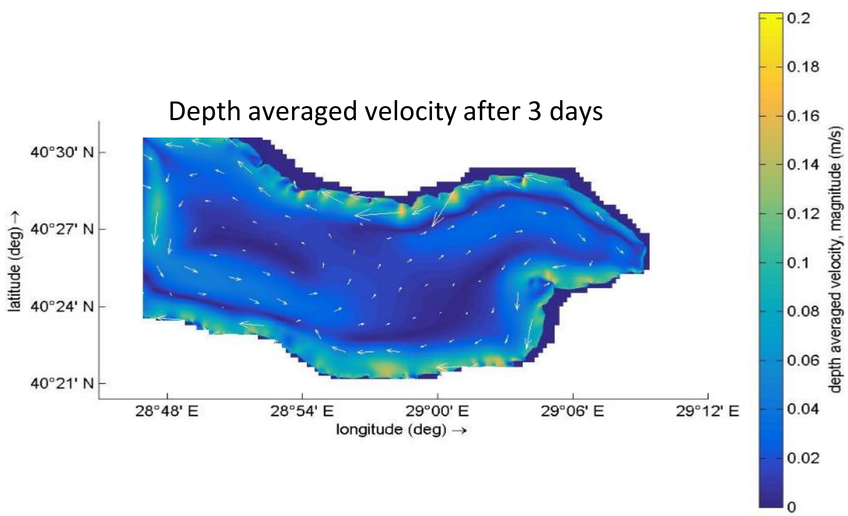

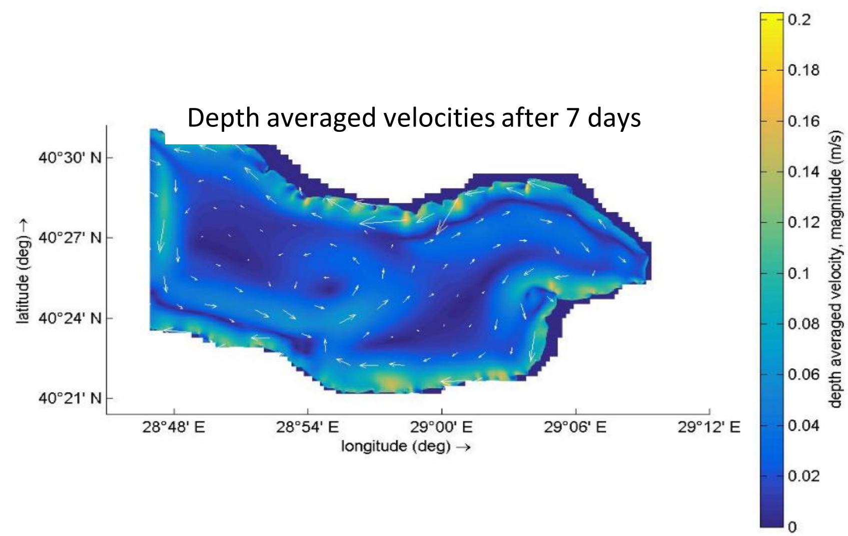

Numerical part: Delft-3D

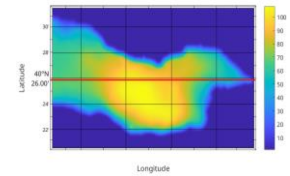

❑ Salinities profile:

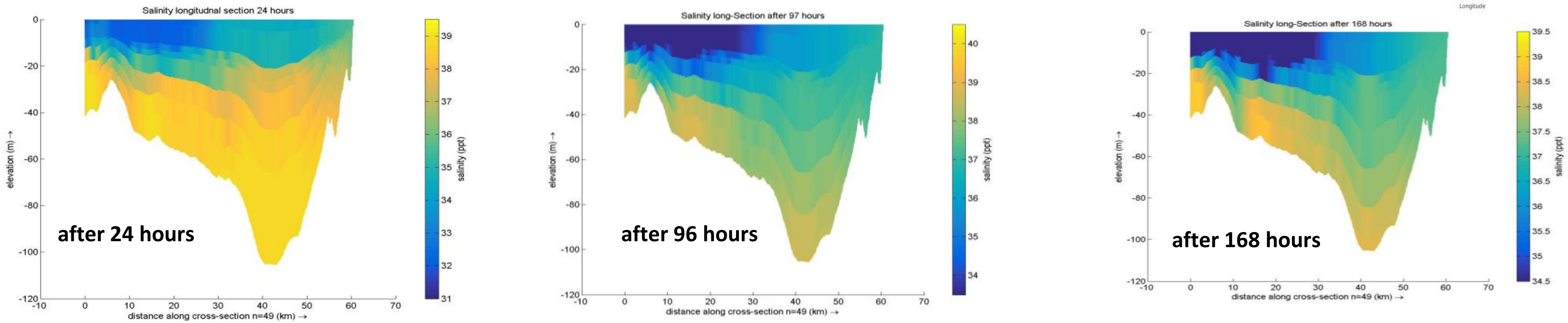

❑ Temperature profile:

after 24 hours

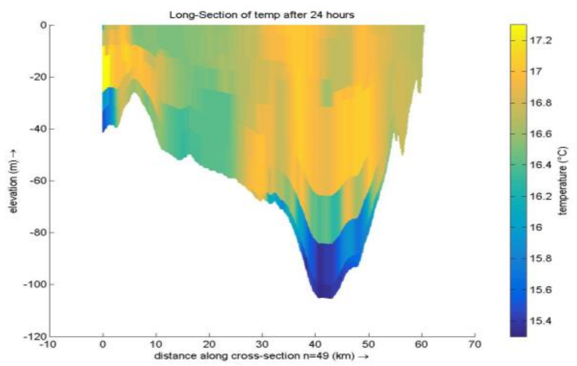

after 96 hours

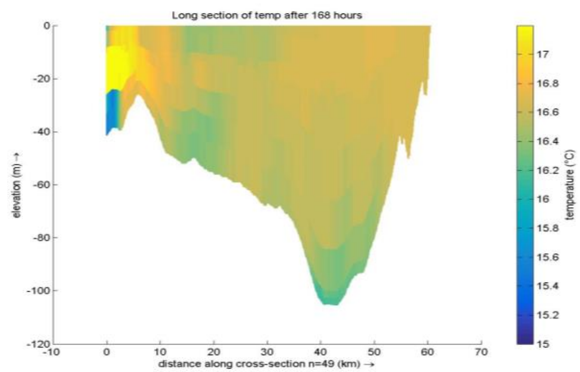

after 168 hours

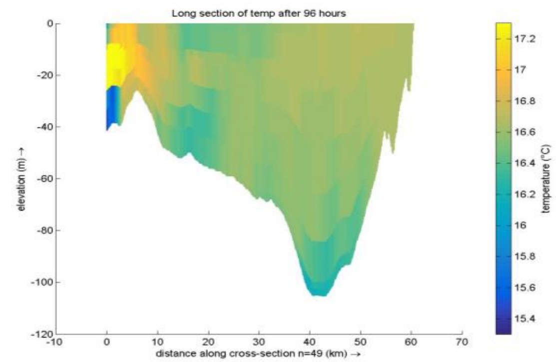

✓ From these figures, you can see non uniform profiles. After 24 hours of the simulation, it shows comparatively low values of the surface temperature.

Numerical part: Delft-3D

❑ Simulation for all region:

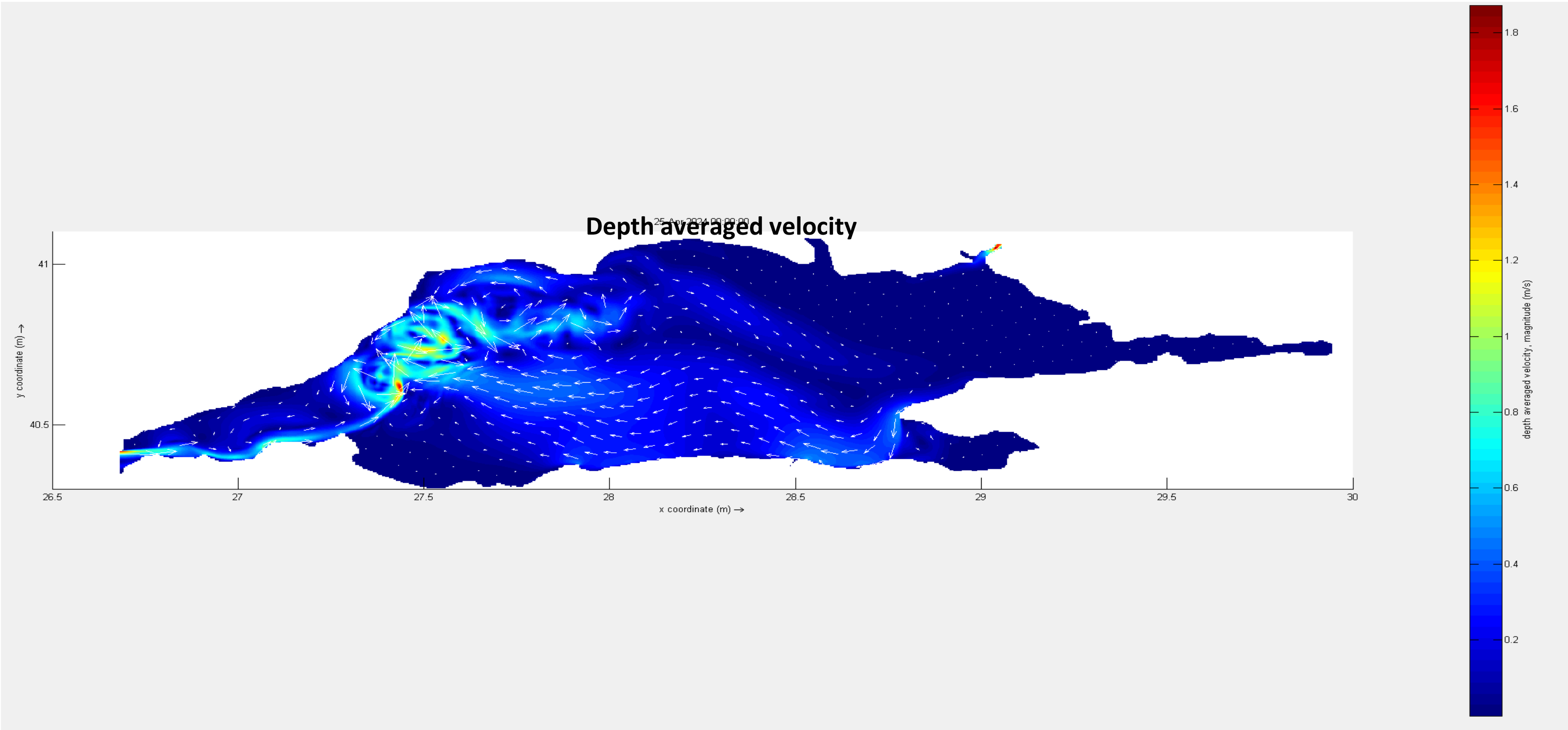

- **The Marmara Sea** plays **a crucial role** in the distribution of oxygen and water masses.
- **Mixing** due to atmospheric conditions and the jet stream from the Bosphorus and salinity flow from Mediterranean sea lead to an increase in the vertical mixing which readouts in the weakening of the stratification in Gemlik Bay.

Numerical part

- ❑Turbulence in the ocean directly controls transport and dispersion of materials in the ocean water.
- ➢ Many such materials directly affect human and ecosystem health and human activities (e.g. microplastic, oil and nutrients and phytoplankton), **making their mixing and transport mechanisms an important topic of investigation**.

❑ Coupling Delft3D- FLOW with CORMIX:

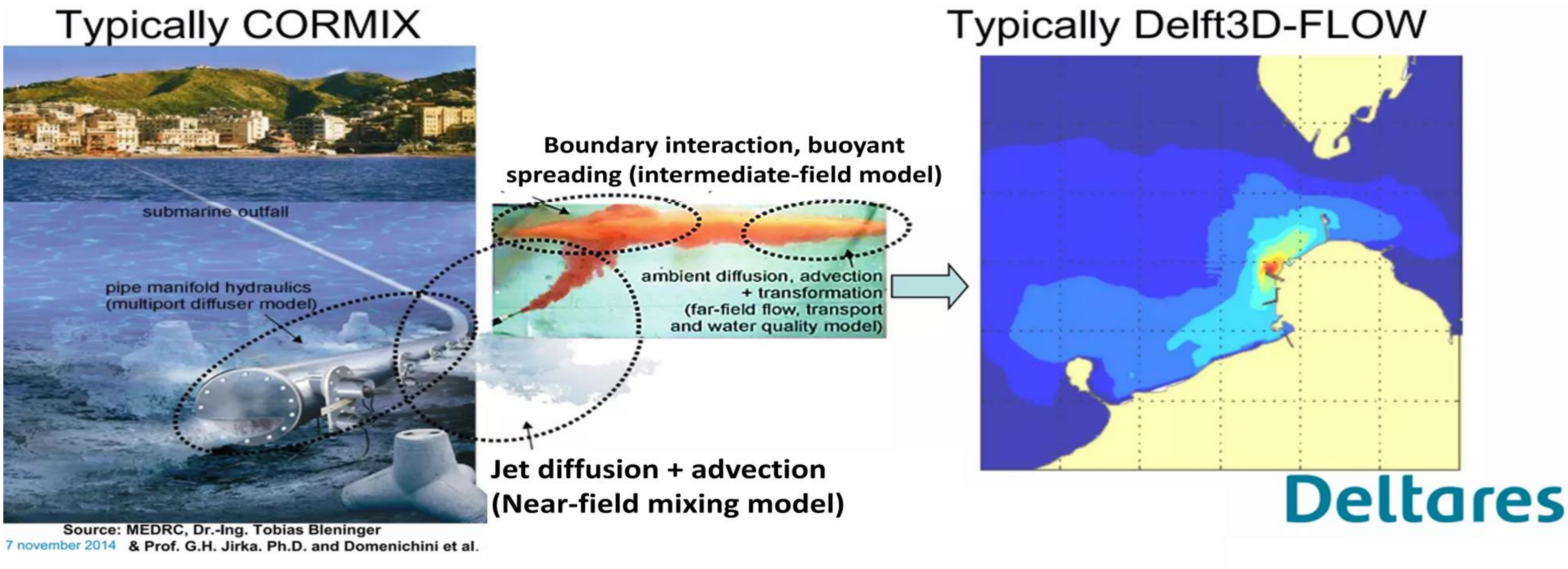

One of the challenges of current oceanic sciences research is **to understand and predict the vertical mixing and horizontal transport of properties** in the Ocean Surface.

Numerical part: CORMIX

❑ By coupling Delft3D- FLOW with CORMIX:

➢ **Coupling of near-field and far field models** is required to accurately and efficiently assess the characteristics of the outfall plume on all spatial scales.

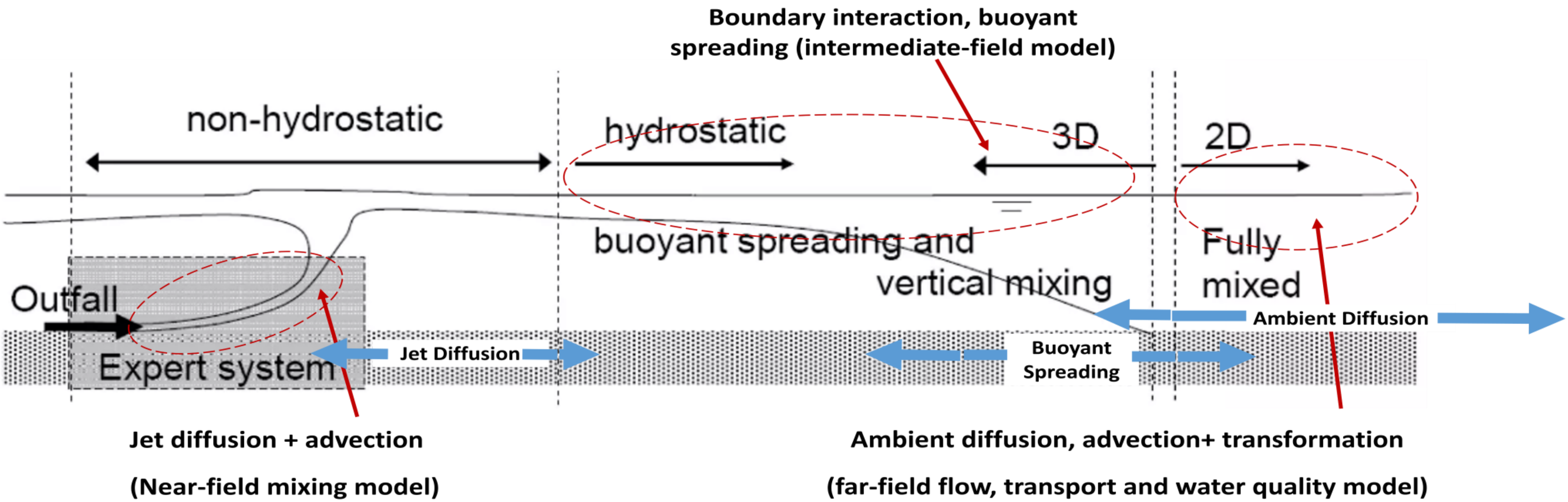

✓ Predicting the vertical distribution of microplastics in the ocean surface mixed layer is necessary for extrapolating surface measurements and comparing observations across conditions.

Numerical part: CORMIX

- **CORMIX** software is broadly accepted as an easy-to-use powerful tool for accurate and reliable point source **mixing analysis**.
- In my project, I will utilize **CORMIX** to further investigate the **sediment transport** in coastal areas and the effect of **pollutants released with sediments**.

✓ It is a specialized software system used for analyzing mixing zones that occur when pollutants are discharged into water bodies

- About CORMIX: There are different simulation models in ***CORMIX*** :
  - CORMIX 1: single port discharges.
  - CORMIX 2: submerged multiport diffusers.
  - CORMIX 3: buoyant surface discharges.
  - DHYDRO: dense brine and/or sediment discharges (single port, submerged multiport, or surface discharges).

Input data in CORMIX:

A: Pollutant Properties

B: Environmental Conditions

C: Discharge Parameters

An Example – Simulation with CORMIX

Test Platform	Current Velocity [m/s]	Mass Discharge [kg/s]	Effluent Concentration [kg/mc]	Effluent Density	Effluent Flowrate [mc/s]	N_legs	(DISTB) [km]	Water Depth (H-D) [m]	Z break [m]	Y break [m]	Nearshore Bottom Slope (i)	Far Slope
AGOSTINO B	0,123	100	1033	1669	0,097	8	15	21,5	8	1500	0,533333	0,1000

Discharge time = *0,599 h* refers to the duration required for an excavator operating at minimum efficency (100 m3/s)

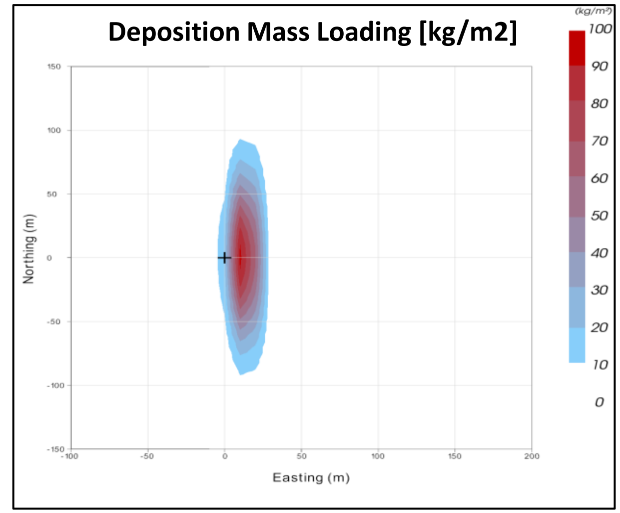

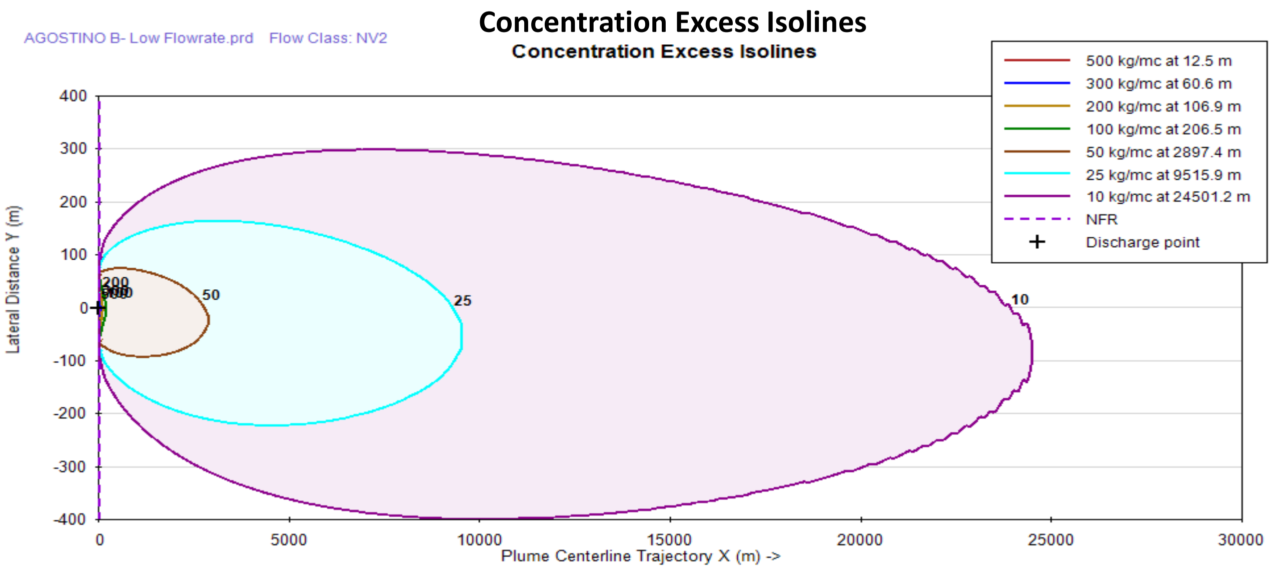

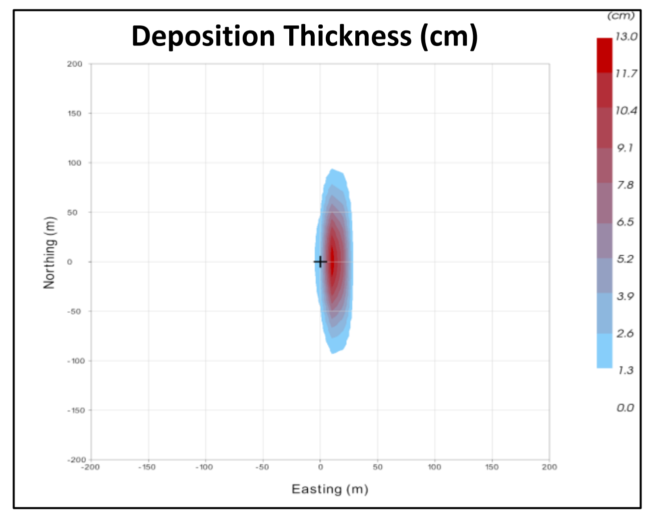

- ✓ **Both erosion and dispersion** play <u>crucial roles</u> in shaping the morphology of sediment beds and influencing sediment transport patterns.

- ❑ The link between morphological changes and bed-exchange processes of erosion and dispersion can be understood through the concept of *particle tracking*.

- ❑ **Particle tracking** is a numerical method used <u>to simulate the movement of individual particles</u> within a fluid or granular system.

- ❑ We performed some **experimental tests** in the laboratory at UNIVPM under monochromatic and bichromatic waves <u>to explore the behavior of the particles</u>.

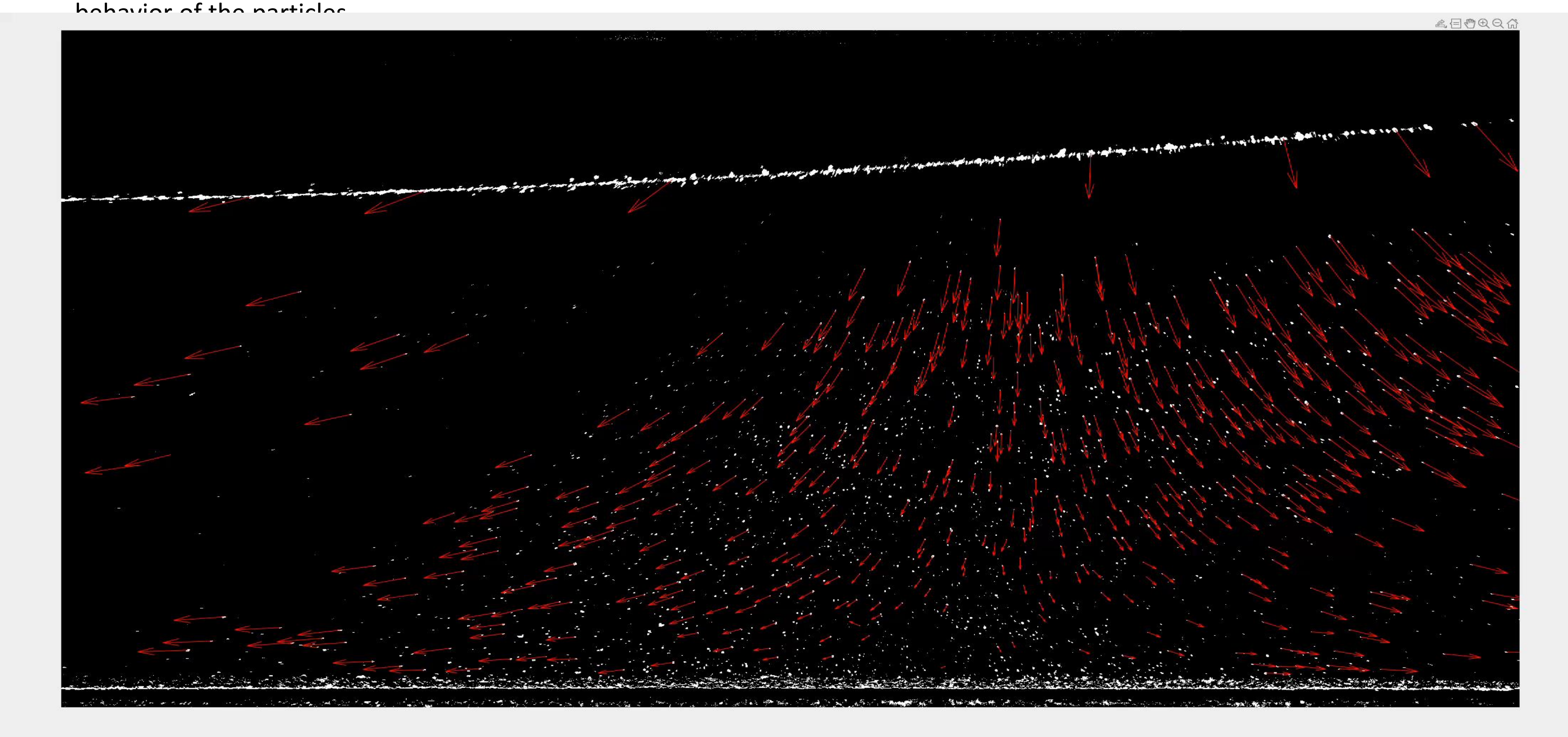

PhD Project: Mixing and transport in the coastal area

- Performing post-processing consists of the proper tracing of particles.
- By reviewing each frame, particle trajectories are then extracted.

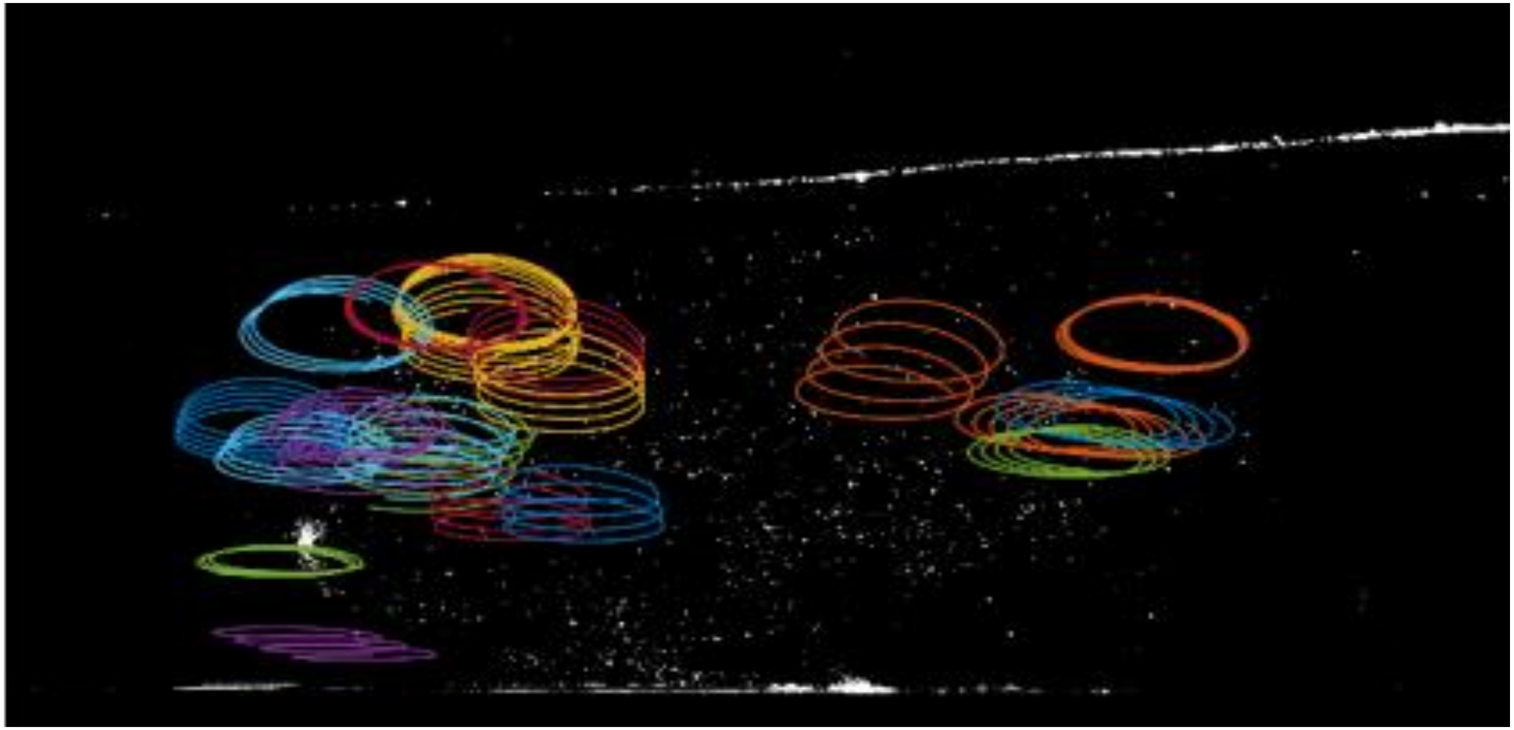

✓ Our objective was to analyze the position and direction of each trajectory with respect to the wave.

✓**So, particle tracking** provides valuable information about the dynamics of erosion and dispersion processes and their impact on morphological changes.

- By combining this approach with other techniques such as field measurements and laboratory experiments, we can gain a comprehensive understanding of sediment transport and bed evolution in natural systems.
- The awareness of plastic pollution and its environmental consequences has grown significantly in recent years.

✓ We will do lab experiments on plastic floaters, using available colored balls

To model physical processes occurring around coastal structures and the motion of suspended particles.

- Different scenarios
  - varying wave conditions
  - tidal level
  - particle characteristics

  will be tested to understand their effects on particle movement and distribution

- Scenarios will be based on the use of:
  1) floating particles with different features (density, size, shape)
  2) groups of particles with different aggregation rates (congested and uncongested configurations)
  3) different flow features (wave height, period, water depth)

Experimental part

- We can have distribution of different densities, shapes, and sizes of plastic debris to investigate the effect of waves and wave-induced currents on the input rate.

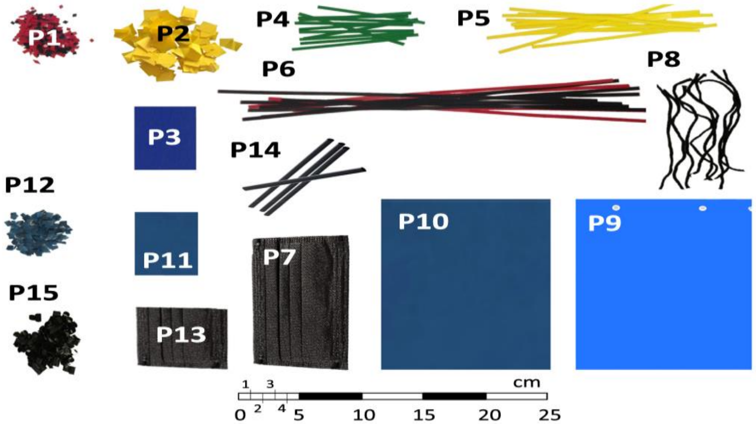

Fig. 2. Plastic debris types (P_i) under study.

Nú˜nez et al (2023)

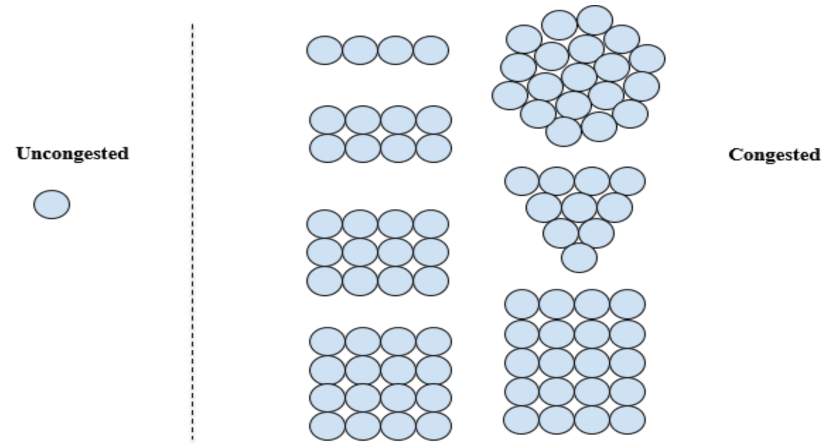

✓ By mitigating plastic pollution, we can help protect marine and coastal ecosystems and preserve the invaluable services they provide.

Field measurement

- **In the case of field experiments**, the video-monitoring system at the Misa River Estuary (nearby UNIVPM) will be used to track surficial sediment transport and circulation patterns around existing coastal structures (e.g., jetty, harbor).

Thank you
for your attention!

Morphodynamic Analysis of the upper confined and unconfined beach profiles during Episodic events

21/04/2024

SEDIMARE Doctoral School -II
University of Nottingham

Buckle Subbiah Elavazhagan

SEDIMARE – DC 05
IH-Cantabria, Universidad de Cantabria

Javier López Lara
Professor, Universidad de Cantabria

María Emilia Maza Fernández
Ass. Professor, Universidad de Cantabria

I INTRODUCTION

01 Numerical models can accommodate the physics behind the coastal processes quite accurately

02 Wave averaged models have limitations in predicting certain aspects of morphodynamics including swash zone dynamics while Lagrangian and two-phase models are highly accurate but with expensive computational needs

03 IH2VOF-SED a Eulerain one phase model employing RANS equations provides a great compromise in-between

04 With IH2VOF-SED model processes behind breaker bar evolution, movement and stabilization, role of infra-gravity waves will be explored

05 With implementations within the model to include submerged vegetation and structures, the model will be put to use for computing the influence of these measures in morphodynamic processes.

06 The final product would be an improved functional 2DV numerical model available for practical use

II Background IH2VOF

- 2DV RANS based solver
- Turbulence is accounted using a k-ε closure model
- Finite difference computational approach in a structured orthogonal mesh
- Free surface reconstruction using Volume of Fluid technique
- Incorporation of solid boundary using partial cell treatment
- Two step projection method is used as numerical solving procedure
- VARANS equations for solved for flows in the porous media
- A well validated model which can different real world scenarios
- Accurately predict runup, overtopping, pressure and forces on the structures

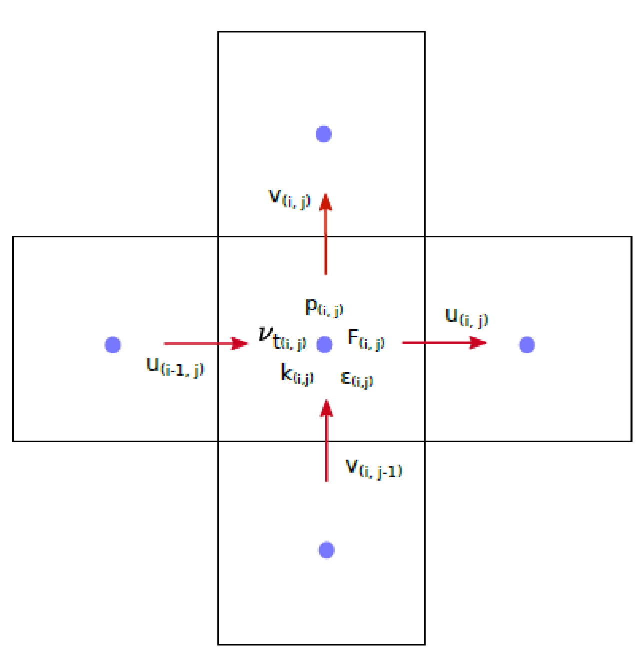

Computed variables

1	1	0.91	0.9	0.9	0.9	0.9	0.9	0.9	0.9	0.9
1	1	0.68	0	0	0	0	0	0	0	0
1	1	1	0.8	0	0	0	0	0	0	0
1	1	1	1	0.89	0	0	0	0	0	0
1	1	1	1	1	0.96	0.31	0	0	0	0
1	1	1	1	1	1	0.99	0.46	0	0	0
1	1	1	1	1	1	1	1	0.61	0	0
1	1	1	1	1	1	1	1	1	0.75	0.07
1	1	1	1	1	1	1	1	1	1	0.86
1	1	1	1	1	1	1	1	1	1	1
1	1	1	1	1	1	1	1	1	1	1

Partial cell Treatment

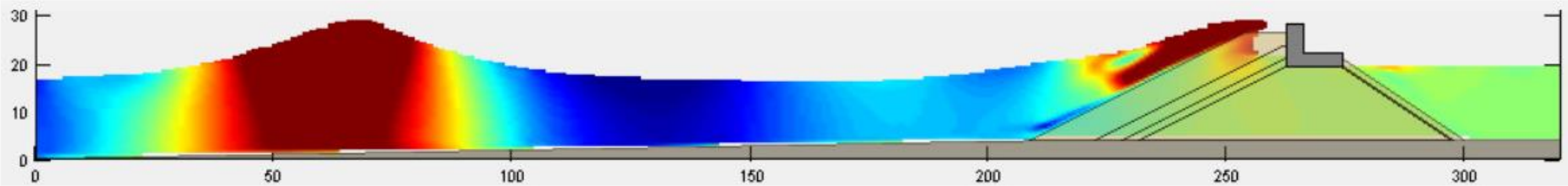

Wave run-up and overtopping over a structure

III Background IH2VOF- SED

Bedload transport is computed by a instantaneous transport rate formula proposed by Roulund et.al 2005

Suspended load transport is computed by solving advective – diffusive equation

Reference Concentration is used for fluid-solid boundary layer, formulation by Smith and McLean, 1977

For seabed displacement a sediment balance equation is used

García-Maribona, J et.al (2021, 2022)

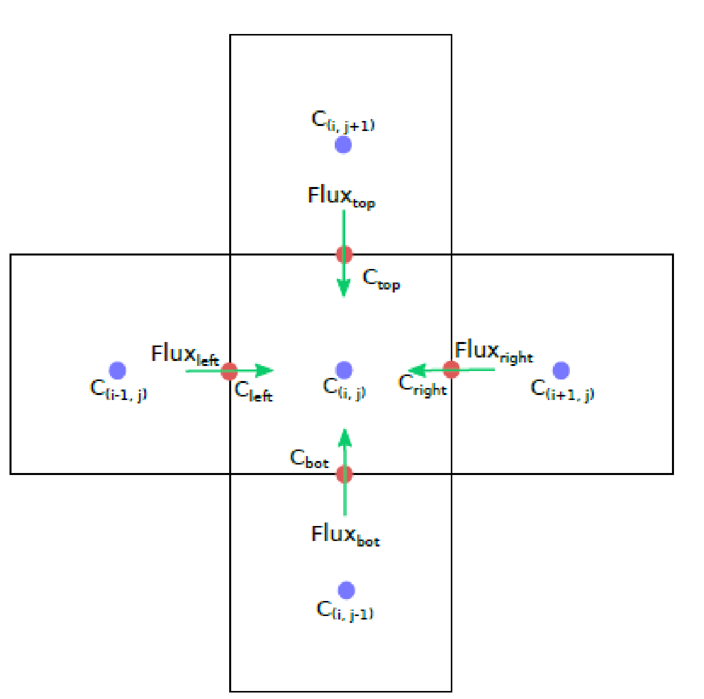

Computed variables

In its current state the implementation is only tested for regular wave erosive condition

The model needs further validation under irregular wave and accretive condition

Incorporation of other schemes to capture vegetative impacts and structural implementation

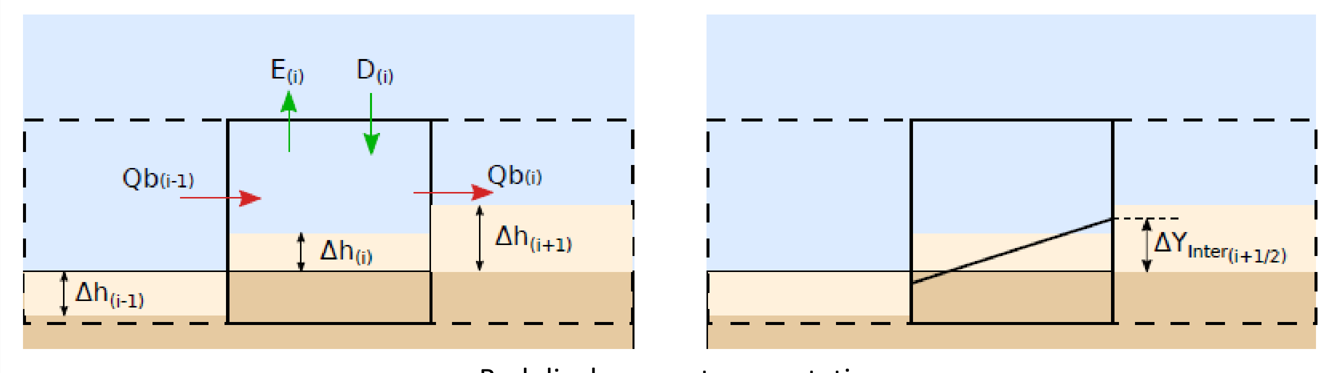

Bed displacement computation

IV Research and Planning

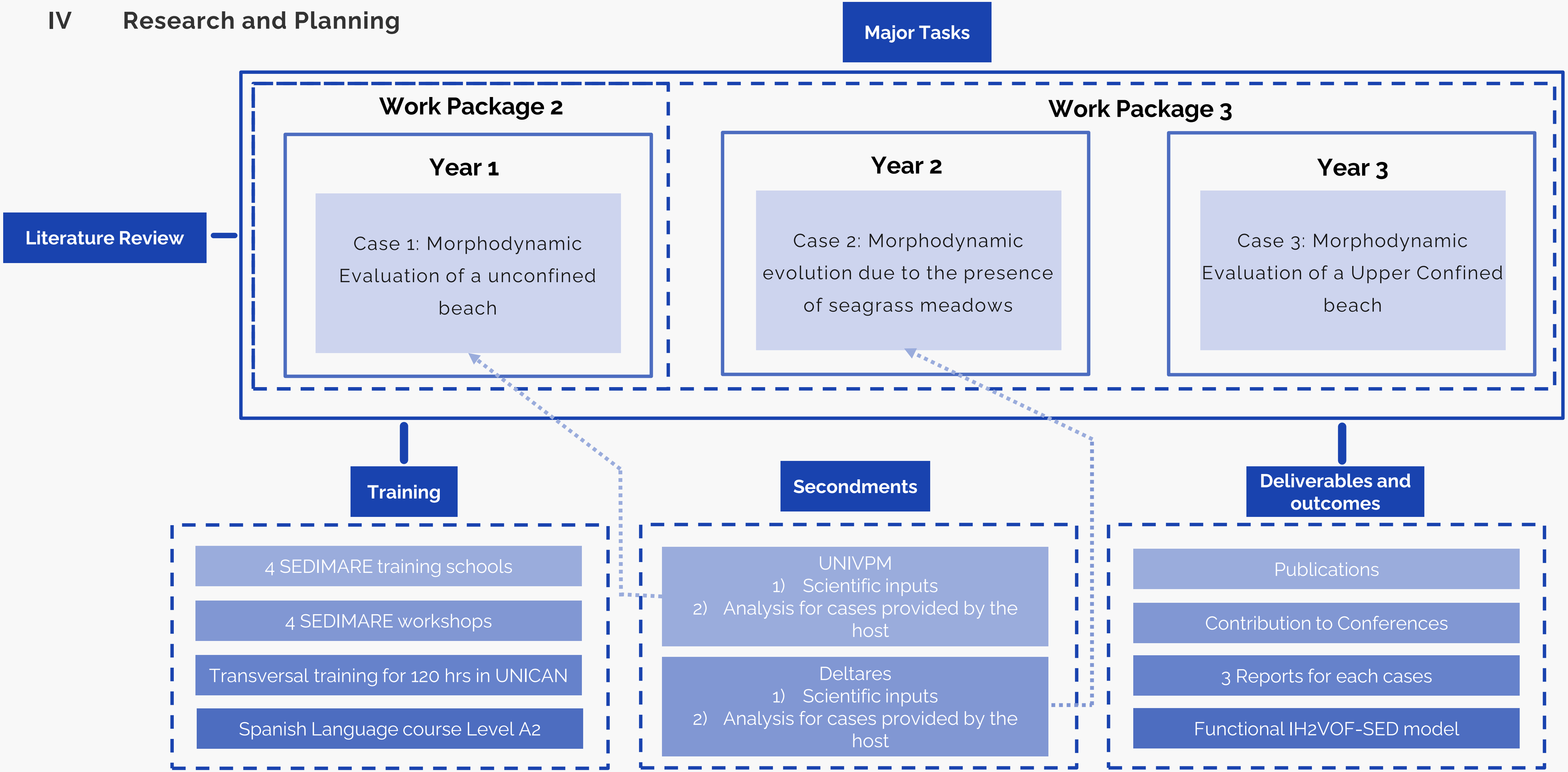

V CASE I – Morphodynamic Evaluation for unconfined beach

OB-1 and WP-2

1. Validation for biochromatic and irregular wave condition

2. Evolution of breaker bar under alternating erosive and accretive Bichromatic waves

3. Inclusion of infragravity waves bound to the short waves to evaluate its influence

Validation case

- Different sequences of alternating erosive and accretive conditions will be tested
- The work will be based on Grossmann et al., 2023)

Wave condition			H_{rms} (m)	T_p (s)	Ω (–)	H_1 (m)	H_2 (m)	f_1 (Hz)	f_2 (Hz)	T_{gr} (s)
B	Benchmark	Random	0.30	4	2.21	n/a	n/a	n/a	n/a	n/a
E1	High energy 1	Bichromatic	0.42	3.7	3.34	0.320	0.320	0.3041	0.2365	14.80
E2	High energy 2	Bichromatic	0.32	3.7	2.54	0.245	0.245	0.3041	0.2365	14.80
A1	Low energy 1	Bichromatic	0.23	4.7	1.44	0.101	0.202	0.2276	0.1979	33.68
A2	Low energy 2	Bichromatic	0.19	5.3	1.05	0.085	0.171	0.2018	0.1755	37.98
A3	Low energy 3	Bichromatic	0.14	5.7	0.72	0.063	0.126	0.1877	0.1632	40.85

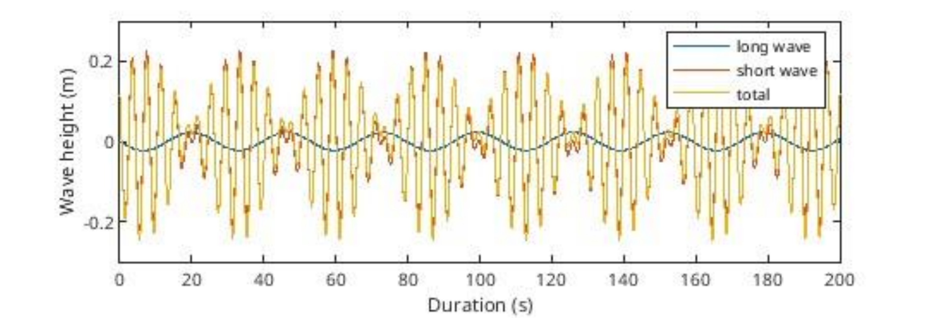

Key expected outputs

1. Breaker bar dynamics in alternating erosive and accretive conditions
2. Role of initial beach profile in the bar dynamics
3. Hydrodynamic and Morphodynamic Processes including infragravity wave release rate influencing the bar generation and evolution

Regular Waves

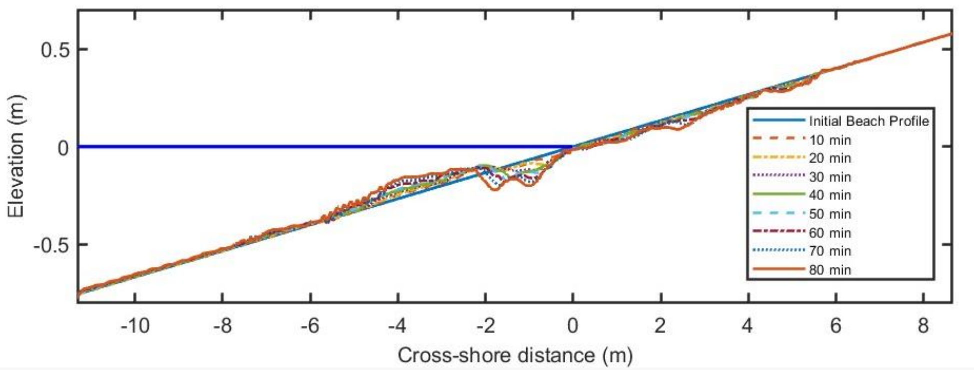

Bichromatic Waves

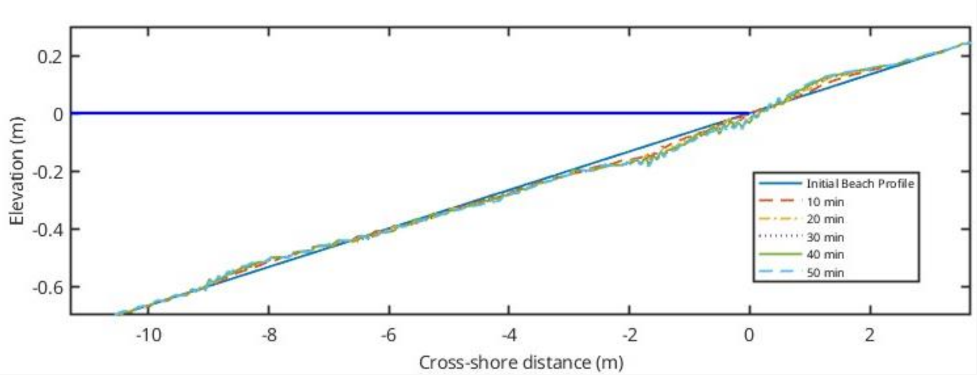

Random Waves

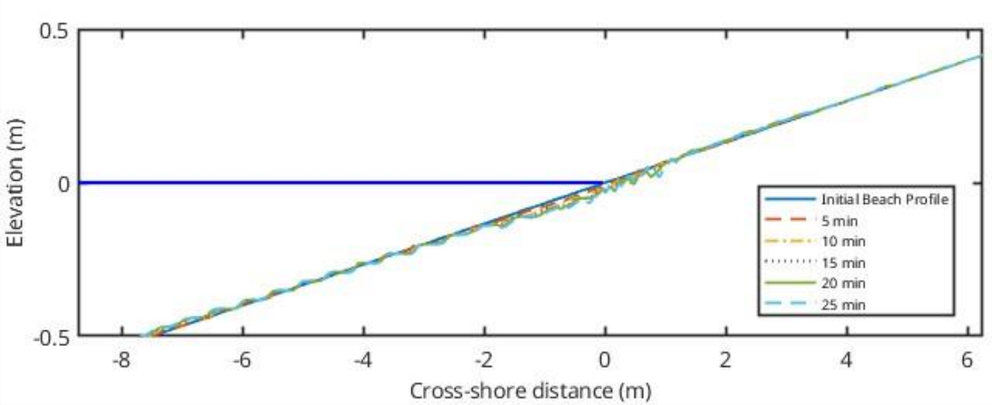

VI CASE II – Morphodynamic evolution due to the presence of seagrass meadow

OB-2 and WP-2,3

1. Development of Numerical scheme to incorporate the impact of Posidonia *Oceania*

2. Validation against CIEM Flume experiments which used a surrogate vegetation model

3. Evaluate the morphodynamic response due to the presence of the seagrass meadow

Validation case

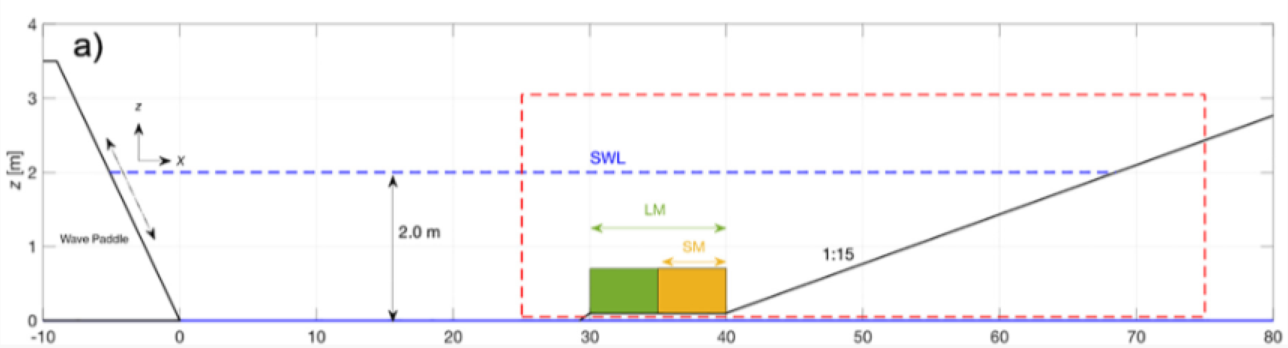

Physical model setup - Astudillo et al., 2022; Astudillo-Gutierrez et al., 2024)

Key expected outputs

1. Functional numerical model incorporating submerged vegetation
2. Role of submerged meadow of different lengths in attenuating waves and velocities
3. Impact of vegetation in breaker bar dynamics

Numerical scheme developed by Maza et al., 2013

$$\overline{F}_{D,i} = \frac{1}{2}\cdot C_D \cdot a \cdot N \cdot \overline{u}_{rel,i} \cdot \left|\overline{u}_{rel,i}\right|$$

$$\frac{\partial u_i}{\partial t} + \overline{u}_j \frac{\partial u_i}{\partial x_j} = -\frac{1}{\rho}\frac{\partial p}{\partial x_i} + g_i + \frac{1}{\rho}\frac{\partial \overline{\tau_{ij}}}{\partial x_j} - \frac{\partial \overline{\left(u'_i u'_j\right)}}{\partial x_j} - \overline{F}_{D,i}$$

Drag force consideration in RANS equation

$$\underbrace{+\rho C_{kp} C_D a N \sqrt{\overline{u}_{rel,j}\overline{u}_{rel,j}}\, k}_{k_w}$$

$$\underbrace{+\rho C_{\varepsilon p} C_D a N \sqrt{\overline{u}_{rel,j}\overline{u}_{rel,j}}\, \varepsilon.}_{\varepsilon_w}$$

Dispersive stresses consideration in K-ε model

$$m_0 \cdot \frac{\partial^2 \xi_i}{\partial t^2} + C \cdot \frac{\partial \xi_i}{\partial t} + \left(E \cdot I \cdot \frac{\partial^4 \xi_i}{\partial z^4}\right) =$$

$$= \frac{1}{2} \cdot \rho \cdot C_D \cdot a \cdot \left(\overline{u} - \frac{\partial \xi_i}{\partial t}\right) \cdot \left|\overline{u} - \partial \frac{\xi_i}{\partial t}\right| + \left(\rho_p - \rho\right) \cdot g \cdot V_p \cdot \frac{\partial \xi_i}{\partial z} + \rho \cdot V_p \cdot \frac{\partial \overline{u}}{\partial t} + \rho \cdot C_m \cdot V_p \cdot \left(\frac{\partial \overline{u}}{\partial t} - \frac{\partial^2 \xi_i}{\partial t^2}\right)$$

Morrison equation for plant motion

VII CASE III – Morphodynamic Evaluation of a Upper Confined beach

OB-3 and WP-2,3

1. Development of Numerical scheme to incorporate coastal structures as non-erodible layers

2. Validation against Delta Flume experiments conducted on dike model with a vertical wall

3. Evaluate the morphodynamic response due to the presence of the seagrass meadow

Validation case

- Large scale Experimental results from WALOWA experiments conducted in Delta flume
- Different tests were conducted by use of Bichromatic waves and Irregular waves

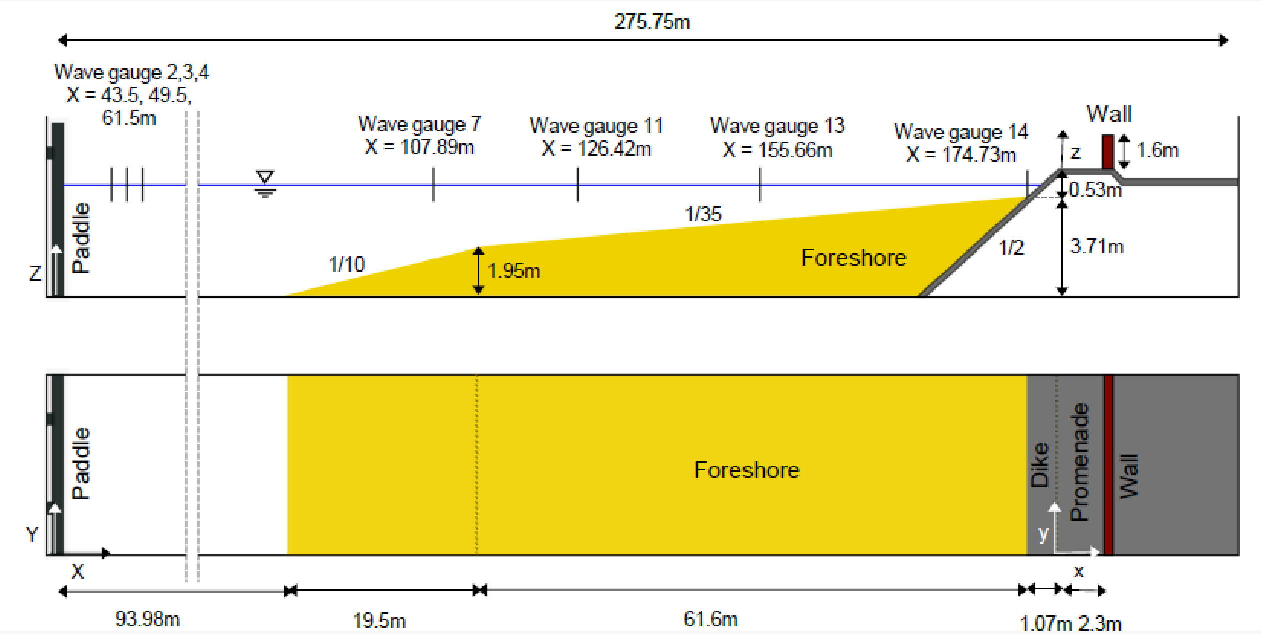

Physical model setup -Streicher et al., 2017)

Key expected outputs

1. Functional numerical model with ability to model structurally confined beaches by incorporating non-erodible layers
2. Impact force and pressure behavior of overtopped waves on vertical structures on top of a dike
3. Scour dynamics

Thank you!

References

1. Astudillo, C., Gracia, V., Cáceres, I., Sierra, J. P., & Sánchez-Arcilla, A. (2022). Beach profile changes induced by surrogate Posidonia Oceanica: Laboratory experiments. *Coastal Engineering*, *175*. https://doi.org/10.1016/j.coastaleng.2022.104144
2. Astudillo-Gutierrez, C., Gracia, V., Cáceres, I., Sierra, J. P., & Sánchez-Arcilla, A. (2024). Influence of seagrass meadow length on beach morphodynamics: An experimental study. *Science of the Total Environment*, *921*. https://doi.org/10.1016/j.scitotenv.2024.170888
3. García-Maribona, J., Lara, J. L., Maza, M., & Losada, I. J. (2021). An efficient RANS numerical model for cross-shore beach processes under erosive conditions. Coastal Engineering, 170. https://doi.org/10.1016/j.coastaleng.2021.103975
4. García-Maribona, J., Lara, J. L., Maza, M., & Losada, I. J. (2022). Analysis of the mechanics of breaker bar generation in cross-shore beach profiles based on numerical modelling. Coastal Engineering, 177. https://doi.org/10.1016/j.coastaleng.2022.104172
5. Grossmann, F., Hurther, D., Sánchez-Arcilla, A., & Alsina, J. M. (2023). Influence of the Initial Beach Profile on the Sediment Transport Processes During Post-Storm Onshore Bar Migration. Journal of Geophysical Research: Oceans, 128(4). https://doi.org/10.1029/2022JC019299
6. Lara, J. L., Losada, I. J., & Guanche, R. (2008). Wave interaction with low-mound breakwaters using a RANS model. Ocean Engineering, 35(13), 1388–1400. https://doi.org/10.1016/j.oceaneng.2008.05.006
7. Lara, J. L., Ruju, A., & Losada, I. J. (2011). Reynolds averaged Navier-Stokes modelling of long waves induced by a transient wave group on a beach. Proceedings of the Royal Society A: Mathematical, Physical and Engineering Sciences, 467(2129), 1215–1242. https://doi.org/10.1098/rspa.2010.0331
8. Maza, M., Lara, J. L., & Losada, I. J. (2013). A coupled model of submerged vegetation under oscillatory flow using Navier-Stokes equations. Coastal Engineering, 80, 16–34. https://doi.org/10.1016/j.coastaleng.2013.04.009
9. Roulund, A., Sumer, B. M., Fredsøe, J., & Michelsen, J. (2005). Numerical and experimental investigation of flow and scour around a circular pile. Journal of Fluid Mechanics, 534, 351–401. https://doi.org/10.1017/S0022112005004507
10. Streicher, M. ;, Kortenhaus, A. ;, Altomare, C. ;, Gruwez, V. ;, Hofland, B. ;, Chen, X. ;, Marinov, K. ;, Scheres, B. ;, Schüttrumpf, H. ;, Hirt, M., Cappietti, L., Esposito, A., Saponieri, A., Valentini, N., Tripepi, G., Pasqualini, D., Di Risio, M., Aristodemo, F., Damiani, L., & Kaste, . . (2017). (Wave Loads on Walls) Large-Scale Experiments in the Delta Flume.

Mathematical modeling and numerical simulations of water-saturated granular materials with emphasis to sediment transport

Evangelos Petridis

UCLouvain
Institute of Mechanics, Materials and Civil Engineering

April 22, 2024

Background

• BSc in Applied Mathematics, Department of Mathematics & Applied Mathematics, University of Crete
Internship: Foundation Of Research and Technology –Hellas (FORTH)
Advisor: Dr. Skarsoulis Emmanuel K.
Subject: Ray tracing in underwater environment with flat bottom

• MSc in Applied and Computational Mathematics, with specialization in "Modelling and Analysis in Science and Technology", Department of Mathematics & Applied Mathematics, University of Crete
MSc Thesis: Dynamics of Airy wavepackets and beams
Supervisor: George N. Makrakis

Project summary

The four parts of my project

• Analysis of mathematical models for flows in porous media and granular mixtures (water-sand).

• Development of advanced computational tools and simulation software for granular mixtures.

• Detailed numerical simulations of shear-driven (Couette) and gravity driven flows of water-sand mixtures. (Emphasis on sediment mobilization and resuspension)

• subgrid (LES) models and reduced models to simulate large-scale sediment mobilization and resuspensions.

Part I

- theoretical work about structural stability and continuous dependence of mathematical models

Part II

- Develop numerical treatment of the stiffness of certain physical parameters (such as granular viscosity)

- perform simulations of sediment dynamics with unprecedented fidelity

Part III

I will focus on the numerical algorithm where I want to

• establish new and accurate modelling approaches and related numerical algorithms for the mobilization and resuspension of sediments

• perform 2D simulations of sediment mobilization and transport due to shear-driven and gravity driven water currents at the laboratory scale

• compared my results with earlier experimental studies and new experiments conducted at UCLouvain

Part IV

In order to improve our understanding of the phenomena of interest and also improve the design of reduced, engineering models for practical applications, I will pursue to

• resolve the relevant turbulent structures of the flow in a computationally efficient manner

• develop of subgrid (LES) models and derive simplified versions of viscous stresses

Progress

- enhanced my theoretical and computational skills
- studied in depth continuum mechanics and thermodynamics of irreversible processes , multi-phase flow modeling, the mathematical model for granular suspensions and the algorithms for its numerical treatment
- studied programming languages (C, Python) and familiarized myself with PETSc which solves linear and nonlinear systems of equations that arise from discretizations of Partial Differential Equations
- completed the intensive advanced course on High Performance Computing offered by UCLouvain
- participated in the first winter school of SEDIMARE, Ancona, Italy
- worked on the analysis of the structural stability of the model for granular mixtures
- attend the course MECA2771: Thermodynamics of irreversible phenomena, UCLouvain

Results

$$\phi\frac{\partial \mathbf{u}}{\partial t} + \phi\boldsymbol{\nabla} p$$
$$= \boldsymbol{\nabla}\cdot(\phi\zeta(\boldsymbol{\nabla}\cdot\mathbf{u})I) + \boldsymbol{\nabla}\cdot\left(\phi\mu\mathbf{V}^d\right) - a^\star(\phi)\mathbf{u} - b^\star(\phi)|\mathbf{u}|\mathbf{u} + \phi\mathbf{f}$$

$$\zeta, \mu > 0$$

$$\boldsymbol{\nabla}\cdot(\phi\mathbf{u}) = 0$$

$$\mathbf{V}^d = \frac{1}{2}(\boldsymbol{\nabla}\mathbf{u} + (\boldsymbol{\nabla}\mathbf{u})^T) - \frac{1}{3}\boldsymbol{\nabla}\cdot\mathbf{u}\ I$$

$$b^\star(\phi) = b(1-\phi) + d(1-\phi)^2\ \ ,\ \ a^\star(\phi) = a(1-\phi)\ ,\ \ a, b, d > 0$$

$$0 < \phi_{\text{min}} \leq \phi \leq \phi_{\text{max}} < 1$$

Results

$$\mathbf{w} = \mathbf{u} - \mathbf{v}\ ,\ \pi = p - q\ ,\ b^\star = \ b_1^\star - b_2^\star = b(1-\phi)\ ,\ \ b = b_1 - b_2$$

$$\Phi = \int_0^t \int_\Omega \phi \mathbf{w}^2 d\mathbf{x} d\eta$$

$$\Phi(t) \leq \frac{c}{2a\lambda^{1/2}\mu^2}(\frac{1}{\phi_{\text{min}}} - 1)^2(\frac{1}{\phi_{\text{max}}} - 1)^{-1}\frac{(\phi_{\text{max}})^{7/2}}{(\phi_{\text{min}})^{9/2}}$$
$$\Big(\int_\Omega \phi|\mathbf{g}|^2 d\mathbf{x}\Big)^2[1 - e^{-2a(\frac{1}{\phi_{\text{max}}}-1)t}]b^2$$

$$\int_\Omega \phi|\mathbf{w}|^2 d\mathbf{x} \leq \frac{c}{\lambda_1^{1/2}\mu^2}(\frac{1}{\phi_{\text{min}}} - 1)^2\frac{(\phi_{\text{max}})^{7/2}}{(\phi_{\text{min}})^{9/2}}\Big(\int_\Omega \phi|\mathbf{g}|^2 d\mathbf{x}\Big)^2 b^2$$

Essential reading

- D.A. Drew and S.L. Passman (1998), *Theory of Multicomponent Fluids*,Springer.
- G. Lebon, D. Jou and J. Casas-Vazquez (2008), *Understanding Non-equilibrium Thermodynamics*, Springer.
- D. Monsorno, C. Varsakelis and M.V. Papalexandris (2016), *A thermo¬mechanical model for granular suspensions*, J. Fluid Mech. 808, pp. 410–440.
- D. Monsorno, A. A. Dimas and M. V. Papalexandris. (2018) *Time-accurate calculation of two-phase granular flows exhibiting compaction, dilatancy andnonlinear rheology*, J. Comput Phys. 372, pp. 799–822.

Research update

Paterno “Jowi” S. Miranda IV, MCE
SEDIMARE Doctoral Candidate #7

p.s.miranda@utwente.nl
jowi.miranda@deltares.nl

patrno4

Deltares
UNIVERSITY OF TWENTE.
SEDIMARE
Sediment Transport and Morphodynamics in Marine and Coastal Waters with Engineering Solutions

Literature review

- **Van Ledden, 2003**
  - Proposed framework for sand-mud erosion modeling
  - Used mud content:
    - despite clay content, $\boldsymbol{P_{clay,crit}}$, showing considerable effect on erosion behavior
    - due to almost fixed $\mathrm{clay:silt}$ ratio in sand-mud environments in Northern Europe
  - Introduced a **critical mud content, $\boldsymbol{P_{mud,crit}}$,** to describe seabed behavior
  - $P_{mud,crit}$ was found to be at ~30%

$$\text{if } P_{mud} \geq P_{mud,crit} \qquad \text{bed behaves like cohesive sediment}$$
$$\text{if } P_{mud} < P_{mud,crit} \qquad \text{bed behaves like non} - \text{cohesive sediment}$$

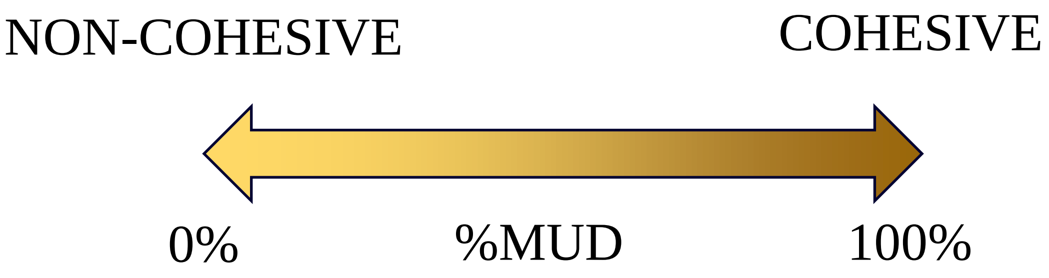

Literature review

- **te Slaa, 2020**
  - Studied deposition and erosion behavior of silt-dominated environments
  - Obtained samples from Yangtze river estuary and tested in laboratory flume
    - Ternary diagram from silt-dominated environment
  - Erosion of silt-dominated is a result of the following sediment parameters:
    - permeability
    - undrained shear strength

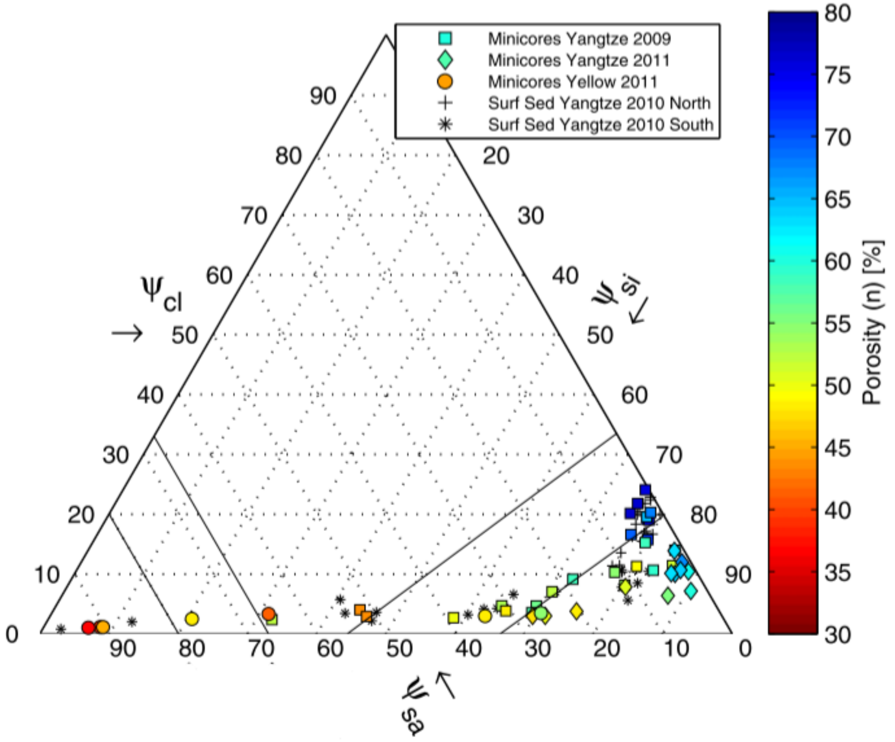

Literature review

- **Colina-Alonso, 2024**
  - Incorporated Van Ledden 2003 framework for sand-mud erosion modeling into Delft 3D
  - Sand-mud interaction mechanisms:
    - Erosion interaction
    - Roughness interaction
  - Result of applying the different mechanisms:

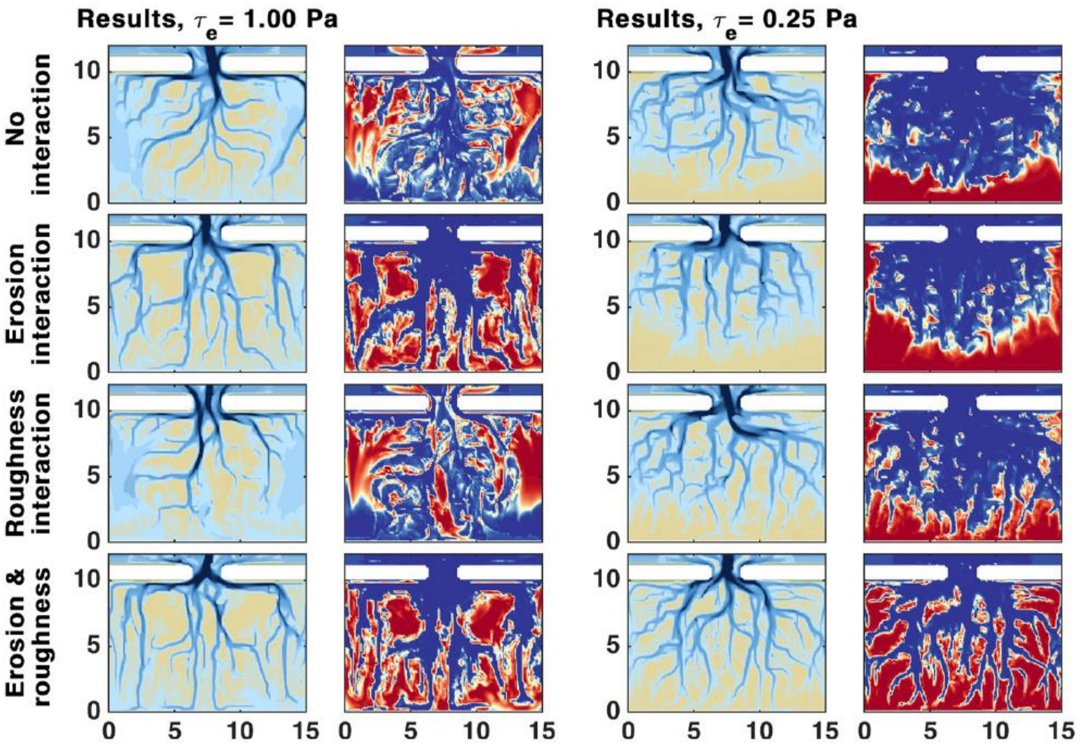

Deltares UNIVERSITY OF TWENTE. SEDIMARE

Sediment Transport and Morphodynamics in Marine and Coastal Waters with Engineering Solutions

Research gap

- Recall, the content of mud

MUD = SILT + CLAY

- From framework of Van Ledden
  - Does not include different mud composition
  - **Hypothesis**: different erosion behavior for *mud with more silt* (i.e. Yangtze river estuary) *vs mud with more clay* (i.e. Scheldt estuary, Wadden Sea)

NON-COHESIVE

COHESIVE

0% %MUD 100%

Silt-dominated

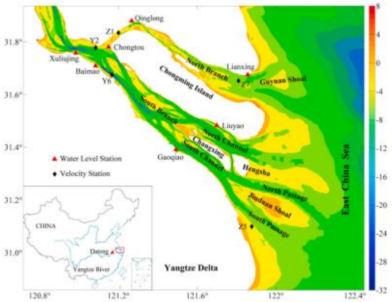

Yangtze river estuary
(Feng et al., 2020)

Clay-dominated
(most of northern Europe)

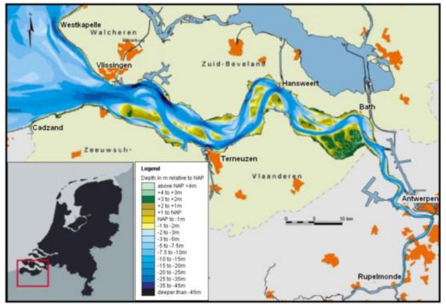

Scheldt Estuary
(Bolle et al., 2010)

Deltares UNIVERSITY OF TWENTE. SEDIMARE
Sediment Transport and Morphodynamics in Marine and Coastal Waters with Engineering Solutions

Research update

- Data collection
  - Pertinent info:
    - %Sand, %Silt, %Clay, D_{50}, τ_{crit}, τ_b vs E
  - From previous studies
    - Panagiotopoulos, I., et al. (1997).
    - Van Ledden, M. (2003).
    - Le Hir, P., et al. (2005).
    - Kothyari, U. C., & Jain, R. K. (2008).
    - Jacobs, Walter. (2011).
    - Perkey, D. W., et al. (2020).
    - van Rijn, L. C. (2020) / MUSA (2022).
    - Yao, P., et al. (2022).

- Compilation of sediment composition in ternary diagram

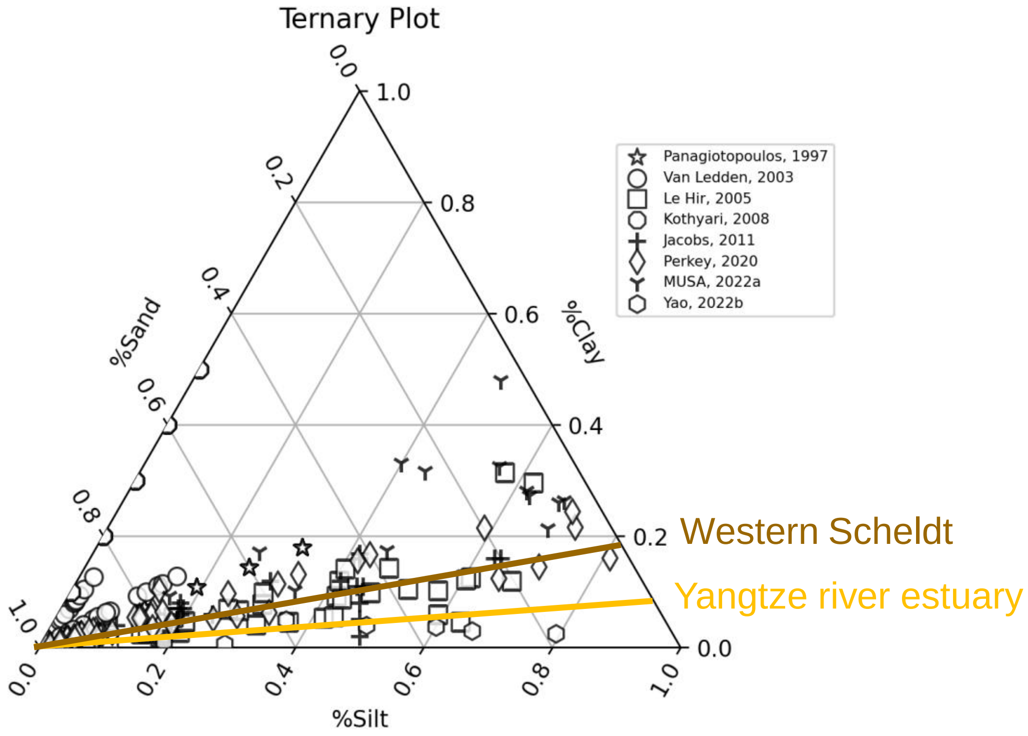

Deltares UNIVERSITY OF TWENTE. SEDIMARE
Sediment Transport and Morphodynamics in Marine and Coastal Waters with Engineering Solutions

Research update

- Schematic diagram of current section of research project

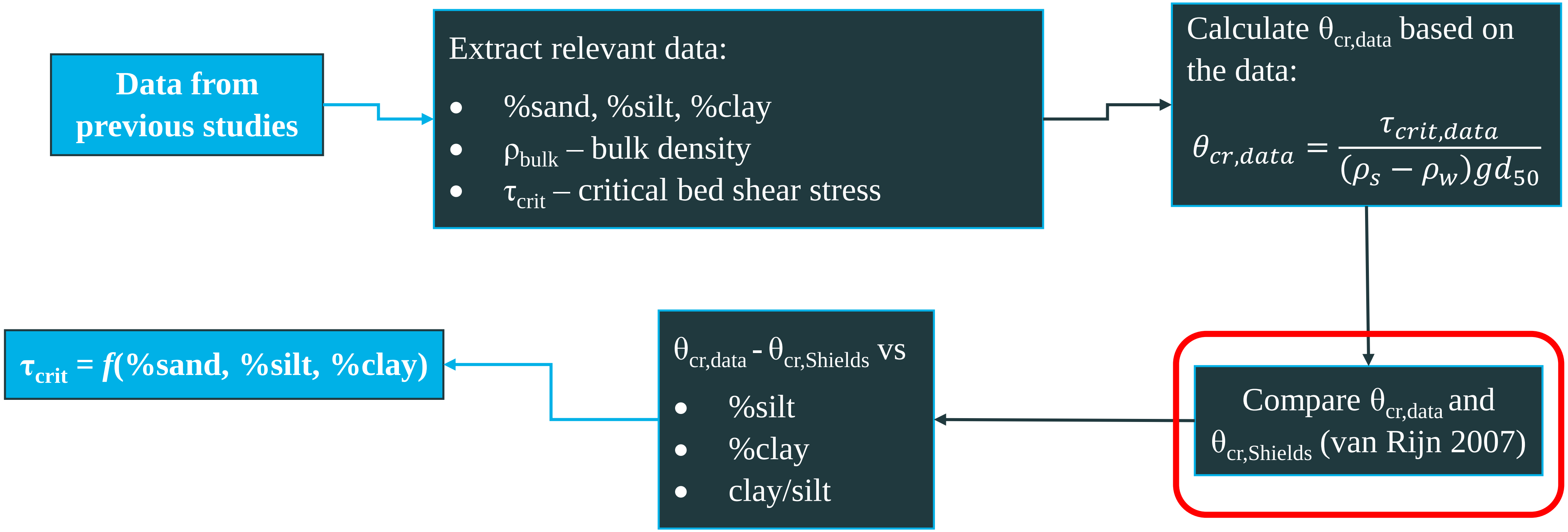

Research update

- Compare Shields parameter from data vs critical Shields parameter from van Rijn, L. C. (2007).

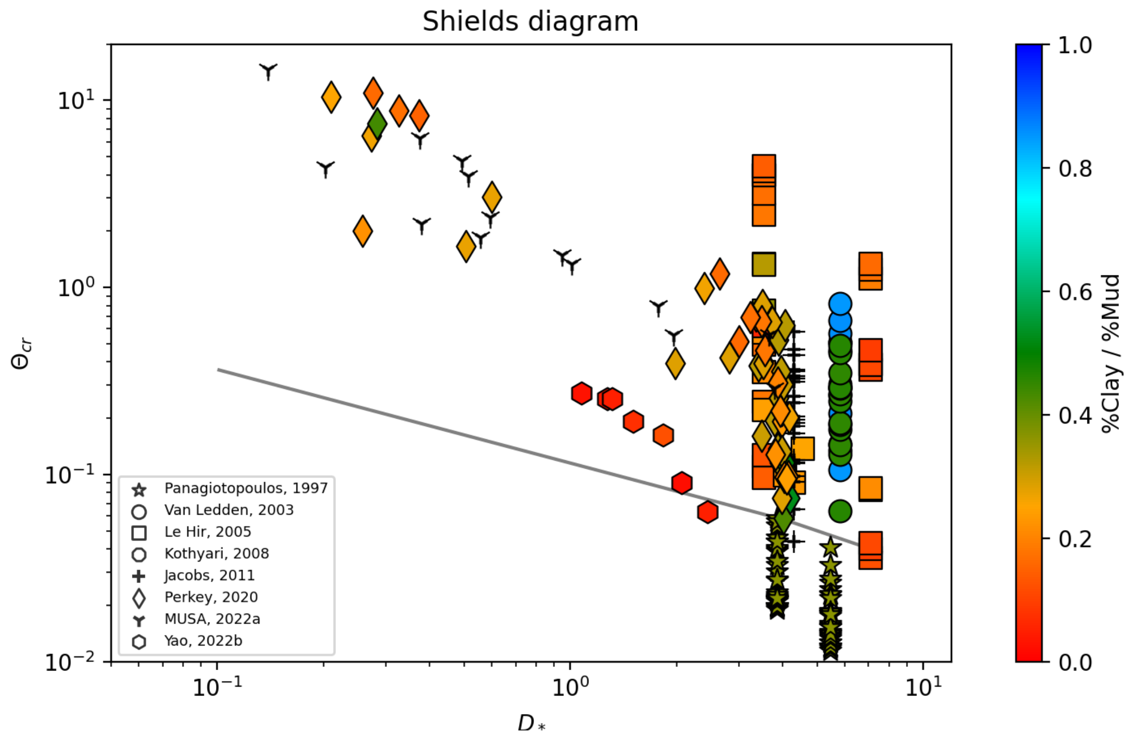

Deltares UNIVERSITY OF TWENTE. SEDIMARE Sediment Transport and Morphodynamics in Marine and Coastal Waters with Engineering Solutions

Research update

Paterno “Jowi” S. Miranda IV, MCE

SEDIMARE Doctoral Candidate #7

p.s.miranda@utwente.nl
jowi.miranda@deltares.nl

patrno4

Deltares

UNIVERSITY OF TWENTE.

SEDIMARE

Sediment Transport and Morphodynamics in Marine and Coastal Waters with Engineering Solutions

SEDIMARE DC8
– CURRENT PROGRESS

MORPHODYNAMICS OF BREACH GROWTH AND BANK EROSION USING LABORATORY EXPERIMENTS

By Siyuan Wang

22-04-2024

DEFINITION

MORPHODYNAMICS OF BREACH GROWTH AND BANK EROSION USING LABORATORY EXPERIMENTS

Bank erosion refers to the process of removing material from a bank which is the land alongside a body of water in geography (Duan, 2005; Sutarto et al., 2014).

Through Hill et al (1993) banks can be divided into three general zones: **toe**, **bank** and **over bank zones**.

Biedenharn et al (1997), Duan (2005), Osman and Thorne (1988) and Sutarto et al (2014) indicated that there are two main modes of bank erosion, which are **hydraulic erosion** and **mechanical failure**.

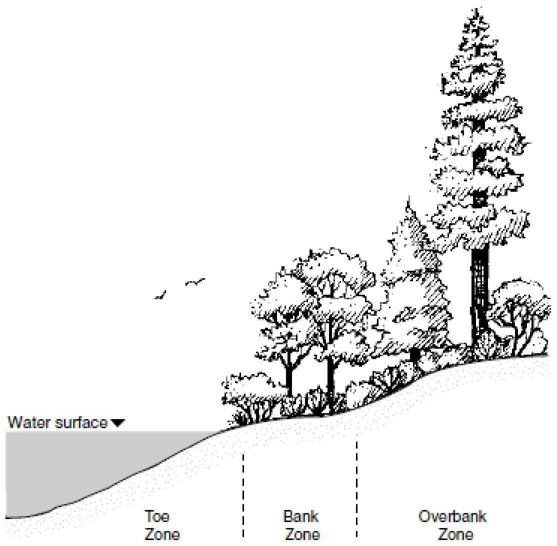

(Hill et al., 1993)

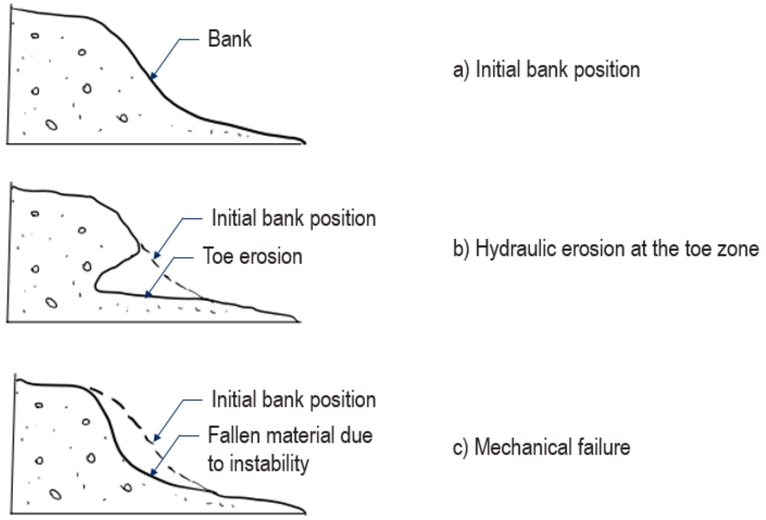

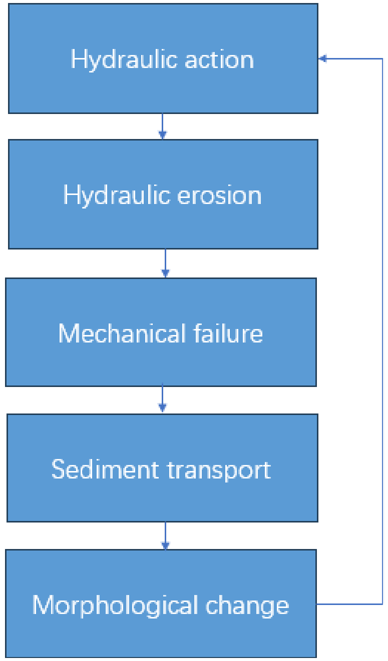

HYDRAULIC EROSION

MORPHODYNAMICS OF BREACH GROWTH AND BANK EROSION USING LABORATORY EXPERIMENTS

Hydraulic erosion is a continuous and uninterrupted process and occurs when the **hydrodynamic forces** surpass the particle resisting **threshold** (Sutarto et al., 2014). This means that the part of the bank in direct contact with these forces, known as the **bank toe**, is typically eroded first, leading to **undercutting**. Research from both field studies and computer models has revealed that this undercutting removes support from the lower part of the bank, creating **overhangs** which can result in mechanical failure (Das et al., 2019; Duan, 2005; Wilson et al., 2007).

MECHANICAL FAILURE

MORPHODYNAMICS OF BREACH GROWTH AND BANK EROSION USING LABORATORY EXPERIMENTS

Regarding **mechanical failure**, non-cohesive and cohesive banks exhibit distinct modes of failure.

For **non-cohesive banks**, mechanical failure is predominantly caused by the **movement of individual particles** on banks that have a slope exceeding the angle of repose. This movement results in a very slightly curved slip surface, a phenomenon known as **plane failure** (ASCE Task Committe, 1998).

Cohesive banks differ from non-cohesive ones, the cohesion among particles in cohesive banks allows for **steeper slopes** than the angle of friction would permit, with very cohesive sediment sometimes having stable vertical failure. This is because the soil can sustain the forces exerted at the top of slopes which are steeper than the friction angle (Thorne, 1978). These internal forces between particles can influence mechanical failure as **circular failure**.

(Soares-Frazão et al., 2007)

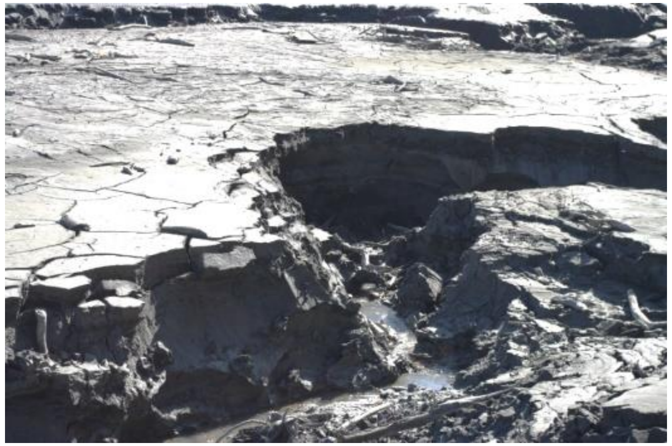

FORCE ANALYSIS OF THRESHOLD OF BANK EROSION

MORPHODYNAMICS OF BREACH GROWTH AND BANK EROSION USING LABORATORY EXPERIMENTS

The forces are the submerged **weight** of the particle (($\overrightarrow{F_G}$) and the hydrodynamic force, which is decomposed into **drag force** (($\overrightarrow{F_D}$) and **lift force** (($\overrightarrow{F_L}$). β is the angle of inclination of flow with respect to the longitudinal axis of the channel, ω is the **downstream angle** and α is the **side slope angle**.

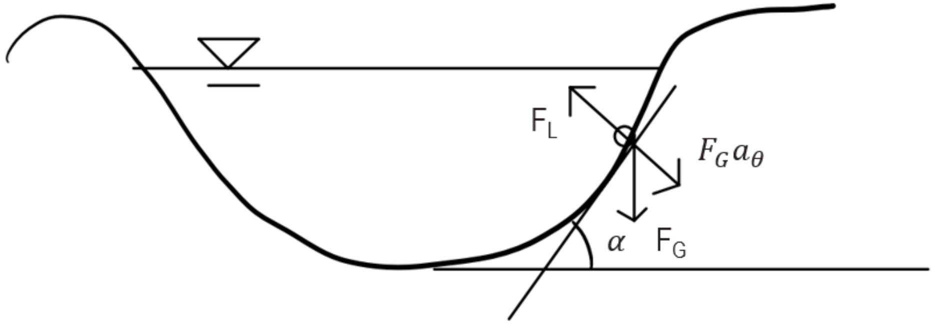

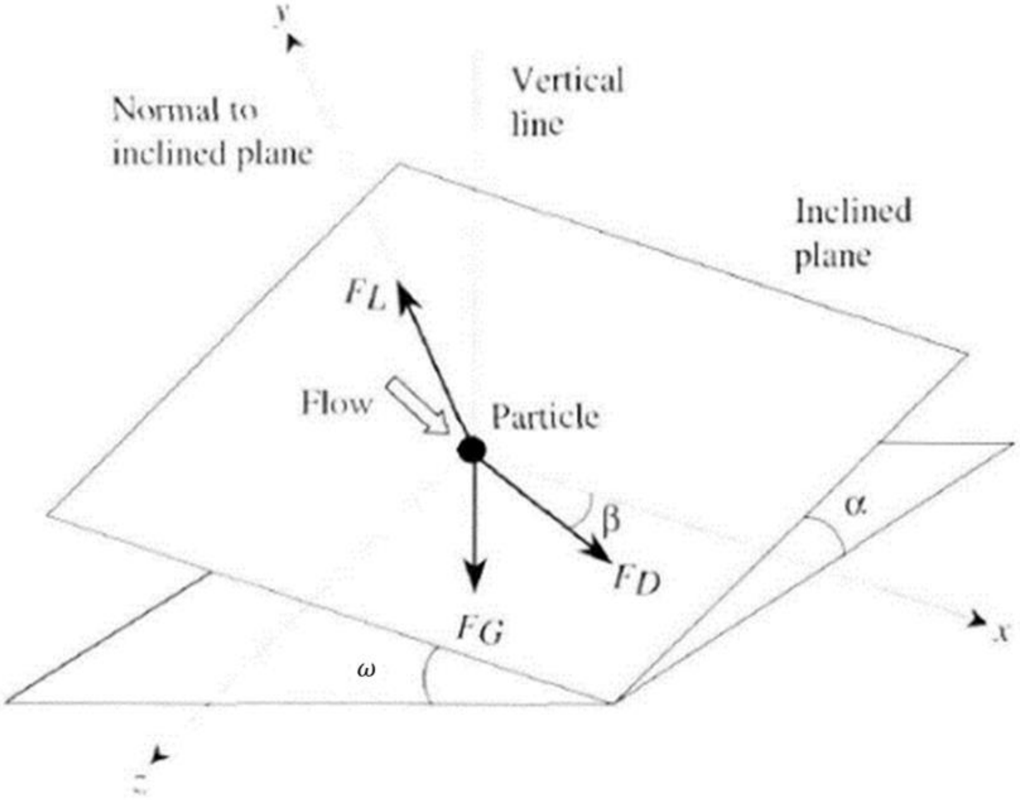

FORCE ANALYSIS OF THRESHOLD OF BANK EROSION

MORPHODYNAMICS OF BREACH GROWTH AND BANK EROSION USING LABORATORY EXPERIMENTS

For **transverse bank slopes**：

$$\tilde{\tau} = \cos\alpha \sqrt{1 - \frac{\tan^2 \alpha}{\tan^2 \phi}}$$

Where $\tilde{\tau}$ is critical shear stress ratio $\tau_c{}^*/\tau_0{}^*$

α is the side slope angle

φ is angle of repose

For **longitudinal bank slopes**：

$$\tilde{\tau} = \cos\omega \left(1 - \frac{\tan \omega}{\tan \phi}\right)$$

Where ω is the downstream angle

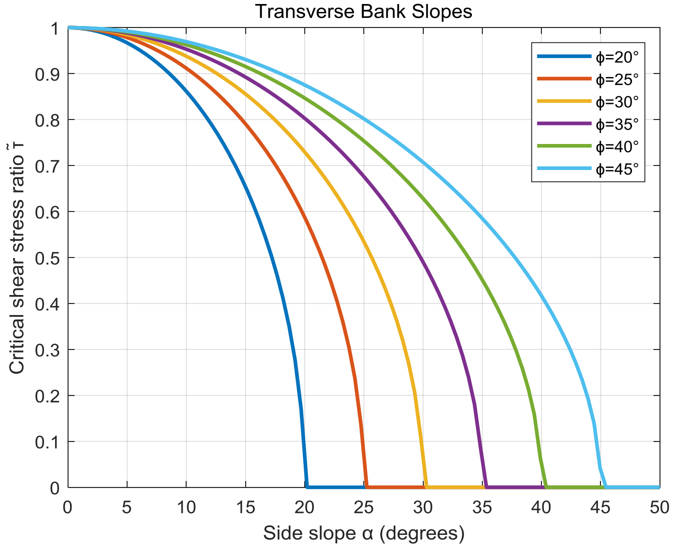

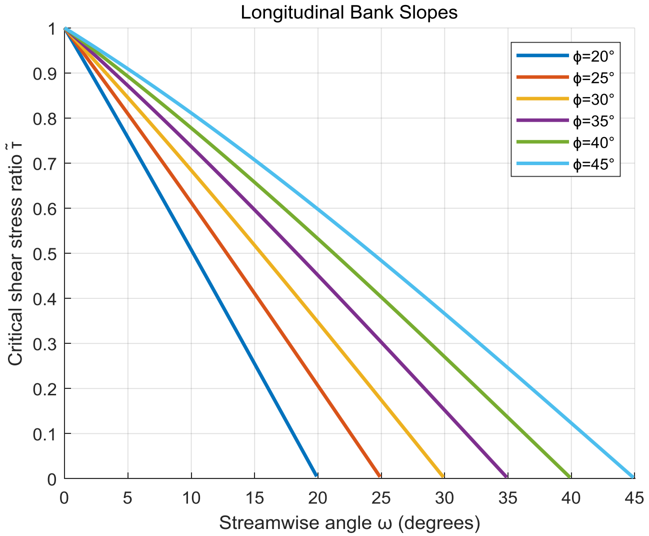

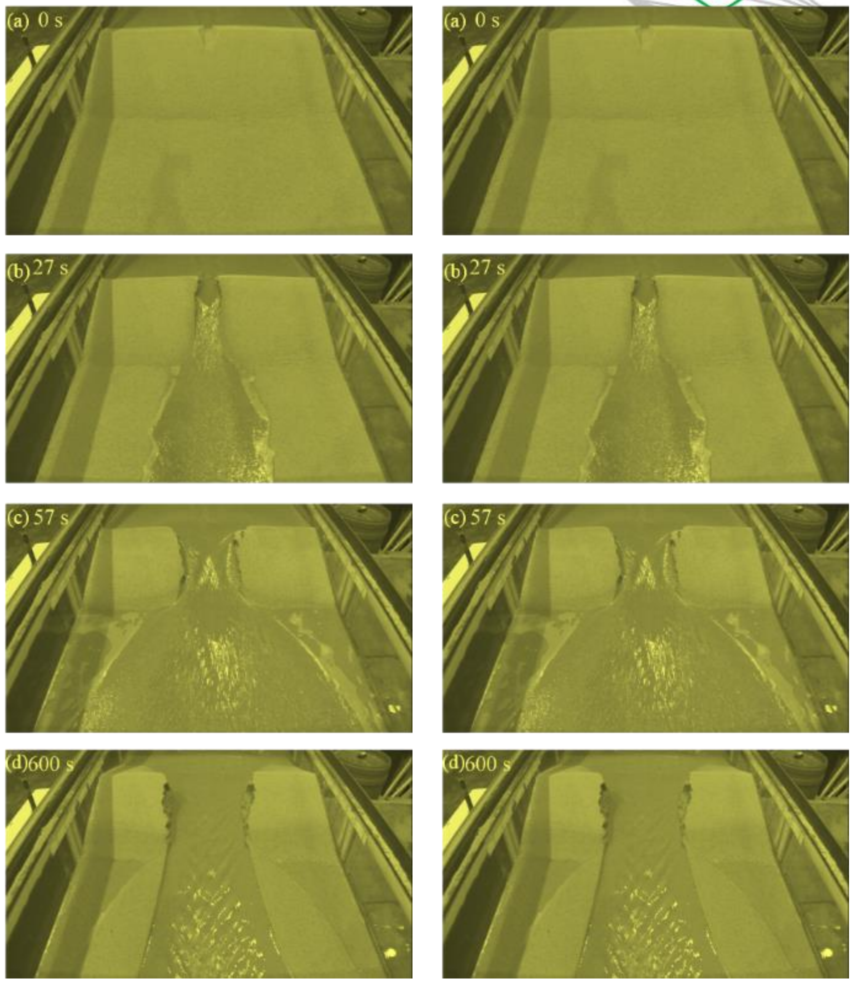

(Experiments by S. Van Emelen)

EXPERIMENT DESIGN

MORPHODYNAMICS OF BREACH GROWTH AND BANK EROSION USING LABORATORY EXPERIMENTS

- Definition of the test dimensions
- Selection of the dike and bank material
- Design of the construction procedure
- Test procedure (constant discharge or prescribed hydrograph)

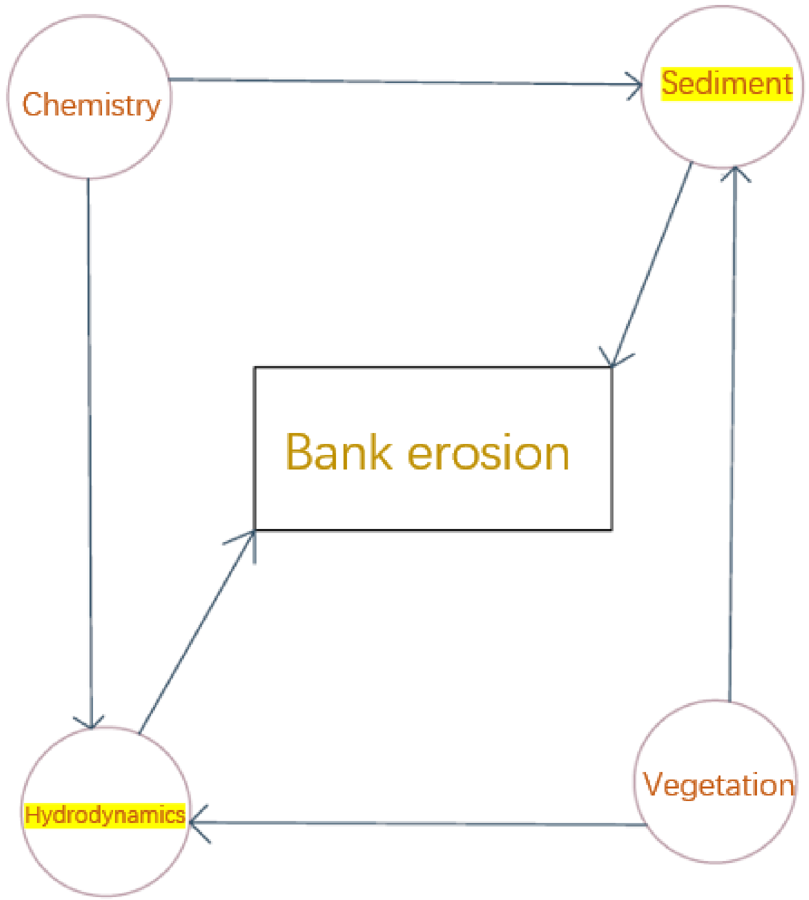

PLANNING

Tasks	2023		2024				2025				2026				2027				2028
	9	12	3	6	9	12	3	6	9	12	3	6	9	12	3	6	9	12	3
EngD																			
Literature review																			
Experiment Design																			
Qualifier							Q-EngD												
Experiment on breach growth																			
Assessment and improvement of formulation																			
Implement formulations in modeling																			
Defence											D-EngD								
PhD																			
Experiment Design																			
Qualifier												Q-PhD							
Experiment on bank erosion																			
Assessment and improvement of formulation																			
Implement formulations in modeling																			
Application to real case																			
Defence																			D-PhD

THANK YOU !

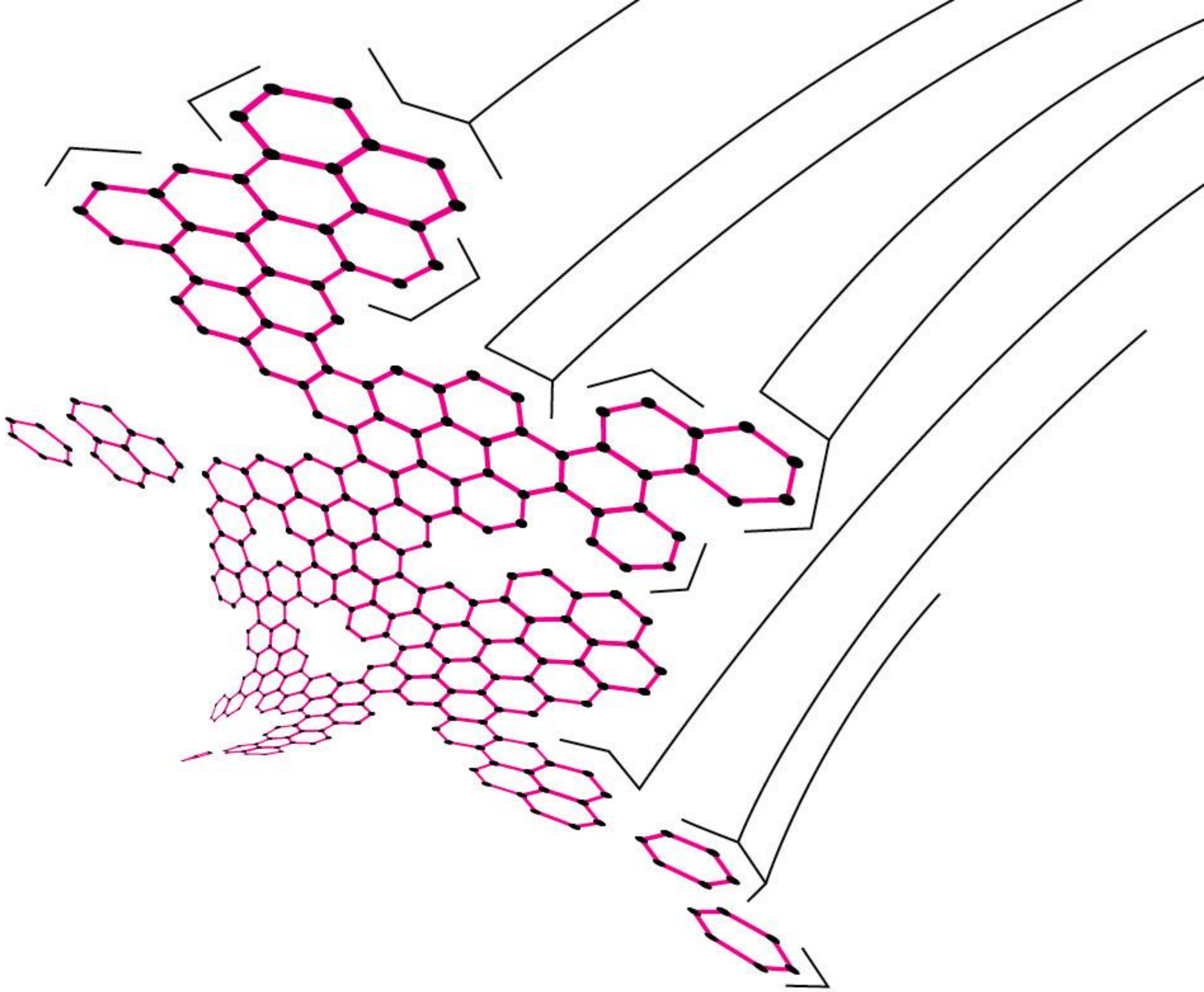

SEDIMARE 2023-2027

Sediment Transport and Morphodynamics in Marine and Coastal Waters with Engineering Solutions

- Eloah Rosas
- e.rosas@fugro.com

Marie Skłodowska-Curie Actions

AUV Operator

- Autonomous Underwater Vehicle Operator – Brazil - 2015

- Pipeline survey Inspection Project in the Offshore platforms in Brazil

ADCP
CTD
Turbidity Sensor
Multi bean
Sonar

Master

SEDIMARE 2023-2027
Sediment Transport and Morphodynamics in Marine and Coastal Waters with Engineering Solutions

Coastal and Marine System – University of Algarve Portugal

Journal of *Marine Science and Engineering*

MDPI

Article

Marine Litter on the Coast of the Algarve: Main Sources and Distribution Using a Modeling Approach

Eloah Rosas [1,*], Flávio Martins [1,2] and João Janeiro [1]

1 Centro de Investigação Marinha e Ambiental (CIMA), Campus de Gambelas, University of Algarve, 8005-139 Faro, Portugal; fmartins@ualg.pt (F.M.); jmjaneiro@ualg.pt (J.J.)
2 Instituto Superior de Engenharia (ISE), Campus de Gambelas, University of Algarve, 8005-139 Faro, Portugal
* Correspondence: egrosas@ualg.pt

Master thesis - Methodology

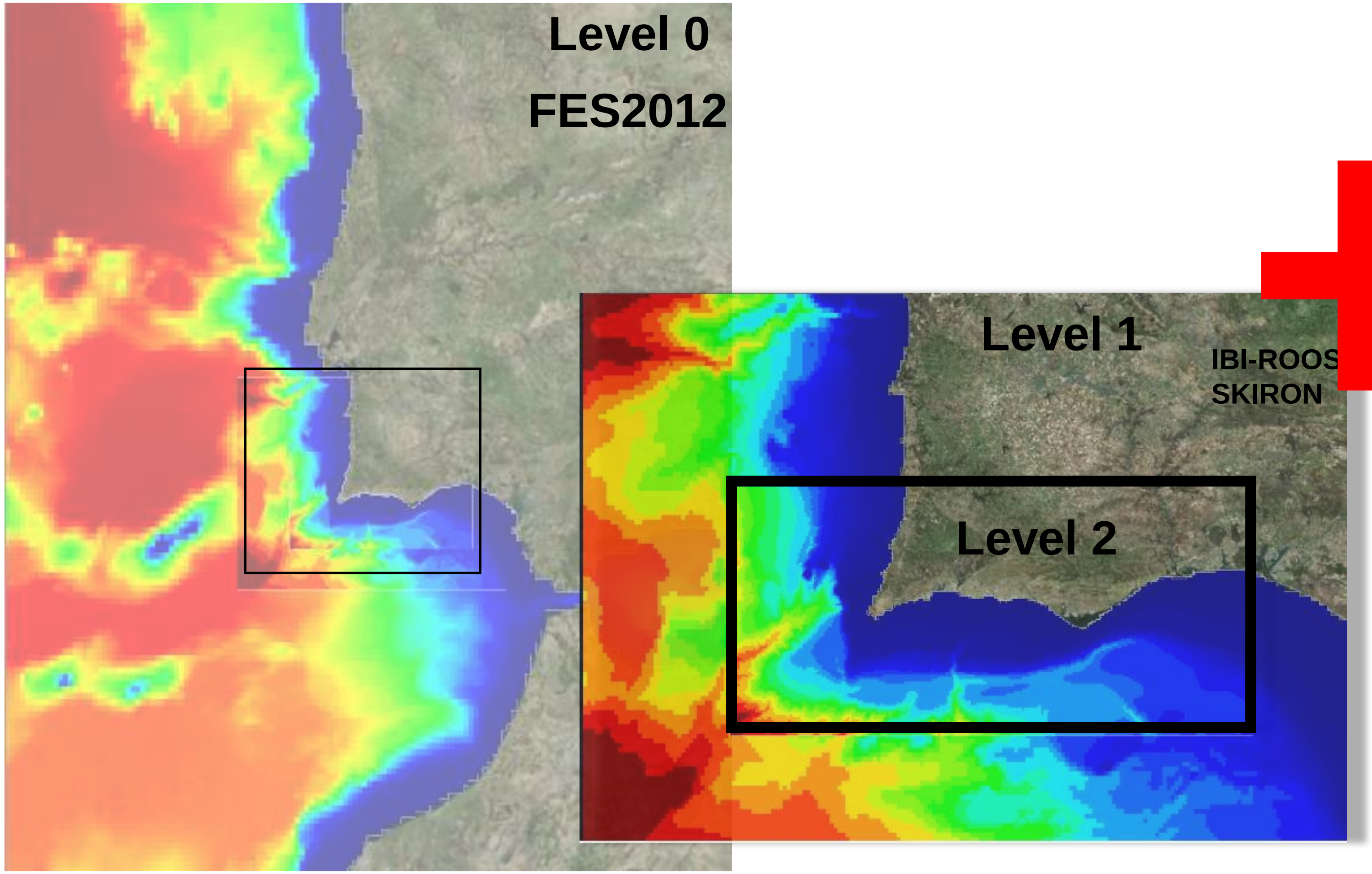

Master – Pathways of Floating litter

SEDIMARE 2023-2027
Sediment Transport and Morphodynamics in Marine and Coastal Waters with Engineering Solutions

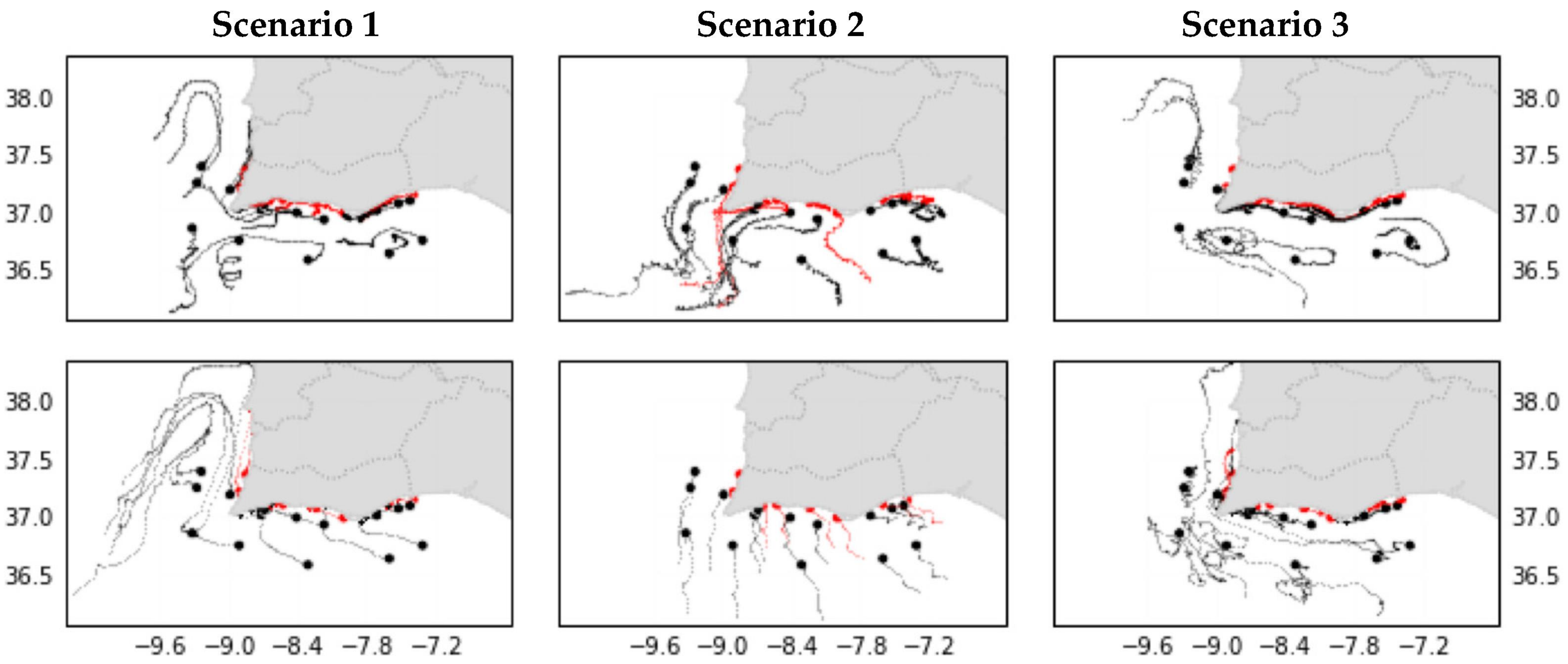

Journal of *Marine Science and Engineering*

MDPI

Article

Pathways and Hot Spots of Floating and Submerged Microplastics in Atlantic Iberian Marine Waters: A Modelling Approach

Eloah Rosas [1,*], Flávio Martins [1,2], Marko Tosic [3], João Janeiro [1], Fernando Mendonça [1] and Lara Mills [1]

1 Centro de Investigação Marinha e Ambiental (CIMA), Campus de Gambelas, University of Algarve, 8005-139 Faro, Portugal
2 Instituto Superior de Engenharia (ISE), Campus de Gambelas, University of Algarve, 8005-139 Faro, Portugal
3 School of Applied Sciences and Engineering, Universidad EAFIT, CRA.49#7S-50, Medellín 050022, Colombia
* Correspondence: egrosas@ualg.pt

Abstract: Plastic pollution has been observed in many marine environments surrounding the Iberian Peninsula, from the surface water to deeper waters, yet studies on their pathways and accumulation areas are still limited. In this study, a global ocean reanalysis model was combined with a particle-tracking Lagrangian model to provide insights into the pathways and accumulation patterns of microplastics originating in southern Portuguese coastal waters (SW Iberian). The study investigates microplastics floating on the surface as well as submerged at different water depths. Model results suggest that the North Atlantic Gyre is the main pathway for microplastics in surface and subsurface waters, transporting the microplastics southwards and eastwards towards the Mediterranean Sea and the Canary Islands. Currents flowing out of the Mediterranean Sea act as the main pathway for microplastics in deep waters, transporting the microplastics along western Iberia. An average residence time of twenty days in the coastal waters suggests that microplastics do not accumulate close to their sources due to their relatively fast transport to adjacent ocean areas. Notably, a significant proportion of microplastics leave the model domain at all depths, implying that SW Iberia may act as a source of microplastics for the adjacent areas, including the Mediterranean Sea, Morocco, the Canary Islands, Western Iberia, and the Bay of Biscay.

Keywords: microplastics; pathways; accumulation; SW Iberia; numerical model

check for updates

Citation: Rosas, E.; Martins, F.; Tosic, M.; Janeiro, J.; Mendonça, F.; Mills, L. Pathways and Hot Spots of Floating and Submerged Microplastics in Atlantic Iberian Marine Waters: A Modelling Approach. *J. Mar. Sci. Eng.* **2022**, *10*, 1640. https://doi.org/10.3390/jmse10111640

Methodology – Microplastic Model

SEDIMARE 2023-2027
Sediment Transport and Morphodynamics in Marine and Coastal Waters with Engineering Solutions

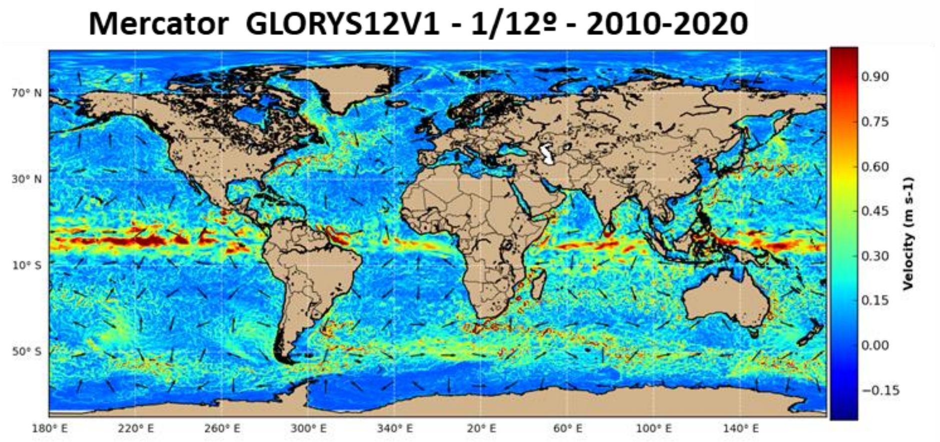

+

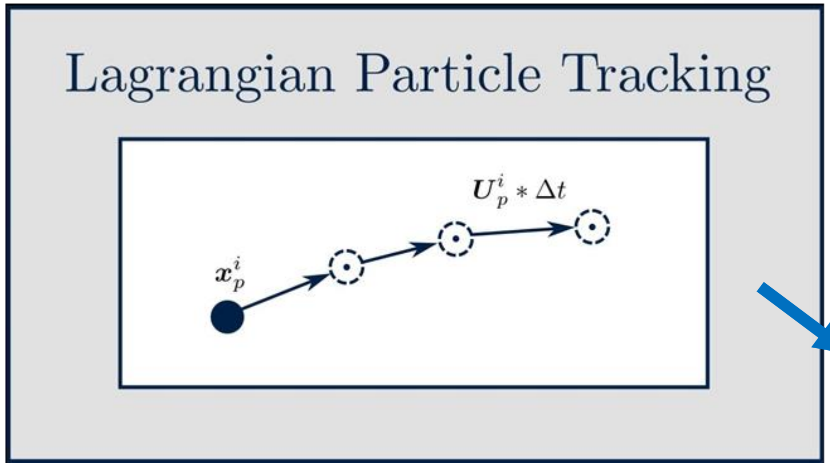

OpenDrift

=

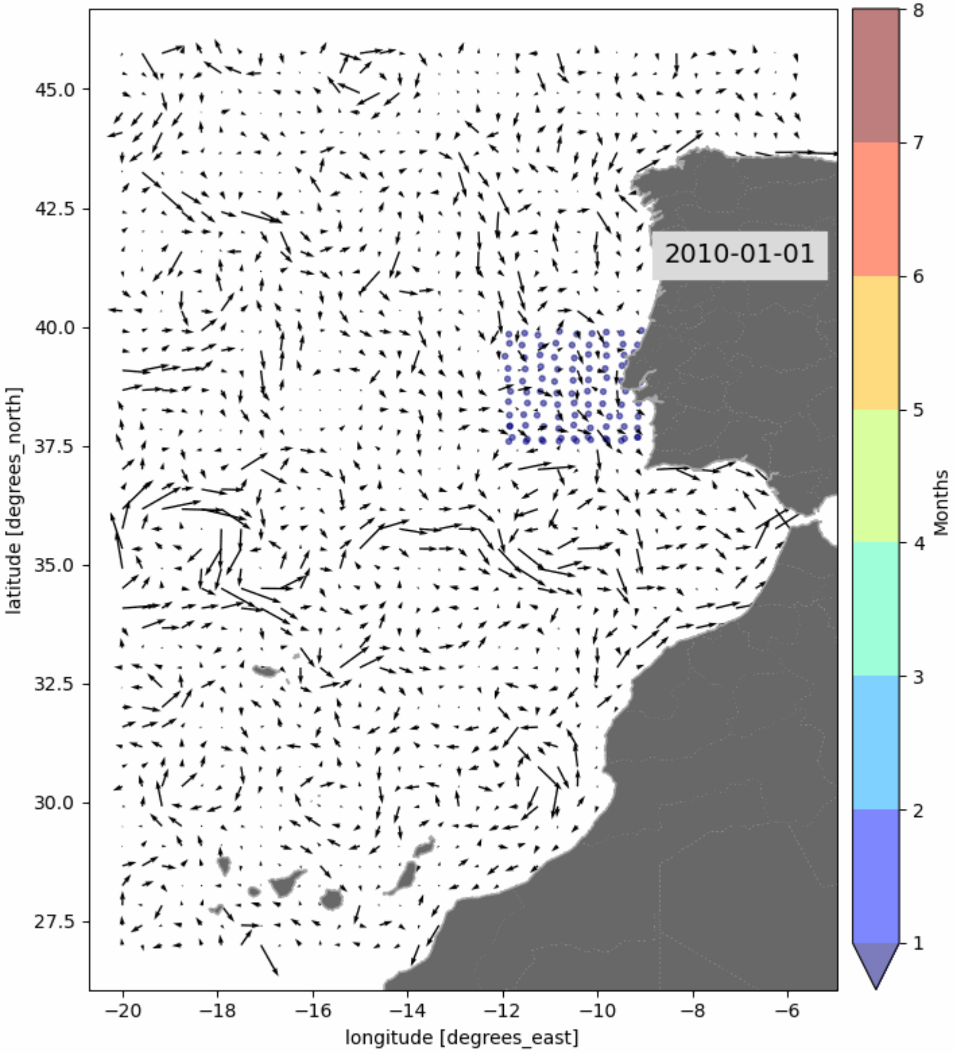

Marie Skłodowska-Curie Actions

FUGRO

Pathways of Microplastics

SEDIMARE 2023-2027
Sediment Transport and Morphodynamics in Marine and Coastal Waters with Engineering Solutions

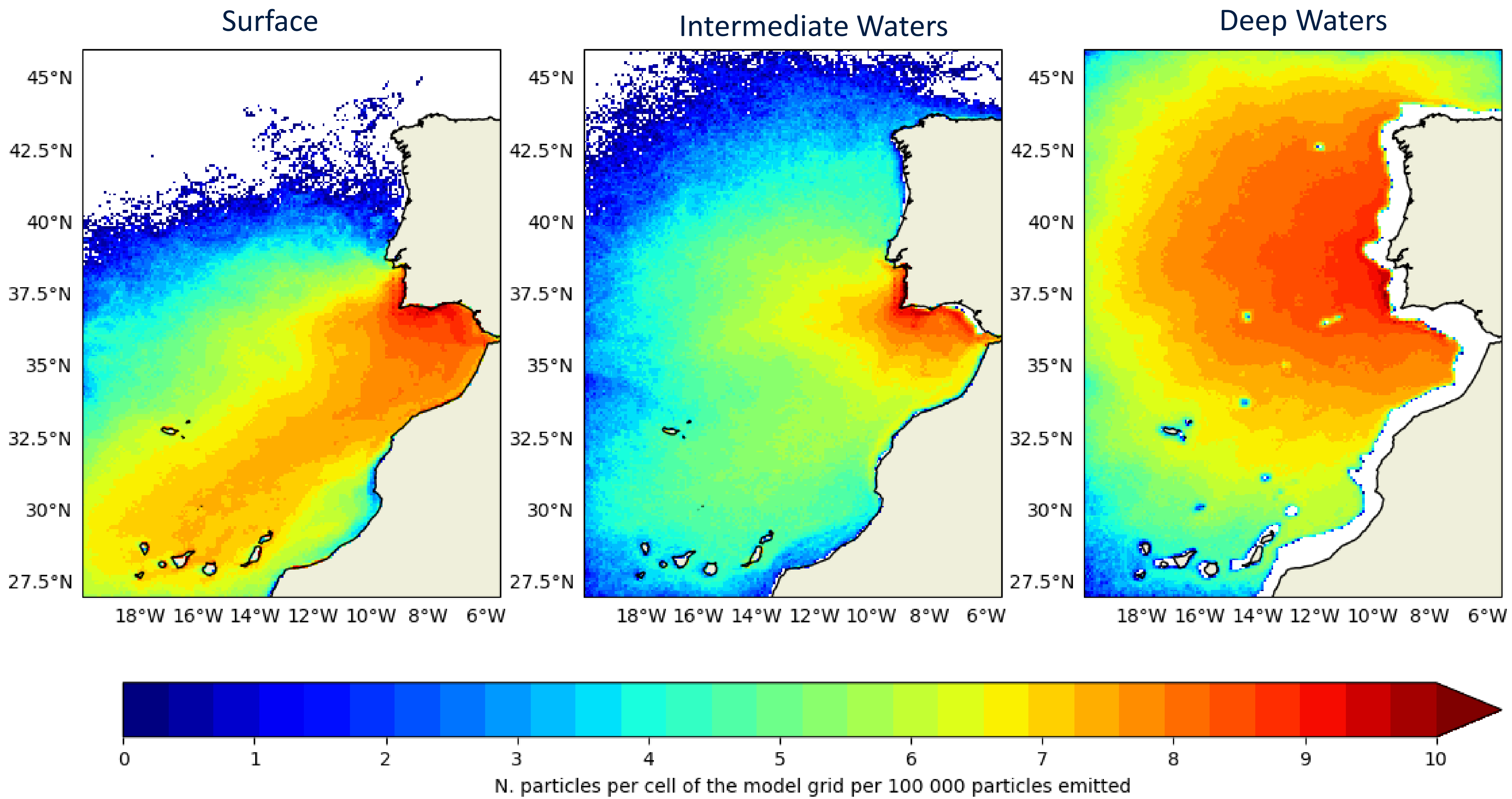

Marie Skłodowska-Curie Actions

FUGRO

Identifying the sources of Microplastics

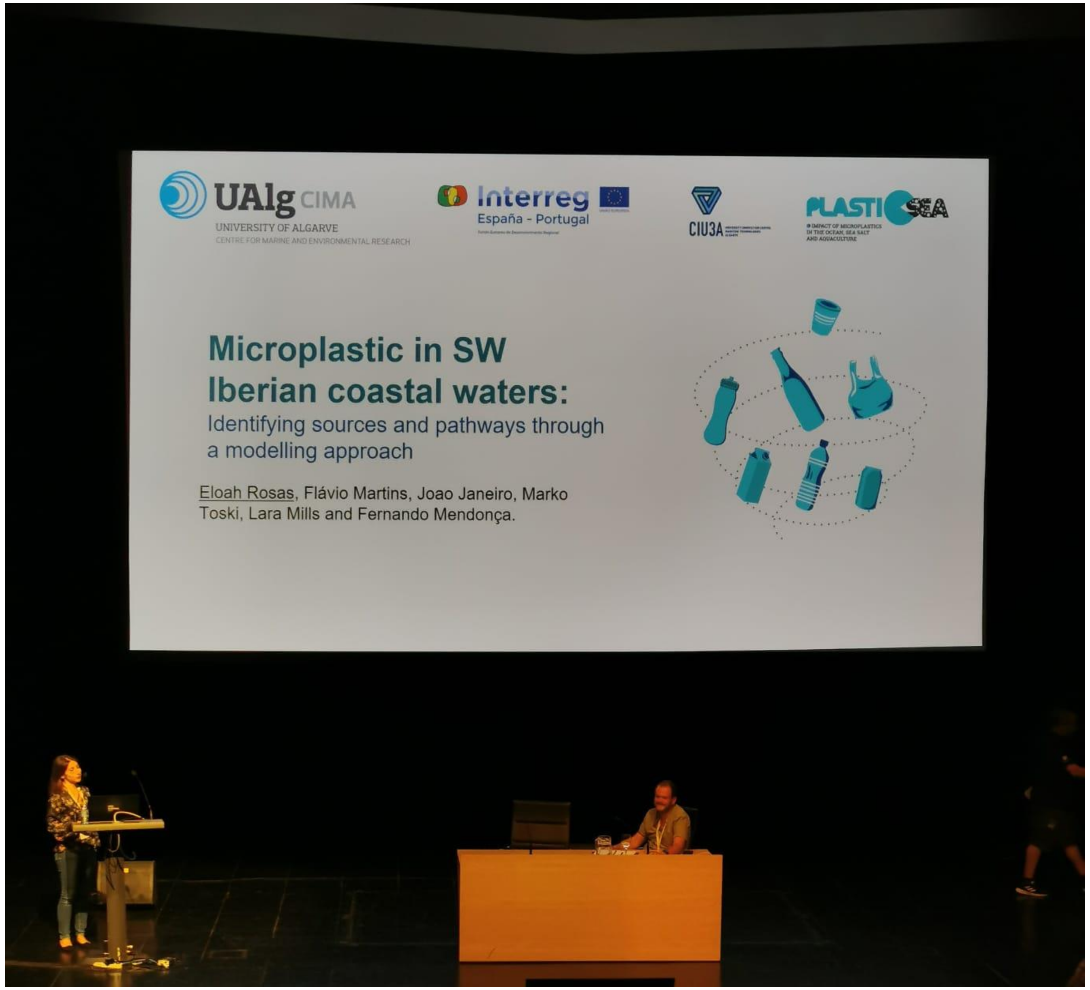

Sources of Microplastic - Methodology

Land	Ocean	Boundaries
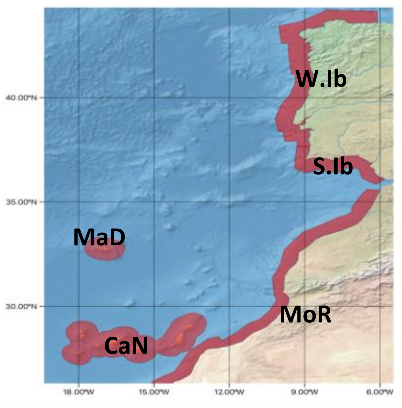	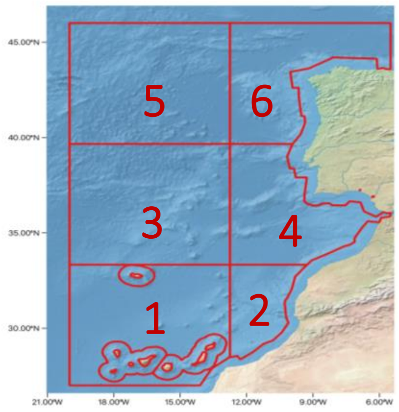	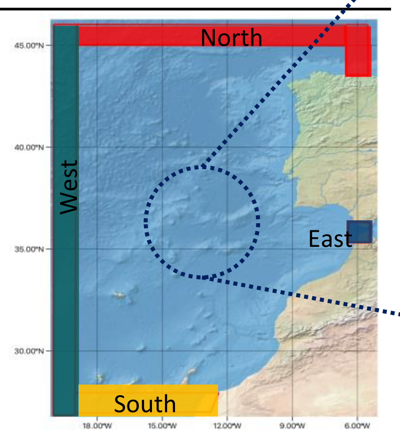

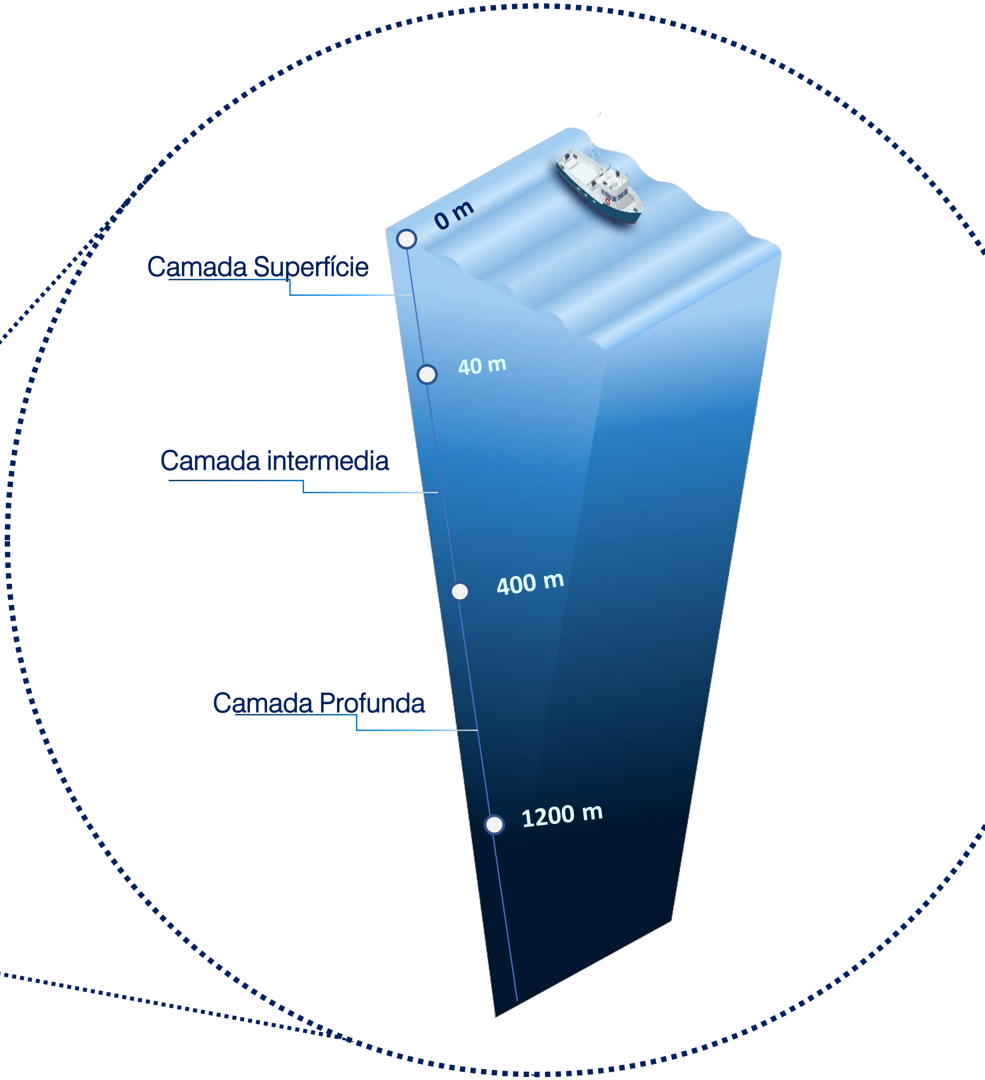

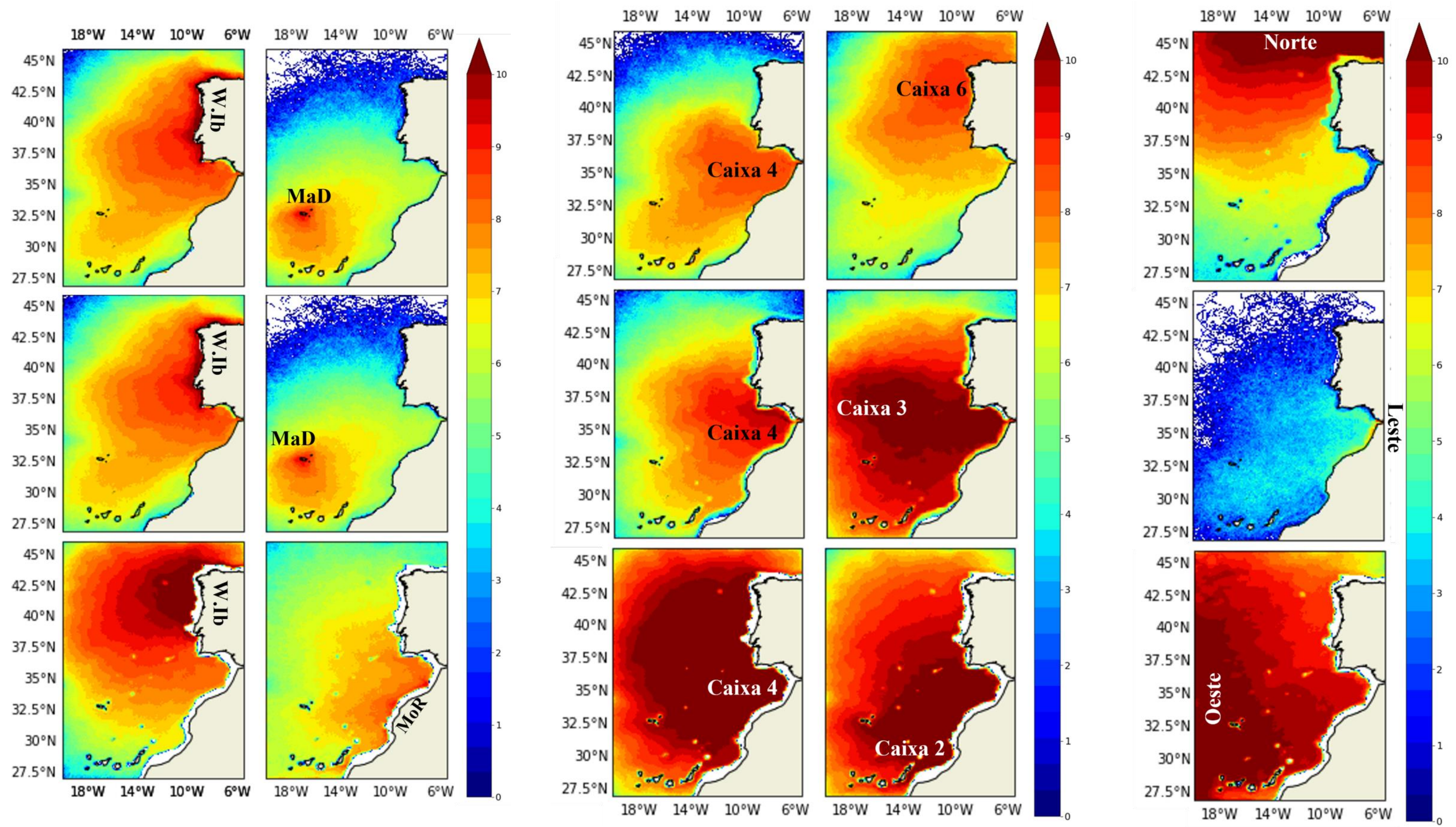

W.Ib
MaD
MoR
Caixa 4
Caixa 6
Caixa 3
Caixa 2
Norte
Leste
Oeste
18°W 14°W 10°W 6°W
45°N 42.5°N 40°N 37.5°N 35°N 32.5°N 30°N 27.5°N
0 1 2 3 4 5 6 7 8 9 10

University + Portuguese Navy

LAUV - Light Autonomous Underwater Vehicle

DVL – Doppler Velocity Log
CTD - Conductivity, Temperature and Depth
ADCP - Acoustic Doppler Current Profiler

Università Politecnica delle Marche
Dipartimento di Ingegneria Civile, Edile e Architettura (DICEA),
MAC - SEDIMARE

Overtopping Breakwater For Energy Conversion (OBREC)

DC10–Saeed Osouli

Supervisors:

Prof. Matteo Postacchini – UNIVPM

DR. Ivan Sabbioni – MAC

Prof. Maurizio Brocchini – UNIVPM

SEDIMARE
1st Network Training School: Numerical Methods in Coastal Hydrodynamics and Sediment Transport
University of Nottingham
April 22-24, 2024

Introduction

- Advantages of an innovative vertical breakwater with an overtopping wave energy converter (2020)

1. Increasing the relative freeboard, reduces the relative overtopping discharge.

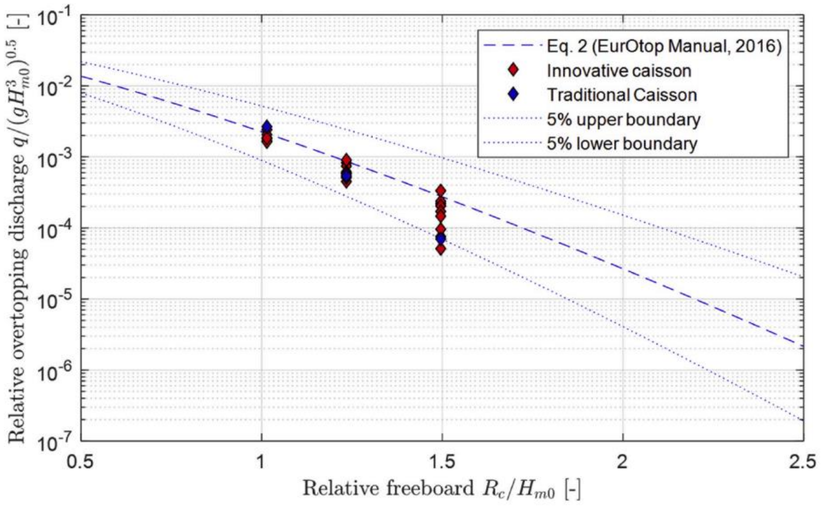

Fig. 8. Measured numerical data of the wave overtopping discharges over the traditional (blue points) and the innovative OBREC caisson (red points). Wave overtopping equation for vertical breakwater (Eq. 7.1 in EurOtop, 2016) with 5% under and upper exceedance limits is reported with blue dotted lines. (For interpretation of the references to colour in this figure legend, the reader is referred to the Web version of this article.)

8

- Overtopping device numerical study: OpenFoam solution verification and evaluation of curved ramps performances (2019)

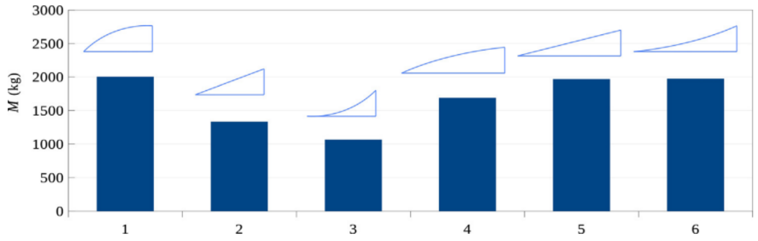

Fig. 19. Average discharge peak for all analyzed ramps shapes.

1. In comparison to the regular ramp shape, curves effect changes by difference with the ratio of H1/L1.

y the

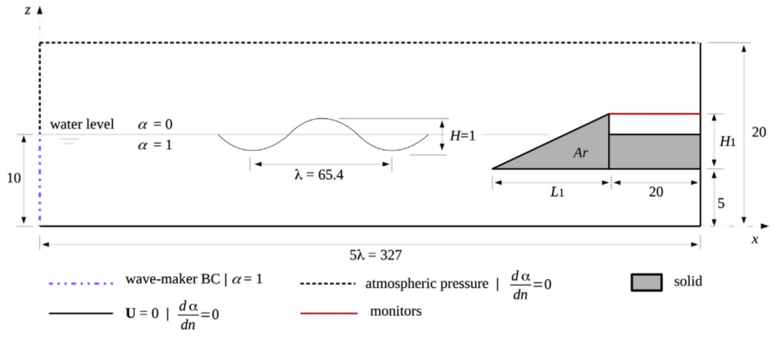

Fig. 6. Schematic domain studied in Martins et al. [16] (dimensions in m; not in scale).

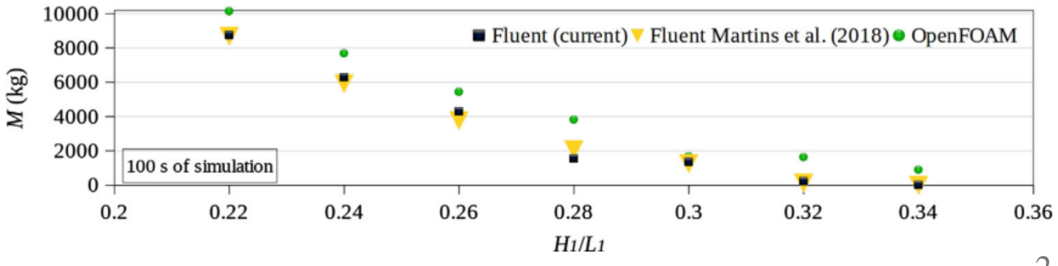

Fig. 13. Water discharge inside the reservoir for all H_1/L_1 studied conditions.

Introduction

- A Simple Model to Assess the Performance of an Overtopping Wave Energy Converter Embedded in a Port Breakwater (2020)

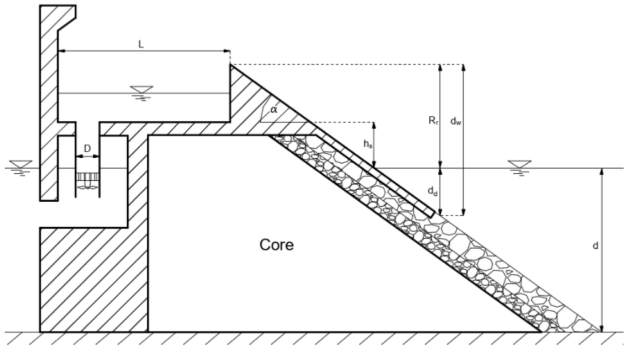

Figure 1. Sketch of an OBREC cross-section and definition of the main geometrical parameters to be considered for design.

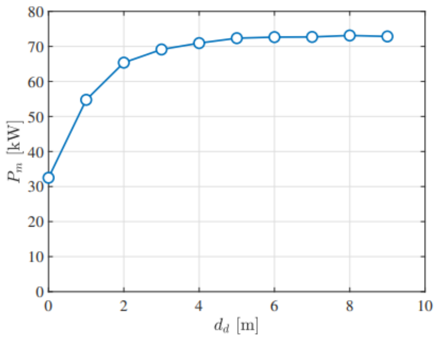

Figure 9. Yearly average output power versus the variation of d_d ($N = 50$, $R_r = 2.5$ m and $h_s = 2$ m).

- Empirical overtopping volume statistics at an OBREC(2019)

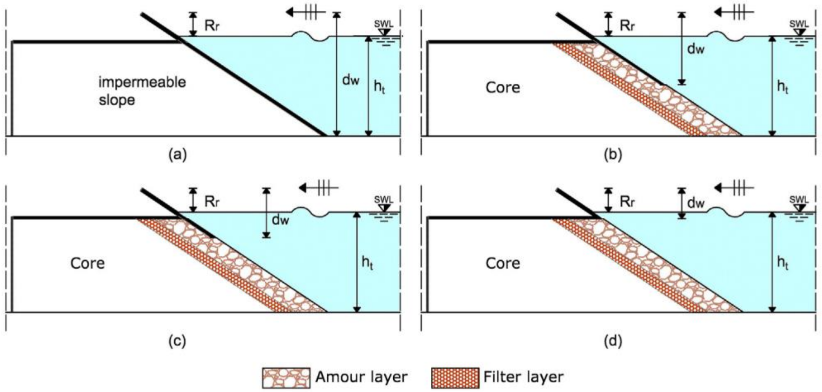

Fig. 3. OBREC configurations analyzed in the present experimental campaign: a) $d_w = 0.274$ m ($d_w^* = 1.0$); b) d_w 0.166 m ($d_w^* = 0.6$); c) $d_w = 0.113$ m ($d_w^* = 0.4$); d) $d_w = 0.064$ m ($d_w^* = 0.2$). R_r indicates the crest free-board and h_t indicates the water depth at the model toe.

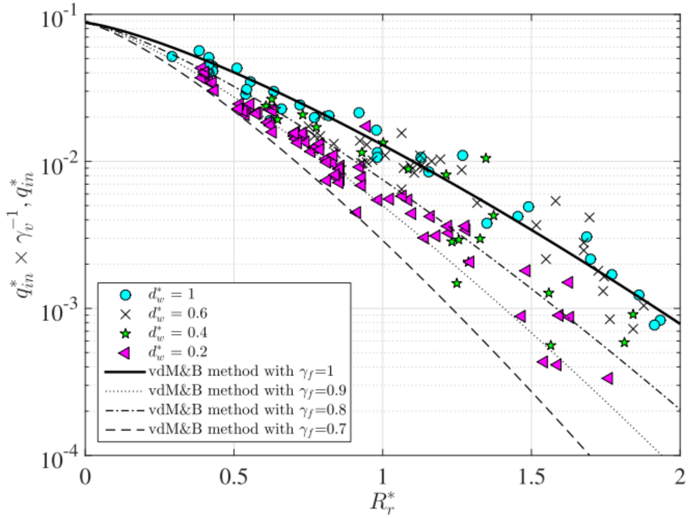

Fig. 8. Comparison of the average wave overtopping rates measured for all configurations tested in the present tests and those estimated by the prediction method of van der Meer and Bruce (2013) adopting four different values of γ_f. The experimental data were corrected using the coefficient γ_V.

Introduction

- Crown Wall Modifications as Response to Wave Overtopping under a Future Sea Level Scenario: An Experimental Parametric Study for an Innovative Composite Seawall (2020)

1. Relative overtopping discharge is plotted against the Iribarren number:

$$\xi_0 = \frac{\tan\alpha}{\sqrt{\frac{H_0}{L_0}}}$$

$\lambda^* = \lambda/\lambda_{small}$, where $\lambda_{small} = 0.10$ and $\lambda = h_{nose}/h_w$

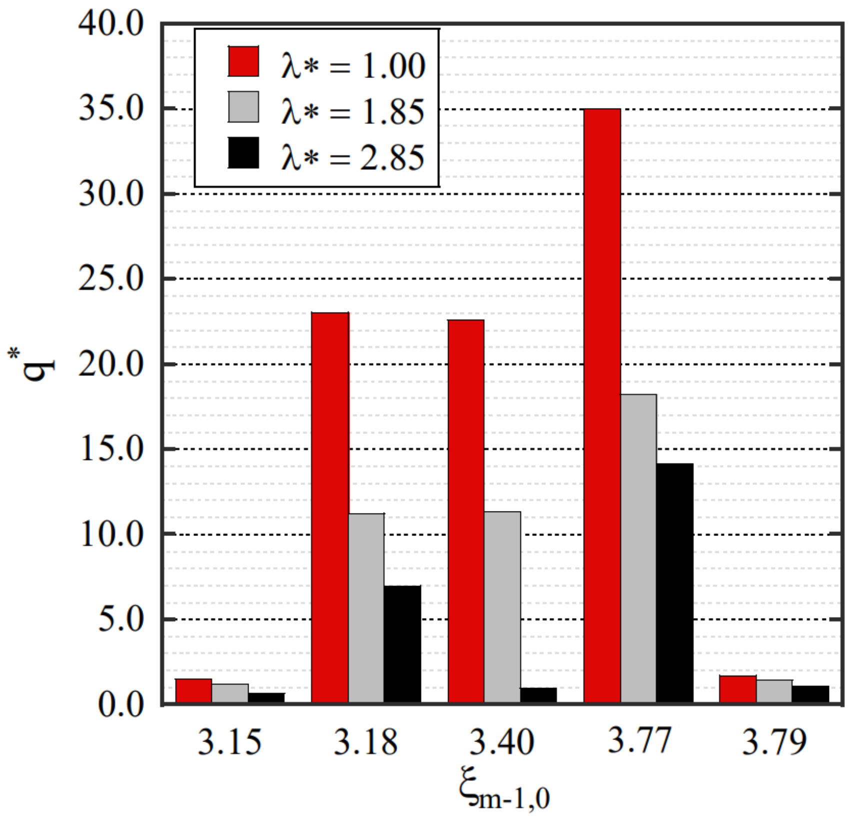

Figure 12. Relative overtopping discharge, q*, against $\xi_{m-1,0}$.

Appl. Sci. **2020**, 10, 2227 8 of 19

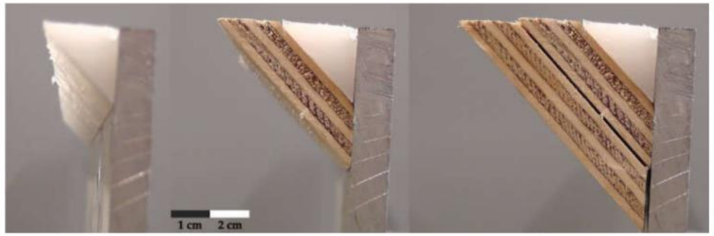

(a) (b) (c)

Figure 7. Photos showing the nose in (**a**) small configuration, (**b**) large configuration and (**c**) extra-large configuration.

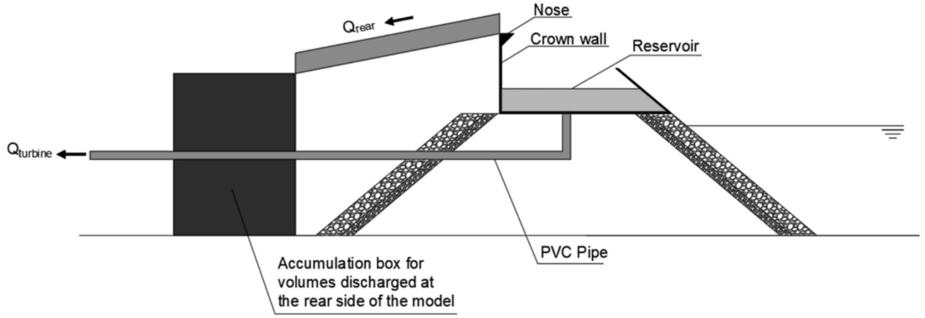

Introduction

- Prototype Overtopping Breakwater for Wave Energy Conversion at Port of Naples **(2016)**

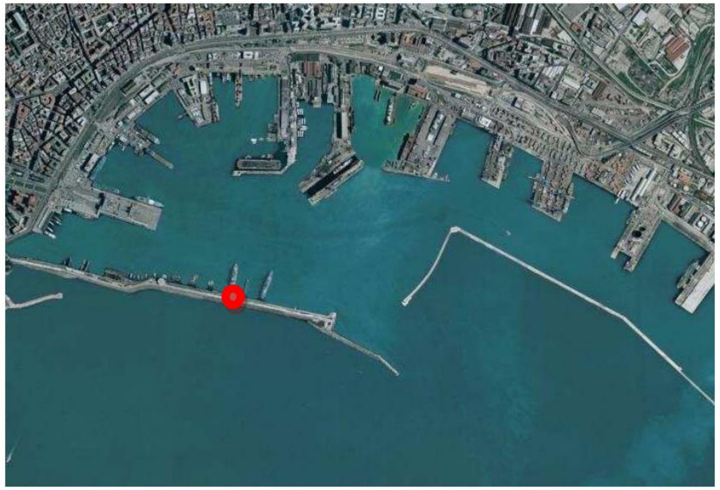
Fig. 2 - Plan view of the location of the OBREC prototype at Naples port (Italy)


Fig. 6 - Antifers handling by mobile crane


Fig. 7 - Construction of micropiles by micropiles drilling rig


Fig. 8 - The bottom slab construction


Fig. 9 - Positioning of the prefabricated ramps


Fig. 10 - OBREC prototype under wave storm

Introduction

- Integrated assessment of the hydraulic and structural performance of the OBREC device in the Gulf of Naples, Italy (2020)

G. Palma, et al. Applied Ocean Research 101 (2020) 102217

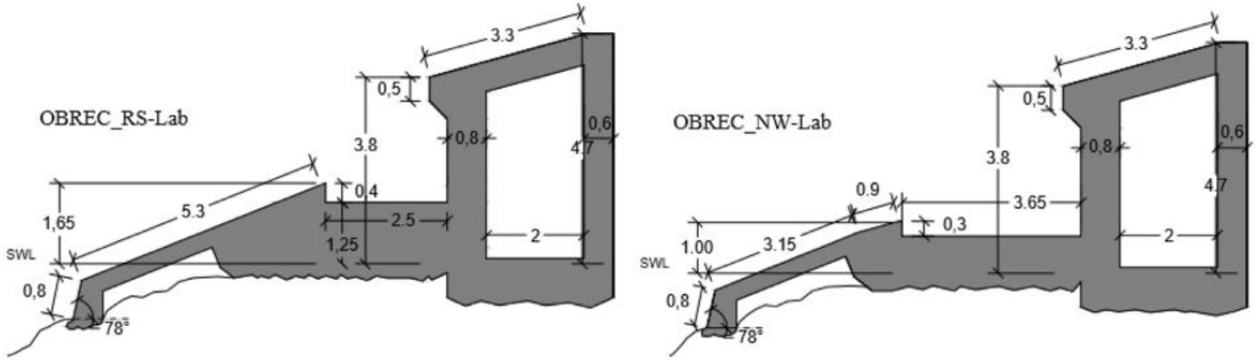

Fig. 2. Cross-sections of the OBREC prototype configurations in the Naples harbour: a) RS-Lab configuration; b) NW-Lab configuration [14].

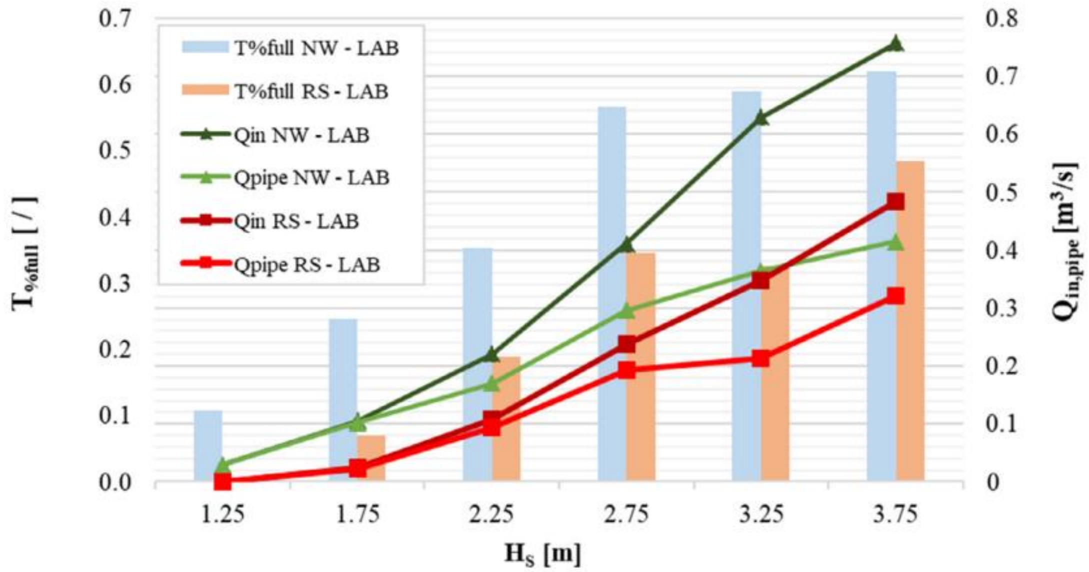

Fig. 16. Comparison between the discharge rate inside the reservoir Q_{in} and inside Q_{pipe} for both the configuration.

1. NW-Lab configuration gives more Q(in the pipe) and T%full.

Introduction

- The Influence of Ramp Shape Parameters on Performance of Overtopping Breakwater for Energy Conversion (2020)

1. They used Flow3D software, and simulations were done within the 60s.
2. Waves with the highest period and significant wave height did not give the maximum result.

Table 2. Ramp shape in polynomial equation expression.

Ramp Shape Name	Polynomial Equation	2D Illustrate	3D Illustration
Linear	$f(x) = -0.34x + 3$		
Convex	$f(x) = -0.037x^2 - 0.009x + 3$		
Concave	$f(x) = 0.037x^2 - 0.66x + 3$		

Table 2. Cont.

Ramp Shape Name	Polynomial Equation	2D Illustrate	3D Illustration
Cubic	$f(x) = -0.015x^3 + 0.191x^2 - 0.924x + 3$		
Cubic (-ve)	$f(x) = 0.015x^3 - 0.191x^2 + 0.27x + 3$		
Quantic	$f(x) = -0.0025x^5 + 0.0543x^4 - 0.415x^3 + 1.29x^2 - 1.729x + 3$		
Quantic(-ve)	$f(x) = 0.0025x^5 - 0.0543x^4 + 0.415x^3 - 1.29x^2 + 1.05x + 3$		

The comparison of overtopping rates at different wave conditions or local monsoon situations is presented in Figure 14. It is shown that the R3 condition gave a higher overtopping discharge rate compared to others. The outcome also indicates that overtopping will gradually increase with increasing wave height (R1–R3). However, the overtopping declined for wave condition R4, although it has a larger wave height compared to other conditions. Theoretically, overtopping rate is relatively proportional to the wave height and period. Among the possible explanations for what happens during R4 condition is being unaware of the effect of the wave number in experiment test. Since R4 have longer wavelength compared to other waves, it produces the least number of overtopping waves within 60 s of the experiment test. This outcome clearly indicates a strong relationship between wave characteristics into overtopping waves and needs an improvement in the experiment setup.

In this study, several wave parameters were used to see an overall effect of ramp shape into overtopping discharge. Four types of normal Malaysian wave characteristics were generated in both simulations and experiment. These waves represent average waves during non-monsoon season (R1), average waves in the year of 2013 (R2), average waves peak waves in the year of 2013 (R3), and average during monsoon season (R4). The corresponding wave parameters are given in Table 3.

Table 3. Statistical average of wave data according to monsoon.

Data Period	Period T_p (s)	Significant Wave Height H_s (m)
Average wave per year (R2)	6.67	1.245
Average Northeast monsoon (R4)	7.74	1.76
Average Southeast monsoon (R1)	4.99	0.79
Average max wave per year (R3)	7.13	1.53 (H_{max})

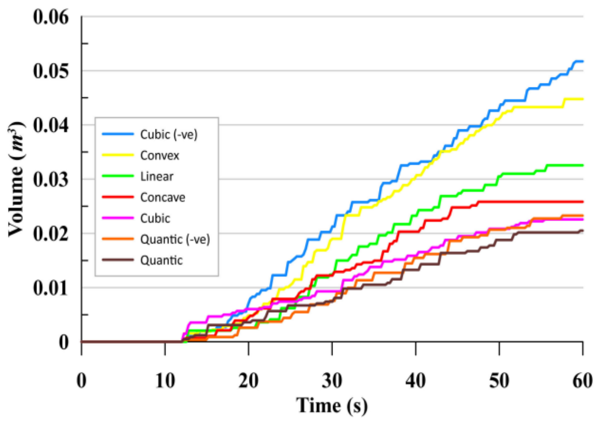

Figure 12. Comparison of overtopping volume for different ramp shapes.

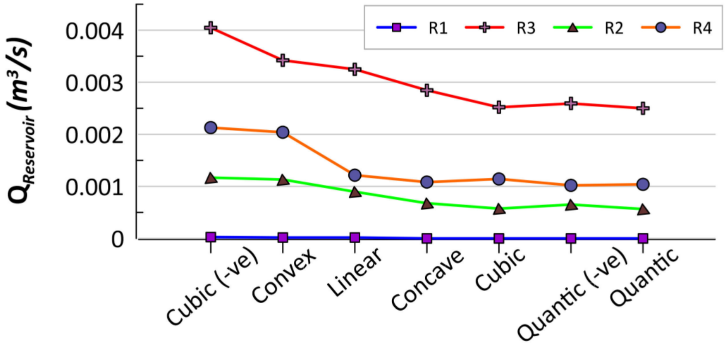

Figure 14. Overtopping rates at different monsoons.

Introduction

- Efficiency evaluation of a ductless Archimedes turbine: Laboratory experiments and numerical simulations

G. Zitti et al. / Renewable Energy 146 (2020) 867–879

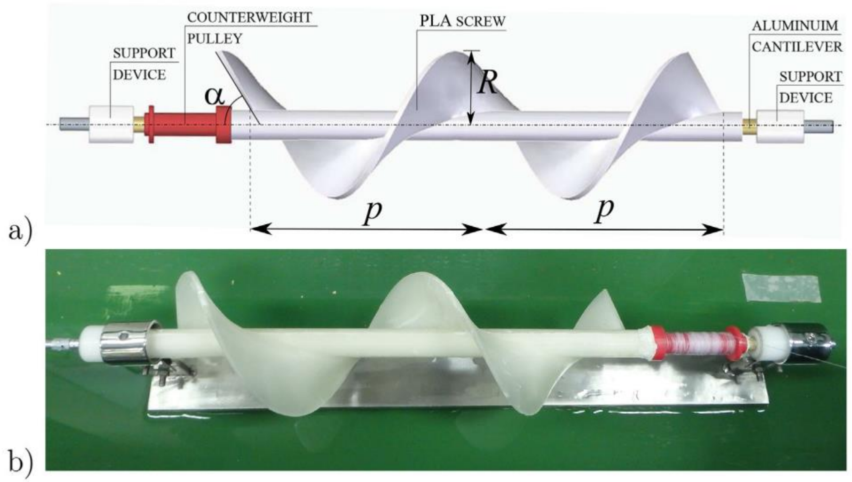

Fig. 3. The screw turbine used for the experiments. a) sketch of the screw turbine model with main components; b) top view of the turbine in the support system.

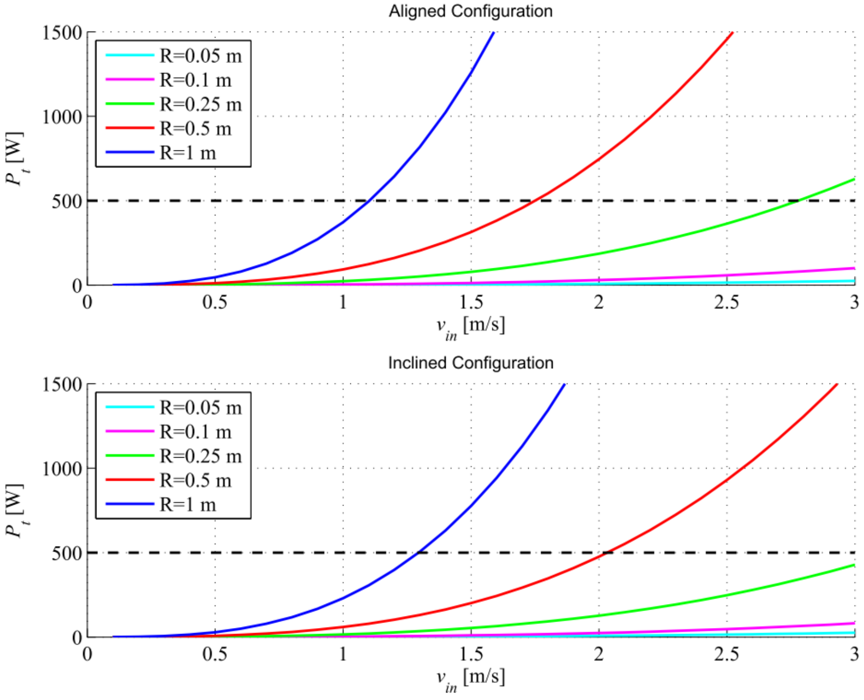

Fig. 12. Power generated by Archimedean-Type Hydrokinetic turbines, with different radii R and for different water flow v_{in}.

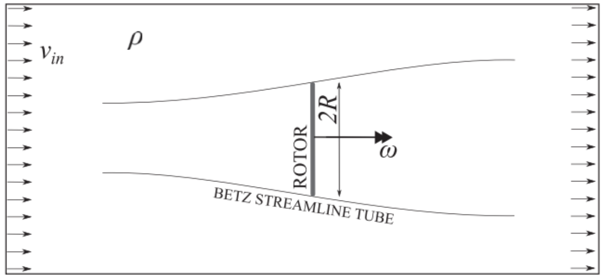

Fig. 1. Sketch of Betz' model.

1. Archimedes screw in the aligned configuration has a good output.

Potential Location of the

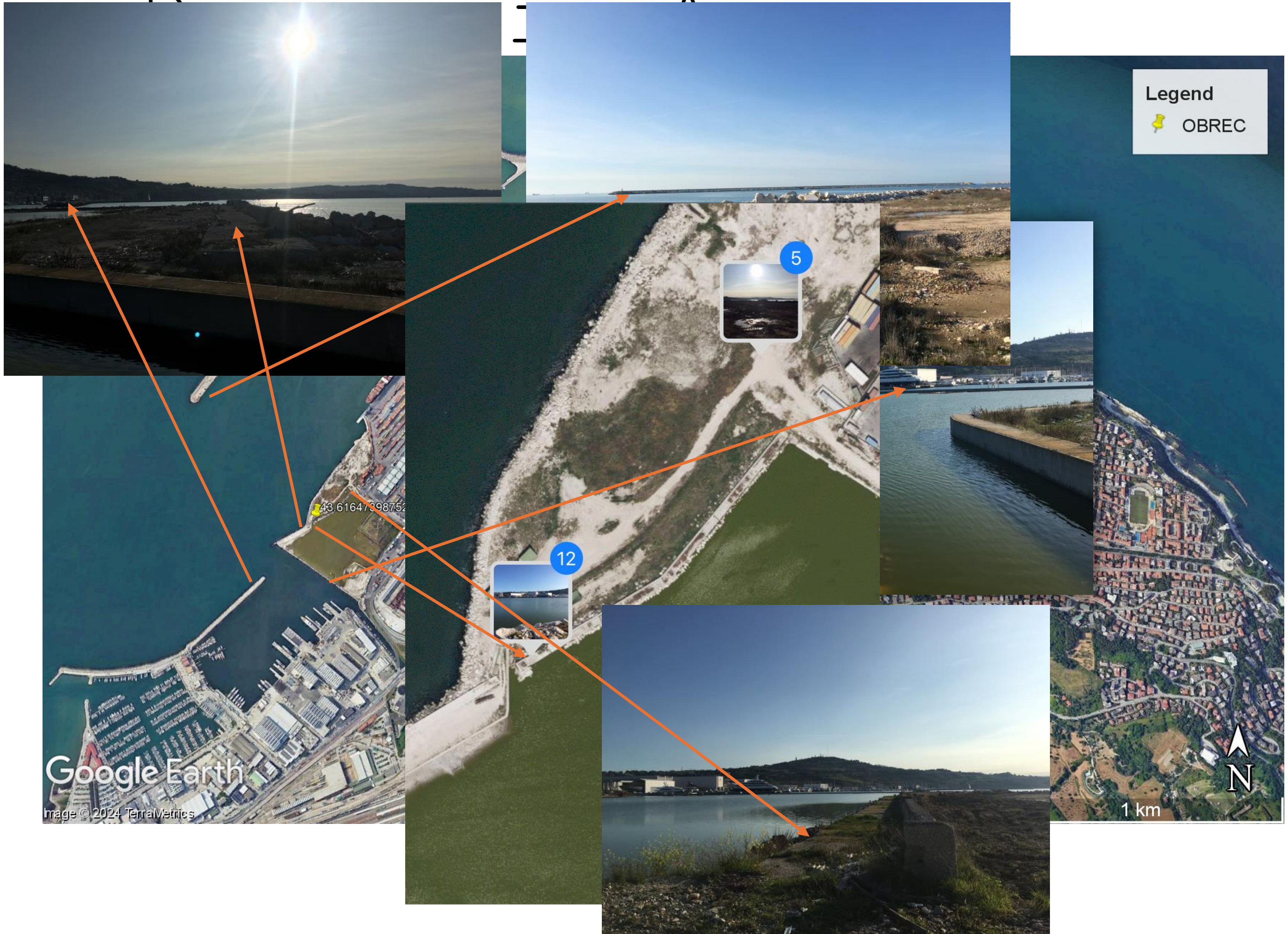

Methodology

Volume conservation:

$$\eta_t + \nabla \cdot M = 0$$

M is the horizontal volume flux.

The depth-averaged horizontal momentum:

$$u_{\alpha,t} + (u_\alpha \cdot \nabla) u_\alpha + g\nabla_\eta + V_1 + V_2 + V_3 + R = 0$$

R: diffusive and dissipative terms (e.g. bottom friction, sub-grid lateral turbulent mixing)

V_1 and V_2 are terms representing the dispersive Boussinesq terms (function of z_α).

V_3 contribution of the order O(μ^2) (function of z_α). $\mu = \frac{h}{l}$

$z_\alpha = \zeta h + \beta\eta$ that $\zeta and \beta$ are constants.

u_α z_α .

- FUNWAVE-TVD (Wave-resolving model) will be used as a shallow water solver.

It is based on Boussinesq-type equations in which Reynolds equations are integrated over the water depth, so the vertical structure is not directly resolved but only modelled. (2DH models)

Bathymetry of the Port of Ancona for FUNWAVE:
Combination of port bathymetry from port Authorities (CAD) and EMODnet data.

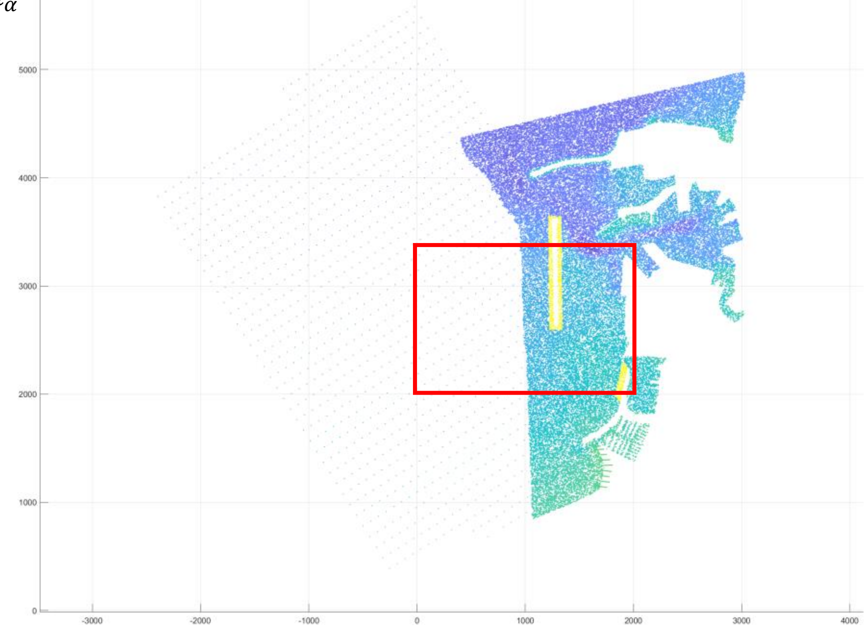

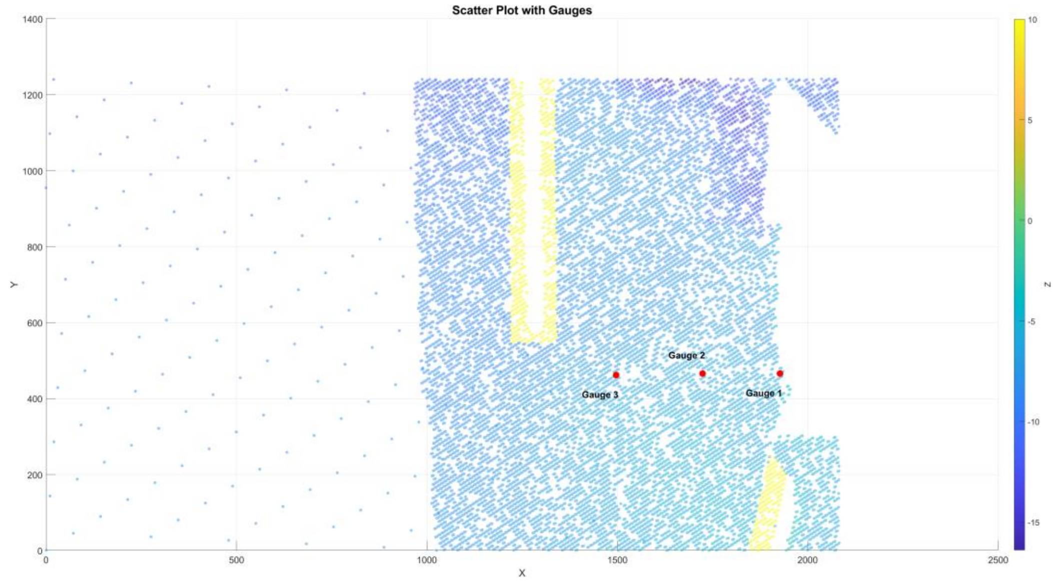

Methodology

- **Wave and Structure Interaction (**
CFD and/or SPH software
- **Designing the conveying system (**
Ansys Fluent, FLOW3D, …
- **Experimental tests**
- **Monitoring of the device (**D3.10**)**

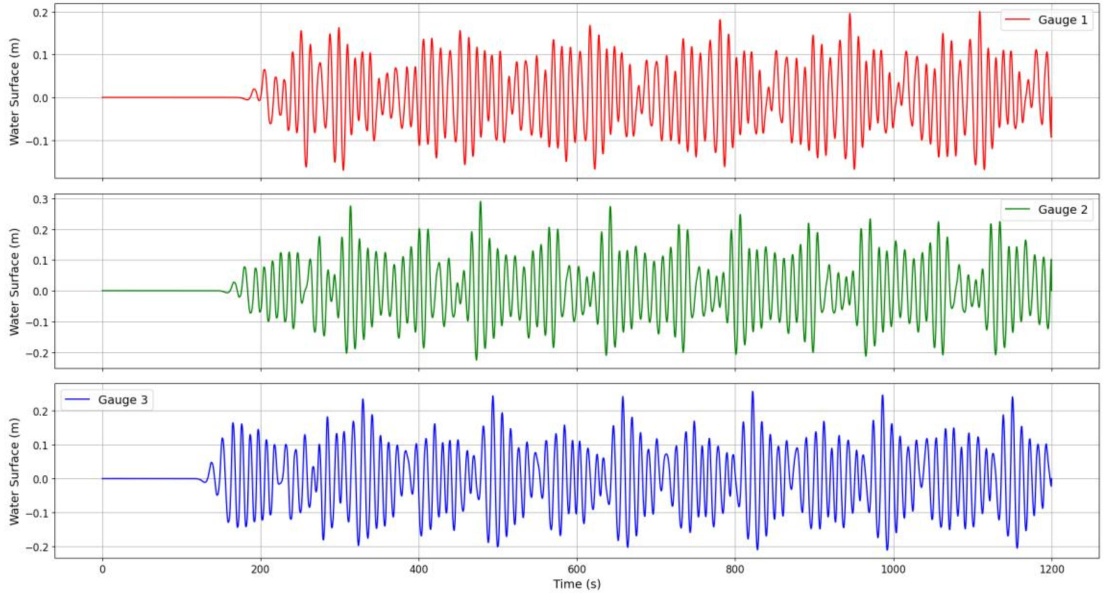

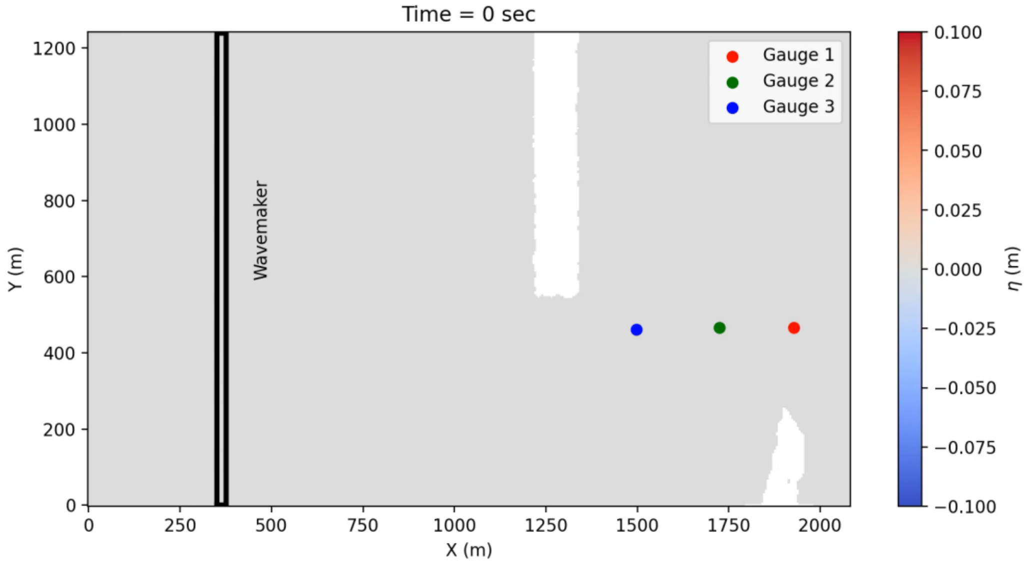

Thank You for Your Attention

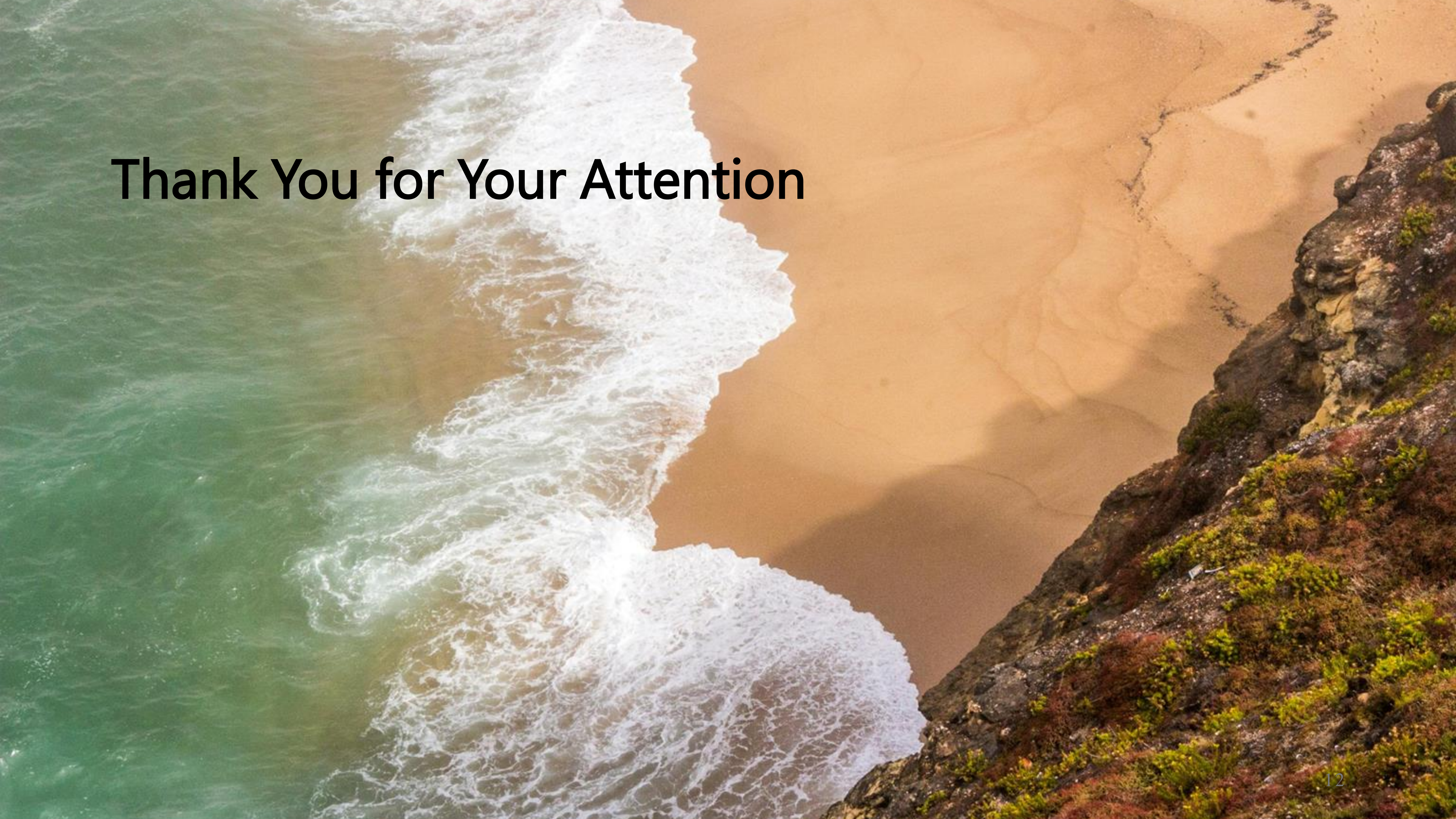

University of Nottingham
UK | CHINA | MALAYSIA

HORIZON EUROPE

Marie Skłodowska-Curie Actions

SEDIMARE 2023-2027
Sediment Transport and Morphodynamics in Marine and Coastal Waters with Engineering Solutions

1st Network Training School: Numerical Methods in Coastal Hydrodynamics And Sediment Transport

University of Nottingham, UK

April 22nd – 24th, 2024

SEDIMARE 2023-2027

Sediment Transport and Morphodynamics in Marine and Coastal Waters with Engineering Solutions

Morphodynamic swash zone modelling

Doctoral Candidate (#11): Quan NGUYEN

Supervising Scientists: Nicholas DODD and Riccardo BRIGANTI

Introduction

The swash zone

Research motivation

- The deficiency of present models is their inability to adequately represent the wave boundary layer, in shoaling, surf and swash zones.
- A recent bottom boundary layer (BBL) sub-model for a fixed bed in the swash zone has shown great performance in predicting with high accuracy water depths and velocities on non-erodible beaches.

➢ Further developed on mobile bed beaches, to improve our capacity to predict coastal accretion and erosion accurately.

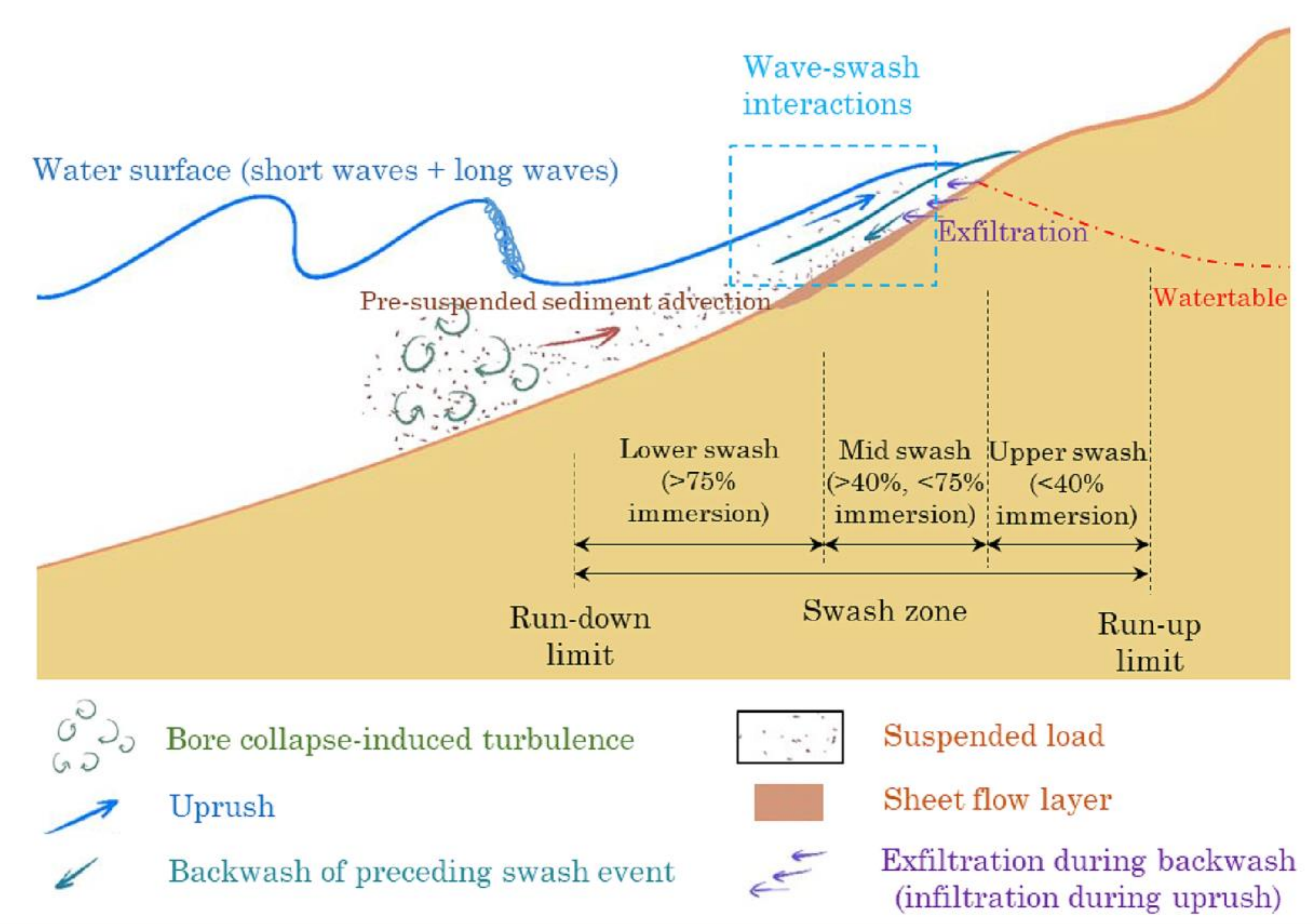

Schematic overview of physical processes in the swash zone (W. Chen et al, 2023).

Swash zone modelling

Hydro-morphodynamical solvers

Solved Equations	
Spatial resolution	Depth-resolving / Depth-averaged
Time resolution	Wave-resolving / Group-averaged
Flow equations	NSWEs / Boussinesq-type / Hybrid
Sediment transport modes	Bed-load / Suspended load / Combined load
Subsurface flow	Excluded / Included
Numerical aspects	
Coupling	Fully-coupled / Uncoupled / Weakly-coupled
Shock treatment	Shock-fitting / Shock-capturing

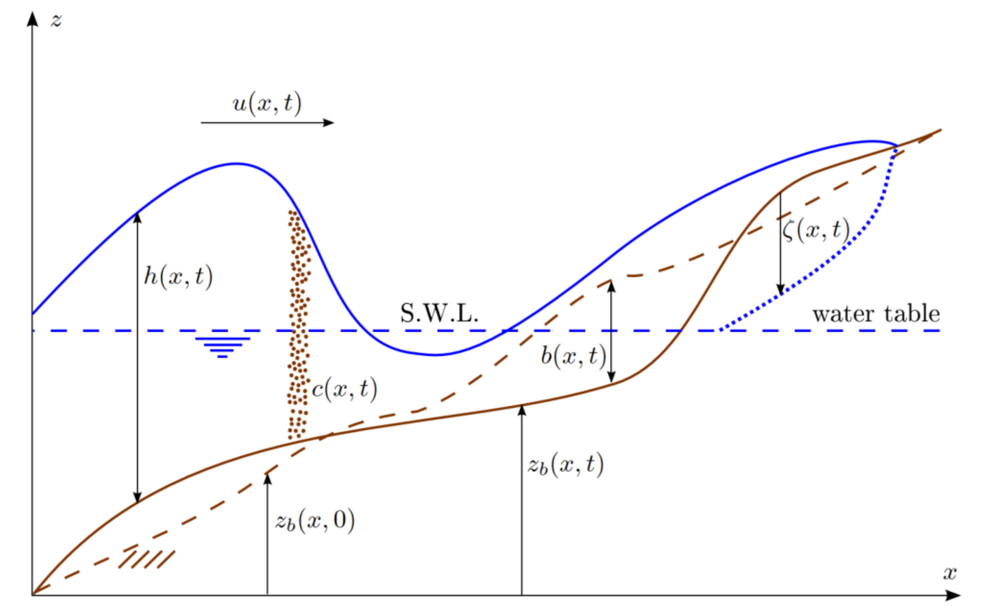

Sketch of the variables involved in a generic morphodynamic swash event (Giorgio Incelli, 2016).

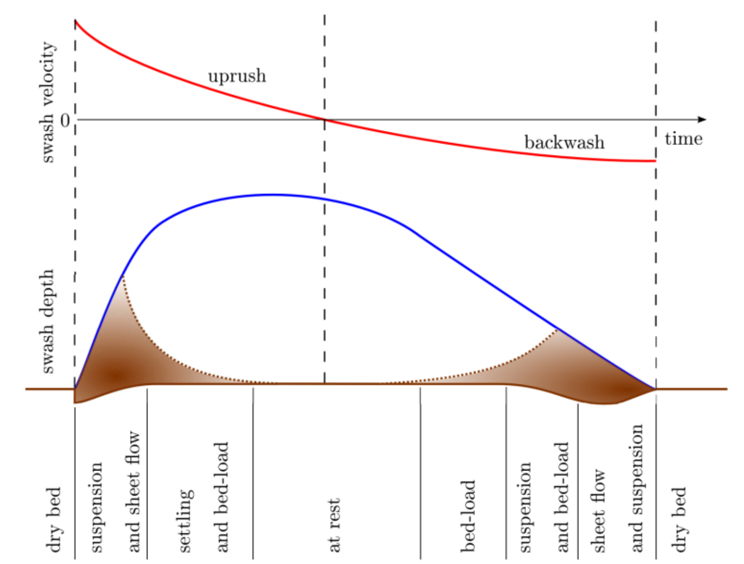

Sketch of the sediment transport processes during a swash cycle (Giorgio, 2016). The figure is modified from Fig. 5 of Masselink and Puleo (2006).

Research Objectives

The development of a morphodynamic swash zone model

- (1) To develop a boundary layer description (sub-model) for a mobile bed that is suitable for incorporation into a NSWE (Nonlinear Shallow Water Wave Equation) morphodynamic solver.
- (2) To validating the resulting morphodynamic solver against laboratory and field data.

Research Methodology

Numerical model

Fully-coupled hydro-morphodynamical numerical solver

Overview

- Depth-averaged, phase-resolving, shock-capturing, and fully-coupled 1-Dimensional model.
- Developed by the Coastal Dynamics and Engineering research group at the University of Nottingham, UK.

Governing equations

- Based on **1D nonlinear shallow water equations (NLSWEs)**
- $\frac{\partial h}{\partial t} + \frac{\partial hU}{\partial x} = 0$
- $\frac{\partial hU}{\partial t} + \frac{\partial\left(hU^2 + \frac{1}{2}gh^2\right)}{\partial x} = -gh\frac{\partial z_B}{\partial x} - \frac{\tau_b}{\rho}$
- **x** is the horizontal abscissa, **t** is time, **U** denotes the depth-averaged horizontal velocity, **h** is the local water depth, $\boldsymbol{z_B}$ is the bed level, **g** is the gravitational acceleration, $\boldsymbol{\tau_b}$ is the bottom shear stress, and **ρ** is the water density.

Spatial discretization

- The **Total Variation Diminishing MacCormack (TVD-MCC) scheme.**

Time stepping

- The **adaptive explicit second-order predictor-corrector scheme** is employed for the main TVD-MCC scheme.
- The **adaptive Runge-Kutta fourth-order scheme** is employed for the bottom boundary equations.

Coupling systems

Bed evolution

- Coupled with the **Exner equation**
- $\frac{\partial z_B}{\partial t} + \xi\frac{\partial q_b}{\partial x} = 0$
- where $\xi = 1/(1-p)$, p being the bed porosity, q_b is the instantaneous bed load sediment transport.
- The system of the **NLSWE** and **Exner equation** in vector form:
- $\frac{\partial \mathbf{W}}{\partial \mathbf{t}} + \frac{\partial \mathbf{F(W)}}{\partial \mathbf{x}} = \mathbf{S}$
- Where $\mathbf{W} = [h, U, z_B]^{\mathrm{T}}$ is the vector of unknowns, $\mathbf{F} = [hU, hU^2 + \frac{1}{2}gh^2, \xi q_b]^2$ is the flux vector, and **S** is the vector of the source terms.

Sediment transport

- Coupled with the **Meyer-Peter and Müller equation**

Seaward Boundary Conditions

- The fully-coupled absorbing-generating seaward boundary conditions, named **Riemann Equation Boundary Conditions** (REBCs).

Bottom Boundary Layer solvers

- The **Momentum integral method**.

Calibration and Validation

1D Dam-break problem

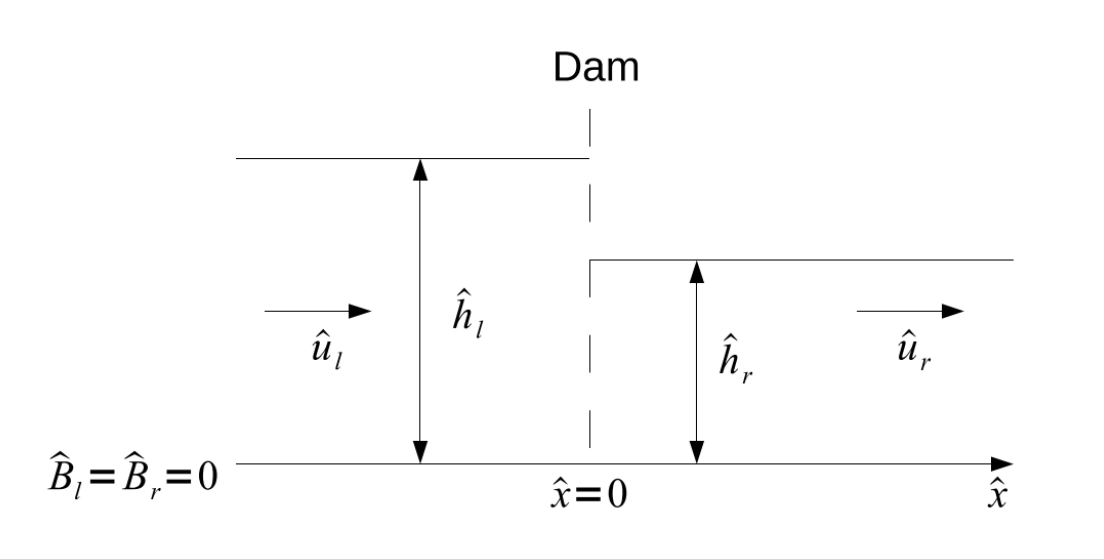

Schematic for the initial conditions of a general dam-break problem. (Fangfang Zhu, 2012)

Laboratory tests

- Intra-swash hydrodynamics and sediment flux for dam-break swash on coarse-grained beaches (O'Donoghue et al., 2016).
- Experimental study of bore-driven swash hydrodynamics on impermeable rough slopes (Kikkert et al., 2012).
- Experimental study of bore-driven swash hydrodynamics on permeable rough slopes (Kikkert et al., 2013).

Research progresses

Numerical simulation of bore-driven swash on impermeable rough slopes

Boundary conditions for numerical simulations

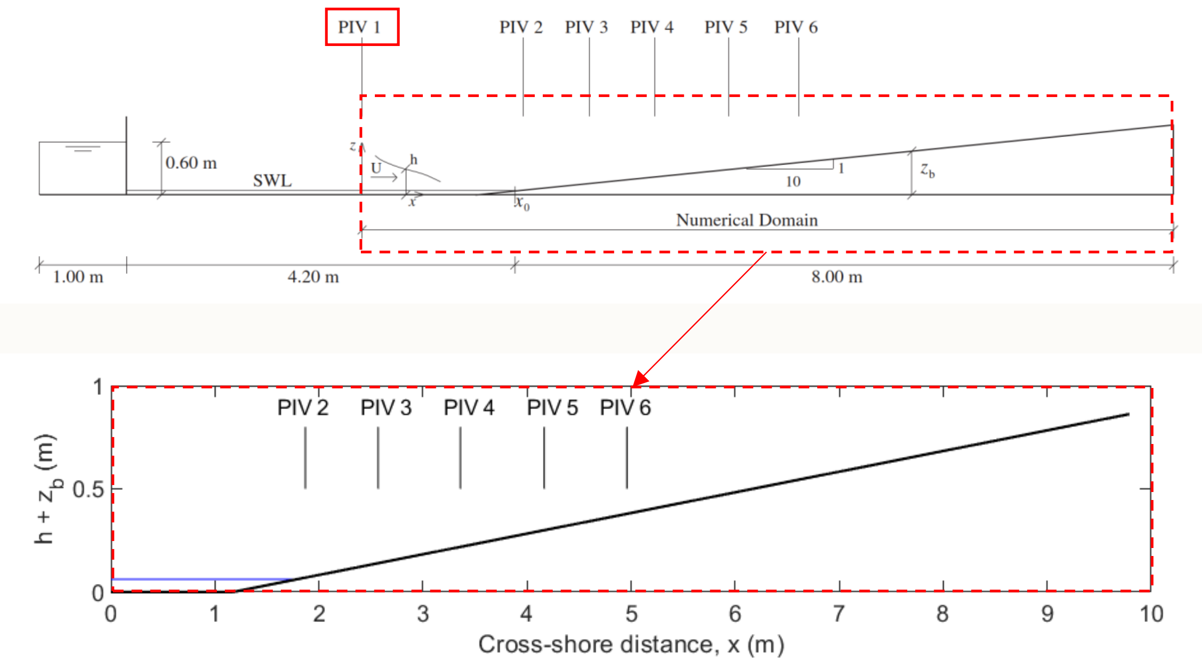

Schematic of the Aberdeen swash facility with the numerical domain used.
(Briganti et al., 2011)

Beach type	Denotation	D_{50}-diameter (mm)
Sand beach	IMP015	1.3
Gravel beach	IMP060	5.4
Gravel beach	IMP100	8.4

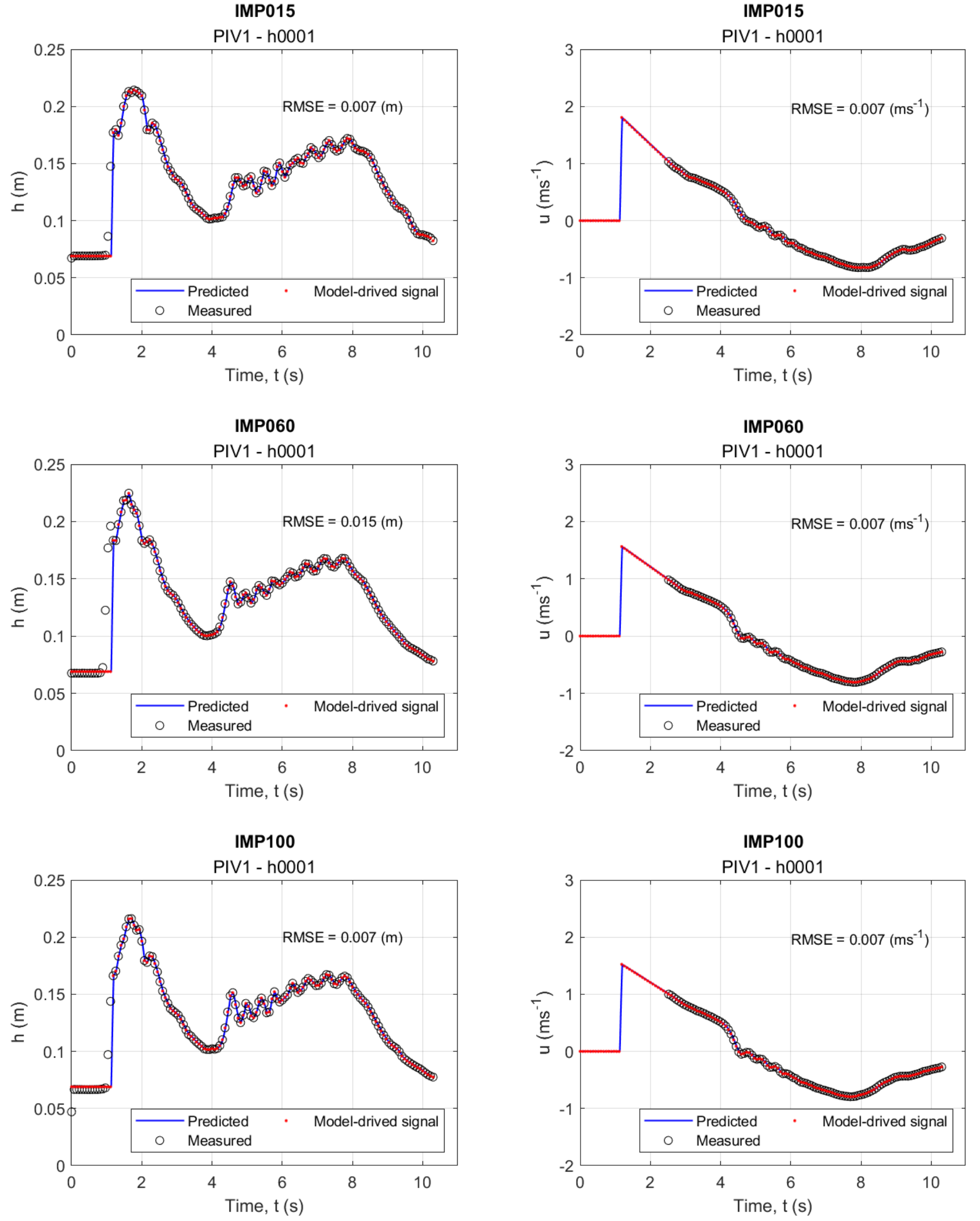

Swash lens simulations

Measured data

Predicted data

IMP015 (sand beach, D_{50} = 1.3 mm)

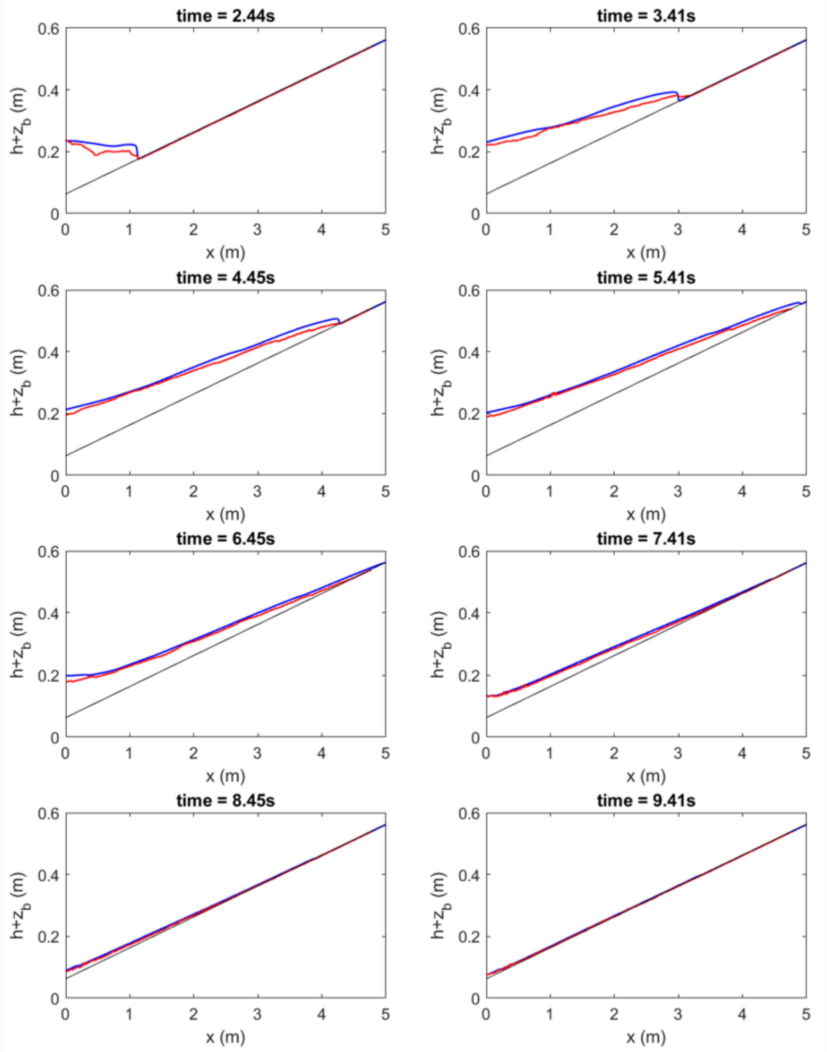

IMP060 (gravel beach, D_{50} = 5.4mm)

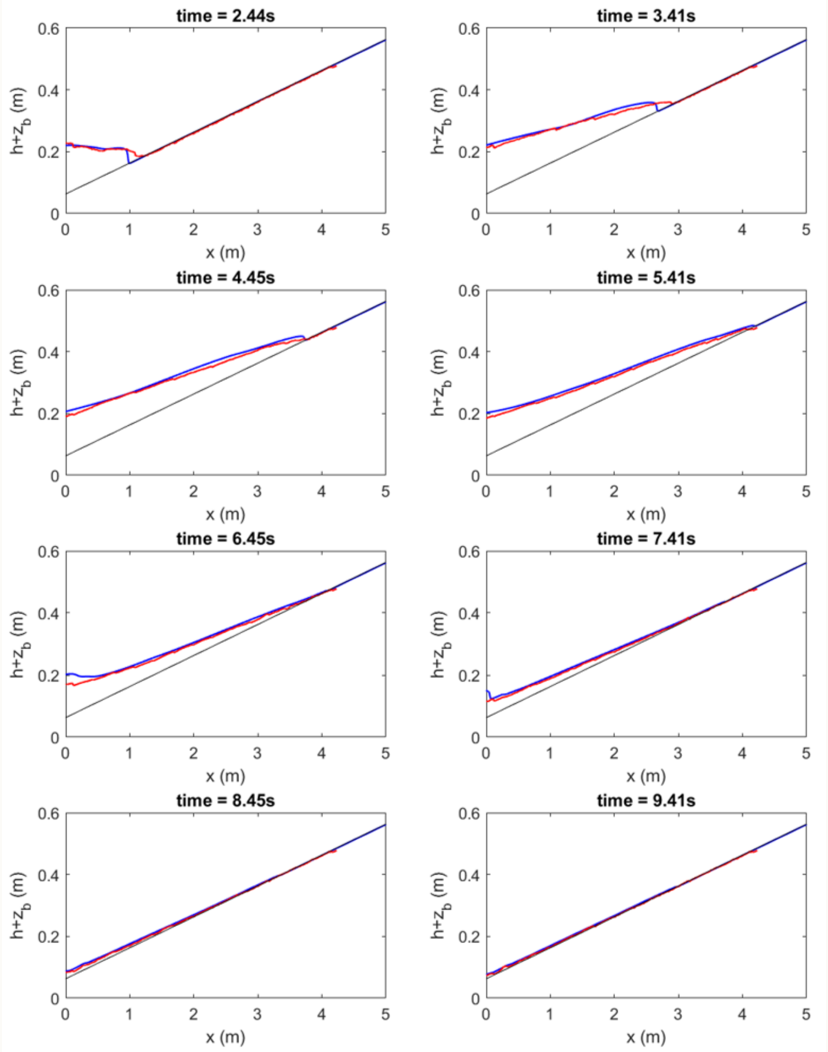

IMP100 (gravel beach, D_{50} = 8.4mm)

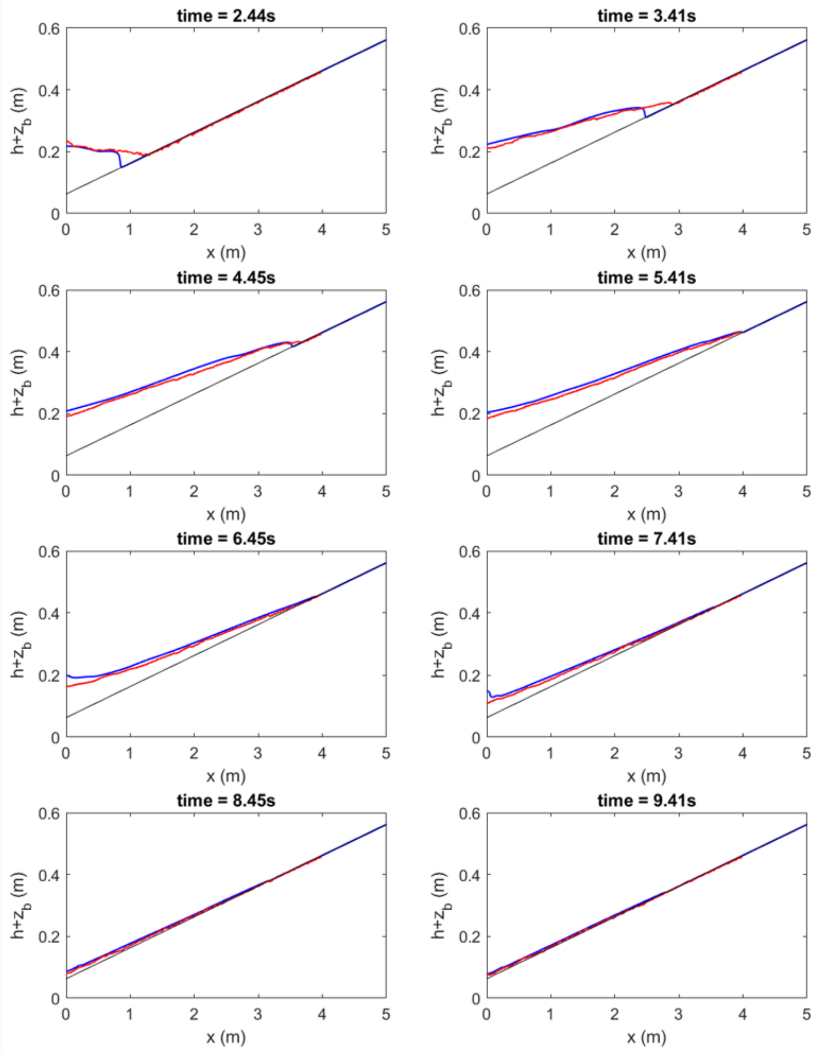

Water depth, Depth-averaged horizontal velocity, and vertical velocity profiles simulations

- ➢ IMP015 (sand beach, D_{50} = 1.3 mm)

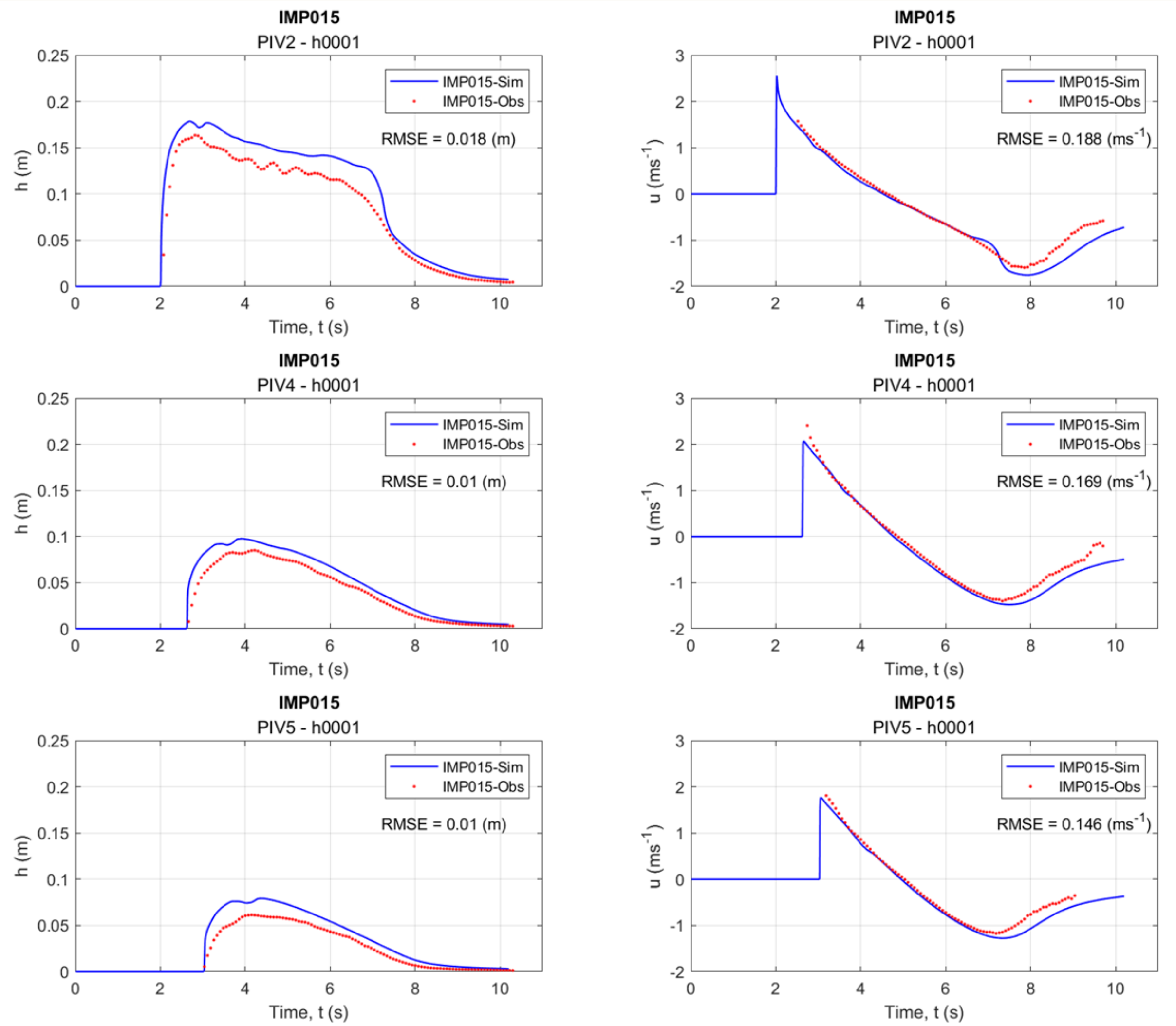

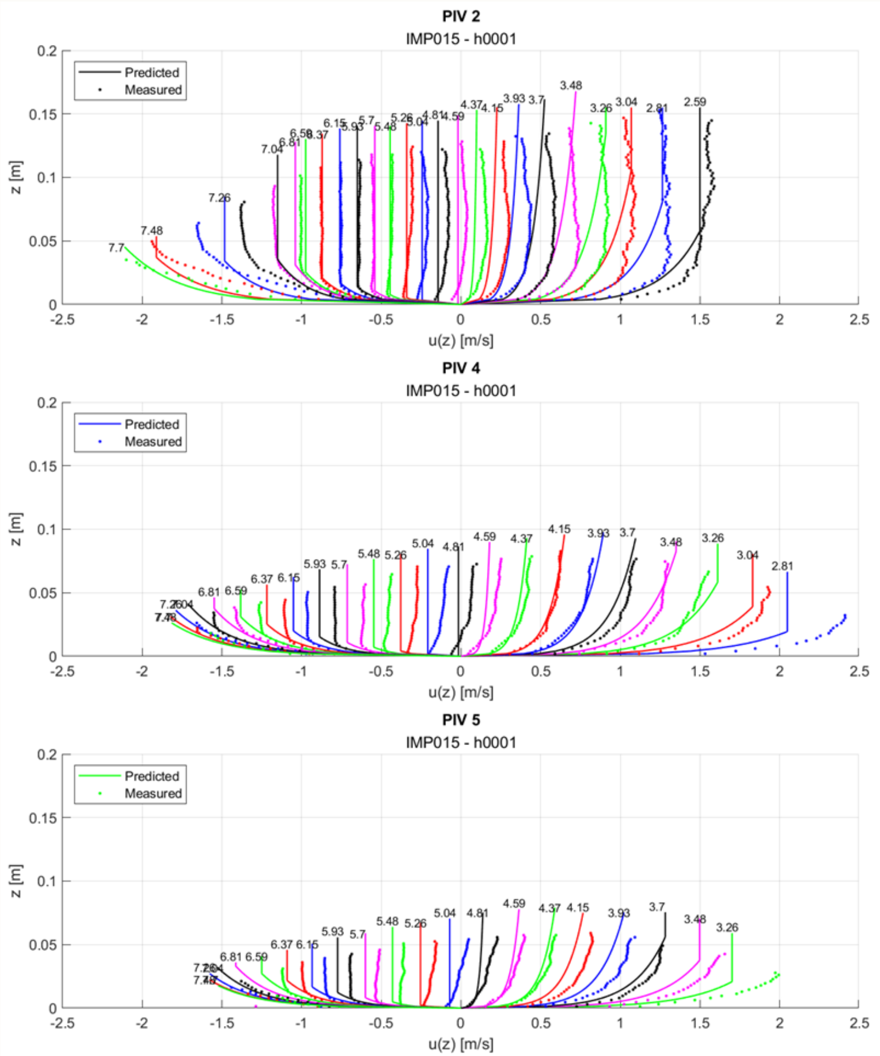

Water depth, Depth-averaged horizontal velocity, and vertical velocity profiles simulations

- IMP060 (gravel beach, D_{50} = 5.4 mm)

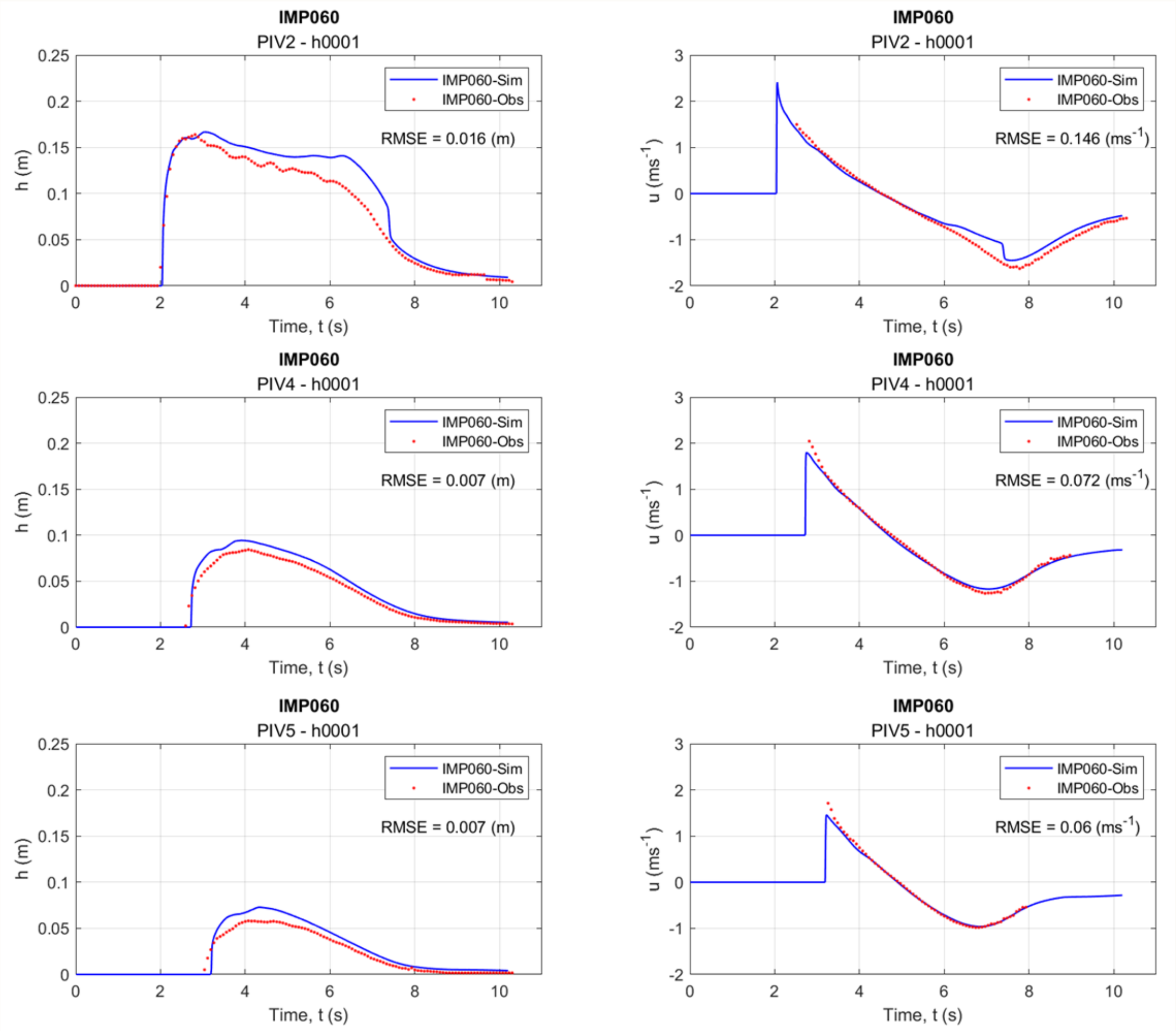

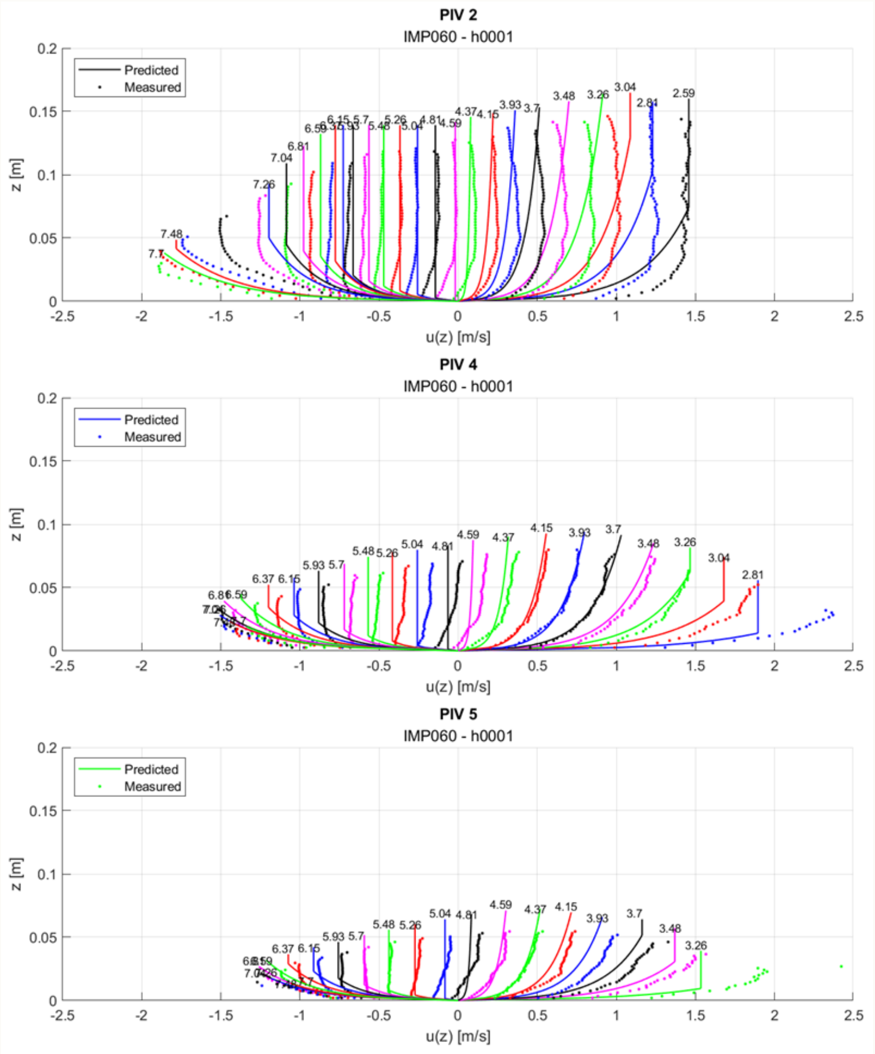

Water depth, Depth-averaged horizontal velocity, and vertical velocity profiles simulations

- IMP100 (gravel beach, D_{50} = 8.4 mm)

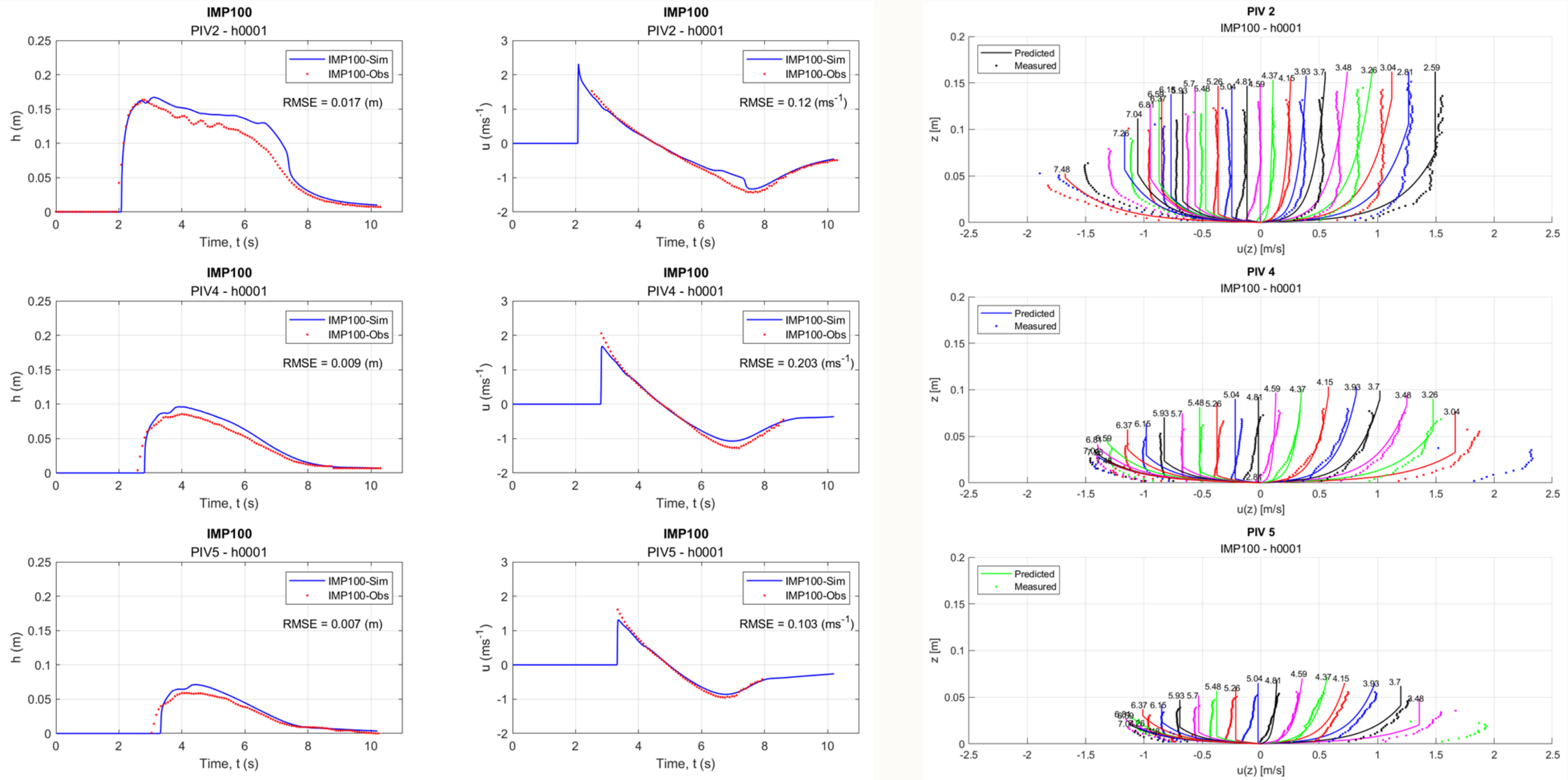

Bottom shear stress simulations

IMP015 (sand beach, D_{50} = 1.3 mm) IMP060 (gravel beach, D_{50} = 5.4mm) IMP100 (gravel beach, D_{50} = 8.4mm)

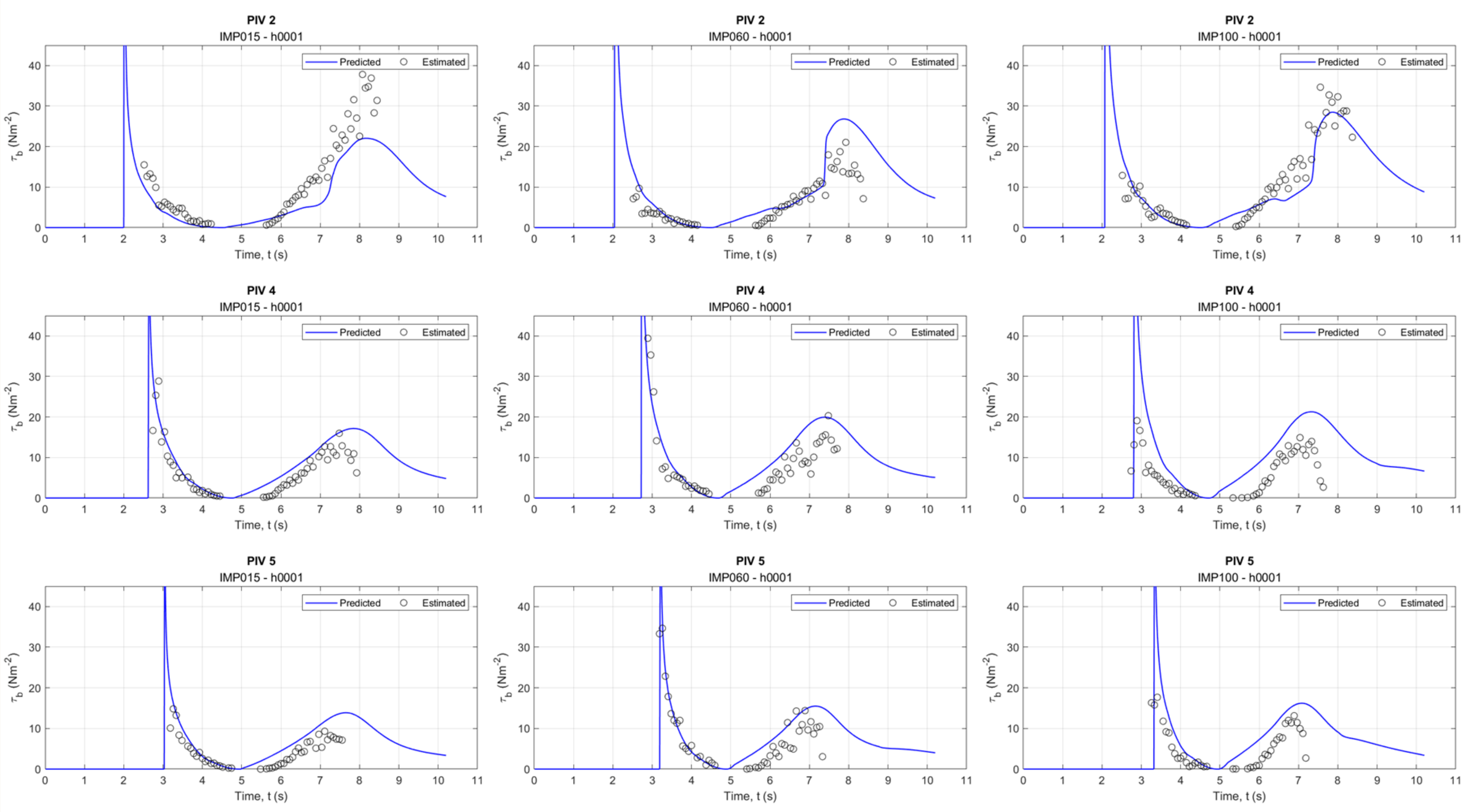

Research plan

Further works

- Numerical simulation of bore-driven swash event on impermeable and permeable rough slopes (<u>for a mobile bed</u>).
- Improving the performance of the numerical simulation of bottom shear stress, which using the momentum integral method for the BBL.
- Incorporating the newly developed boundary layer sub-model, with a focus on the mobile bed, into a NSWE morphodynamic solver.
- Implementing sensitivity analysis that considering the in/exfiltration and their effect on the boundary layer, possible phase effect, and the effect of bore turbulence.

University of Nottingham
UK | CHINA | MALAYSIA

HORIZON EUROPE

Marie Skłodowska-Curie Actions

SEDIMARE 2023-2027
Sediment Transport and Morphodynamics in Marine and Coastal Waters with Engineering Solutions

Thank you

Quan NGUYEN

"Q2Dmorfo: a reduced complexity model for long term coastal dynamics" (Invited Speaker Albert Falqués, Universitat Politècnica de Catalunya)

SEDIMARE School
Numerical Methods in Coastal Hydrodynamics and Sediment Transport
University of Nottingham

http://df.upc.edu/morfos

23/04/2024

Modelling long term and large scale coastal morphodynamics

Albert Falqués
Universitat Politècnica de Catalunya

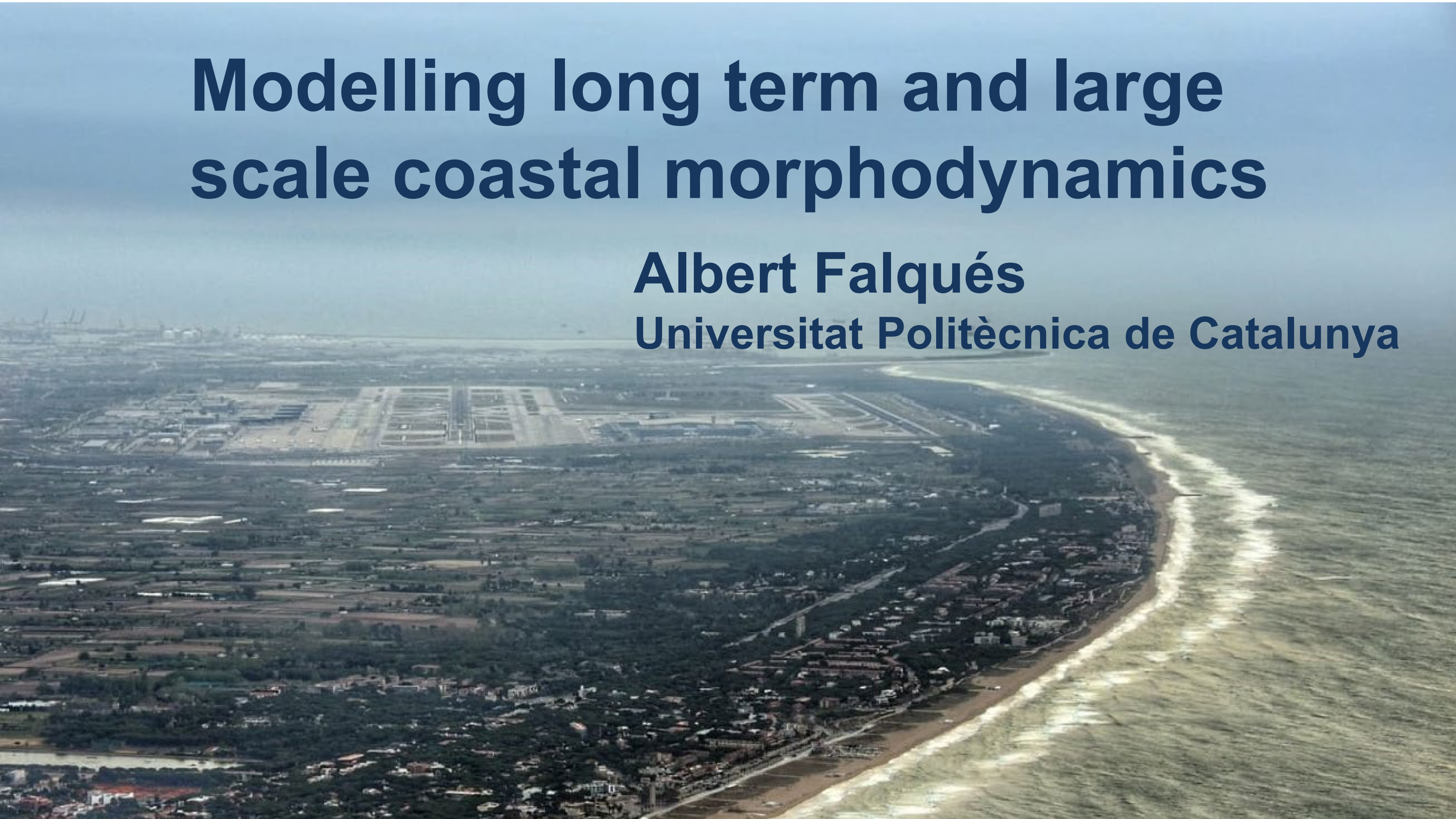

OUTLINE:

1) Aim: long term & large scale
2) Different types of models
3) The Q2Dmorfo model
4) Application: Zandmotor meganourishment
5) Application: shoreline sandwaves
6) Take-home message

OUTLINE:

1) **Aim: long term & large scale**
2) Different types of models
3) The Q2Dmorfo model
4) Application: Zandmotor meganourishment
5) Application: shoreline sandwaves
6) Take-home message

1) Aim: long term & large scale

AIM: Long term evolution (10-100 yr) of sandy coasts at large length scales (10-100 Km)

Llobregat river delta,
South of Barcelona,
Catalonia

Zandmotor meganourishment
Near den Haag.
The Netherlands

OUTLINE:

1) Aim: long term & large scale
2) **Different types of models**
3) The Q2Dmorfo model
4) Application: Zandmotor meganourishment
5) Application: shoreline sandwaves
6) Take-home message

2) Different types of models

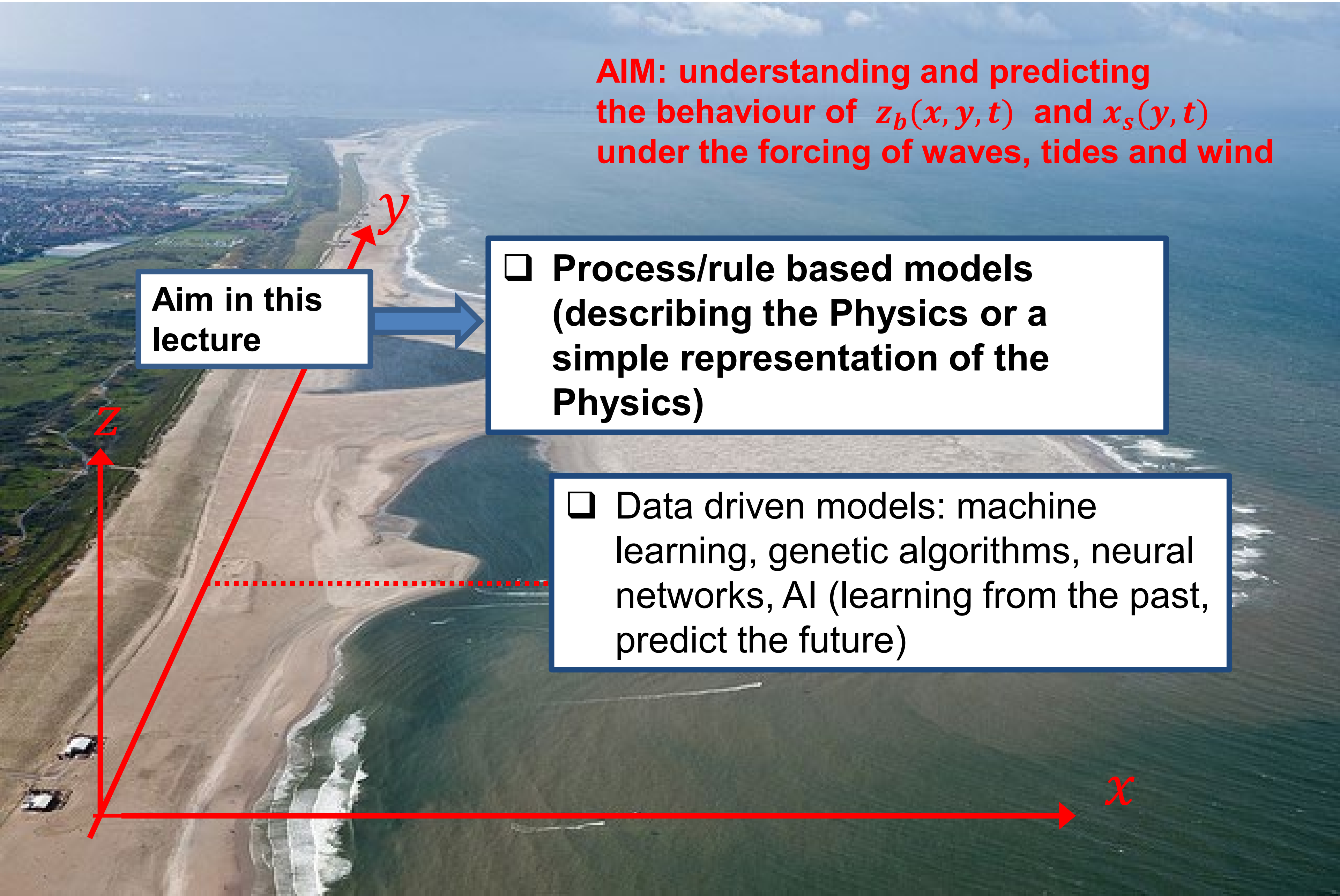

AIM: understanding and predicting the behaviour of $z_b(x, y, t)$ and $x_s(y, t)$ under the forcing of waves, tides and wind

Aim in this lecture

- ❑ **Process/rule based models (describing the Physics or a simple representation of the Physics)**

- ❑ Data driven models: machine learning, genetic algorithms, neural networks, AI (learning from the past, predict the future)

2) Different types of models

Morfos http://df.upc.edu/morfos UPC

Too time consuming, not able for large-scale and long-term

3D – wave-resolving

- ➢ Reynolds-averaged equations with individual waves in 3D

3D – wave-averaged

- ➢ …s-averaged equations …ean currents in 3D
- ➢ …re treated on average: energy spectrum $E(\omega,\theta)(x,y,t)$

2D – wave-resolving

- ➢ Average on the z coordinate (shallow water, Boussinesq, …)
- ➢ Individual waves

decreasing complexity

2D – wave-averaged

- ➢ Shallow water equations for the mean currents
- ➢ Waves are treated on average: energy spectrum

⇨ Very common; so-called: **coastal area models** or **2DH models**

2) Different types of models

3D – wave-resolving

- ➢ Reynolds-averaged equations with individual waves in 3D

3D – wave-averaged

s-averaged equations
ean currents in 3D
re treated on average:
energy spectrum $E(\omega,\theta)(x,y,t)$

te
q, …)

Too time consuming, not able for large-scale and long-term

Can deal with:

- ✓ **A few Km's of coast**
- ✓ **From days to months**
- X **BUT NO for several years or decades:**
  - ➢ **Computational cost**
  - ➢ **Small scale error accumulation**

decreasing complexity

2D – wave-a

- ➢ Shallow water equations for the mean currents
- ➢ Waves are treated on average: energy s

⇨ Very common; so-called: **co**

NEED FOR SIMPLER MODELS ("reduced-complexity models")

One-line coastline models

surf zone “collapsed” in one line

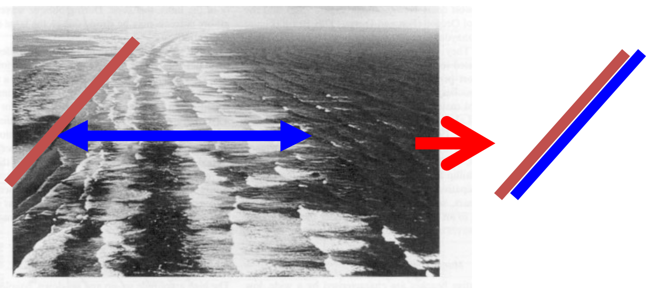

Only one unknown: $\boxed{x_s(y,t)}$

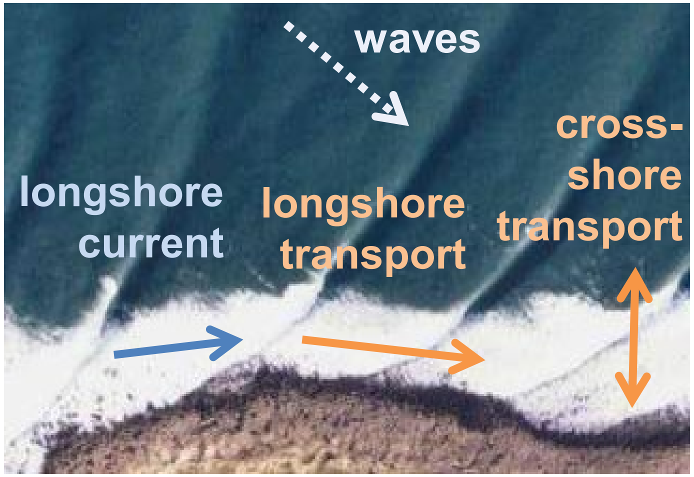

Essential simplifications:

- Shoreline movement is governed just by gradients in longshore transport
- Alongshore sediment transport is computed parametrically from the waves
- Cross-shore sediment transport is not explicitly considered (instantaneous translation of the cross-shore profile according to shoreline displacement)
- Hydrodynamics not resolved (only waves)

One-line governing equation

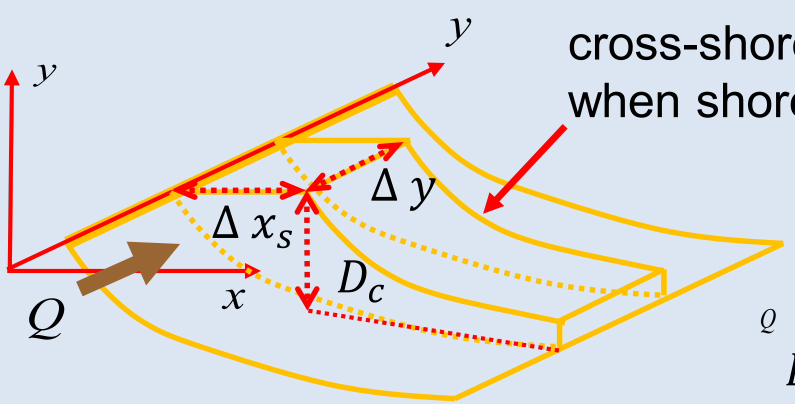

cross-shore profile translation when shoreline moves

sediment volume conservation:

$$D_c\, \Delta x_s\, \Delta y = -\Delta Q\, \Delta t$$

$$\frac{\partial x_s}{\partial t} = -\frac{1}{D_c}\frac{\partial Q}{\partial y}$$

$$Q(y,t) = \int_{x_s}^{\infty} q_y(x,y,t)\, dx = \text{ total transport rate } m^3/s$$

$$Q = Q_0(H_b)\ \sin\left(2(\theta_b - \frac{\partial x_s}{\partial y})\right)$$

$$\left|\frac{\partial x_s}{\partial y}\right| \ll 1 \quad ; \quad H_b\,, \theta_b \text{ do not depend on } \frac{\partial x_s}{\partial y}$$

Pelnard-Considère equation (1956):

$$\frac{\partial x_s}{\partial t} = a\frac{\partial^2 x_s}{\partial y^2}$$

$$a = 2\,\frac{Q_0\ \cos 2\theta_b}{D_c}$$

Can we improve one-line models to include a description of cross-shore transport better tan just profile translation ?

Equilibrium shoreline models (parameterization of cross-shore processes)

shoreline $x_s(t)$ at a particular alongshore location or alongshre average

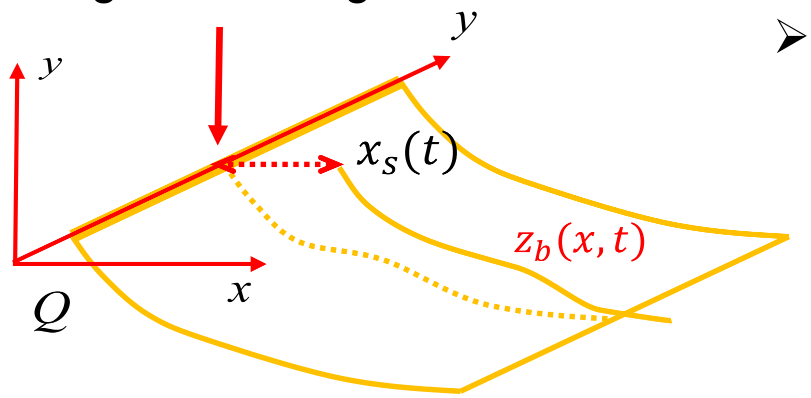

Initial idea by Miller & Dean, 2004

Concept at any given beach:

- ➢ equilibrium shoreline position = function (wave forcing)
- ➢ shoreline evolves towards moving equilibrium

$$\boxed{\frac{dx_s}{dt} = -\,k^{\pm}\,\gamma\,\Delta W}$$

$$k^{\pm} = \begin{cases} k^{+} & \Delta W > 0 \\ k^{-} & \Delta W < 0 \end{cases}$$

$\gamma =$ wave thrust

$\Delta W =$ disequilibrium magnitude

Basically, two ways of formulation:

- ❑ Yates et al., 2009. $\Delta W = E - E_{eq}(x_s)$ $\quad \gamma = E^{1/2}$
- ❑ Splinter et al., 2014. $\Delta W = \dfrac{\Omega - \Omega_{eq}}{\sigma_\Omega}$ $\quad \gamma = P^{1/2}$
  $\Omega_{eq} =$ f(past values of Ω with decreasing weight)

$$E = \frac{1}{8}\rho g H_{rms}^2$$

$$\Omega = \frac{H_s}{w T_p}$$

$$P = c_g\,E$$

How to include cross-shore processes into one-line models ?
Extended one-line models

- ❑ **alongshore:** one-line

- ❑ **cross-shore:**
  - ➢ equilibrium shoreline
  - ➢ other approximations

Type	Model name	Autors	Characteristics
one-line		Pelnard-Considère 1956	1-line longshore
	GENESIS	Gravens et al. 1991	1-line longshore
	CEM	Ashton 2006	1-line longshore - cellular
One-line alongshore + equilibrium shoreline cross-shore	CoSMoS-COAST	Vitousek et al. 2017	1-line longshore + equilibrium shoreline + Bruun
	LX-Shore	Robinet et al. 2018	1-line longshore (cellular) + equilibrium shoreline + Bruun
	COCOONED	Antolinez et al. 2019	1-line longshore + equilibrium shoreline
	IH-LANS	Alvarez-Cuesta et al. 2021	1-line longshore + equilibrium shoreline + Bruun
		Tran & Berthélemy 2020	1-line longshore + equilibrium shoreline - embayed beach
One-line alongshore + «something» cross-shore	UNIBEST		1-line + detailed cross-shore processes
	MIKE 21 Shoreline Morphology		1-line longshore + cross-shore profile translation
	ShorelineS	Roelvink 2020	1-line (curvilinear-cellular) + optional cross-shore transport
	ShoreTrans	McCarroll 2021	1-line longshore + cross-shore profile translation + Bruun
N-lines	NLINE	Dabees 2000	N-lines

OUTLINE:

1) Aim: long term & large scale
2) Different types of models
3) **The Q2Dmorfo model**
4) Application: Zandmotor meganourishment
5) Application: shoreline sandwaves
6) Take-home message

Q2Dmorfo: A different way to include cross-shore processes in a shoreline model

One-line extended models: $\Delta\, x_s \;=\; \Delta x_s^L \;+\; \Delta x_s^C \;+\; \Delta x_s^B$

- Δx_s: Total shoreline displacement
- Δx_s^L: one-line
- Δx_s^C: cross-shore
- Δx_s^B: Bruun Rule

- Any nonlinear interaction between components/processes is excluded
- Sediment conservation is not explicitly considered

- An alternative to one-line extended models
- Several advantages
- Complexity in between 2DH models and one-line models
- Roughly inspired in N-lines models

Falqués et al., 2006, 2008; van den Berg et al., 2012; Arriaga et al., 2017

Q2Dmorfo

Essential simplification:

- **Sediment transport is computed parametrically in 2DH from the waves without resolving the mean hydrodynamics**

onshore wave transformation and breaking

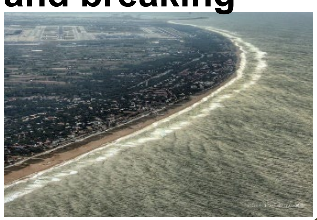

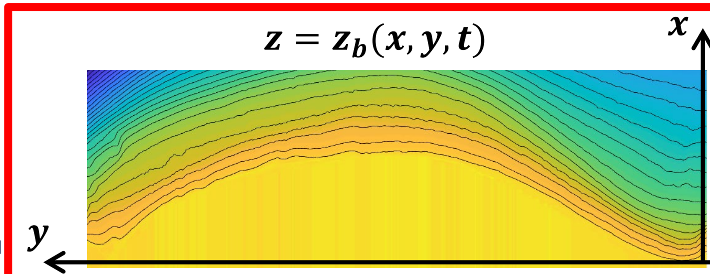

bed level updating: sediment volume conservation

tides

~~currents, mean sea level~~

sediment transport computation

wind

BUT the 2D bathymetry is resolved approximately !

3) The Q2Dmorfo model

	2DH	One-line extended	Q2Dmorfo
Mean Hydrodynamics	✓	✗	✗
Longshore transport	✓	✓	✓
Cross-shore transport	✓		✓
Bathymetry	✓	✗	✓
Coastline	✓	✓	✓
Mean sea level changes	✓		✓

Dynamic equation

$$\frac{\partial z_b}{\partial t} + \frac{\partial q_x}{\partial x} + \frac{\partial q_y}{\partial y} = 0$$

sediment conservation at each horizontal cell

Unknown: bed level $z = z_b(x, y, t)$

Sediment flux $(m^3/m \cdot s)$ $\vec{q}(x, y, t)$

- must be evaluated at each cell, either submerged or dry
- depends on bed level, mean sea level, waves, wind …
- very versatile: any process whose sediment flux can be parameterized can be included

sediment porosity p is included in $\vec{q}$

The equation is solved in all the domain $L_x \times L_y$ both submerged and dry beach

Sediment transport

Sediment flux $\vec{q}$ is decomposed as:

- **"longshore": transport by the wave-driven longshore current**
- **"cross-shore": transport by wave nonlinearities, undertow, gravity**
  - A longshore diffusive component is also added

At each grid point, the local shore-normal and longshore directions must be defined

The local cross-shore direction, $\hat{n}$, is defined from an averaged bathymetry (running average) representing the overall trend of the coastline (filtering out the relatively small morphological features)

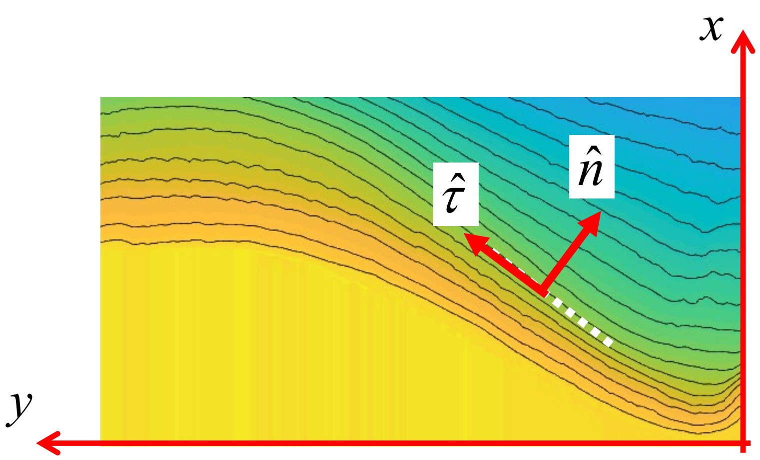

3) The Q2Dmorfo model

Sediment transport: “longshore”

$$\vec{q} = \vec{q}_L + \vec{q}_N + \vec{q}_D$$

- $\vec{q}_L$: longshore transport
- $\vec{q}_N$: cross-shore transport
- $\vec{q}_D$: diffusive transport

longshore transport

$$\boxed{\vec{q}_L = f(x')\,Q(y)\,\hat{\tau}}$$

$f(x')$

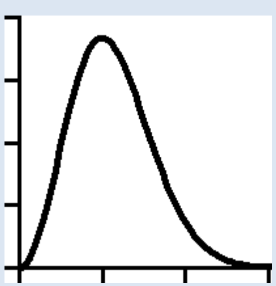

x'

total transport rate m^3/s;
e.g., CERC formula

$$Q = \mu H_b^{5/2} \sin(2(\theta_b - \phi_s))$$

$$f(x') = \frac{4}{\sqrt{\pi} L^3} x'^2\, e^{-(x'/L)^2}$$

$$L = 0.8 X_b + X_{sz}$$

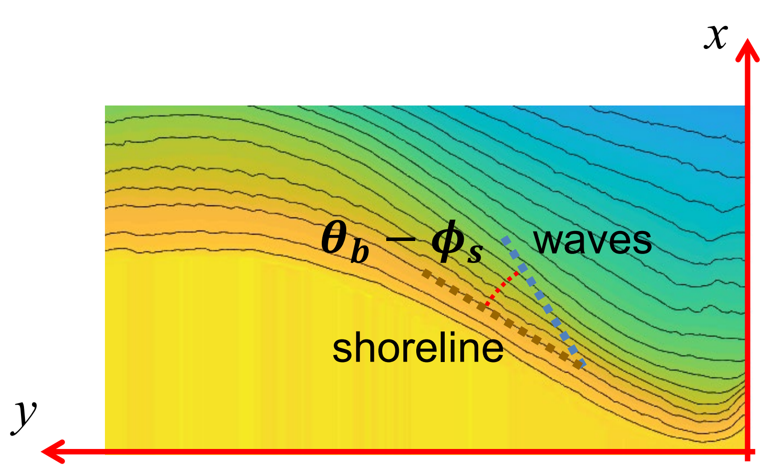

Sediment transport: “cross-shore”

$$\vec{q} = \underbrace{\vec{q}_L}_{\text{longshore transport}} + \underbrace{\vec{q}_N}_{\text{cross-shore transport}} + \underbrace{\vec{q}_D}_{\text{diffusive transport}}$$

It is based on the concept of equilibrium cross-shore beach profile: equilibrium bed slope is such that the gravity downslope transport balances the other transport sources and there is no net cross-shore transport

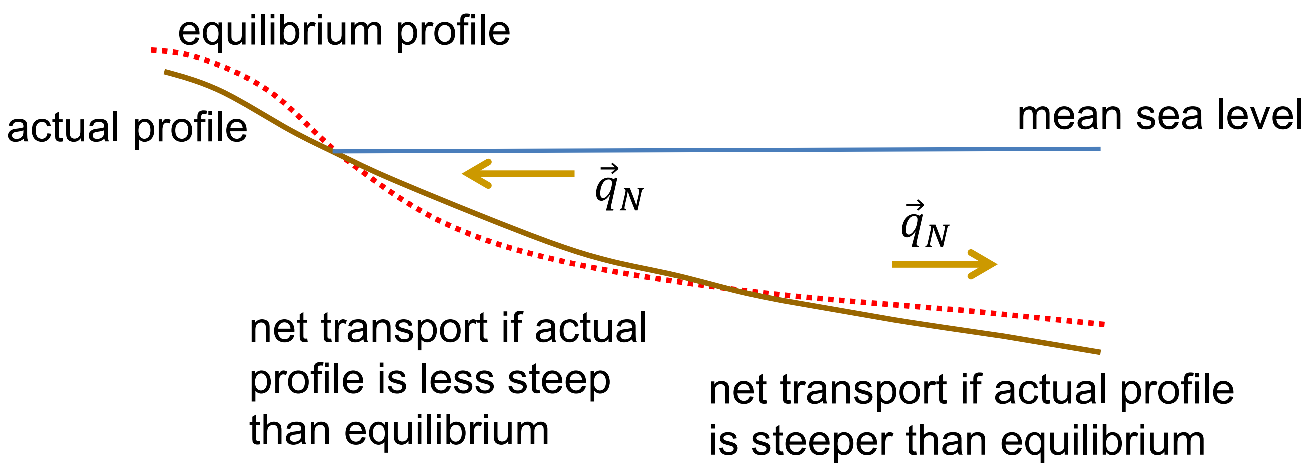

3) The Q2Dmorfo model

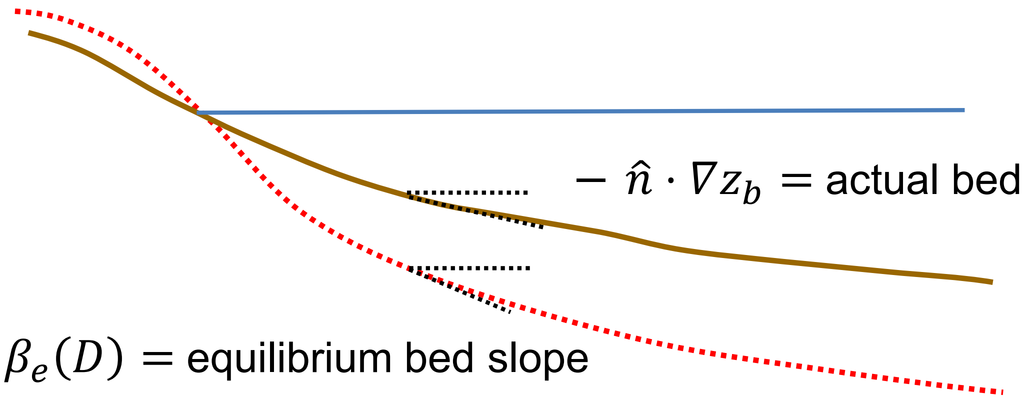

$-\,\hat{n}\cdot\nabla z_b$ = actual bed slope

$\beta_e(D)$ = equilibrium bed slope

$$\boxed{\vec{q}_N = -\gamma(D)\,\left(\hat{n}\cdot\nabla z_b + \beta_e(D)\right)\hat{n}}$$

$\gamma(D)$ = stirring factor

relaxation to the equilibrium profile

The equilibrium profile is prescribed

3) The Q2Dmorfo model

Sediment transport: diffusive longshore

$$\vec{q} = \vec{q}_L + \vec{q}_N + \vec{q}_D$$

longshore transport ($\vec{q}_L$) | cross-shore transport ($\vec{q}_N$) | diffusive transport ($\vec{q}_D$)

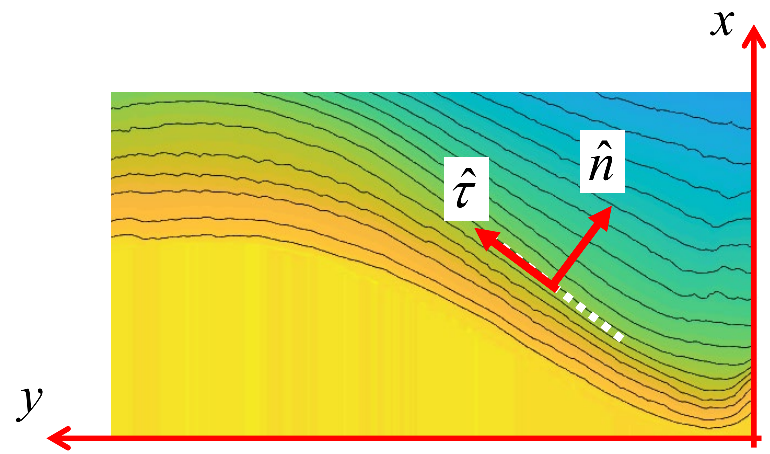

alongshore diffusive transport

$$\boxed{\vec{q}_D = -\gamma(D)\,\left(\hat{\tau}\cdot\nabla z_b\right)\hat{\tau}}$$

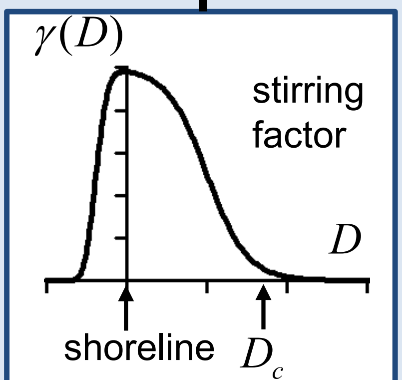

smoothes morphodynamic noise in the alongshore direction

Q2Dmorfo: SUMMARY

- Q2Dmorfo: reduced complexity model

  Main simplifications with respect to 2DH models:
  - Nearshore hydrodynamics is not resolved
  - Sediment transport is computed parametrically from wave field

  Main improvement with respect to one-line shoreline models
  - Bathymetry and sediment fluxes are treated like 2DH models
  - Changes in mean sea level incorporated

- Adequate to study the long term behaviour of large (or not so large) coastline stretches

- Main limitations:
  - It cannot describe the surf zone features like sand bars and rip channels
  - It cannot cope with extremely curved shorelines:
    e.g. developing sandy spits
  - Coastal structures can only be currently included as hard lateral boundaries

OUTLINE:

1) Aim: long term & large scale
2) Different types of models
3) The Q2Dmorfo model
4) **Application: Zandmotor meganourishment**
5) Application: shoreline sandwaves
6) Take-home message

4) Application: Zandmotor mega - nourishment

Beach meganourishment in the Delfland coast, southern Dutch coast (2011)

- $21 \cdot 10^6\ m^3$ sand
- $\approx$ 2 km x 1 km

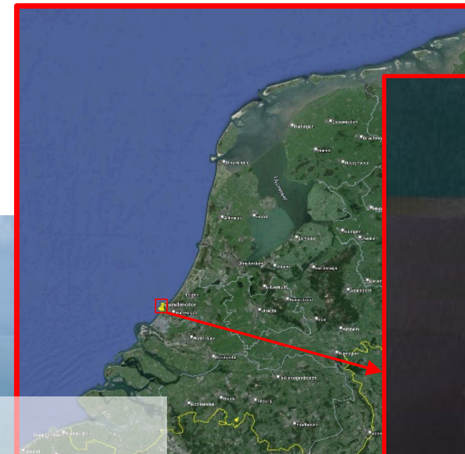

Evolution under sea level rise up to 2100 ?

Arriaga et al., 2017

Ribas et al., 2023

Data

- **Initial bathymetry** January 2012

measured | smoothed and extended

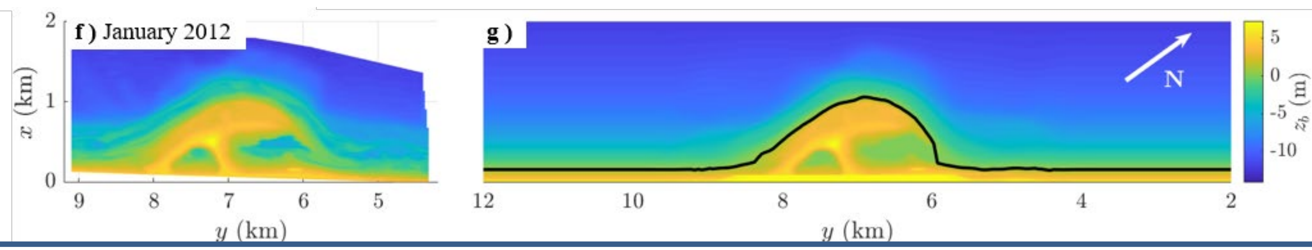

- **Mean sea level** one-month extract

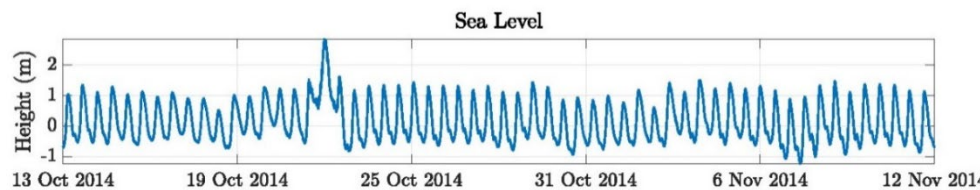

$z_s(t)$

- **Waves at the offshore boundary** one-month extract

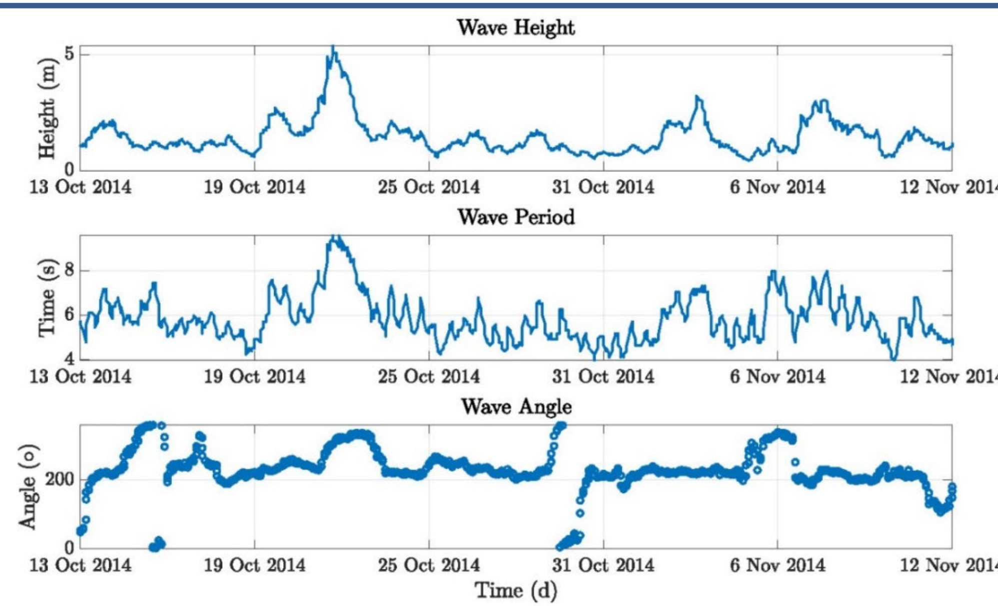

$H_s(t)$

$T_p(t)$

$\theta(t)$

- **Equilibrium beah profile:** from historical Jarkus data (1990-2009)

4) Application: Zandmotor mega - nourishment

End of calibration: April 2013

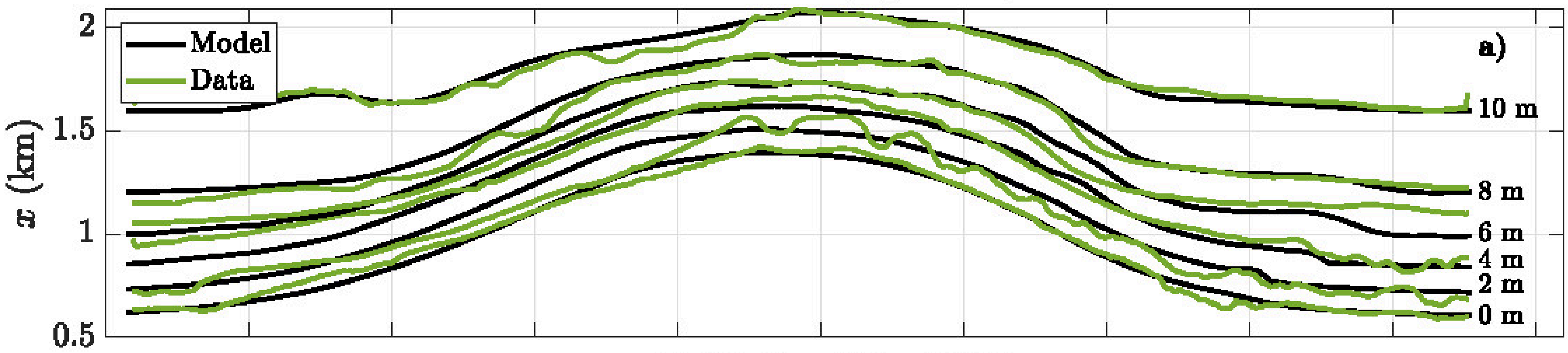

Validation: August 2019

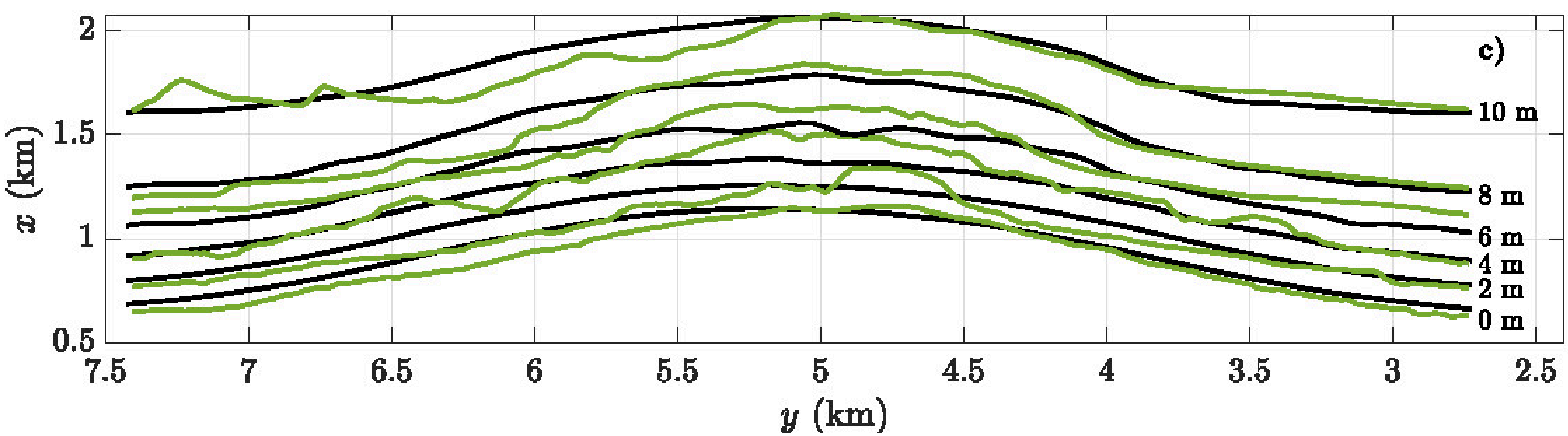

Long term projections

- **Forcing projection: waves**

Existing studies show that not significant changes are expected in the Dutch coast during the XXI century

Wave time series = repetition of the measured waves from 2010 to 2019
(a single realization !)

one-month extract

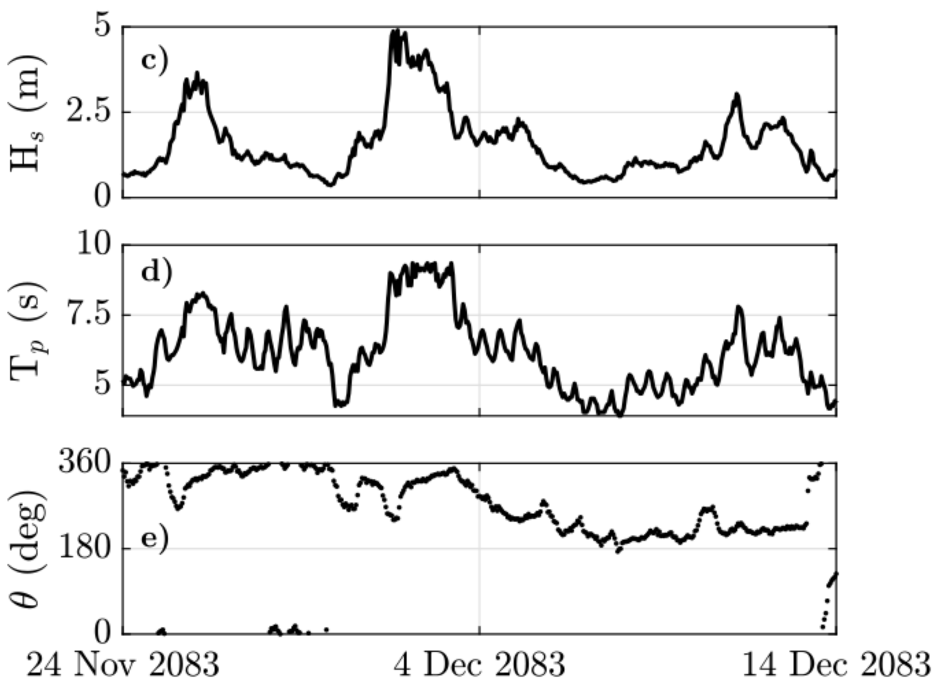

Morphodynamic projections: results

Mean sea level rise scenario RCP8.5 ($\Delta z_s = 0.8$ m)

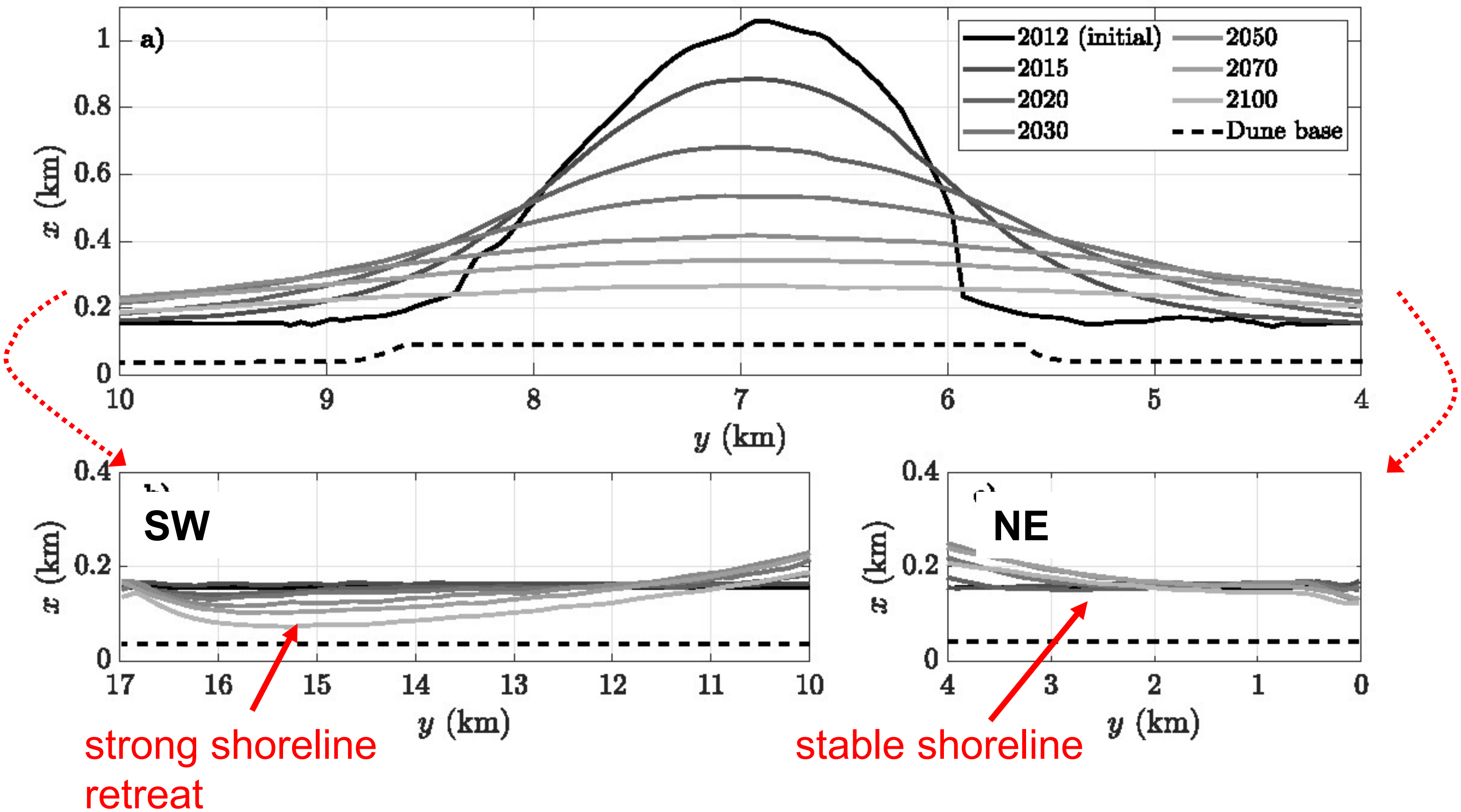

4) Application: Zandmotor mega - nourishment

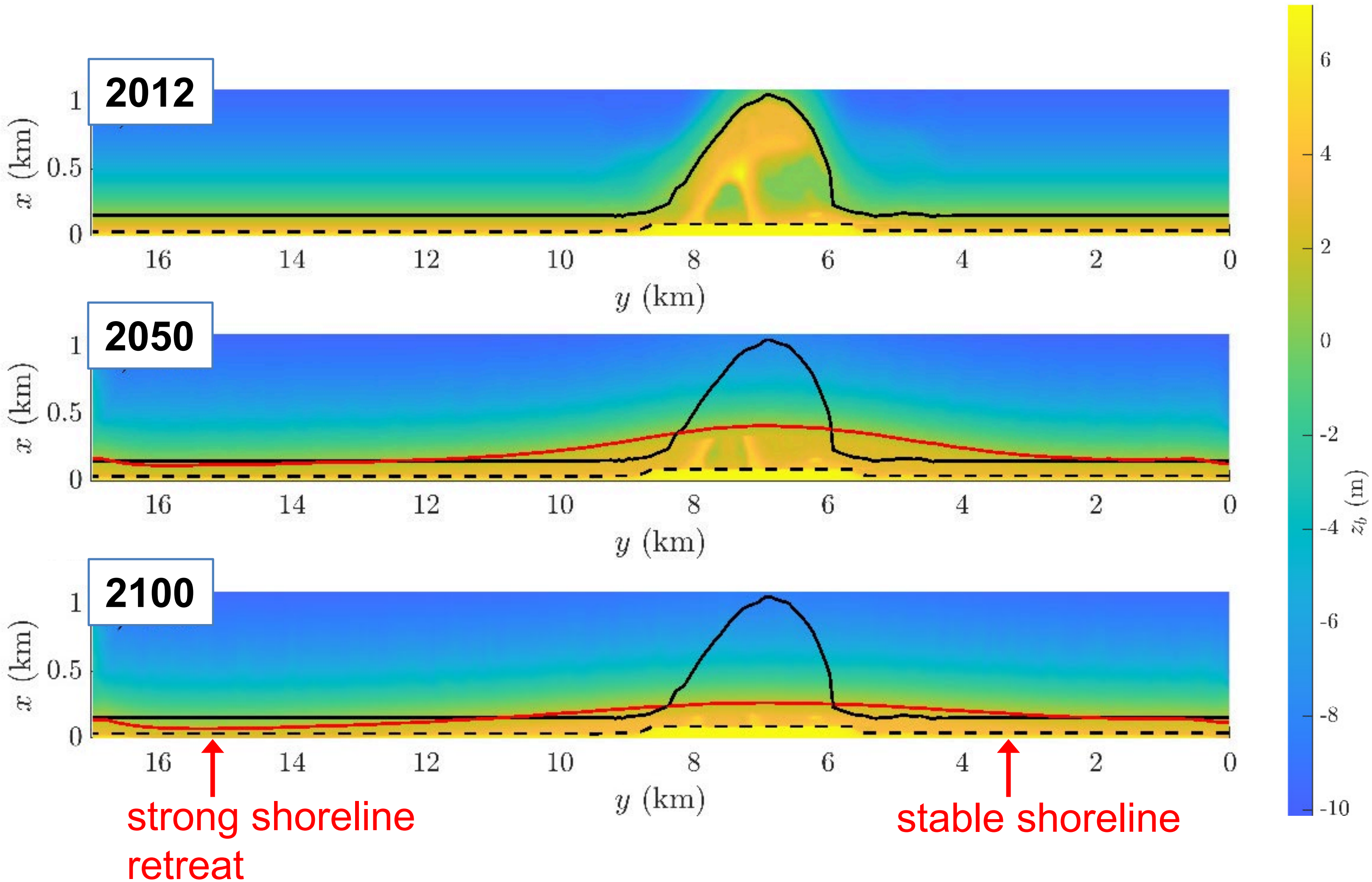

Zandmotor mega-nourishment: SUMMARY

- ❑ Calibrated version of the model successfully reproduce evolution from 2012 to 2019
- ❑ Zandmotor will diffuse and feed adjacent beaches.
- ❑ Diffusivity is 2.5 less than that computed with Pelnard-Considère equation (due to dominant wave obliquity)
- ❑ Shoreline retreat $\approx$ 50% passive flooding and 50% offshore sediment transport
- ❑ Morphological evolution strongly alongshore variable.
- ❑ SW coast strong recession, NE keeps stable

OUTLINE:

1) Aim: long term & large scale
2) Different types of models
3) The Q2Dmorfo model
4) Application: Zandmotor meganourishment
5) **Application: shoreline sandwaves**
6) Take-home message

High-angle wave shoreline instability (HAWI)

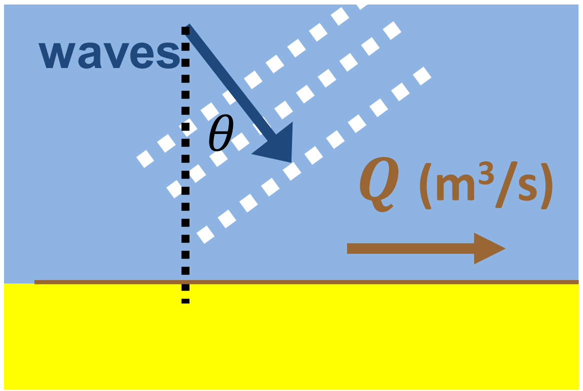

shoreline perturbation

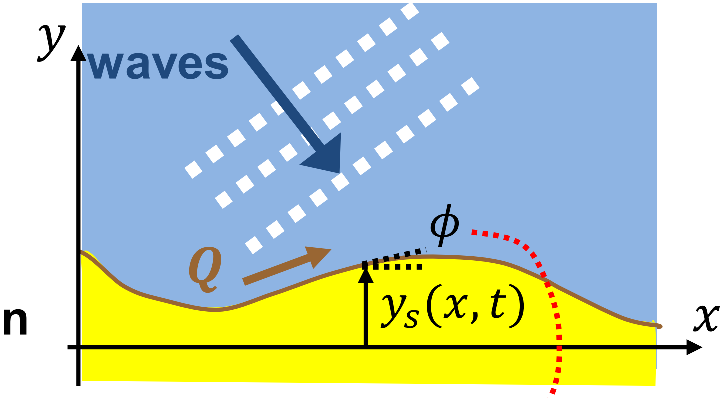

$$Q \sim \mu\, H_b^{5/2} \sin\, 2\theta_b \quad \Rightarrow \quad Q \sim \mu\, H_b^{5/2} \sin\, 2(\theta_b - \phi)$$

- one-line approximation
- sediment conservation
- if $H_b\,, \theta_b \;\approx$ unaltered

$$\frac{\partial y_s}{\partial t} = \varepsilon\, \frac{\partial^2 y_s}{\partial x^2}$$

$\boldsymbol{\varepsilon > 0}$ if $\theta_b < 45^o$

Rectilinear shoreline is stable
Free perturbations tend to decay

5) Application: shoreline sand waves

Is this instability observed in nature?

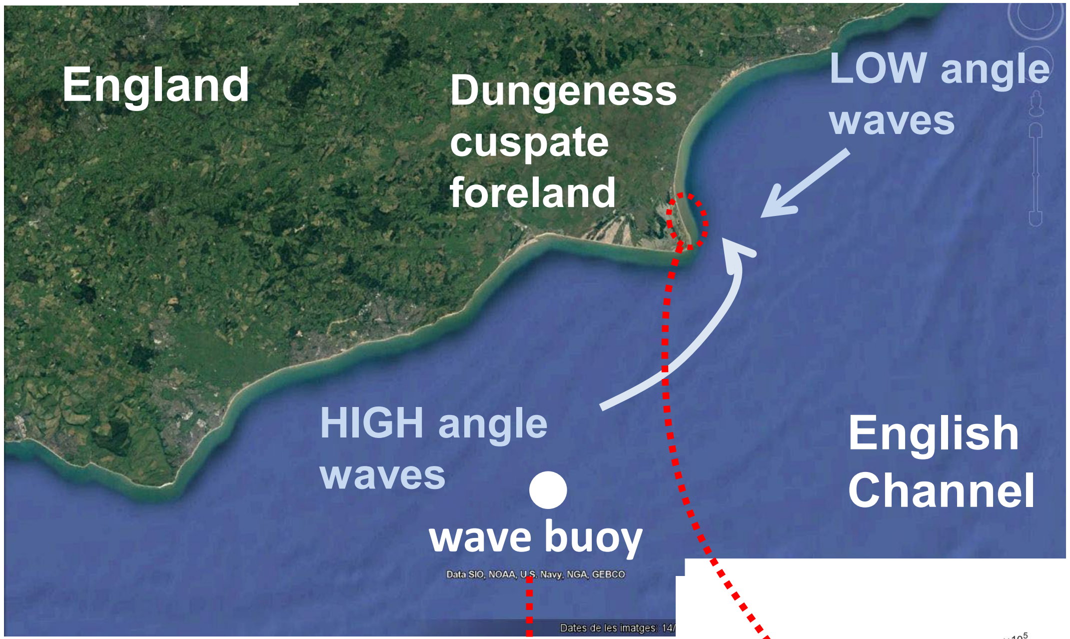

Arriaga et al., 2018

Shoreline sandwave formation event

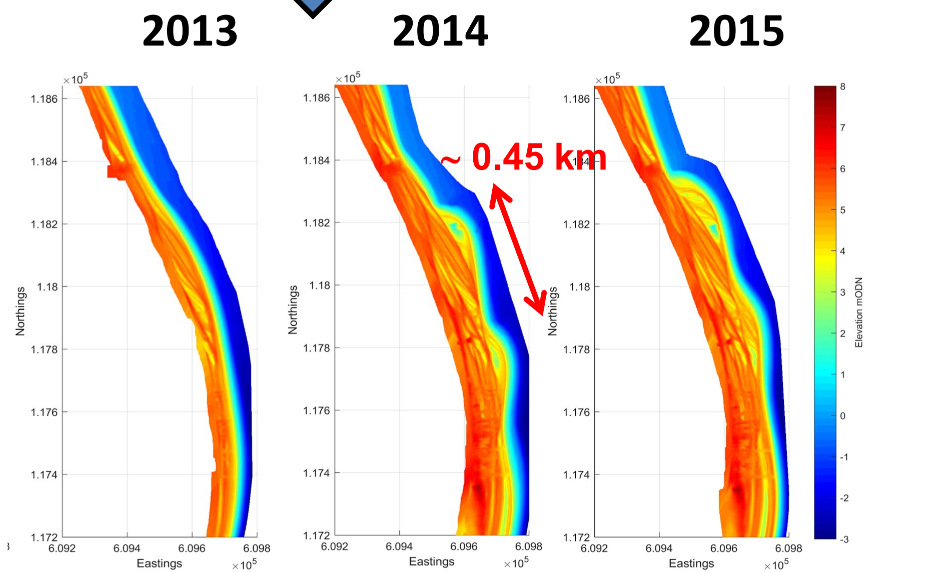

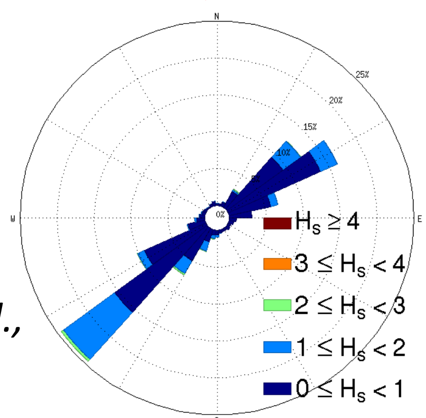

From Arriaga et al., OD, 2018

TAKE-HOME MESSAGE

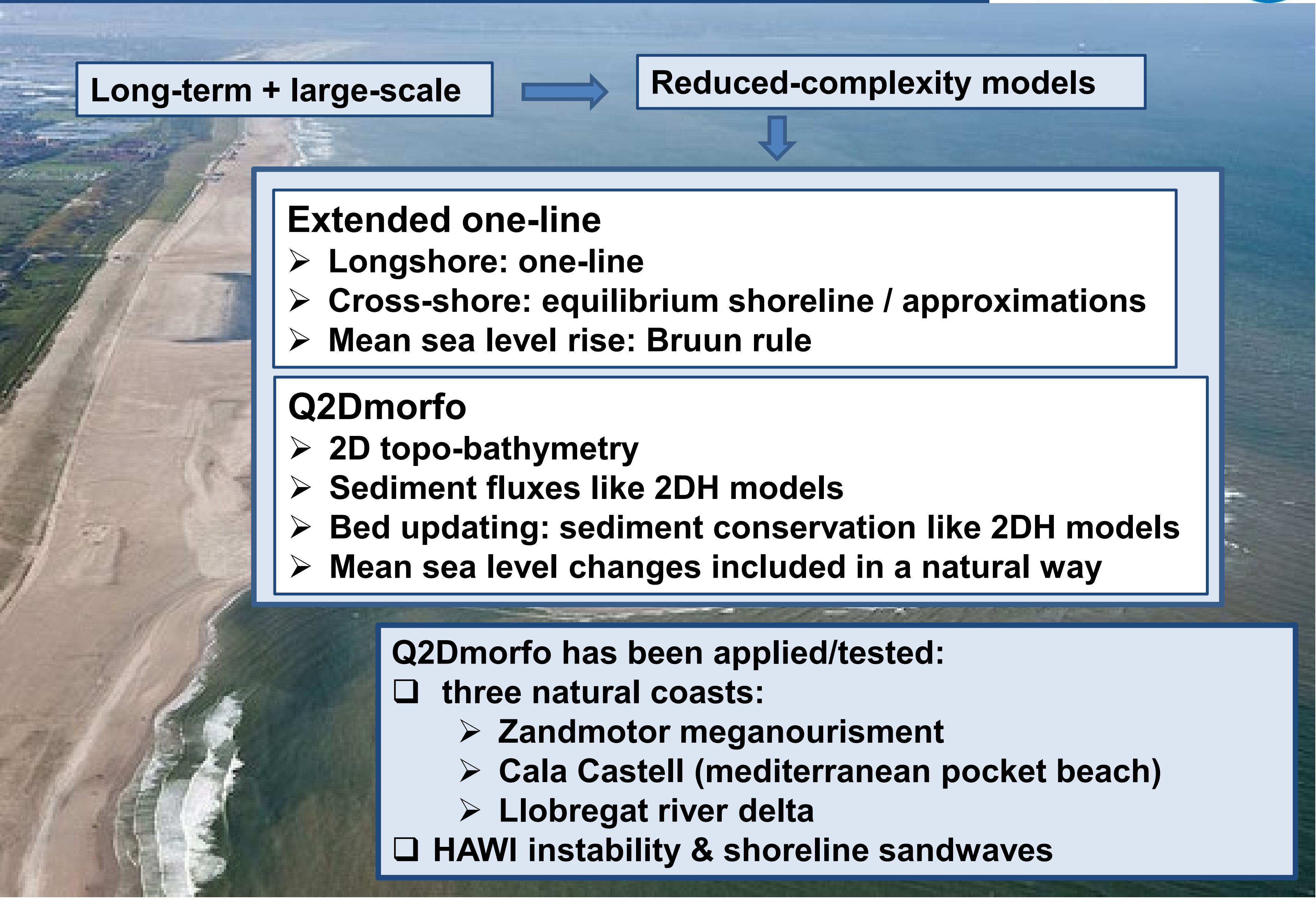

Long-term + large-scale → **Reduced-complexity models**

Extended one-line

- Longshore: one-line
- Cross-shore: equilibrium shoreline / approximations
- Mean sea level rise: Bruun rule

Q2Dmorfo

- 2D topo-bathymetry
- Sediment fluxes like 2DH models
- Bed updating: sediment conservation like 2DH models
- Mean sea level changes included in a natural way

Q2Dmorfo has been applied/tested:

- three natural coasts:
  - Zandmotor meganourisment
  - Cala Castell (mediterranean pocket beach)
  - Llobregat river delta
- HAWI instability & shoreline sandwaves

Thank you for your attention !

Cala Castell (Costa Brava, Catalonia)

albert.falques@upc.edu

REFERENCES

Morfos
http://df.upc.edu/morfos
UPC

- Alvarez-Cuesta et al. 2021, Modelling long-term shoreline evolution in highly anthropized coastal areas. Part 1: Model description and validation, Coastal Enginnering; doi.org/10.1016/j.coastaleng.2021.103960
- Antolinez et al. 2019, Predicting Climate-Driven Coastlines With a Simple and Efficient Multiscale Model, JGR Earth Surface ; doi.org/10.1029/2018JF004790
- Arriaga et al. 2017, Modeling the long-term diffusion and feeding capability of a mega-Nourishment, Coastal Engineering ; dx.doi.org/10.1016/j.coastaleng.2016.11.011
- Ashton et al. 2006, High-angle wave instability and emergent shoreline shapes: 1. Modeling of sand waves, flying spits, and capes, JGR; doi:10.1029/2005JF000422.
- Arriaga et al. 2018, Formation events of shoreline sand waves on a gravel beach, Ocean Dynamics; doi.org/10.1007/s10236-018-1157-5
- Dabees 2000, Efficient modelling of beach evolution, PhD thesis, Queen’s University
- Falqués 2003, On the diffusivity in coastline dynamics, GRL ; doi:10.1029/2003GL017760
- Falqués et al. 2006, An alternative to existint N-line shoreline models, , EGS General Assembly,
- Falqués et al. 2008, Q2D-morfo: a medium to long term model for beach morphodynamics, RCEM Conference
- Gravens et al. 1991, Technical Report CERC-89-19, GENESIS: Generalized model for simulating shoreline change
- McCarroll et al. 2021, A rules-based shoreface translation and sediment budgeting tool for estimating coastal change: ShoreTrans, , Marine Geology; doi.org/10.1016/j.margeo.2021.106466
- Miller and Dean 2004, A simple new shoreline change model, Coastal Engineering; doi:10.1016/j.coastaleng.2004.05.006
- Pelnard-Considère 1956, Essai de theorie de l’evolution des formes de rivage en plages de sable et de galets, in 4th Journees de l’Hydraulique, Les Energies de la Mer, pp. III – 1.
- Ribas et al. 2023, Impact of mean sea-level rise on the long-term evolution of a mega-nourishment, Climatic Change; doi.org/10.1007/s10584-023-03503-6

REFERENCES

- Robinet et al. 2018, A reduced-complexity shoreline change model combining longshore and cross-shore processes: The LX-Shore model, Environment Modelling and Software,; https://doi.org/10.1016/j.envsoft.2018.08.010
- Roelvink 2020, Efficient Modeling of Complex Sandy Coastal Evolution at Monthly to Century Time Scales , Frontiers in marine Science, https://doi.org/10.3389/fmars.2020.00535
- Splinter et al. 2014, A generalized equilibrium model for predicting daily to interannual shoreline response, JGR Earth Surface; dx.doi.org/10.1002/2014JF003106
- Tran and Barthelemy 2020, Combined longshore and cross-shore shoreline model for closed embayed beaches, Coastal Engineering; https://doi.org/10.1016/j.coastaleng.2020.103692
- Van den Berg et al. 2012, Modeling large scale shoreline sand waves under oblique wave incidence, JGR, doi:10.1029/2011JF002177.
- Vitousek et al. 2017, A model integrating longshore and cross-shore processes for predicting long-term Shoreline response to climate change, JGR Earth Surface, dx.doi.org/10.1002/2016JF004065
- Yates et al. 2009, Equilibrium shoreline response: Observations and modeling, JGR; doi:10.1029/2009JC005359

“Find your course in choosing between coarse grids, fine grids, unstructured grids, quadtree grids and subgrids” (N. Volp, UTWENTE)

grids, quadtree grids and subgrids

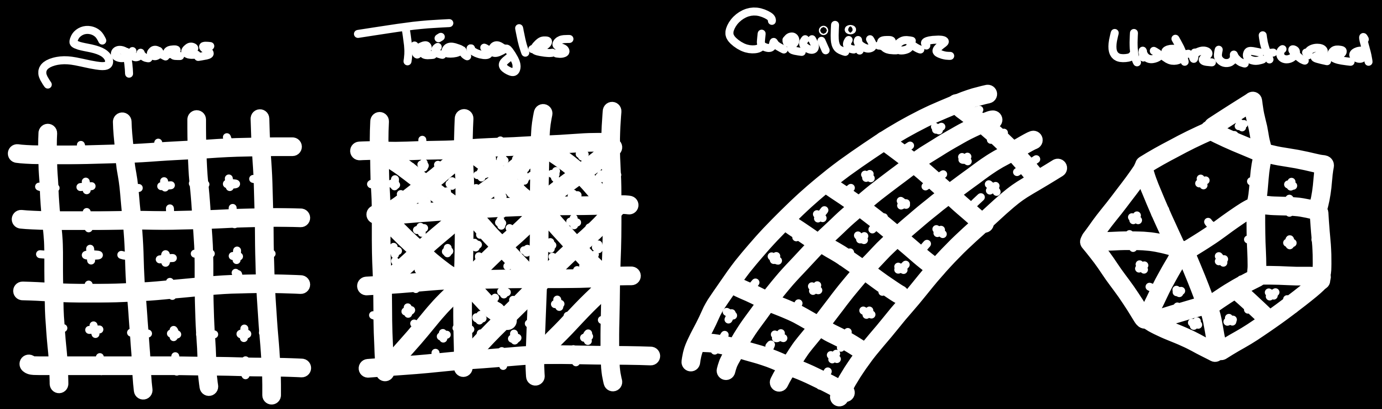

Dealing with grids in hydro- en morphodynamics

Nelen & Schuurmans

UNIVERSITY OF TWENTE.

dr. Nicolette Volp
University of Twente & Nelen en Schuurmans

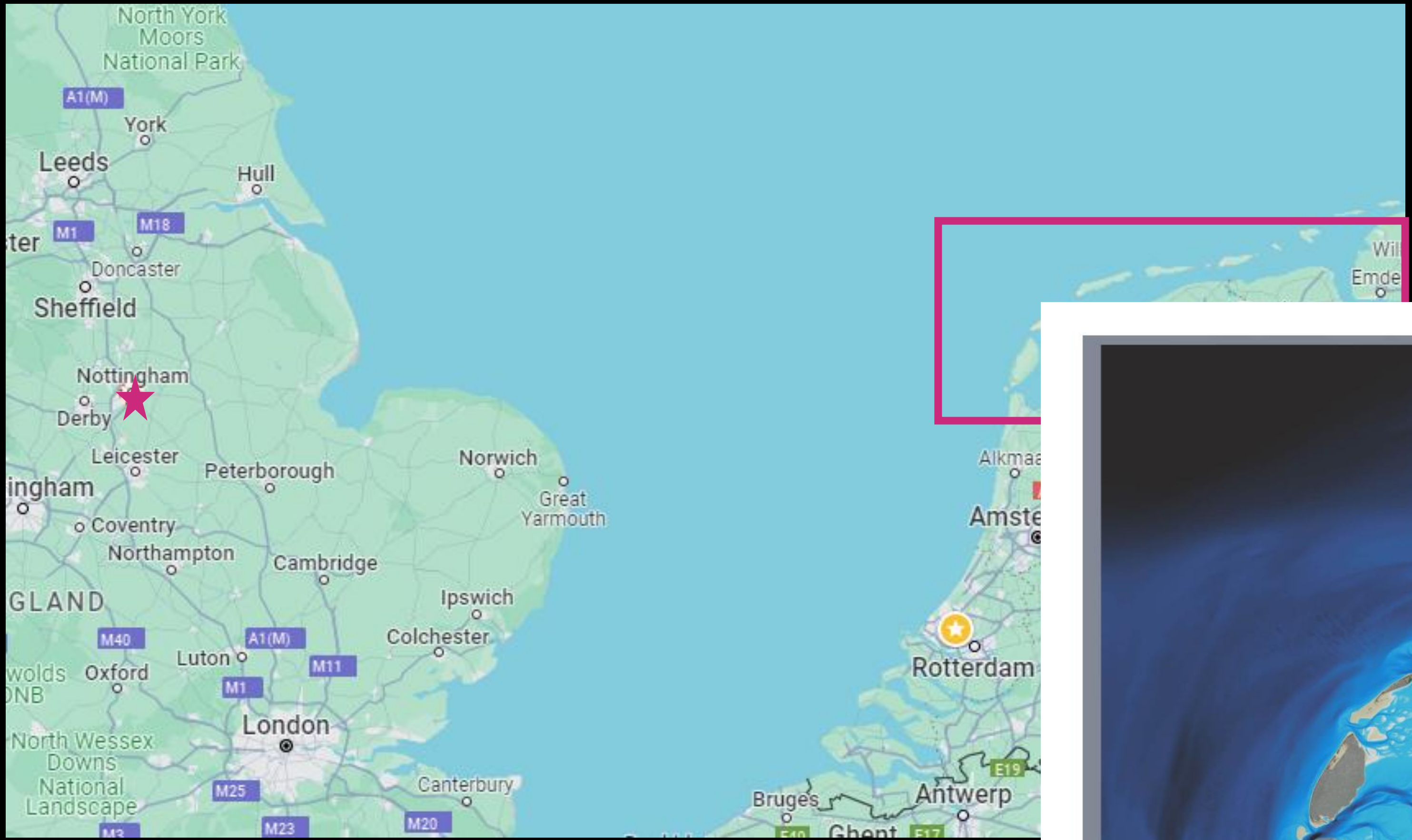

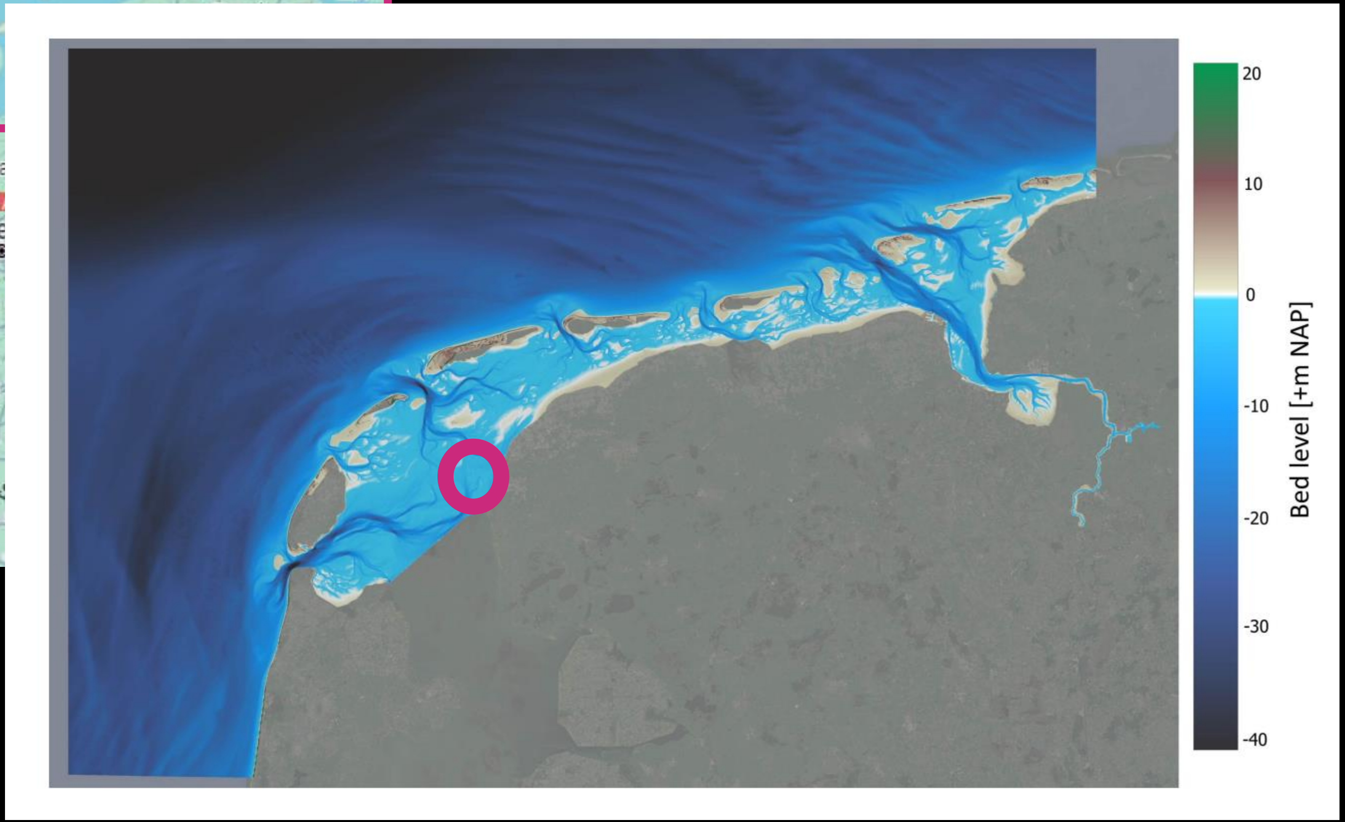

From: Google Maps

From: Reinder Boorsma MSc. Project

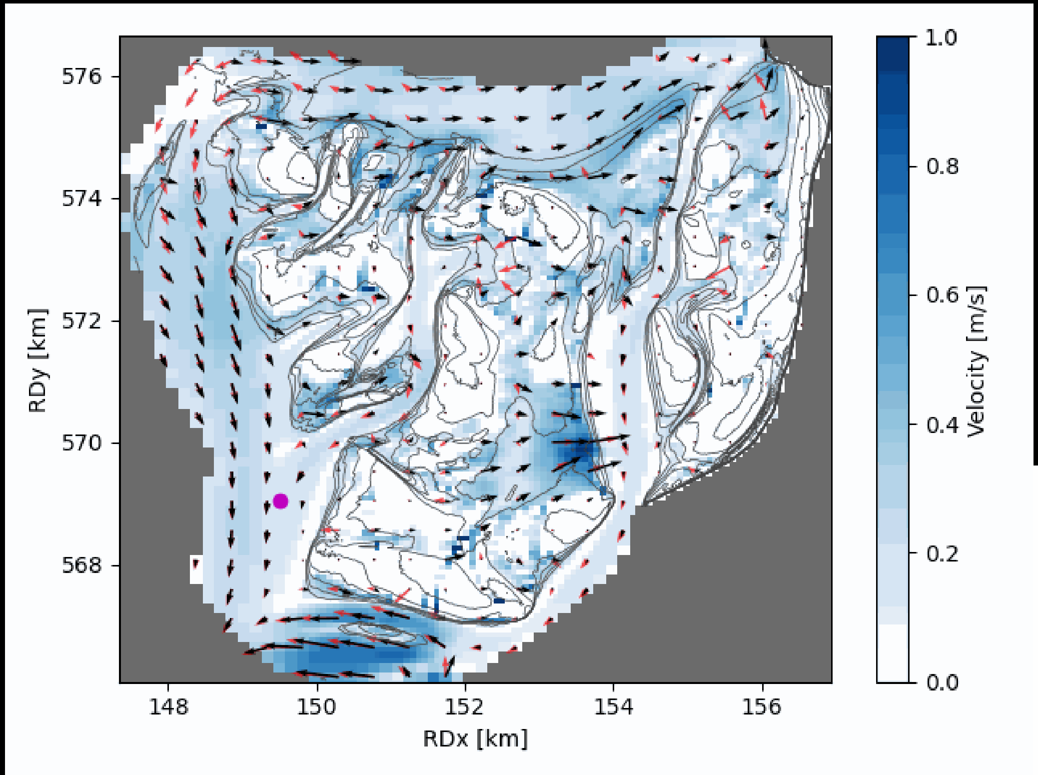

RDy [km]
576
574
572
570
568
148
150
152
154
156
RDx [km]
Velocity [m/s]
1.0
0.8
0.6
0.4
0.2
0.0

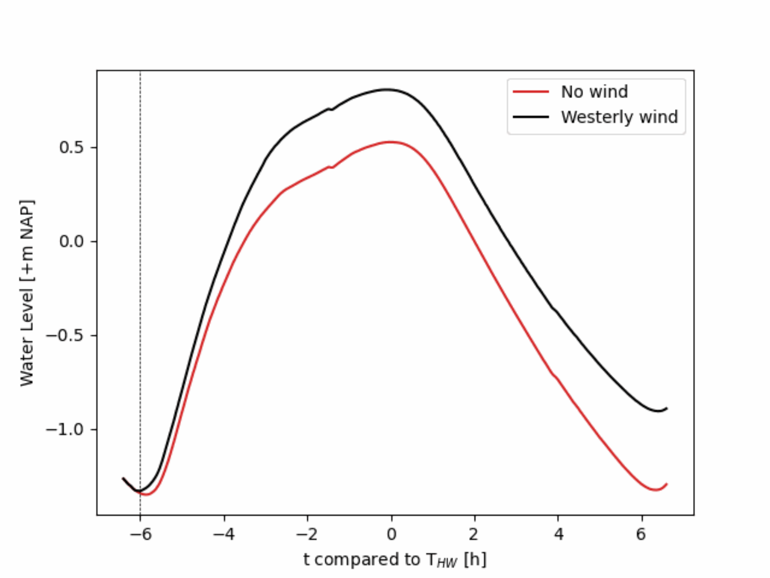

No wind
Westerly wind
Water Level [+m NAP]
0.5
0.0
−0.5
−1.0
−6
−4
−2
0
2
4
6
t compared to T_{HW} [h]

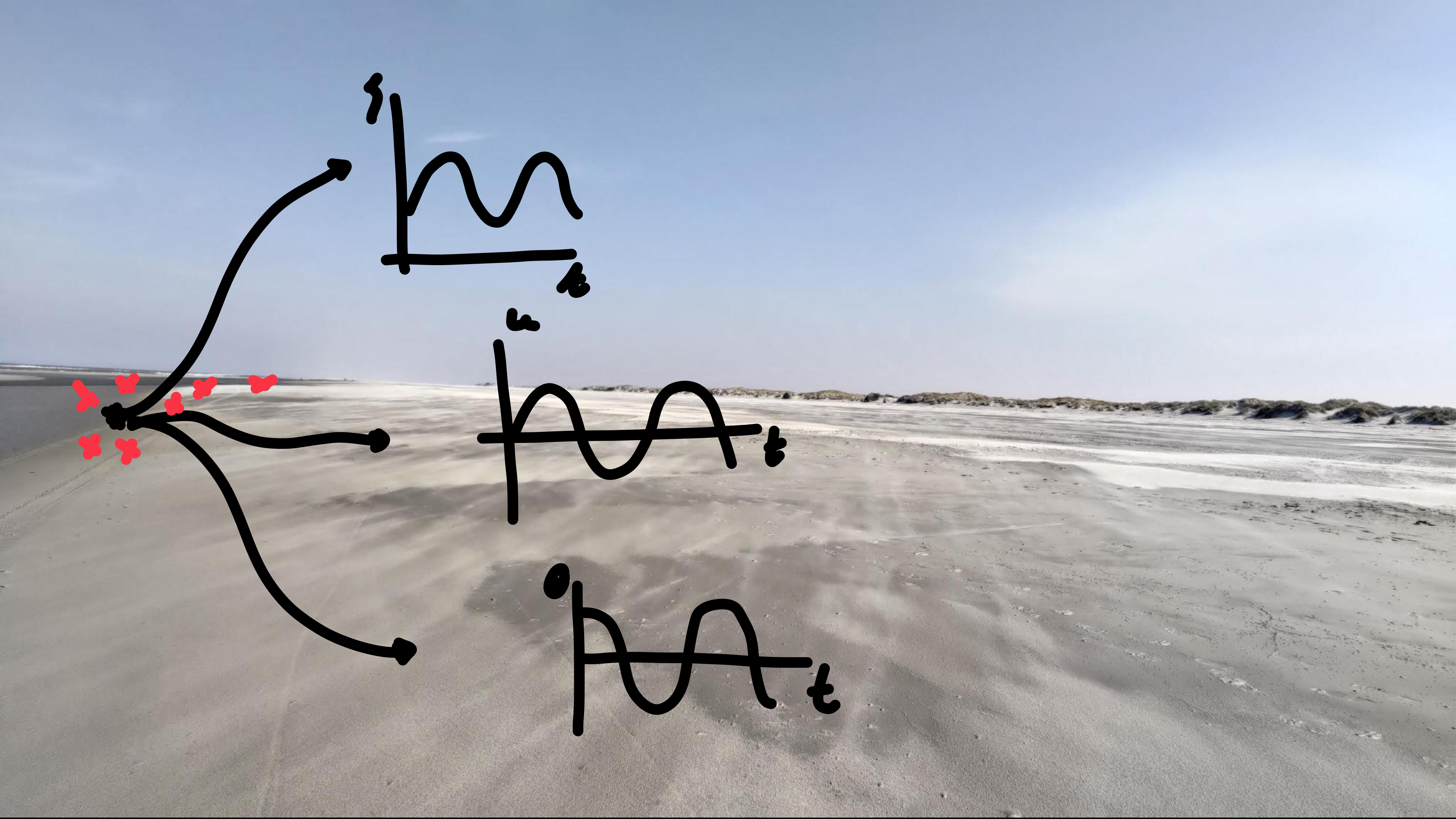
t
t
t

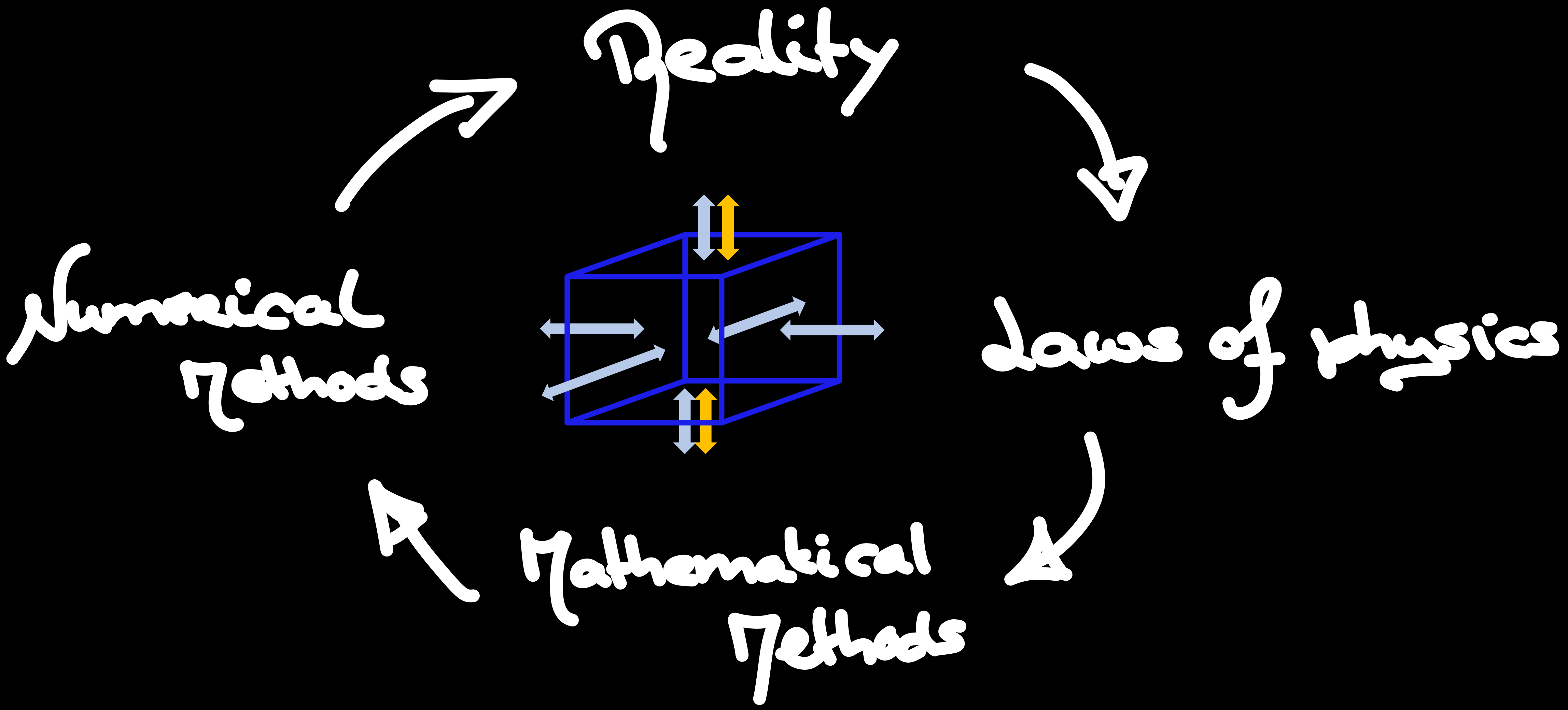
Reality
Laws of physics
Mathematical Methods
Numerical Methods

Some Conclusions

- Get to know your grid
- Choose your resolution wisely
- Be careful with grid size transitions
- Subgrid is cool

The equations

→ Conservation of mass

$$\rho \frac{dV}{dt} = \sum \rho Q_{in} - \sum \rho Q_{out}$$

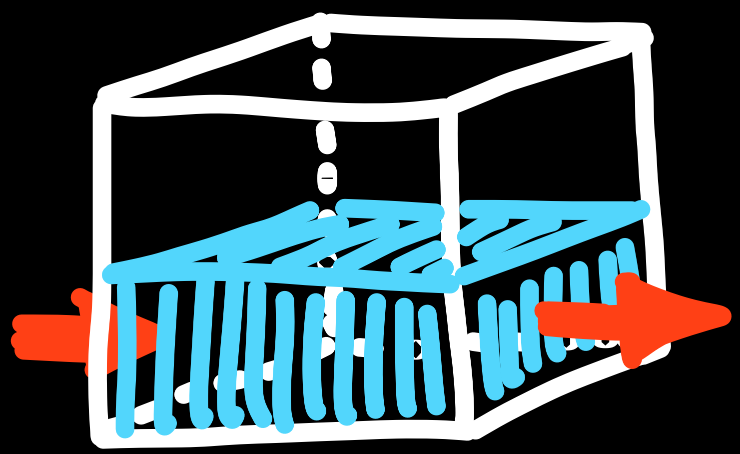

The equations

→ Conservation of mass $\rho \frac{dV}{dt} = \sum \rho Q_{in} - \sum \rho Q_{out}$

→ Conservation of momentum

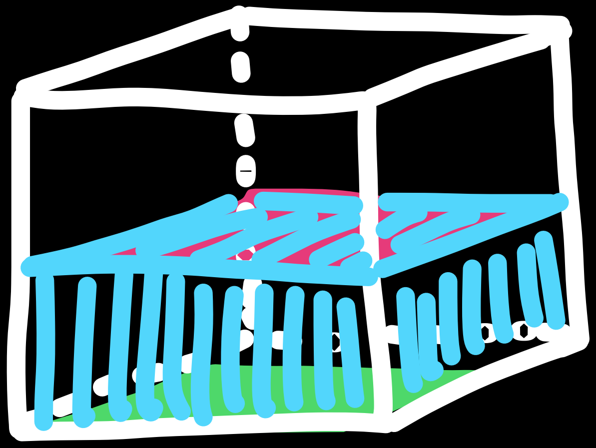

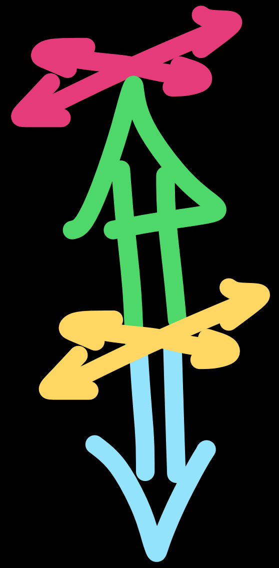

$$\frac{dp}{dt} = \tilde{F}_G + \tilde{F}_f + \tilde{F}_w + \ldots$$

The equations : an example

2D Depth Averaged Shallow Water Equations :

$$\frac{\partial u}{\partial t} + u\frac{\partial u}{\partial x} + v\frac{\partial u}{\partial y} + g\frac{\partial \zeta}{\partial x} + \frac{c_f}{h}u|u| = 0$$

$$\frac{\partial v}{\partial t} + u\frac{\partial v}{\partial x} + v\frac{\partial v}{\partial y} + g\frac{\partial \zeta}{\partial y} + \frac{c_f}{h}v|u| = 0$$

$$\frac{\partial h}{\partial t} + (uh)_x + (vh)_y = 0$$

Grids

- Water level, full velocity vector

Grids

- Water level, full velocity vector
- Water level
- Full velocity vector

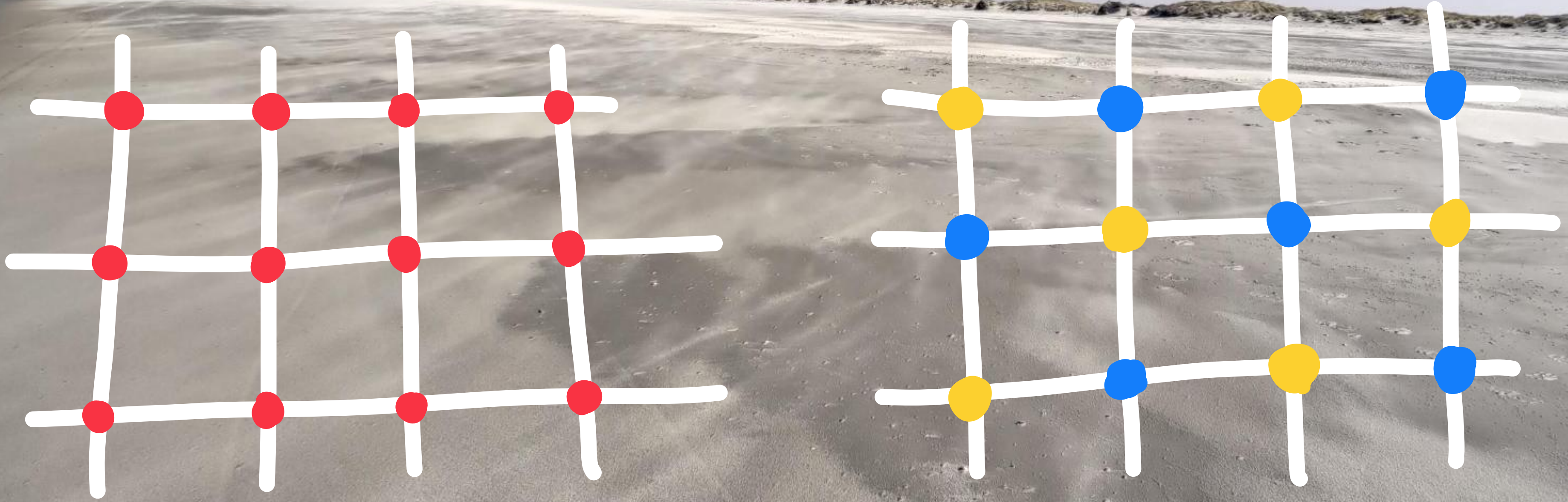

Grids

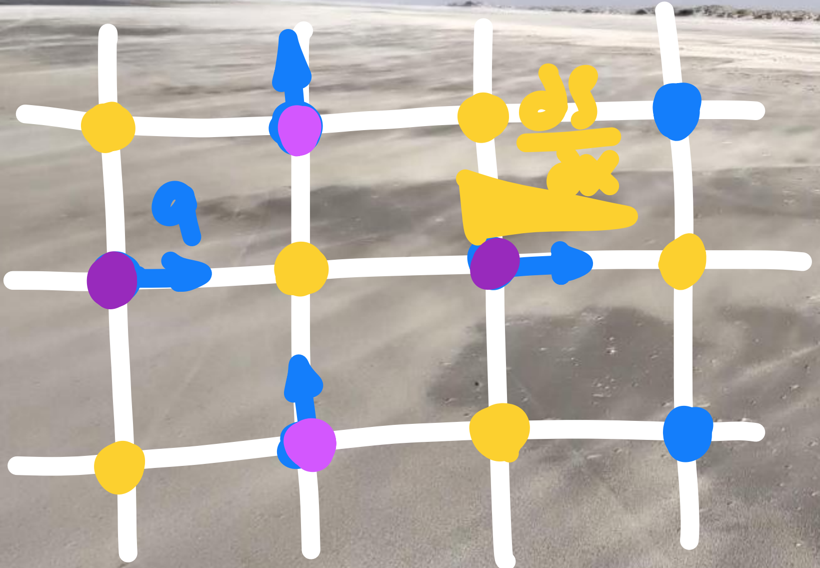

x-component velocity

y-component velocity

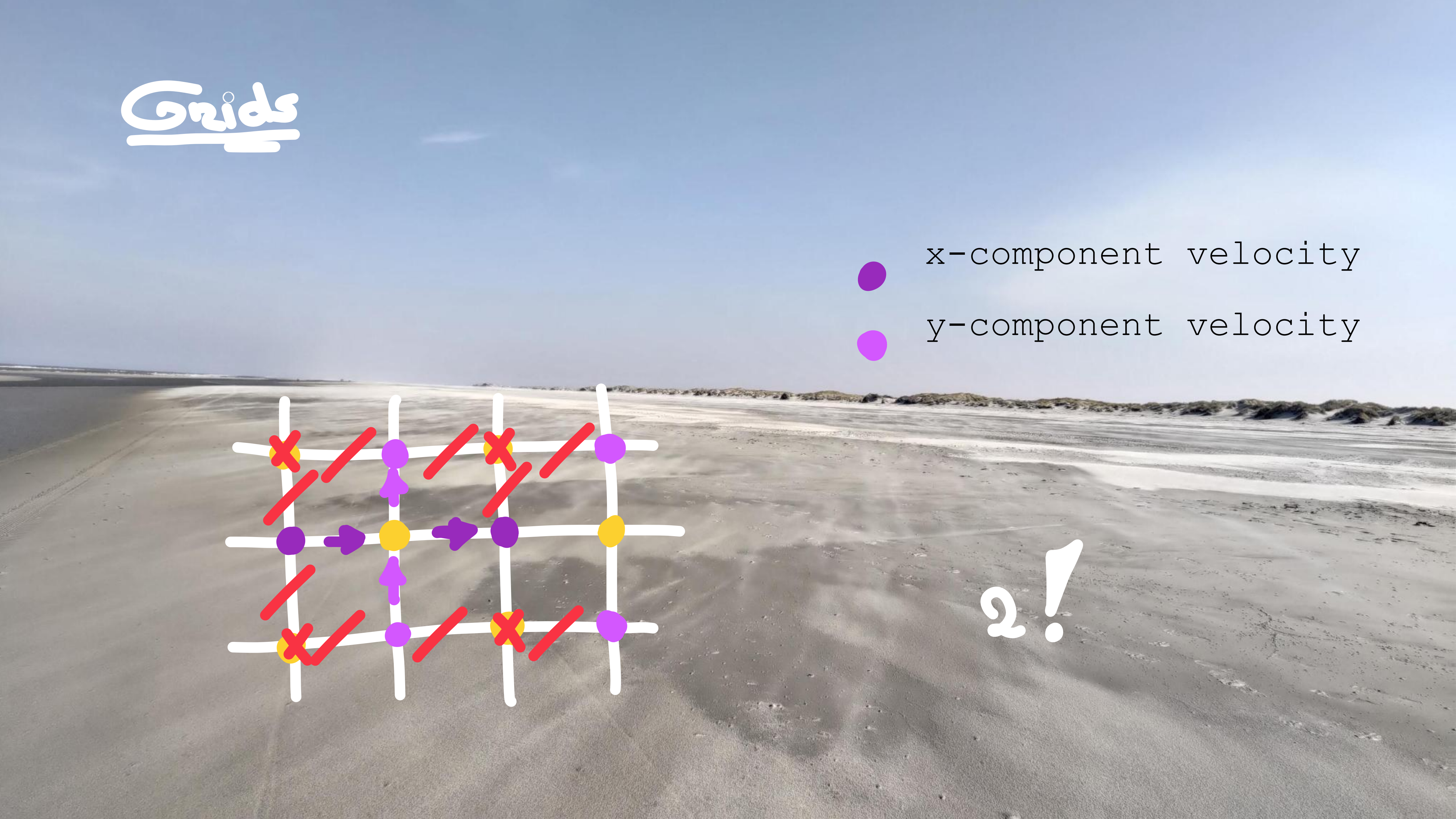
Grids
x-component velocity
y-component velocity
2!

Grid Resolution

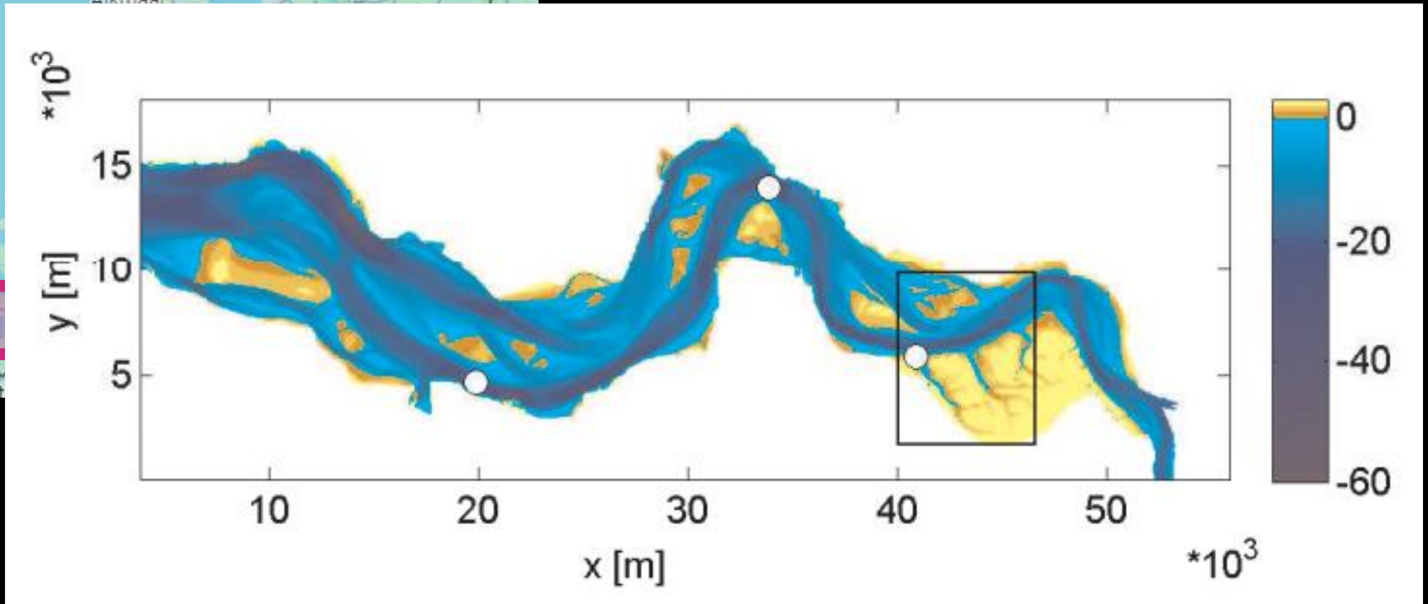

From: Google Maps

From: Nicolette Volp, Phd Thesis

Grid Resolution

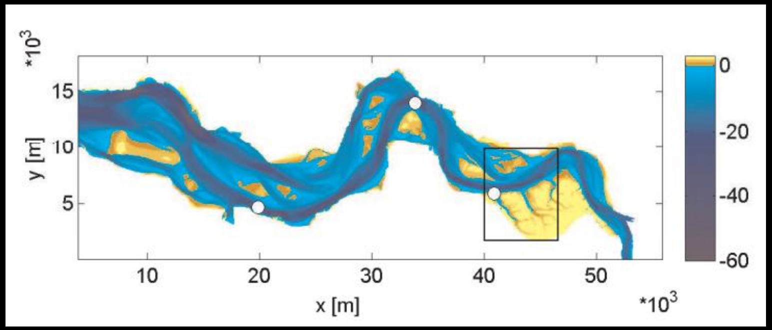

$\Delta x = 40\,m$

$\Delta x = 400\,m$

$\Delta x = 960\,m$

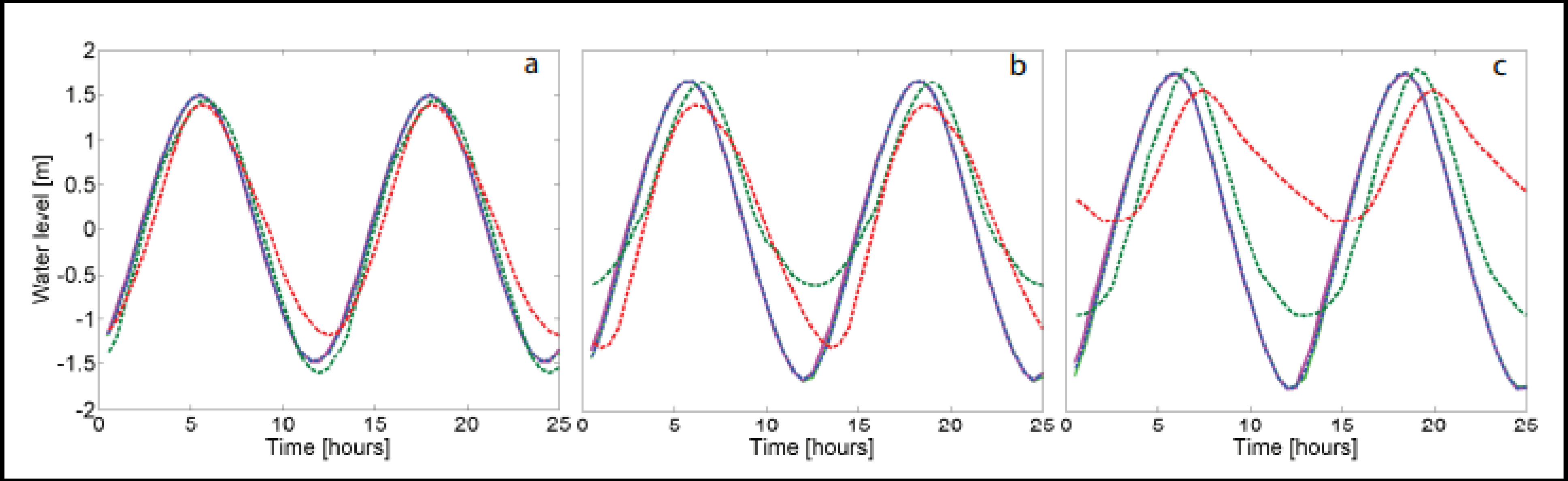

From: Nicolette Volp, Phd Thesis

The discretization Error

$$\frac{dc}{dx} = f(c,x) \Rightarrow \frac{c_{m+1} - c_m}{\Delta x} = f_m$$

Consistency:

$$\lim_{\Delta x \to 0} \frac{c(x+\Delta x) - c(x)}{\Delta x} - f(c,x) = 0$$

The discretization Error

$$\frac{dc}{dx} = f(c,x) \rightarrow \frac{c_{n+1} - c_n}{\Delta x} = f_n \qquad \lim_{\Delta x \to 0} \frac{c(x+\Delta x) - c(x)}{\Delta x} - f(c,x) = 0$$

Taylor

$$c(x_0+\Delta x) = c(x_0) + \Delta x \left.\frac{dc}{dx}\right|_{x_0} + \frac{\Delta x^2}{2!} \left.\frac{d^2c}{dx^2}\right|_{x_0} + \frac{\Delta x^3}{3!} \left.\frac{d^3c}{dx^3}\right|_{x_0} + \dots$$

The discretization Error

$$\frac{dc}{dx} = f(c,x) \rightarrow \frac{c_{n+1} - c_n}{\Delta x} = f_n \qquad \lim_{\Delta x \to 0} \frac{c(x+\Delta x) - c(x)}{\Delta x} - f(c,x) = 0$$

$$c(x+\Delta x) = c(x) + \Delta x \left.\frac{dc}{dx}\right|_{x_0} + \frac{\Delta x^2}{2!} \left.\frac{d^2c}{dx^2}\right|_{x_0} + \frac{\Delta x^3}{3!} \left.\frac{d^3c}{dx^3}\right|_{x_0} + \dots$$

$$\lim_{\Delta x \to 0} \frac{c(x_0) + \Delta x \left.\frac{dc}{dx}\right|_{x_0} + \frac{\Delta x^2}{2!} \frac{d^2c}{dx^2} + \dots - c(x_0)}{\Delta x} - f(c,x_0)$$

The discretization Error

$$\frac{dc}{dx} = f(c,x) \rightarrow \frac{c_{n+1}-c_n}{\Delta x} = f_n \qquad \lim_{\Delta x \to 0} \frac{c(x+\Delta x)-c(x)}{\Delta x} - f(c,x) = 0$$

$$c(x_0+\Delta x) = c(x_0) + \Delta x \frac{dc}{dx}\Big|_{x_0} + \frac{\Delta x^2}{2!}\frac{d^2c}{dx^2}\Big|_{x_0} + \frac{\Delta x^3}{3!}\frac{d^3c}{dx^3}\Big|_{x_0} + \cdots$$

$$\lim_{\Delta x \to 0} \frac{\cancel{c(x_0)} + \cancel{\Delta x} \frac{dc}{dx}\Big|_{x_0} + \frac{\Delta x^{\cancel{2}}}{2!}\frac{d^2c}{dx^2} + \cdots - \cancel{c(x_0)}}{\cancel{\Delta x}} - f(c,x_0)$$

The discretization Error

$$\frac{dc}{dx} = f(c,x) \rightarrow \frac{c_{n+1}-c_n}{\Delta x} = f_n \qquad \lim_{\Delta x \to 0} \frac{c(x+\Delta x)-c(x)}{\Delta x} - f(c,x) = 0$$

$$c(x_0+\Delta x) = c(x_0) + \Delta x \left.\frac{dc}{dx}\right|_{x_0} + \frac{\Delta x^2}{2!}\left.\frac{d^2c}{dx^2}\right|_{x_0} + \frac{\Delta x^3}{3!}\left.\frac{d^3c}{dx^3}\right|_{x_0} + \cdots$$

$$\lim_{\Delta x \to 0} \frac{\cancel{c(x_0)} + \cancel{\Delta x}\cancel{\left.\frac{dc}{dx}\right|_{x_0}} + \frac{\Delta x^{\cancel{2}}}{2!}\frac{d^2c}{dx^2} + \cdots - \cancel{c(x_0)}}{\cancel{\Delta x}} - \cancel{f(c,x_0)}$$

$$= \lim_{\Delta x \to 0} \frac{\Delta x}{2!}\frac{d^2c}{dx^2} + \cdots$$

Intermezzo

https://www.menti.com/alswr9ueqrxs

A Simple Example

$$\frac{d^2y}{dx^2} = 12x^2 \quad \Bigg| \quad \left.\frac{dy}{dx}\right|_{x=-1} = -4 \qquad y\Big|_{x=1} = -1$$

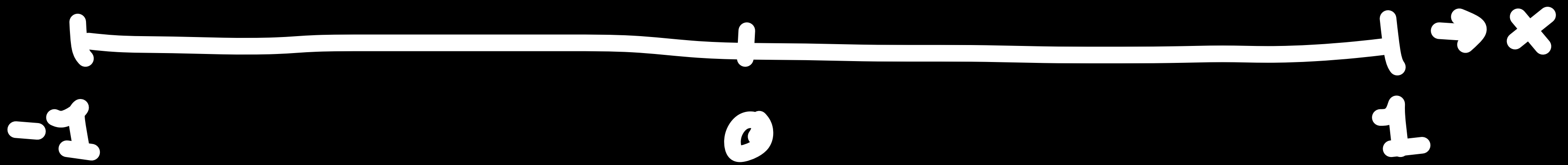

$$y = x^4$$

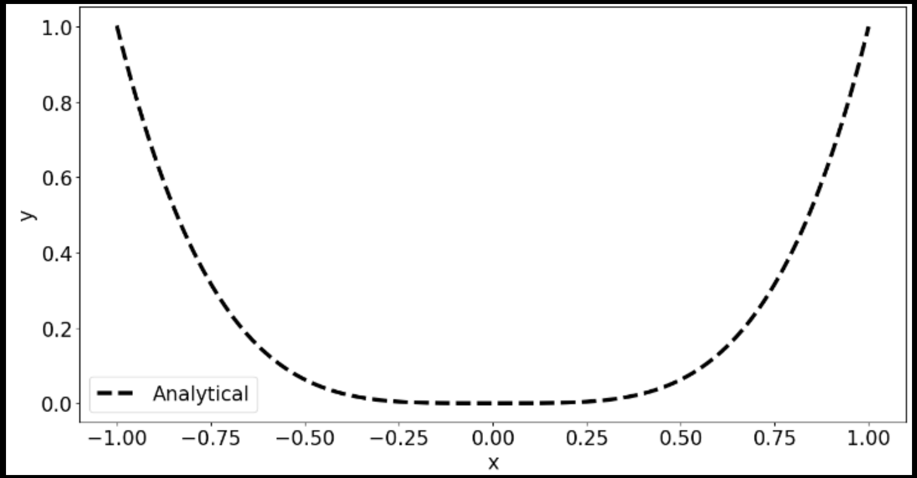

Lets Check that Error

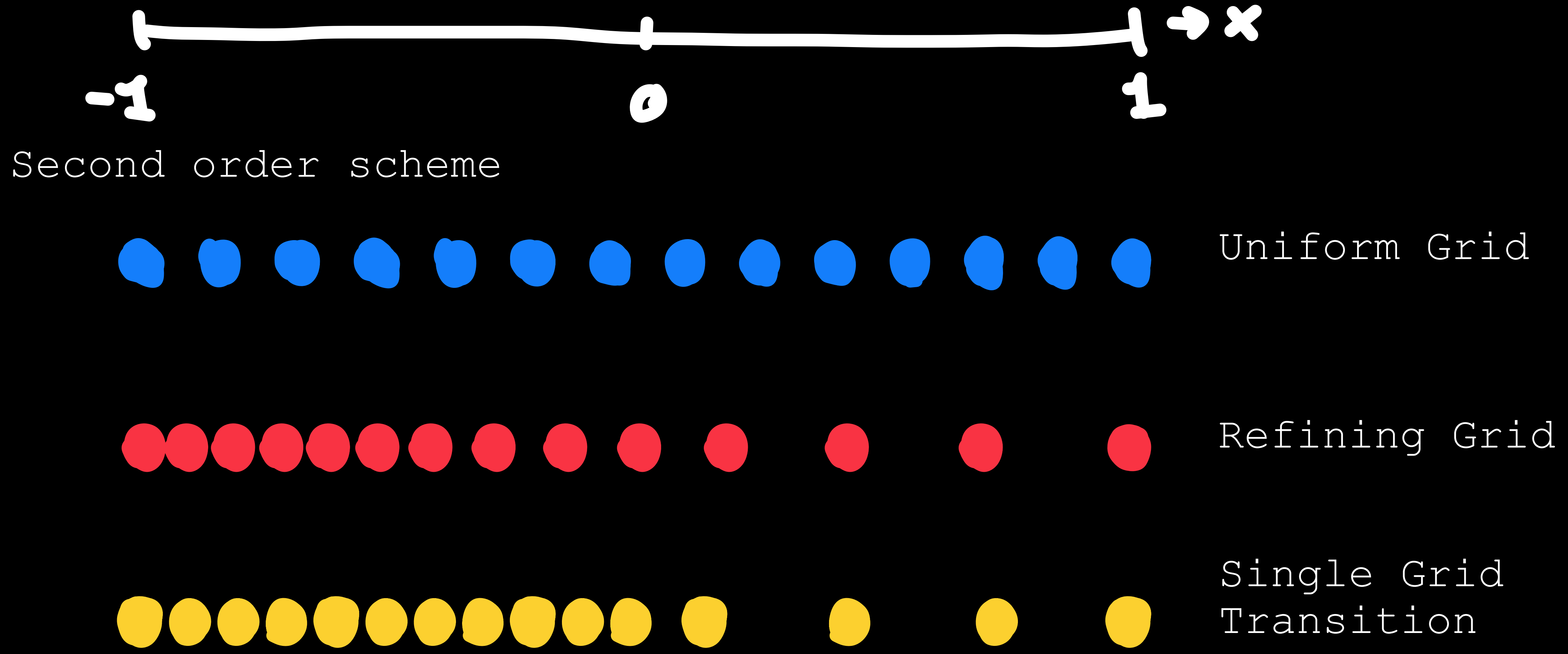

Lets Check that Error

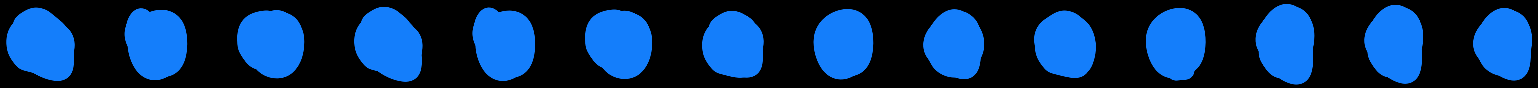

Uniform Grid

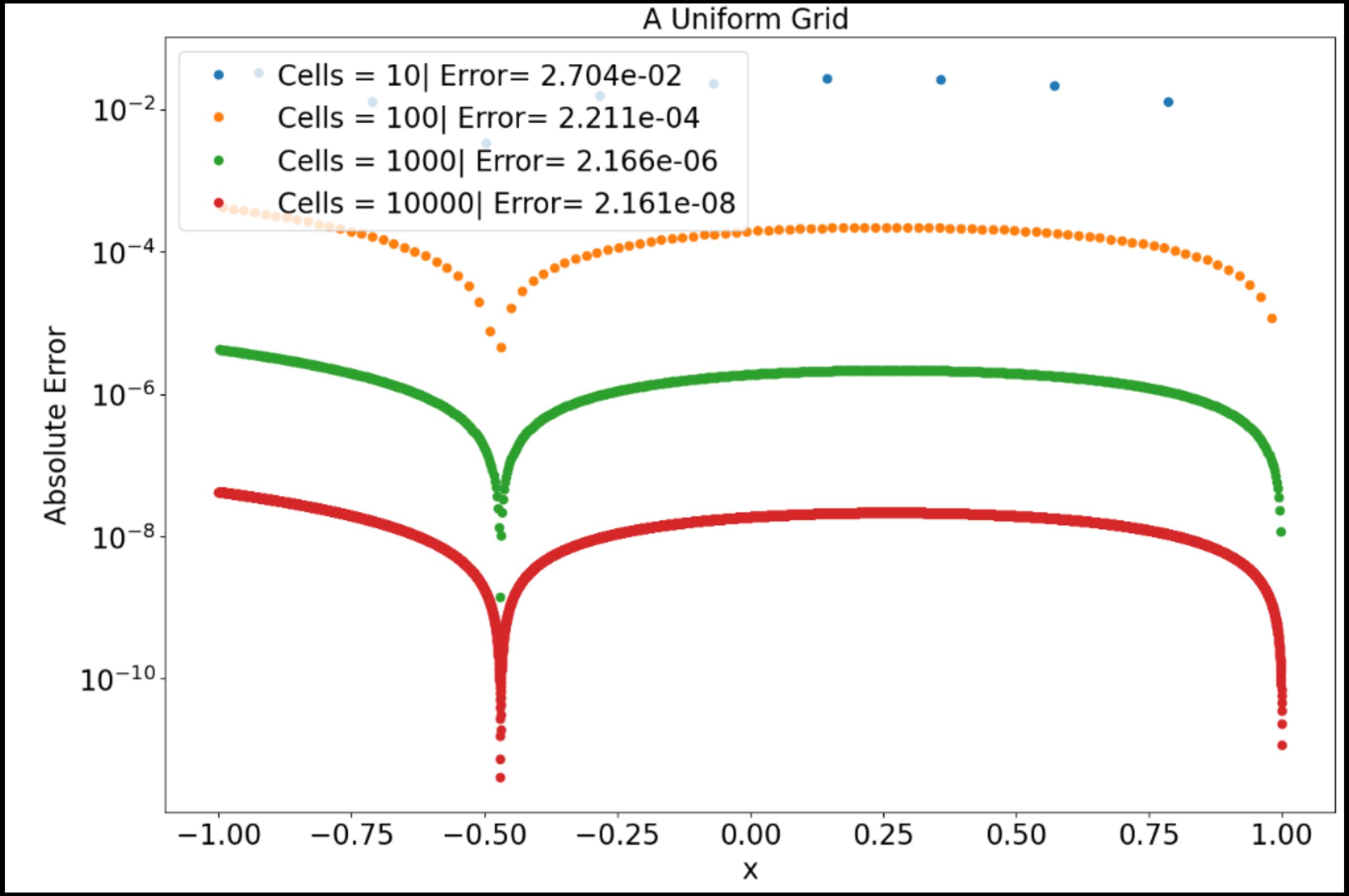

Lets Check that Error

Refining Grid

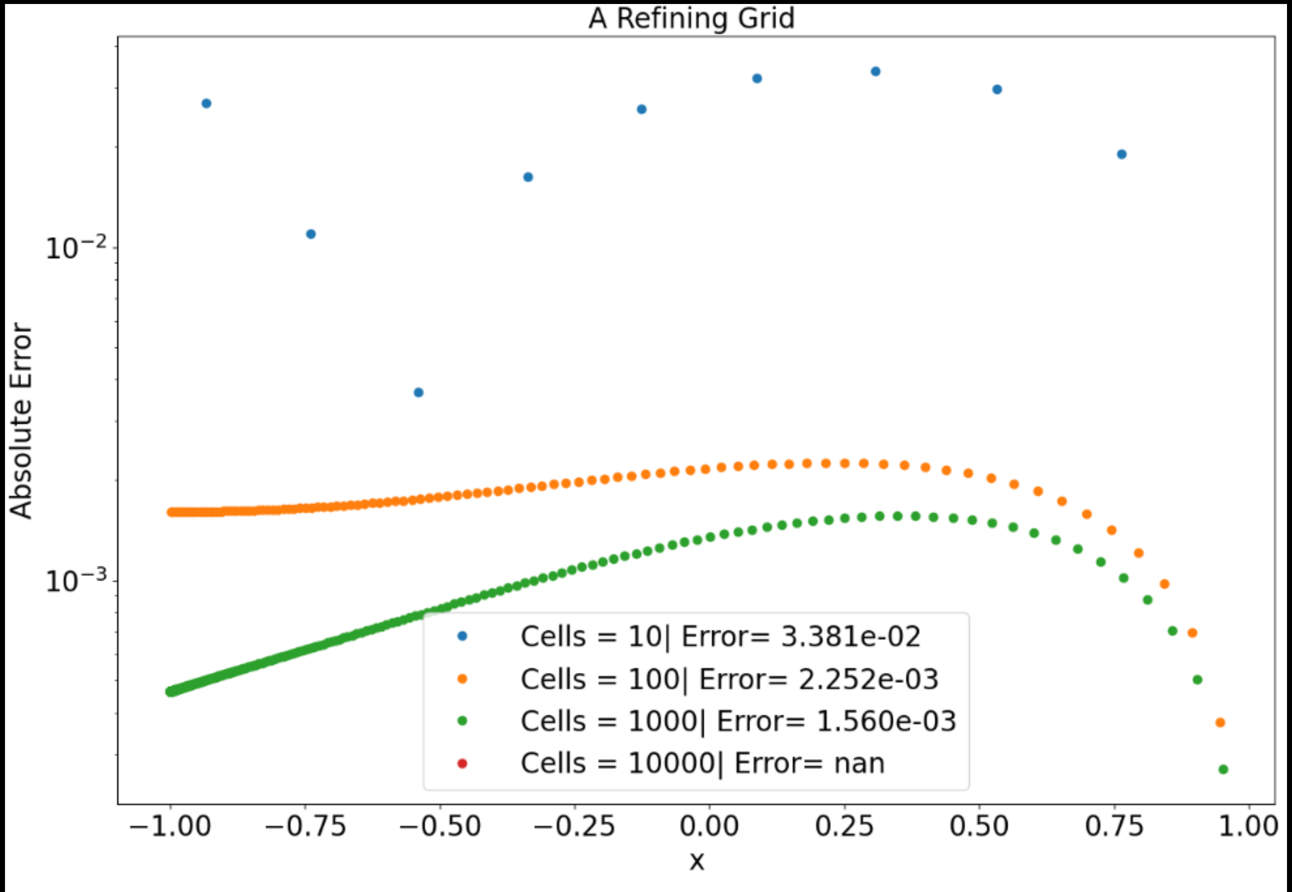

Lets Check that Error

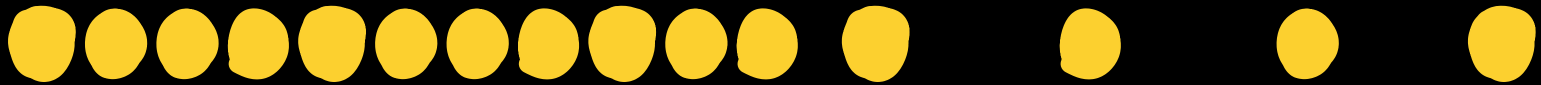

Single Grid
Transition

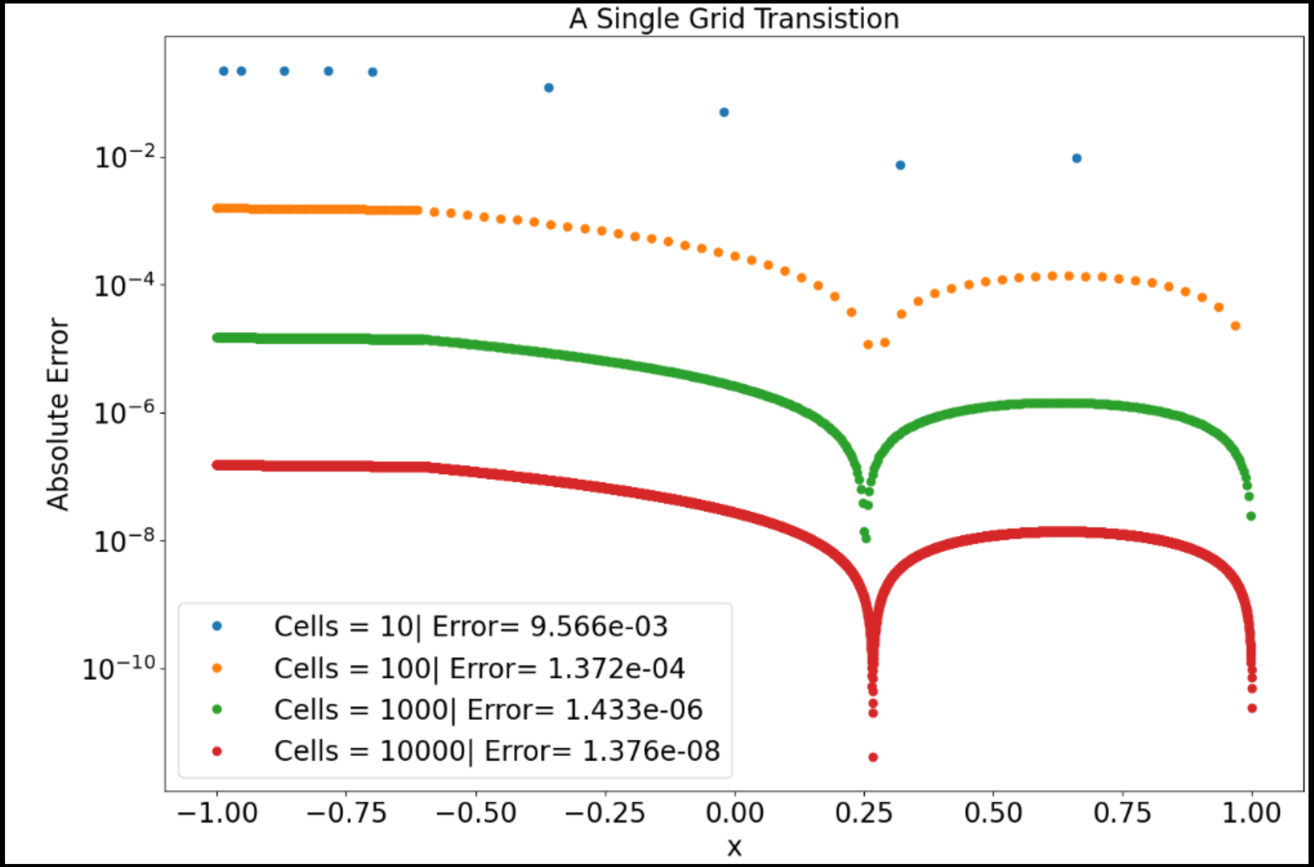

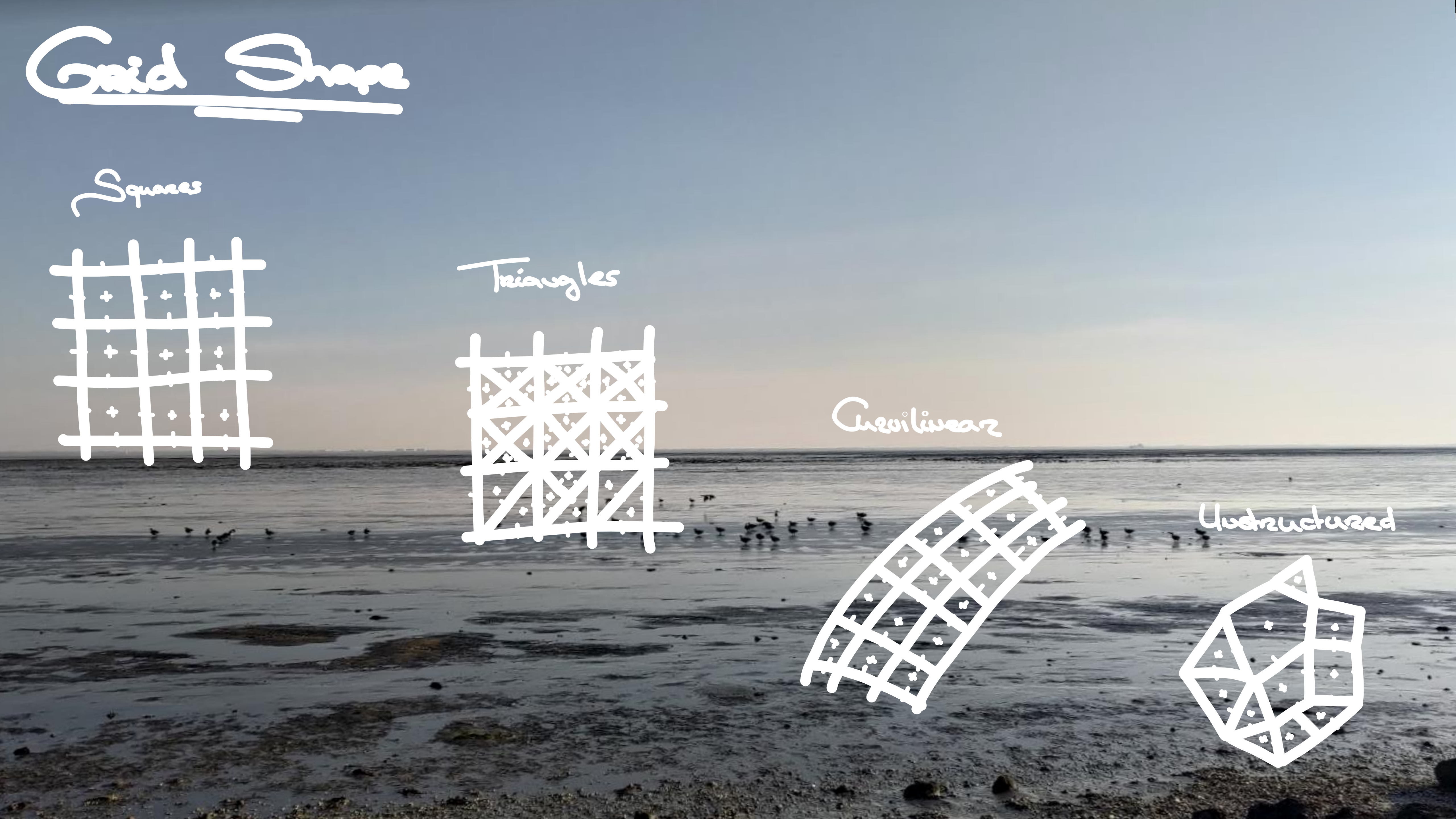
Grid Shape
Squares
Triangles
Curvilinear
Unstructured

Grid Shape

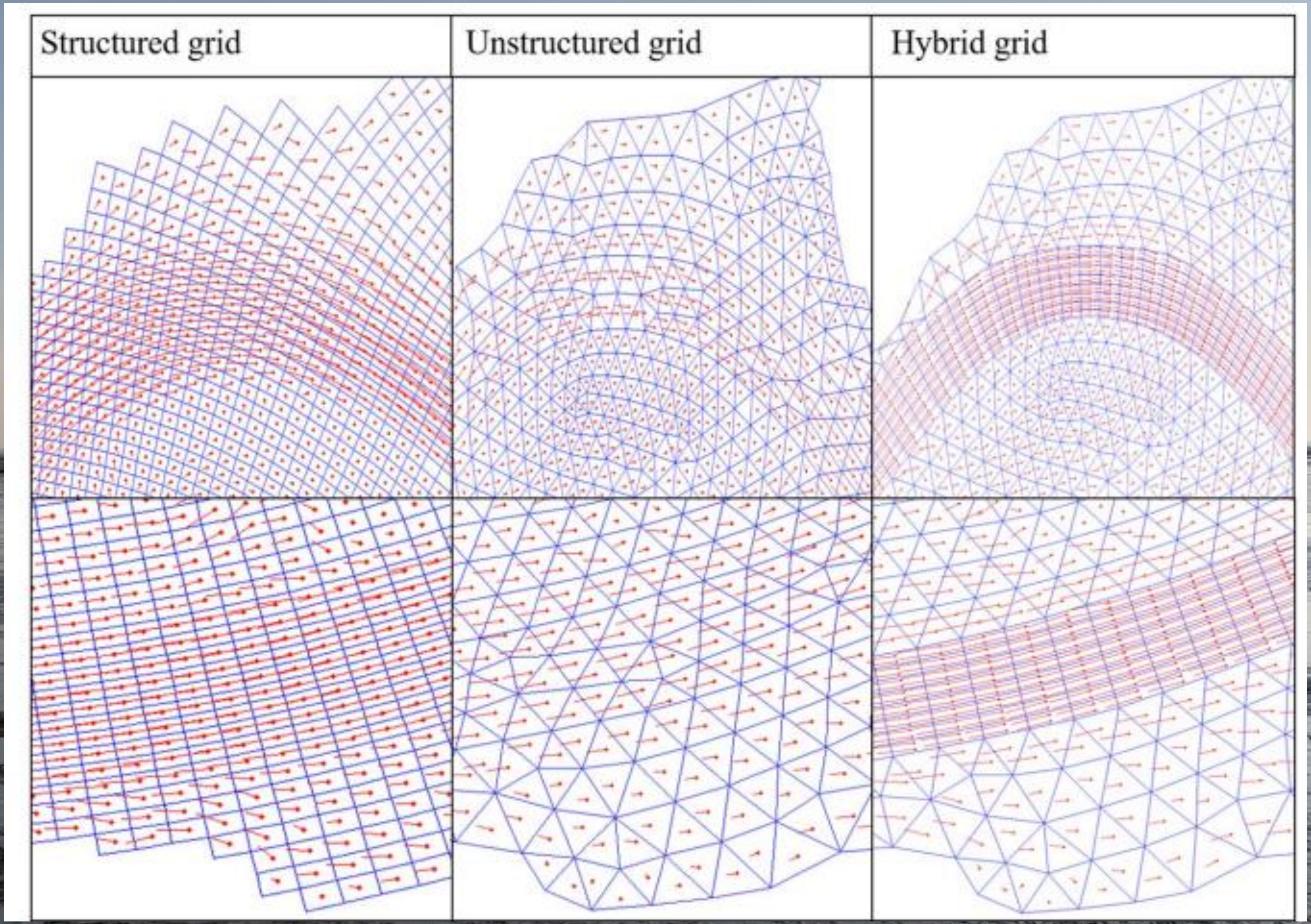

From: Bomers et al 2019

Bathymetry

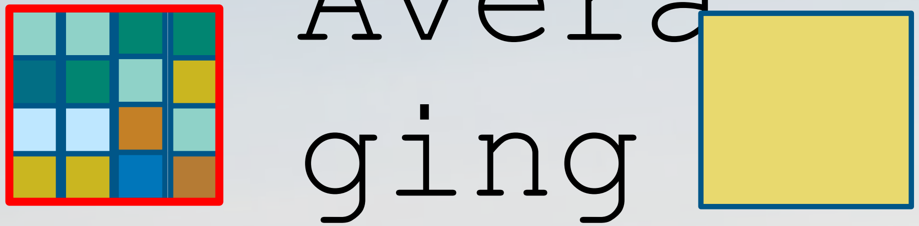

Averaging

Corners

Unstructured

Unstructured

Bathymetry

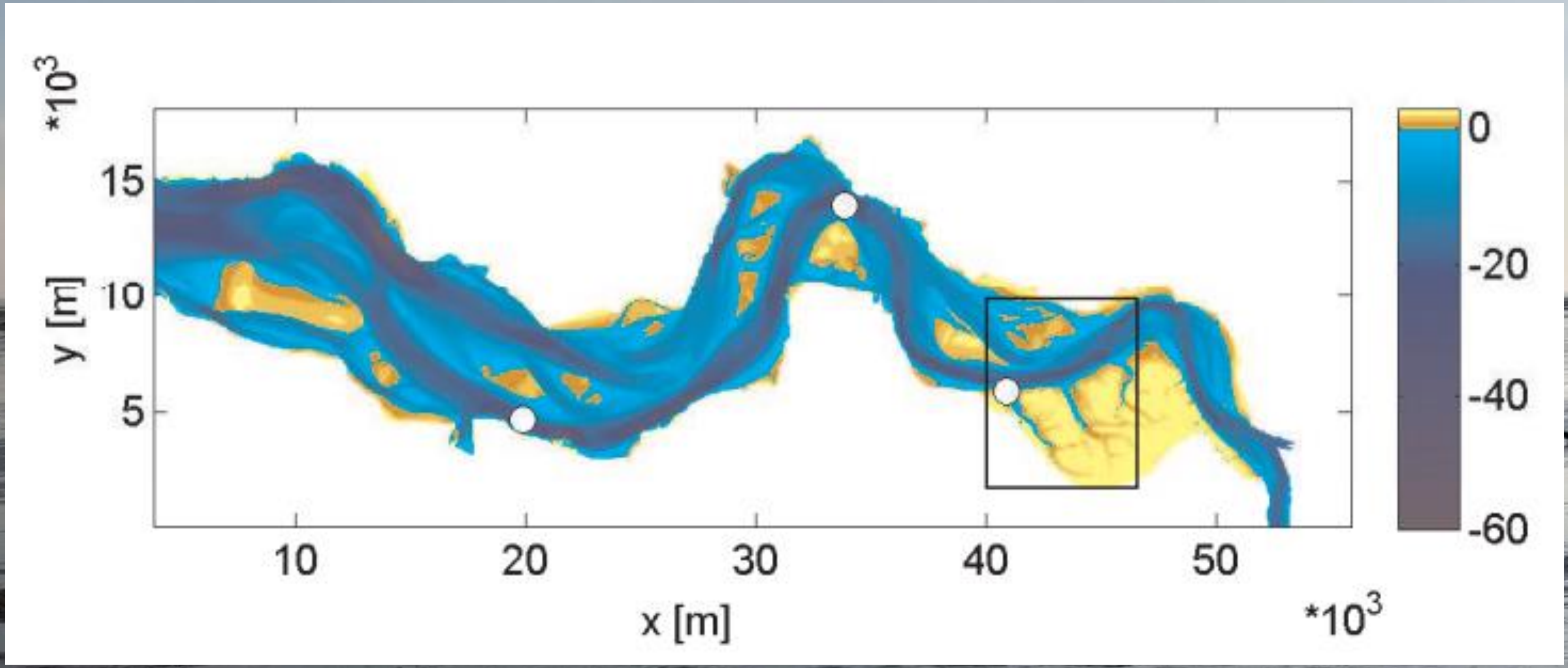

Subgrid Bathymetry

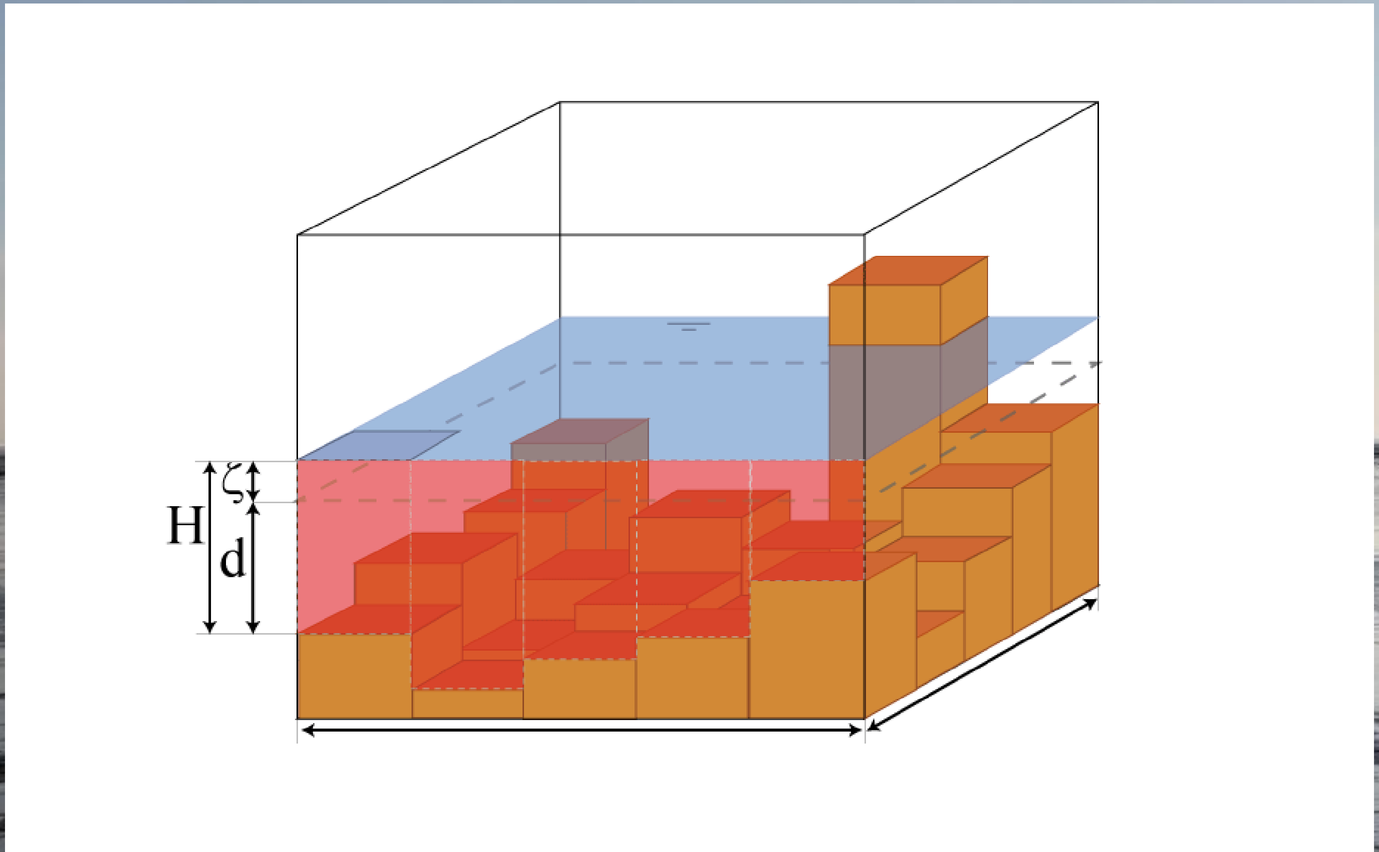

Casulli 2009`, Bates, Defina 2009 …

Subgrid Bathymetry

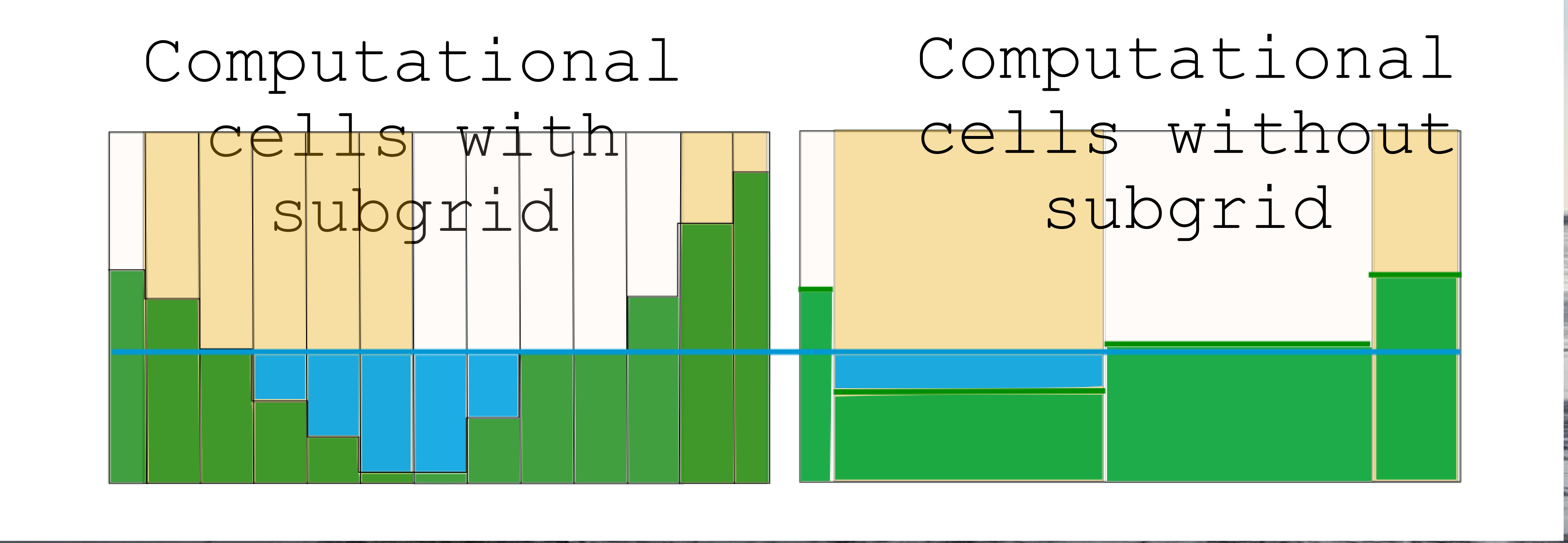

Subgrid Bathymetry

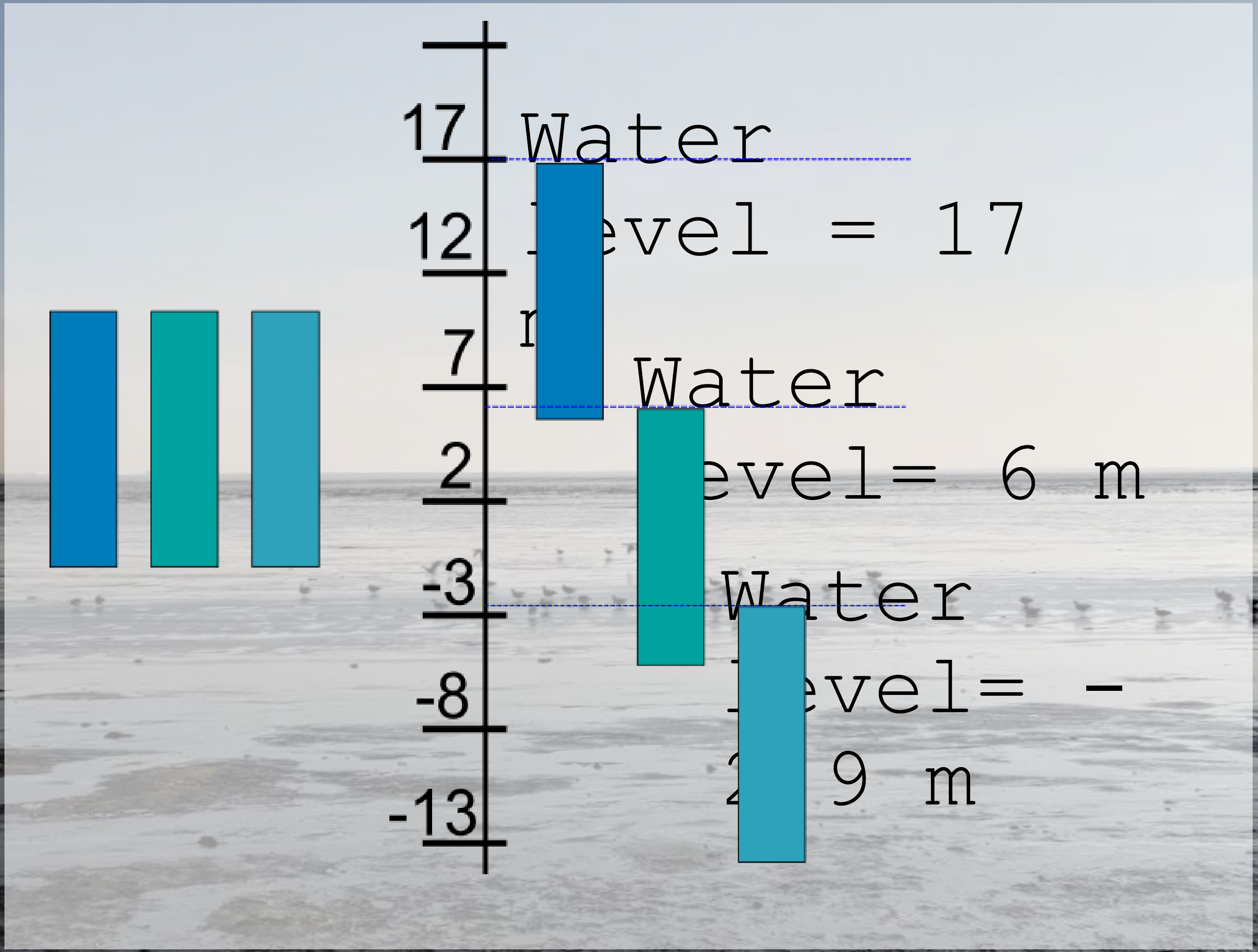

Subgrid Bathymetry

$$\frac{dV(\zeta)}{d\zeta} = non - lineair$$

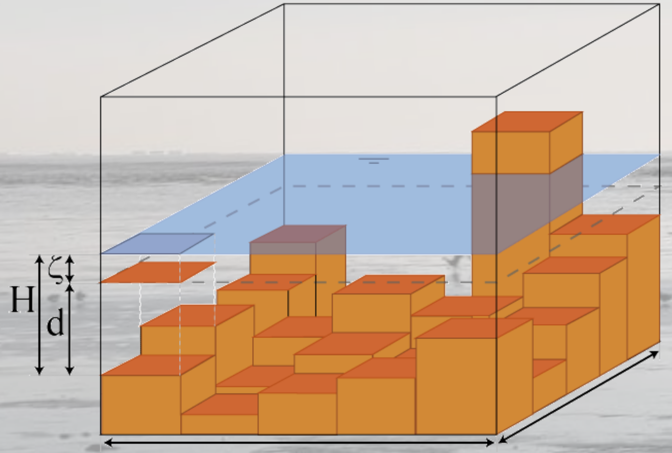

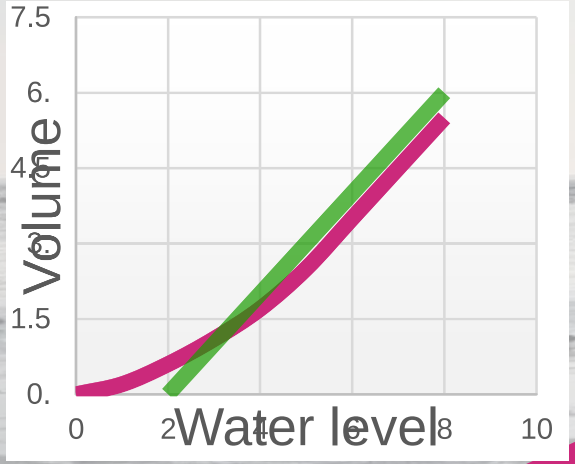

Automatic flooding and drying

Casulli 2009, Casulli &

High Resolution Morphodynamics

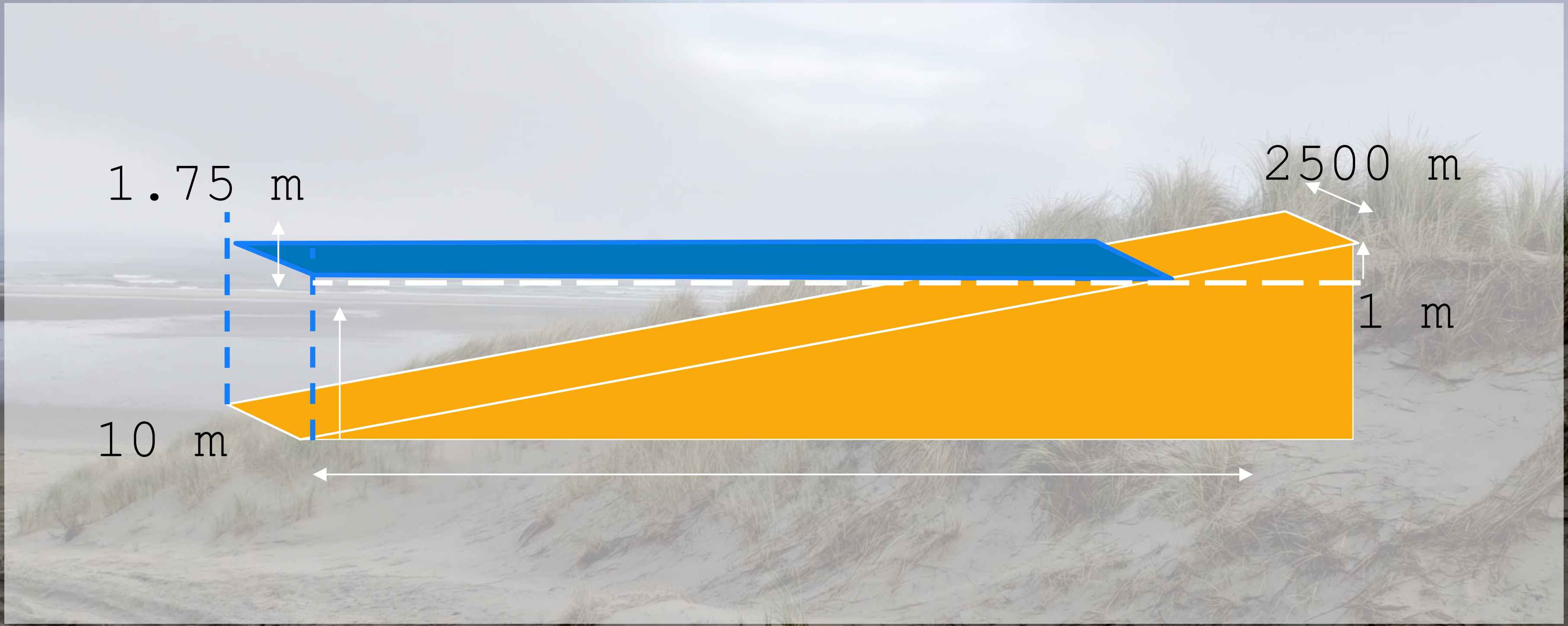

High Resolution Morphodynamics

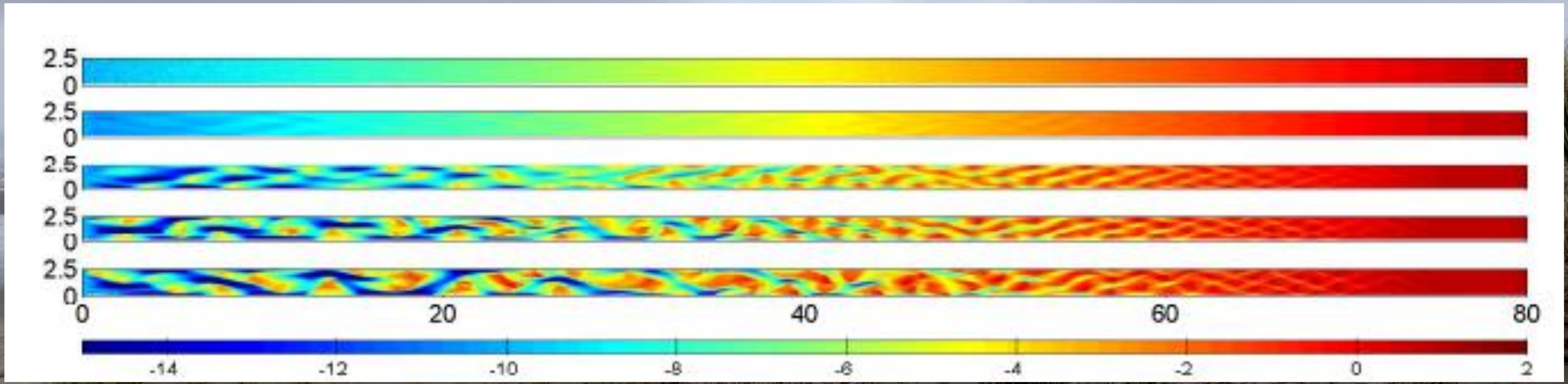

Volp et al 2017

High Resolution Morphodynamics

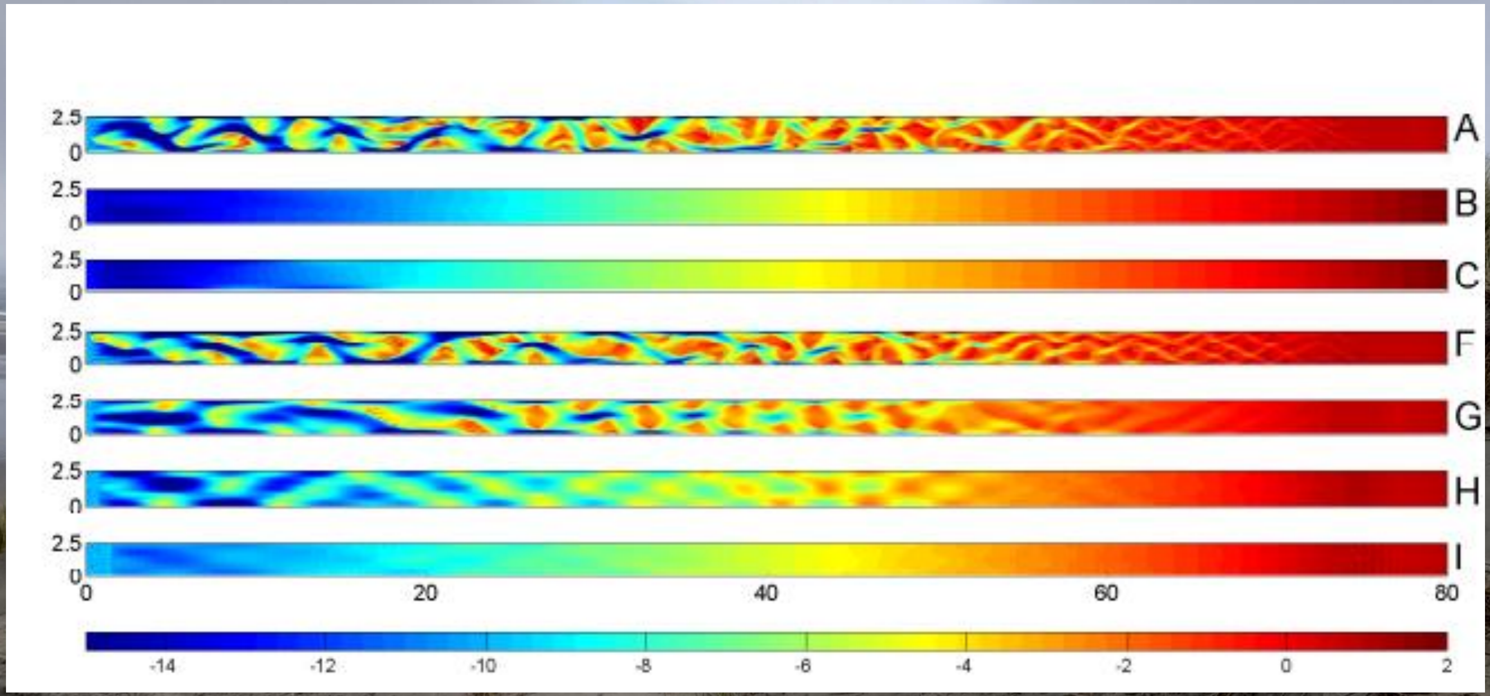

Volp et al 2017

High Resolution Morphodynamics

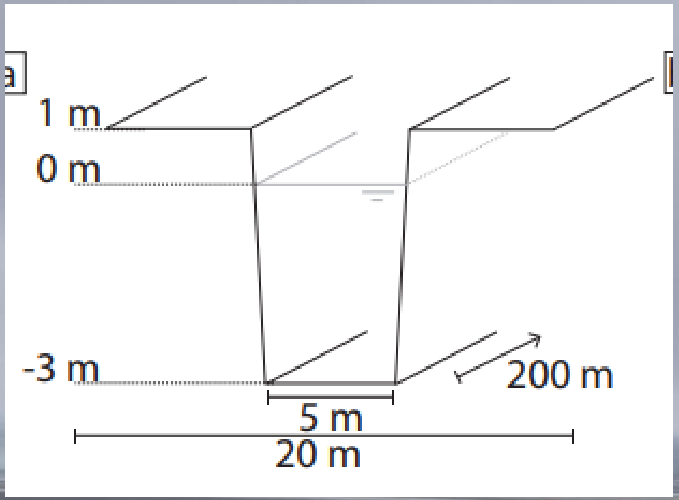

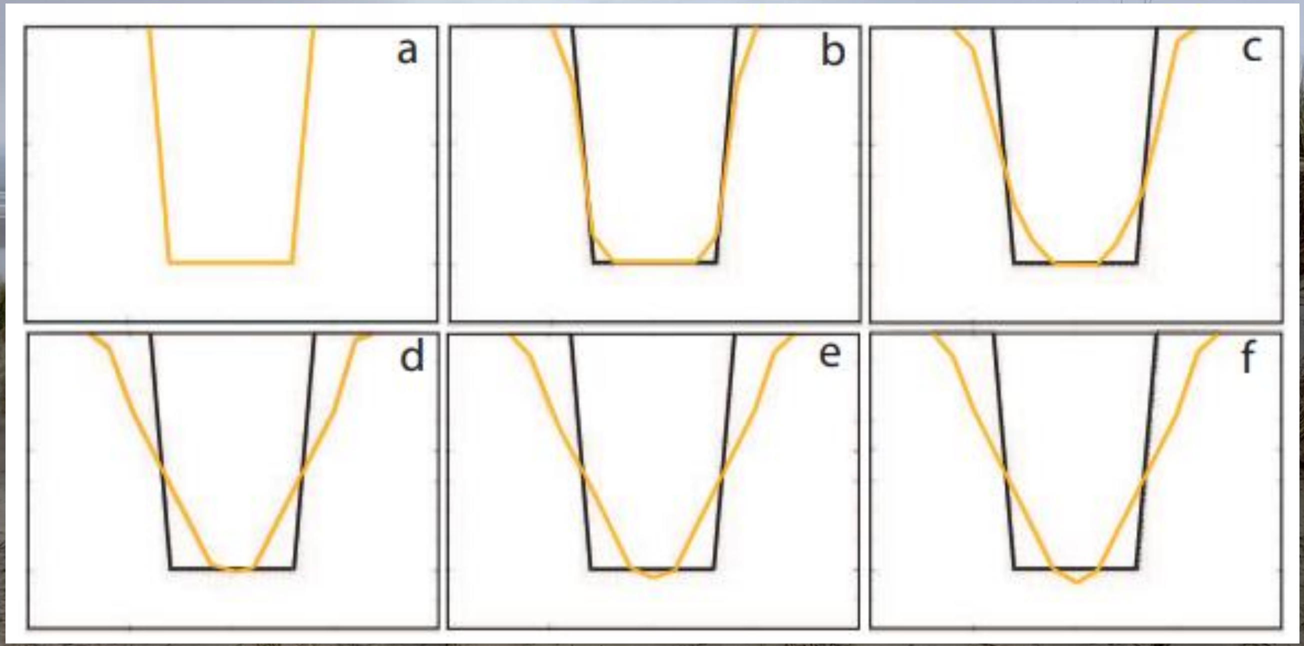

Volp et al 2017

Some Conclusions

- Get to know your grid
- Choose your resolution wisely
- Be careful with grid size transitions
- Subgrid is cool

?

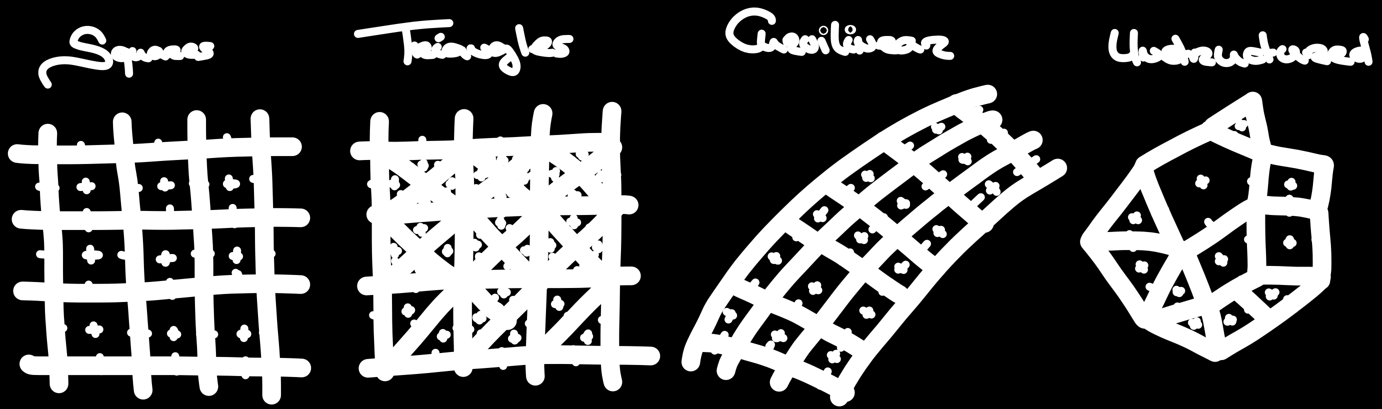

Dealing with grids in hydro- en morphodynamics

dr. Nicolette Volp
University of Twente & Nelen en Schuurmans

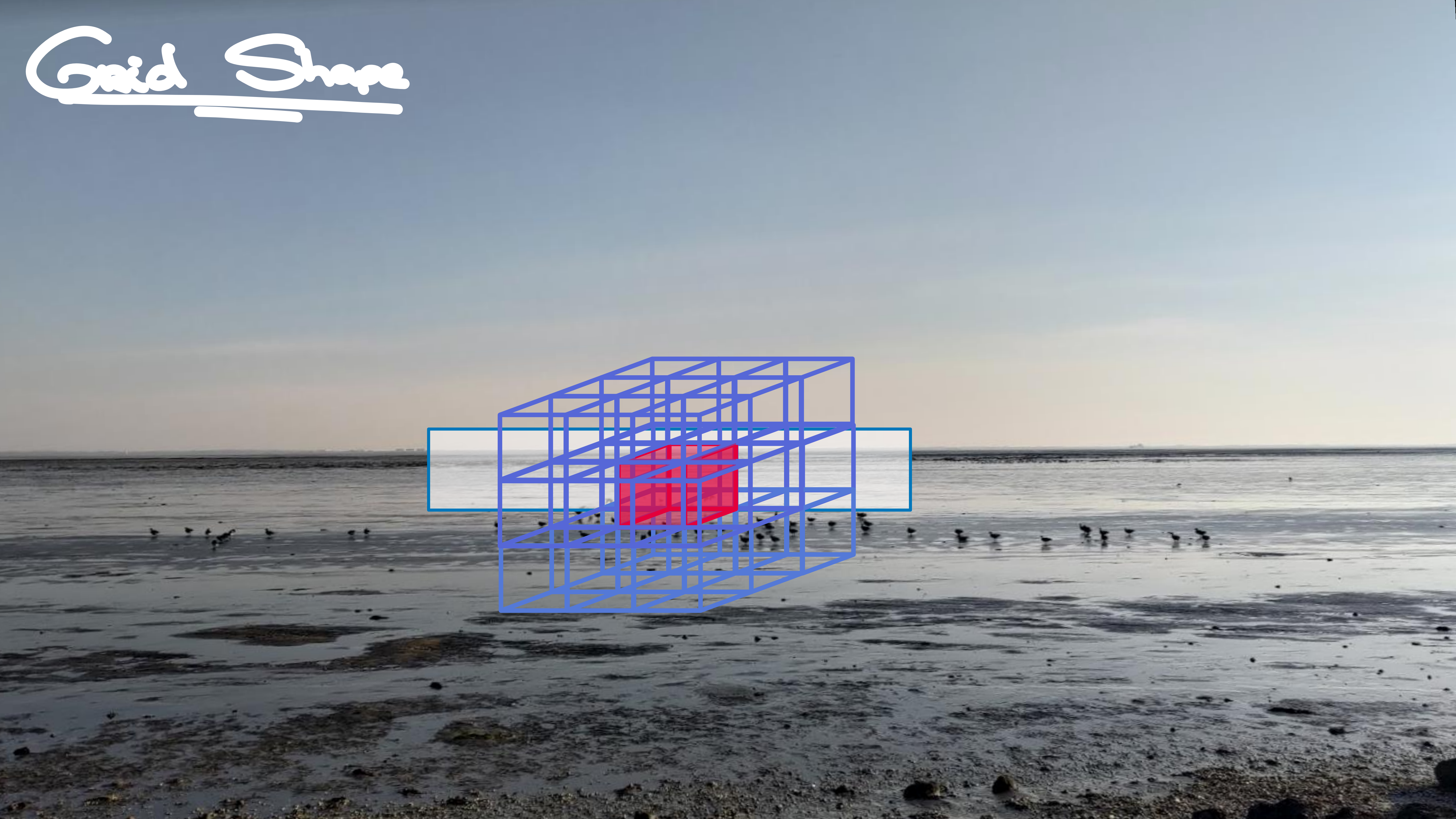
Grid Shape

“Modelling of coupled hydrodynamics, sediment transport and bed morphodynamics”
(A. Dimas, UPATRAS)

HYDRAULIC ENGINEERING LABORATORY
DEPARTMENT OF CIVIL ENGINEERING
UNIVERSITY OF PATRAS

Modelling of coupled hydrodynamics, sediment transport and bed morphodynamics

Athanassios A. Dimas

Professor

Leftheriotis, G.A., and Dimas, A.A., 2022. Morphodynamics of vortex ripple creation under constant and changing oscillatory flow conditions. *Coastal Engineering*, 177.

Oyarzun, G., Chalmoukis, I.A., Leftheriotis, G.A., and Dimas, A.A., 2020. A GPU-based algorithm for efficient LES of high Reynolds number flows in heterogeneous CPU/GPU supercomputers. *Applied Mathematical Modelling*, 85, 141-156.

Dimas, A.A. and Leftheriotis, G.A., 2019. Mobility parameter and sand grain size effect on sediment transport over vortex ripples in the orbital regime. *Journal of Geophysical Research – Earth Surface*, 124(1), 2-20.

Acknowledgments

This work was implemented under the Initial Training Network SEDITRANS, funded by the EU program Marie Sklodowska Curie Actions (MSCA), and was also supported by computational time granted from the Greek Research & Technology Network (GRNET) in the National HPC facility – ARIS – under project ID CoastHPC.

Outline

1. Motivation
2. Objectives
3. Methodology
   - Governing equations
   - Immersed boundary method
   - Numerical implementation
4. Results
   - Orbital vortex ripples
   - Validation
   - Mobile vs fixed bed ripples
5. Conclusions

Motivation

- Cascade: wave-induced turbulent oscillatory flow → interaction with a coastal sandy seabed (sediment transport and bed morphodynamics) → generation of bed forms (ripples, dunes, bars)

- Coastal Engineering: bed morphodynamics is a critical factor in modeling nearshore processes at a larger scale → design of coastal protection measures/structures

Objectives

Physics

- Focus on vortex ripples (Bagnold 1946), which have a strong influence on:
  - near-bed boundary layer hydrodynamics,
  - sediment transport mechanisms,
  - bed morphodynamics.
- Effect of related non-dimensional parameters on sediment transport.
- Mechanisms regarding the morphodynamic development of vortex ripples.

Modeling and Computing

- High Reynolds number cases →
  - implementation of large-eddy simulation (LES) formulation,
  - implementation of a hybrid CPU-GPU parallel algorithm for supercomputing use.

Methodology

Wave-Induced Oscillatory Flow

Near-bed (outside the wave boundary layer) horizontal velocity over flat bed (constant depth):

$$u_o = U_o \cos(kx - \omega t) \quad \text{or} \quad u_o(t) = U_o\left(\cos(\omega t) + B\cos(2\omega t)\right)$$

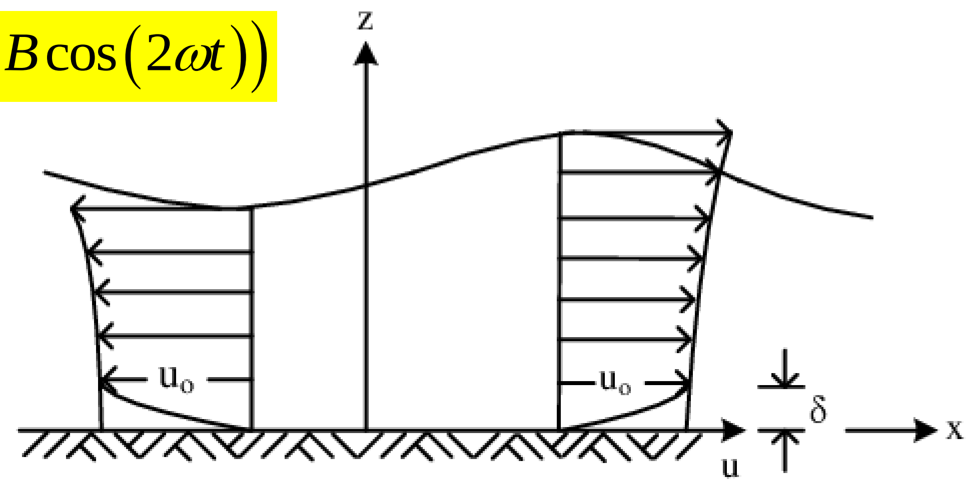

where t is time, x is the horizontal coordinate, U_o is the velocity amplitude, $a_o = U_o/\omega$ is the orbital motion amplitude, $\omega = 2\pi/T$ is the wave radial frequency, T is the wave period, $k = 2\pi/L$ is the wavenumber, L is the wavelength and B is the wave skewness.

Reynolds number: $$\mathrm{Re} = \frac{U_o \alpha_o}{\nu}$$

Methodology

Flow Equations (non-dimensional)

Continuity equation: $$\frac{\partial u_i}{\partial x_i} = 0$$

Navier-Stokes equations: $$\frac{\partial u_i}{\partial t} + \frac{\partial}{\partial x_j}\left(u_i u_j\right) = -\frac{\partial p}{\partial x_i} - \frac{\partial \tau_{ij}}{\partial x_j} + \frac{1}{\mathrm{Re}}\frac{\partial^2 u_i}{\partial x_j \partial x_j} + f_i$$

where u_i is the resolved velocity field according to LES formalism.

Dynamic pressure: $p = P_o + P$ where P_o is the externally imposed pressure field.

Subgrid-scale (SGS) stresses (Smagorinsky 1963): $$\boxed{\tau_{ij} = -2D_{wall}\nu_{sgs}S_{ij} = -2D_{wall}\left(C_s\Delta\right)^2 |S| S_{ij}}$$

$$|S| = \left(2S_{ij}S_{ij}\right)^{1/2}$$

$$\Delta = \left(\Delta x_1 \Delta x_2 \Delta x_3\right)^{1/3}$$

$$D_{wall} = 1 - \exp\left[-\left(\frac{r^+}{\mathrm{A}^+}\right)^3\right]$$

Methodology

Wave-Induced Sediment Transport

Sediment transport: bed load and suspended load.

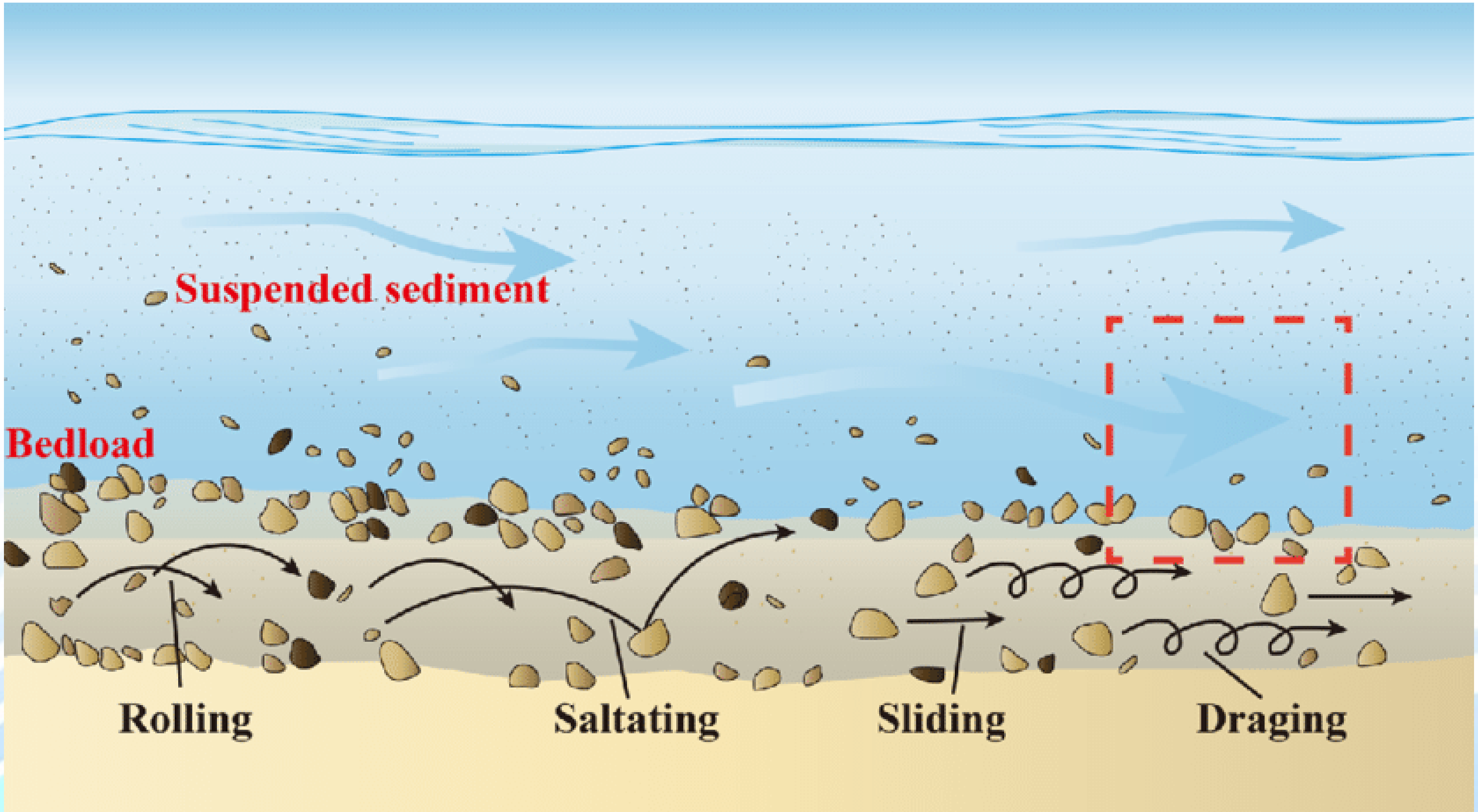

Methodology

Sediment Transport Equations (Bed Load)

Bed load transport rate (Engelund and Fredsøe, 1976):

$$\frac{q_b}{\sqrt{(S-1)\,gD_g^3}} = \begin{cases} \operatorname{sgn}(\theta)\dfrac{5\pi}{3}\left[1+\left(\dfrac{\pi}{6}\dfrac{\mu_d}{|\theta|-\theta_c}\right)^4\right]^{-\frac{1}{4}}\left(\sqrt{|\theta|}-0.7\sqrt{\theta_c}\right), & (|\theta|>\theta_c) \\ 0 & , (|\theta|\le\theta_c) \end{cases}$$

Shields number: $\theta = \dfrac{\tau_b}{\rho_w (S-1)\,gD_g^3}$

Critical Shields number: $\theta_c(D_g, S)$

Median grain diameter: D_g

Sediment specific gravity: S

Dynamic friction coefficient: $\mu_d \approx 0.5\mu_s$

Methodology

Sediment Transport Equations (Suspended Load)

Advection-diffusion equation for the suspended sediment concentration:

$$\frac{\partial c}{\partial t} + u_j \frac{\partial c}{\partial x_j} - w_s \frac{\partial c}{\partial x_3} = \frac{1}{\sigma \mathrm{Re}} \frac{\partial^2 c}{\partial x_j \partial x_j} - \frac{\partial \chi_i}{\partial x_i} + f_c$$

where w_s is

the sediment fall velocity:

$$\frac{w_s D_g}{\nu} = \begin{cases} D_*^3/18 & D_*^3 < 39 \\ D_*^{2.1}/6 \quad \text{for} & 39 < D_*^3 < 10^4 \\ 1.05 D_*^{1.5} & 10^4 < D_*^3 \le 3 \cdot 10^6 \end{cases} \quad \text{where} \quad D_* = D_g \left(\frac{(S-1)g}{\nu^2} \right)^{1/3}$$

σ is the Schmidt number, χ_j is the SGS turbulent term (Zedler and Street 2001): $\chi_j = \frac{\nu_{sgs}}{\sigma_t} \frac{\partial c}{\partial x_j}$

and σ_t is the turbulent Schmidt number.

In coastal sediment transport modeling, it is usual to set $\sigma = \sigma_t = 1$.

Methodology

Bed Evolution Equation

Conservation of sediment mass →

Exner equation:

$$\frac{\partial z_b}{\partial t} + \frac{1}{1-n}\frac{\partial}{\partial t}\int_{x_3 \geq z_b} c\,dx_3 = -\frac{1}{1-n}\left(\frac{\partial q_1}{\partial x_1} + \frac{\partial q_2}{\partial x_2}\right)$$

where $q_{1,2} = \left(q_b + q_s\right)_{1,2}$ is the total sediment flux rate and n is the bed sediment porosity.

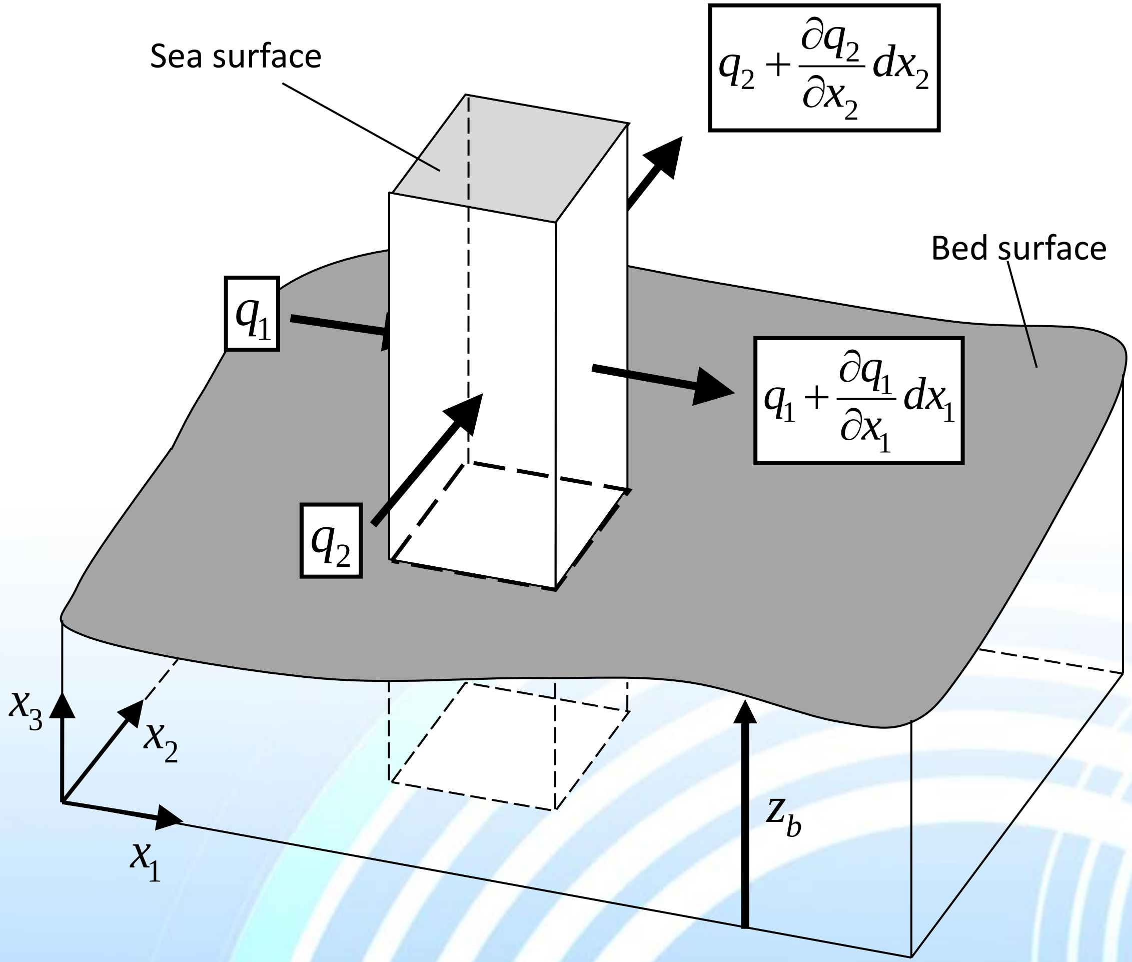

Methodology

Hybrid Computing

In-house code capable to run on either CPU only or CPU+GPU architectures. Switching between architectures is done only using different compilation flags.

Intra node: CPU -> shared memory approach OpenACC (similar to OpenMP)

GPU -> stream processing (CUDA or OpenACC)

Inter node: MPI communications

The code parallelization follows a domain decomposition approach:

- Divide domain in parts with same workload.
- Each sub-domain is solved in a computing node.
- Discretizations that require unknowns from other sub-domains perform MPI communications.

Results

Orbital Vortex Ripples

Their creation on a sandy bed depends on two non-dimensional parameters.

The mobility parameter: $\psi = \frac{U_o^2}{(S-1)gD_g}$

The ratio: $\frac{a_o}{D_g} = \frac{d_o/2}{D_g}$

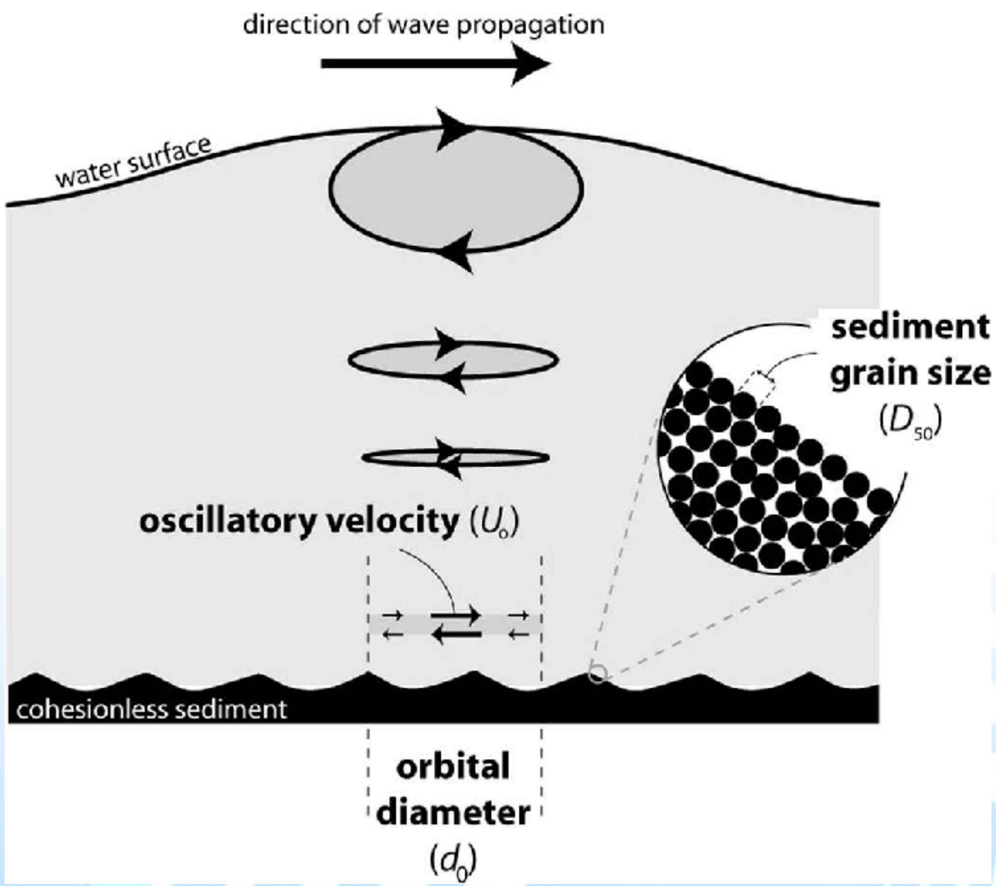

Ripple dimensions according to Nielsen (1992):

$$h_r/a_o = 0.275 - 0.022 \times \psi^{0.5}$$

$$L_r/a_o = 2.2 - 0.345 \times \psi^{0.34}$$

Orbital ripples correspond to $a_o/D_g < 1000$ and vortex ripples to $h_r/L_r > 0.1$, i.e., $\psi < 100$.

Note: $\psi > 300 \rightarrow$ sheet flow

Results

Cases

ψ	L_r/a_o	h_r/a_o	h_r/L_r	$\Delta x_{1,2}/a_o$	$\Delta x_3/a_o$
20	1.245	0.177	0.142	0.014	0.002-0.02
50	0.895	0.119	0.134	0.010	0.002-0.02
80	0.669	0.078	0.117	0.008	0.002-0.02

$a_o/D_g = 250,\ 500,\ 1000$

$u_o(t) = U_o\left(\cos(\omega t) + B\cos(2\omega t)\right)$ $\quad B = 0.176$

$\mathrm{Re} = 10^5$

Grid: $256 \times 256 \times 450$ cells

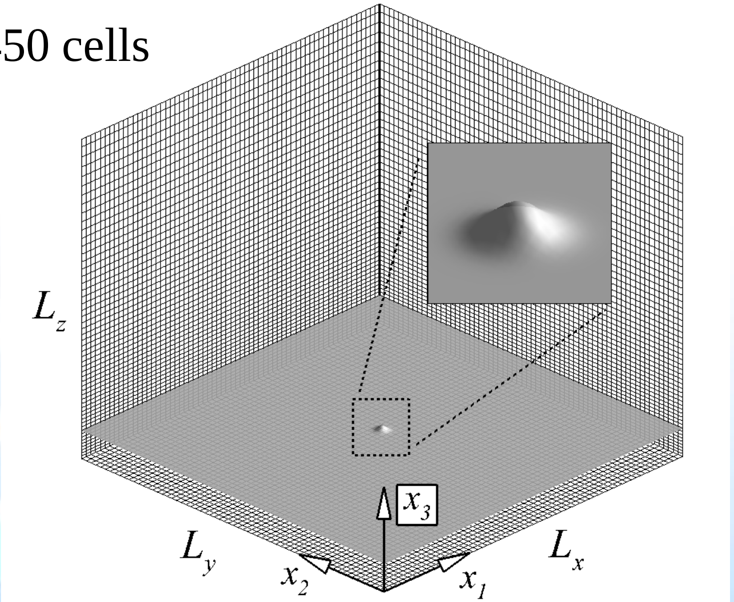

Mobile bed (every 4th node is shown)

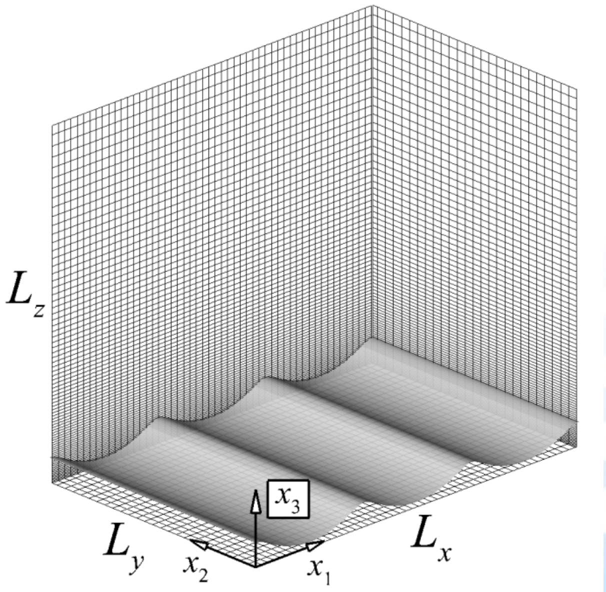

Fixed bed (every 5th node is shown)

Results

Bed evolution and ripple creation initiating from a flat bed
($0 < t < 200T$, $\psi = 50$, Re = 23,163, $a_o/D_g = 500$)

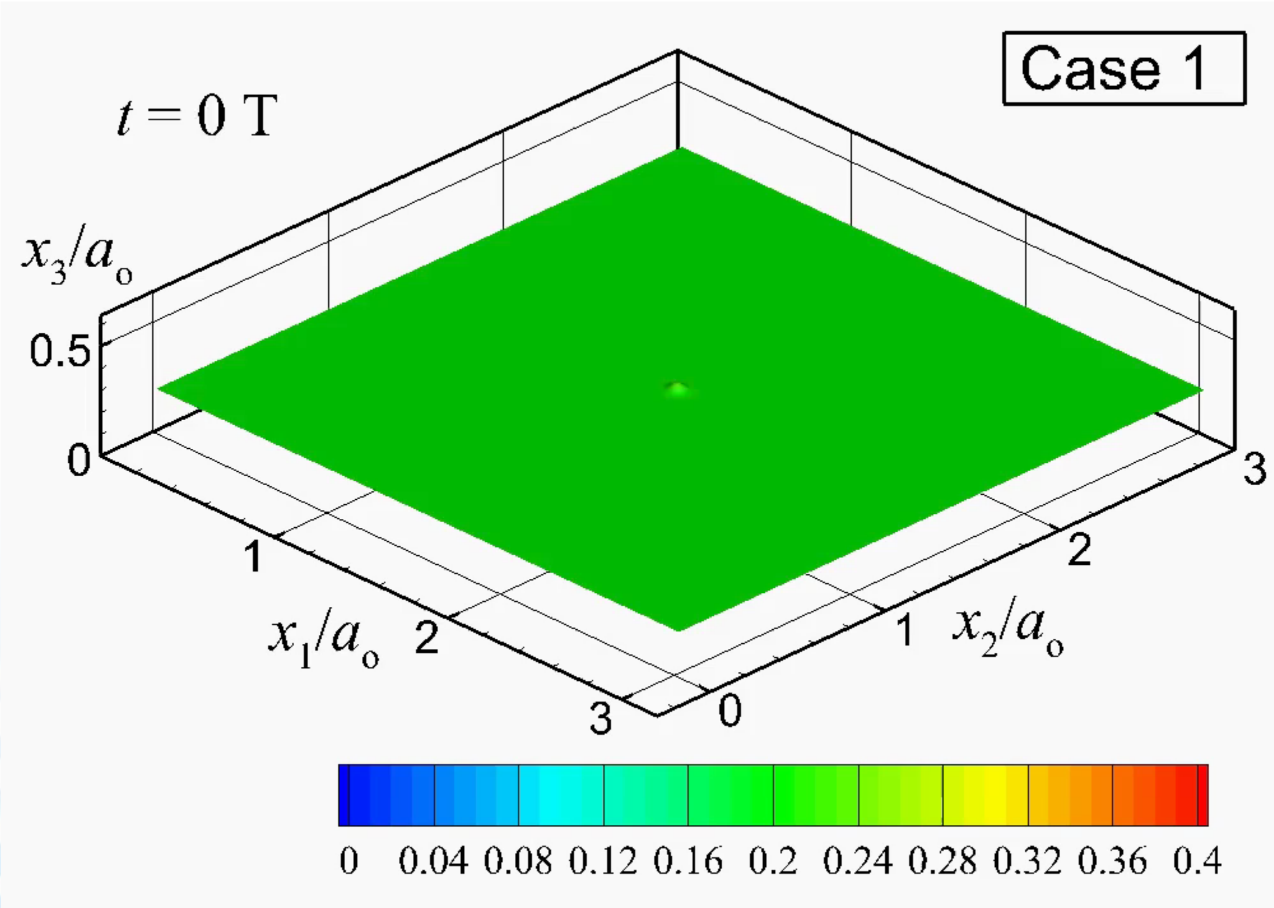

	L_r/a_o	h_r/a_o	h_r/L_r
Simulation	0.89	0.14	0.157
Nielsen	0.895	0.119	0.133

Comparison with Nielsen (1992)

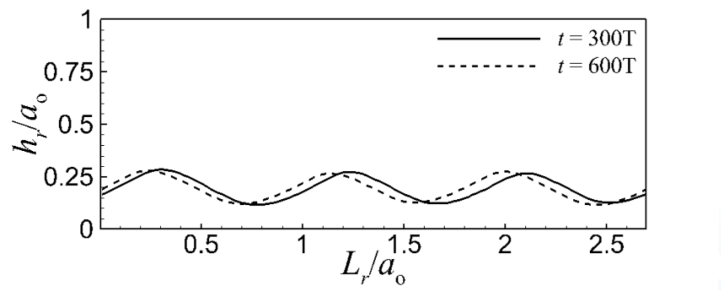

Ripple migration in equilibrium state

Results

Bed evolution and ripple creation initiating from a flat bed

(ψ = 50, a_o/D_g = 500)

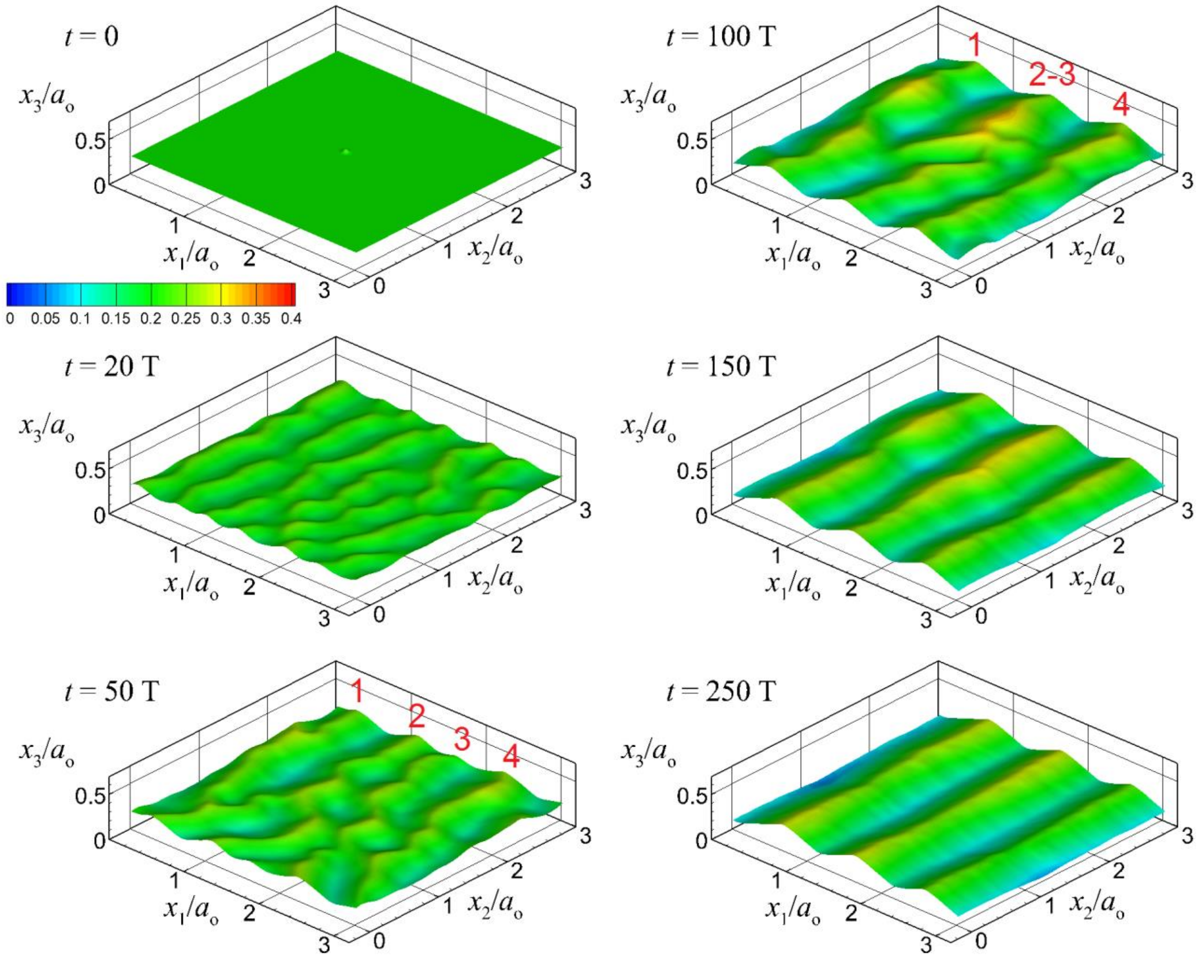

Results

Spanwise-averaged vorticity (left) and suspended sediment concentration (right)
(ψ = 50, a_o/D_g = 500)

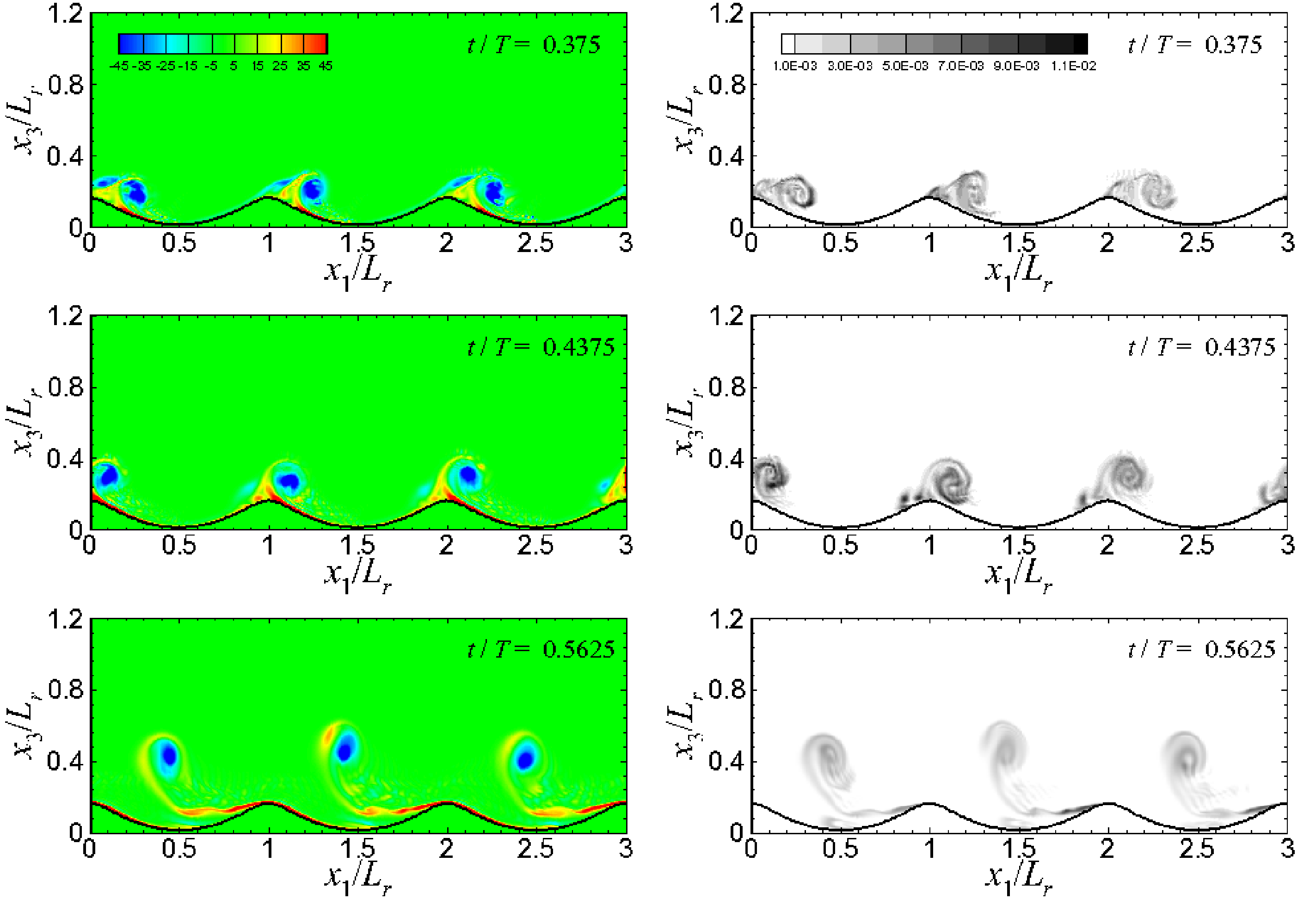

Results (Validation)

Parameters according to the experiment Mr5b63 in Van der Werf et al. (2007).

$$\psi = 42 \qquad L_r/a_o = 0.9535$$

$$a_o/D_g = 990 \qquad h_r/a_o = 0.1767$$

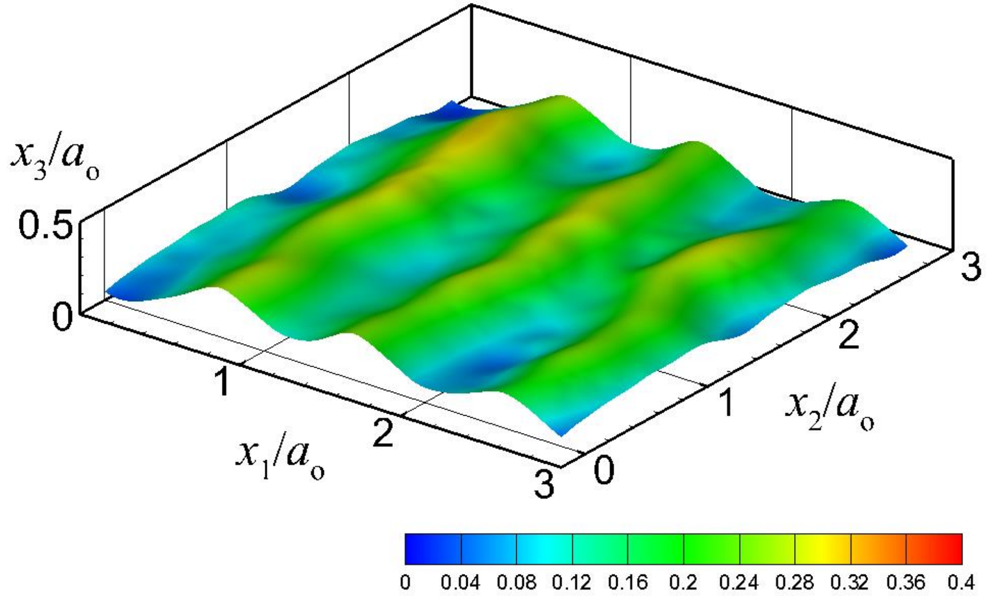

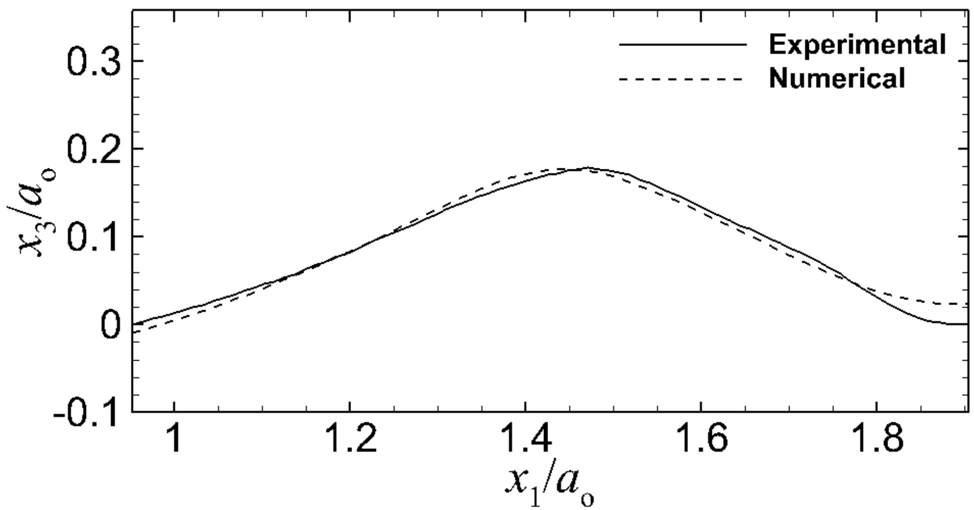

Bed after 500 wave periods (left) and ripple profile comparison (right).

Results (Validation)

Parameters according to the experiment Mr5b63 in Van der Werf et al. (2007).

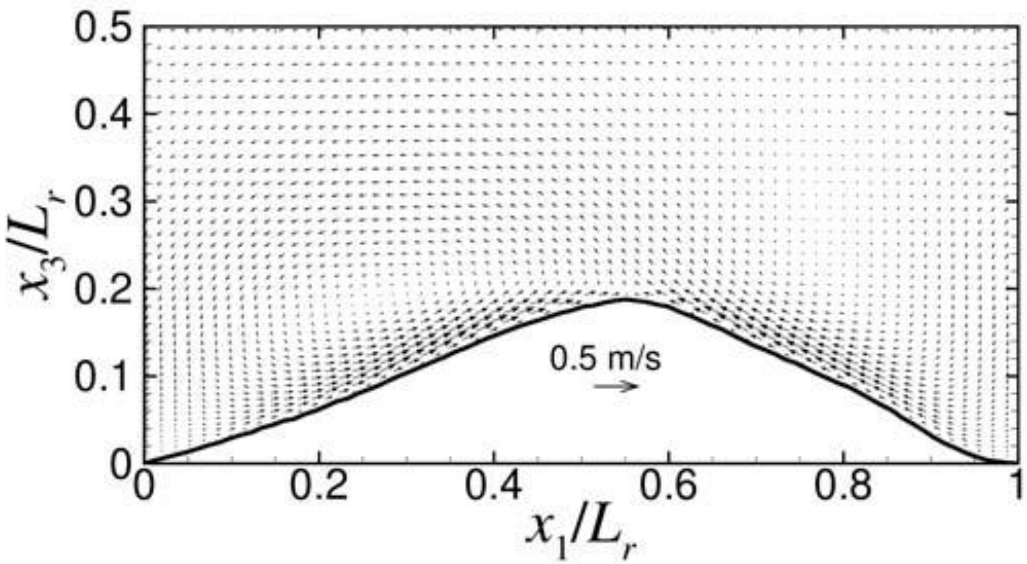

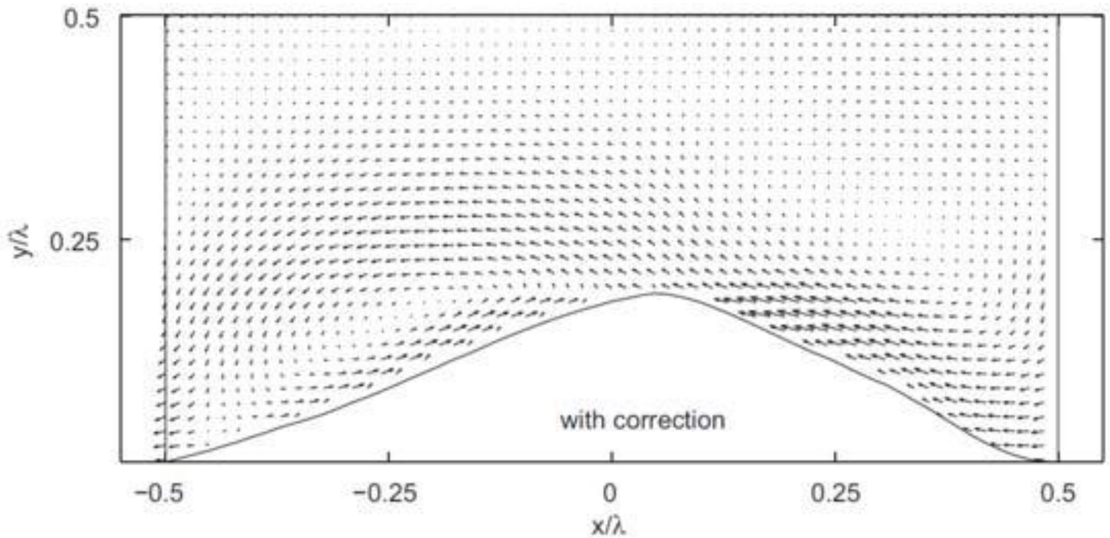

Time- and spanwise-averaged velocity comparison between numerical (left) and experimental (right) results.

Results (Validation)

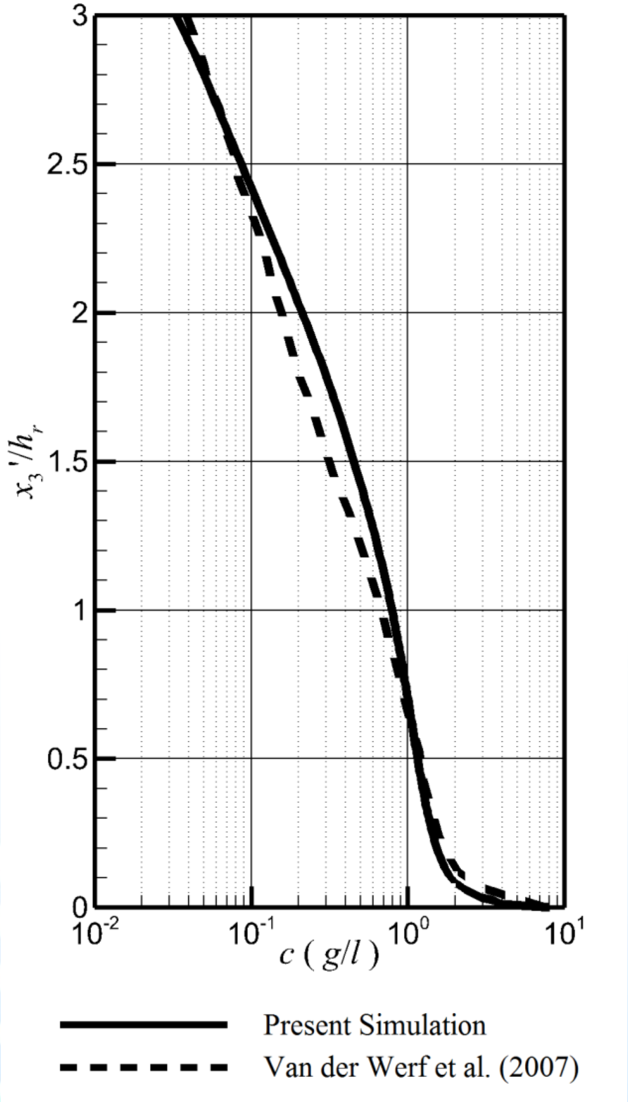

Time- and horizontally-averaged concentration of the suspended sediment according to the parameters in the experiment Mr5b63 in Van der Werf et al. (2007).

Mean bed, suspended and net load comparison.

	$\langle Q_b \rangle$ (mm^2/s)	$\langle Q_s \rangle$ (mm^2/s)	$\langle Q_{tot} \rangle$ (mm^2/s)
Numerical Results	6.1	-10.2	-4.1
Van der Werf et al. (2008)	6.9 ± 1	-10.6 ± 1.7	-3.7 ± 0.7

Results

Mobile ripple evolution and spanwise-averaged vorticity for mobile and fixed ripples (ψ = 50, a_o/D_g = 500)

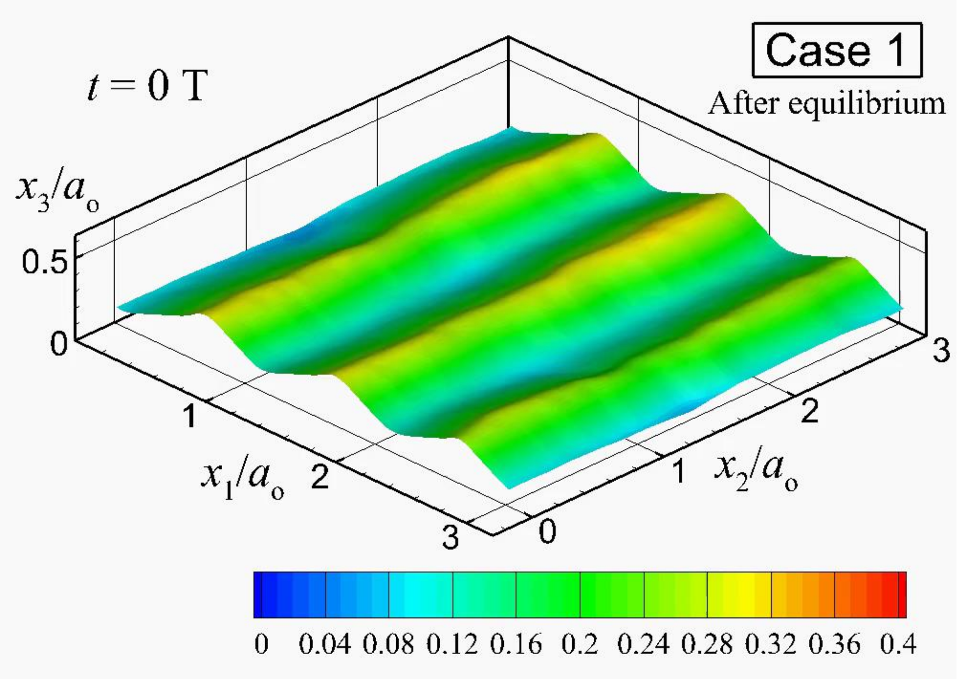

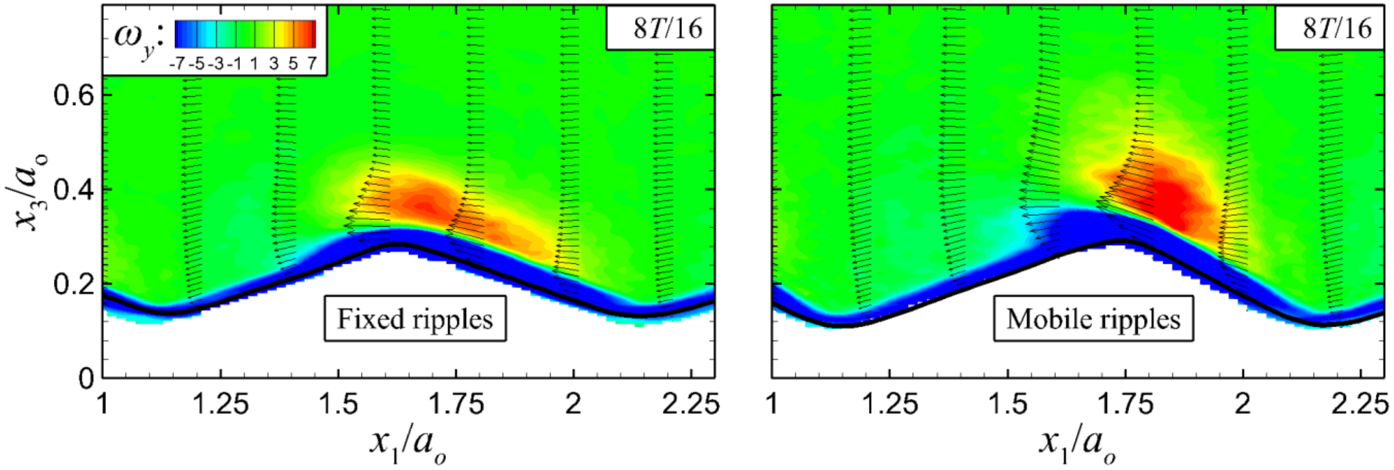

Results

Net bed load parameter $\langle\Phi_b\rangle$ (left) and net suspended load parameter $\langle\Phi_s\rangle$ (right) as functions of the mobility parameter ψ and the relative sand grain size a_o/D_g.

$$\Phi_{b,s} = \frac{q_{b,s}}{\sqrt{(S-1)\,gD_g^3}}$$

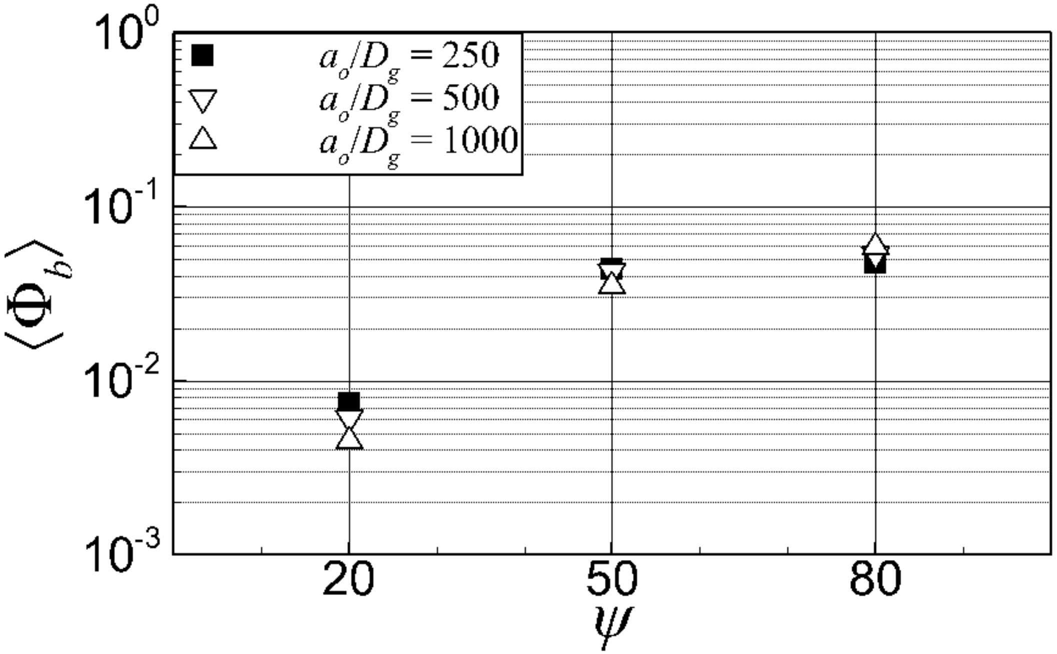

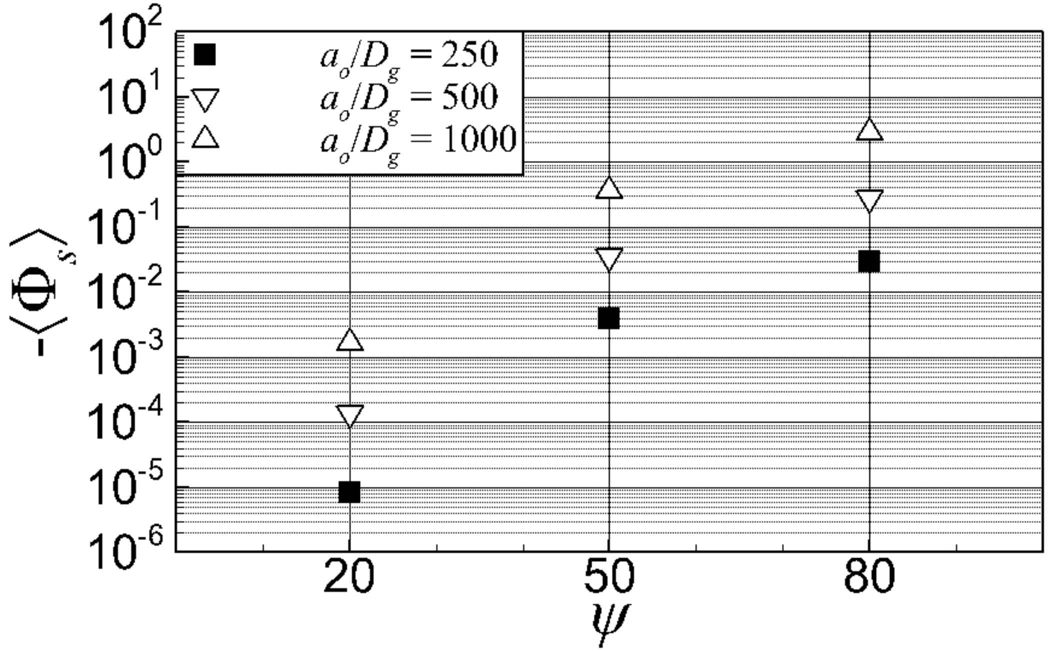

Results

Ripple widening or shortening
(ψ = 50, a_o/D_g = 500)

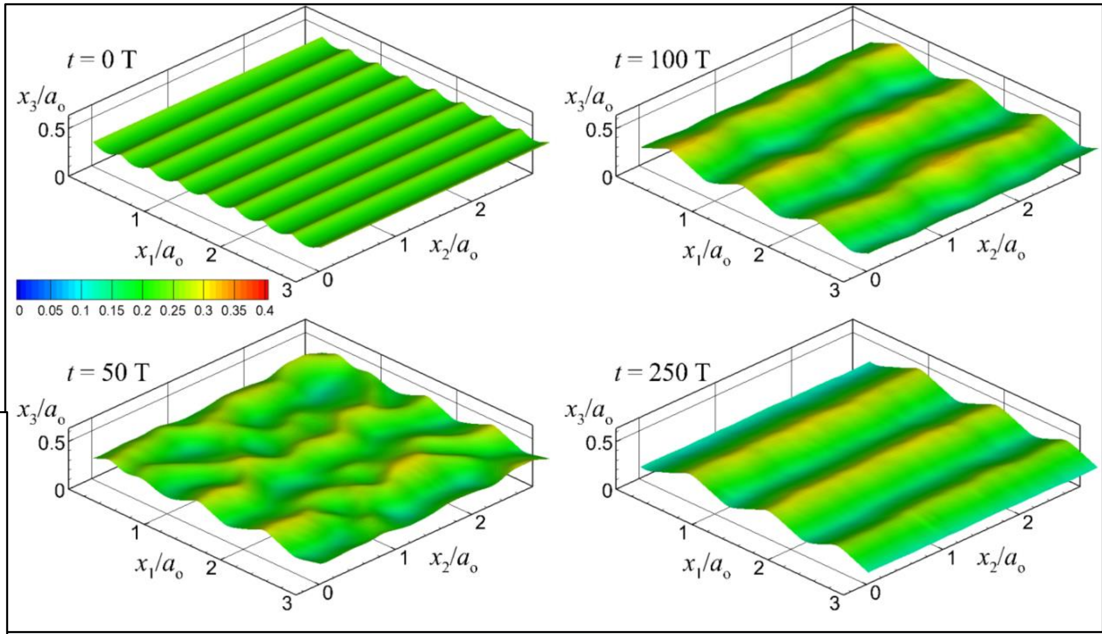

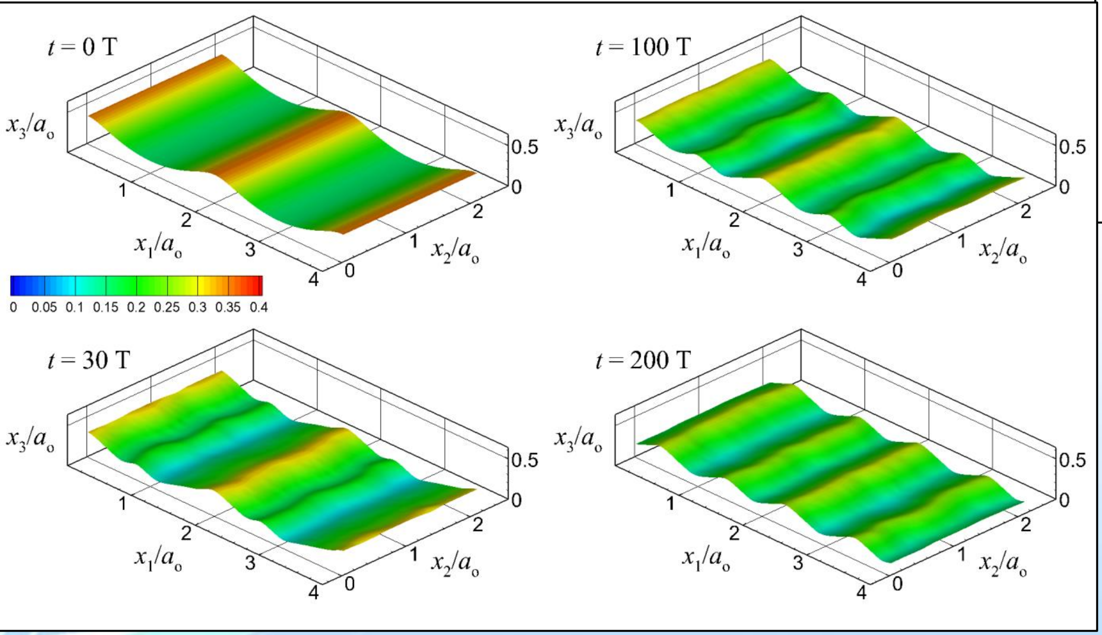

Results

Ripple re-orientation, driven by oblique (45°) oscillatory flow (ψ = 50, a_o/D_g = 500)

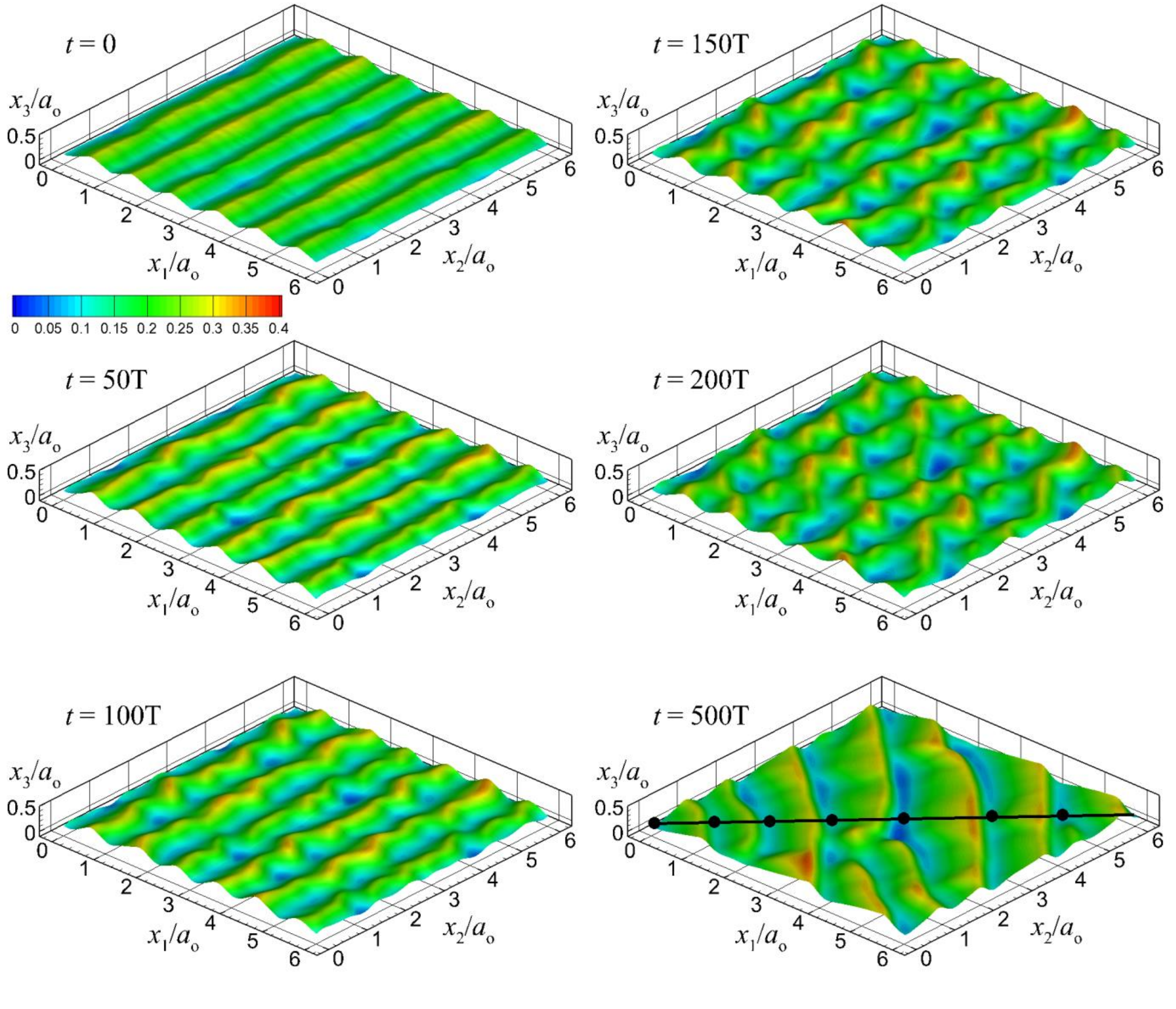

Results

Comparison of 4 different implementation strategies for using the computing node:

CPUs: → MPI

→ MPI+OPENMP

→ MPI+OPENACC

GPUs: → MPI+OPENACC

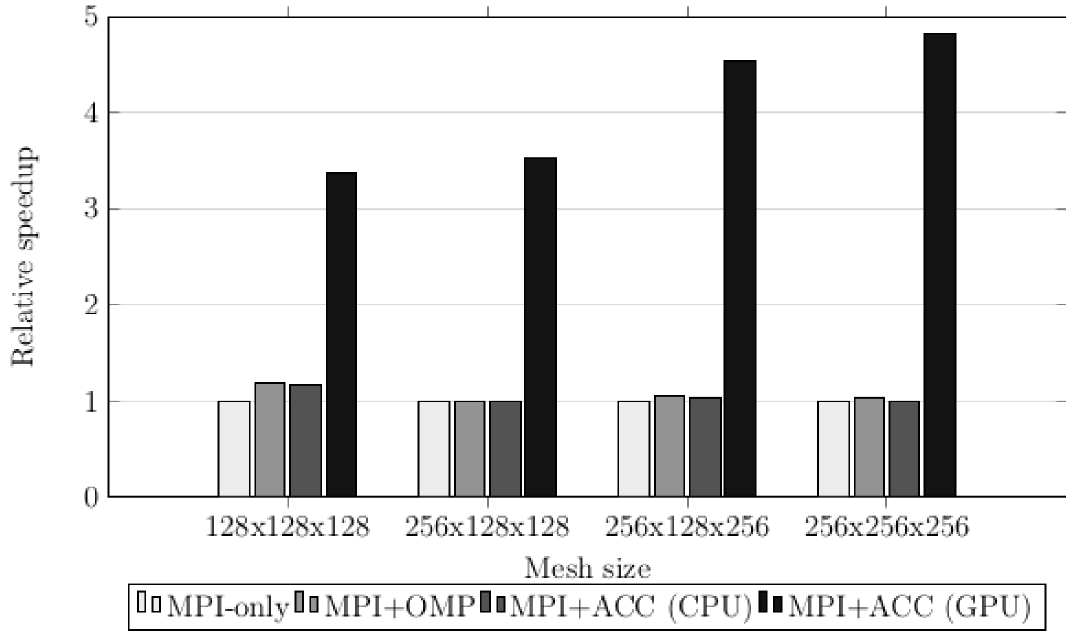

Relative speedup over MPI-only:

- All CPU implementations obtain nearly same performance.
- GPU performance depends on the problem size but it is much faster than the CPU-only.

Timings:

- 2 hrs / wave period, 30 million grid cells (20 CPU processors, 0.5 PF machine, OPENMP)
- 3 hrs / wave period, 400 million grid cells (512 hybrid nodes, 25 PF machine, OPENACC)

Conclusions

Sedimen transport

- Net bed load in the wave direction; its magnitude increases linearly with D_g/a_o.
- The effect of ψ on the net bed load is stronger for $\psi < 50$ than for $\psi > 50$.
- Net suspended load in the opposite to the wave direction; its magnitude increases with increasing ψ and a_o/D_g.
- The relative contribution of bed load versus suspended load on the total sediment load was found to depend on both ψ and a_o/D_g.
- For $\psi > 50$ and $a_o/D_g > 500$, the suspended load is the dominant mode.

Morphodynamics

- Model predicts ripple creation, growth, merging, and re-orientation.
- Under the same hydrodynamic forcing, the bed reaches the same equilibrium state regardless of its initial geometry, and ripples are eventually oriented perpendicular to the flow direction, regardless of their initial orientation or shape.
- Predicted sediment transport loads and ripple dimensions in accordance with experimental and empirically obtained results.
- Comparing fixed and mobile bed cases, bed load did not present substantial differences but suspended load demonstrated a strong increase by a factor of about three in mobile cases.

"Blending coastal morphodynamic models and observations through data assimilation"
(M. Alvarez, FIHAC)

Blending coastal morphodynamic models and observations through data assimilation

SEDIMARE school, University of Nottingham

23/04/2024

Moisés Álvarez-Cuesta(alvcuestam@unican.es)

Climate risks, adaptation and resiliency group

Instituto de Hidráulica Ambiental de la Universidad de Cantabria - IHCantabria

Background

- 2012-2016 BSc Civil Engineering (U. Cantabria, exchange year at Princeton University)
- 2016-2019 MSc Civil Engineering (U. Cantabria and École des Ponts (Paris))
- 2019-2022 Phd in Coastal Engineering (U. Cantabria - IHCantabria)
- 2022-present Post-doc at Climate risks, adaptation and resiliency group (IHCantabria)

Research lines

- Coastal impacts of climate change (erosion and flooding)
- Data assimilation and machine learning applied to coastal impact forecasting

Index

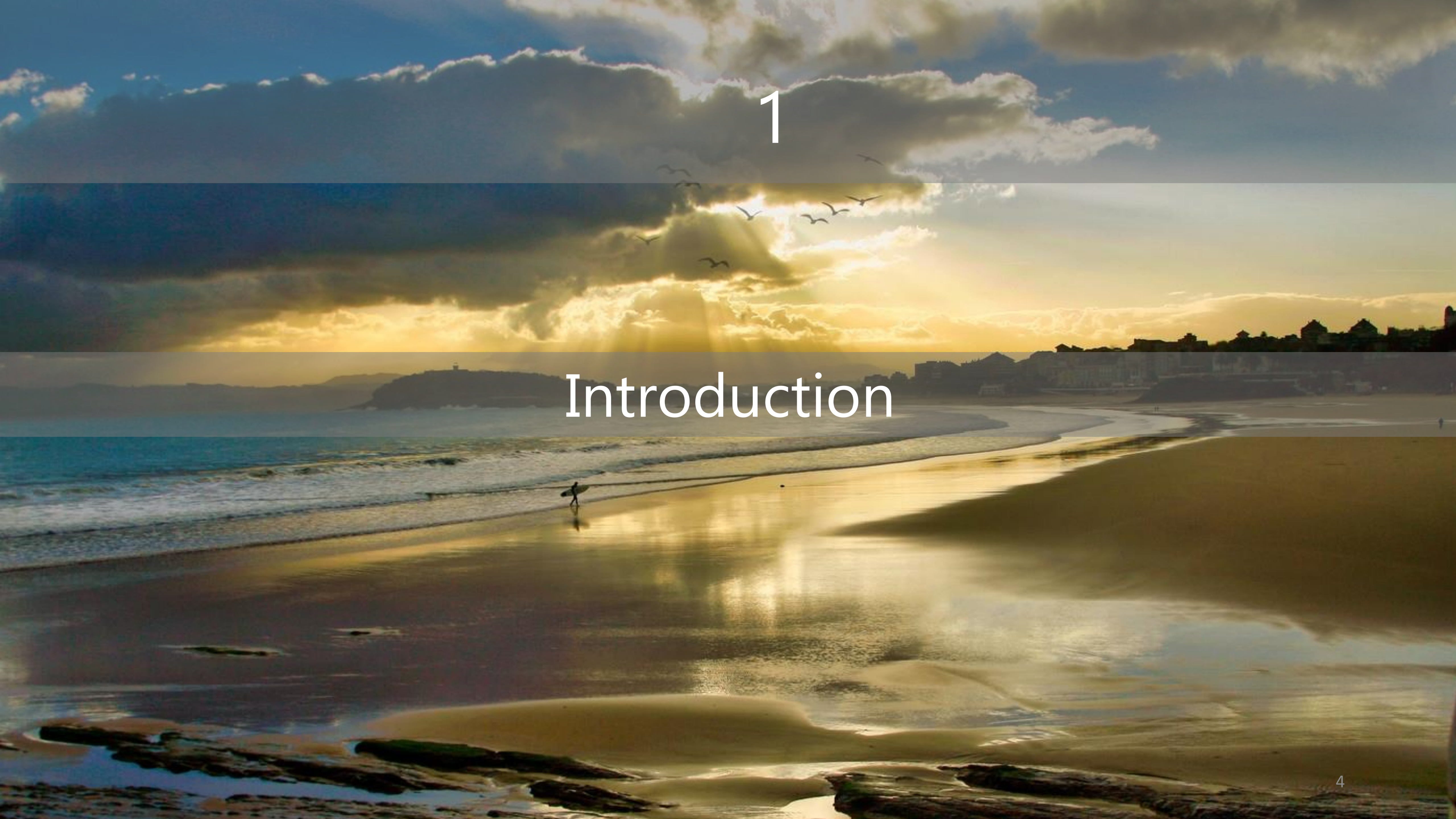

1

Introduction

Future

SLR

Jevrejeva et al., (2016)
Hermans et al., (2021)

Waves

Hemer et al., (2013)
Lobeto et al., (2021)

Extreme events

Bloemendaal et al., (2022)
Gori et al., (2022)

What will be the future of our coasts?

"the future of the coastline will be what we engineer it to be"

Vitousek et al. (2017)

Key questions to answer

Where?

When?

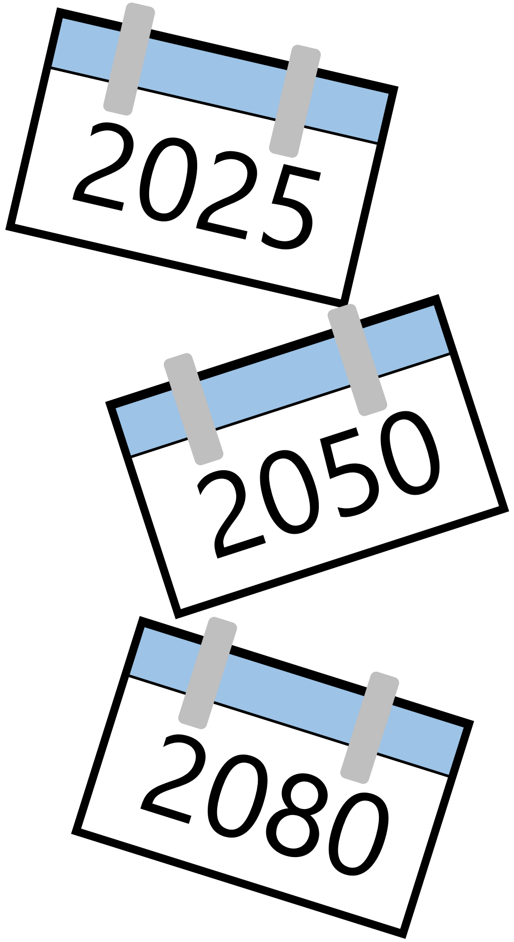

How?

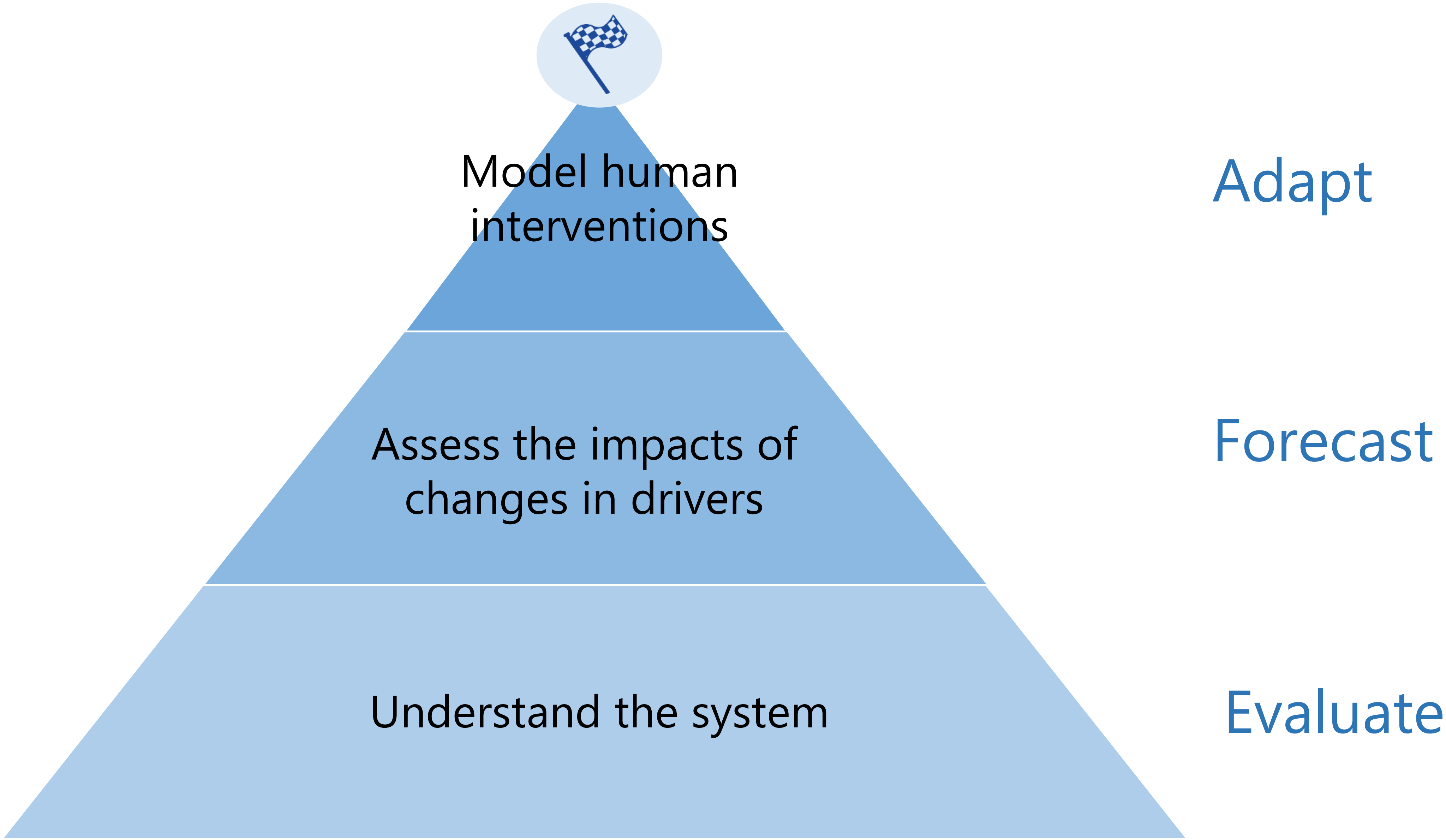
Model human interventions
Assess the impacts of changes in drivers
Understand the system
Adapt
Forecast
Evaluate

Evaluate, forecast and adapt

1.- Classical coastal engineering problem
2.- Climate change

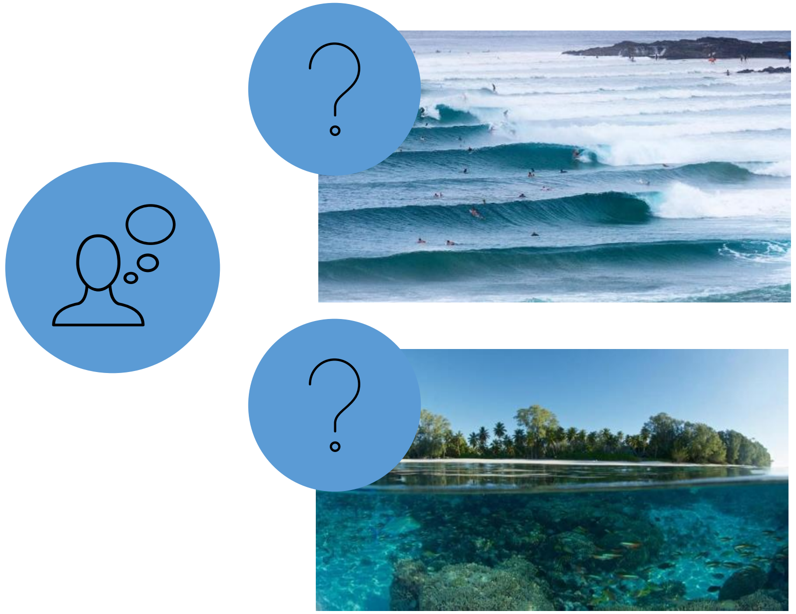

Probabilistic methods

Computationally efficient

Temporal scale (decades)

Spatial scale (10’s km)

Adaptation measures

Observations

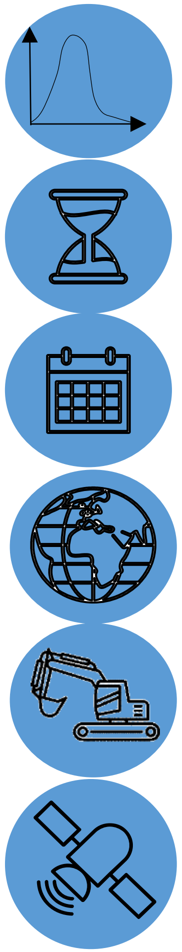

Main goal: **improve** the assessment of **coastal impacts** (erosion and flooding) to produce more accurate risk assessments to support **climate change adaptation**.

1. **Evaluate**. Development of a **shoreline evolution model** accounting for the main physical processes, the effect of man man-made intervention and enhanced by data assimilation
2. **Project.** Development of a methodology to **forecast** the **coastal evolution** considering erosion and flooding accounting for the **climate uncertainty**.
3. **Adapt**. Development of a long-term **coastal model** capable of solving **complex coastal environments.**

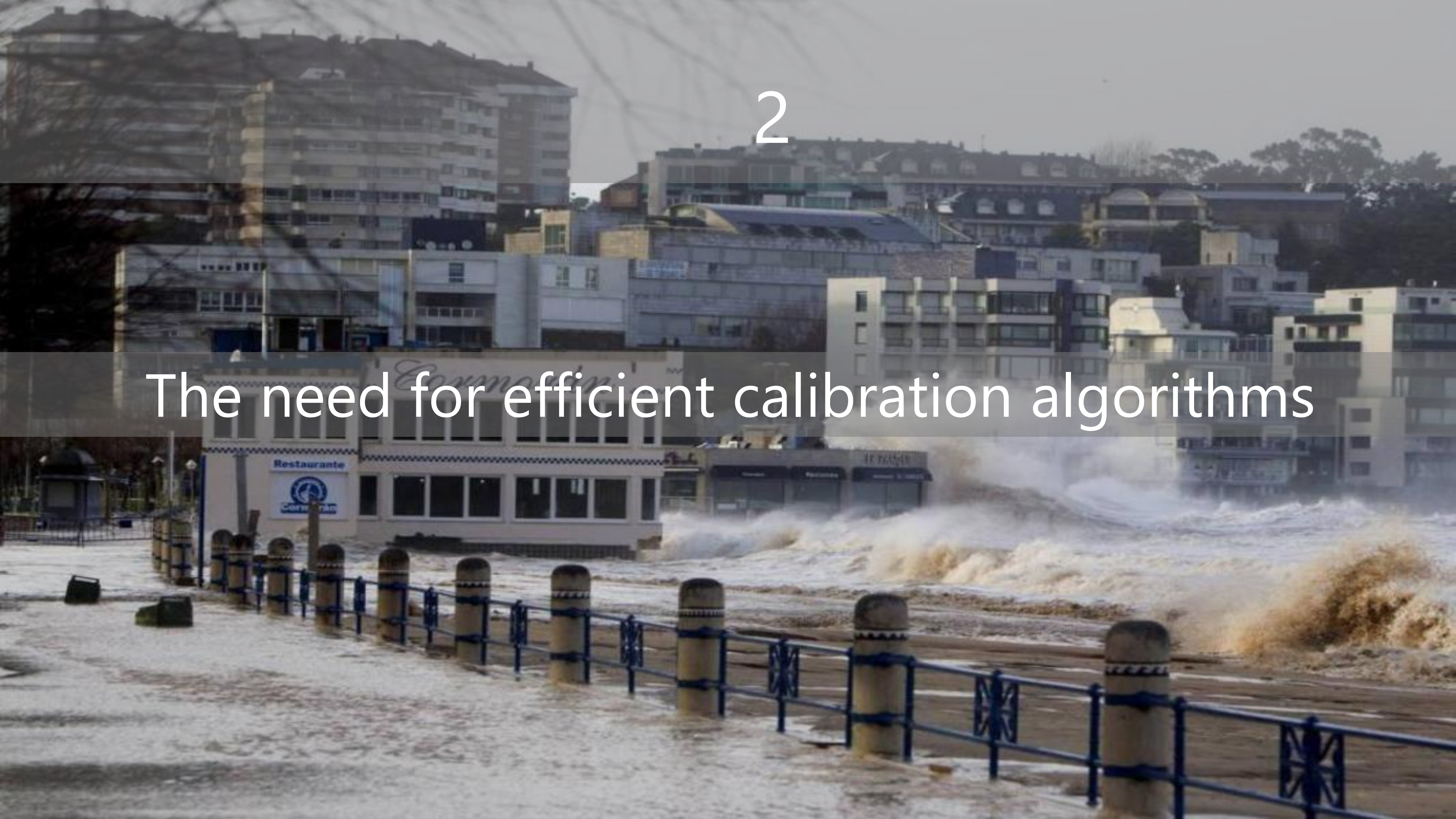

2

The need for efficient calibration algorithms

Process-based models

Hydrodynamics

Sed. transport

↓

Morphodynamics

-Time scales Storms $\mathcal{O}(days)$
-Spatial scales $\mathcal{O}(10^2\text{m})$

Physics-based models

Cross-shore

Longshore

↓

Shoreline

-Time scales $\mathcal{O}$(years)
-Spatial scales $\mathcal{O}(10^2\text{km})$

Empirical models

in situ Measures

Remote sensing

↓

Shoreline

-Spatio-temporal scales
f(data)

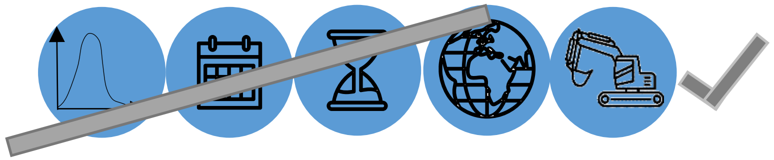

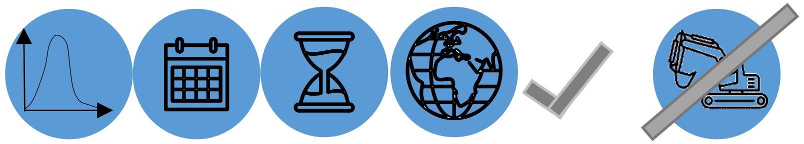

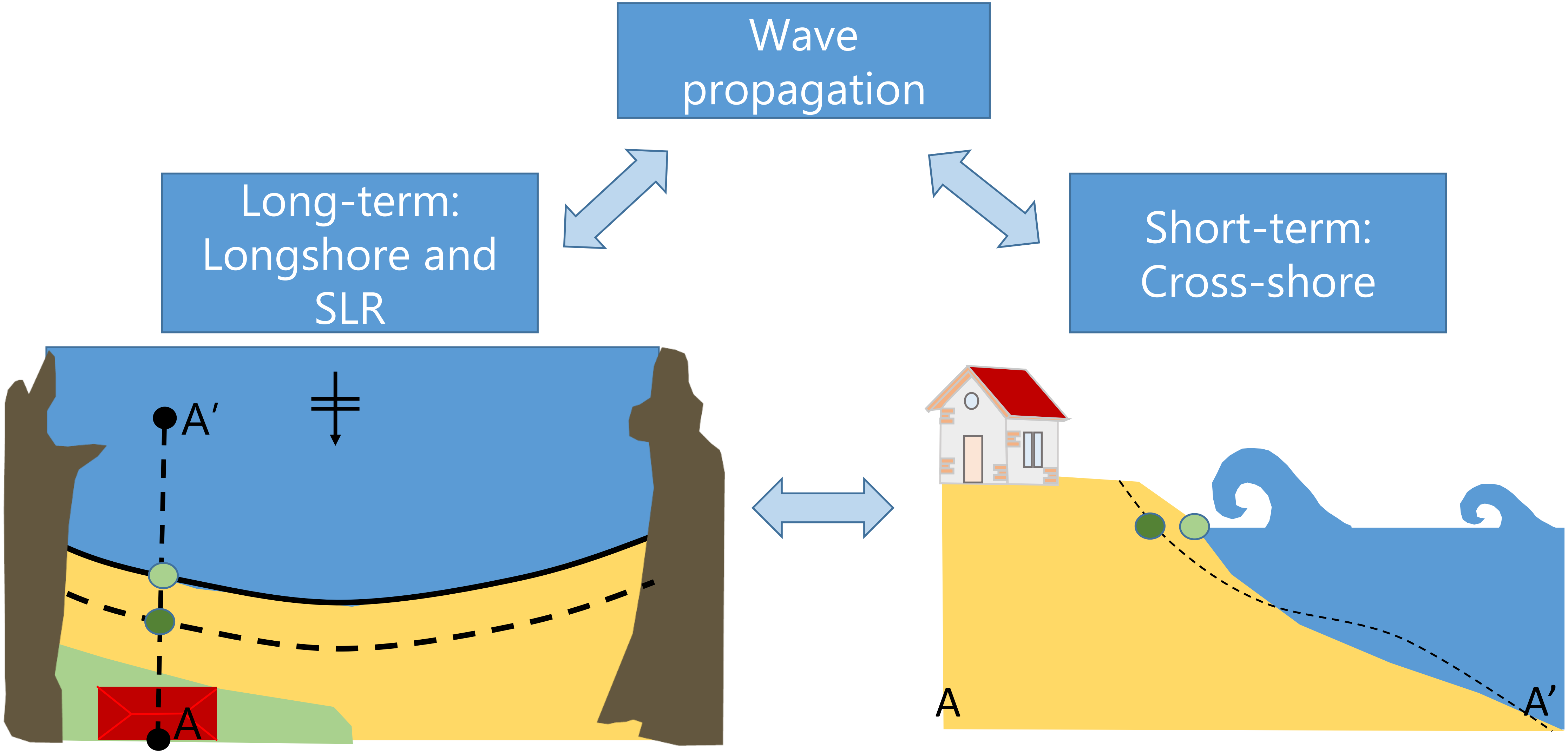
Wave propagation
Long-term: Longshore and SLR
Short-term: Cross-shore
A′
A
A
A’

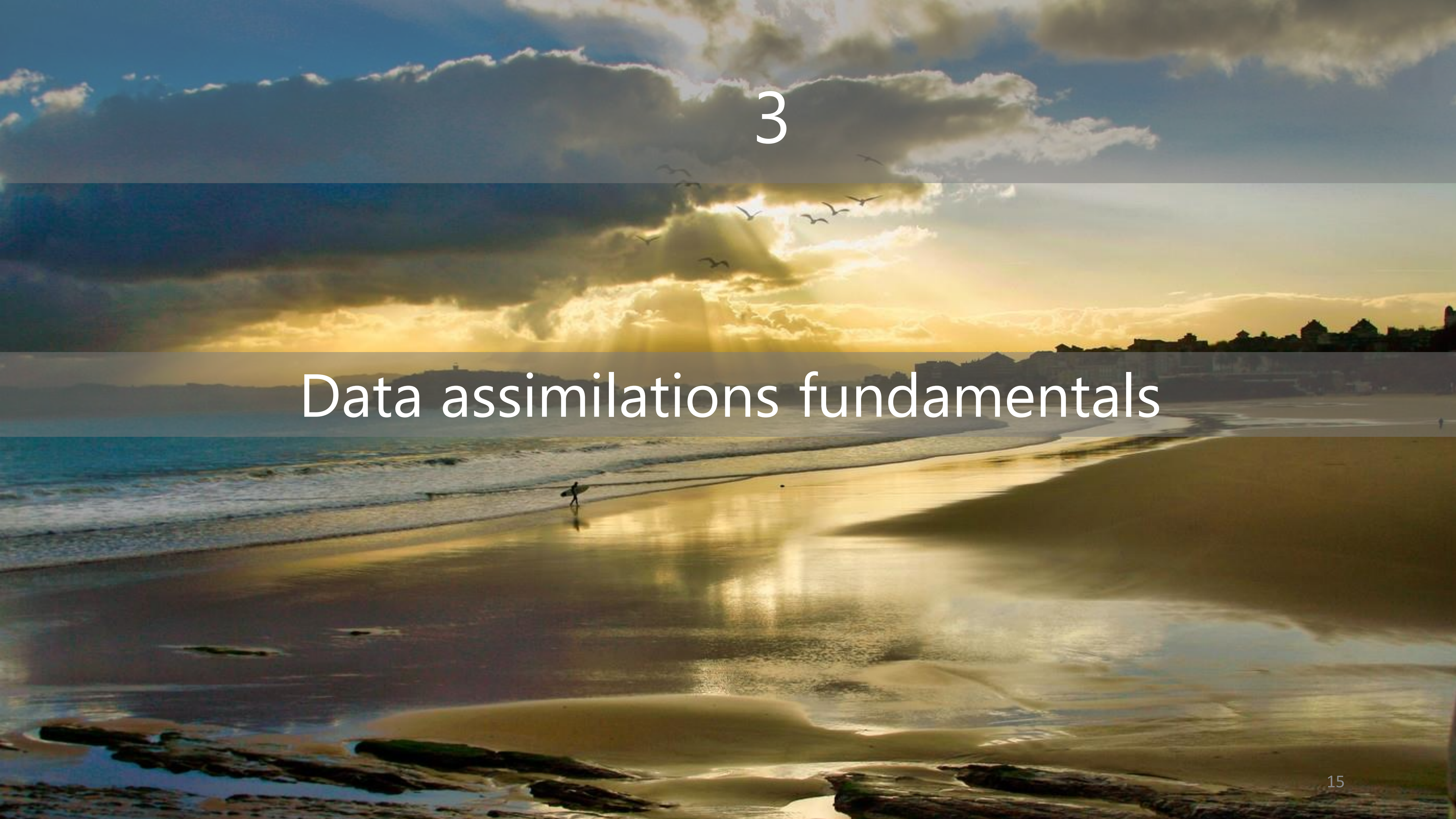
3
Data assimilations fundamentals

DA vs AI

DA

“Data assimilation is a process used in various fields to improve the accuracy of models and forecasts by integrating observed data into them.”

$$Y = F\,(x)$$

Processes + data

AI

“Artificial intelligence is based on algorithms and mathematical models that allow machines to process large amounts of data, identify patterns and make decisions or take actions based on those patterns.”

$$Y = F\,(x)$$

Data

DA vs calibration

DA

- Ground truth is assume to be a weighted mean of the model and the observations: state= model+observations
- Model and observations are considered to be uncertain
- One or reduced number (<100) of model runs
- New observations can be integrated easily

Standard calibration

- Adjust the model to fit the observations: state=model
- No uncertainty is considered in the model nor in the observations
- Many model runs
- New observations require recalibration

DA ingredients

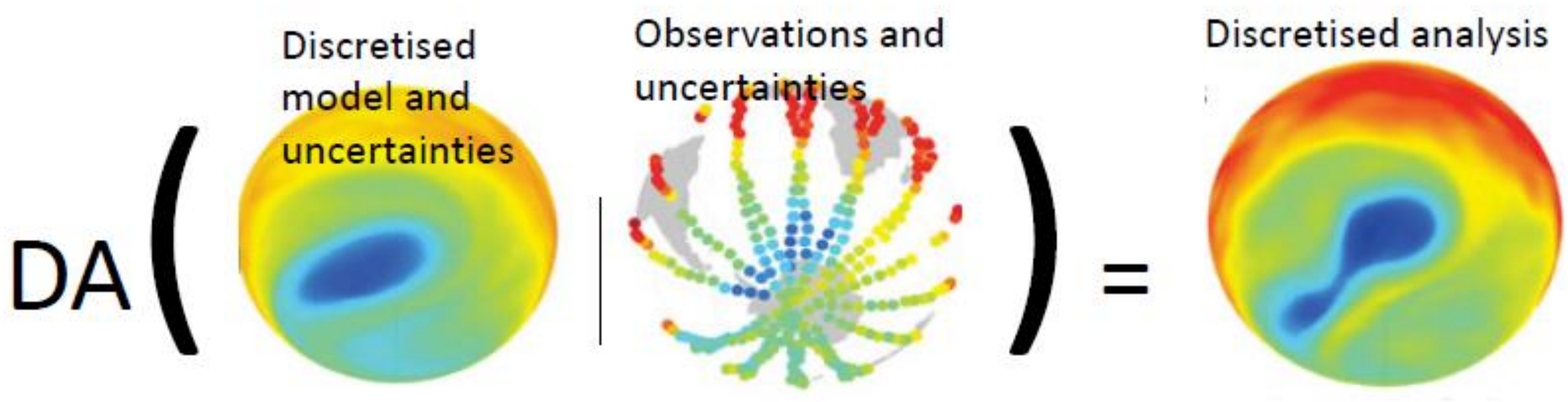

$$p(\mathbf{x}|\mathbf{y}) = \frac{p(\mathbf{x})p(\mathbf{y}|\mathbf{x})}{p(\mathbf{y})}$$

$p(\mathbf{x})$ PDF of the state (model forecast)

$p(\mathbf{y}|\mathbf{x})$ PDF of the observations given a state

$p(\mathbf{x}|\mathbf{y})$ PDF of the state considering the observations

DA ingredients

- Gaussianity (mean and covariance)

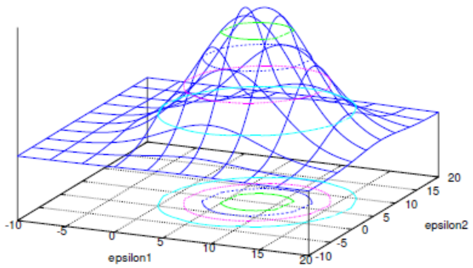

- Vector of vectors

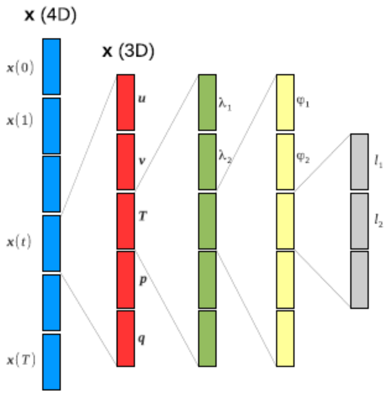

- Forward model: $\mathbf{x}_{i+1}^{f} = \mathcal{M}_i(\mathbf{x}_i^a)$
- Observation operator: $\mathbf{y}_{\mathrm{i+1}} = \mathcal{H}\left(\mathbf{x}_{\mathrm{i+1}}^{t}\right) + \epsilon$
- B matrix

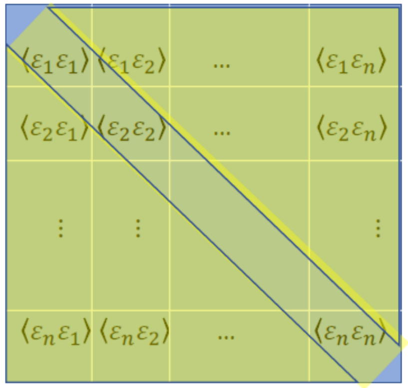

- R matrix (usually uncorrelated)

2 families of DA methods

Sequential

- "Estimation theory"
- Forecast state minimises the variance of the forecast error
- One observation at a time
- A given time step estimate is influenced by the last observation
- Model equations are not respected when assimilating an observation

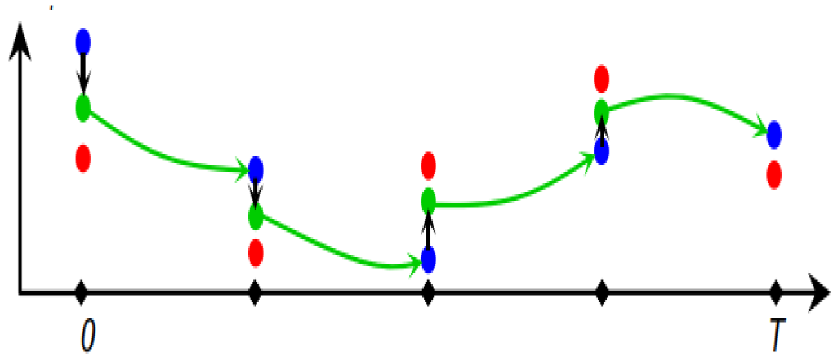

Variational

- "Optimal control theory"
- Forecast state minimises a cost function
- Several observations at a time
- A given time step estimate is influenced by previous and future observations
- Model equations are respected inside a time window (strong-constraint)

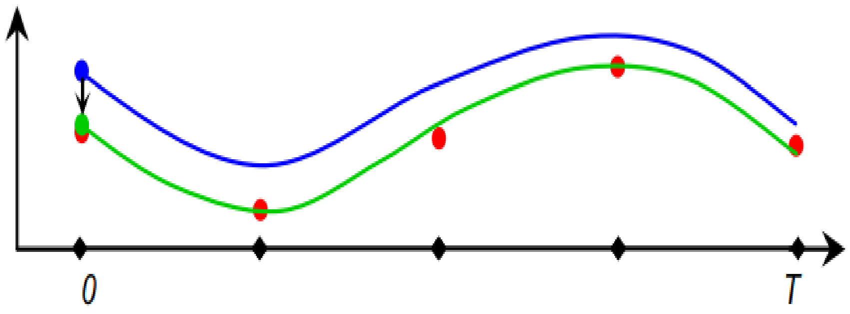

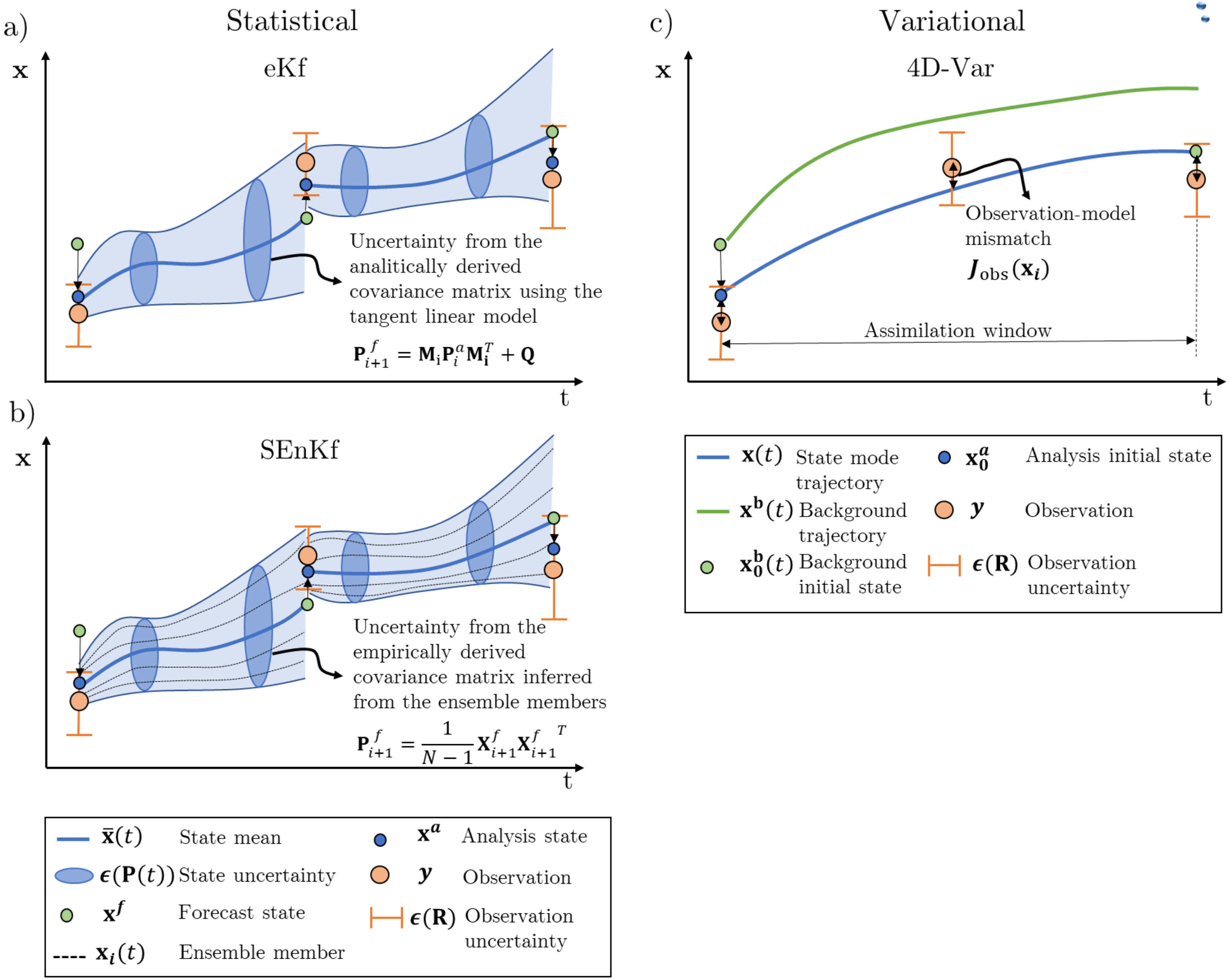
a)
Statistical
eKf
x
t
Uncertainty from the analitically derived covariance matrix using the tangent linear model
$\mathbf{P}^f_{i+1} = \mathbf{M}_i\mathbf{P}^a_i\mathbf{M}^T_i + \mathbf{Q}$
b)
SEnKf
x
t
Uncertainty from the empirically derived covariance matrix inferred from the ensemble members
$\mathbf{P}^f_{i+1} = \frac{1}{N-1}\mathbf{X}^f_{i+1}\mathbf{X}^{f\,T}_{i+1}$
$\bar{\mathbf{x}}(t)$ State mean
$\epsilon(\mathbf{P}(t))$ State uncertainty
$\mathbf{x}^f$ Forecast state
$\mathbf{x}_i(t)$ Ensemble member
$\mathbf{x}^a$ Analysis state
$\boldsymbol{y}$ Observation
$\epsilon(\mathbf{R})$ Observation uncertainty
c)
Variational
4D-Var
x
t
Observation-model mismatch
$J_{\mathrm{obs}}(\mathbf{x}_i)$
Assimilation window
$\mathbf{x}(t)$ State mode trajectory
$\mathbf{x}^b(t)$ Background trajectory
$\mathbf{x}^b_0(t)$ Background initial state
$\mathbf{x}^a_0$ Analysis initial state
$\boldsymbol{y}$ Observation
$\epsilon(\mathbf{R})$ Observation uncertainty

4

Data assimilation and shoreline modelling

Observation requirements

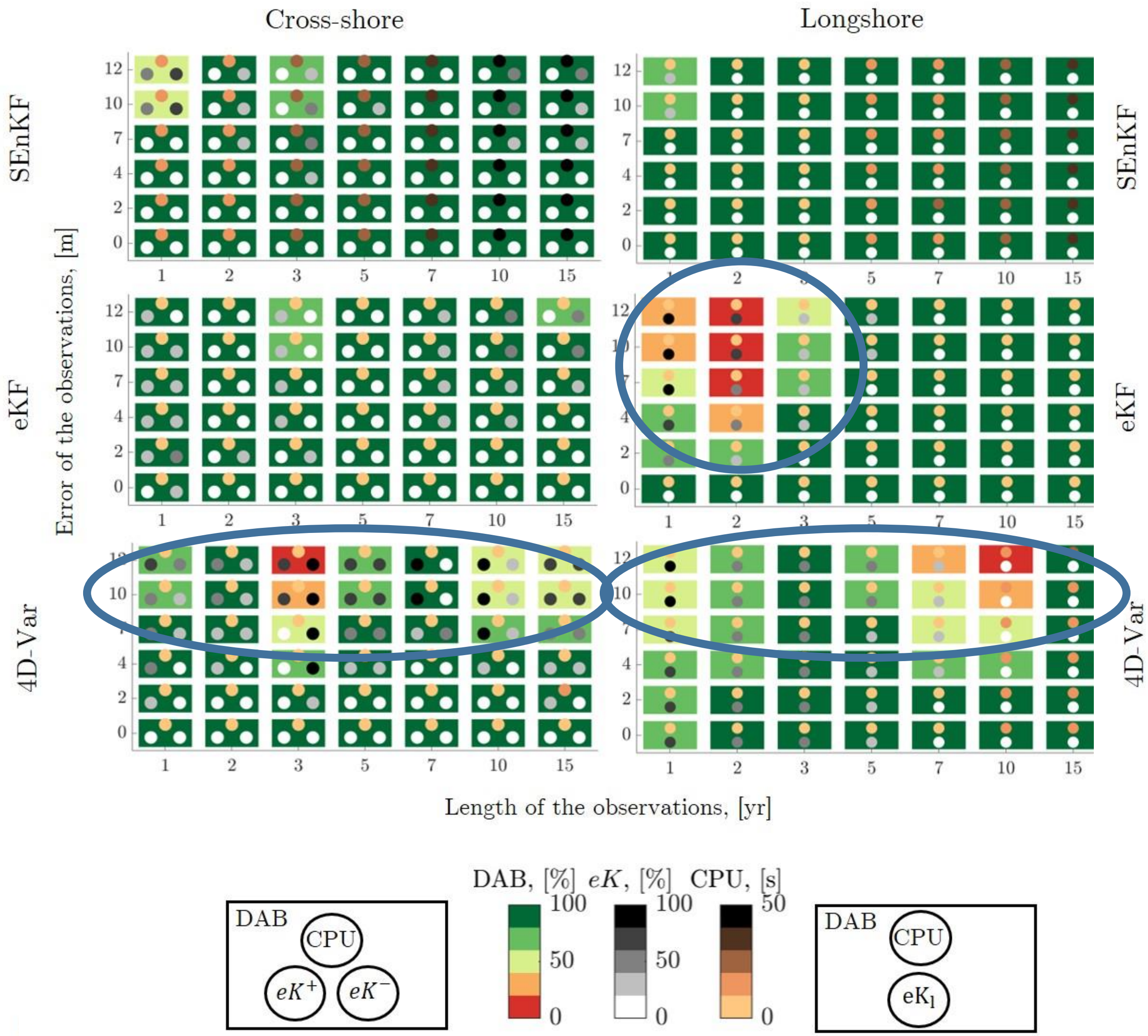

- eKf needs longer time series when errors are big
- 4D-Var performs poorly with noise
- The frequency of the observations is not relevant

Prior system knowledge (evolution)

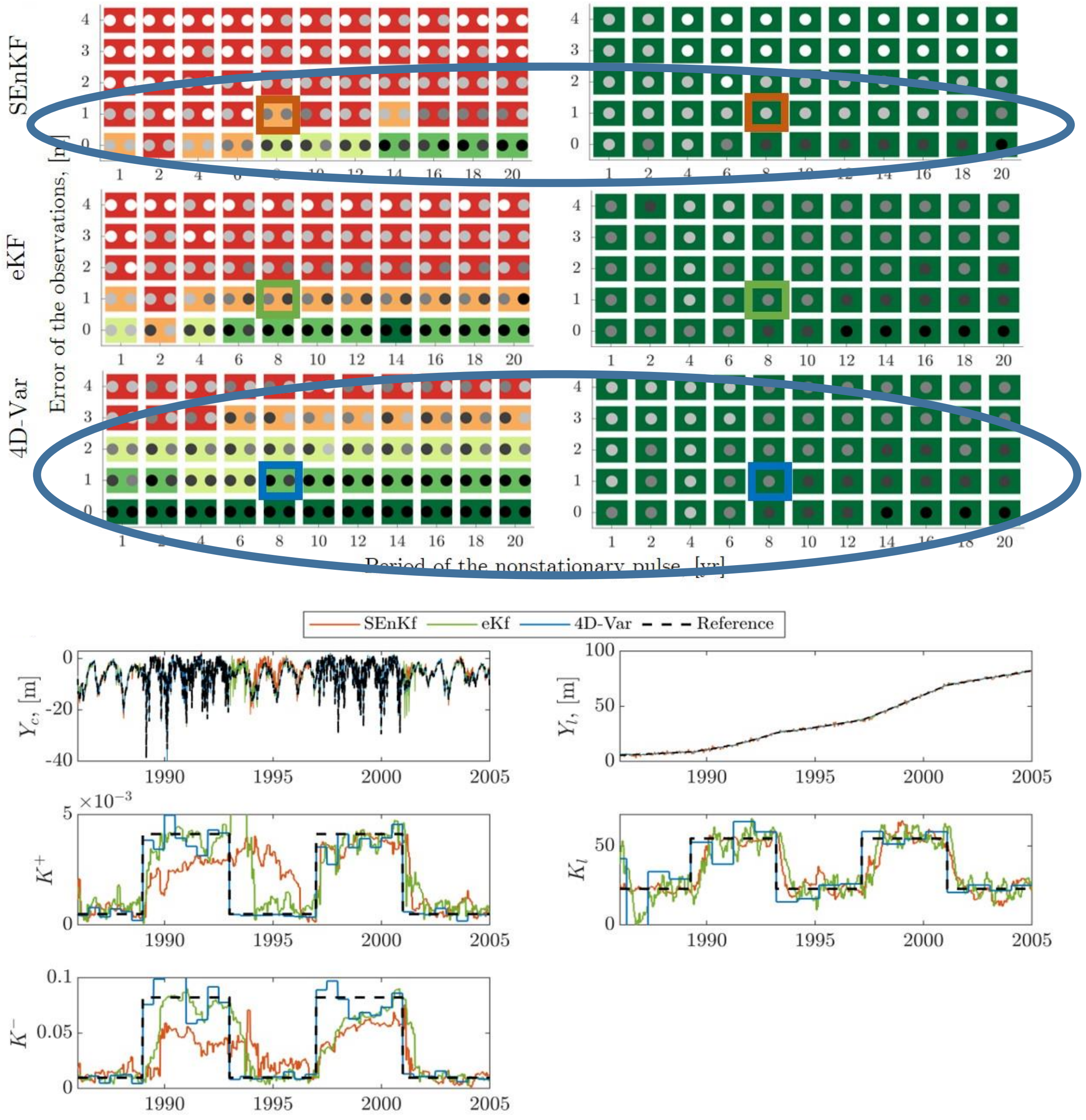

- The noise in the observations is key
- SEnKf performs poorly when errors are big
- 4D-Var is the best performing algorithm

Prior system knowledge (initial state)

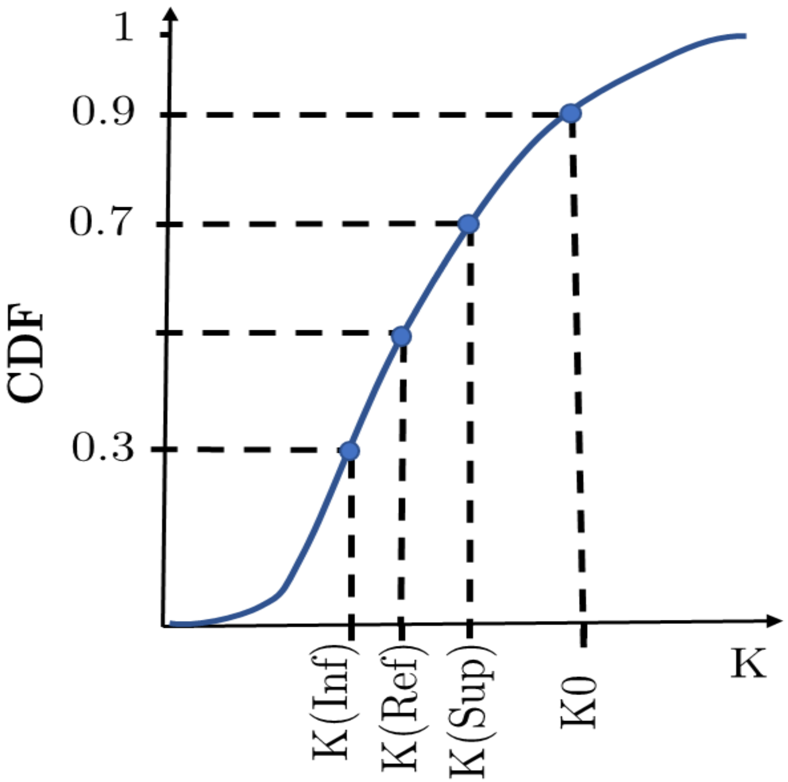

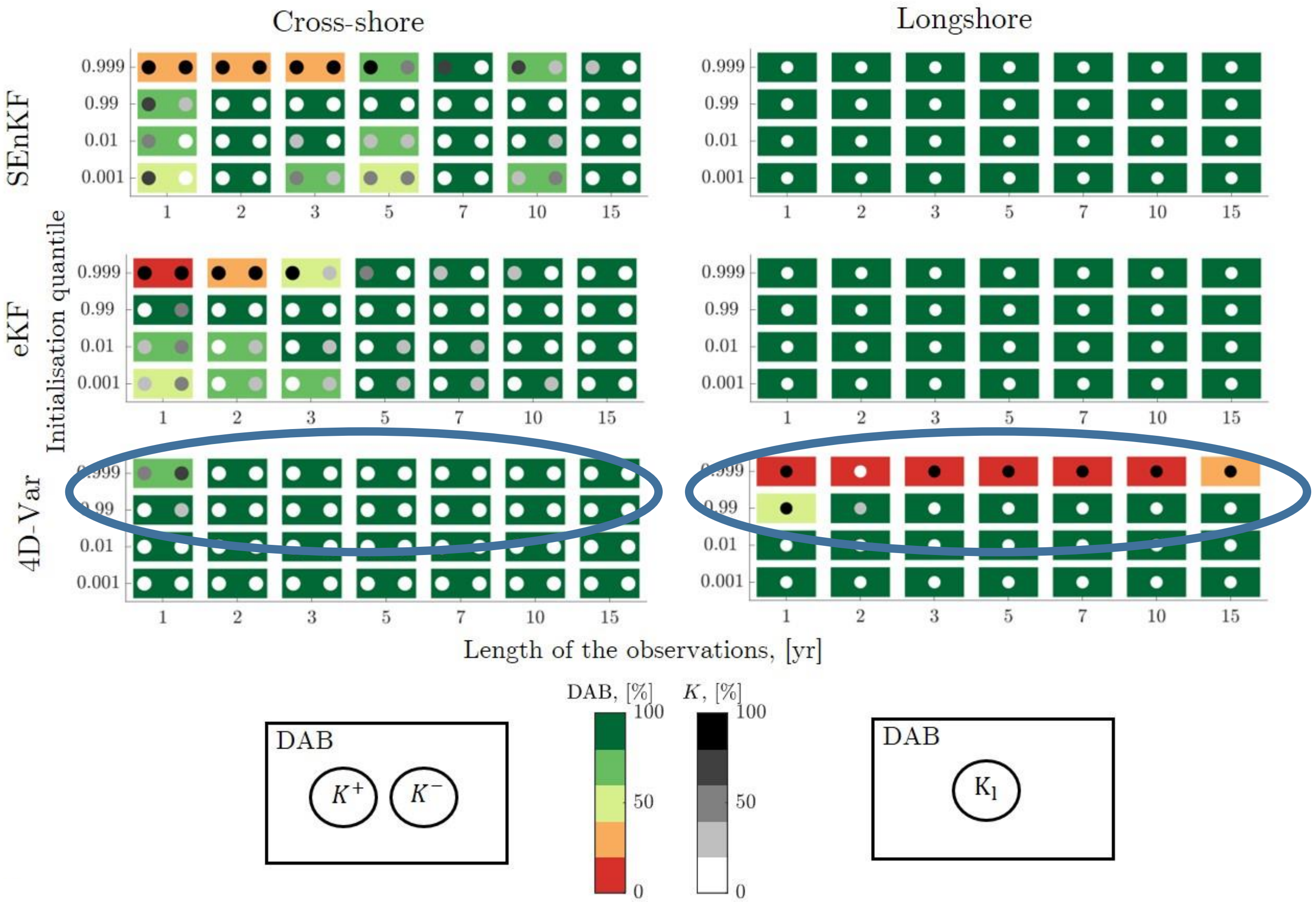

- 4D-Var is the best algorithm for cross-shore processes
- 4D-Var is the worst algorithm for longshore processes

Real case application

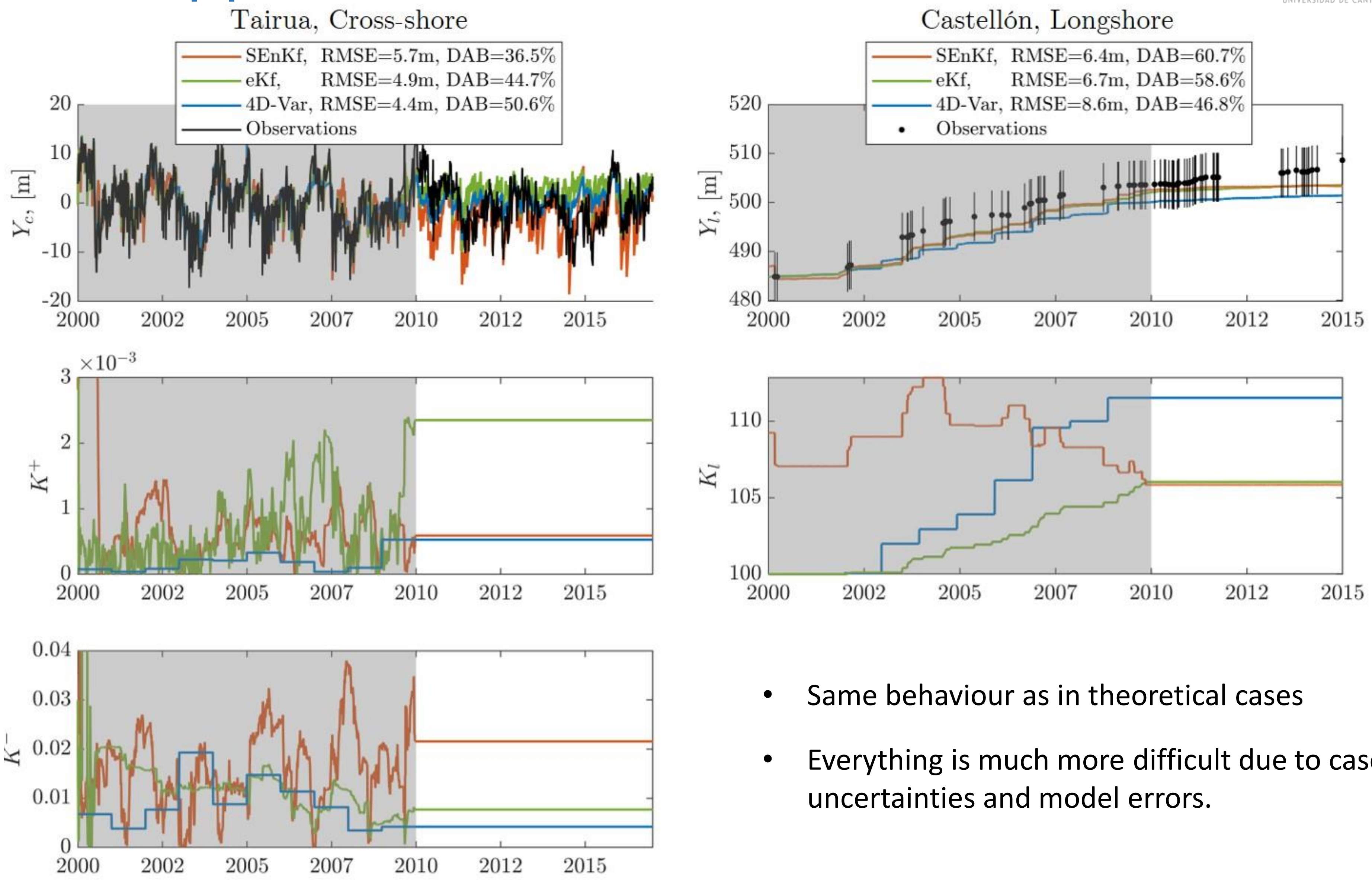

- Same behaviour as in theoretical cases
- Everything is much more difficult due to cascading uncertainties and model errors.

Summary

	DA Method	Performance with low quality data	Performance with limited observations	Performance with reduced prior system knowledge.	Performance in tracking system nonstationnarity	CPU efficiency	Ease of Implementation
Cross-shore	SEnKF	***	***	**	*	*	***
	eKF	***	**	**	**	***	**
	4D-Var	*	***	***	***	**	*
Longshore	SEnKF	***	***	***	**	*	***
	eKF	**	*	***	***	**	**
	4D-Var	**	**	**	***	**	*

- Which method to use?
- It depends ...

Alvarez-Cuesta, M., Toimil, A., & Losada, I. J. (2024). Which data assimilation method to use and when: unlocking the potential of observations in shoreline modelling. *Environmental Research Letters*, *19*(4), 044023.

5

Practical application of DA and real-world morphodynamic models

Application to a real case

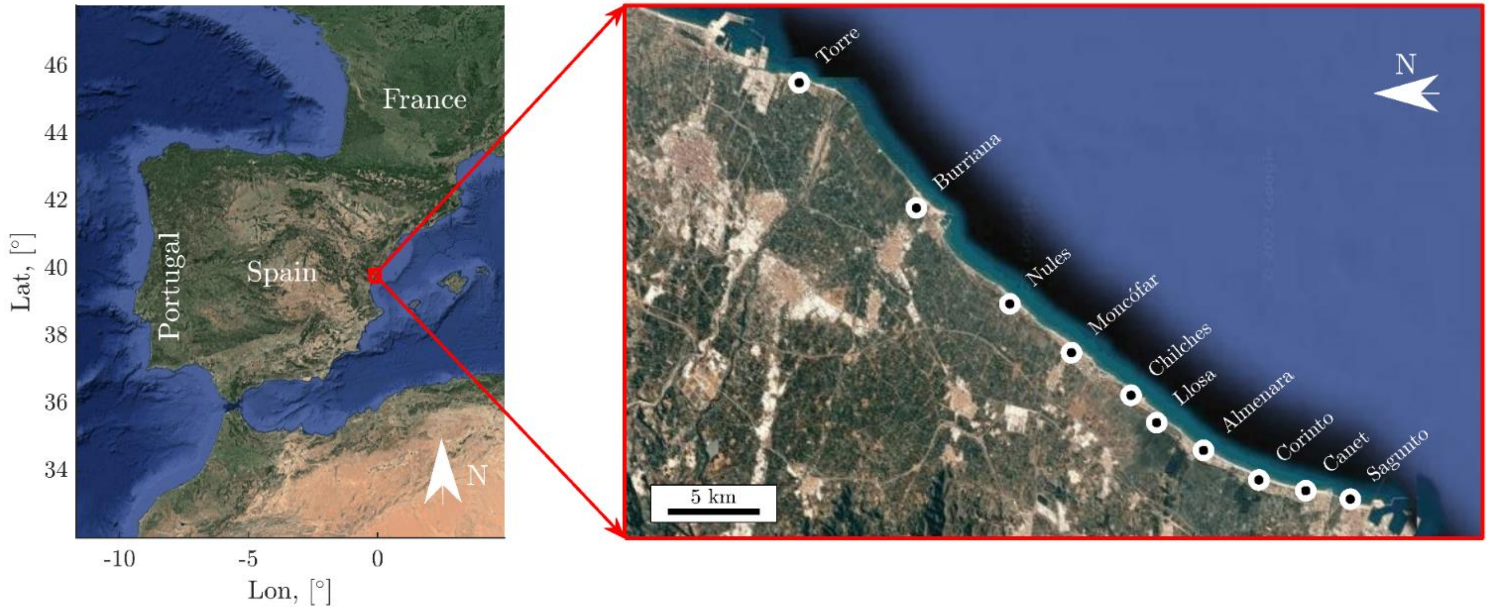

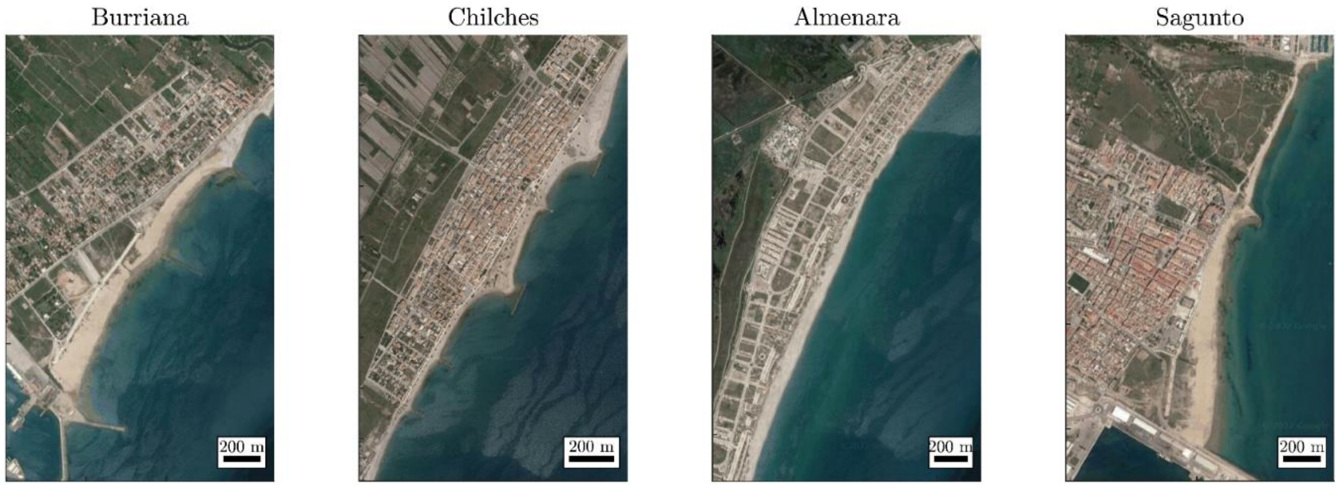

Preprocessing

SWAN grid

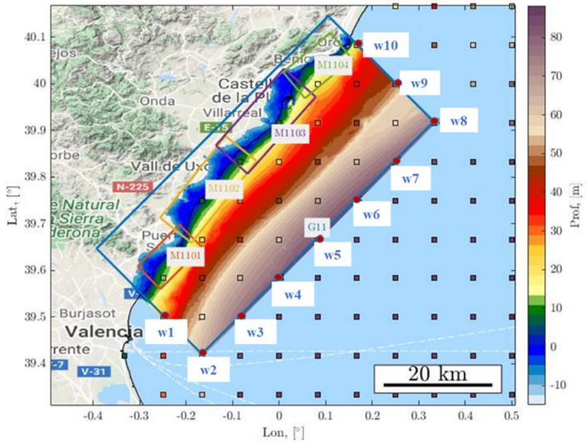

Sediments

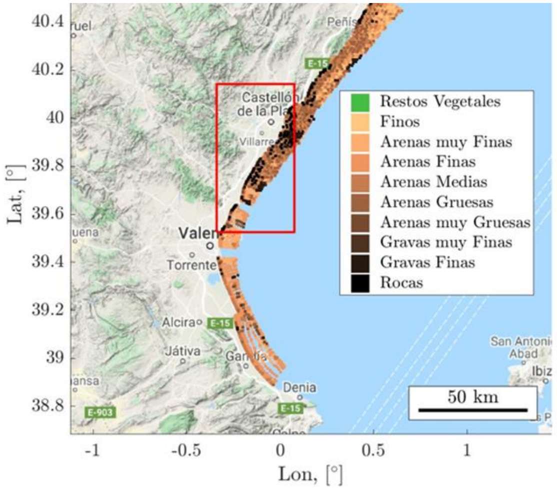

Transects

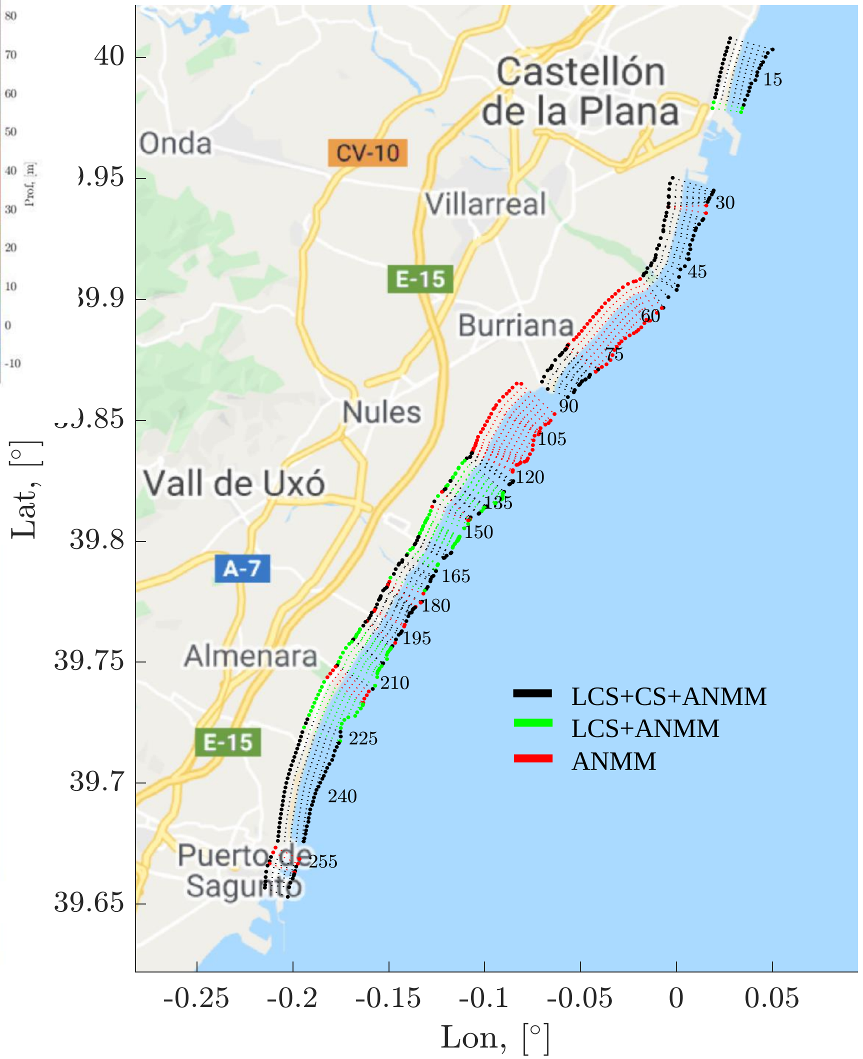

Observations (CoastSat, Vos et al. 2019)

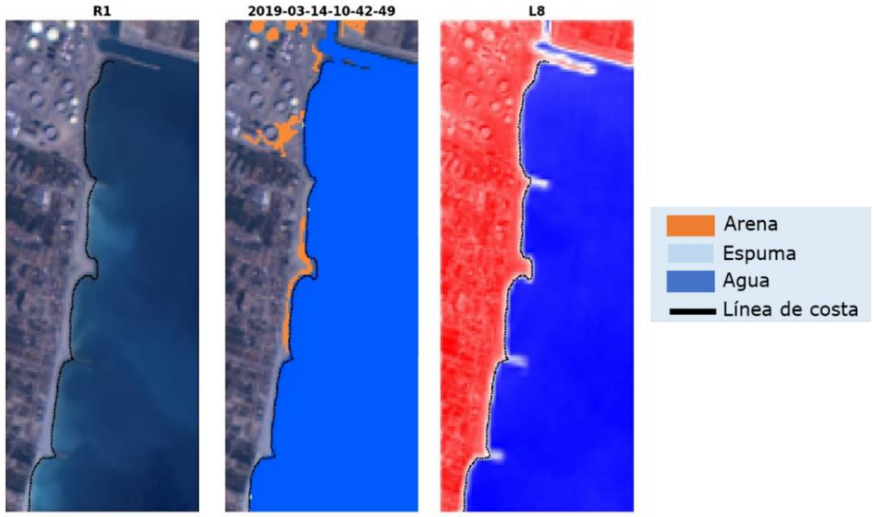

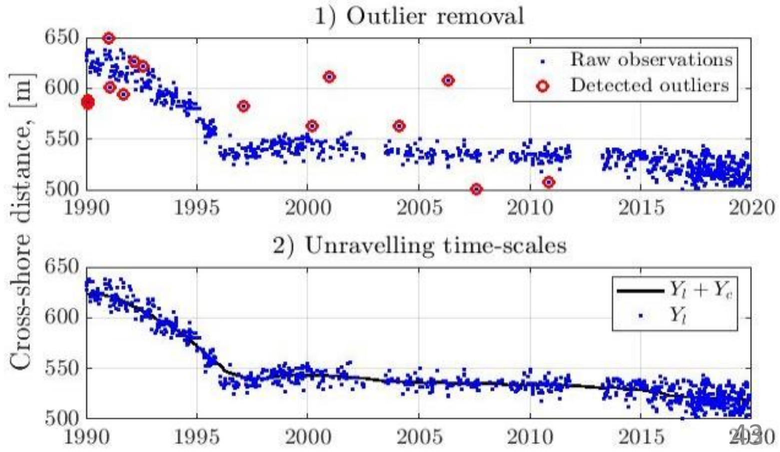

Governing equation

$$\underbrace{\frac{\partial Y}{\partial t}}_{\text{Shoreline changes}} = \underbrace{-\frac{1}{B+d_c}\frac{\partial Q}{\partial x} + \frac{1}{B+d_c} q + \boxed{vlt}}_{\frac{\partial Y_l}{\partial t}\ \text{Longshore}} + \underbrace{\boxed{K_c}\left[Y_c^{eq} - Y_c\right]}_{\frac{\partial Y_c}{\partial t}\ \text{Cross-shore}}$$

1.- Wave breaking

2.- Structures

3.- Free parameters

$$Q = \boxed{K_e}\boxed{K_l}\boxed{H_b^{2.5}}\left[\sin(2\boxed{\alpha}) - \frac{1}{\tan\beta_s}\frac{d\boxed{H_b}}{dx}\right]$$

USACE (1984)
O&B (1980)

$$Y_c^{eq} = \Delta y0 + \Delta Y_{eq} + R_{ANMM}$$

$$\Delta Y_{eq} = -\boxed{W_b}\left(\frac{0.106\boxed{H_b} + MM + MA}{B + \boxed{d_b}}\right)$$

M&D (2004)
Bruun (1962)
Toimil et al. (2017)

Results

200m Transects

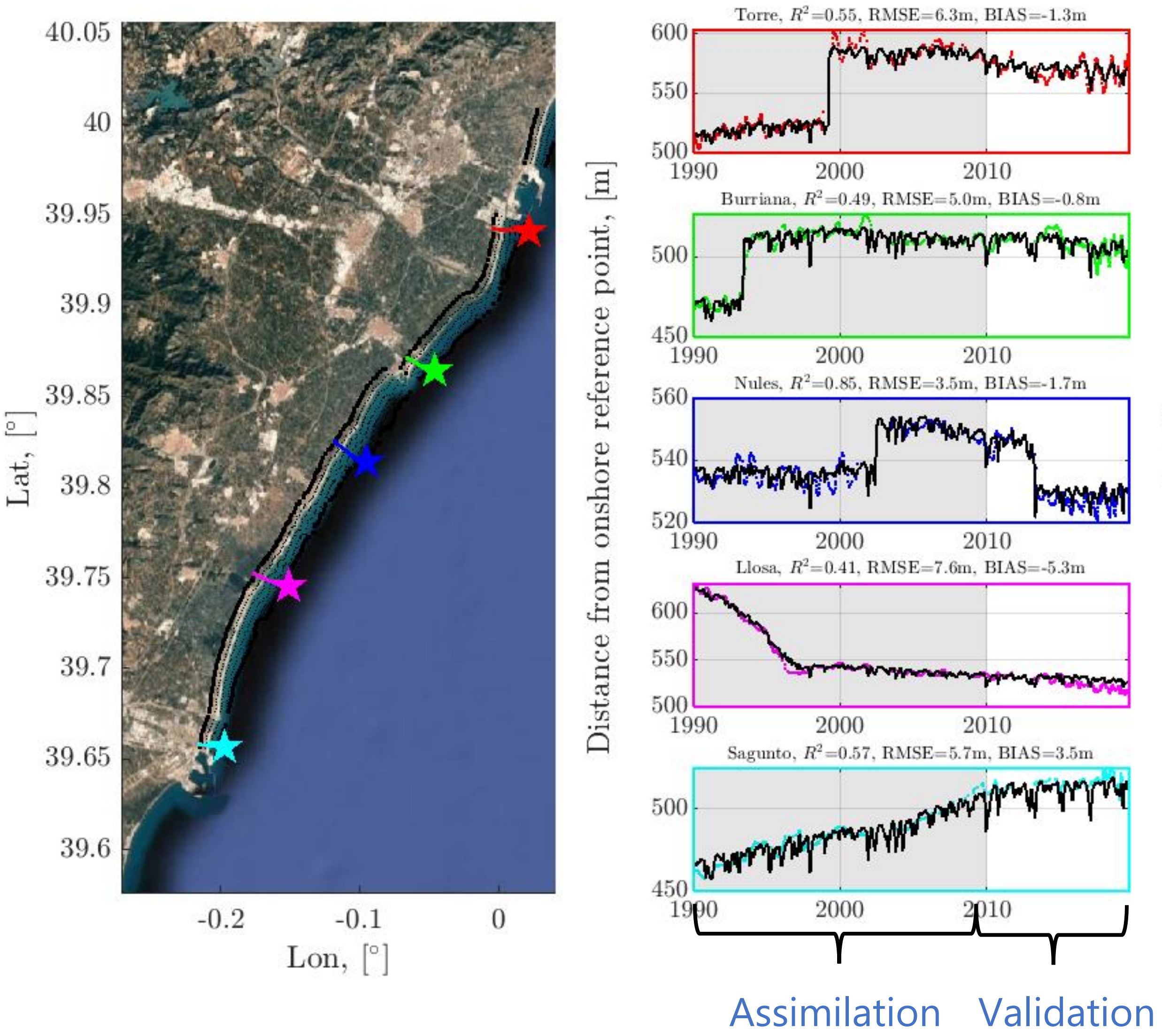

15m Transects

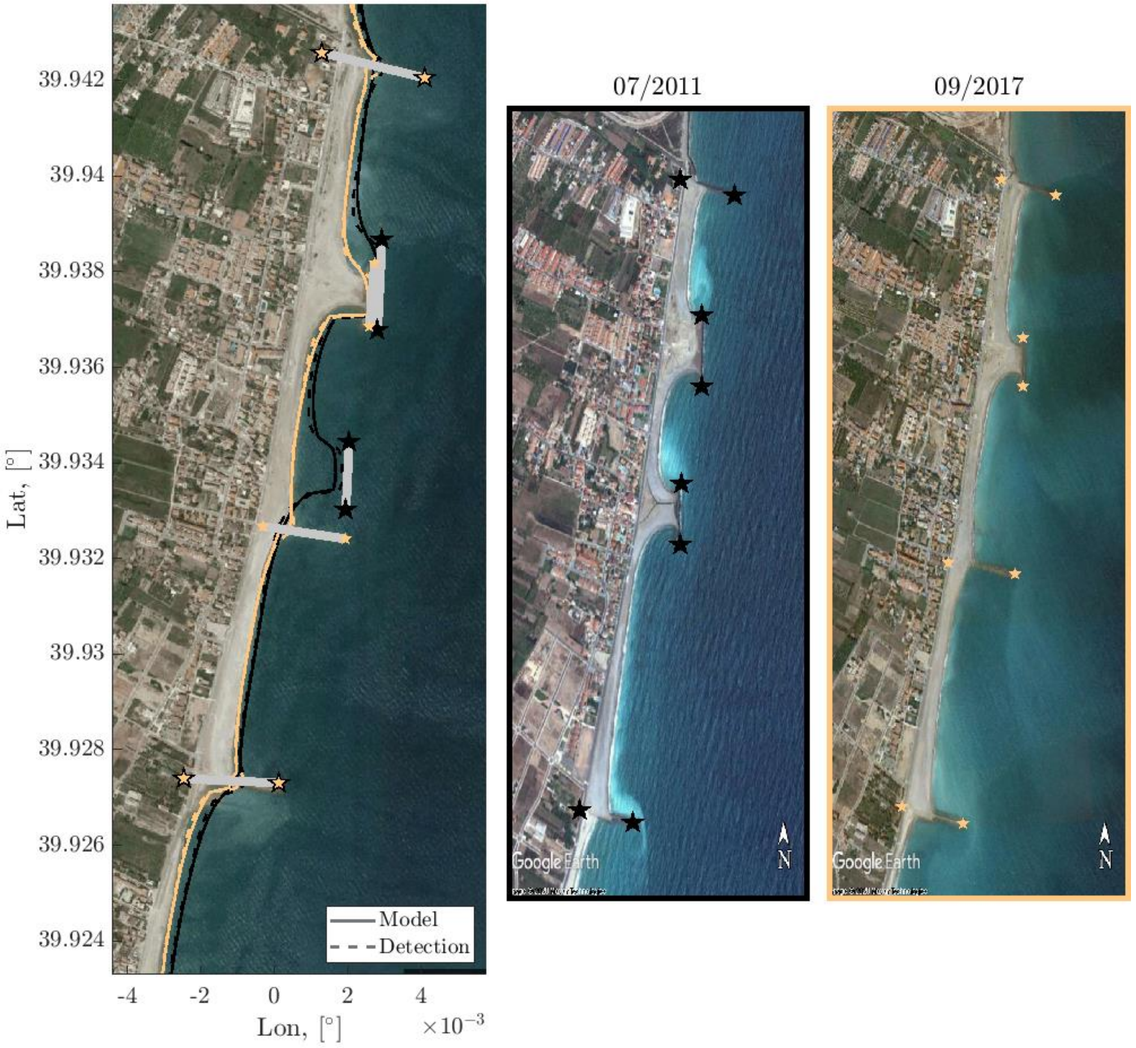

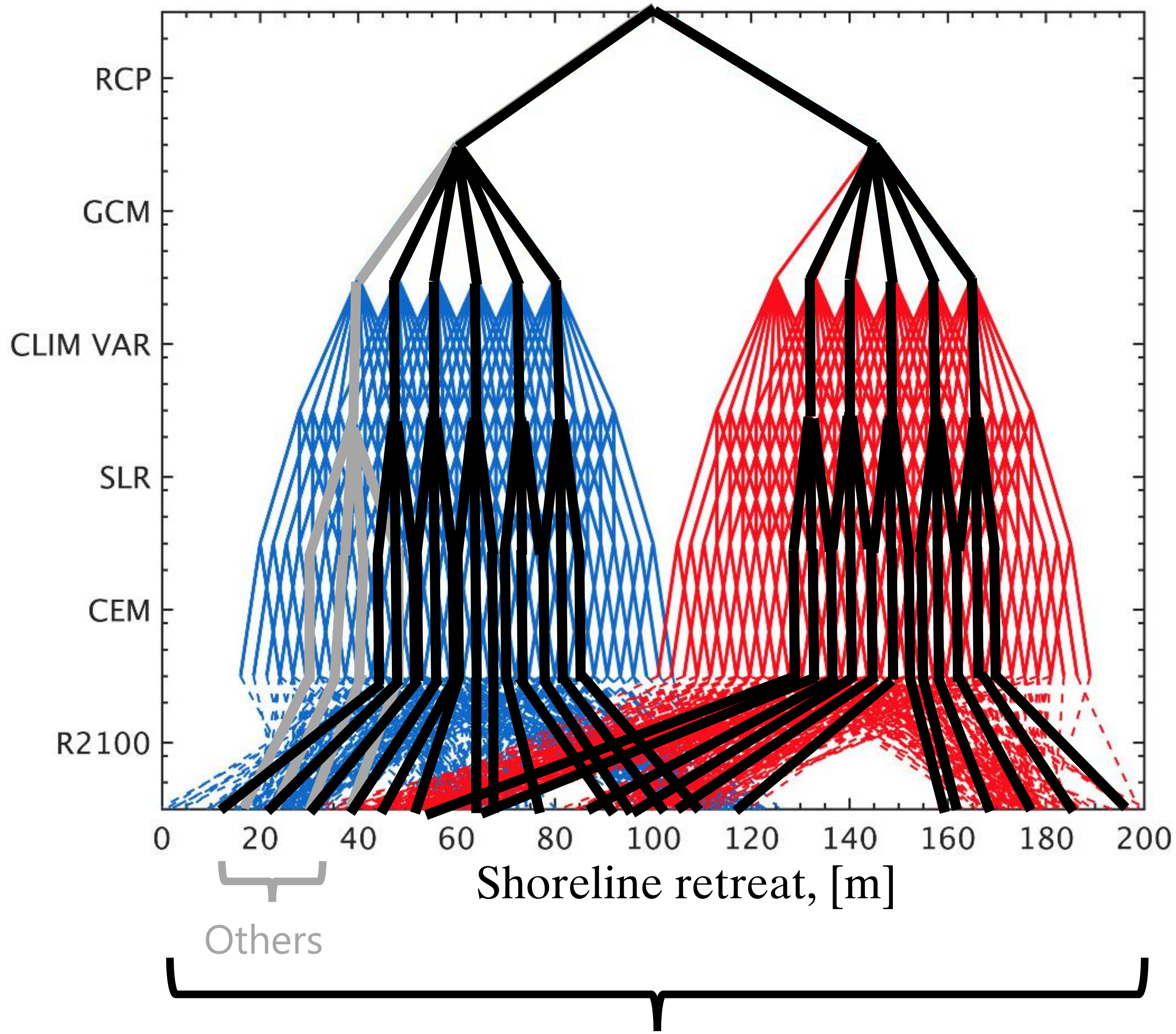

Toimil, A., Camus, P., Losada, I. J., & Alvarez-Cuesta, M. (2021). Visualising the uncertainty cascade in multi-ensemble probabilistic coastal erosion projections. *Frontiers in Marine Science*, *8*, 683535.

IHcantabria INSTITUTO DE HIDRÁULICA AMBIENTAL UNIVERSIDAD DE CANTABRIA
FUNDACION INSTITUTO DE HIDRÁULICA AMBIENTAL DE CANTABRIA

Shoreline forecast

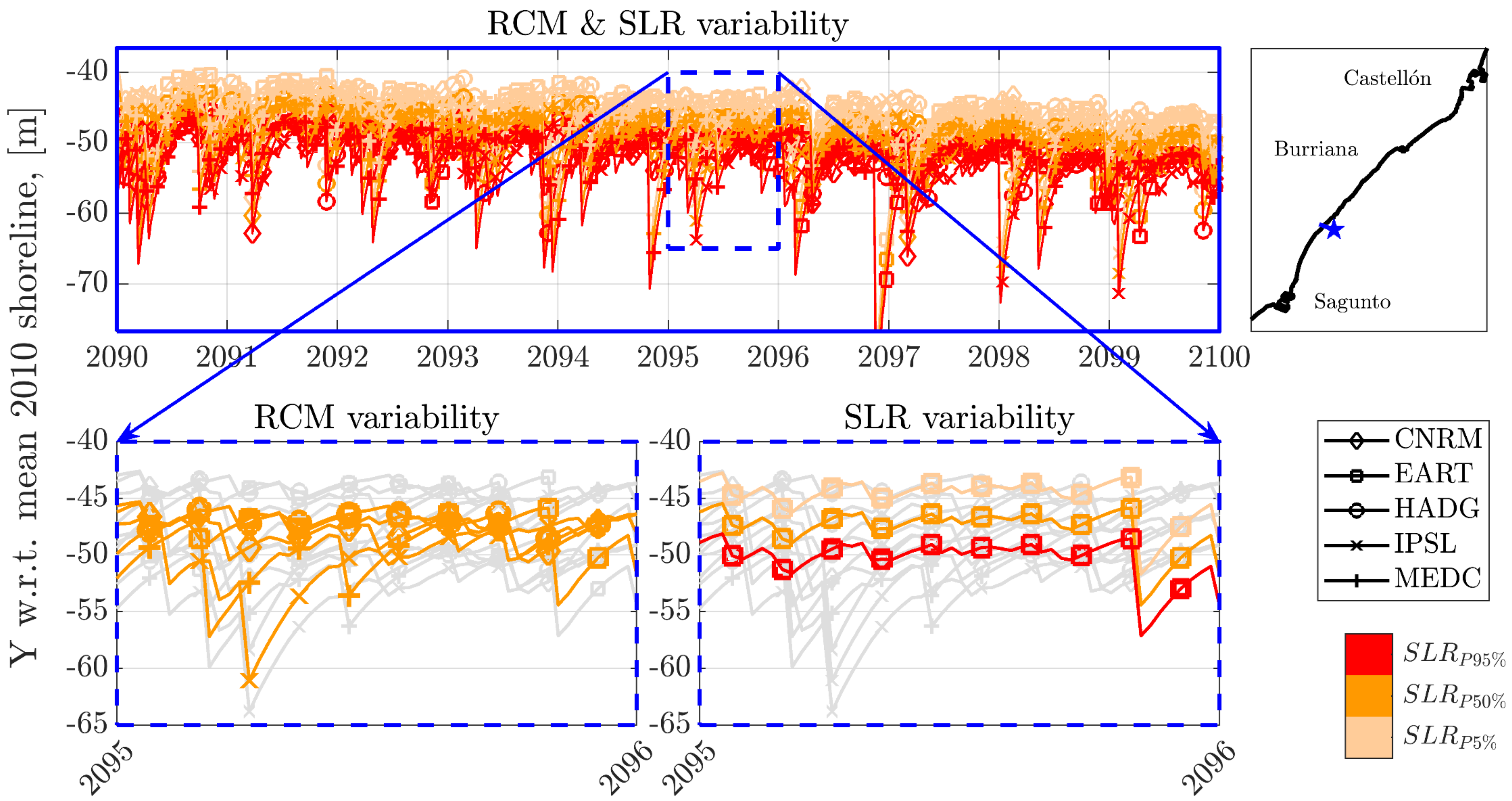

Alvarez-Cuesta, M., Toimil, A., & Losada, I. J. (2021). Reprint of: Modelling long-term shoreline evolution in highly anthropized coastal areas. Part 2: Assessing the response to climate change. *Coastal Engineering*, *169*, 103985.

Nonstationary extreme retreats

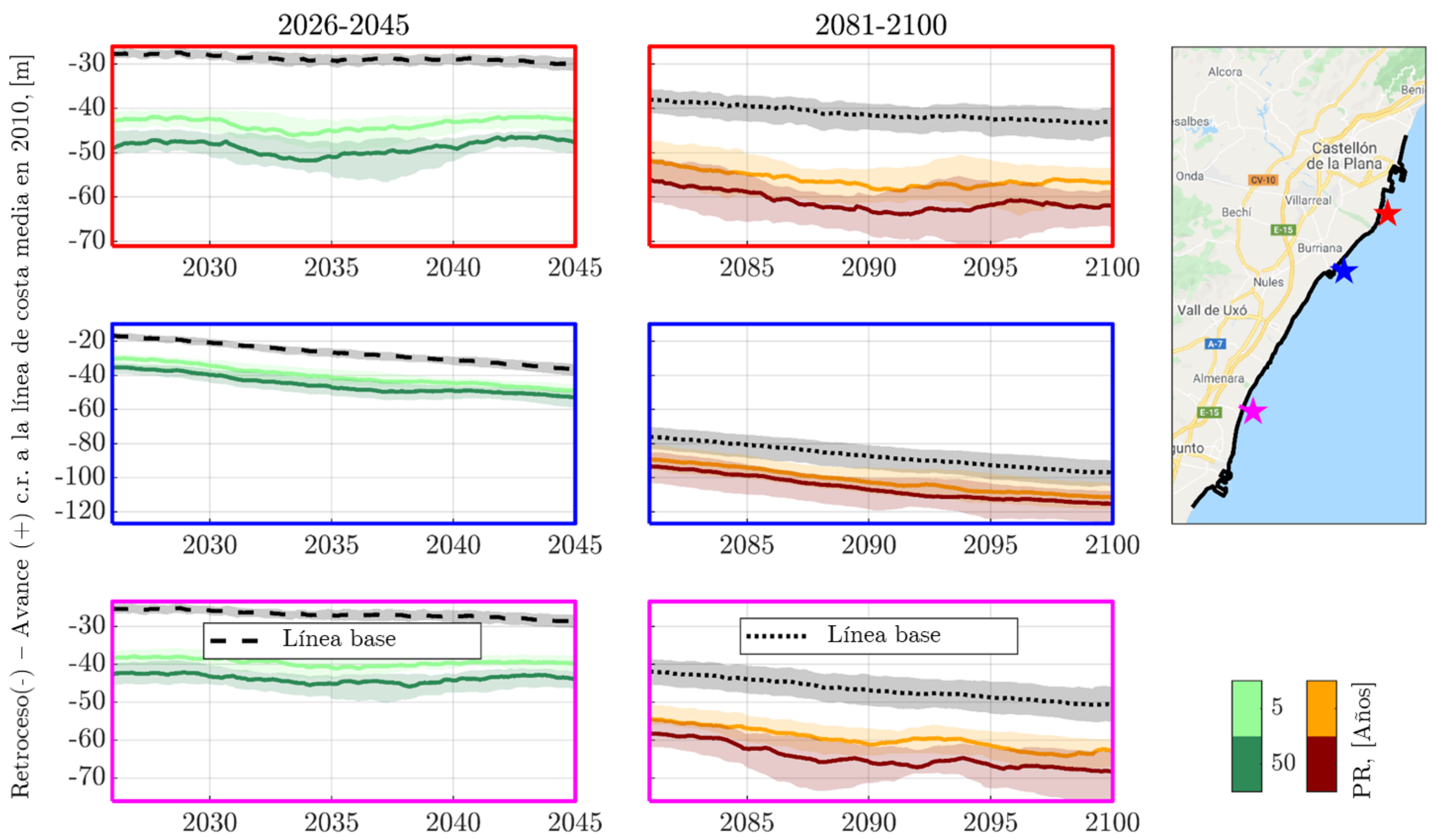

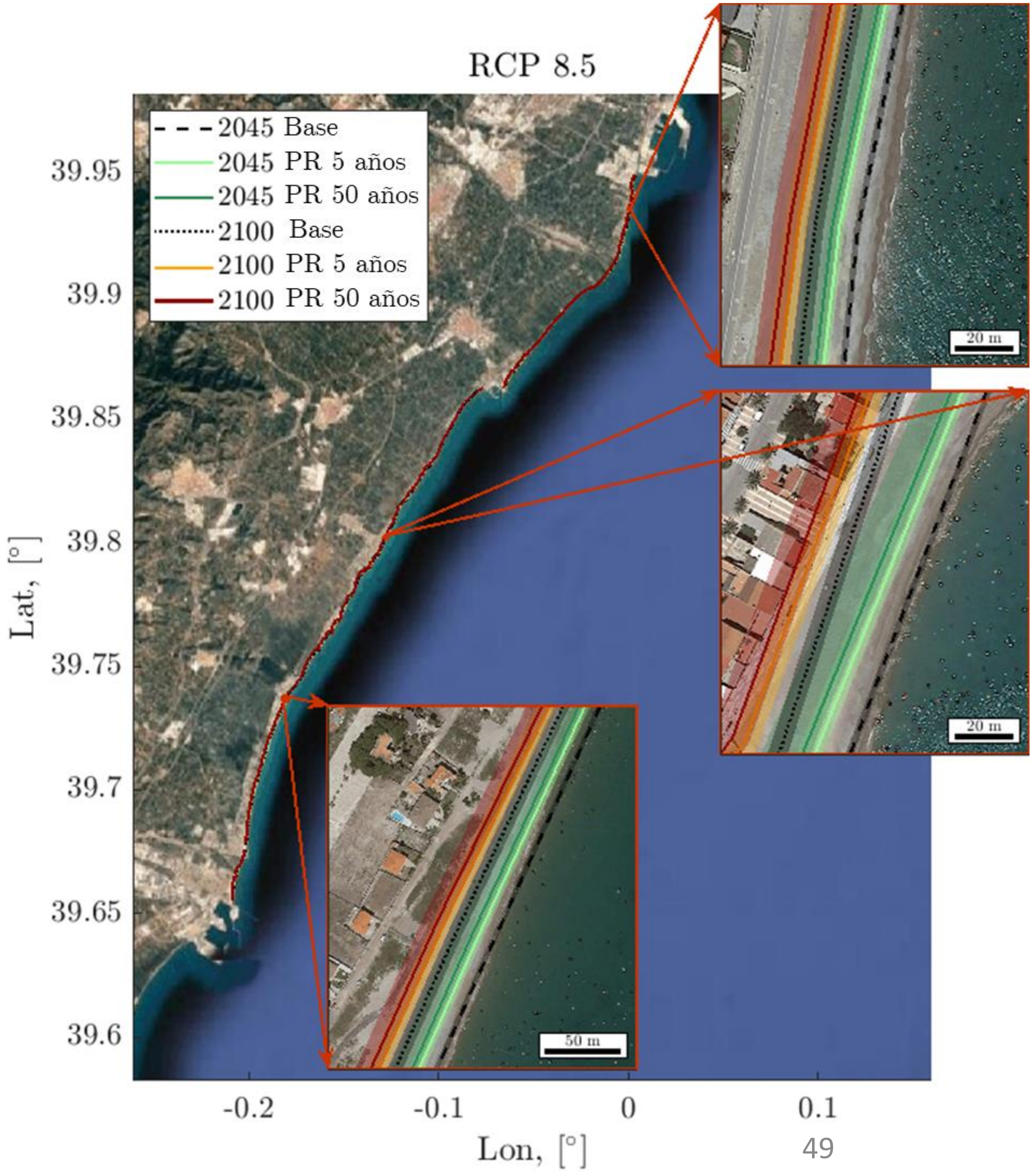

Profile translation

ShoreTrans, McCarrol et al. (2020)

IH-LANS

$$\frac{\partial Y}{\partial t} = \boxed{\frac{\partial Y_l}{\partial t}} + \boxed{\frac{\partial Y_c}{\partial t}}$$

$$\Delta V_i = (Y_{l,i} - Y_{l,2020})(B + d_c)$$

$$SLR_i = SLR_i - SLR_{2020}$$

$$Y_{c,ref}$$

Longshore

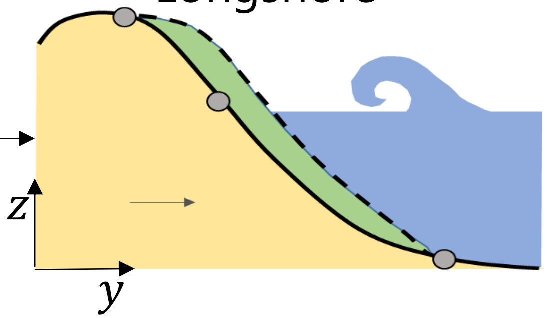

SLR

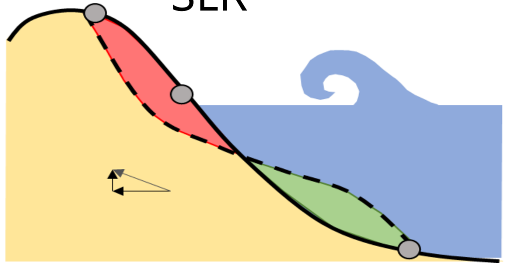

Cross-shore (storms)

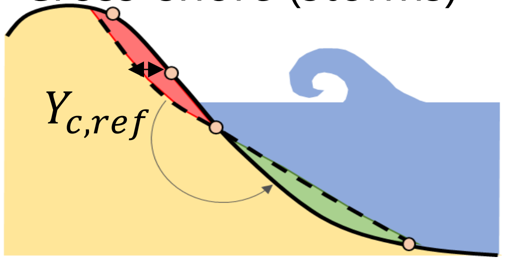

Longshore processes

$$z_i(y) = z_{2020}(y - \Delta Y) + \mathrm{ANMM_i}$$

$$\Delta Y\ ??$$

$$\min_{\Delta Y} \int_{y_b+\Delta Y}^{y_{dc}+\Delta Y} [z_i(y) - z_{2020}(y)]dy + \Delta V_i$$

Cross-shore processes

Kinsela et al. (2017)

$$V_{ero} = V_{acr}$$

Thanks for your attention!

Moisés Álvarez-Cuesta(alvcuestam@unican.es)

Climate risks, adaptation and resiliency group

Instituto de Hidráulica Ambiental de la Universidad de Cantabria - IHCantabria

“Wave resolving numerical modelling of swash zone hydro- and morphodynamics” (R. Briganti, UNOTT)

University of Nottingham
UK | CHINA | MALAYSIA

Wave resolving numerical modelling of swash zone hydro- and morphodynamics

Presenter:

Dr. Riccardo Briganti

Outline

Sediment transport → Overview of numerical challenges and models → Part 1: Description of bottom boundary layer → Part 2: Sediment transport modelling in XBeach → Conclusions

Context and motivations

- Sandy beaches evolution plays a key role in coastal vulnerability

- The direct effect of the trends in frequency of storms on beaches profiles evolution is still difficult to predict (IPCC, 2014)

- Swash zone hydro-morphodynamics:
  - region alternatively wet or dry
  - important for bedforms (e.g. cusps, and coarse sediment beaches)
  - exchange of sediments between swash and surf zones

Cusps in Peru. Credit: coastalcare.org

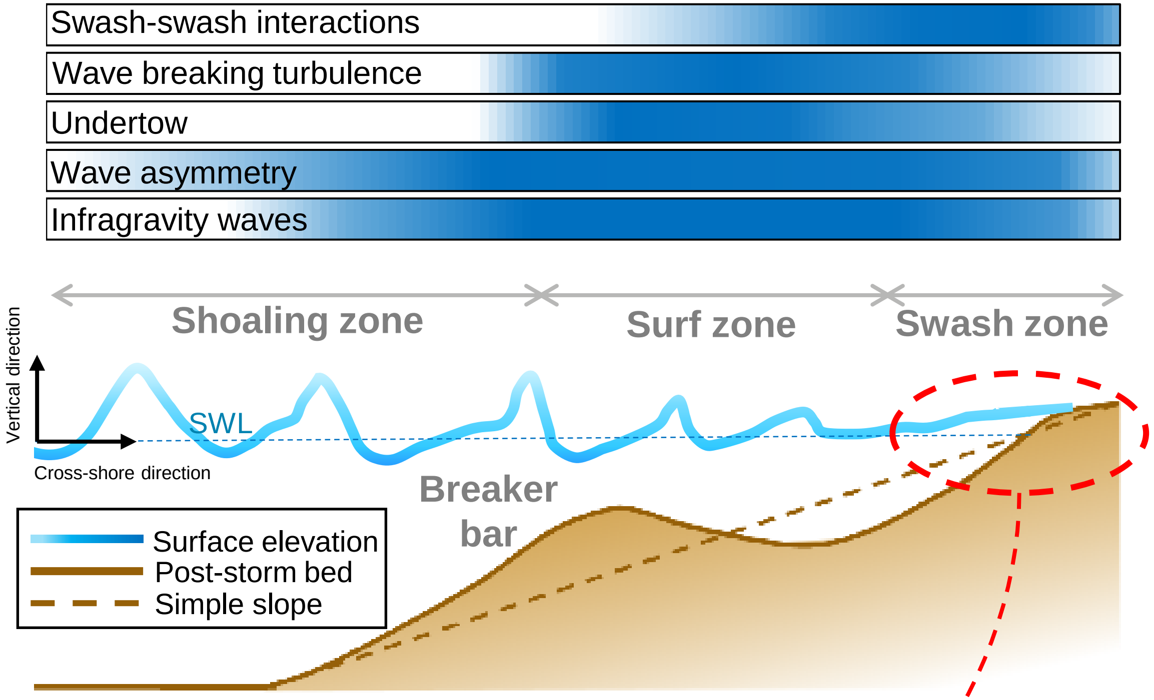

The swash zone in Torvaianicq. Credit Dr Giulia Mancini

Basic concepts in sediment transport

Sediment is transported by flows in different modes, traditionally these are defined as:
-Bed load
-Suspended load
-Sheet flow is a condition of thin, highly concentrated sediments (>50% in volume) close to the bed, it is associated to bed load, although it is actually very different.

The flow in the swash zone is highly unsteady and transitions among the three modes occur within a single wave period.

Chen et al. (2023)

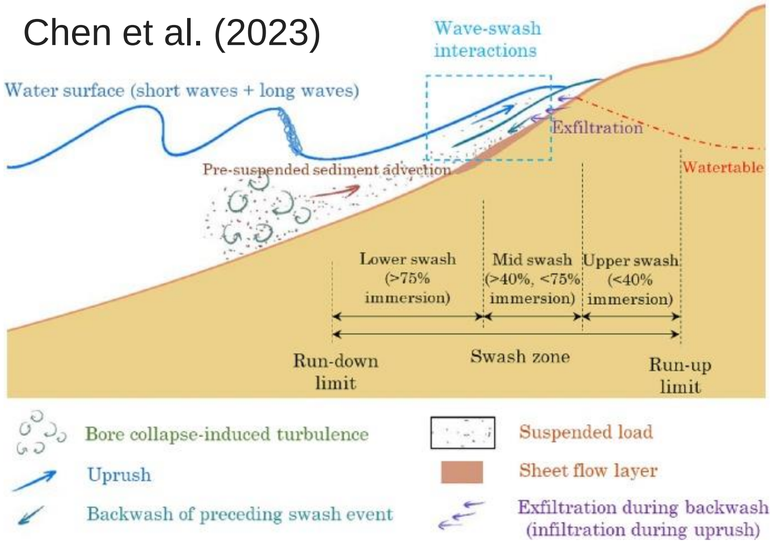

Chardón-Maldonado et al. (2016)

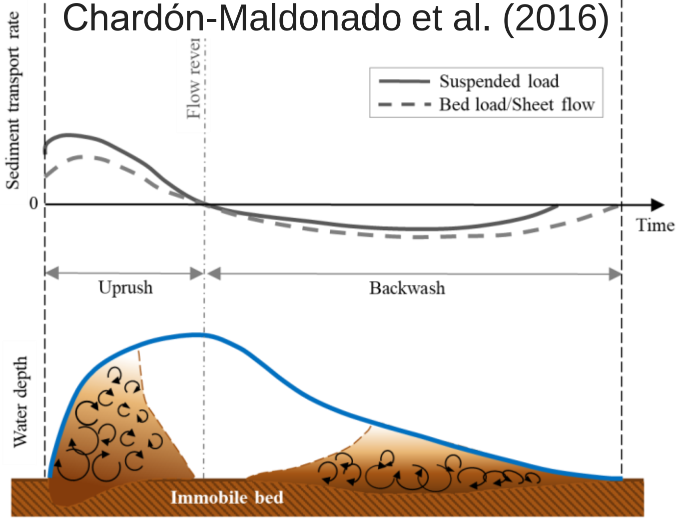

Recent reviews:

Chardón-Maldonado, P., Pintado-Patiño, J.C. and Puleo, J.A., 2016. Advances in swash-zone research: Small-scale hydrodynamic and sediment transport processes. *Coastal Engineering*, *115*, pp.8-25.

Chen, W., Van Der Werf, J.J. and Hulscher, S.J.M.H., 2023. A review of practical models of sand transport in the swash zone. *Earth-Science Reviews*, *238*, p.104355.

Numerical modelling of swash processes

Traditional classifications of numerical models for coastal hydrodynamic (wave driven) processes are based on

- The time scales resolved:
  - **Wave resolving** (or **phase resolving**): models that describe processes within individual waves, e.g. intra-swash cycle.
  - **Wave averaging** (or **phase averaging**): models that describe processes at temporal scale larger than wave period, intra-wave processes are modelled (e.g. dissipation due to wave breaking, radiation stress).

- The spatial scales/dimension resolved:
  - **Two dimensional, depth averaging** models: capable of describing horizontal hydrodynamic processes (e.g. wave refraction, diffraction). Often referred as 2DH (or 1DH if one-dimensional propagation is considered).
  - **Three dimensional, depth resolving** models: capable of resolving both horizontal and vertical (within the water column), processes (e.g. wave breaking generated turbulence. Often referred as 2DV.

Combinations: e.g., wave resolving, 2DH models (such those we develop at UoN), wave resolving 2DV models (e.g. IH2VOF); wave averaging, depth resolving models exist, e.g. for wave induced circulation, we do not discuss them here.

“Intermediate” types: e.g. some 2DH wave model provide a description of some processes within the water column, e.g. description of the vertical velocity (Boussinesq-type models, SWASH), description of the bottom boundary layer (e.g. UoN and UNIVPM models, based on NLSWE).

Numerical modelling of sediment transport and morphodynamics

Available approaches:

Phase resolving

-Depth resolving (2DV) hydrodynamics eqs + particle methos (e.g. DEM: SediFOAM, SedFOAM, SPH)

-Depth resolving (2DV) hydrodynamics eqs + continuum approximation for particles (e.g. IH2VOF-SED and Kranemborg et al, 2024)

-**Depth integrating hydrodynamics eqs + continuum approximation for sediments** (e.g. Xbeach NH, UoN/UNIVPM models)

-Depth integrating phase averaging hydrodynamics equations + continuum approximation for particles (many engineering oriented models e.g. Delft3D, see Chen et al. 2023)

We focus on the depth integrating approach. Models for swash include:

-A set of depth integrated hydrodynamic equations, time averaged on scales comparable to one or multiple wave periods (e.g. XBeach hydrostatic governing equations), or not phased averaged (e.g. NH-NLSWE, Boussinesq-type equations, NLSWE).

-A continuity equations for sediments (e.g. Exner equation)

-A transport equation for suspended sediment concentration, and one equation for bed load sediment flux.

Numerical modelling of sediment transport and morphodynamics

Bottom shear stress and turbulence in wave motion are the key parameters/processes that determine the mobilisation and entrainment of sediment particles in the flow.

Depth averaging and phase resolving models (focus on work carried out at the UoN).
Bed load only for now, example:

-Description of the boundary layer in NLSWE+Exner solvers

-Numerical modelling of the intra-wave sediment transport on sandy beaches using Non-hydrostatic NLSWE + Exner solvers (

$$\frac{\partial h}{\partial t} + \frac{\partial hU}{\partial x} = 0$$

$$\frac{\partial hU}{\partial t} + \frac{\partial \left(hU^2 + \frac{1}{2}gh^2\right)}{\partial x} = -gh\frac{\partial z_b}{\partial x} - \frac{\tau_b}{\rho}.$$

$$\frac{\partial z_b}{\partial t} + \xi\frac{\partial q_s}{\partial x} = 0,$$

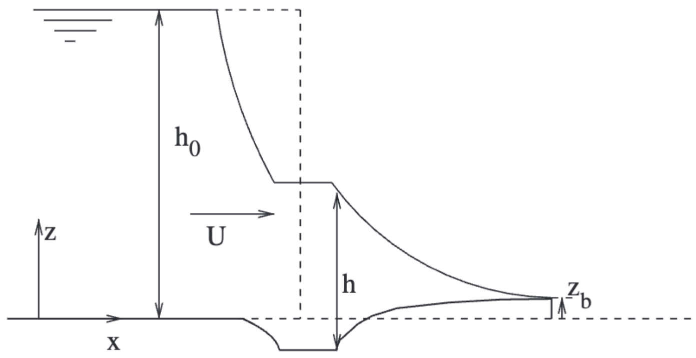

Part 1: Aims and objectives

To improve the numerical modelling of the bottom boundary layer in the swash zone:

OBJECTIVES

- Include the spatial gradient in the momentum integral model for the BBL
- Include this formulation in a specified time interval, method of characteristics (STI-MOC) solver of the NLSWE
- Validate the solver against experimental results (Kikkert et al., 2012)
- comparing the results with the original momentum integral model

Part 1: NLSWE and bottom boundary layer model

We used the NLSWE

$$\frac{\partial h}{\partial t} + h\frac{\partial u}{\partial x} + u\frac{\partial h}{\partial x} = 0$$

$$\frac{\partial u}{\partial t} + u\frac{\partial u}{\partial x} = -g\frac{\partial h}{\partial x} - g\frac{\partial B}{\partial x} - \frac{1}{\rho}\frac{\tau}{h}$$

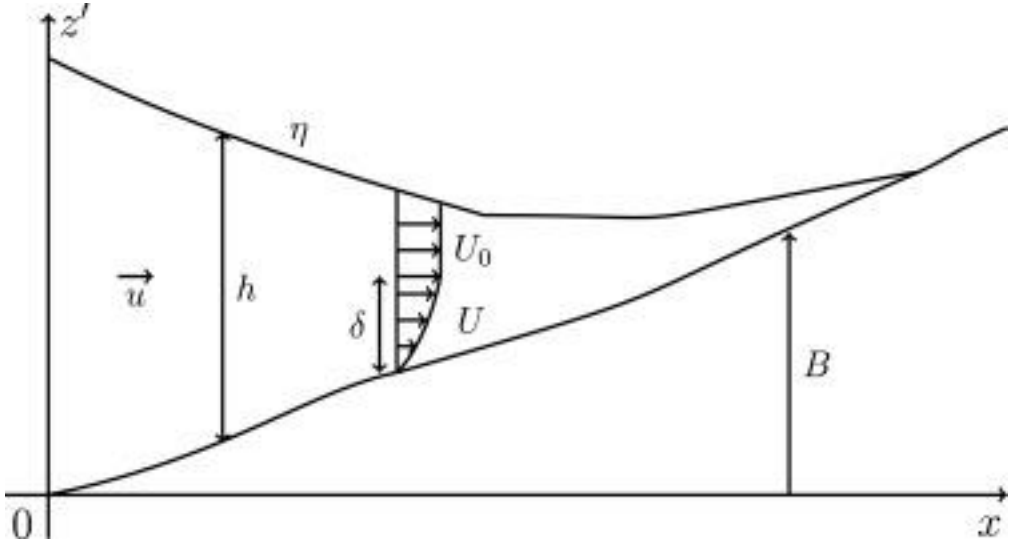

See the figure for symbols: note that u *i*s the depth averaged velocity U is the velocity in the bottom boundary layer, U_0 is the free stream (depth uniform) velocity.

We solve the NLSWE for h and u and the bottom boundary layer equation provides τ for the next step.

Zhu et al. (2022) solve the NLSWE using the STI MOC solve (SF)r of Zhu and Dodd, (2015)

Part 1: NLSWE and bottom boundary layer model

Why the bottom boundary layer (BBL) is so important in the swash zone?

Bed shear stress depends on the structure of the flow near the bottom, swash flows are very energetic near the tip, as many dam-break type flows, where intense sediment transport occurs (Spinewine and Capart, 2013).

The logarithmic structure of the BBL is used, however, this is not valid around flow reversal

Shear stress is highest at the tip, and in mid-flow reversal.

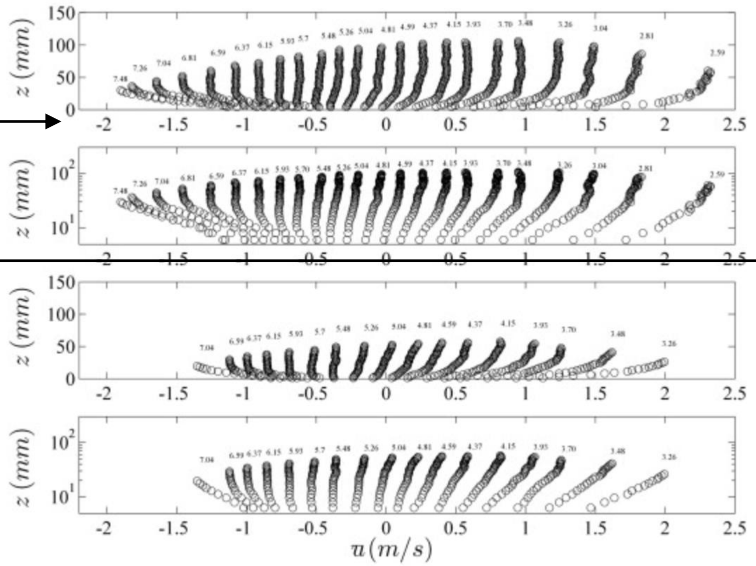

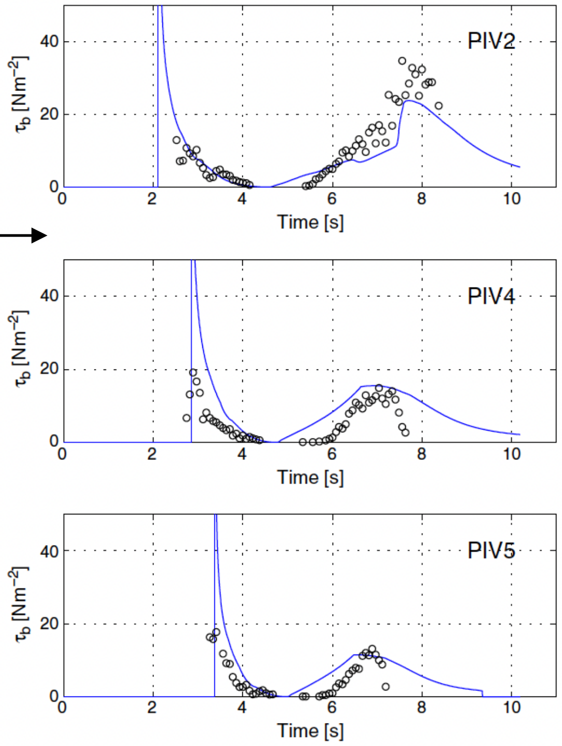

2DV solvers are capable of resolving the BBL, however they need suitable high resolution in proximity of the bed.

In 2DH we can use Chezy formulation or simplified BBL models.

References

Spinewine, B. and Capart, H., 2013. Intense bed-load due to a sudden dam-break. Journal of Fluid Mechanics, 731, pp.579-614.

Part 1: NLSWE and bottom boundary layer model

Relationship between the bed shear stress and bottom boundary layer

The horizontal velocity *u(x, z, t)* inside the boundary layer is approximated using the logarithmic law:

$$u(x, y, z, t) = \frac{U_f}{\kappa} \ln\left(\frac{z}{z_0}\right)$$

where U_f is the friction velocity, z the vertical coordinate, z_0 s the height at which the velocity is assumed to be zero, κ is the von Karman constant (=0.4).

$$U_f = \sqrt{\frac{\tau_b}{\rho}}$$

where τ_b is the bottom shear stress and ρ is the water density. Following the original momentum integral method (Fredsøe and Deigaard, 1993), U_f is determined by computing the integral:

$$-U_f = \int_{z_0}^{z_0+\delta} \frac{\partial}{\partial t}(U_0 - u(x, y, z, t))dz$$

where δ is the thickness of the boundary layer.

Reference:

Fredsøe, J., Deigaard, R., 1993. Mechanics of Coastal Sediment Transport. Vol. 3 of Advanced Series on Ocean Engineering. World Scientific, Singapore.

Modelling the bottom boundary layer

The solution of the equation

$$\frac{\partial U}{\partial t} + U\frac{\partial U}{\partial x} = -g\frac{\partial h}{\partial x} - g\frac{\partial B}{\partial x} + \frac{1}{\rho}\frac{\partial \tau}{\partial z}$$

Is simplified by transforming it in a PDE in Z:

$$Z = \frac{U_0}{U_f \kappa} = ln\left(\frac{z_0 + \delta}{z_0}\right)$$

In Zhu et al. (2022) the complete solution is derived and validated
We used Kikkert et al. (2012)

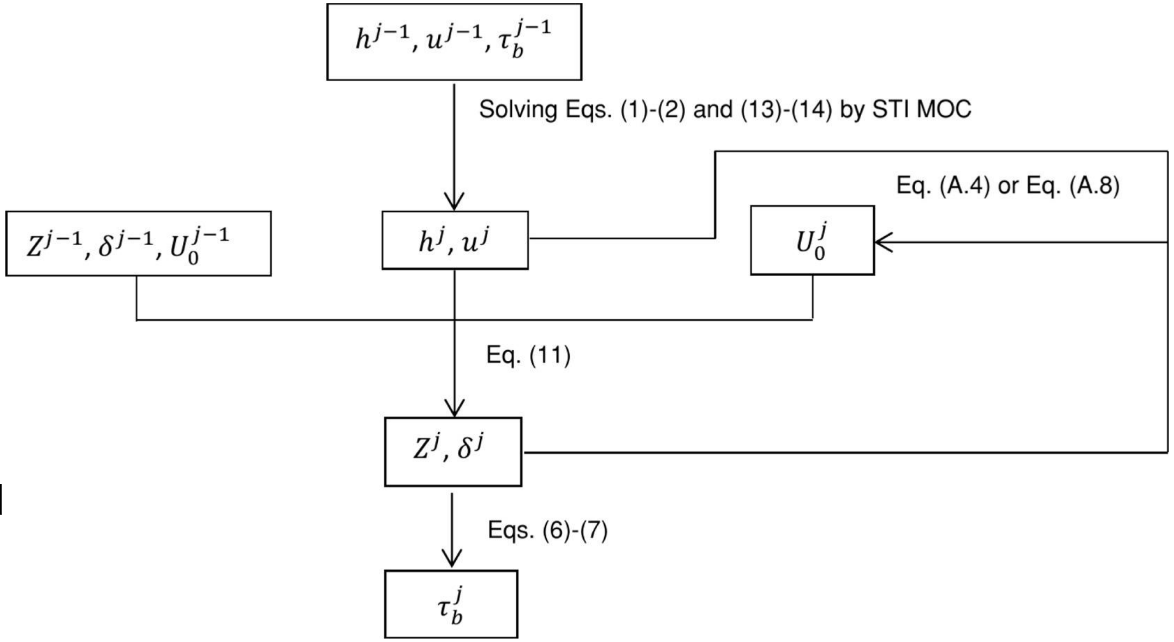

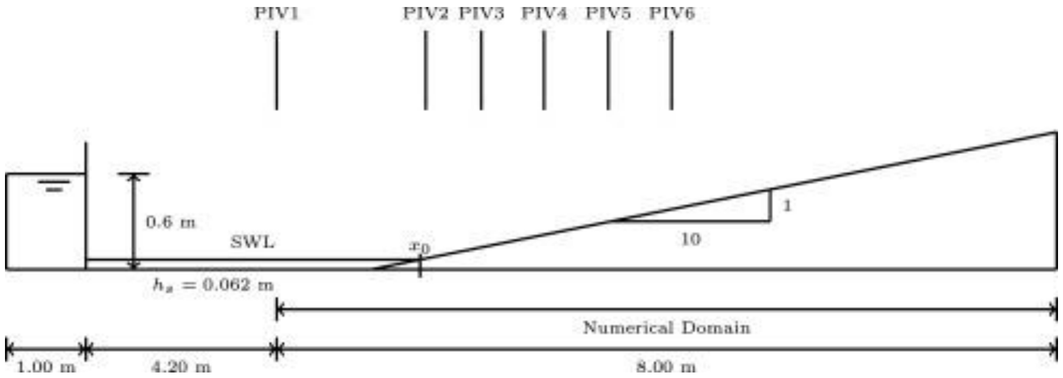

Modelling the bottom boundary layer

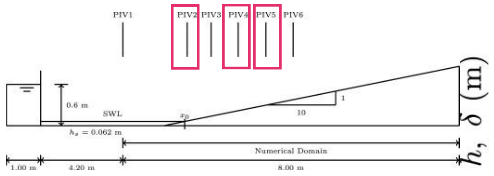

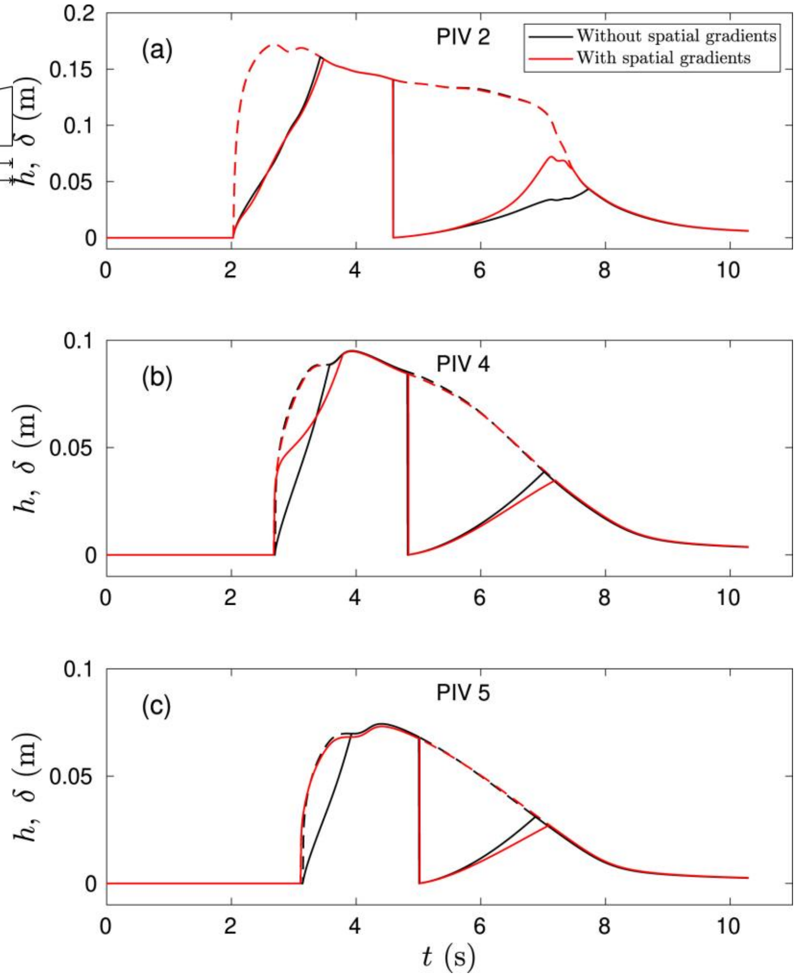

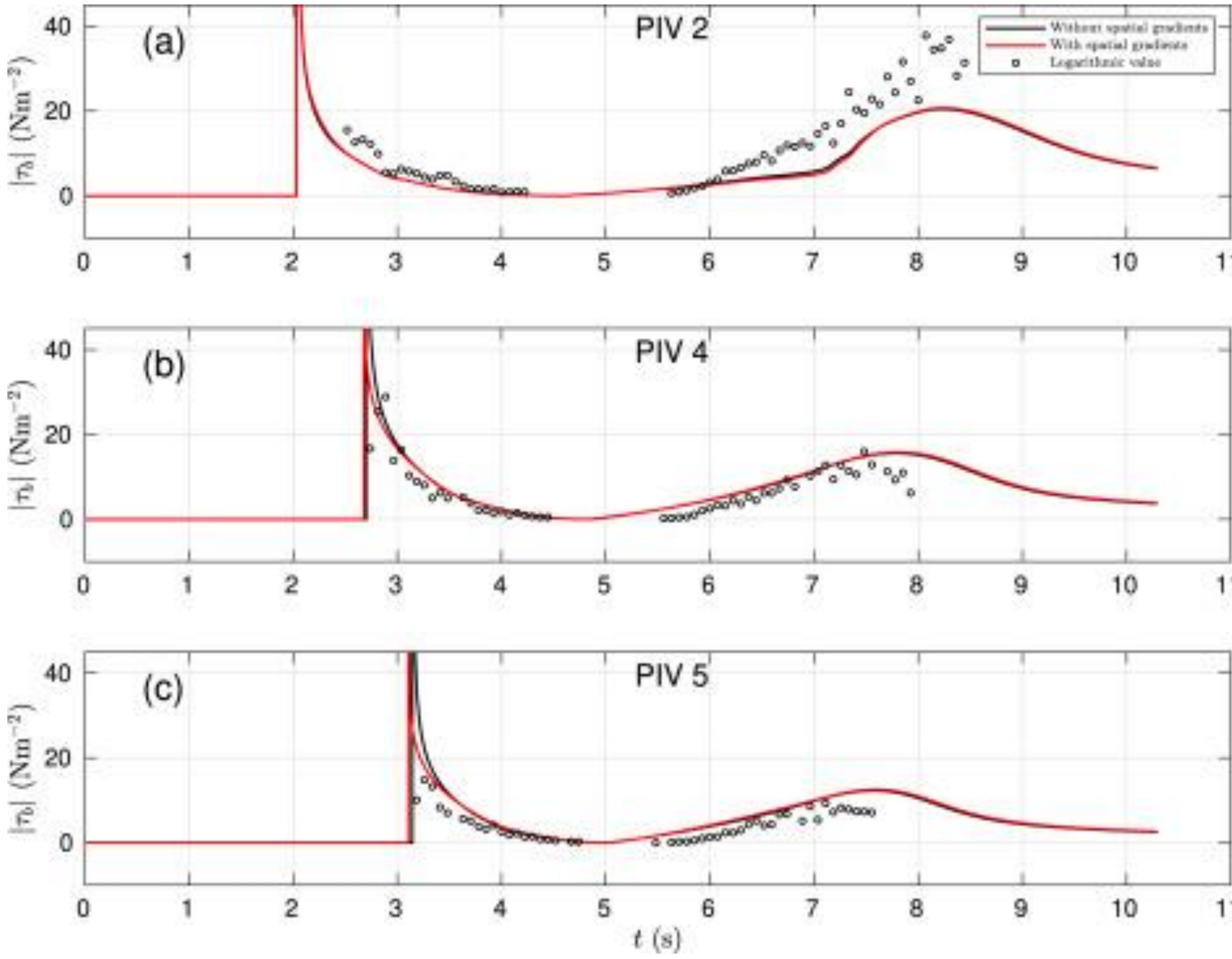

The model including spatial gradients predicts lower τ at bore arrival, unfortunately this is the region of higher uncertainty in the measurements of velocity from which τ is computed for the experiments.

Conclusions: part 1

☺ The inclusion of spatial gradients in the bottom boundary layer model is theoretically more appropriate for highly non-linear waves.

☹ The solution of the momentum integral becomes more complex, with singularity at flow reversal as in the version of the method without spatial gradients.

☺ Validation cases indicate an improvement in the accuracy of the flow description, in terms of RMSE

☹ Uncertainty in the measurement of flow velocity still limit our capability of choosing best modelling for the bed shear stress at the bore arrival (i.e. at the tip of the swash lens). We don't know how accurate is any method in that region.

Part 2: Non-hydrostatic XBeach

Few existing numerical models are able to resolve the complex morphodynamics in the swash zone, limiting their use in coastal engineering practice

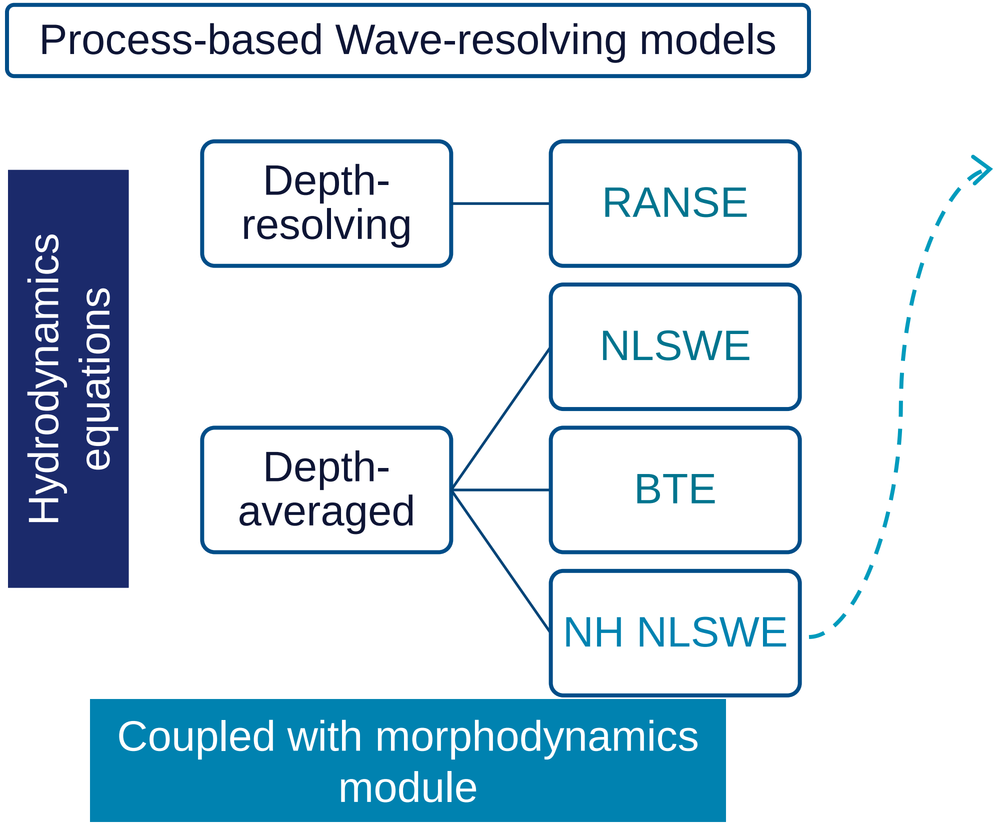

NON-HYDROSTATIC XBEACH (XBNH)

- wave-by-wave flow and surface elevation variations due to short wave
- intra-wave bed changes at time scales of storms

- morphodynamics response lacks an extended validation in the context of sandy beaches
- available formulations developed for the Wave Averaged Sediment Transport (XBNH-WAST)

- Inaccurate prediction of beach profile evolution under bichromatic wave groups related to inaccuracies in the modelled suspended sediment concentration (Ruffini et al., 2020)

Reference

Ruffini, G., Briganti, R., Alsina, J.M., Brocchini, M., Dodd, N. and McCall, R., 2020. Numerical modeling of flow and bed evolution of bichromatic wave groups on an intermediate beach using nonhydrostatic XBeach. Journal of Waterway, Port, Coastal, and Ocean Engineering, 146(1), p.04019034.

Part 2: Aims and objectives

To improve the numerical modelling of the intra-wave sediment transport on sandy beaches using a depth-averaged wave-resolving framework by:

OBJECTIVES

- improving a depth-averaged non-hydrostatic, wave-resolving framework (e.g., the open-source Non-hydrostatic XBeach) to represent the complexity of the swash zone and its mutual feedback with the surf zone
- verifying the performance and robustness of the developed model against semi-analytical solutions and experimental studies
- modelling relevant engineering scenarios by simulating laboratory experiments involving representative wave conditions in order to compare numerical results with measurements
- comparing the morphodynamic response of the improved model with the available sediment transport formulations in the selected framework

Methodology

- Two subroutines for the **Intra-Wave Sediment Transport** (**XBNH-IWST**) including the effects of wave breaking-induced turbulence were newly developed

XBNH-IWST

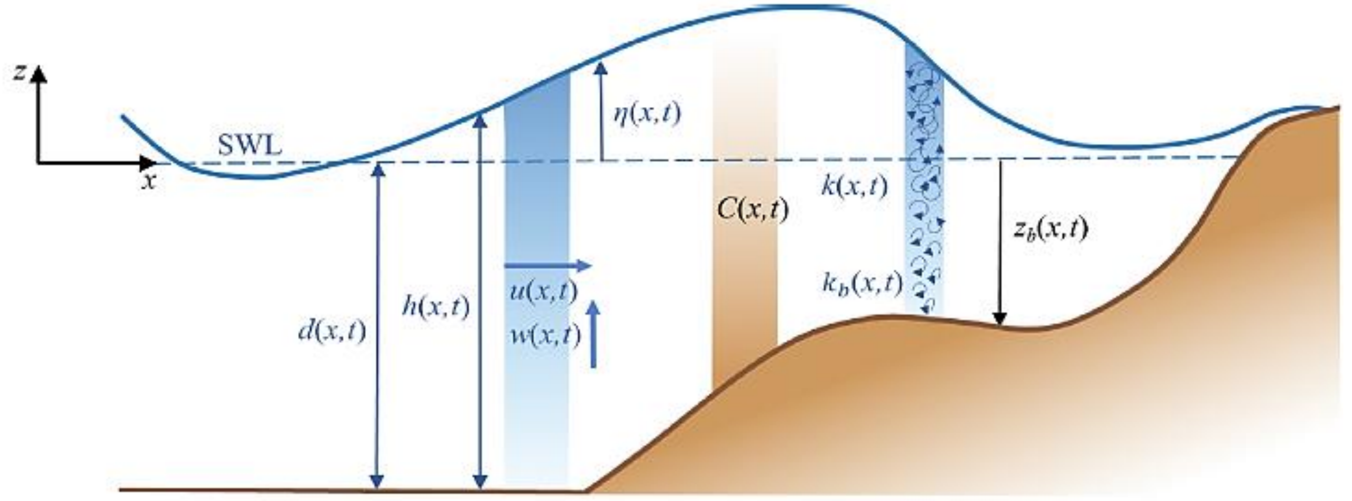

Hydrodynamics:

1DH – Non-hydrostatic Non Linear Shallow Water Equations
+ additional models for horizontal viscosity for the Hydrostatic Front Approximation (HFA) for wave-breaking

Sediment transport:

Pritchard and Hogg (2003) (suspended load)
Meyer-Peter Muller (1948) (bed load)

+ Wave breaking-induced turbulence model based on a depth-averaged Turbulent Kinetic Energy (TKE) balance equation

Bed-updating:

Exner-type equation

Notation	
x, z	Cross-shore and vertical coordinates
t	Time
η	Water surface elevation
h, d	Total and still water depth
d_z	Distance from the bed level, z_b
u, w	Depth-averaged horizontal and vertical velocities
C	Depth-averaged suspended sediment concentration
k, k_b	Depth-averaged TKE and near-bed TKE

Reference
Mancini, G., Briganti, R., McCall, R., Dodd, N. and Zhu, F., 2021. Numerical modelling of intra-wave sediment transport on sandy beaches using a non-hydrostatic, wave-resolving model. Ocean Dynamics, 71(1), pp.1-20.

Methodology

Hydrodynamics:

$$\frac{\partial h}{\partial t} + h\frac{\partial u}{\partial x} + u\frac{\partial h}{\partial x} = 0$$

$$\frac{\partial u}{\partial t} + u\frac{\partial u}{\partial x} - \frac{\partial}{\partial x}\left(\upsilon_h \frac{\partial u}{\partial x}\right) = -\frac{1}{\rho}\left(\frac{\partial(\rho p_{nh} + \rho g \eta)}{\partial x}\right) - \frac{1}{\rho}\frac{\tau_b}{h}$$

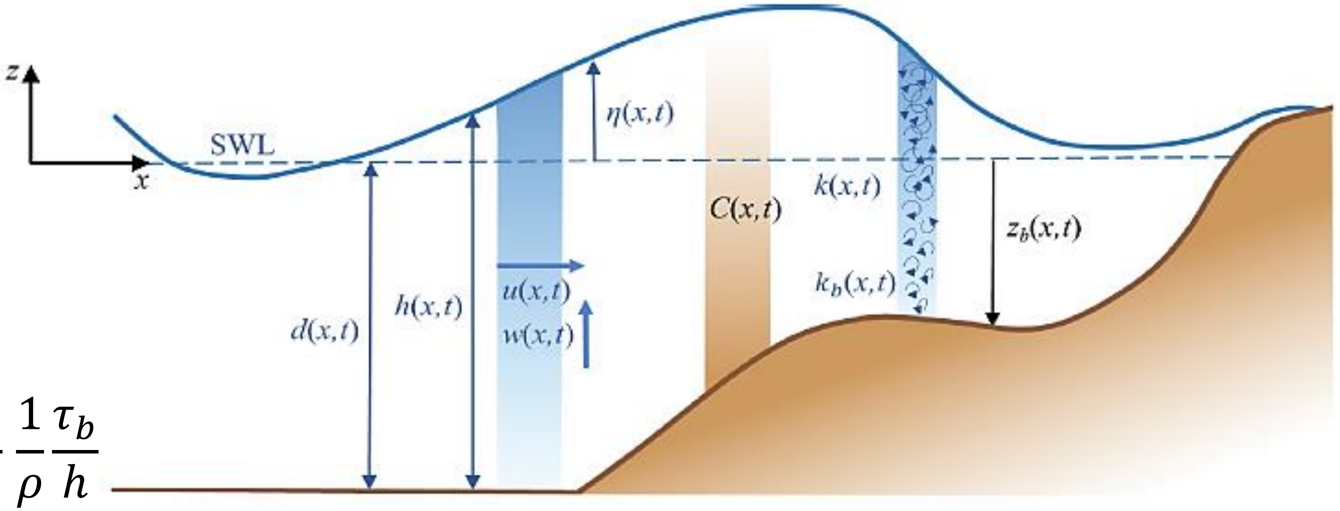

p_{nh} is the dynamic pressure. The solver allows multiple layers of fluid. Here only one is used. Note slight change in symbols for consistency with XBeach literature

Bed-updating:

Exner-type equation

$$(1 - n_b)\frac{\partial z_b}{\partial t} + E - D + \frac{\partial q_b}{\partial x} = 0$$

q_b is the bed load sediment flux, $E - D$ is the difference between erosion and deposition terms, E and D respectively

Notation	
x, z	Cross-shore and vertical coordinates
t	Time
η	Water surface elevation
h, d	Total and still water depth
d_z	Distance from the bed level, z_b
u, w	Depth-averaged horizontal and vertical velocities
C	Depth-averaged suspended sediment concentration
k, k_b	Depth-averaged TKE and near-bed TKE

Methodology

XB NH-IWST morphodynamics modelling:

- Pritchard and Hogg (2003) transport equation:

$$\frac{\partial hC}{\partial t}+\frac{\partial\left[\left(huC+D_C h\frac{\partial C}{\partial x}\right)S_{sl}\right]}{\partial x}=m_e\left(\frac{\tau_b-\tau_{cr}}{\tau_{ref}}\right)^R-w_s C_{nb}=\mathrm{E}-\mathrm{D}$$

Mobility parameter which determines the erodibility of the sediment as suspended load

$$C_{nb}=CK_C,\quad K_C\geq 1$$ Shape factor depending on flow and sediment properties

- Meyer-Peter Muller (1948) formulation for bed load transport

- Exner-type equation for bed-updating

+TKE effects included through bed shear stress modelling

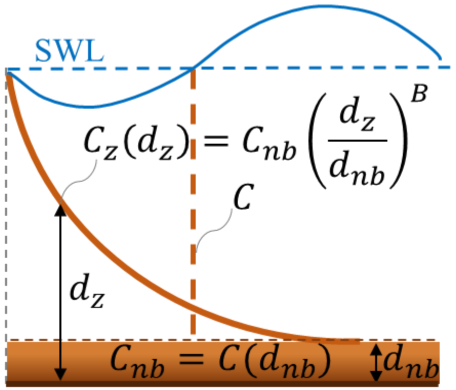

C = model output
C_z = computed in the aftermath of numerical simulations

Notation	
B	Rouse number
C	Depth-averaged suspended sediment concentration
C_{nb}	Near-bed csediment oncentration
C_z	Parametric distribution of suspended sediment concentration
D_C	Diffusion coefficient
D_{50}	Median grain diameter
$R>0$	Numerical exponent
S_{sl}	Bed slope effects coefficient
τ_b	Bed shear stress
τ_{ref}	Reference bed shear stress
τ_{cr}	Critical bed shear stress

Methodology

XB NH-IWST wave breaking-induced turbulence modelling:

- Turbulent Kinetic Energy (TKE) balance equation:

$$\frac{\partial hk}{\partial t} + \frac{\partial huk}{\partial x} = Source_k - Sink_k$$

  - **R13 turbulence model:** based on the roller surface model for the wave energy dissipation used in Reniers et al. (2013)
  - **KW92-A09 turbulence model:** based on the time-varying wave energy model of Kobayashi and Wurjanto (1992) and Alsina et al. (2009) study (**used for XBNH-IWST validation**)

- near-bed TKE model:

$$k_b = k\left[min\left(\frac{1}{exp(\frac{h}{l_m}) - 1}, 1\right)\right]$$

Included in bed shear stress modelling

Results

XBNH-IWST sediment transport model verification

- with the of Zhu and Dodd (2015) high-accuracy STI-MOC solution for a solitary wave over an erodible sloped bed

XBNH-IWST turbulence model verification

- with the Ting and Kirby (1994) laboratory experiments for plunging and spilling breakers over a fixed bed

XBNH-IWST validation

- with the Alsina et al. (2016) laboratory experiments
- with the Young et al. (2010) laboratory experiments

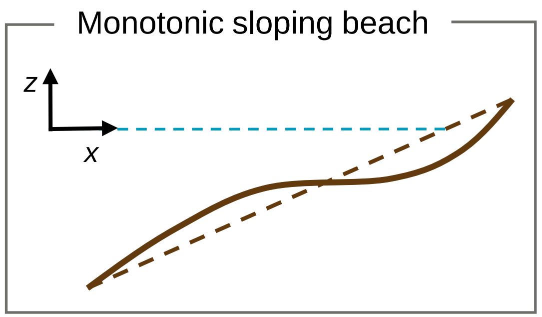

- with the Van der Zanden et al. (2017) experiments

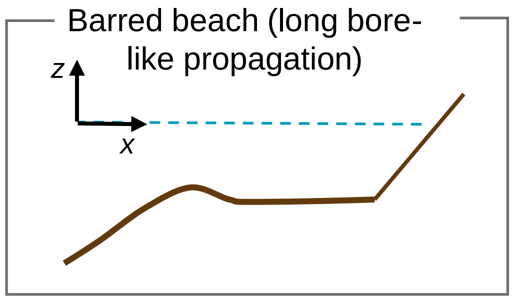

References
Young, Y.L., Xiao, H. and Maddux, T., 2010. Hydro-and morpho-dynamic modeling of breaking solitary waves over a fine sand beach. Part I: Experimental study. Marine Geology, 269(3-4), pp.107-118.
Ting, F.C. and Kirby, J.T., 1994. Observation of undertow and turbulence in a laboratory surf zone. Coastal Engineering, 24(1-2), pp.51-80.
van Der Zanden, J., Hurther, D., Cáceres, I., O’donoghue, T. and Ribberink, J.S., 2017. Suspended sediment transport around a large-scale laboratory breaker bar. Coastal engineering, 125, pp.51-69.

Results: model verification

XBNH-IWST sediment transport model verification

- with the of Zhu and Dodd (2015) high-accuracy numerical solution for a solitary wave over an erodible sloped bed:
  - Model parameters set up like Zhu and Dodd (2015) + well-mixing, dynamic pressure off
  - Same sediment transport formulations used in the two models

Final bed levels and changes

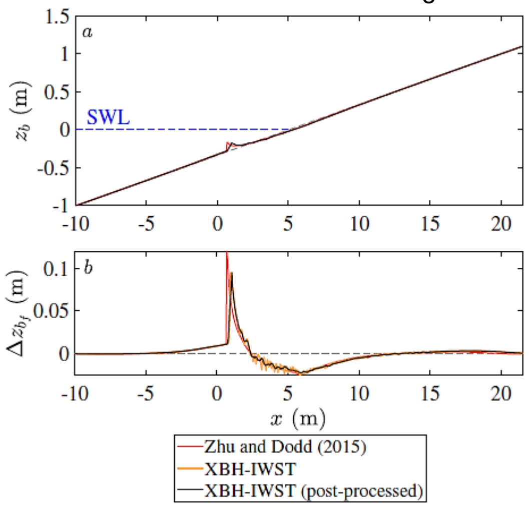

Time series of sediment concentration

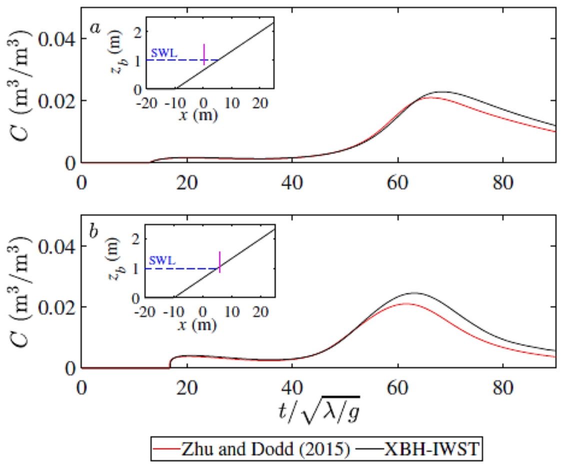

Verification indicated that the Pritchard and Hogg (2003) transport equation performs qualitatively and quantitatively well when compared with a high-accuracy numerical solution of NLSWE

XBNH-IWST wave breaking TKE model verification

- with the Ting and Kirby (1994) laboratory experiments for plunging and spilling breakers over a fixed bed:
  - Sensitivity analysis and calibration of TKE model
  - Verification of additional horizontal viscosity models for HFA (i.e., wave-breaking)

Time varying phase-averaged quantities in the inner surf zone

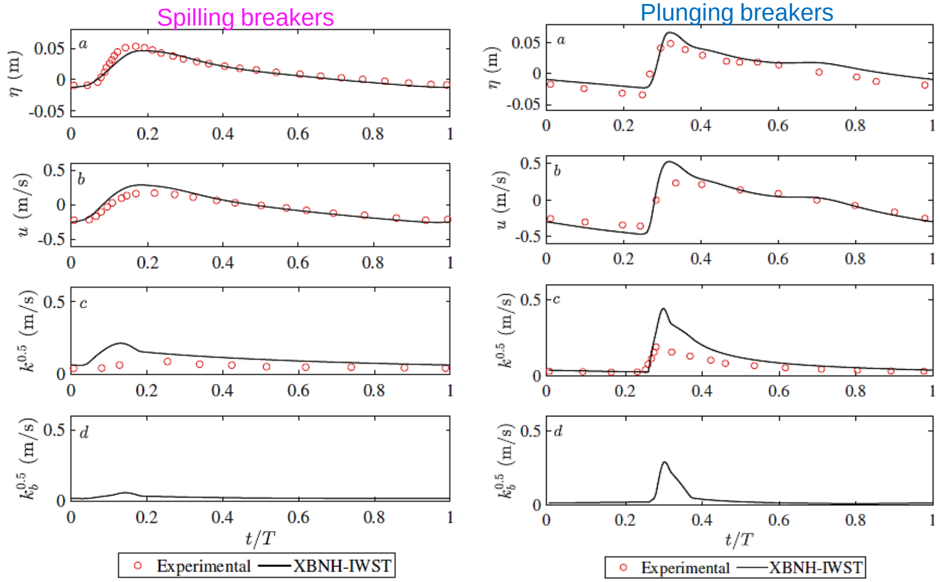

The accuracy in the prediction of *k* is higher for the plunging breakers, for which *k* was observed to vary over the water depth less than for the spilling breakers in the experiments

Results: model validation

- Numerical simulations of the Young et al. (2010) laboratory experiments:

  - Consecutive, non-interacting solitary waves over a sandy sloped beach
  - Initial bed: result of previous runs on the nominal 1:15 sloped bed level, hence near-equilibrium profile beach state
  - To be consistent with experiments, reflection due to the finite size of the flume was was taken into account in the numerical simulations

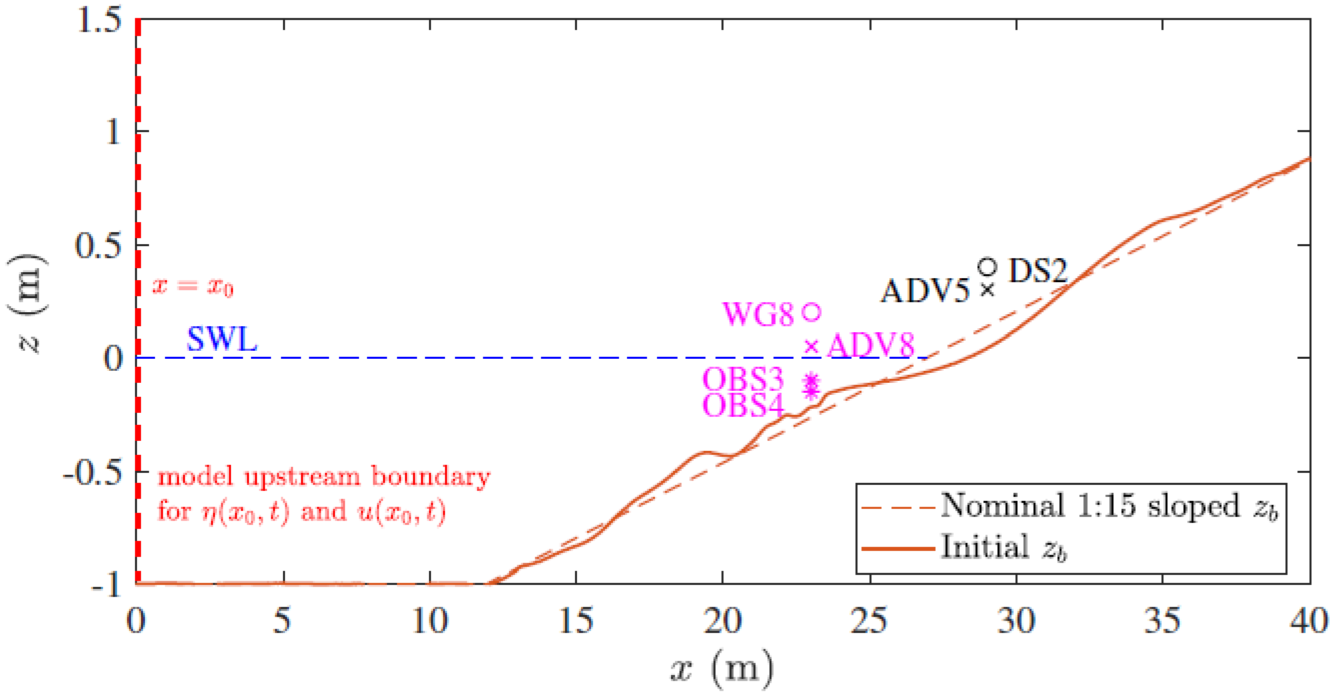

Results: model validation

Time series of flow and sediment transport quantities

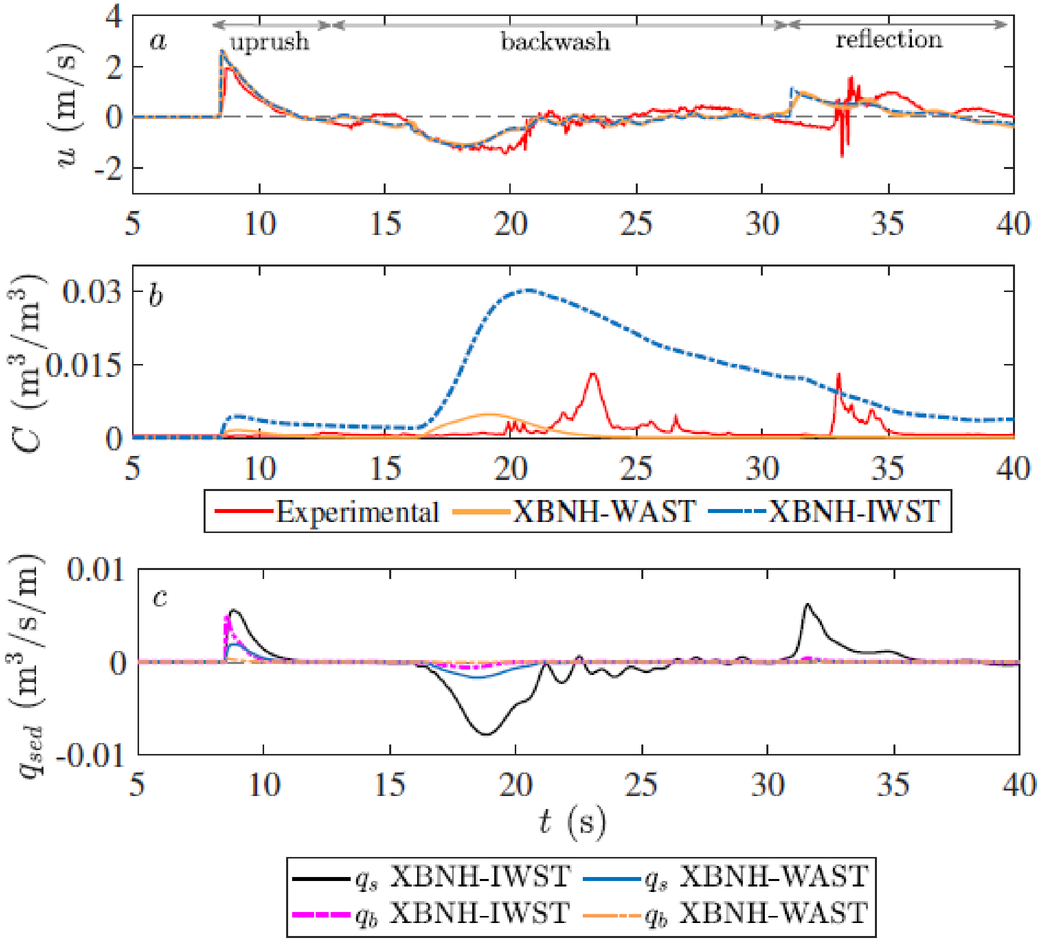

Final bed levels and changes after 3 waves

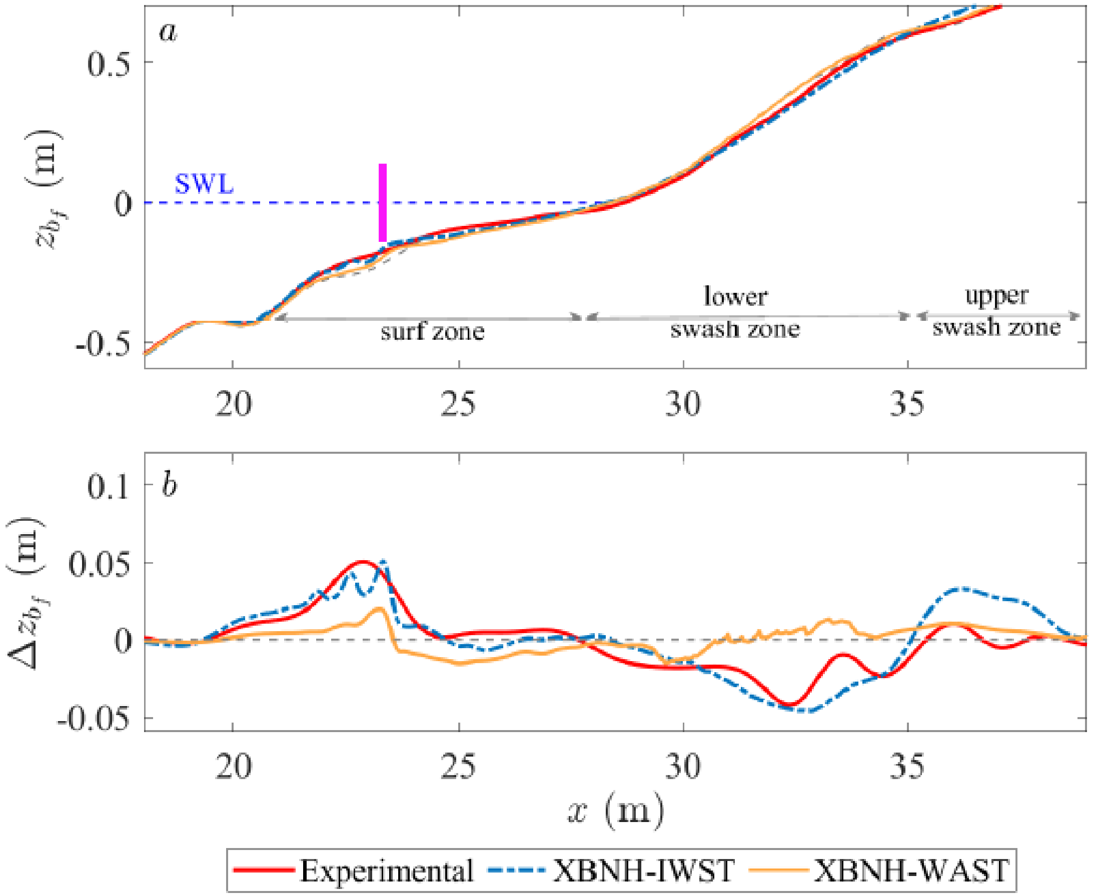

As for the Alsina et al. (2016) case, XBNH-IWST overestimates *C* at the backwash but it can reproduce the suspension close to flow reversal unlike XBNH-WAST

nRMSE (XBNH-IWST) < nRMSE (XBNH-WAST) by 35%
RMSTE (XBNH-IWST) < RMSTE (XBNH-WAST) by 84%

Results: model validation

- Numerical simulations of the Van der Zanden et al. (2016) laboratory experiments:

  - Regular plunging breakers (first order wave theory) over a barred beach (long-bore like propagation over the shelf extending shoreward of the breaker bar trough)
  - Detailed mesurements of velocity and TKE, including near-bed TKE
  - Assessment of XBNH-IWST modelling of wave breaking-generated TKE and its morphodynamics response in the surf zone

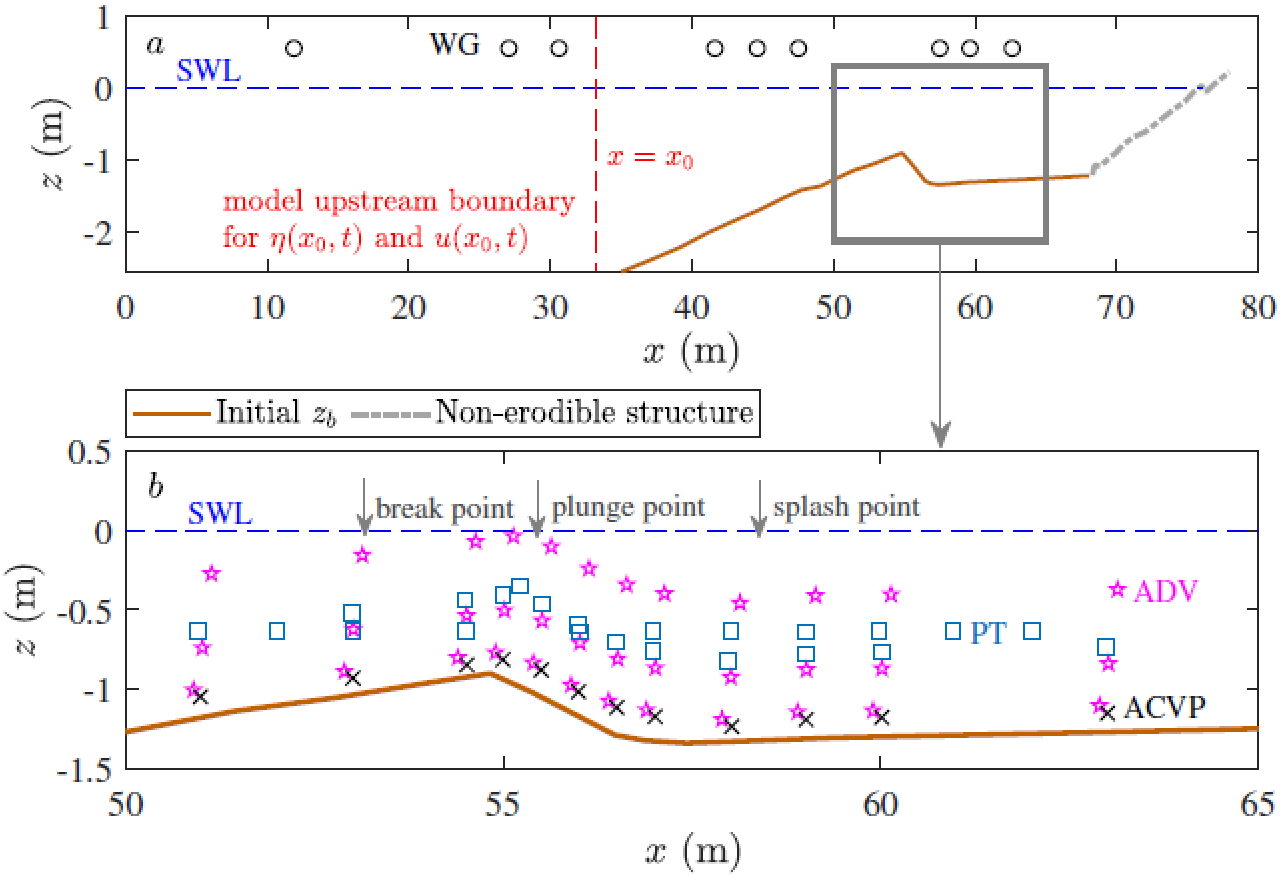

The experiments consisted of 6 runs of 15 mins each. The bed profile was measured prior to the first run and after every 30 mins

Conclusions: part 2

☺ XBNH-IWST improves the prediction of suspended sediment concentration close to flow reversal, and in turn, of swash morphodynamics compared to XBNH-WAST

☹ However, the prediction of suspended sediment concentration with XBNH-IWST is not accurate, especially at the backwash stage of the flow, and breakers bar development is not properly captured

☺ For monotonic sloping beaches XBNH-IWST performs better when the initial bed level is closer to the morphodynamic equilibrium (i.e., the bed has already evolved) than for an initial uniform sloped bed

☹ Results for Van der Zanden et al. (2016) case show that XBNH-IWST does not properly obtain the experimental spatial gradient of the flow velocity in the surf zone, and therefore, the observed bar evolution

References

Briganti, R., Dodd, N., Pokrajac, D. and O'Donoghue, T., 2011. Non linear shallow water modelling of bore-driven swash: Description of the bottom boundary layer. *Coastal Engineering*, *58*(6), pp.463-477.

Zhu, F. and Dodd, N., 2015. The morphodynamics of a swash event on an erodible beach. *Journal of Fluid Mechanics*, *762*, pp.110-140.

Ruffini, G., Briganti, R., Alsina, J.M., Brocchini, M., Dodd, N. and McCall, R., 2020. Numerical modeling of flow and bed evolution of bichromatic wave groups on an intermediate beach using nonhydrostatic XBeach. Journal of Waterway, Port, Coastal, and Ocean Engineering, 146(1), p.04019034.

Mancini, G., Briganti, R., McCall, R., Dodd, N. and Zhu, F., 2021. Numerical modelling of intra-wave sediment transport on sandy beaches using a non-hydrostatic, wave-resolving model. *Ocean Dynamics*, *71*(1), pp.1-20.

Zhu, F., Dodd, N., Briganti, R., Larson, M. and Zhang, J., 2022. A logarithmic bottom boundary layer model for the unsteady and non-uniform swash flow. *Coastal Engineering*, *172*, p.104048.

Thank you for your attention!

“Modelling eddies and coherent structures in the coastal area.” (M. Postacchini, UNIVPM)

Marie Skłodowska-Curie Actions

SEDIMARE

Sediment Transport and Morphodynamics in Marine and Coastal Waters with Engineering Solutions

MODELLING EDDIES AND COHERENT STRUCTURES IN THE COASTAL AREA

_THE ROLE OF MACRO-VORTICES

Matteo Postacchini

Department of Civil and Building Engineering, and Architecture

UNIVERSITÀ POLITECNICA DELLE MARCHE (Ancona)

DEFINITIONS

- **EDDY**
  - *"A current of water or air running contrary to the main current (especially, a circular current: whirlpool)"* (Merriam-Webster)
- **COHERENT STRUCTURE**
  - *"A coherent structure is a connected turbulent fluid mass with instantaneously phase-correlated vorticity over its spatial extent"* (Hussain, *J.FluidMech.*1986)

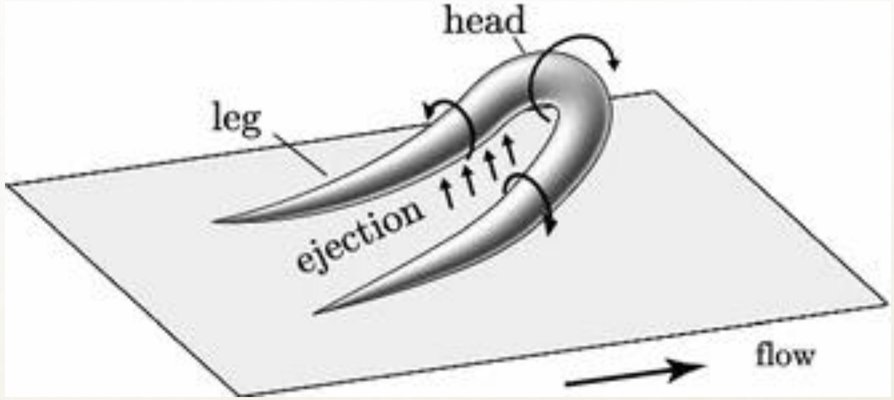

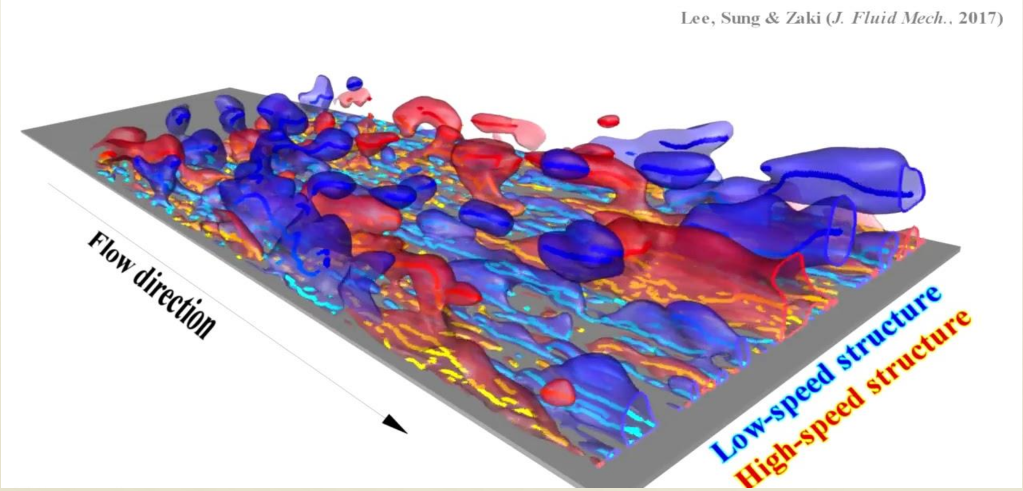

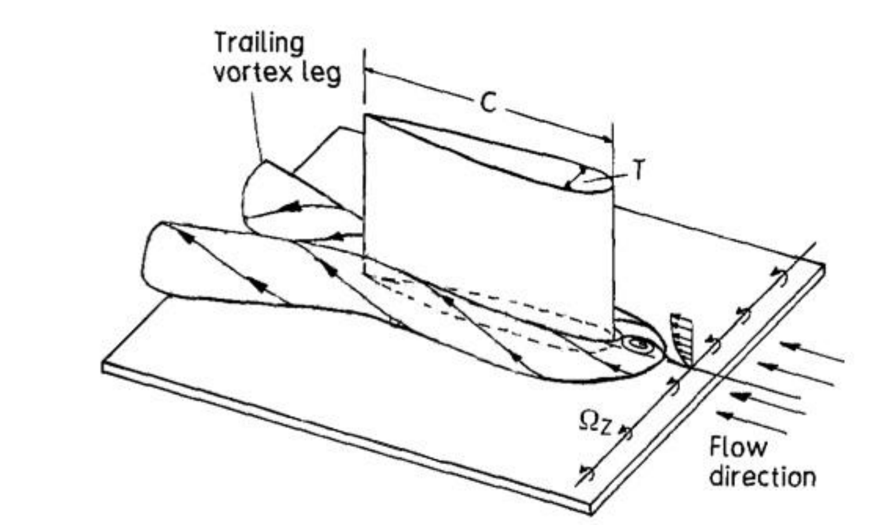

MATTEO POSTACCHINI
UNIVERSITÀ POLITECNICA DELLE MARCHE (Ancona)

WHY STUDYING EDDIES?
WHAT IS THEIR ROLE IN THE COASTAL REGION?

- Wave propagation in the nearshore
  - ➢ generation of short-crested waves
    - breaking → edge (vertical) vortices
    - rip currents
  - ➢ interaction with submerged structures (e.g. pipelines)
    - generation of horizontal vorticity
  - ➢ interaction with emerged structures (e.g. vertical cylinders)
    - generation of complex vorticity patterns

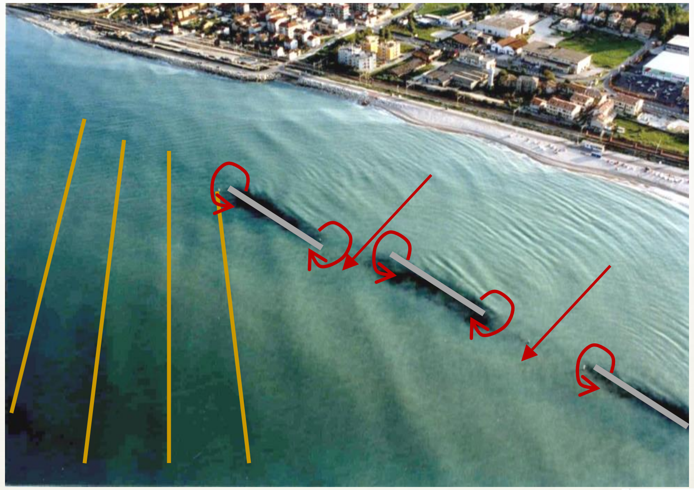

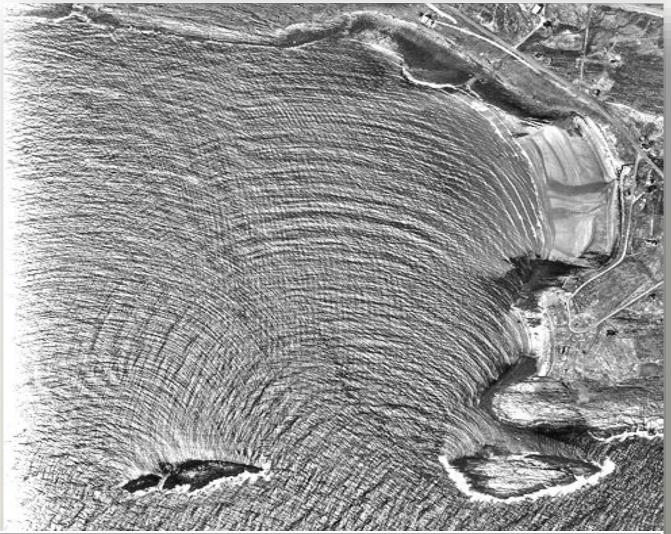

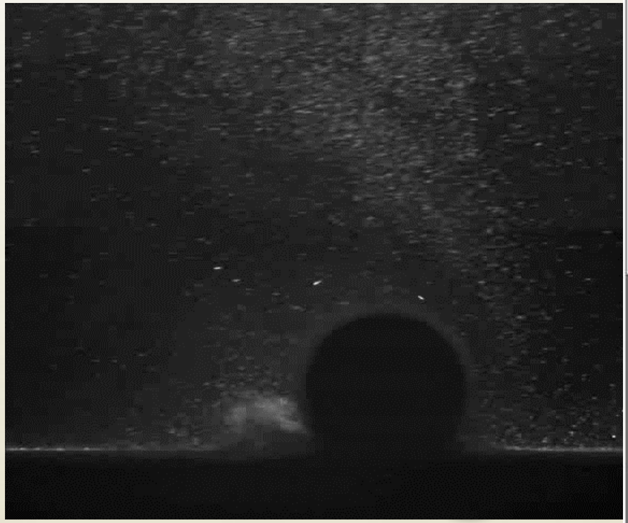

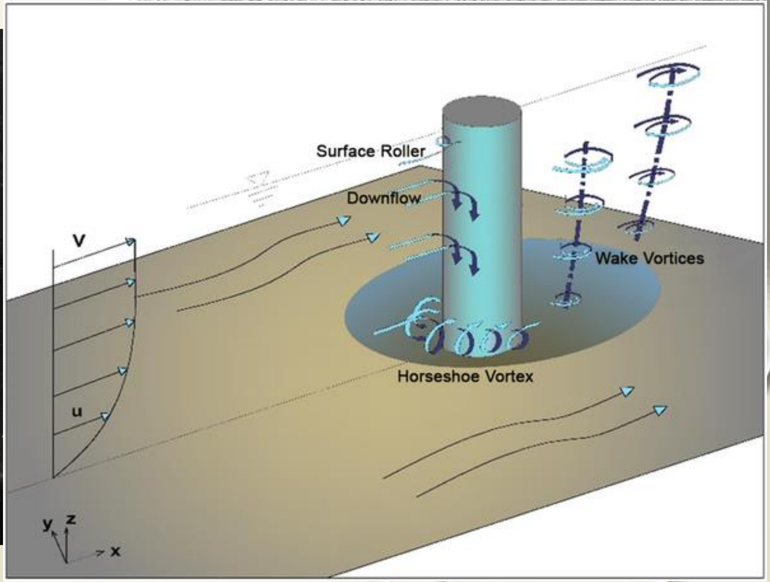

MATTEO POSTACCHINI
UNIVERSITÀ POLITECNICA DELLE MARCHE (Ancona)

WHY STUDYING EDDIES?
WHAT IS THEIR ROLE IN THE COASTAL REGION?

- Among the main issues
  - coastal erosion
  - scour
  - structure stability
  - coastal safety

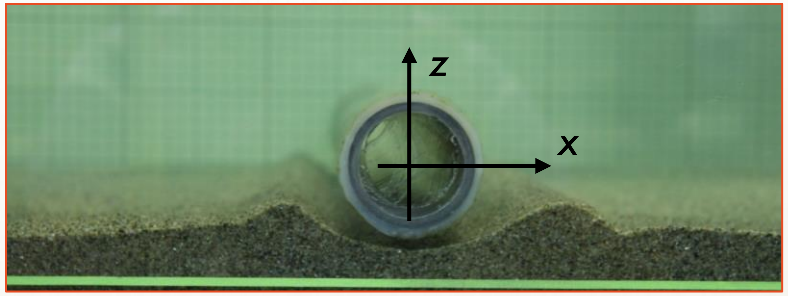

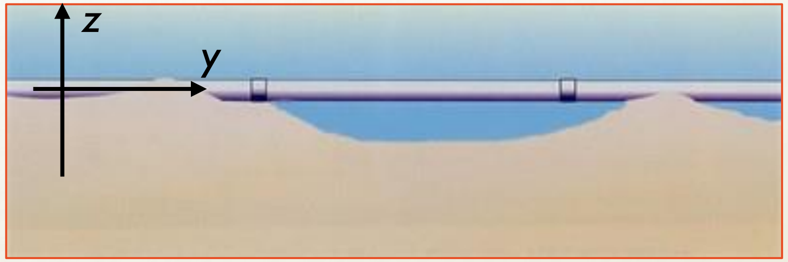

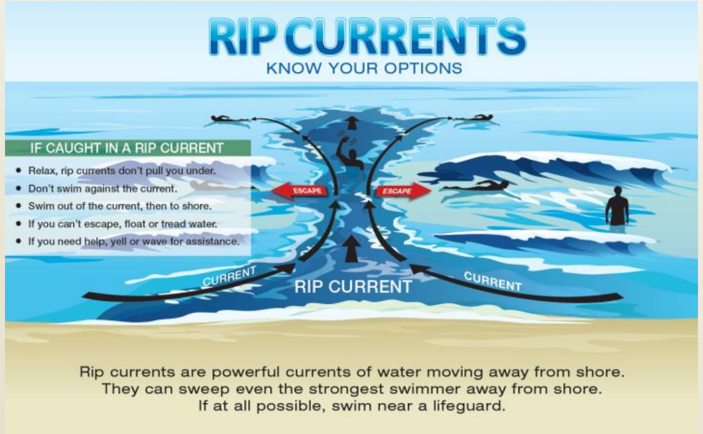

August 2013,
Haeundae Beach (South Korea)

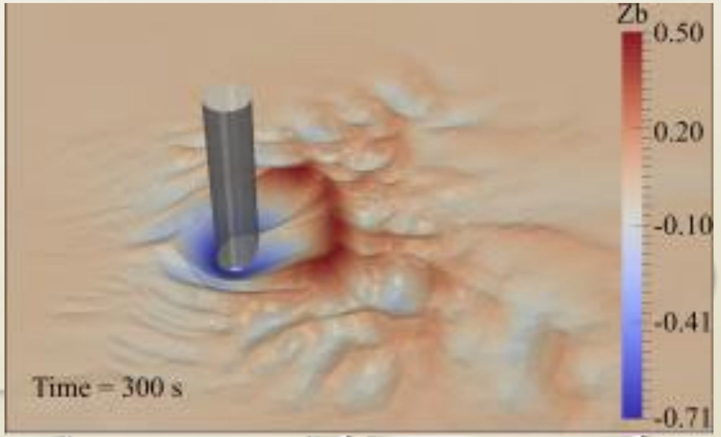

MATTEO POSTACCHINI
UNIVERSITÀ POLITECNICA DELLE MARCHE (Ancona)

(ALMOST) HORIZONTAL VORTICITY

_non-breaking waves over a rectangular structure

Lab experiments

- wave flume (30x0.6x0.9)m^3
- cnoidal waves over a vertical barrier
  - structure: D=(6-12)cm
  - water level: h=24cm
  - waves: T=2s, H/h=0.05-0.25
- PIV measurements

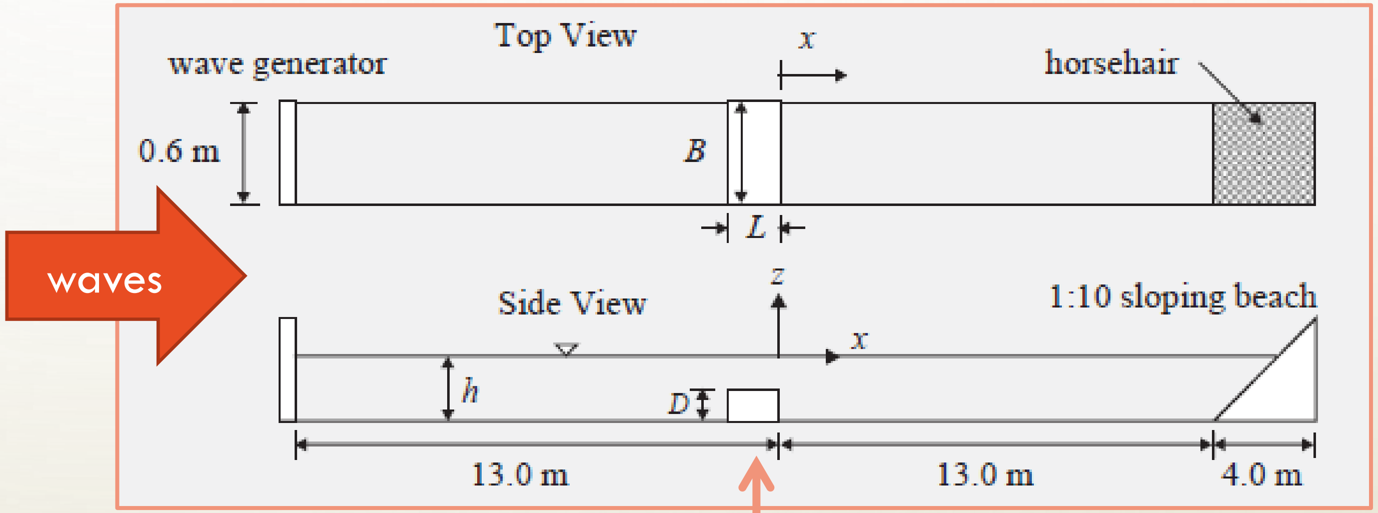

Adapted from Chang *et al.* (*Coast. Eng.*, 2005)

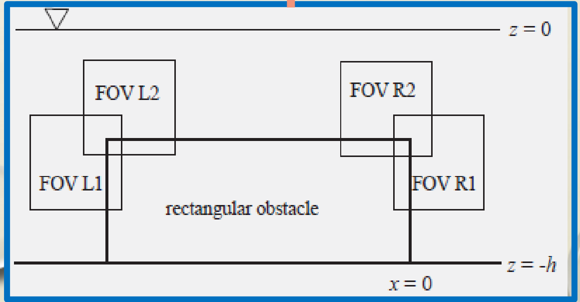

MATTEO POSTACCHINI
UNIVERSITÀ POLITECNICA DELLE MARCHE (Ancona)

(ALMOST) HORIZONTAL VORTICITY

_non-breaking waves over a rectangular structure

Adapted from *Chang et al.* (*Coast. Eng.*, 2005)

Findings at the weather side

- little anti-clockwise vortex ***(phase a)***
- generation of clockwise vortex reaching its maximum vorticity during wave crest ***(phase f)***
- split of clockwise vortex into two vortices ***(phase h)***

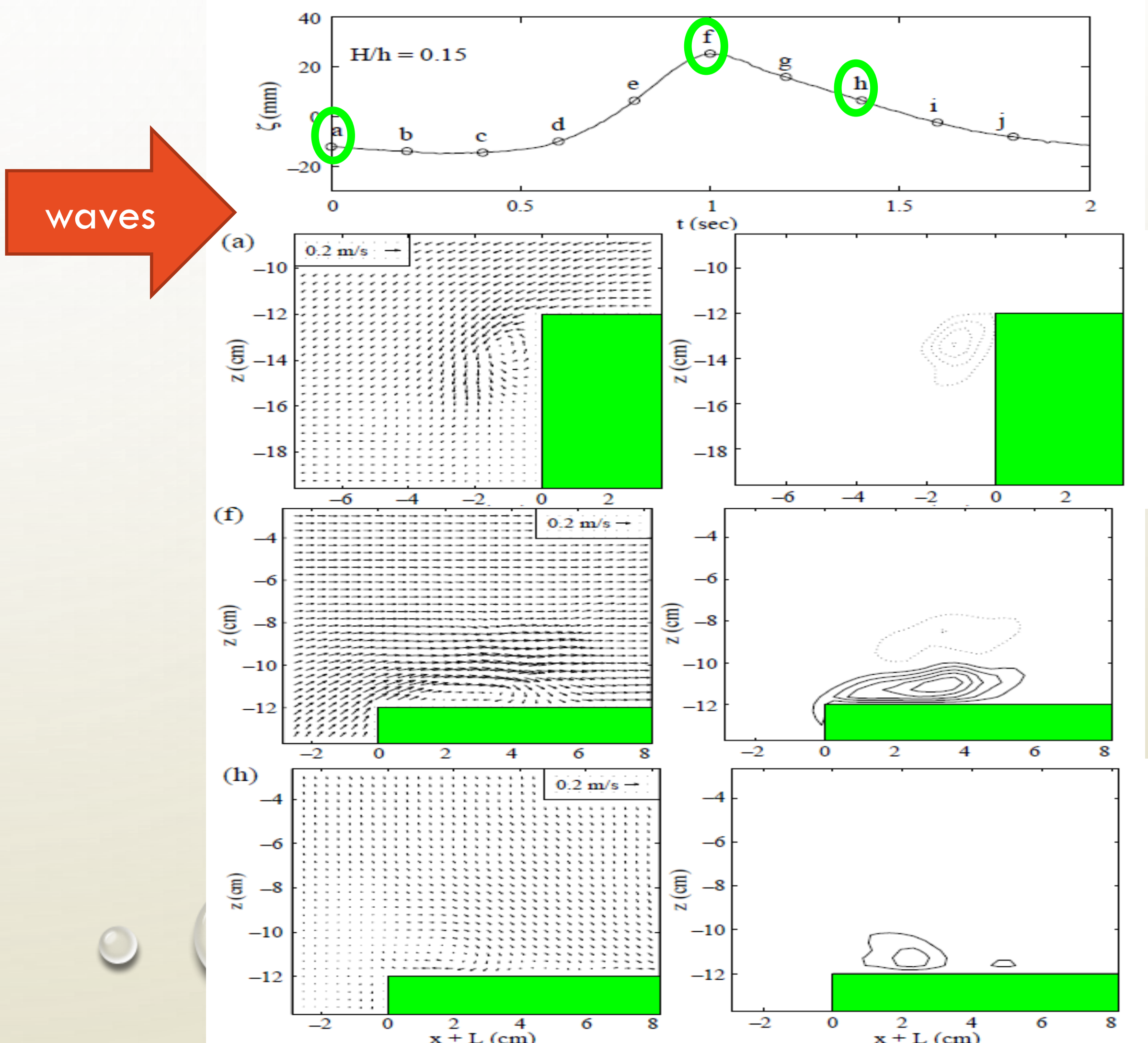

MATTEO POSTACCHINI
UNIVERSITÀ POLITECNICA DELLE MARCHE (Ancona)

(ALMOST) HORIZONTAL VORTICITY

_non-breaking waves over a rectangular structure

Adapted from *Chang et al. (Coast. Eng., 2005)*

Findings at the lee side

- anti-clockwise vortex above the obstacle ***(phase a)***
- flow separation/jet-like flow around the top corner, forming a clockwise vortex, then convected along x ***(phase f)***
    - vortex motion limited to nearby area
    - jet-like flow pattern not clearly observed at the weather side
- anti-clockwise vortex generated at the top corner and upward motion of clockwise vortex ***(phase j)***
- vortices last much longer in the case of <u>solitary waves</u>

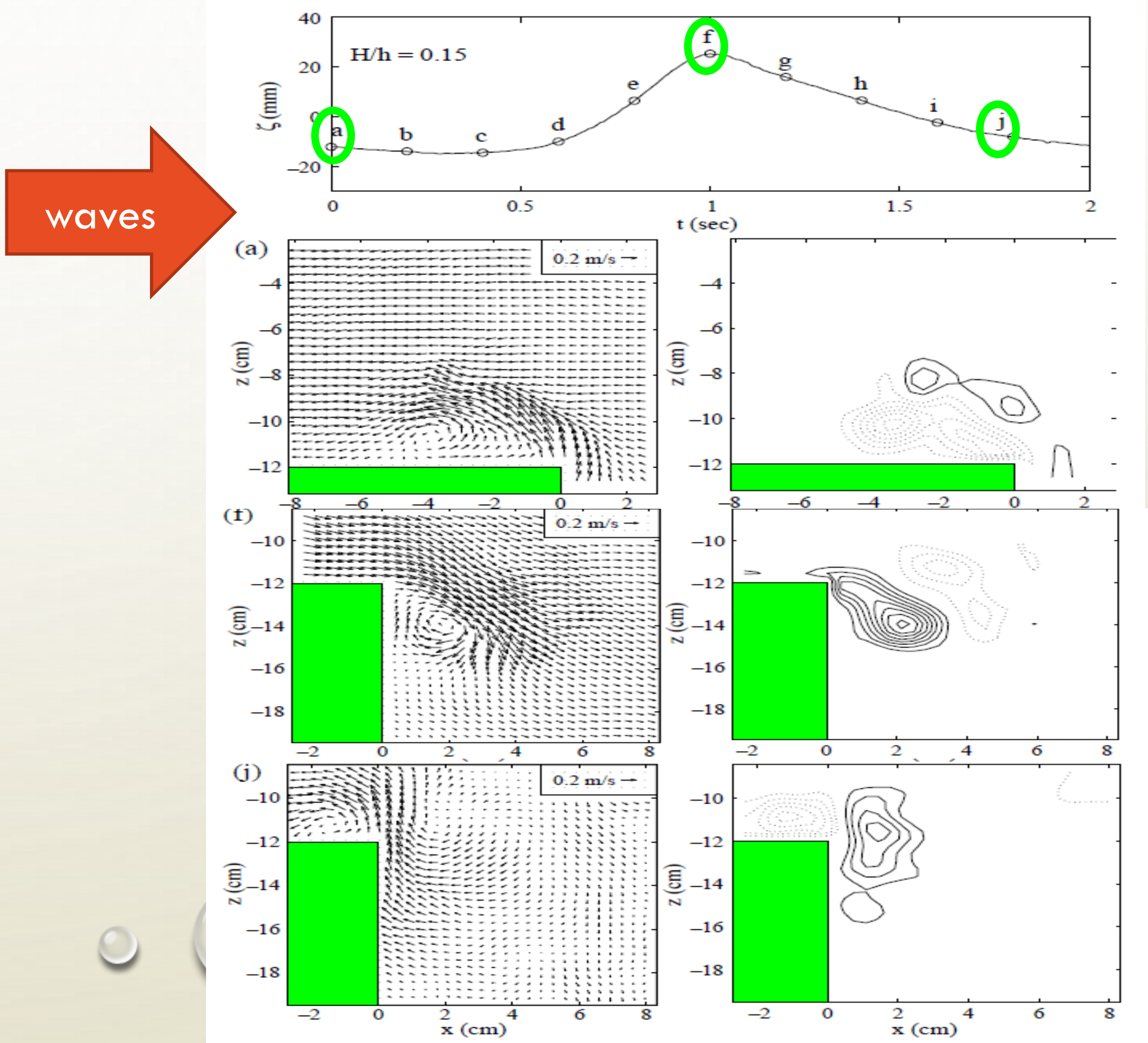

(ALMOST) HORIZONTAL VORTICITY

_breaking waves over a rectangular structure

Lab experiments

- wave flume $(22x0.5x0.76)m^3$
- solitary waves over a vertical barrier
  - h=14cm, H/h=0.5
- PIV measurements

Adapted from *Wu et al.* (*Coast. Eng.*, 2012)

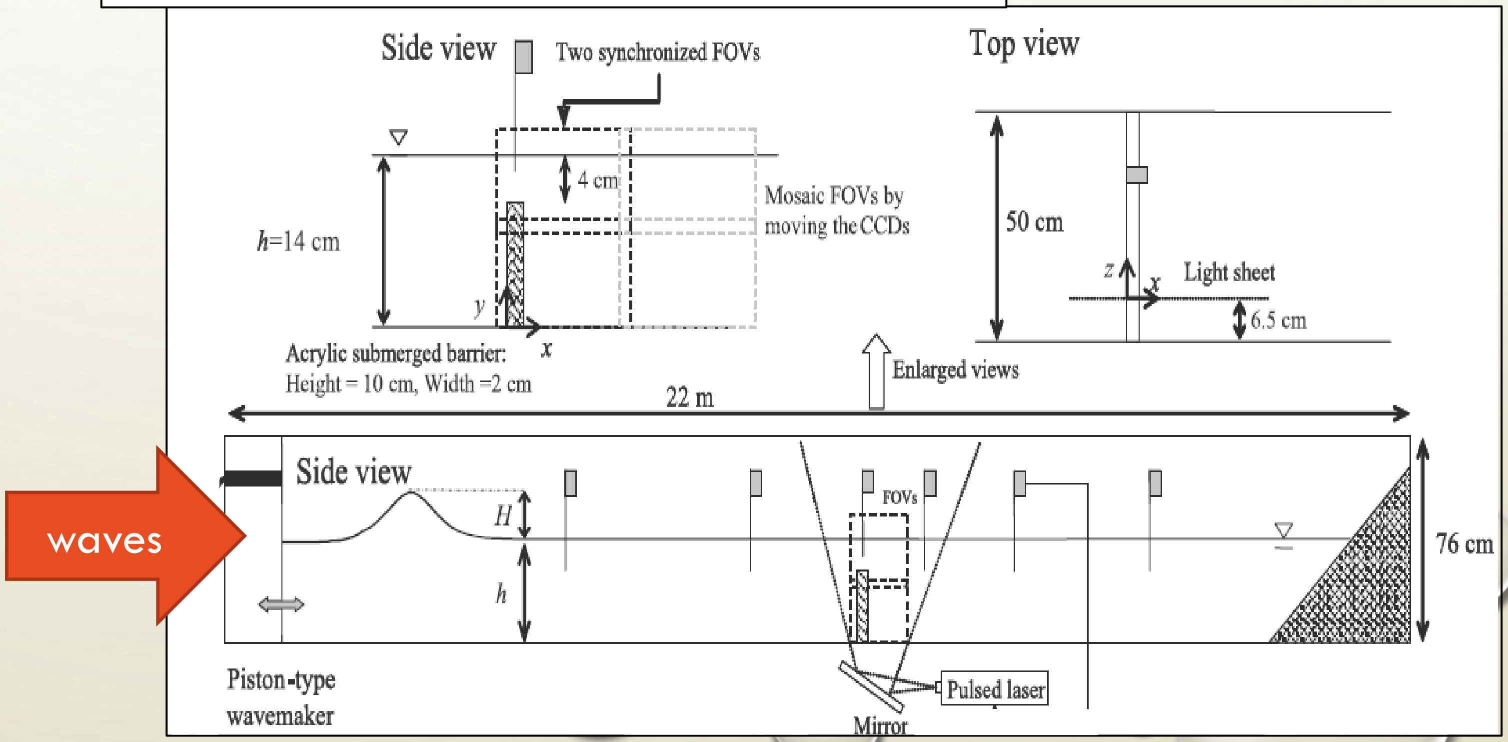

MATTEO POSTACCHINI
UNIVERSITÀ POLITECNICA DELLE MARCHE (Ancona)

(ALMOST) HORIZONTAL VORTICITY

_breaking waves over a rectangular structure

Numerical simulations

- COBRAS *(Wu et al., Coast.Eng. 2012)*
  - 2D scheme solving Reynolds-Averaged Navier-Stokes (RANS) equations
  - nonlinear k-ε equations for the turbulent kinetic energy (k) and the turbulent dissipation rate (ε)

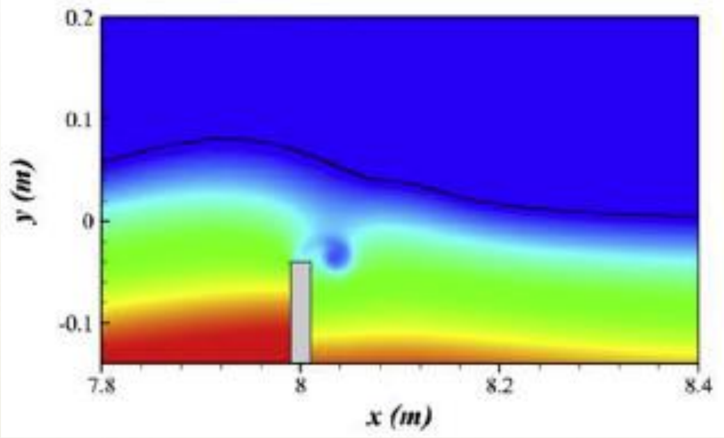

- CIP-based model *(Wang et al., Oc.Eng. 2018)*
  - 2D Constrained Interpolation Profile method to solve hyperbolic-type equations
  - non-uniform and staggered Cartesian grid
  - semi-Lagrangian scheme, mainly applied in fields of physics and electromagnetism
  - continuity + 2D N-S equations

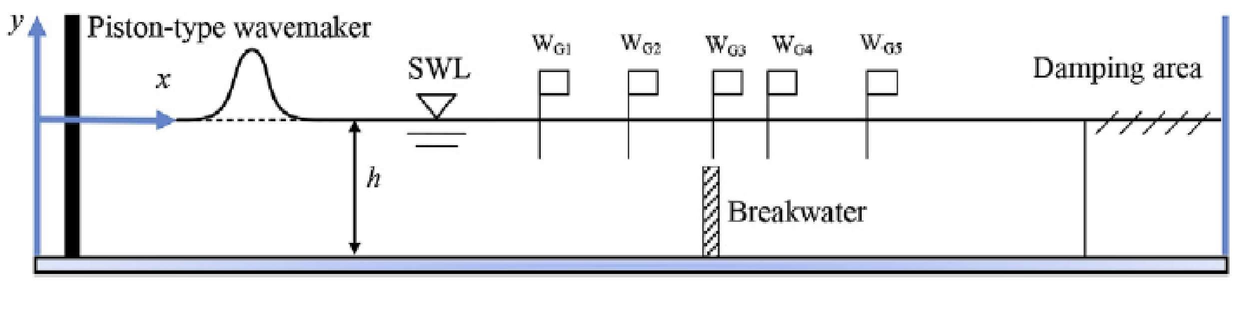

Fig. 1. Schematic view of numerical model.

(ALMOST) HORIZONTAL VORTICITY

_breaking waves over a rectangular structure

Exp-COBRAS comparison (*Wu et al.*, 2012)

- large clockwise vortex generated by flow separation (similar to non-breaking-wave case)
- smaller anti-clockwise vortex:
    1. intact wave form approaching the structure
    2. free-surface bulging and double wave crest
    3. "backward breaking" (sort of hydraulic jump)
    4. air-water mixing + anti-clockwise vortex
- interaction between counter-rotating eddies

Courtesy of *Prof. Shih-Chun Hsiao*

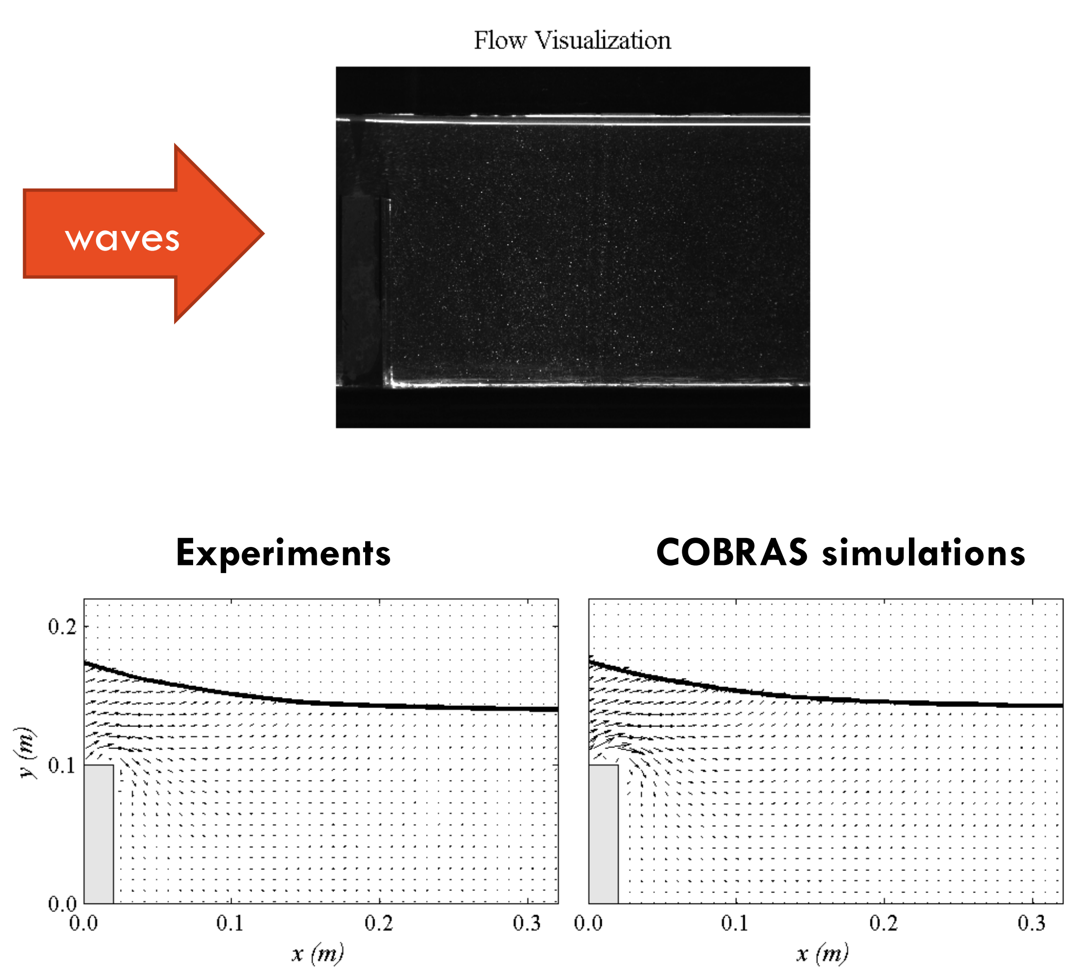

(ALMOST) HORIZONTAL VORTICITY

_breaking waves over a rectangular structure

Exp-CIP comparison (*Wang et al.*, 2018)

- large clockwise vortex generated by flow separation (similar to non-breaking-wave case)
- smaller anti-clockwise vortex:
    1. intact wave form approaching the structure
    2. free-surface bulging and double wave crest
    3. “backward breaking” (sort of hydraulic jump)
    4. air-water mixing + anti-clockwise vortex
- interaction between counter-rotating eddies
- <u>additional **vortex** generated at bed</u>

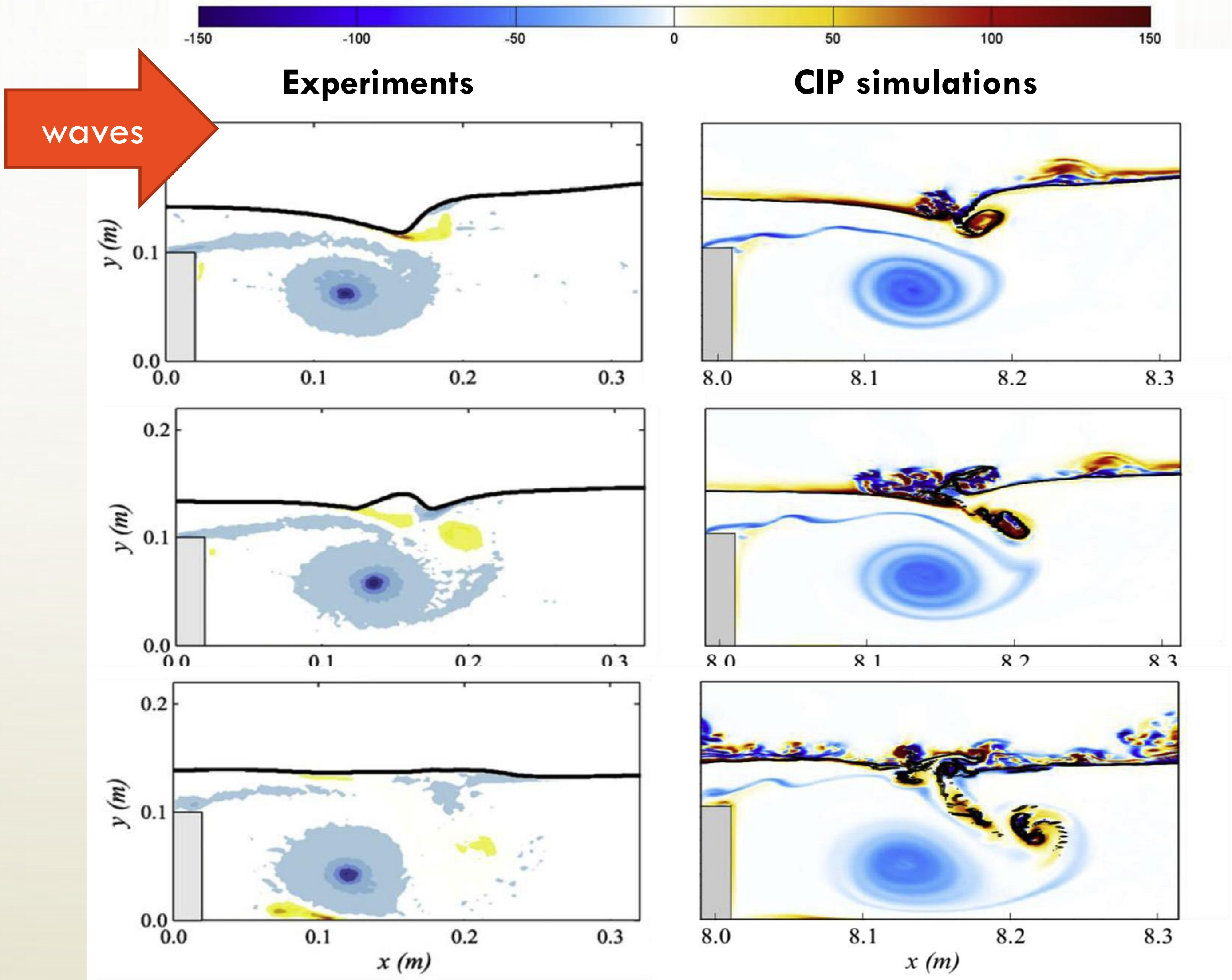

Adapted from *Wang et al. (Oc.Eng., 2018)*

MATTEO POSTACCHINI
UNIVERSITÀ POLITECNICA DELLE MARCHE (Ancona)

(ALMOST) HORIZONTAL VORTICITY

clockwise vortex from flow separation due to waves over obstacles of various size/shape

- ruled by wave characteristics, obstacle geometry, soil type (e.g., grain size, porosity)

anti-clockwise vortex at the surface due to wave breaking

- driven by impinging jet (function of wave characteristics)
- interaction between counter-rotating vortices

wave - structure - soil
→ vortex features (e.g., strength, energy)

- potential soil erosion close to or relatively far from structure (case of vortex-vortex interaction)
- potential structure damages or failure

MATTEO POSTACCHINI
UNIVERSITÀ POLITECNICA DELLE MARCHE (Ancona)

(ALMOST) VERTICAL VORTICITY

_short-crested waves

Wave breaking → transfer of momentum between atmosphere and ocean

- *Open ocean* (deep waters) → breaking forced by wind stress
  - development of <u>vortex ring</u> around breaking area, where flow topology requires the horizontal ring segment as a <u>connection</u> between counter-rotating vertical vortices developing at the edges of the breaking region

Adapted from *Peregrine (Eur.J.Mech.B/Fluids, 1999)*

waves **in deep** waters

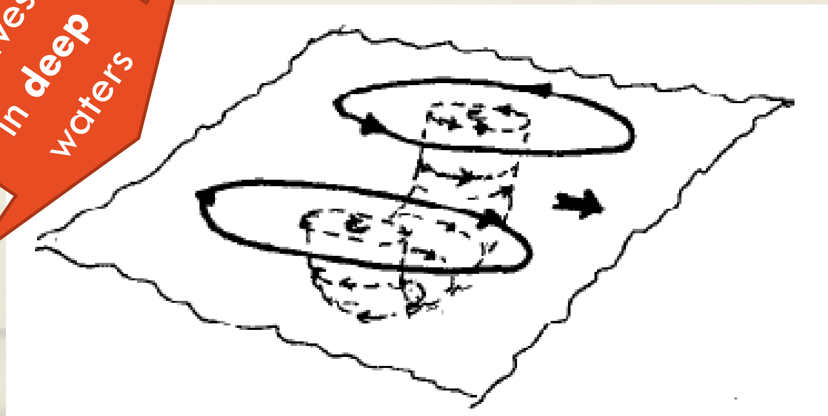

MATTEO POSTACCHINI
UNIVERSITÀ POLITECNICA DELLE MARCHE (Ancona)

(ALMOST) VERTICAL VORTICITY

_short-crested waves

Wave breaking → transfer of momentum between atmosphere and ocean

- *Coastal region*
  - short-crested waves → finite-length breakers/bores
  - *Peregrine* (1998,1999):
    - <u>rate of change of circulation around closed loop</u> crossing a breaker = <u>wave energy dissipation</u> across wave front (head loss): $\frac{\partial \Gamma}{\partial t} = E_D = \frac{g(h_2 - h_1)^3}{4 h_1 h_2}$

    (h_2 , h_1: water depths behind and in front of breaking wave)
    - longshore <u>differential wave energy dissipation</u> (e.g., at breaker edges) forces a jump in <u>potential vorticity</u> (due to changes in h_2 and h_1): $\Delta\Omega \propto \frac{\partial E_D}{\partial y}$

Adapted from *Peregrine (Eur.J.Mech.B/Fluids, 1999)*

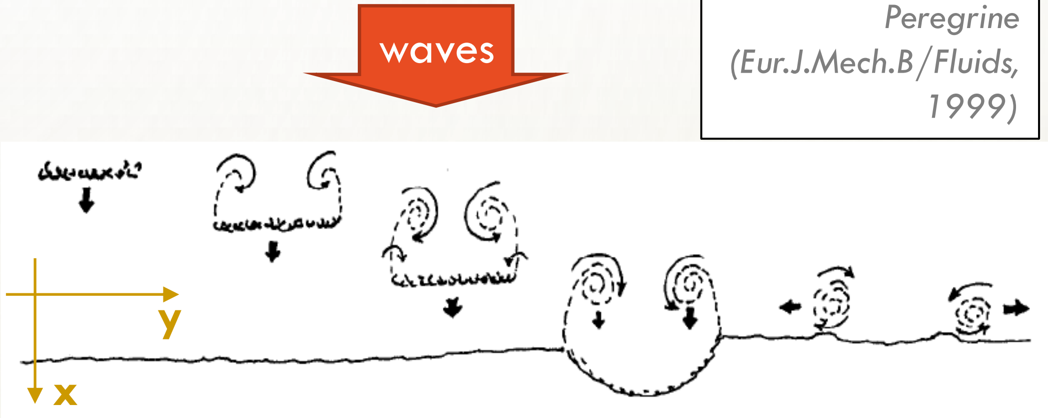

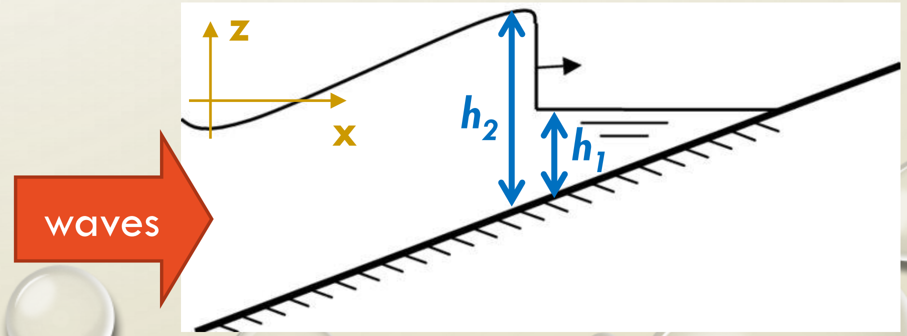

(ALMOST) VERTICAL VORTICITY

_short-crested wave breaking and vortex generation

- From *long-crested* to *short-crested* waves in the nearshore
  - ***submerged structures***
    - breaking over the structure and generation of short breakers
  - ***cross-sea***
    - induced by wave processes (e.g., reflection, refraction, diffraction)
    - honeycomb structure and breaking
- Vortex *generation* at breaker edges
- Typical *mechanisms* of motion
  - ❑ **self-advection** – driven by bed depth
  - ❑ **mutual advection** – vortex interaction

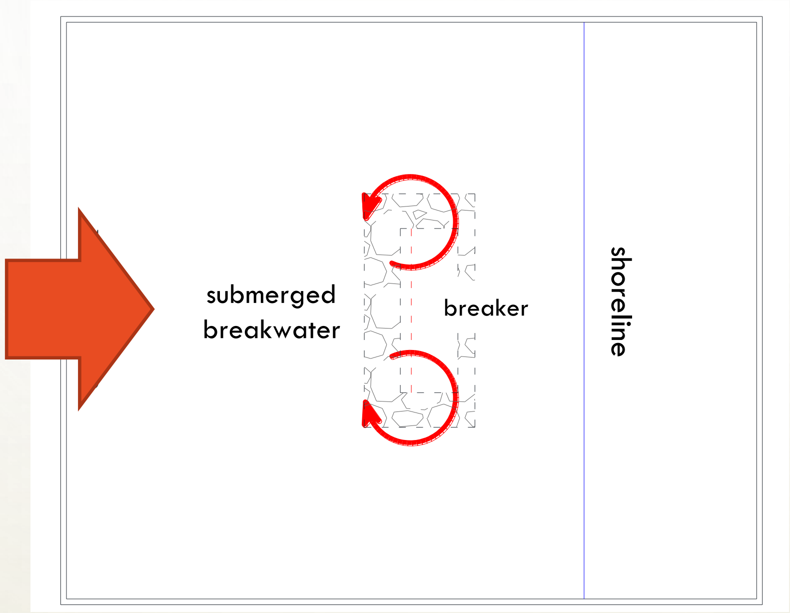

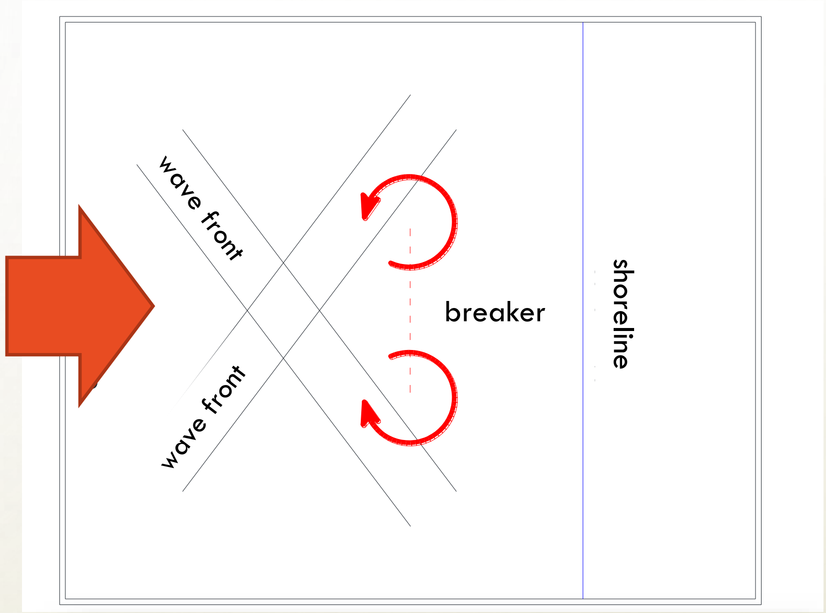

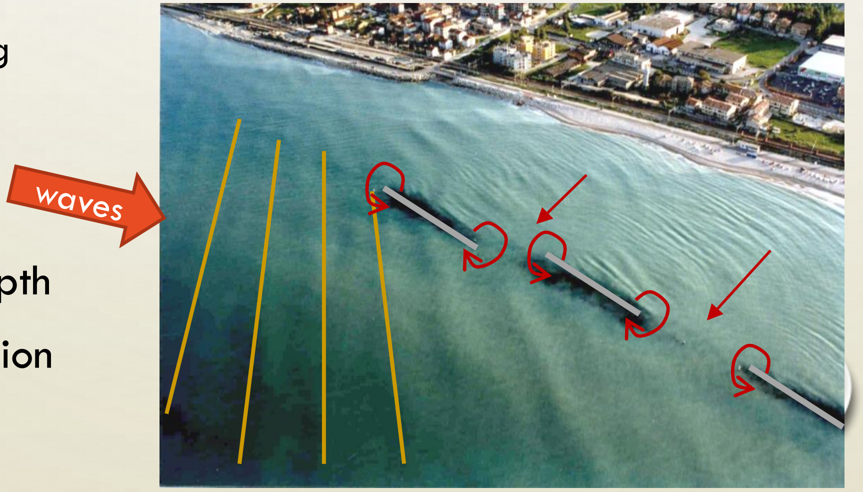

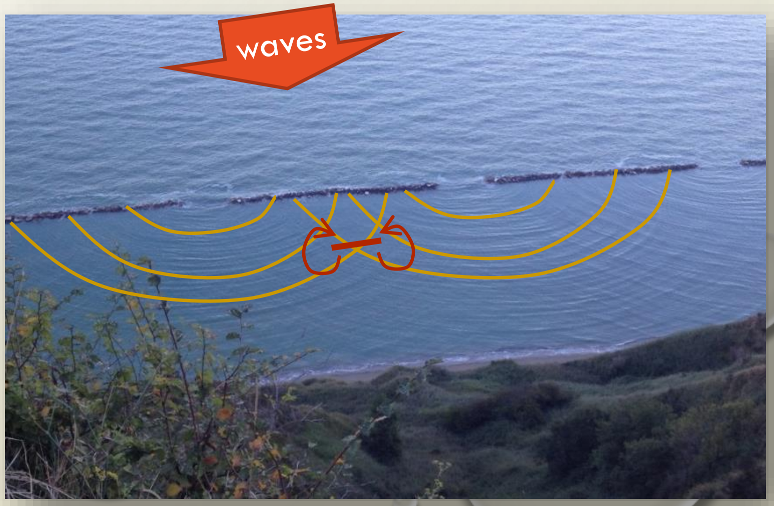

MATTEO POSTACCHINI
UNIVERSITÀ POLITECNICA DELLE MARCHE (Ancona)

(ALMOST) VERTICAL VORTICITY

- *Surf zone* as source for turbulent eddy structures
  - <u>2D inverse cascade</u> (transfer of energy from small-scale vorticity to larger structures)
- *Short waves* due to different nearshore processes
  - "dipolar vorticity structure" at breaker edges

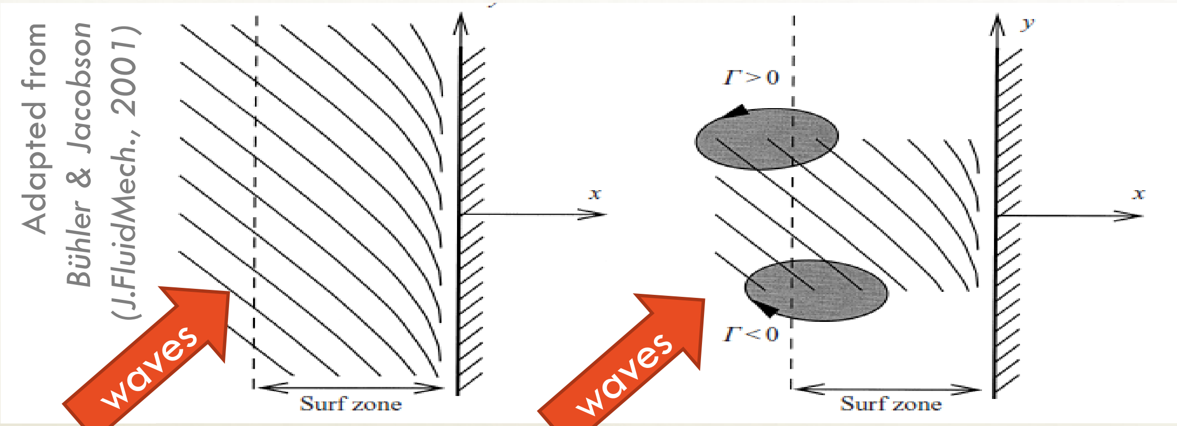

- *Alongshore current* due to breaking over submerged bars
  - <u>long-crested</u>: strong current over the bar crest
  - <u>short-crested</u>: large landward shift over barred beaches (e.g.,~50m, *Kirby & Derakhti*, 2019) and weak over planar beaches (*Bühler & Jacobson*, 2001)

_*short-crested waves*

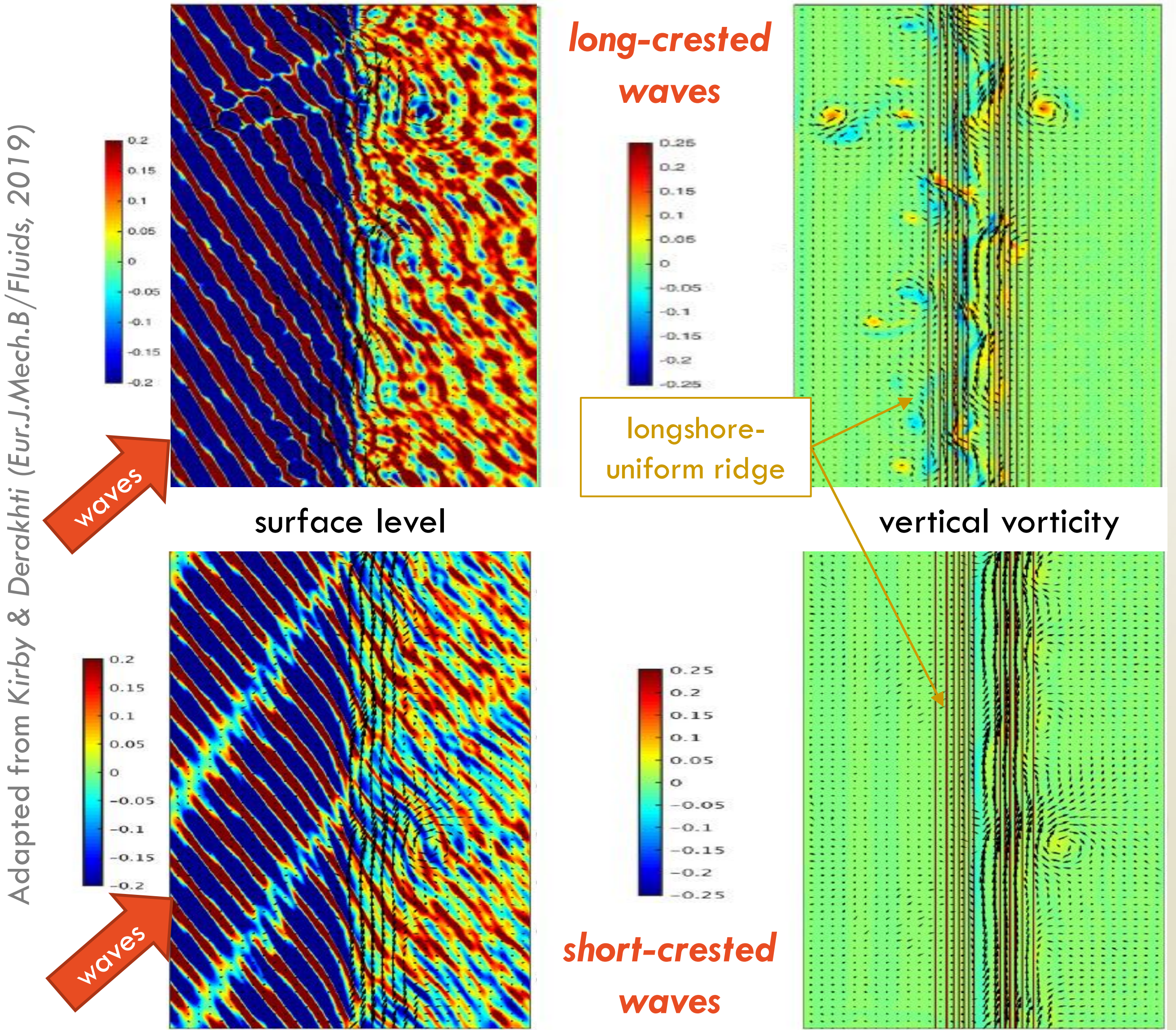

MATTEO POSTACCHINI
UNIVERSITÀ POLITECNICA DELLE MARCHE (Ancona)

(ALMOST) VERTICAL VORTICITY

- **2DH simulations**
  - FUNWAVE - depth-averaged Boussinesq-type model
  - short-crested waves traveling over a barred beach
  - breaking over bar crest (x~650m)
  - counter-rotating vortices at breaker edges
  - well-organized (seaward) **rip currents** at incident wave nodes (dashed lines)
  - nearshore breaking and **further rip currents**
- **3D simulations**
  - TRUCHAS – Large Eddy Simulations (LES) code
  - Peregrine (1999)'s **vortex loop** evolving towards a horseshoe vortex, then aligning with mean flow

_short-crested waves

Adapted from
Kirby & Derakhti
(Eur.J.Mech.B/Fluids, 2019)

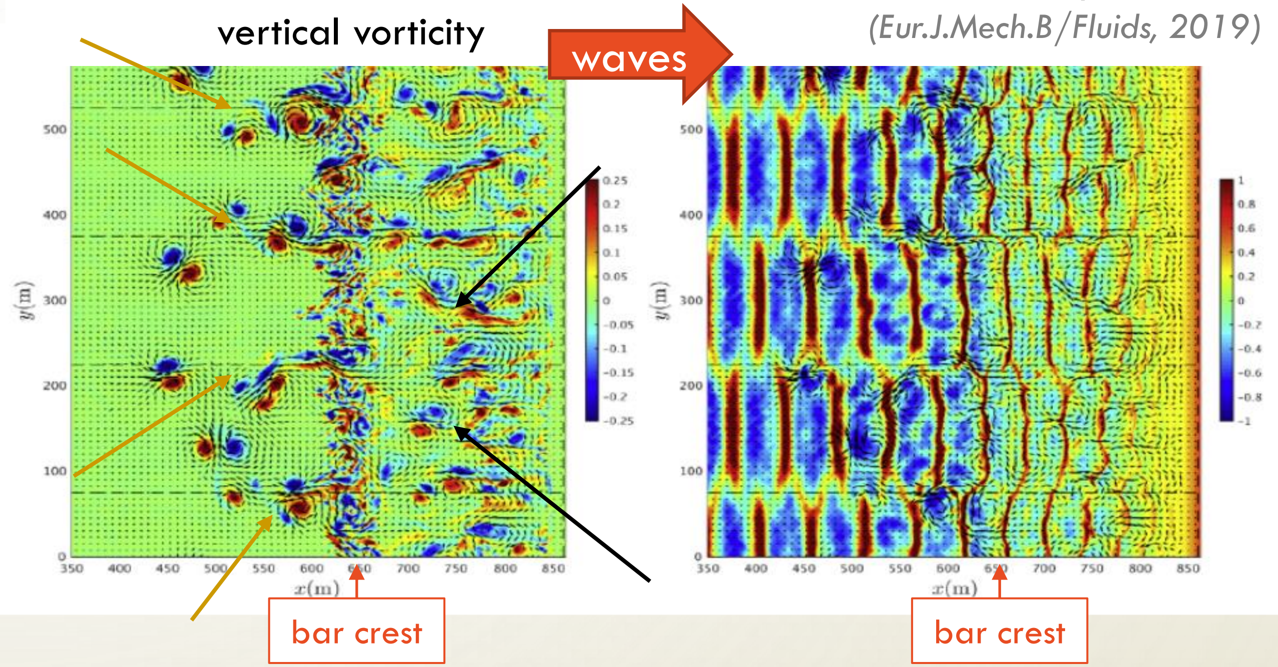

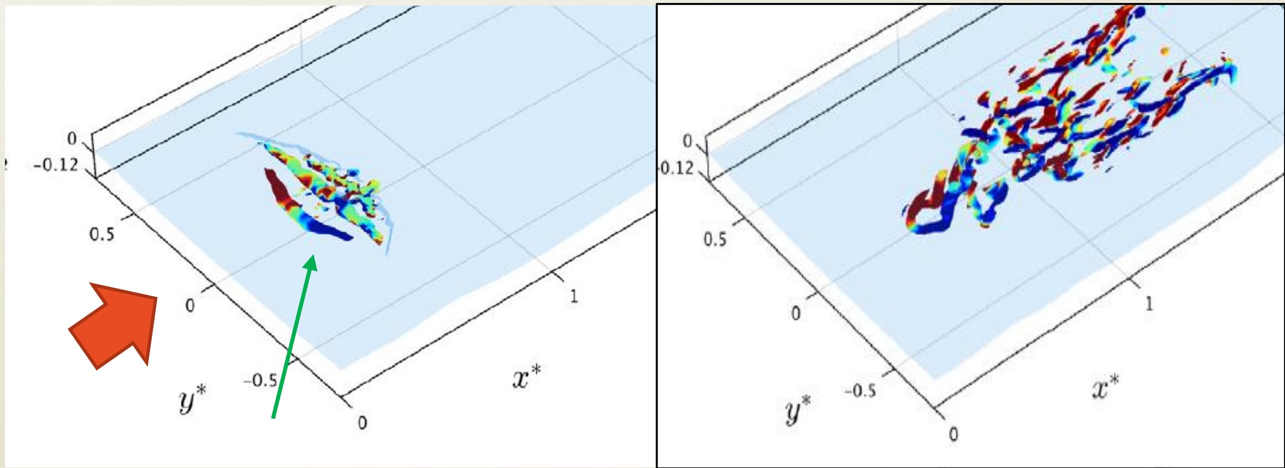

MATTEO POSTACCHINI
UNIVERSITÀ POLITECNICA DELLE MARCHE (Ancona)

(ALMOST) VERTICAL VORTICITY

_breaking over submerged structures

- **Numerical simulations**
  - Nonlinear Shallow Water Equations (NSWE)
    - 2DH depth-averaged model
  - regular wave train (H=1m, T=10s) over submerged breakwater
- **Findings**
  - <u>vortex generation</u> along the lateral boundaries
  - <u>shoreward motion</u> (mutual advection)
  - <u>self-advection</u> around the structure + detachment
  - motion nearby the structure (self-advection and interaction among vortices)
  - vortex <u>dissipation</u>

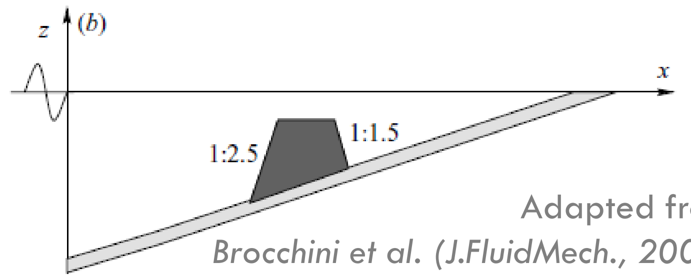

Adapted from Brocchini et al. (J.FluidMech., 2004)

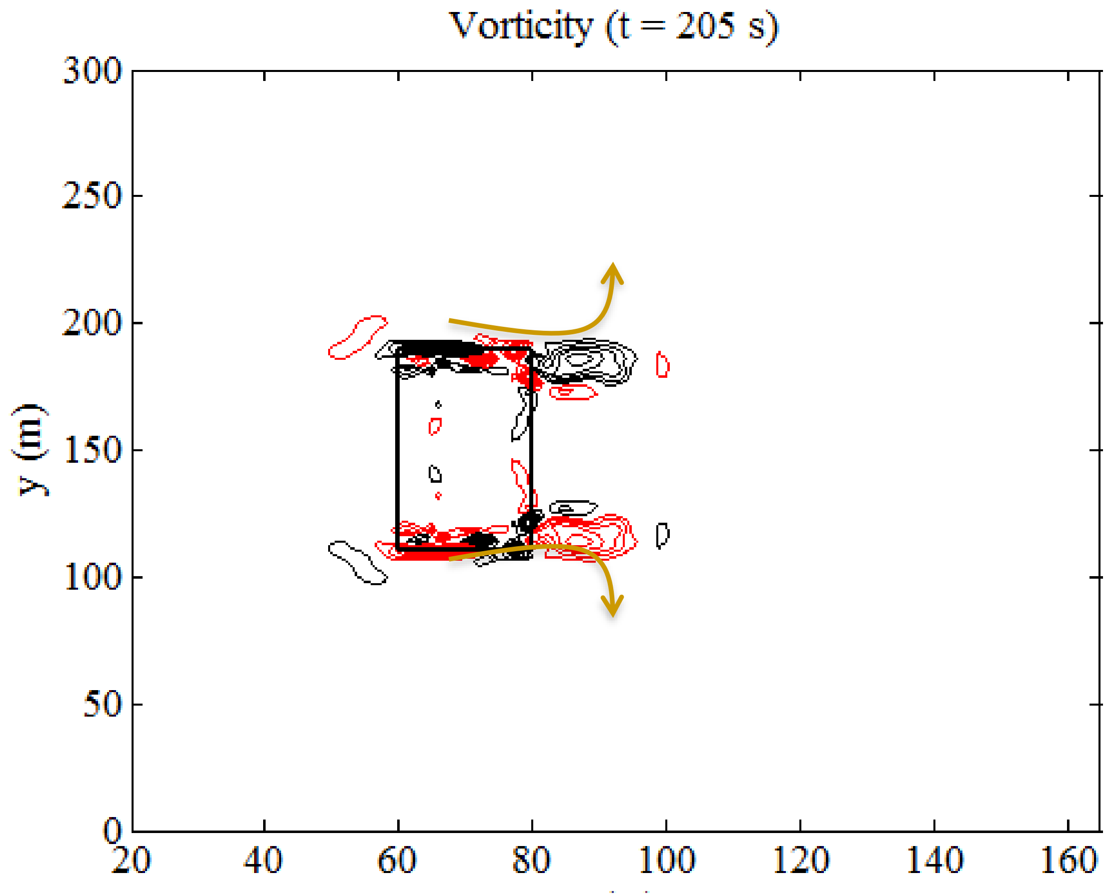

Adapted from *Postacchini & Brocchini (IDRA 2014)*

MATTEO POSTACCHINI
UNIVERSITÀ POLITECNICA DELLE MARCHE (Ancona)

(ALMOST) VERTICAL VORTICITY

counter-rotating vortices at the edges of short-crested breakers

- induced by submerged finite-length obstacles or intersecting waves

vortex motion ruled by **self-advection** and **mutual interaction**

- dispersion mechanism and inverse cascade

- important role in rip-current generation/development

breakwater or **cross-sea characteristics** define pattern of vortex pairs

- swimmers'/beach-goers' <u>safety</u>

- <u>morphological changes</u>, especially close to structures/at breaking locations, in the rip channel, where vortices migrate

CONCLUDING REMARKS

<ins>coherent structures in the coastal region</ins> at the basis of *engineering*, *environmental*, *safety* issues

almost horizontal vorticity generates from <ins>interaction</ins> with submerged obstacles

- bed erosion (e.g., at structure toe) or **scouring** process

- potential **structure instability**

almost vertical vorticity generates from short-crested breakers

- interaction, shoreward-seaward motion, <ins>rip currents</ins>

- erosion-deposition patterns

- people **safety**

THANKS
FOR YOUR ATTENTION

“Calibration and verification of sediment transport models in the real world” (M. Knaapen, HRW)

hr wallingford

Calibration and validation for morphological modelling in consultancy

Michiel Knaapen

Overview

- Data availability and quality
- Derived data/pseudo data
- Model input data sources
- Calibration parameters
- Project examples
  - Poole & Christchurch Bays
  - Texas

Data: Publicly available

Data availability

Water levels

- Almost every port has a tide gauge
- Accurate satellite data

Data availability

https://www.ndbc.noaa.gov/

Wave & current data

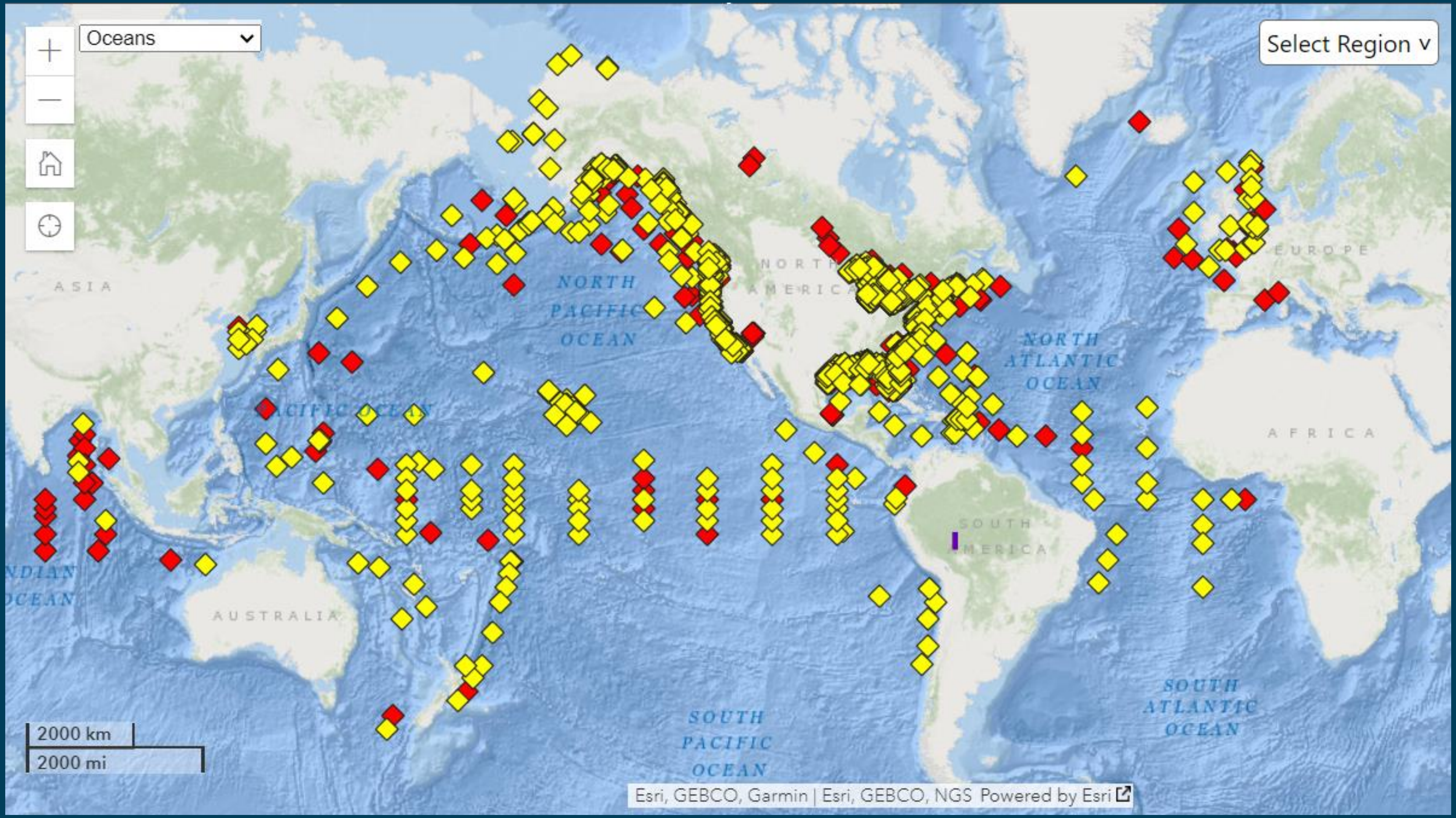

*There are more buoys around

Data availability

Wave data & current data

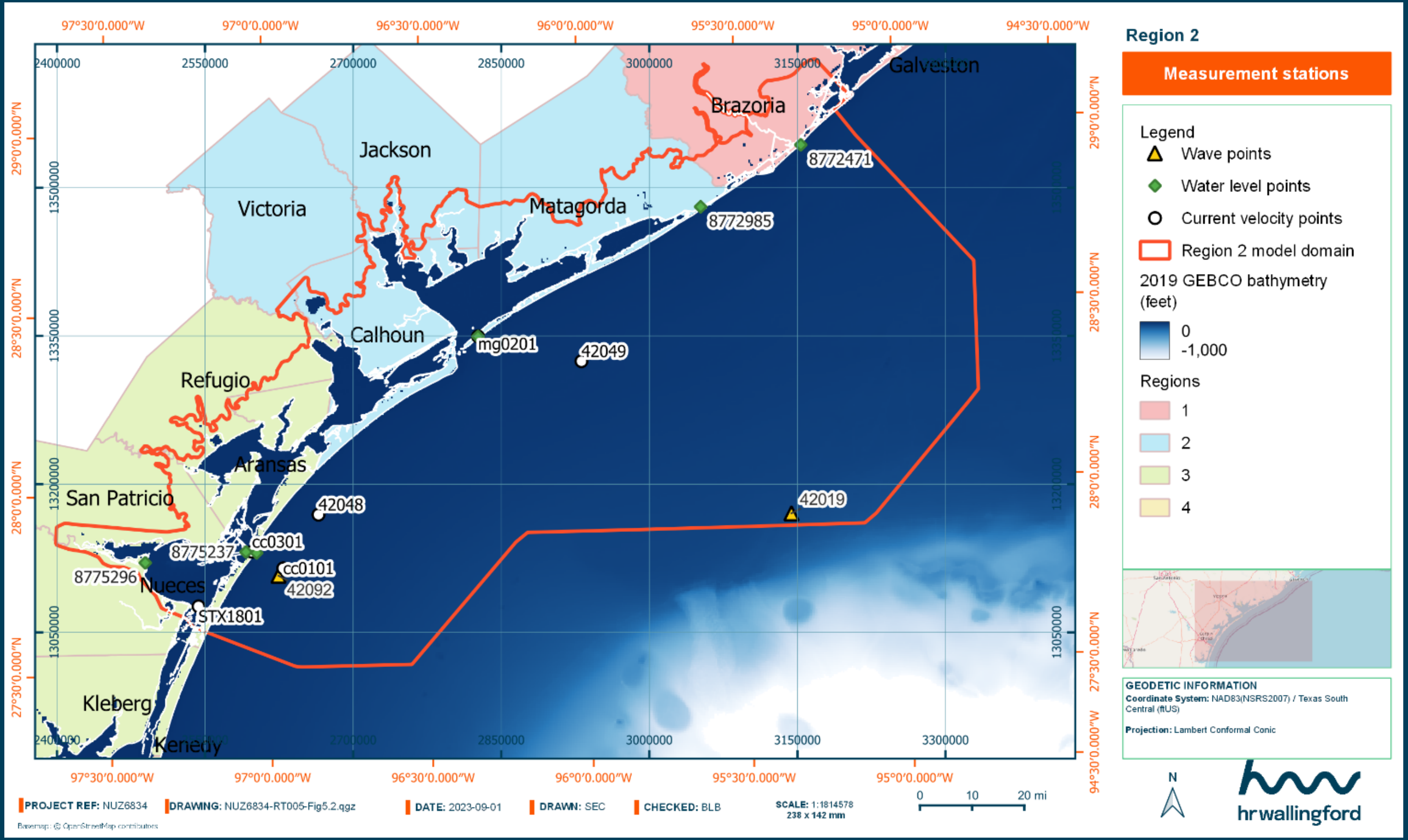

hr wallingford

Data availability

Current data

Generally only surface currents

If profiles are available, it will be missing

- the top 0.5-1m and
- bottom 0.5-1m

Data availability

Sediments

Sediment transport cannot be measured directly

Data availability

Sediments

Concentration data is very rare outside specific research locations (Duck/Egmond/…)

- Taken during calm conditions
- Short period
- calm conditions
- Never taken near the bed

Data availability

Sediments

Seabed composition:

Low resolution

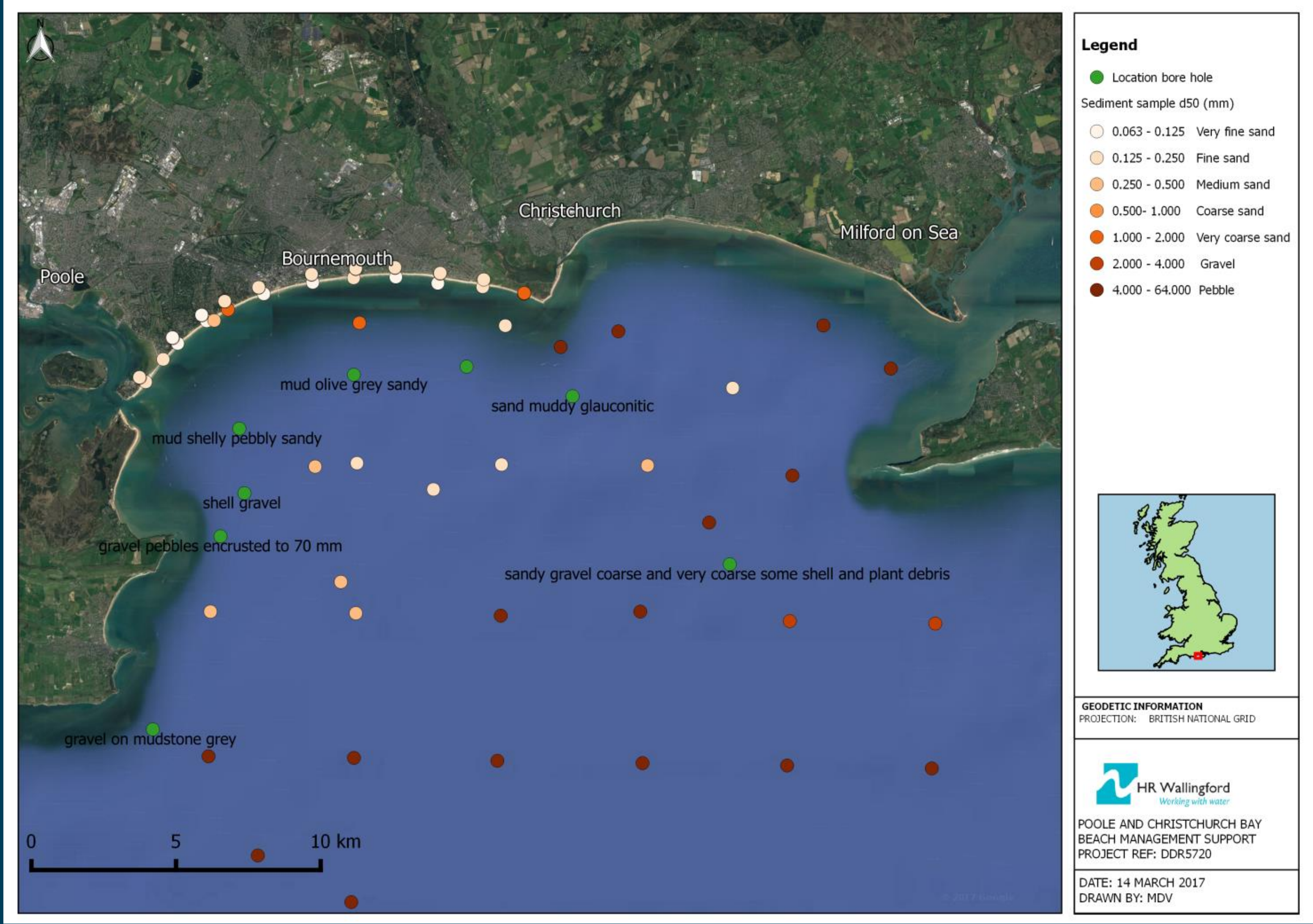

Data availability

Sediments

Seabed composition:

Grain size distributions

Median size

Sediment fractions (clay/silt/mud/gravel)

Classification

Project dependent data cover short period of time

Water levels for Extreme level analysis

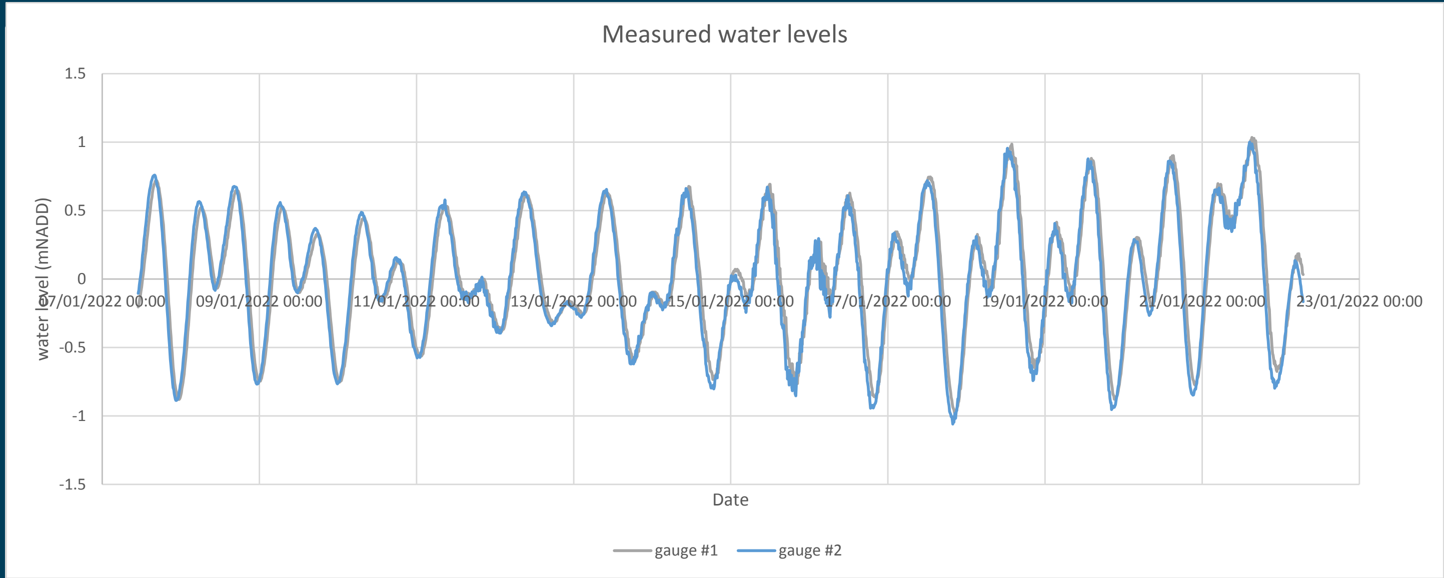

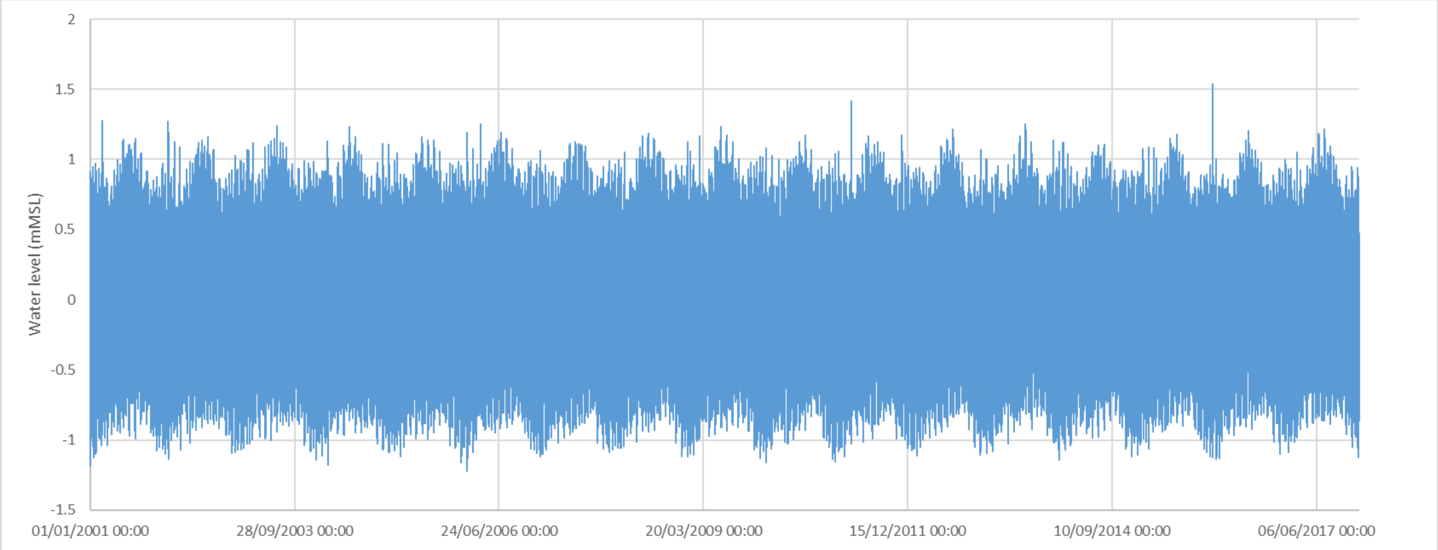

hrwallingford

Project dependent data

Wave measurements for Extreme level analysis and sediment transport

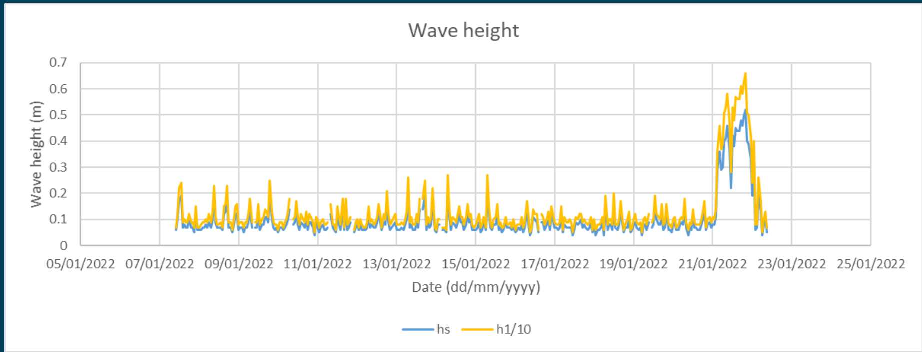

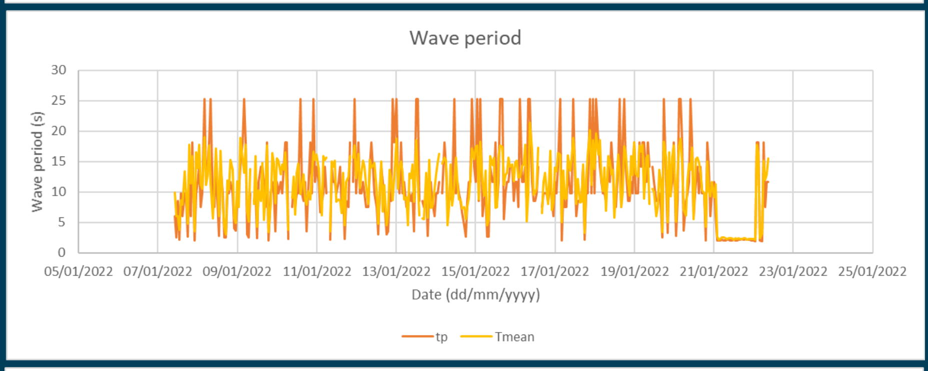

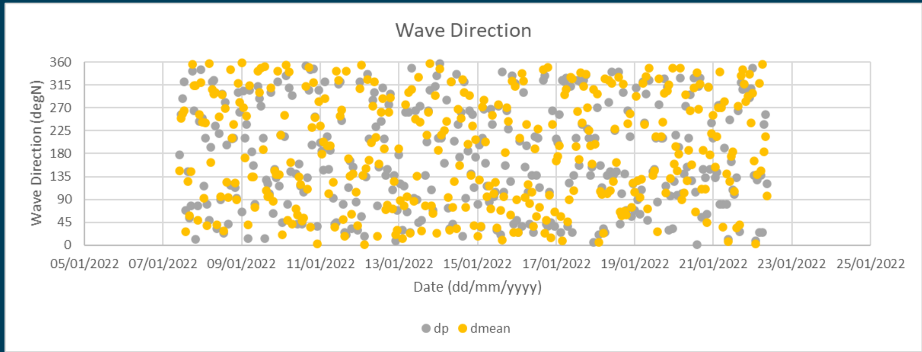

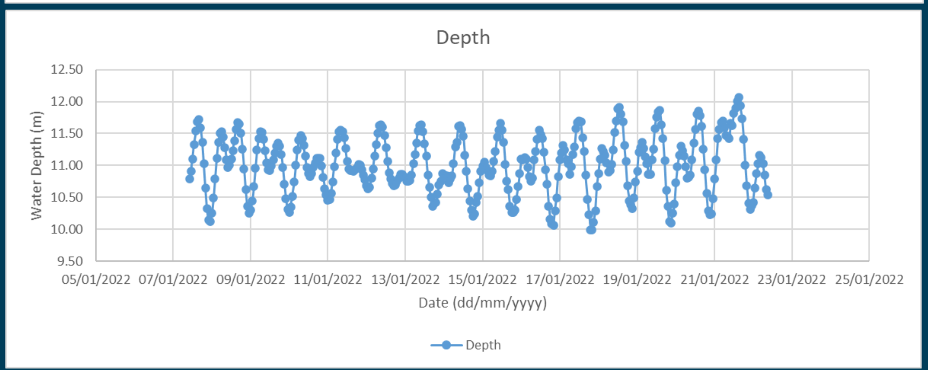

hr wallingford

Uncertainties in sediment transport

- To improve form a factor 2-5, we do need verification
- Against local measurements
  - sediment transport or

$$Qs = \int_{o}^{h} u\, C$$

- Qs= suspended load transport
- U = velocity
- C =concentration
- h = water depth

So needs velocities and concentrations in same location

Shoreline morphology

Modelled sediment budgets compared to observed shoreline retreat

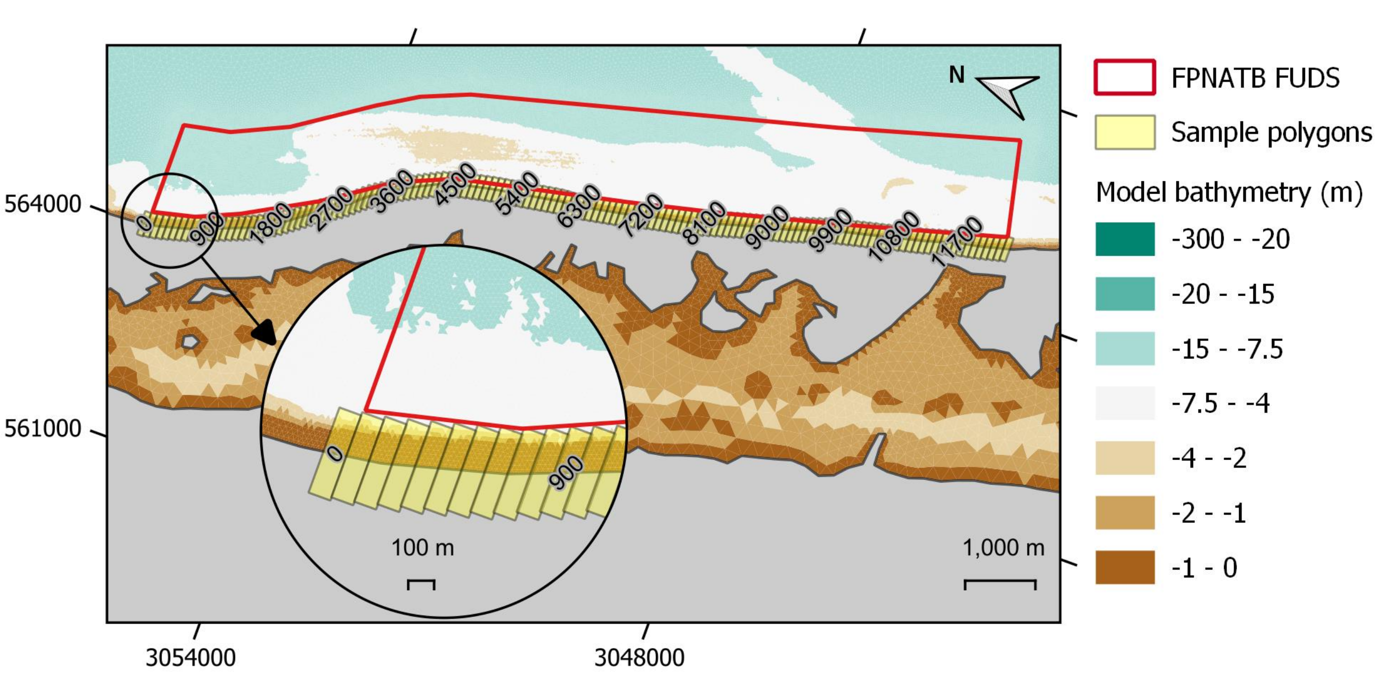

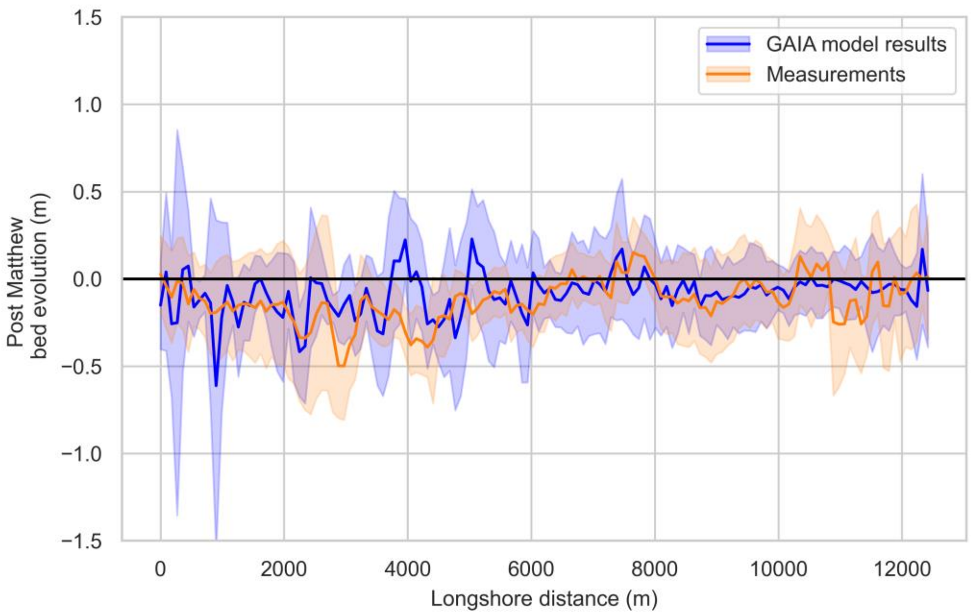

hrwallingford

CHALLENGING ACCEPTED KNOWLEDGE ON THE LITTORAL DRIFT IN TEXAS

Michiel Knaapen

Belen Blanco & Richard Lewis

Soft solutions for coastal management

- Increasing number of nourishments
- Nourishment disappearing
- Need more sources for sediment

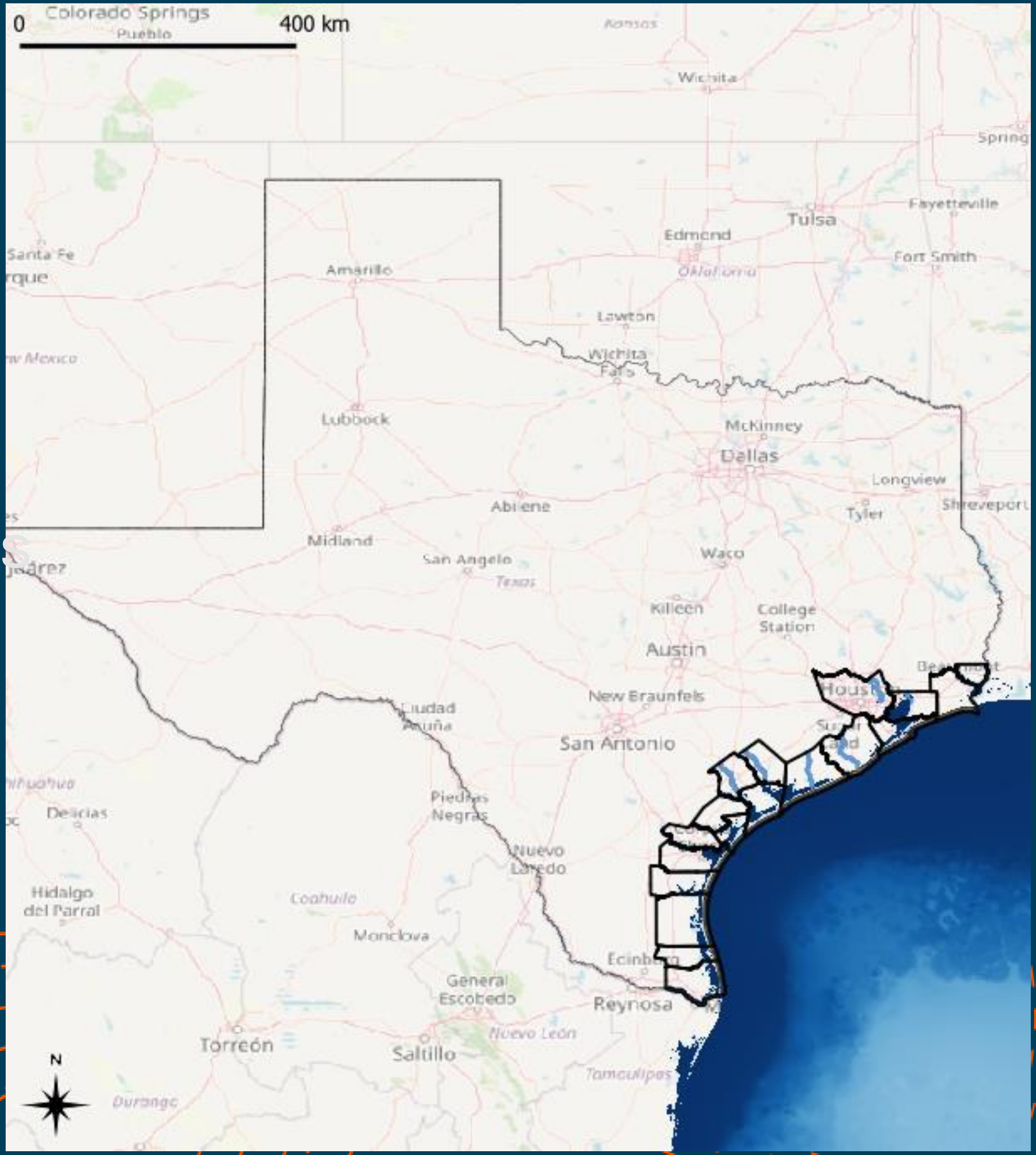

TEXAS GENERAL LAND OFFICE
ESTABLISHED 1836

hrwallingford

Existing knowledge

Literature based on McGowen et al (1977)

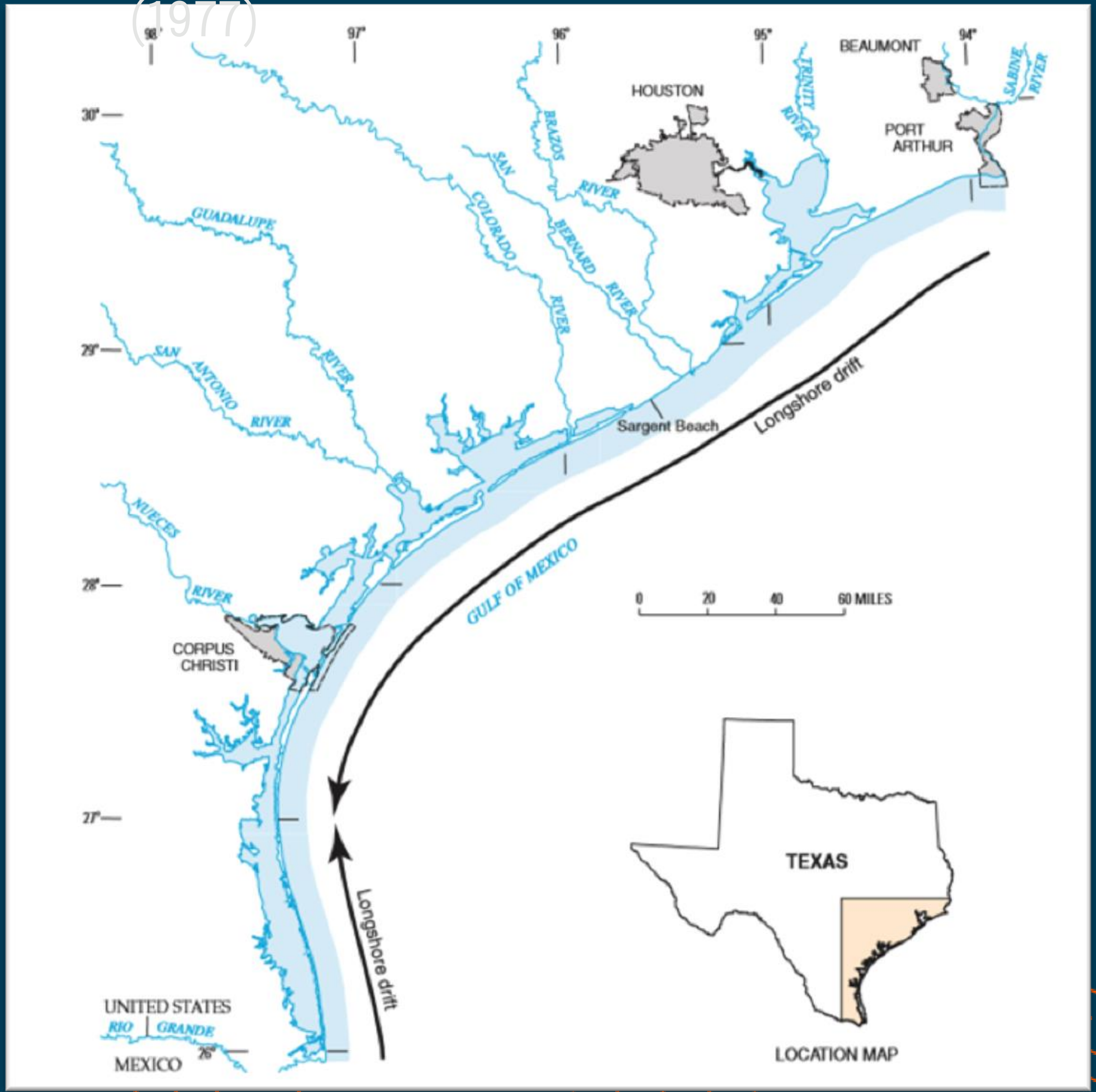

Based on littoral drift due to waves from sector E-S, ignoring currents

hr wallingford

Mapping the sediment transport pathways in detail

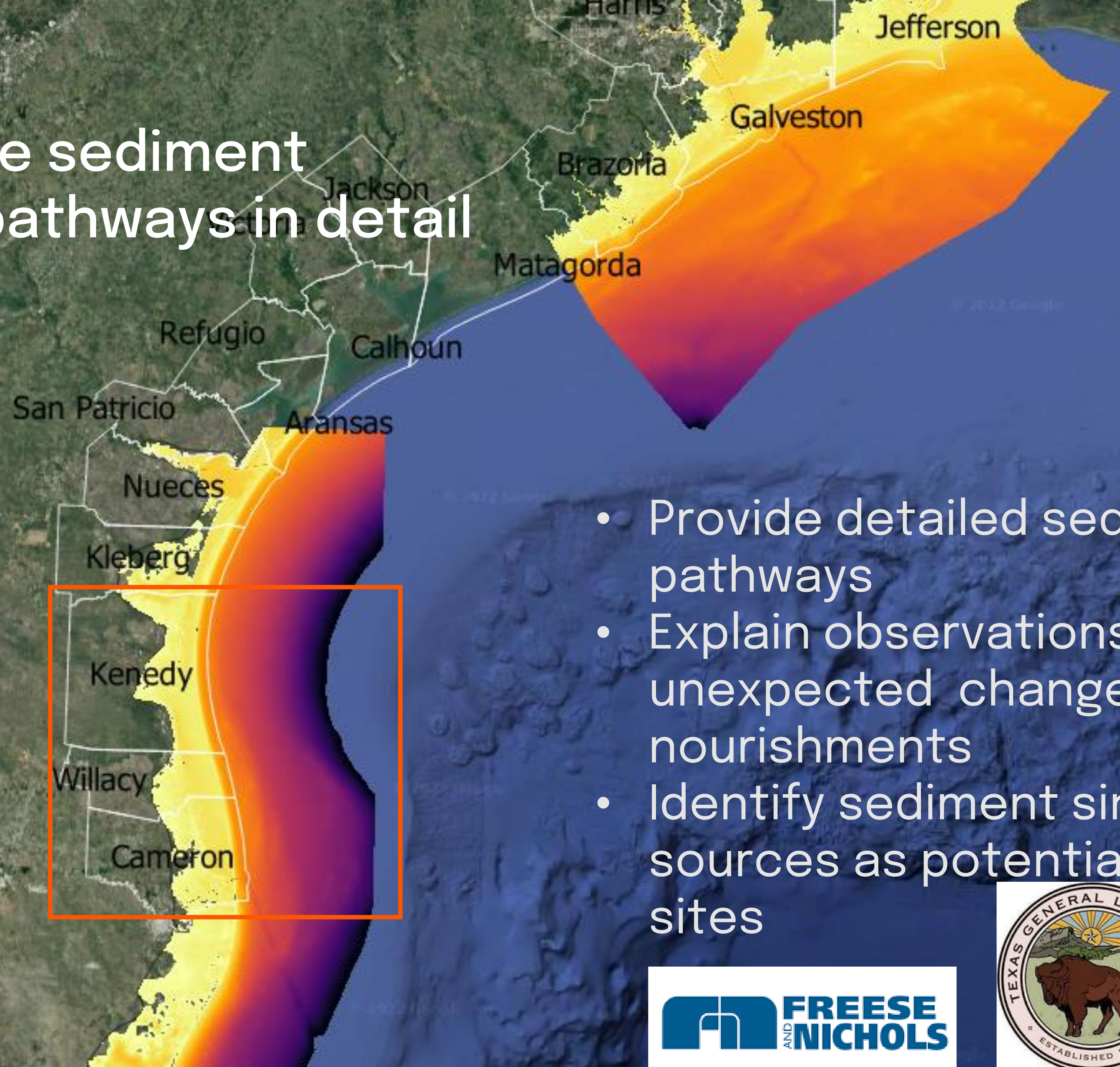

- Provide detailed sediment pathways
- Explain observations unexpected changes nourishments
- Identify sediment sinks and sources as potential borrow sites

The model: TELEMAC-TOMAWAC-SISYPHE

http://www.opentelemac.org/

Model set-up sand transport modelling

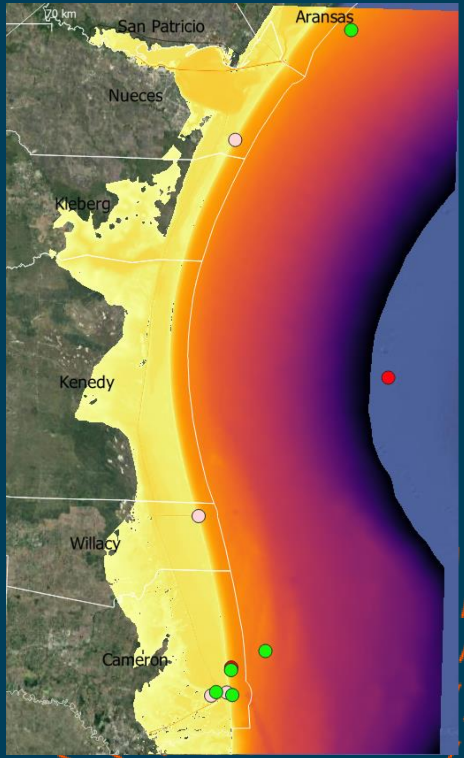

Mesh

- 500,000 nodes;
- 10m at breaker line;
- 5km on offshore boundary;
- barrier islands in bathymetry

hr wallingford

Model set-up sand transport modelling
(Following Knaapen TUC 2019)

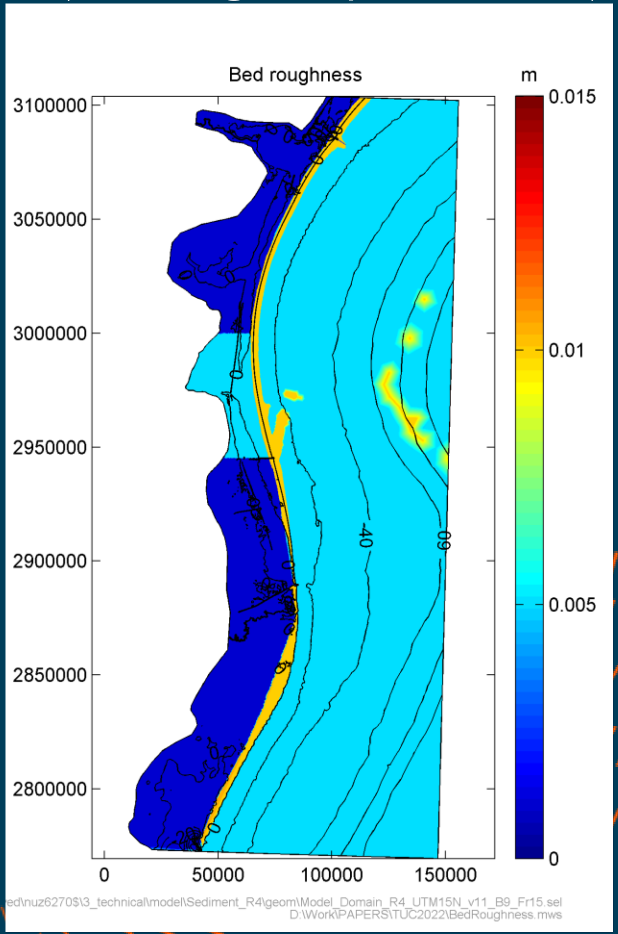

Model setting:

- Waves: TOMAWAC
- Currents: TELEMAC 2D

Model settings as close to default as possible, exceptions:

- Numerical stability settings
- Smagorinski turbulence model
- Friction: Nikuradse, spatially varying

hr wallingford

Model set-up sand transport modelling

(Following Knaapen TUC 2019)

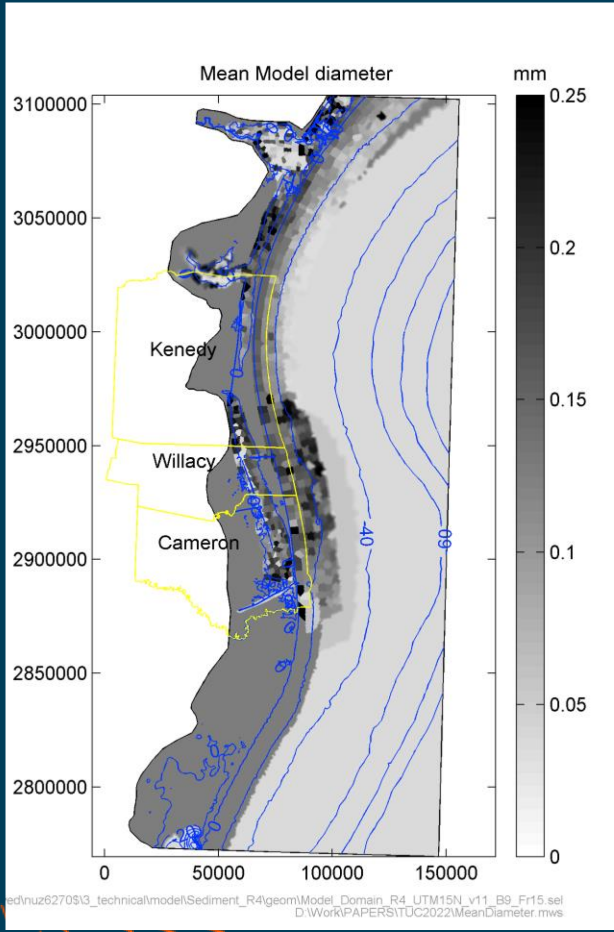

Model setting:

- Waves: TOMAWAC
- Currents: TELEMAC 2D
- Sediment: SISYPHE

Model settings as close to default as possible, exceptions:

- Bedload sediment transport: Soulsby-van Rijn
- Suspended sediment transport: Soulsby-van Rijn
- Settling lag
- Grain size: Spatially varying; 5 sediment classes (silt & sand)

hr wallingford

Calibration/Validation data

Waves: 2 points (red)
Currents: 5 points (green)
Levels: 4 points (pink)

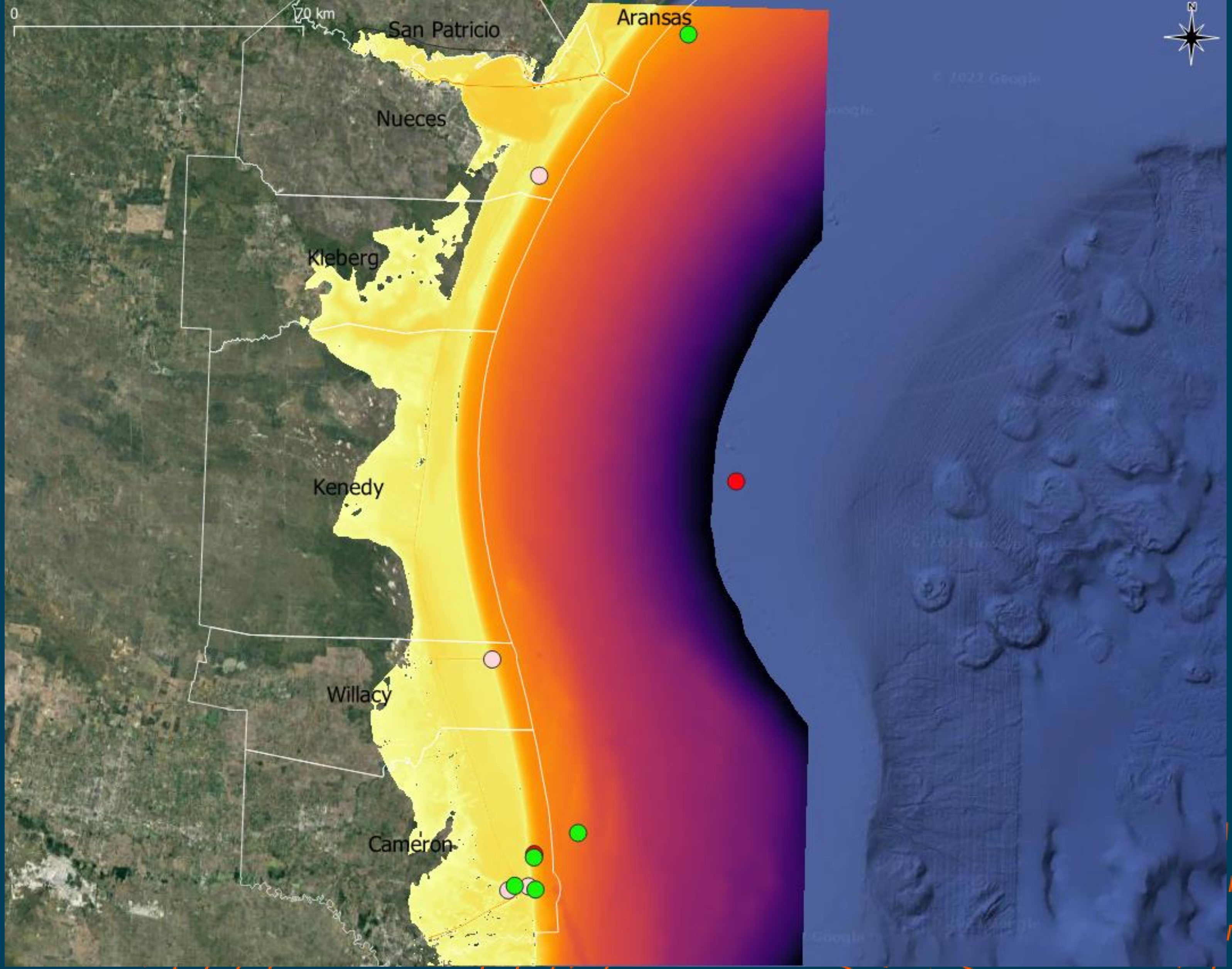

hrwallingford

Validation results nearshore waves

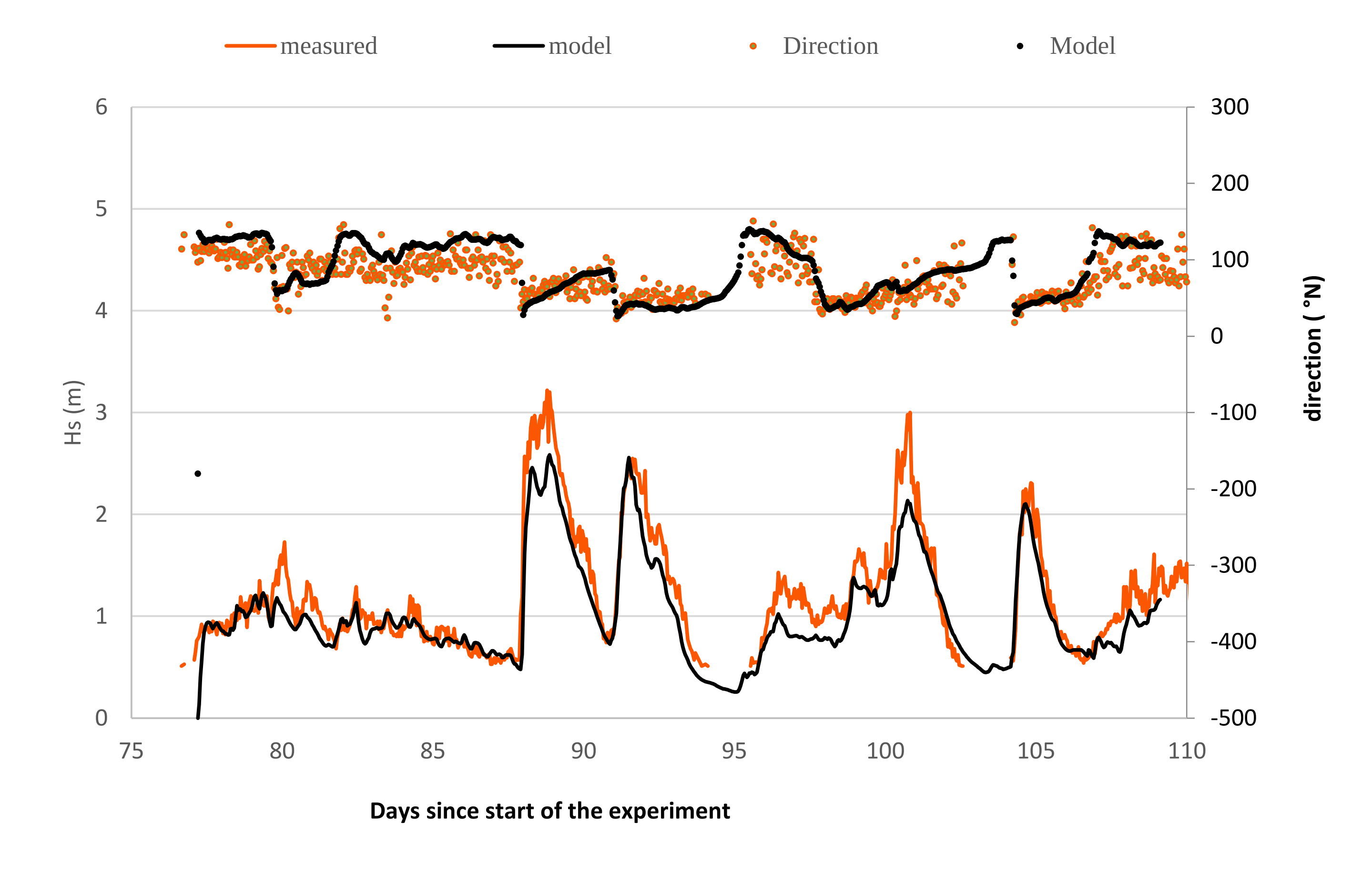

hr wallingford

Validation results nearshore currents

hr wallingford

Error statistics validation

Variable	Location		RMSE	Skill
Water level (m)	Aransas Pass	Inlet	0.29	0.93
	Bob Hall Pier	Coast	0.29	0.93
	South Padre Island	Inlet	0.27	0.89
	Port Isabel	Laguna	0.28	0.94
Velocity (m/s)	Tabs Buoy D	Ocean	0.14	0.55
	Tabs Buoy J	Ocean	0.06	0.66
	South Padre Island September*	Coast	0.06	0.60
	South Padre Island November*	Coast	0.11	0.89
Wave height (m)	NDBC 42045	Ocean	0.28	0.85
	South Padre Island November*	Coast	0.14	0.95

*Engel et al (2019)

Channel sedimentation

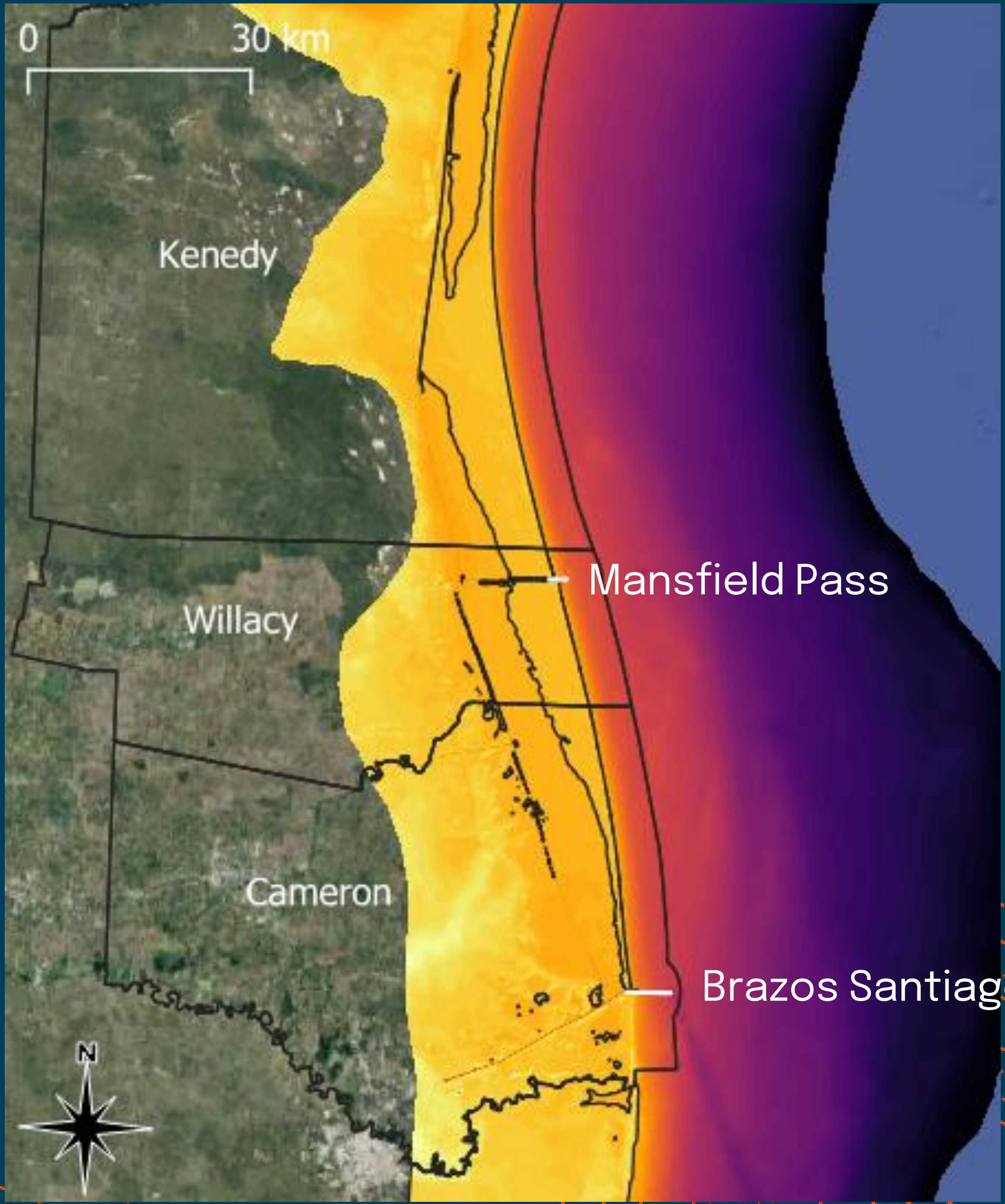

hrwallingford

Channel sedimentation outside Brazos Santiago Pass

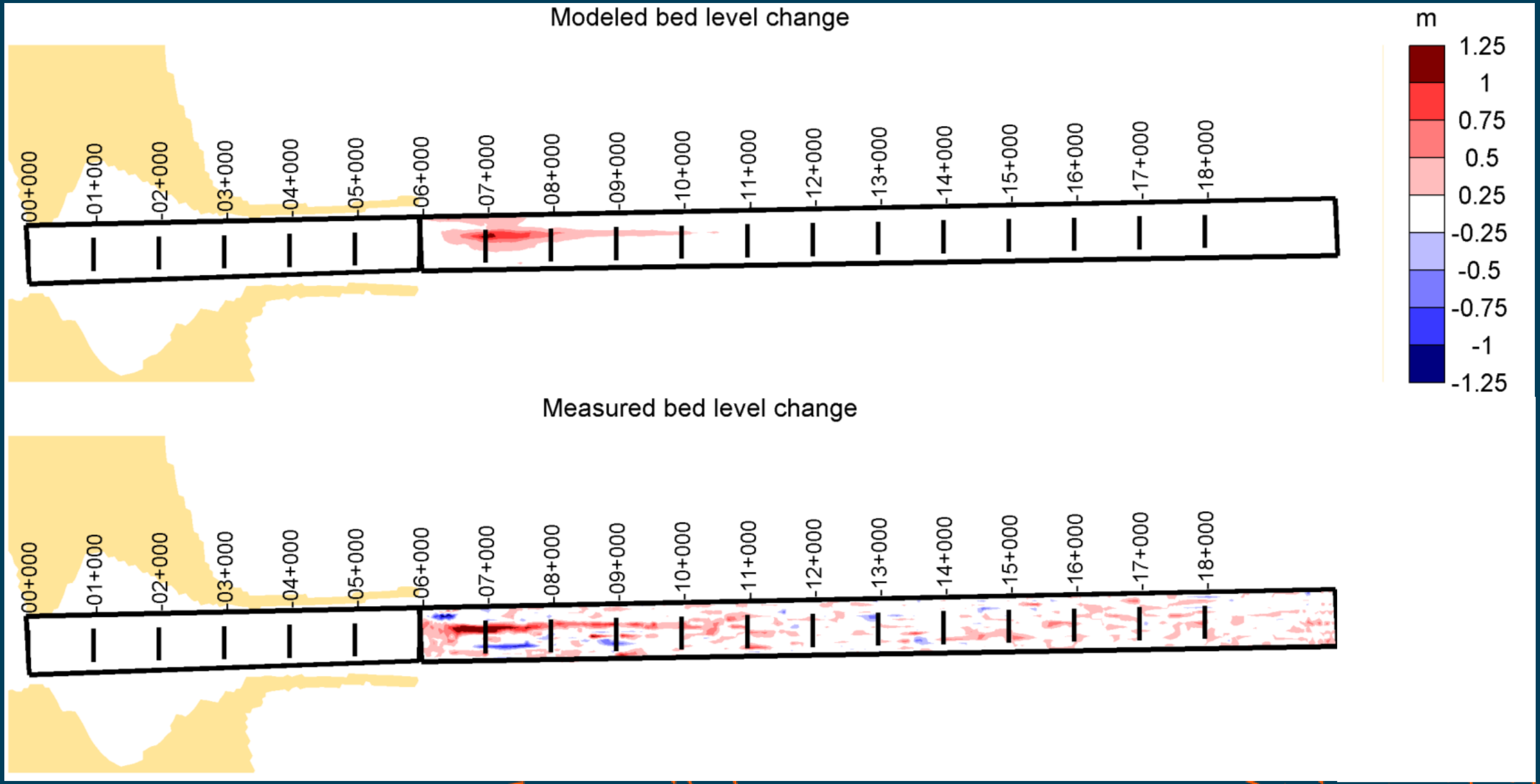

hr wallingford

Quantification evolution 3 months

Channel	Measured infill	Model infill	Error
	m^3/y	m^3/y	%
Brazos Santiago jetties	62,000*	58,000	-6
Brazos Santiago outer	78,000	73,000	-6
Mansfield jetties	-45,000	-22,000	-51

*Includes correction of reference

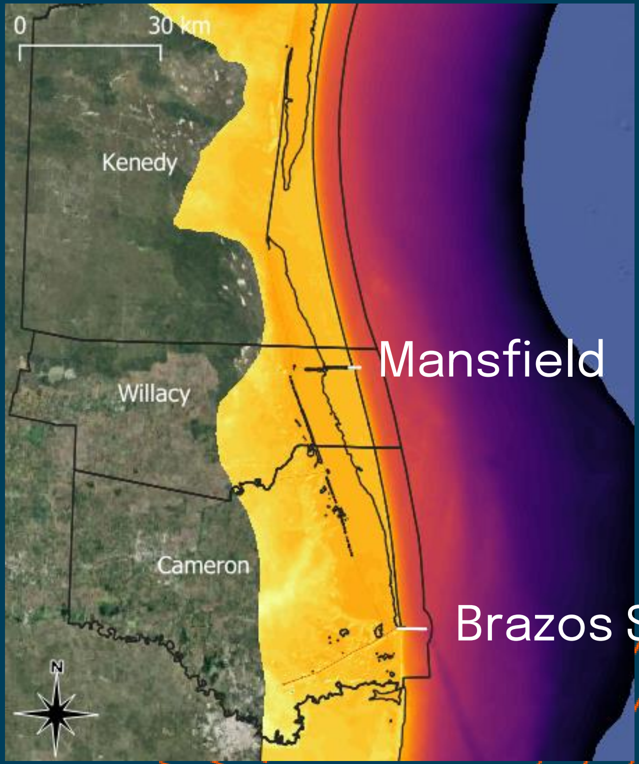

hr wallingford

Quantification long-term infill /dredging volumes

Channel	Measured infill	Model infill	Error
	m³/y	m³/y	%
Brazos Santiago jetties	115,000	147,000	28
Brazos Santiago outer	154,000	124,000	19
Mansfield jetties	27,000	41,000	52
Mansfield outer	2,000	0	-100

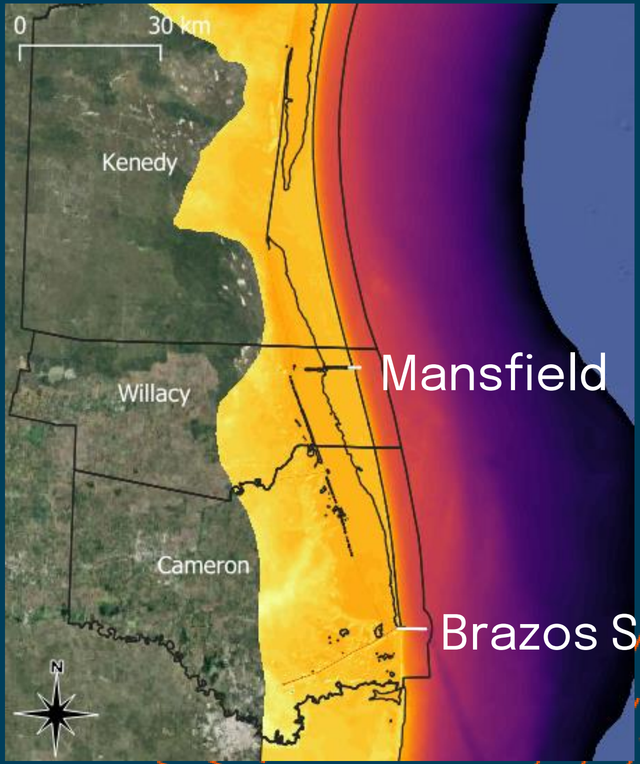

hr wallingford

Area modelling changes the conventional knowledge on littoral drift in Texas

Conclusion:

- Even thought the current velocities in the Gulf of Mexico are low, they cannot be neglected in nearshore sediment transport calculations

Area modelling changes the conventional knowledge on littoral drift in Texas

Implications:

- Placement of dredged material:
  - Placement sites north of the entrance channel
  - Sediment could rapidly return to channel
- Location of Nourishment:
  - Distance offshore might effect direction of movement
- Breakwaters/groynes:
  - The length of the groyne might influence not only the magnitude but also the direction of sediment bypassing